frontiers | Research Topics

Effects of alcohol use on immunity and immune responses

Edited by
Suhas Sureshchandra, Samantha Yeligar, Derrick R. Samuelson and Ilhem Messaoudi

Published in
Frontiers in Immunology

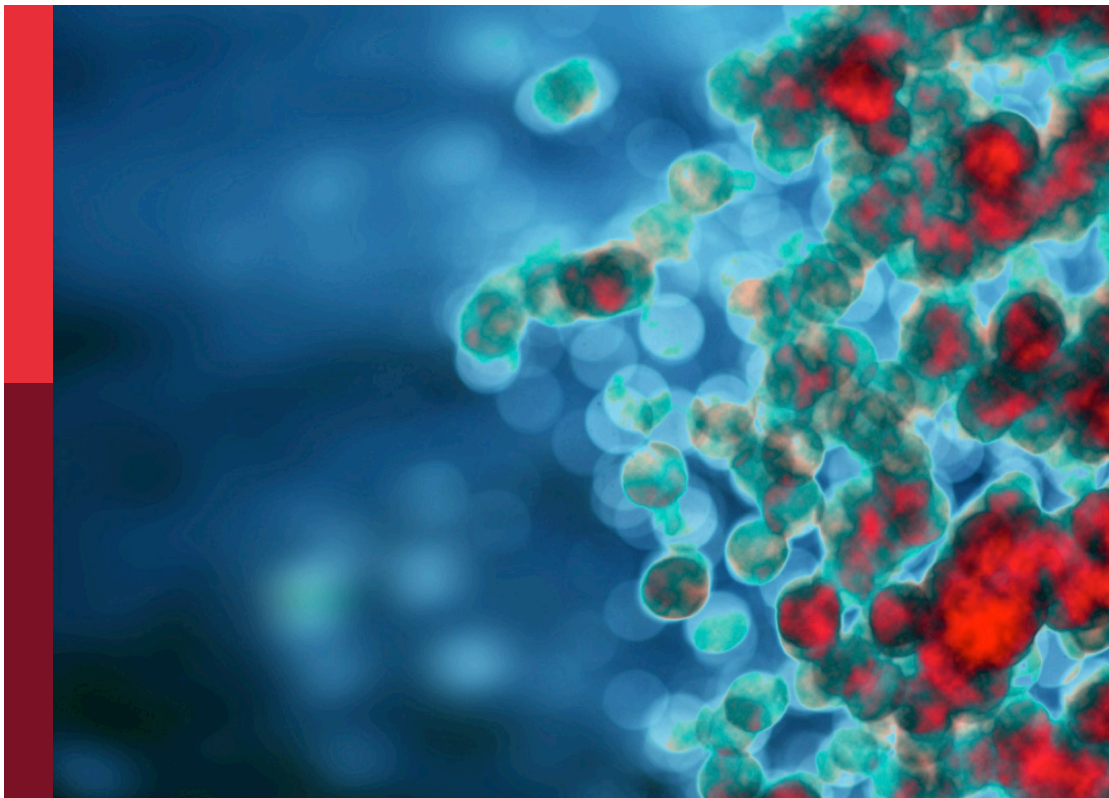

ISSN 1664-8714
ISBN 978-2-8325-4059-6
DOI 10.3389/978-2-8325-4059-6

About Frontiers

Frontiers is more than just an open access publisher of scholarly articles: it is a pioneering approach to the world of academia, radically improving the way scholarly research is managed. The grand vision of Frontiers is a world where all people have an equal opportunity to seek, share and generate knowledge. Frontiers provides immediate and permanent online open access to all its publications, but this alone is not enough to realize our grand goals.

Frontiers journal series

The Frontiers journal series is a multi-tier and interdisciplinary set of open-access, online journals, promising a paradigm shift from the current review, selection and dissemination processes in academic publishing. All Frontiers journals are driven by researchers for researchers; therefore, they constitute a service to the scholarly community. At the same time, the *Frontiers journal series* operates on a revolutionary invention, the tiered publishing system, initially addressing specific communities of scholars, and gradually climbing up to broader public understanding, thus serving the interests of the lay society, too.

Dedication to quality

Each Frontiers article is a landmark of the highest quality, thanks to genuinely collaborative interactions between authors and review editors, who include some of the world's best academicians. Research must be certified by peers before entering a stream of knowledge that may eventually reach the public - and shape society; therefore, Frontiers only applies the most rigorous and unbiased reviews. Frontiers revolutionizes research publishing by freely delivering the most outstanding research, evaluated with no bias from both the academic and social point of view. By applying the most advanced information technologies, Frontiers is catapulting scholarly publishing into a new generation.

What are Frontiers Research Topics?

Frontiers Research Topics are very popular trademarks of the *Frontiers journals series*: they are collections of at least ten articles, all centered on a particular subject. With their unique mix of varied contributions from Original Research to Review Articles, Frontiers Research Topics unify the most influential researchers, the latest key findings and historical advances in a hot research area.

Find out more on how to host your own Frontiers Research Topic or contribute to one as an author by contacting the Frontiers editorial office: frontiersin.org/about/contact

Effects of alcohol use on immunity and immune responses

Topic editors

Suhas Sureshchandra — University of California, Irvine, United States
Samantha Yeligar — Emory University, United States
Derrick R. Samuelson — University of Nebraska Medical Center, United States
Ilhem Messaoudi — University of Kentucky, United States

Citation

Sureshchandra, S., Yeligar, S., Samuelson, D. R., Messaoudi, I., eds. (2023). *Effects of alcohol use on immunity and immune responses*. Lausanne: Frontiers Media SA. doi: 10.3389/978-2-8325-4059-6

Table of contents

05 The Impact of Alcohol Use Disorder on Tuberculosis: A Review of the Epidemiology and Potential Immunologic Mechanisms
Gregory W. Wigger, Tara C. Bouton, Karen R. Jacobson, Sara C. Auld, Samantha M. Yeligar and Bashar S. Staitieh

18 Ethanol Intoxication Impairs Respiratory Function and Bacterial Clearance and Is Associated With Neutrophil Accumulation in the Lung After *Streptococcus pneumoniae* Infection
Holly J. Hulsebus, Kevin M. Najarro, Rachel H. McMahan, Devin M. Boe, David J. Orlicky and Elizabeth J. Kovacs

32 Alcohol-Induced Glycolytic Shift in Alveolar Macrophages Is Mediated by Hypoxia-Inducible Factor-1 Alpha
Niya L. Morris, David N. Michael, Kathryn M. Crotty, Sarah S. Chang and Samantha M. Yeligar

47 Alcohol Impairs Immunometabolism and Promotes Naïve T Cell Differentiation to Pro-Inflammatory Th1 $CD4^+$ T Cells
Patrick M. McTernan, Danielle E. Levitt, David A. Welsh, Liz Simon, Robert W. Siggins and Patricia E. Molina

60 Hyaladherins May be Implicated in Alcohol-Induced Susceptibility to Bacterial Pneumonia
Kathryn M. Crotty and Samantha M. Yeligar

69 Ethanol Induces Secretion of Proinflammatory Extracellular Vesicles That Inhibit Adult Hippocampal Neurogenesis Through G9a/GLP-Epigenetic Signaling
Jian Zou, T. Jordan Walter, Alexandra Barnett, Aaron Rohlman, Fulton T. Crews and Leon G. Coleman Jr

83 Acute Intoxication With Alcohol Reduces Trauma-Induced Proinflammatory Response and Barrier Breakdown in the Lung *via* the Wnt/β-Catenin Signaling Pathway
Laurens Noack, Katrin Bundkirchen, Baolin Xu, Severin Gylstorff, Yuzhuo Zhou, Kernt Köhler, Phatcharida Jantaree, Claudia Neunaber, Aleksander J. Nowak and Borna Relja

100 Malondialdehyde Acetaldehyde-Adduction Changes Surfactant Protein D Structure and Function
Claire G. Nissen, Deanna D. Mosley, Kusum K. Kharbanda, Dawn M. Katafiasz, Kristina L. Bailey and Todd A. Wyatt

109 Transcriptional and Epigenetic Regulation of Monocyte and Macrophage Dysfunction by Chronic Alcohol Consumption
Delphine C. Malherbe and Ilhem Messaoudi

125 Innate lymphocytes: Role in alcohol-induced immune dysfunction
Karla Ruiz-Cortes, Daniel N. Villageliu and Derrick R. Samuelson

137 Chronic alcohol administration alters metabolomic profile of murine bone marrow
Tássia Tatiane Pontes Pereira, Filipe Fideles Duarte-Andrade, Jéssica Gardone Vitório, Taiane do Espírito Santo Pereira, Flavia Rayssa Braga Martins, Jéssica Amanda Marques Souza, Nathália Luisa Malacco, Eliza Mathias Melo, Carolina Raíssa Costa Picossi, Ernani Pinto, Ricardo Santiago Gomez, Mauro Martins Teixeira, Adriana Nori de Macedo, Gisele André Baptista Canuto and Frederico Marianetti Soriani

146 Chronic ethanol exposure impairs alveolar leukocyte infiltration during pneumococcal pneumonia, leading to an increased bacterial burden despite increased CXCL1 and nitric oxide levels
Flávia Rayssa Braga Martins, Maycon Douglas de Oliveira, Jéssica Amanda Marques Souza, Celso Martins Queiroz-Junior, Francisco Pereira Lobo, Mauro Martins Teixeira, Nathalia Luisa Malacco and Frederico Marianetti Soriani

frontiers in Immunology

REVIEW
published: 31 March 2022
doi: 10.3389/fimmu.2022.864817

The Impact of Alcohol Use Disorder on Tuberculosis: A Review of the Epidemiology and Potential Immunologic Mechanisms

Gregory W. Wigger[1*], *Tara C. Bouton*[2], *Karen R. Jacobson*[2], *Sara C. Auld*[1,3], *Samantha M. Yeligar*[1,4] *and Bashar S. Staitieh*[1]

[1] Division of Pulmonary, Allergy, Critical Care and Sleep Medicine, Department of Medicine, Emory University School of Medicine, Atlanta, GA, United States, [2] Section of Infectious Diseases, Department of Medicine, Boston University School of Medicine, Boston, MA, United States, [3] Rollins School of Public Health, Emory University, Atlanta, GA, United States, [4] Atlanta VA Medical Center, Atlanta, GA, United States

OPEN ACCESS

Edited by:
Bruno Rivas-Santiago, Unidad de Investigación Biomédica de Zacatecas (IMSS), Mexico

Reviewed by:
Katrin Doris Mayer-Barber, National Institutes of Health (NIH), United States
Roberta Provvedi, University of Padua, Italy
Alejandra Montoya-Rosales, Biomark Life Sciences, Mexico

***Correspondence:**
Gregory W. Wigger
gwigger@emory.edu

Specialty section:
This article was submitted to Nutritional Immunology, a section of the journal Frontiers in Immunology

Received: 28 January 2022
Accepted: 09 March 2022
Published: 31 March 2022

Citation:
Wigger GW, Bouton TC, Jacobson KR, Auld SC, Yeligar SM and Staitieh BS (2022) The Impact of Alcohol Use Disorder on Tuberculosis: A Review of the Epidemiology and Potential Immunologic Mechanisms. Front. Immunol. 13:864817. doi: 10.3389/fimmu.2022.864817

Globally, an estimated 107 million people have an alcohol use disorder (AUD) leading to 2.8 million premature deaths each year. Tuberculosis (TB) is one of the leading causes of death globally and over 8% of global TB cases are estimated to be attributable to AUD. Social determinants of health such as poverty and undernutrition are often shared among those with AUD and TB and could explain the epidemiologic association between them. However, recent studies suggest that these shared risk factors do not fully account for the increased risk of TB in people with AUD. In fact, AUD has been shown to be an independent risk factor for TB, with a linear increase in the risk for TB with increasing alcohol consumption. While few studies have focused on potential biological mechanisms underlying the link between AUD and TB, substantial overlap exists between the effects of alcohol on lung immunity and the mechanisms exploited by *Mycobacterium tuberculosis* (*Mtb*) to establish infection. Alcohol misuse impairs the immune functions of the alveolar macrophage, the resident innate immune effector in the lung and the first line of defense against *Mtb* in the lower respiratory tract. Chronic alcohol ingestion also increases oxidative stress in the alveolar space, which could in turn facilitate *Mtb* growth. In this manuscript, we review the epidemiologic data that links AUD to TB. We discuss the existing literature on the potential mechanisms by which alcohol increases the risk of TB and review the known effects of alcohol ingestion on lung immunity to elucidate other mechanisms that *Mtb* may exploit. A more in-depth understanding of the link between AUD and TB will facilitate the development of dual-disease interventions and host-directed therapies to improve lung health and long-term outcomes of TB.

Keywords: alcohol, alcohol use disorder (AUD), tuberculosis, alveolar macrophage (AM), innate immunity, oxidative stress

1 INTRODUCTION

Alcohol misuse is a significant global health issue with wide-ranging and pervasive consequences. In 2016, 5.3% of all global deaths were attributable to alcohol consumption, and alcohol misuse was the 7th leading risk factor for premature death and disability (1, 2). Alcohol use disorder (AUD) has been linked to an increased susceptibility to pulmonary infections and their associated complications for over 200 years (3). More recently, AUD has been found to be an independent risk factor for acute respiratory distress syndrome (ARDS) with a two to four-fold increased risk compared to individuals without AUD (4, 5). Similarly, persons with AUD have an increased risk for bacterial pneumonia and its associated morbidity and mortality (6–11). They also suffer from a higher incidence of serious complications from pneumonia, including bacteremia, parapneumonic effusion, and empyema (9, 12–14). AUD causes a variety of detrimental effects on the lungs including increased alveolar oxidative stress, immune impairments, and alterations in the metabolism of pulmonary cells.

Despite advances in diagnosis and treatment, tuberculosis (TB) is the second leading infectious killer worldwide, only recently surpassed by COVID-19 (15). While the global TB incidence rate has been decreasing annually since 2000, the most recent World Health Organization (WHO) global TB data reported an increase in TB mortality for the first time in 20 years, driven in large part by disruption of TB control programs from the COVID-19 pandemic (15).

The recognition of the association between alcohol and TB occurred even before the causative agent of TB was known. As early as the 19th century, physicians noted the increased incidence of infections, like TB and other causes of pneumonia, among patients that consumed alcohol (3, 16). The co-occurrence of excessive alcohol intake and TB has been continually noted since that time. AUD is one of the most common global risk factors for TB, second only to undernutrition and, notably, ahead of HIV and smoking (15). In this critical review, we will parse the complex relationship between alcohol and TB. We highlight recent epidemiologic work demonstrating a direct relationship between alcohol misuse and TB. We discuss mechanisms by which alcohol causes lung injury and suppresses lung immunity *via* increases in oxidative stress and impairments to the pulmonary innate immune system. For each of these biological pathways impacted by alcohol, we will highlight the potential mechanisms that might favor *Mtb* infection and dissemination.

2 ALCOHOL AND TB EPIDEMIOLOGY

Epidemiologic data support a clear relationship between alcohol and TB and reveal the various biologic, immunologic, and clinical impacts that alcohol may have on patients with TB (**Figure 1**).

2.1 Risk of Infection

The risk of both latent TB infection (LTBI) and active TB disease is higher among persons with alcohol use disorders (AUD) than those without AUD (17). For example, one study in New York City found a 28-fold higher rate of active TB disease among those with AUD as compared to age-matched individuals without AUD (18). Other studies have documented a dose-response relationship between active TB and alcohol consumption, with the risk of TB rising as a person's daily alcohol consumption increases (19, 20).

While improvements in diagnostics and broader access to treatment have led to global declines in TB incidence since 2000 (21), cases of TB associated with AUD are on the rise, particularly among men (22, 23). It is estimated that 8-15% of global TB deaths are attributable to alcohol misuse and AUD (15, 20, 24). In high-income countries where non-communicable diseases, including diabetes and AUD, have a greater prevalence, over 35% of TB deaths among those under the age of 65 are linked to alcohol misuse (25).

Although the interactions between poverty, social marginalization, alcohol misuse, and TB remain complicated and difficult to disentangle, their overlap does not fully explain the increased risk of TB with AUD. Studies examining the relationship between AUD and TB have shown that AUD remains a significant independent risk factor for TB, with a relative risk of 2.9, even after controlling for confounders such as comorbidities, lifestyle, or social determinants of health (20, 24, 26–28).

2.2 Risk of Transmission and Severity

Individuals with TB and AUD are more infectious and have more clinically severe TB. Analyses of TB outbreaks have shown clustered TB spread and transmission among persons with AUD, and drinking venues and bars have been identified as sites of TB transmission (29–31). Further, molecular epidemiology studies have shown individuals with AUD are more likely to reflect recent TB transmission and to be part of a transmission cluster (32, 33). While this increased transmission may be due to the social marginalization often seen with AUD, it could also be due to an increased mycobacterial burden in persons with AUD. Cases of TB associated with AUD have higher rates of acid-fast bacilli (AFB) detected in sputum samples and increased *Mtb* bacterial load compared to TB without an AUD association (25, 26). Both of these characteristics have previously been associated with more severe TB features, including cavitation, as well as increased *Mtb* transmission and thus may explain some of the increased transmissibility of TB in AUD (25, 26, 34–36). Those with AUD and TB are more likely to present with pulmonary rather than extrapulmonary TB (25, 26). More of their lungs are affected by TB and they are predisposed to advanced, cavitary disease at the time of presentation (25, 26, 35, 37).

2.3 Treatment Outcomes

For those who initiate treatment, patients with TB and AUD have worse clinical outcomes, including increased time to culture conversion, incidence of TB treatment failure, rate of disease relapse, and risk of death (25, 28, 38–43). Again, the intersection of alcohol and certain social determinants complicates the interpretation of these data. For example, it is known that

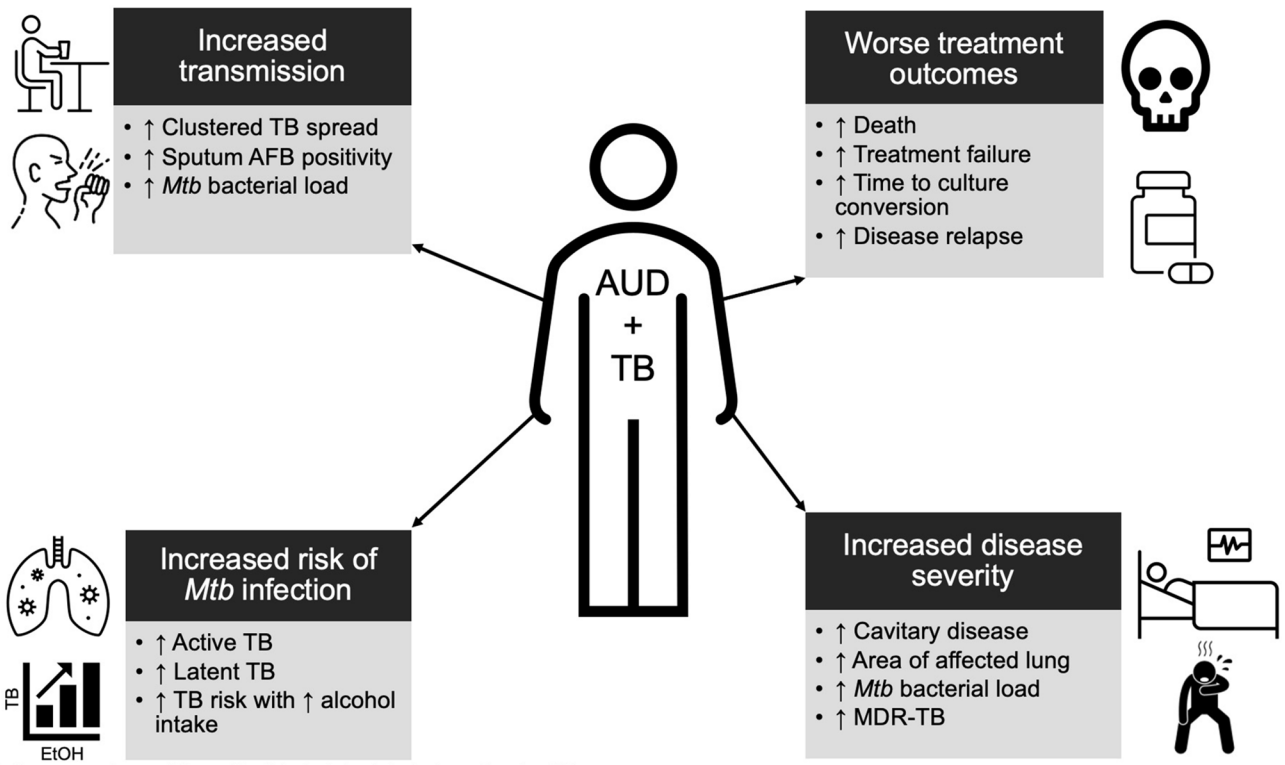

FIGURE 1 | Summary schema of the epidemiologic data of alcohol use disorder (AUD) and tuberculosis (TB). Individuals with AUD are at a higher risk for TB, more infectious, have more severe disease, and are more likely to experience poor outcomes. See main text for further details.

AUD has been associated with delays in accessing TB care and poor adherence to TB treatment, both of which may contribute to the more advanced, severe disease at the time of diagnosis and inadequate therapy (44, 45). More recent data indicate an increased incidence of multi-drug resistant TB in people with AUD, possibly due to poor treatment adherence as well as comorbidities associated with AUD that impact immune function and metabolism (43, 46, 47). However, as described above, poor TB outcomes persist among individuals with AUD even when controlling for behaviors that impact access to and retention in treatment (e.g., individuals with AUD lost to treatment follow-up) (28). A two- to four-fold increased risk of death remains for those with TB associated with AUD compared to those without AUD even when only considering patients being actively treated for TB (25, 48, 49).

2.4 Efficacy of Treatment

Alcohol-associated metabolic dysfunction and adverse drug effects have been a concern regarding individuals with AUD and TB. Studies have shown alcohol's potential impact on the metabolism, absorption, and resultant concentrations of several TB drugs including isoniazid, rifampicin, and fluoroquinolones (50–58). Proper drug concentrations are essential for successful TB treatment. Sub-therapeutic concentrations are predictive of poor outcomes in TB, including death or disease relapse, while supra-therapeutic concentrations can lead to adverse events and treatment interruptions (59). Historically, such concerns have led to the exclusion of individuals with AUD from studies of TB preventative therapy. However, clinical trials are underway investigating the true benefit vs. harm of TB preventative therapy in persons with AUD (60). Alcohol intervention programs may also play an important role in the future of treatment for TB associated with AUD. Previous studies have shown a desire for such programs among TB patients, and the initiation of intervention programs led to favorable outcomes with improved treatment adherence in individuals with AUD and TB (61, 62).

3 MECHANISMS OF TB IN AUD

3.1 Oxidative Stress

The lung's constant exposure to the external environment and resultant processing of inhaled smoke, dust particles, microbes, toxins, etc. generates free radicals, including reactive oxygen species (ROS) and reactive nitrogen species (RNS), that are released into the alveolar environment. In the lungs, there are efficient antioxidant defense systems, including antioxidant enzymes and antioxidant stores, that defend against oxidants and other reactive species (63, 64). Maintaining a balanced

oxidation-reduction (redox) state is essential for key cellular functions, such as proliferation, differentiation, and apoptosis (63). Redox balance can alter protein structure and reactivity as well as cell signaling pathways (65). These alterations can result in a release of inflammatory mediators and cytokines with subsequent macrophage activation, polymorphonuclear (PMN) cell recruitment, inflammation, and tissue damage (64). The redox state can be assessed by measuring thiol/disulfide couples including glutathione (GSH) and glutathione disulfide (GSSG), the primary thiol redox system within the alveoli (63). Epithelial lining fluid of a healthy lung has abundant extracellular GSH in order to detoxify oxidants and free radicals (63–65). Oxidative stress in the lung results when its antioxidant capacity is depleted. Both chronic alcohol ingestion as well as *Mtb* infection increase oxidative stress.

3.1.1 Alcohol Increases Pulmonary Oxidative Stress

AUD increases pulmonary oxidative stress and induces an oxidized microenvironment within the lung through a variety of mechanisms. AUD depletes antioxidant stores, including GSH, within the pulmonary environment (66). GSH serves as the primary reducing agent in the alveolar space, acting as a substrate in a reaction with glutathione peroxidase that detoxifies peroxides in the lung including hydrogen peroxide and lipid peroxides (67). AUD alters pulmonary GSH homeostasis, resulting in an oxidation of GSH stores to form GSSG and oxidation of the GSH/GSSG redox potential (66, 68–70). Alcohol-induced depletion of GSH impairs an essential defense mechanism against oxidative stress in the lung.

There are a number of mechanisms through which alcohol depletes pulmonary GSH stores. First, alcohol induces mitochondrial dysfunction which decreases ATP generation and, in turn, may decrease GSH synthesis (68, 71). GSH can also be synthesized by reduction of GSSG, which utilizes NADPH as the electron donor. However, alcohol may reduce NADPH availability, resulting in decreased capacity for reduction and less GSH (71). Alcohol also increases ROS generation which then oxidizes GSH, further depleting GSH stores (71–73). A primary mechanism by which alcohol impairs GSH is its effects on the protein nuclear factor (erythroid-derived 2)-like 2 (Nrf2). Since Nrf2 is a transcription factor that activates hundreds of antioxidant genes and innate immune effectors (74), alcohol-mediated decreases in Nrf2 activation critically impairs the lung redox balance of those with AUD. Downstream effects from Nrf2 impairment include a diminished antioxidant response to oxidative stress and drained GSH stores (74).

AUD further increases alveolar oxidative stress by enhancing the expression and activity of NADPH oxidases (Nox). Nox proteins are membrane-associated enzymes that catalyze the reduction of molecular oxygen to superoxide and hydrogen peroxide, thus serving as major sources of ROS in the lungs. In alcohol-fed mice and rats, increased Nox expression increases alveolar oxidative stress (72, 73, 75). AUD depletes alveolar macrophage levels of peroxisome proliferator-activated receptor gamma (PPARγ) which, in turn, upregulates Nox proteins (76). Nox activity is likely further enhanced by the increase in TGFβ expression seen with AUD, which also upregulates particular Nox proteins (77, 78).

The increased oxidative stress within the alveolar microenvironment of individuals with AUD has important implications for pulmonary innate immunity. GSH deficiency increases alveolar epithelial intercellular permeability and diminishes surfactant synthesis (69, 79, 80). The oxidative stress associated with upregulated Nox protein expression impairs alveolar macrophage phagocytosis in alcohol-fed mice (72, 76). In environments of limited GSH, alveolar macrophage phagocytosis and microbe clearance are also compromised (68, 71). Supplementation of GSH has been demonstrated to restore alveolar macrophage function (71, 81, 82).

3.1.2 *Mtb* Increases Pulmonary Oxidative Stress

Infection with *Mtb* has also been shown to increase oxidative stress and deplete antioxidant levels in the lungs. People with active TB disease had lower circulating levels of serum thiol and increased levels of its oxidized product serum disulfide (83). More broadly, mycobacterial infections, including *Mtb* and *Mycobacterium abscessus* (a rapid growing mycobacterium), have been associated with increased oxidative stress, as shown by decreases in total serum antioxidant capacity, total GSH, and increased lipid peroxidation (84–86). Treatment with antioxidants, including N-acetylcysteine (a precursor to GSH), have been shown to reduce oxidative stress as well as intracellular and pulmonary *Mtb* burden, while improving cell viability (84, 85).

Nrf2 is also an important aspect of the response to *Mtb*. Its expression is upregulated in *Mtb* infection due to the associated increase in ROS and oxidative stress (87, 88). Studies done *in vitro* with human macrophages have demonstrated benefit with pharmacologic Nrf2. Specifically, Nrf2 activation decreased oxidative injury, mitochondrial depolarization, and *Mtb*-induced ROS production in addition to inhibiting programmed necrosis of the macrophage (89).

An increase in oxidative stress, in the context of *Mtb* infection, allows for enhanced mycobacterial growth and survival. *Mtb* grows *in vitro* at a faster rate in more oxidized environments, as in the lung apices where clinical TB disease is most common (90). These observations are supported by a series of experiments with *M. abscessus* where increased intracellular growth was seen in more oxidized environments (86).

3.1.3 Pulmonary Oxidative Stress: AUD and *Mtb* Overlap

Taken together, the co-occurrence of AUD and *Mtb* infection likely results in a significant increase in pulmonary oxidative stress state which benefits *Mtb*. First, the combination of oxidative stress and impairments in antioxidant defenses, particularly the depletion of GSH stores and Nrf2 inhibition by alcohol, may sufficiently derange immune function and facilitate *Mtb* infection and growth. Second, *Mtb*'s growth and survival improves in oxidative environments, making the oxidized alveoli in those with AUD a more ideal environment for *Mtb*. Collectively, alcohol-induced oxidative stress may generate the

ideal combination for *Mtb* infection: an oxidized alveolus and an impaired host response.

3.2 Pulmonary Innate Immunity

The pulmonary innate immune system is a multilayered system for defense against pathogens, detection of tissue damage, and maintaining pulmonary tissue integrity and homeostasis (91). Chronic alcohol misuse exerts a wide range of effects on this system resulting in impairments of several vital functions of innate immunity (92, 93). Its adverse effects impact the basic defense and barrier functions of the cilia and alveolar epithelium as well as the functions of specialized cells including alveolar macrophages and PMNs. For example, AUD inhibits neutrophil margination, influx from the peripheral circulation into the alveolar space, and subsequent pathogen clearance and killing during infection (92, 94–96). Antigen-presenting cells (APCs) of the innate immune system, necessary for adaptive immune activation, have a decreased peripheral presence and impaired activity due to alcohol (97, 98).

Alongside the growing understanding of the negative impacts of alcohol, the understanding of *Mtb* infection and host-pathogen interactions is also evolving. With the increased occurrence and severity of TB with AUD, it is likely that *Mtb* exploits alcohol-mediated impairments in pulmonary innate immunity to establish infection and disseminate. Previous research has elucidated alcohol's deleterious effects on pulmonary mucociliary function, alveolar epithelium, and the alveolar macrophage. Given this breadth of information, in addition to the alveolar macrophage being first line of defense in the alveolar space and the dominant cell type that *Mtb* infects, we will spend the remaining portion of this section reviewing the specific effects of chronic alcohol misuse on the pulmonary innate immunity and how these alcohol-mediated alterations may intersect with *Mtb* pathogenicity.

3.2.1 Pulmonary Mucociliary Function

Ciliated airway cells are the first line of defense against inhaled pathogens and clear foreign particles from the lung. Chronic alcohol use repetitively exposes airways to ethanol eliminated from the bronchial circulation in exhaled breath. This repetitive injury impairs the integrity and function of airway cell cilia, ultimately leading to desensitization and resistance to motility, a phenomenon referred to as alcohol-induced ciliary dysfunction (99–101).

In the context of *Mtb*, this ciliary dysfunction facilitates transmission of airborne pathogens like *Mtb* into the lower airways, making it more likely that inhaled microbes will establish infection (102). Given that ciliary dysfunction has been associated with mycobacterial pulmonary infections, alcohol-induced ciliary dysfunction represents a likely mechanism by which AUD could predispose the host to *Mtb* infection (103).

3.2.2 Alveolar Epithelium

Chronic alcohol use is also known to disrupt the pulmonary epithelial structure and function. AUD prevents the formation of a reliable, physical barrier of the alveolar epithelium by impairing tight junctions within its monolayer. Tight junctions are an important aspect of the epithelium as they closely associate cells and limit the passage of water, proteins, and other solutes across cell layers (104). Chronic alcohol ingestion alters the expression and interaction of essential components of the tight junctions, including claudin-1, claudin-5, claudin-7, occludin, and zonula occludens-1, resulting in a five-fold increase in pulmonary epithelial permeability (79, 105–107). People with AUD have increased alveolar-capillary permeability which predisposes them to the development of non-cardiogenic pulmonary edema compared to individuals without AUD (108, 109). Experiments in animal models support this mechanism of injury, with chronic alcohol consumption in rats increasing susceptibility to edematous lung injury (69). Alcohol also increases TGF-β1 expression while inhibiting granulocyte/macrophage colony-stimulating factor (GM-CSF) in the alveolar space, both of which have been implicated in disrupting and increasing the permeability of the alveolar epithelium (77, 110, 111). Lastly, AUD reduces the alveolar epithelial cell synthesis of surfactant, an important pattern recognition molecule that binds to various microbes and targets them for immune clearance (112, 113). Surfactant proteins have been shown to function as an opsonin that increases the *Mtb*-macrophage interaction and upregulates phagocytosis (114). Although the mechanism by which *Mtb* gains access to the lung interstitium from the alveolus is not fully understood, the putative mechanisms proposed in the literature include direct infection of alveolar epithelial cells and migration of *Mtb*-infected macrophages across the alveolar epithelium (115, 116). Both scenarios would be significantly more likely in the setting of alcohol-induced tight junction impairments and the more permeable alveolar epithelium of the alcohol-affected lung.

3.2.3 Alveolar Macrophage

3.2.3.1 Key Functions

The alveolar macrophage is essential for maintaining homeostasis of the lower airways through phagocytosis, removal of debris, and efferocytosis. It is also the first line of pulmonary immune defense in the alveolar space, responsible for recognizing, ingesting, and clearing pathogens, as well as release of cytokines and chemokines to recruit PMNs and monocytes to the site of invasion. Through a multitude of pathways and effects, AUD causes significant alveolar macrophage dysfunction, impairing phagocytosis, pathogen clearance, and cytokine release (71, 72, 76, 81, 82, 117–120).

AUD interferes with the maturation and terminal differentiation of the alveolar macrophage through inhibition of multiple signaling pathways. Alcohol interferes with GM-CSF signaling by downregulating GMCSF-Rβ expression on the alveolar macrophage surface resulting in impaired phagocytic function (117). Impairing GM-CSF signaling results in diminished expression of PU.1, a GM-CSF-dependent regulatory transcription factor required for normal alveolar macrophage cell development and

differentiation as well as alveolar macrophage phagocytosis, pathogen killing, and cytokine production (118, 119, 121, 122). In addition to its previously mentioned role in oxidative defensive, Nrf2 additionally participates in alveolar macrophage maturation by increasing PU.1 expression by binding to its promoter region. Alcohol's inhibition of Nrf2 has been shown to also be responsible for the decreased PU.1 expression of AUD (123).

Mtb's interaction with the innate immune system is an ongoing area of interest and research. The alveolar macrophage is the primary cell that *Mtb* infects once it enters the lower respiratory tract (115, 116). Once phagocytosed by the alveolar macrophage, *Mtb* actively blocks phagosome maturation and fusion with the lysosome to ensure its survival and establish its intracellular niche (115, 124). In some cases, the alveolar macrophage is able to achieve successful intracellular killing of *Mtb*, likely through IFNγ and nitric oxide synthase signaling pathways (124). However, when *Mtb* evades killing, it replicates and eventually disrupts the phagosome membrane allowing *Mtb* into the alveolar macrophage cytosol for further replication. After infecting the alveolar macrophage, *Mtb* then gains access to the lung interstitium, where granuloma formation occurs (115). Subsequent host-pathogen interactions determine whether infection is cleared or if there is progression to latent TB infection or active TB disease, however a discussion of these later events is beyond the scope of this review (115).

GM-CSF is known to be an important for the innate immune response to mycobacterial infections, particularly with its role in restricting bacillary growth and promoting mycobacterial clearance (125–127). Patients with mycobacterial pulmonary infections have higher rates of GM-CSF signaling dysfunction compared to healthy controls (128). Further, treatment with recombinant GM-CSF (rGM-CSF) prior to mycobacterial infection enhanced intracellular killing and phagolysosomal fusion after *Mtb* infection as well as intracellular mycobacterial killing and superoxide anion release after *Mycobacterium avium complex* (MAC) infection (125, 129). Inhibiting GM-CSF by neutralizing GM-CSF antibodies prior to *Mtb* exposure dampens the proinflammatory cytokine release and neutrophil recruitment and increases *Mtb* burden in mouse macrophages (127). Thus, alcohol's downregulation of GMCSF-Rβ on AMs and subsequent decreased GM-CSF expression likely contribute to an impaired response to *Mtb* infection.

Alcohol-induced impairments in innate immunity provide multiple avenues for facilitating *Mtb* infection. Data is limited on alcohol's specific effects on the alveolar macrophage in the case of *Mtb* infection, however multiple studies have investigated other mycobacterial infections including MAC. Several studies done *in vitro* using human macrophages demonstrated that exposure to alcohol enhanced the intracellular growth of MAC and diminished the macrophage response to inflammatory cytokines (130, 131). Chronic exposure to alcohol also diminished macrophage production of bactericidal, innate immune effectors in response to MAC infection in a mouse model (132). Additional experiments showed increased dissemination, impaired pulmonary granuloma formation, and increased mycobacterial burden in alcohol-fed mice following mycobacterial infection (130, 133).

3.2.3.2 Alveolar Macrophage Phenotype

Macrophages act as surveillance for the innate immune system, recognizing pathogens and tissue damage *via* pathogen-associated molecular patterns (PAMPs), damage-associated molecular patterns (DAMPs), and pattern recognition receptors. They have robust phagocytic and killing abilities and act as initiators of the inflammatory response. They function as antigen presenting cells that assist in the activation of the adaptive immune system. Further, macrophages participate in tissue repair, tissue remodeling, and maintain homeostasis (91). This plasticity in macrophage function occurs in response to surrounding physiologic state and cellular signaling and is referred to as macrophage phenotype (134).

Two paradigmatic states of the macrophage were initially described. The first being the "pro-inflammatory" or "classically activated" macrophage that responds to bacteria, viruses, lipopolysaccharide (LPS), and interferon gamma (IFNγ). It produces proinflammatory cytokines and chemokines like interleukin (IL)-12 and tumor necrosis factor alpha (TNFα), induces further inflammation and IFNγ release, and attracts neutrophils, natural killer (NK) cells, and lymphocytes to the site of infection (135). It relies heavily on glycolysis and fatty acid synthesis and a decrease in mitochondrial respiration (136). The second paradigmatic activation state is the "anti-inflammatory" or "alternatively activated" macrophage that is stimulated by IL-4 and participates in wound healing and tissue repair. It produces anti-inflammatory cytokines including IL-10 and IL-13 to reduce inflammation and promote tissue growth (135). Its metabolism is dependent on the tricarboxylic acid cycle (TCA) cycle and enhanced fatty acid oxidation (136). While macrophage differentiation was previously considered to be dichotomous and terminal, recent research suggests a more dynamic spectrum of activation and function. Depending on various extracellular signals, what were previously defined as all "anti-inflammatory" macrophages can exhibit dramatic differences in physiology, including overlap in function with some "pro-inflammatory" macrophages (137). Studies looking at gene expression of macrophages in pathologic conditions have demonstrated heterogenous activation and functionality as well as significant overlap in gene expression whether stimulated with LPS or IL-10 (138–140). Further data showed macrophage functional pattern changes with duration of stimuli and that they are capable of completely changing their phenotype based on the surrounding microenvironment (135, 141, 142). Overall, data collectively support the idea that macrophages are dynamic, plastic, and capable of displaying multiple, distinct, functional patterns.

Chronic alcohol exposure impacts alveolar macrophage functionality and makes phenotyping the alveolar macrophage in the context of alcohol misuse a complex issue (134). At baseline, alveolar macrophages isolated from animal models of chronic alcohol ingestion have increased IL-13 and TGF-β_1 production, both associated with suppression of inflammation, as well as

decreased phagocytic ability (77, 78, 143). These findings are likely due, at least in part, to alcohol-induced oxidative stress in the alveolar environment (as discussed previously). However, when exposed to alcohol and PAMPs, such as LPS, alveolar macrophages exhibit an exaggerated inflammatory response. In studies utilizing AMs from subjects with AUD, alveolar macrophages produce increased proinflammatory cytokines, including TNFα, IFNγ, IL-1β, and IL-6, in response to LPS stimulation compared to persons without AUD (144–146). Despite this elevation in inflammatory signals, multiple studies note a persistent decrease in alveolar macrophage phagocytosis when exposed to bacterial pathogens or PAMPs (72, 76, 117). This overexuberant response to pathogen stimulation has been postulated to be a contributing factor in the elevated risk for disproportionate inflammatory states, like ARDS, in people with AUD (147). While some of these phenotypic changes are related to the alcohol-induced oxidative stress in the lung, chronic alcohol exposure also alters alveolar macrophage metabolism (76, 82). AUD been shown to impair LPS-induced glycolytic response and induce mitochondrial derangements in the alveolar macrophage which can alter its cytokine response and contribute to phagocytosis impairments (148–150).

Mtb has also been noted to induce phenotypic changes in the alveolar macrophage after infection. In the early stages of infection, *Mtb* induces a robust production of inflammatory cytokines, increased phagocytosis, and upregulation of glycolysis from the alveolar macrophage (151–155). Glycolysis is important to the immune response because glycolytic inhibition results in an increased mycobacterial burden (156). Once intracellular, *Mtb* itself attempts to evade the macrophage's killing processes by secreting virulence factors that inhibit the alveolar macrophage's expression of the nuclear factor-κB (NF-κB) and IFNγ, ultimately promoting *Mtb*'s intracellular survival (151, 157). Following the initial response to *Mtb*, alveolar macrophages increase production of anti-inflammatory cytokines, including IL-10 and TGF-β, with decreased glycolysis and increased oxidative phosphorylation and free fatty acid metabolism (151, 158–162). Successful treatment of TB leads to resolution of these phenotypic changes to the macrophage (163).

Further work is clearly necessary to fully understand the relationship between AUD, *Mtb*, and alveolar macrophage function. The quiescent, baseline state of alveolar macrophages in subjects with AUD with increased expression of TGF-β_1 may provide more favorable conditions for *Mtb* infection and facilitate intracellular proliferation. Further, glycolysis is integral to the macrophage's response to *Mtb*: a decreased glycolytic reserve has been associated with *Mtb* infection and risk factors for TB (156, 164). Alcohol's impairments of LPS-induced glycolysis may contribute to alveolar macrophage dysfunction and increase the risk of *Mtb* infection in those with AUD.

4 CONCLUSION AND FUTURE DIRECTIONS

Increasing rates of AUD pose a significant barrier to reaching the global goal of TB elimination. AUD is a risk factor for TB infection, severe disease, transmission, and associated death.

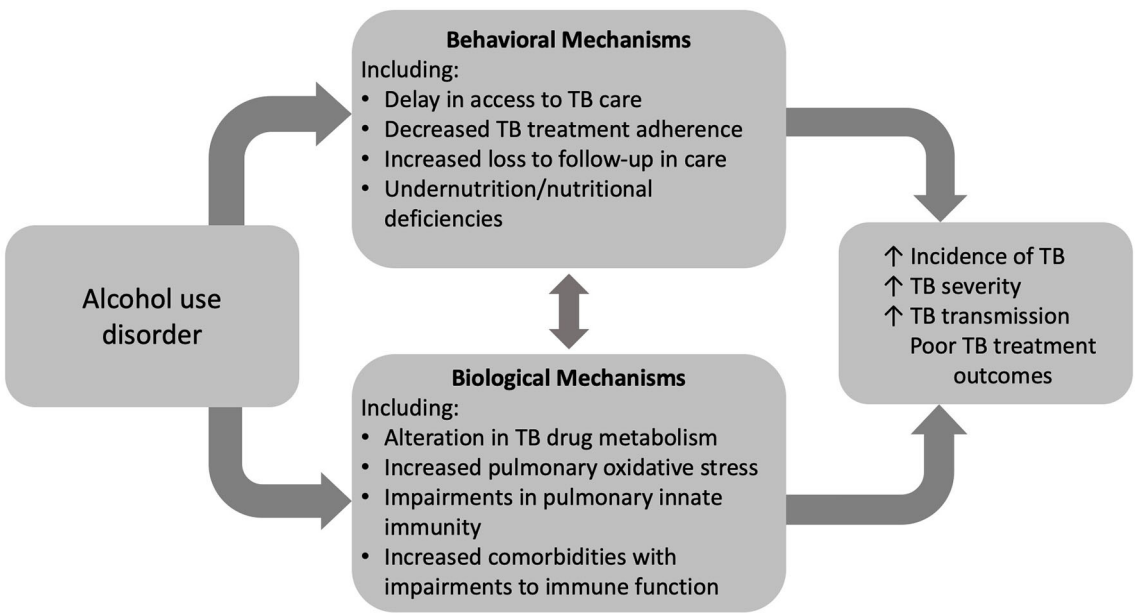

FIGURE 2 | Alcohol use disorder (AUD) influences tuberculosis (TB) care and outcomes through both behavioral and biologic mechanisms.

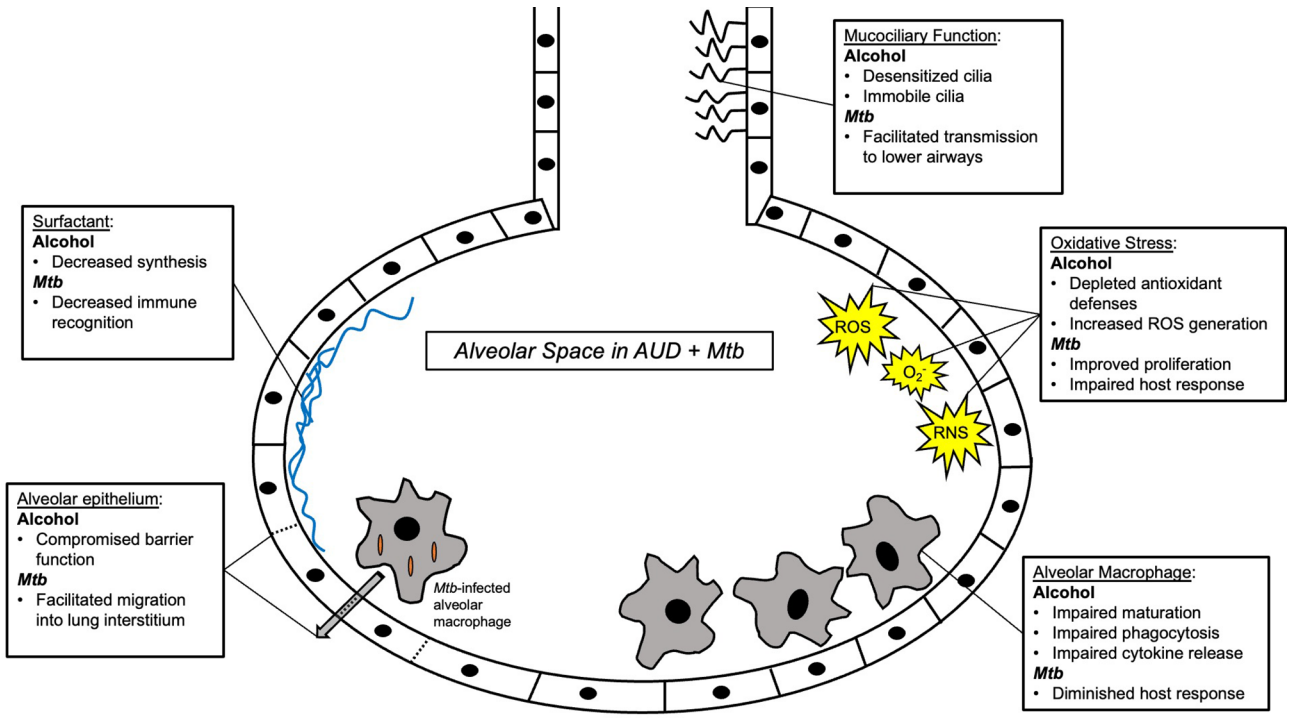

FIGURE 3 | Summary schema of the alveolar space in alcohol use disorder (AUD) and Mycobacterium tuberculosis (Mtb) infection. Multiple components of innate immunity are affected by AUD, including macrophages, surfactant, the alveolar epithelium, and the alveolar oxidative state. See main text for further details.

Despite behavioral determinants of health linking AUD and TB disease, compelling evidence supports a biological impact of alcohol on TB risk and disease (**Figure 2**). The impact of alcohol on oxidative stress in the alveolar environment as well as impairments to the alveolar epithelium, alveolar macrophage, and remainder of the pulmonary innate immune system may facilitate *Mtb* infection and evasion of host defenses (**Figure 3**). To date, research directly investigating the mechanistic causes of TB in persons with AUD has been limited. Future investigations into the roles of innate immunity and oxidative stress specifically in alcohol and TB are needed. A better understanding of these causal pathways will lead to the development of host-directed therapies and better treatment outcomes in individuals with AUD and TB.

AUTHOR CONTRIBUTIONS

Design and conception - GW. Drafting and revising manuscript – GW, TB, KJ, SA, SY, and BS. All authors contributed to the article and approved the submitted version.

FUNDING

This study was funded by the National Heart, Lung, and Blood Institute [T32 HL116271], the National Institute of Allergy and Infectious Diseases (NIAID) [K23 AI152930; R01 AI119037; K23 AI134182], and the National Institute on Alcohol Abuse and Alcoholism (NIAAA) [R01 AA026086; K08 AA024512].

REFERENCES

1. WHO. *Alcohol: Fact Sheet 2018* . Available at: https://www.who.int/en/news-room/fact-sheets/detail/alcohol.
2. Alcohol GBD and Drug Use C. The Global Burden of Disease Attributable to Alcohol and Drug Use in 195 Countries and Territories, 1990-2016: A Systematic Analysis for the Global Burden of Disease Study 2016. *Lancet Psychiatry* (2018) 5(12):987–1012. doi: 10.1016/S2215-0366(18)30337-7
3. Rush B. *An Inquiry Into the Effects of Ardent Spirits Upon the Human Body and Mind : With an Account of the Means of Preventing, and of the Remedies for Curing Them. 4th ed.* Philadelphia: Printed for Thomas Dobson. Archibald Bartram (1805).
4. Moss M, Bucher B, Moore FA, Moore EE, Parsons PE. The Role of Chronic Alcohol Abuse in the Development of Acute Respiratory Distress Syndrome in Adults. *JAMA* (1996) 275(1):50–4. doi: 10.1001/jama.275.1.50
5. Moss M, Parsons PE, Steinberg KP, Hudson LD, Guidot DM, Burnham EL, et al. Chronic Alcohol Abuse is Associated With an Increased Incidence of Acute Respiratory Distress Syndrome and Severity of Multiple Organ Dysfunction in Patients With Septic Shock. *Crit Care Med* (2003) 31(3):869–77. doi: 10.1097/01.CCM.0000055389.64497.11
6. Happel KI, Nelson S. Alcohol, Immunosuppression, and the Lung. *Proc Am Thorac Soc* (2005) 2(5):428–32. doi: 10.1513/pats.200507-065JS

7. Mehta AJ, Guidot DM. Alcohol Abuse, the Alveolar Macrophage and Pneumonia. *Am J Med Sci* (2012) 343(3):244–7. doi: 10.1097/MAJ.0b013e31823ede77
8. Simou E, Britton J, Leonardi-Bee J. Alcohol and the Risk of Pneumonia: A Systematic Review and Meta-Analysis. *BMJ Open* (2018) 8(8):e022344. doi: 10.1136/bmjopen-2018-022344
9. Fernandez-Sola J, Junque A, Estruch R, Monforte R, Torres A, Urbano-Marquez A. High Alcohol Intake as a Risk and Prognostic Factor for Community-Acquired Pneumonia. *Arch Intern Med* (1995) 155(15):1649–54. doi: 10.1001/archinte.155.15.1649
10. Clark BJ, Williams A, Feemster LM, Bradley KA, Macht M, Moss M, et al. Alcohol Screening Scores and 90-Day Outcomes in Patients With Acute Lung Injury. *Crit Care Med* (2013) 41(6):1518–25. doi: 10.1097/CCM.0b013e318287f1bb
11. O'Brien JM Jr, Lu B, Ali NA, Martin GS, Aberegg SK, Marsh CB, et al. Alcohol Dependence is Independently Associated With Sepsis, Septic Shock, and Hospital Mortality Among Adult Intensive Care Unit Patients. *Crit Care Med* (2007) 35(2):345–50. doi: 10.1097/01.CCM.0000254340.91644.B2
12. Chalmers JD, Singanayagam A, Murray MP, Scally C, Fawzi A, Hill AT. Risk Factors for Complicated Parapneumonic Effusion and Empyema on Presentation to Hospital With Community-Acquired Pneumonia. *Thorax* (2009) 64(7):592–7. doi: 10.1136/thx.2008.105080
13. Gentile JH, Sparo MD, Mercapide ME, Luna CM. Adult Bacteremic Pneumococcal Pneumonia Acquired in the Community. A Prospective Study on 101 Patients. *Medicina (B Aires)* (2003) 63(1):9–14.
14. Plevneshi A, Svoboda T, Armstrong I, Tyrrell GJ, Miranda A, Green K, et al. Population-Based Surveillance for Invasive Pneumococcal Disease in Homeless Adults in Toronto. *PloS One* (2009) 4(9):e7255. doi: 10.1371/journal.pone.0007255
15. WHO G. *Global Tuberculosis Report 2020*. (2020), Glob Tuberc Rep.
16. Osler W. *The Principles and Practice of Medicine, Designed for the Use of Practitioners and Students of Medicine. 3d ed*. New York: D. Appleton and company (1898). p. xvii, 1 , 1181.
17. Puryear SB, Fatch R, Beesiga B, Kekibiina A, Lodi S, Marson K, et al. Higher Levels of Alcohol Use Are Associated With Latent Tuberculosis Infection in Adults Living With Human Immunodeficiency Virus. *Clin Infect Dis* (2021) 72(5):865–8. doi: 10.1093/cid/ciaa527
18. Friedman LN, Sullivan GM, Bevilaqua RP, Loscos R. Tuberculosis Screening in Alcoholics and Drug Addicts. *Am Rev Respir Dis* (1987) 136(5):1188–92. doi: 10.1164/ajrccm/136.5.1188
19. Francisco J, Oliveira O, Felgueiras O, Gaio AR, Duarte R. How Much is Too Much Alcohol in Tuberculosis? *Eur Respir J* (2017) 49(1):1–4. doi: 10.1183/13993003.01468-2016
20. Imtiaz S, Shield KD, Roerecke M, Samokhvalov AV, Lonnroth K, Rehm J. Alcohol Consumption as a Risk Factor for Tuberculosis: Meta-Analyses and Burden of Disease. *Eur Respir J* (2017) 50(1):1–13. doi: 10.1183/13993003.00216-2017
21. Fan CY, Katsuyama M, Yabe-Nishimura C. PKCdelta Mediates Up-Regulation of NOX1, a Catalytic Subunit of NADPH Oxidase, via Transactivation of the EGF Receptor: Possible Involvement of PKCdelta in Vascular Hypertrophy. *Biochem J* (2005) 390(Pt 3):761–7. doi: 10.1042/BJ20050287
22. Collaborators GBDA. Alcohol Use and Burden for 195 Countries and Territories, 1990-2016: A Systematic Analysis for the Global Burden of Disease Study 2016. *Lancet* (2018) 392(10152):1015–35. doi: 10.1016/S0140-6736(18)31310-2
23. Collaborators GBDT. Global, Regional, and National Sex Differences in the Global Burden of Tuberculosis by HIV Status, 1990-2019: Results From the Global Burden of Disease Study 2019. *Lancet Infect Dis* (2021) 22(2):222–41. doi: 10.1016/S1473-3099(21)00449-7
24. Rehm J, Samokhvalov AV, Neuman MG, Room R, Parry C, Lonnroth K, et al. The Association Between Alcohol Use, Alcohol Use Disorders and Tuberculosis (TB). A Systematic Review. *BMC Public Health* (2009) 9:450. doi: 10.1186/1471-2458-9-450
25. Volkmann T, Moonan PK, Miramontes R, Oeltmann JE. Tuberculosis and Excess Alcohol Use in the United States, 1997-2012. *Int J Tuberc Lung Dis* (2015) 19(1):111–9. doi: 10.5588/ijtld.14.0516
26. Fiske CT, Hamilton CD, Stout JE. Alcohol Use and Clinical Manifestations of Tuberculosis. *J Infect* (2009) 58(5):395–401. doi: 10.1016/j.jinf.2009.02.015
27. Lonnroth K, Williams BG, Stadlin S, Jaramillo E, Dye C. Alcohol Use as a Risk Factor for Tuberculosis - a Systematic Review. *BMC Public Health* (2008) 8:289. doi: 10.1186/1471-2458-8-289
28. Ragan EJ, Kleinman MB, Sweigart B, Gnatienko N, Parry CD, Horsburgh CR, et al. The Impact of Alcohol Use on Tuberculosis Treatment Outcomes: A Systematic Review and Meta-Analysis. *Int J Tuberc Lung Dis* (2020) 24(1):73–82. doi: 10.5588/ijtld.19.0080
29. Kline SE, Hedemark LL, Davies SF. Outbreak of Tuberculosis Among Regular Patrons of a Neighborhood Bar. *N Engl J Med* (1995) 333(4):222–7. doi: 10.1056/NEJM199507273330404
30. Diel R, Meywald-Walter K, Gottschalk R, Rusch-Gerdes S, Niemann S. Ongoing Outbreak of Tuberculosis in a Low-Incidence Community: A Molecular-Epidemiological Evaluation. *Int J Tuberc Lung Dis* (2004) 8(7):855–61.
31. Classen CN, Warren R, Richardson M, Hauman JH, Gie RP, Ellis JH, et al. Impact of Social Interactions in the Community on the Transmission of Tuberculosis in a High Incidence Area. *Thorax* (1999) 54(2):136–40. doi: 10.1136/thx.54.2.136
32. Nava-Aguilera E, Andersson N, Harris E, Mitchell S, Hamel C, Shea B, et al. Risk Factors Associated With Recent Transmission of Tuberculosis: Systematic Review and Meta-Analysis. *Int J Tuberc Lung Dis* (2009) 13(1):17–26.
33. Fok A, Numata Y, Schulzer M, FitzGerald MJ. Risk Factors for Clustering of Tuberculosis Cases: A Systematic Review of Population-Based Molecular Epidemiology Studies. *Int J Tuberc Lung Dis* (2008) 12(5):480–92.
34. Lohmann EM, Koster BF, le Cessie S, Kamst-van Agterveld MP, van Soolingen D, Arend SM. Grading of a Positive Sputum Smear and the Risk of Mycobacterium Tuberculosis Transmission. *Int J Tuberc Lung Dis* (2012) 16(11):1477–84. doi: 10.5588/ijtld.12.0129
35. Wang H, Hosford J, Lauzardo M. The Effect of Alcohol Use on the Clinical Presentation of Tuberculosis. *J Mycobac Dis* (2012) 2(5):2–5. doi: 10.4172/2161-1068.1000123
36. Palaci M, Dietze R, Hadad DJ, Ribeiro FK, Peres RL, Vinhas SA, et al. Cavitary Disease and Quantitative Sputum Bacillary Load in Cases of Pulmonary Tuberculosis. *J Clin Microbiol* (2007) 45(12):4064–6. doi: 10.1128/JCM.01780-07
37. Kan CK, Ragan EJ, Sarkar S, Knudsen S, Forsyth M, Muthuraj M, et al. Alcohol Use and Tuberculosis Clinical Presentation at the Time of Diagnosis in Puducherry and Tamil Nadu, India. *PloS One* (2020) 15(12):e0240595. doi: 10.1371/journal.pone.0240595
38. Przybylski G, Dabrowska A, Trzcinska H. Alcoholism and Other Socio-Demographic Risk Factors for Adverse TB-Drug Reactions and Unsuccessful Tuberculosis Treatment - Data From Ten Years' Observation at the Regional Centre of Pulmonology, Bydgoszcz, Poland. *Med Sci Monit* (2014) 20:444–53. doi: 10.12659/MSM.890012
39. Shin SS, Pasechnikov AD, Gelmanova IY, Peremitin GG, Strelis AK, Mishustin S, et al. Treatment Outcomes in an Integrated Civilian and Prison MDR-TB Treatment Program in Russia. *Int J Tuberc Lung Dis* (2006) 10(4):402–8.
40. de Albuquerque Mde F, Ximenes RA, Lucena-Silva N, de Souza WV, Dantas AT, Dantas OM, et al. Factors Associated With Treatment Failure, Dropout, and Death in a Cohort of Tuberculosis Patients in Recife, Pernambuco State, Brazil. *Cad Saude Publica* (2007) 23(7):1573–82. doi: 10.1590/S0102-311X2007000700008
41. Thomas BE, Thiruvengadam K SR, Kadam D, Ovung S, Sivakumar S, Bala Yogendra Shivakumar SV, et al. Smoking, Alcohol Use Disorder and Tuberculosis Treatment Outcomes: A Dual Co-Morbidity Burden That Cannot be Ignored. *PloS One* (2019) 14(7):e0220507. doi: 10.1371/journal.pone.0220507
42. Duraisamy K, Mrithyunjayan S, Ghosh S, Nair SA, Balakrishnan S, Subramoniapillai J, et al. Does Alcohol Consumption During Multidrug-Resistant Tuberculosis Treatment Affect Outcome? A Population-Based Study in Kerala, India. *Ann Am Thorac Soc* (2014) 11(5):712–8. doi: 10.1513/AnnalsATS.201312-447OC
43. Fleming MF, Krupitsky E, Tsoy M, Zvartau E, Brazhenko N, Jakubowiak W, et al. Alcohol and Drug Use Disorders, HIV Status and Drug Resistance in a Sample of Russian TB Patients. *Int J Tuberc Lung Dis* (2006) 10(5):565–70.

44. Storla DG, Yimer S, Bjune GA. A Systematic Review of Delay in the Diagnosis and Treatment of Tuberculosis. *BMC Public Health* (2008) 8:15. doi: 10.1186/1471-2458-8-15
45. Moro RN, Borisov AS, Saukkonen J, Khan A, Sterling TR, Villarino ME, et al. Factors Associated With Noncompletion of Latent Tuberculosis Infection Treatment: Experience From the PREVENT TB Trial in the United States and Canada. *Clin Infect Dis* (2016) 62(11):1390–400. doi: 10.1093/cid/ciw126
46. Lasebikan VO, Ige OM. Alcohol Use Disorders in Multidrug Resistant Tuberculosis (MDR-TB) Patients and Their non-Tuberculosis Family Contacts in Nigeria. *Pan Afr Med J* (2020) 36:321. doi: 10.11604/pamj.2020.36.321.17118
47. Ignatyeva O, Balabanova Y, Nikolayevskyy V, Koshkarova E, Radiulyte B, Davidaviciene E, et al. Resistance Profile and Risk Factors of Drug Resistant Tuberculosis in the Baltic Countries. *Tuberculosis (Edinb)* (2015) 95(5):581–8. doi: 10.1016/j.tube.2015.05.018
48. Mathew TA, Ovsyanikova TN, Shin SS, Gelmanova I, Balbuena DA, Atwood S, et al. Causes of Death During Tuberculosis Treatment in Tomsk Oblast, Russia. *Int J Tuberc Lung Dis* (2006) 10(8):857–63.
49. Kattan JA, Sosa LE, Lobato MN. Tuberculosis Mortality: Death From a Curable Disease, Connecticut, 2007-2009. *Int J Tuberc Lung Dis* (2012) 16 (12):1657–62. doi: 10.5588/ijtld.12.0169
50. Olsen H, Morland J. Ethanol-Induced Increase in Drug Acetylation in Man and Isolated Rat Liver Cells. *Br Med J* (1978) 2(6147):1260–2. doi: 10.1136/bmj.2.6147.1260
51. Koriakin VA, Sokolova GB, Grinchar NA, Iurchenko LN. Pharmacokinetics of Isoniazid in Patients With Pulmonary Tuberculosis and Alcoholism. *Probl Tuberk* (1986) 12):43–6.
52. Ortenberg ZA. Pharmacokinetics of Isoniazid, PAS, and Cycloserin in Acute and Chronic Alcoholic Intoxication (Experimental Study). *Probl Tuberk* (1978) 9):60–4.
53. Lester D. The Acetylation of Isoniazid in Alcoholics. *Q J Stud Alcohol* (1964) 25:541–3. doi: 10.15288/qjsa.1964.25.541
54. Thomas BH, Solomonraj G. Drug Interactions With Isoniazid Metabolism in Rats. *J Pharm Sci* (1977) 66(9):1322–6. doi: 10.1002/jps.2600660930
55. Wilcke JT, Dossing M, Angelo HR, Askgaard D, Ronn A, Christensen HR. Unchanged Acetylation of Isoniazid by Alcohol Intake. *Int J Tuberc Lung Dis* (2004) 8(11):1373–6.
56. Kimerling ME, Phillips P, Patterson P, Hall M, Robinson CA, Dunlap NE. Low Serum Antimycobacterial Drug Levels in non-HIV-Infected Tuberculosis Patients. *Chest* (1998) 113(5):1178–83. doi: 10.1378/chest.113.5.1178
57. Ferrando R, Garrigues TM, Bermejo MV, Martin-Algarra R, Merino V, Polache A. Effects of Ethanol on Intestinal Absorption of Drugs: In *Situ* Studies With Ciprofloxacin Analogs in Acute and Chronic Alcohol-Fed Rats. *Alcohol Clin Exp Res* (1999) 23(8):1403–8. doi: 10.1111/j.1530-0277.1999.tb04363.x
58. Merino V, Martin-Algarra RV, Rocher A, Garrigues TM, Freixas J, Polache A. Effects of Ethanol on Intestinal Absorption of Drugs. I. *In Situ* Studies With Ciprofloxacin Analogs in Normal and Chronic Alcohol-Fed Rats. *Alcohol Clin Exp Res* (1997) 21(2):326–33. doi: 10.1111/j.1530-0277.1997.tb03768.x
59. Pasipanodya JG, McIlleron H, Burger A, Wash PA, Smith P, Gumbo T. Serum Drug Concentrations Predictive of Pulmonary Tuberculosis Outcomes. *J Infect Dis* (2013) 208(9):1464–73. doi: 10.1093/infdis/jit352
60. Hahn J. *Alcohol Drinkers' Exposure to Preventive Therapy for TB (ADEPTT)*. Identifier NCT0330229. (2017). Available at: https://clinicaltrials.gov/ct2/show/NCT03302299.
61. Thomas B, Suhadev M, Mani J, Ganapathy BG, Armugam A, Faizunnisha F, et al. Feasibility of an Alcohol Intervention Programme for TB Patients With Alcohol Use Disorder (AUD)–a Qualitative Study From Chennai, South India. *PloS One* (2011) 6(11):e27752. doi: 10.1371/journal.pone.0027752
62. Thomas B, Watson B, Senthil EK, Deepalakshmi A, Balaji G, Chandra S, et al. Alcohol Intervention Strategy Among Tuberculosis Patients: A Pilot Study From South India. *Int J Tuberc Lung Dis* (2017) 21(8):947–52. doi: 10.5588/ijtld.16.0693
63. Moriarty-Craige SE, Jones DP. Extracellular Thiols and Thiol/Disulfide Redox in Metabolism. *Annu Rev Nutr* (2004) 24:481–509. doi: 10.1146/annurev.nutr.24.012003.132208
64. Rahman I, Yang SR, Biswas SK. Current Concepts of Redox Signaling in the Lungs. *Antioxid Redox Signal* (2006) 8(3-4):681–9. doi: 10.1089/ars.2006.8.681
65. Go YM, Jones DP. Thiol/disulfide Redox States in Signaling and Sensing. *Crit Rev Biochem Mol Biol* (2013) 48(2):173–81. doi: 10.3109/10409238.2013.764840
66. Moss M, Guidot DM, Wong-Lambertina M, Ten Hoor T, Perez RL, Brown LA. The Effects of Chronic Alcohol Abuse on Pulmonary Glutathione Homeostasis. *Am J Respir Crit Care Med* (2000) 161(2 Pt 1):414–9. doi: 10.1164/ajrccm.161.2.9905002
67. Rahman I, MacNee W. Oxidative Stress and Regulation of Glutathione in Lung Inflammation. *Eur Respir J* (2000) 16(3):534–54. doi: 10.1034/j.1399-3003.2000.016003534.x
68. Liang Y, Yeligar SM, Brown LA. Chronic-Alcohol-Abuse-Induced Oxidative Stress in the Development of Acute Respiratory Distress Syndrome. *Scientific World Journal* (2012) 2012:740308. doi: 10.1100/2012/740308
69. Holguin F, Moss I, Brown LA, Guidot DM. Chronic Ethanol Ingestion Impairs Alveolar Type II Cell Glutathione Homeostasis and Function and Predisposes to Endotoxin-Mediated Acute Edematous Lung Injury in Rats. *J Clin Invest* (1998) 101(4):761–8. doi: 10.1172/JCI1396
70. Velasquez A, Bechara RI, Lewis JF, Malloy J, McCaig L, Brown LA, et al. Glutathione Replacement Preserves the Functional Surfactant Phospholipid Pool Size and Decreases Sepsis-Mediated Lung Dysfunction in Ethanol-Fed Rats. *Alcohol Clin Exp Res* (2002) 26(8):1245–51. doi: 10.1111/j.1530-0277.2002.tb02663.x
71. Liang Y, Harris FL, Brown LA. Alcohol Induced Mitochondrial Oxidative Stress and Alveolar Macrophage Dysfunction. *BioMed Res Int* (2014) 2014:371593. doi: 10.1155/2014/371593
72. Yeligar SM, Harris FL, Hart CM, Brown LA. Ethanol Induces Oxidative Stress in Alveolar Macrophages *via* Upregulation of NADPH Oxidases. *J Immunol* (2012) 188(8):3648–57. doi: 10.4049/jimmunol.1101278
73. Wagner MC, Yeligar SM, Brown LA, Michael Hart C. PPARgamma Ligands Regulate NADPH Oxidase, eNOS, and Barrier Function in the Lung Following Chronic Alcohol Ingestion. *Alcohol Clin Exp Res* (2012) 36 (2):197–206. doi: 10.1111/j.1530-0277.2011.01599.x
74. Jensen JS, Fan X, Guidot DM. Alcohol Causes Alveolar Epithelial Oxidative Stress by Inhibiting the Nuclear Factor (Erythroid-Derived 2)-Like 2-Antioxidant Response Element Signaling Pathway. *Am J Respir Cell Mol Biol* (2013) 48(4):511–7. doi: 10.1165/rcmb.2012-0334OC
75. Polikandriotis JA, Rupnow HL, Elms SC, Clempus RE, Campbell DJ, Sutliff RL, et al. Chronic Ethanol Ingestion Increases Superoxide Production and NADPH Oxidase Expression in the Lung. *Am J Respir Cell Mol Biol* (2006) 34(3):314–9. doi: 10.1165/rcmb.2005-0320OC
76. Yeligar SM, Mehta AJ, Harris FL, Brown LA, Hart CM. Peroxisome Proliferator-Activated Receptor Gamma Regulates Chronic Alcohol-Induced Alveolar Macrophage Dysfunction. *Am J Respir Cell Mol Biol* (2016) 55(1):35–46. doi: 10.1165/rcmb.2015-0077OC
77. Bechara RI, Brown LA, Roman J, Joshi PC, Guidot DM. Transforming Growth Factor Beta1 Expression and Activation is Increased in the Alcoholic Rat Lung. *Am J Respir Crit Care Med* (2004) 170(2):188–94. doi: 10.1164/rccm.200304-478OC
78. Brown SD, Brown LA. Ethanol (EtOH)-Induced TGF-Beta1 and Reactive Oxygen Species Production are Necessary for EtOH-Induced Alveolar Macrophage Dysfunction and Induction of Alternative Activation. *Alcohol Clin Exp Res* (2012) 36(11):1952–62. doi: 10.1111/j.1530-0277.2012.01825.x
79. Guidot DM, Modelska K, Lois M, Jain L, Moss IM, Pittet JF, et al. Ethanol Ingestion via Glutathione Depletion Impairs Alveolar Epithelial Barrier Function in Rats. *Am J Physiol Lung Cell Mol Physiol* (2000) 279(1):L127–35. doi: 10.1152/ajplung.2000.279.1.L127
80. Brown LA, Harris FL, Bechara R, Guidot DM. Effect of Chronic Ethanol Ingestion on Alveolar Type II Cell: Glutathione and Inflammatory Mediator-Induced Apoptosis. *Alcohol Clin Exp Res* (2001) 25(7):1078–85. doi: 10.1111/j.1530-0277.2001.tb02320.x
81. Brown LA, Ping XD, Harris FL, Gauthier TW. Glutathione Availability Modulates Alveolar Macrophage Function in the Chronic Ethanol-Fed Rat. *Am J Physiol Lung Cell Mol Physiol* (2007) 292(4):L824–32. doi: 10.1152/ajplung.00346.2006

82. Yeligar SM, Harris FL, Hart CM, Brown LA. Glutathione Attenuates Ethanol-Induced Alveolar Macrophage Oxidative Stress and Dysfunction by Downregulating NADPH Oxidases. *Am J Physiol Lung Cell Mol Physiol* (2014) 306(5):L429–41. doi: 10.1152/ajplung.00159.2013
83. Demir E, Giden R, Sak ZHA, Demir Giden Z. Thiol-Disulphide Homoeostasis as a Novel Oxidative Stress Biomarker in Lung Tuberculosis Patient. *Int J Clin Pract* (2021) 75(5):e13998. doi: 10.1111/ijcp.13998
84. Palanisamy GS, Kirk NM, Ackart DF, Shanley CA, Orme IM, Basaraba RJ. Evidence for Oxidative Stress and Defective Antioxidant Response in Guinea Pigs With Tuberculosis. *PloS One* (2011) 6(10):e26254. doi: 10.1371/journal.pone.0026254
85. Amaral EP, Conceicao EL, Costa DL, Rocha MS, Marinho JM, Cordeiro-Santos M, et al. N-Acetyl-Cysteine Exhibits Potent Anti-Mycobacterial Activity in Addition to its Known Anti-Oxidative Functions. *BMC Microbiol* (2016) 16(1):251. doi: 10.1186/s12866-016-0872-7
86. Oberley-Deegan RE, Rebits BW, Weaver MR, Tollefson AK, Bai X, McGibney M, et al. An Oxidative Environment Promotes Growth of Mycobacterium Abscessus. *Free Radic Biol Med* (2010) 49(11):1666–73. doi: 10.1016/j.freeradbiomed.2010.08.026
87. Rothchild AC, Olson GS, Nemeth J, Amon LM, Mai D, Gold ES, et al. Alveolar Macrophages Generate a Noncanonical NRF2-Driven Transcriptional Response to Mycobacterium Tuberculosis In Vivo. *Sci Immunol* (2019) 4 (37):1–14. doi: 10.1126/sciimmunol.aaw6693
88. Rockwood N, Costa DL, Amaral EP, Du Bruyn E, Kubler A, Gil-Santana L, et al. Mycobacterium Tuberculosis Induction of Heme Oxygenase-1 Expression Is Dependent on Oxidative Stress and Reflects Treatment Outcomes. *Front Immunol* (2017) 8:542. doi: 10.3389/fimmu.2017.00542
89. Sun Q, Shen X, Ma J, Lou H, Zhang Q. Activation of Nrf2 Signaling by Oltipraz Inhibits Death of Human Macrophages With Mycobacterium Tuberculosis Infection. *Biochem Biophys Res Commun* (2020) 531(3):312–9. doi: 10.1016/j.bbrc.2020.07.026
90. Meylan PR, Richman DD, Kornbluth RS. Reduced Intracellular Growth of Mycobacteria in Human Macrophages Cultivated at Physiologic Oxygen Pressure. *Am Rev Respir Dis* (1992) 145(4 Pt 1):947–53. doi: 10.1164/ajrccm/145.4_Pt_1.947
91. Chaudhuri N, Sabroe I. Basic Science of the Innate Immune System and the Lung. *Paediatr Respir Rev* (2008) 9(4):236–42. doi: 10.1016/j.prrv.2008.03.002
92. Zhang P, Bagby GJ, Happel KI, Summer WR, Nelson S. Pulmonary Host Defenses and Alcohol. *Front Biosci* (2002) 7:d1314–30. doi: 10.2741/A842
93. Kany S, Janicova A, Relja B. Innate Immunity and Alcohol. *J Clin Med* (2019) 8(11):1–31. doi: 10.3390/jcm8111981
94. Hallengren B, Forsgren A. Effect of Alcohol on Chemotaxis, Adherence and Phagocytosis of Human Polymorphonuclear Leucocytes. *Acta Med Scand* (1978) 204(1-2):43–8. doi: 10.1111/j.0954-6820.1978.tb08396.x
95. Boe DM, Nelson S, Zhang P, Bagby GJ. Acute Ethanol Intoxication Suppresses Lung Chemokine Production Following Infection With Streptococcus Pneumoniae. *J Infect Dis* (2001) 184(9):1134–42. doi: 10.1086/323661
96. Malacco N, Souza JAM, Martins FRB, Rachid MA, Simplicio JA, Tirapelli CR, et al. Chronic Ethanol Consumption Compromises Neutrophil Function in Acute Pulmonary Aspergillus Fumigatus Infection. *Elife* (2020) 9:1–23. doi: 10.7554/eLife.58855
97. Laso FJ, Vaquero JM, Almeida J, Marcos M, Orfao A. Chronic Alcohol Consumption is Associated With Changes in the Distribution, Immunophenotype, and the Inflammatory Cytokine Secretion Profile of Circulating Dendritic Cells. *Alcohol Clin Exp Res* (2007) 31(5):846–54. doi: 10.1111/j.1530-0277.2007.00377.x
98. Szabo G, Catalano D, White B, Mandrekar P. Acute Alcohol Consumption Inhibits Accessory Cell Function of Monocytes and Dendritic Cells. *Alcohol Clin Exp Res* (2004) 28(5):824–8. doi: 10.1097/01.ALC.0000127104.80398.9B
99. Wyatt TA, Gentry-Nielsen MJ, Pavlik JA, Sisson JH. Desensitization of PKA-Stimulated Ciliary Beat Frequency in an Ethanol-Fed Rat Model of Cigarette Smoke Exposure. *Alcohol Clin Exp Res* (2004) 28(7):998–1004. doi: 10.1097/01.ALC.0000130805.75641.F4
100. Wyatt TA, Sisson JH. Chronic Ethanol Downregulates PKA Activation and Ciliary Beating in Bovine Bronchial Epithelial Cells. *Am J Physiol Lung Cell Mol Physiol* (2001) 281(3):L575–81. doi: 10.1152/ajplung.2001.281.3.L575
101. Price ME, Case AJ, Pavlik JA, DeVasure JM, Wyatt TA, Zimmerman MC, et al. S-Nitrosation of Protein Phosphatase 1 Mediates Alcohol-Induced Ciliary Dysfunction. *Sci Rep* (2018) 8(1):9701. doi: 10.1038/s41598-018-27924-x
102. Torrelles JB, Schlesinger LS. Integrating Lung Physiology, Immunology, and Tuberculosis. *Trends Microbiol* (2017) 25(8):688–97. doi: 10.1016/j.tim.2017.03.007
103. Noone PG, Leigh MW, Sannuti A, Minnix SL, Carson JL, Hazucha M, et al. Primary Ciliary Dyskinesia: Diagnostic and Phenotypic Features. *Am J Respir Crit Care Med* (2004) 169(4):459–67. doi: 10.1164/rccm.200303-365OC
104. Schneeberger EE, Lynch RD. Structure, Function, and Regulation of Cellular Tight Junctions. *Am J Physiol* (1992) 262(6 Pt 1):L647–61. doi: 10.1152/ajplung.1992.262.6.L647
105. Fernandez AL, Koval M, Fan X, Guidot DM. Chronic Alcohol Ingestion Alters Claudin Expression in the Alveolar Epithelium of Rats. *Alcohol* (2007) 41(5):371–9. doi: 10.1016/j.alcohol.2007.04.010
106. Koval M. Claudin Heterogeneity and Control of Lung Tight Junctions. *Annu Rev Physiol* (2013) 75:551–67. doi: 10.1146/annurev-physiol-030212-183809
107. Schlingmann B, Overgaard CE, Molina SA, Lynn KS, Mitchell LA, Dorsainvil White S, et al. Regulation of Claudin/Zonula Occludens-1 Complexes by Hetero-Claudin Interactions. *Nat Commun* (2016) 7:12276. doi: 10.1038/ncomms12276
108. Burnham EL, Halkar R, Burks M, Moss M. The Effects of Alcohol Abuse on Pulmonary Alveolar-Capillary Barrier Function in Humans. *Alcohol Alcohol* (2009) 44(1):8–12. doi: 10.1093/alcalc/agn051
109. Berkowitz DM, Danai PA, Eaton S, Moss M, Martin GS. Alcohol Abuse Enhances Pulmonary Edema in Acute Respiratory Distress Syndrome. *Alcohol Clin Exp Res* (2009) 33(10):1690–6. doi: 10.1111/j.1530-0277.2009.01005.x
110. Pelaez A, Bechara RI, Joshi PC, Brown LA, Guidot DM. Granulocyte/macrophage Colony-Stimulating Factor Treatment Improves Alveolar Epithelial Barrier Function in Alcoholic Rat Lung. *Am J Physiol Lung Cell Mol Physiol* (2004) 286(1):L106–11. doi: 10.1152/ajplung.00148.2003
111. Overgaard CE, Schlingmann B, Dorsainvil White S, Ward C, Fan X, Swarnakar S, et al. The Relative Balance of GM-CSF and TGF-Beta1 Regulates Lung Epithelial Barrier Function. *Am J Physiol Lung Cell Mol Physiol* (2015) 308(12):L1212–23. doi: 10.1152/ajplung.00042.2014
112. Guidot DM, Brown LA. Mitochondrial Glutathione Replacement Restores Surfactant Synthesis and Secretion in Alveolar Epithelial Cells of Ethanol-Fed Rats. *Alcohol Clin Exp Res* (2000) 24(7):1070–6. doi: 10.1111/j.1530-0277.2000.tb04652.x
113. Wright JR, Borron P, Brinker KG, Folz RJ. Surfactant Protein A: Regulation of Innate and Adaptive Immune Responses in Lung Inflammation. *Am J Respir Cell Mol Biol* (2001) 24(5):513–7. doi: 10.1165/ajrcmb.24.5.f208
114. Ferguson JS, Schlesinger LS. Pulmonary Surfactant in Innate Immunity and the Pathogenesis of Tuberculosis. *Tuber Lung Dis* (2000) 80(4-5):173–84. doi: 10.1054/tuld.2000.0242
115. Pai M, Behr MA, Dowdy D, Dheda K, Divangahi M, Boehme CC, et al. Tuberculosis. *Nat Rev Dis Primers* (2016) 2:16076. doi: 10.1038/nrdp.2016.76
116. Cohen SB, Gern BH, Delahaye JL, Adams KN, Plumlee CR, Winkler JK, et al. Alveolar Macrophages Provide an Early Mycobacterium Tuberculosis Niche and Initiate Dissemination. *Cell Host Microbe* (2018) 24(3):439–46 e4. doi: 10.1016/j.chom.2018.08.001
117. Brown SD, Gauthier TW, Brown LA. Impaired Terminal Differentiation of Pulmonary Macrophages in a Guinea Pig Model of Chronic Ethanol Ingestion. *Alcohol Clin Exp Res* (2009) 33(10):1782–93. doi: 10.1111/j.1530-0277.2009.01017.x
118. Joshi PC, Applewhite L, Ritzenthaler JD, Roman J, Fernandez AL, Eaton DC, et al. Chronic Ethanol Ingestion in Rats Decreases Granulocyte-Macrophage Colony-Stimulating Factor Receptor Expression and Downstream Signaling in the Alveolar Macrophage. *J Immunol* (2005) 175(10):6837–45. doi: 10.4049/jimmunol.175.10.6837
119. Joshi PC, Applewhite L, Mitchell PO, Fernainy K, Roman J, Eaton DC, et al. GM-CSF Receptor Expression and Signaling is Decreased in Lungs of Ethanol-Fed Rats. *Am J Physiol Lung Cell Mol Physiol* (2006) 291(6):L1150–8. doi: 10.1152/ajplung.00150.2006
120. Joshi PC, Mehta A, Jabber WS, Fan X, Guidot DM. Zinc Deficiency Mediates Alcohol-Induced Alveolar Epithelial and Macrophage Dysfunction in Rats.

Am J Respir Cell Mol Biol (2009) 41(2):207–16. doi: 10.1165/rcmb.2008-0209OC
121. Shibata Y, Berclaz PY, Chroneos ZC, Yoshida M, Whitsett JA, Trapnell BC. GM-CSF Regulates Alveolar Macrophage Differentiation and Innate Immunity in the Lung Through PU.1. *Immunity* (2001) 15(4):557–67. doi: 10.1016/S1074-7613(01)00218-7
122. Lloberas J, Soler C, Celada A. The Key Role of PU.1/SPI-1 in B Cells, Myeloid Cells and Macrophages. *Immunol Today* (1999) 20(4):184–9. doi: 10.1016/S0167-5699(99)01442-5
123. Staitieh BS, Fan X, Neveu W, Guidot DM. Nrf2 Regulates PU.1 Expression and Activity in the Alveolar Macrophage. *Am J Physiol Lung Cell Mol Physiol* (2015) 308(10):L1086–93. doi: 10.1152/ajplung.00355.2014
124. Russell DG. Mycobacterium Tuberculosis and the Intimate Discourse of a Chronic Infection. *Immunol Rev* (2011) 240(1):252–68. doi: 10.1111/j.1600-065X.2010.00984.x
125. Bryson BD, Rosebrock TR, Tafesse FG, Itoh CY, Nibasumba A, Babunovic GH, et al. Heterogeneous GM-CSF Signaling in Macrophages is Associated With Control of Mycobacterium Tuberculosis. *Nat Commun* (2019) 10 (1):2329. doi: 10.1038/s41467-019-10065-8
126. Mishra A, Singh VK, Actor JK, Hunter RL, Jagannath C, Subbian S, et al. GM-CSF Dependent Differential Control of Mycobacterium Tuberculosis Infection in Human and Mouse Macrophages: Is Macrophage Source of GM-CSF Critical to Tuberculosis Immunity? *Front Immunol* (2020) 11:1599. doi: 10.3389/fimmu.2020.01599
127. Benmerzoug S, Marinho FV, Rose S, Mackowiak C, Gosset D, Sedda D, et al. GM-CSF Targeted Immunomodulation Affects Host Response to M. Tuberculosis Infection. *Sci Rep* (2018) 8(1):8652. doi: 10.1038/s41598-018-26984-3
128. Kim K, Waterer G, Thomson R, Yang IA, Nashi N, Tan DB, et al. Levels of Anti-Cytokine Antibodies may be Elevated in Patients With Pulmonary Disease Associated With non-Tuberculous Mycobacteria. *Cytokine* (2014) 66 (2):160–3. doi: 10.1016/j.cyto.2014.01.005
129. Suzuki K, Lee WJ, Hashimoto T, Tanaka E, Murayama T, Amitani R, et al. Recombinant Granulocyte-Macrophage Colony-Stimulating Factor (GM-CSF) or Tumour Necrosis Factor-Alpha (TNF-Alpha) Activate Human Alveolar Macrophages to Inhibit Growth of Mycobacterium Avium Complex. *Clin Exp Immunol* (1994) 98(1):169–73. doi: 10.1111/j.1365-2249.1994.tb06625.x
130. Bermudez LE, Young LS. Ethanol Augments Intracellular Survival of Mycobacterium Avium Complex and Impairs Macrophage Responses to Cytokines. *J Infect Dis* (1991) 163(6):1286–92. doi: 10.1093/infdis/163.6.1286
131. Bermudez LE. Effect of Ethanol on the Interaction Between the Macrophage and Mycobacterium Avium. *Alcohol* (1994) 11(2):69–73. doi: 10.1016/0741-8329(94)90046-9
132. Bermudez LE, Young LS, Martinelli J, Petrofsky M. Exposure to Ethanol Up-Regulates the Expression of Mycobacterium Avium Complex Proteins Associated With Bacterial Virulence. *J Infect Dis* (1993) 168(4):961–8. doi: 10.1093/infdis/168.4.961
133. Mason CM, Dobard E, Zhang P, Nelson S. Alcohol Exacerbates Murine Pulmonary Tuberculosis. *Infect Immun* (2004) 72(5):2556–63. doi: 10.1128/IAI.72.5.2556-2563.2004
134. Murray PJ, Allen JE, Biswas SK, Fisher EA, Gilroy DW, Goerdt S, et al. Macrophage Activation and Polarization: Nomenclature and Experimental Guidelines. *Immunity* (2014) 41(1):14–20. doi: 10.1016/j.immuni.2014.06.008
135. Malyshev I, Malyshev Y. Current Concept and Update of the Macrophage Plasticity Concept: Intracellular Mechanisms of Reprogramming and M3 Macrophage "Switch" Phenotype. *BioMed Res Int* (2015) 2015:341308. doi: 10.1155/2015/341308
136. O'Neill LA, Kishton RJ, Rathmell J. A Guide to Immunometabolism for Immunologists. *Nat Rev Immunol* (2016) 16(9):553–65. doi: 10.1038/nri.2016.70
137. Edwards JP, Zhang X, Frauwirth KA, Mosser DM. Biochemical and Functional Characterization of Three Activated Macrophage Populations. *J Leukoc Biol* (2006) 80(6):1298–307. doi: 10.1189/jlb.0406249
138. Pettersen JS, Fuentes-Duculan J, Suarez-Farinas M, Pierson KC, Pitts-Kiefer A, Fan L, et al. Tumor-Associated Macrophages in the Cutaneous SCC Microenvironment are Heterogeneously Activated. *J Invest Dermatol* (2011) 131(6):1322–30. doi: 10.1038/jid.2011.9
139. Lang R, Patel D, Morris JJ, Rutschman RL, Murray PJ. Shaping Gene Expression in Activated and Resting Primary Macrophages by IL-10. *J Immunol* (2002) 169(5):2253–63. doi: 10.4049/jimmunol.169.5.2253
140. Laskin DL, Weinberger B, Laskin JD. Functional Heterogeneity in Liver and Lung Macrophages. *J Leukoc Biol* (2001) 70(2):163–70. doi: 10.1189/jlb.70.2.163
141. Wells CA, Ravasi T, Faulkner GJ, Carninci P, Okazaki Y, Hayashizaki Y, et al. Genetic Control of the Innate Immune Response. *BMC Immunol* (2003) 4:5. doi: 10.1186/1471-2172-4-5
142. Stout RD, Suttles J. Functional Plasticity of Macrophages: Reversible Adaptation to Changing Microenvironments. *J Leukoc Biol* (2004) 76 (3):509–13. doi: 10.1189/jlb.0504272
143. Curry-McCoy TV, Venado A, Guidot DM, Joshi PC. Alcohol Ingestion Disrupts Alveolar Epithelial Barrier Function by Activation of Macrophage-Derived Transforming Growth Factor Beta1. *Respir Res* (2013) 14:39. doi: 10.1186/1465-9921-14-39
144. Gaydos J, McNally A, Guo R, Vandivier RW, Simonian PL, Burnham EL. Alcohol Abuse and Smoking Alter Inflammatory Mediator Production by Pulmonary and Systemic Immune Cells. *Am J Physiol Lung Cell Mol Physiol* (2016) 310(6):L507–18. doi: 10.1152/ajplung.00242.2015
145. O'Halloran EB, Curtis BJ, Afshar M, Chen MM, Kovacs EJ, Burnham EL. Alveolar Macrophage Inflammatory Mediator Expression is Elevated in the Setting of Alcohol Use Disorders. *Alcohol* (2016) 50:43–50. doi: 10.1016/j.alcohol.2015.11.003
146. Crews FT, Bechara R, Brown LA, Guidot DM, Mandrekar P, Oak S, et al. Cytokines and Alcohol. *Alcohol Clin Exp Res* (2006) 30(4):720–30. doi: 10.1111/j.1530-0277.2006.00084.x
147. Yeligar SM, Chen MM, Kovacs EJ, Sisson JH, Burnham EL, Brown LA. Alcohol and Lung Injury and Immunity. *Alcohol* (2016) 55:51–9. doi: 10.1016/j.alcohol.2016.08.005
148. Romero F, Shah D, Duong M, Stafstrom W, Hoek JB, Kallen CB, et al. Chronic Alcohol Ingestion in Rats Alters Lung Metabolism, Promotes Lipid Accumulation, and Impairs Alveolar Macrophage Functions. *Am J Respir Cell Mol Biol* (2014) 51(6):840–9. doi: 10.1165/rcmb.2014-0127OC
149. Slovinsky WS, Shaghaghi H, Para R, Romero F, Summer R. Alcohol-Induced Lipid Dysregulation Impairs Glycolytic Responses to LPS in Alveolar Macrophages. *Alcohol* (2020) 83:57–65. doi: 10.1016/j.alcohol.2019.08.009
150. Morris NL, Harris FL, Brown LAS, Yeligar SM. Alcohol Induces Mitochondrial Derangements in Alveolar Macrophages by Upregulating NADPH Oxidase 4. *Alcohol* (2021) 90:27–38. doi: 10.1016/j.alcohol.2020.11.004
151. Lugo-Villarino G, Verollet C, Maridonneau-Parini I, Neyrolles O. Macrophage Polarization: Convergence Point Targeted by Mycobacterium Tuberculosis and HIV. *Front Immunol* (2011) 2:43. doi: 10.3389/fimmu.2011.00043
152. Braverman J, Sogi KM, Benjamin D, Nomura DK, Stanley SA. HIF-1alpha Is an Essential Mediator of IFN-Gamma-Dependent Immunity to Mycobacterium Tuberculosis. *J Immunol* (2016) 197(4):1287–97. doi: 10.4049/jimmunol.1600266
153. Shi L, Salamon H, Eugenin EA, Pine R, Cooper A, Gennaro ML. Infection With Mycobacterium Tuberculosis Induces the Warburg Effect in Mouse Lungs. *Sci Rep* (2015) 5:18176. doi: 10.1038/srep18176
154. Gleeson LE, Sheedy FJ, Palsson-McDermott EM, Triglia D, O'Leary SM, O'Sullivan MP, et al. Cutting Edge: Mycobacterium Tuberculosis Induces Aerobic Glycolysis in Human Alveolar Macrophages That Is Required for Control of Intracellular Bacillary Replication. *J Immunol* (2016) 196 (6):2444–9. doi: 10.4049/jimmunol.1501612
155. Lachmandas E, Beigier-Bompadre M, Cheng SC, Kumar V, van Laarhoven A, Wang X, et al. Rewiring Cellular Metabolism *via* the AKT/mTOR Pathway Contributes to Host Defence Against Mycobacterium Tuberculosis in Human and Murine Cells. *Eur J Immunol* (2016) 46 (11):2574–86. doi: 10.1002/eji.201546259
156. Huang L, Nazarova EV, Tan S, Liu Y, Russell DG. Growth of Mycobacterium Tuberculosis *In Vivo* Segregates With Host Macrophage Metabolism and Ontogeny. *J Exp Med* (2018) 215(4):1135–52. doi: 10.1084/jem.20172020
157. Benoit M, Desnues B, Mege JL. Macrophage Polarization in Bacterial Infections. *J Immunol* (2008) 181(6):3733–9. doi: 10.4049/jimmunol.181.6.3733
158. Almeida AS, Lago PM, Boechat N, Huard RC, Lazzarini LC, Santos AR, et al. Tuberculosis is Associated With a Down-Modulatory Lung Immune

Response That Impairs Th1-Type Immunity. *J Immunol* (2009) 183(1):718–31. doi: 10.4049/jimmunol.0801212
159. Bonecini-Almeida MG, Ho JL, Boechat N, Huard RC, Chitale S, Doo H, et al. Down-Modulation of Lung Immune Responses by Interleukin-10 and Transforming Growth Factor Beta (TGF-Beta) and Analysis of TGF-Beta Receptors I and II in Active Tuberculosis. *Infect Immun* (2004) 72(5):2628–34. doi: 10.1128/IAI.72.5.2628-2634.2004
160. Hackett EE, Charles-Messance H, O'Leary SM, Gleeson LE, Munoz-Wolf N, Case S, et al. Mycobacterium Tuberculosis Limits Host Glycolysis and IL-1beta by Restriction of PFK-M *via* MicroRNA-21. *Cell Rep* (2020) 30(1):124–36 e4. doi: 10.1016/j.celrep.2019.12.015
161. Shi L, Jiang Q, Bushkin Y, Subbian S, Tyagi S. Biphasic Dynamics of Macrophage Immunometabolism During Mycobacterium Tuberculosis Infection. *mBio* (2019) 10(2):e02550-18. doi: 10.1128/mBio.02550-18
162. Mohareer K, Medikonda J, Vadankula GR, Banerjee S. Mycobacterial Control of Host Mitochondria: Bioenergetic and Metabolic Changes Shaping Cell Fate and Infection Outcome. *Front Cell Infect Microbiol* (2020) 10:457. doi: 10.3389/fcimb.2020.00457
163. Raju B, Hoshino Y, Belitskaya-Levy I, Dawson R, Ress S, Gold JA, et al. Gene Expression Profiles of Bronchoalveolar Cells in Pulmonary TB. *Tuberculosis (Edinb)* (2008) 88(1):39–51. doi: 10.1016/j.tube.2007.07.003
164. Gleeson LE, O'Leary SM, Ryan D, McLaughlin AM, Sheedy FJ, Keane J. Cigarette Smoking Impairs the Bioenergetic Immune Response to Mycobacterium Tuberculosis Infection. *Am J Respir Cell Mol Biol* (2018) 59(5):572–9. doi: 10.1165/rcmb.2018-0162OC

Conflict of Interest: The authors declare that the research was conducted in the absence of any commercial or financial relationships that could be construed as a potential conflict of interest.

frontiers | Frontiers in Immunology

ORIGINAL RESEARCH
published: 04 May 2022
doi: 10.3389/fimmu.2022.884719

Ethanol Intoxication Impairs Respiratory Function and Bacterial Clearance and Is Associated With Neutrophil Accumulation in the Lung After *Streptococcus pneumoniae* Infection

Holly J. Hulsebus[1,2], *Kevin M. Najarro*[1], *Rachel H. McMahan*[1], *Devin M. Boe*[1,2], *David J. Orlicky*[3] *and Elizabeth J. Kovacs*[1,2*]

[1] Department of Surgery, Division of GI, Trauma and Endocrine Surgery, University of Colorado Anschutz Medical Campus, Aurora, CO, United States, [2] Immunology Graduate Program, University of Colorado Anschutz Medical Campus, Aurora, CO, United States, [3] Department of Pathology, University of Colorado Anschutz Medical Campus, Aurora, CO, United States

OPEN ACCESS

Edited by:
Suhas Sureshchandra, University of California, Irvine, United States

Reviewed by:
Frederico Marianetti Soriani, Federal University of Minas Gerais, Brazil
Prajwal Gurung, The University of Iowa, United States
Leon Coleman Jr., University of North Carolina at Chapel Hill, United States

***Correspondence:**
Elizabeth J. Kovacs
elizabeth.kovacs@cuanschutz.edu

Specialty section:
This article was submitted to Nutritional Immunology, a section of the journal Frontiers in Immunology

Received: 26 February 2022
Accepted: 11 April 2022
Published: 04 May 2022

Citation:
Hulsebus HJ, Najarro KM, McMahan RH, Boe DM, Orlicky DJ and Kovacs EJ (2022) Ethanol Intoxication Impairs Respiratory Function and Bacterial Clearance and Is Associated With Neutrophil Accumulation in the Lung After Streptococcus pneumoniae Infection. Front. Immunol. 13:884719. doi: 10.3389/fimmu.2022.884719

Alcohol consumption is commonplace in the United States and its prevalence has increased in recent years. Excessive alcohol use is linked to an increased risk of infections including pneumococcal pneumonia, mostly commonly caused by *Streptococcus pneumoniae*. In addition, pneumonia patients with prior alcohol use often require more intensive treatment and longer hospital stays due to complications of infection. The initial respiratory tract immune response to *S. pneumoniae* includes the production of pro-inflammatory cytokines and chemokines by resident cells in the upper and lower airways which activate and recruit leukocytes to the site of infection. However, this inflammation must be tightly regulated to avoid accumulation of toxic by-products and subsequent tissue damage. A majority of previous work on alcohol and pneumonia involve animal models utilizing high concentrations of ethanol or chronic exposure and offer conflicting results about how ethanol alters immunity to pathogens. Further, animal models often employ a high bacterial inoculum which may overwhelm the immune system and obscure results, limiting their applicability to the course of human infection. Here, we sought to determine how a more moderate ethanol exposure paradigm affects respiratory function and innate immunity in mice after intranasal infection with 10^4 colony forming units of *S. pneumoniae.* Ethanol-exposed mice displayed respiratory dysfunction and impaired bacterial clearance after infection compared to their vehicle-exposed counterparts. This altered response was associated with increased gene expression of neutrophil chemokines *Cxcl1* and *Cxcl2* in whole lung homogenates, elevated concentrations of circulating granulocyte-colony stimulating factor (G-CSF), and higher

neutrophil numbers in the lung 24 hours after infection. Taken together, these findings suggest that even a more moderate ethanol consumption pattern can dramatically modulate the innate immune response to *S. pneumoniae* after only 3 days of ethanol exposure and provide insight into possible mechanisms related to the compromised respiratory immunity seen in alcohol consumers with pneumonia.

Keywords: alcohol, inflammation, innate immunity, lung function, macrophage, leukocyte

INTRODUCTION

The immune system is influenced by a myriad of environmental factors, including alcohol consumption. In 2019, 69% of U.S. adults aged 26 years or older reported alcohol use in the past month (1). Importantly, social stresses associated with the COVID-19 pandemic have led to increased sales of alcoholic beverages: sales were 3.6% higher in March 2020 and 15.5% higher in April 2021 when compared to a 3-year average from the same month in 2017-2019 (2). Further, alcohol-related deaths have been rising at an astonishingly quick pace in recent years: fatalities due to alcohol rose by 25.9% between 2019 and 2020, compared to a 16.6% increase in age-adjusted mortality rates from all causes (3). Based on this rapidly escalating prevalence of alcohol consumption, we will likely continue to see a rise alcohol-associated morbidity and mortality well into the future.

Alcohol's effects on the immune system vary based on the amount and duration of consumption. Broadly speaking, alcohol intake can be classified as "moderate" or "excessive" (4). The U.S. Centers for Disease Control and Prevention describe "moderate" alcohol intake as 1-2 drinks per day for males or 1 drink per day for a female (4). "Excessive" alcohol consumption includes binge drinking, or that which brings blood alcohol concentration (BAC) above the "legal limit" for driving (80 mg/dL; usually 5 + drinks for a male or 4+ drinks for a female within 2 hours) and heavy drinking, considered 14+ drinks per week for a male or 7+ drinks for a female (5). In addition, human studies characterize "alcohol use disorder" (AUD) as the inability to modify or discontinue alcohol use despite adverse consequences to one's personal or work life, and is clinically measured by several social and psychological parameters (6).

Epidemiological studies have shown that moderate alcohol intake is generally associated with protective health effects, such as decreased risk of cardiovascular disease [reviewed in (7)], lower concentrations of circulating inflammatory biomarkers (8), and lower risk of all-cause mortality in humans (9). In contrast, other studies have found an increased risk for all-cause mortality in adults with heavy alcohol consumption [> 14 and > 7 drinks per week for men and women, respectively (9), or 5+ drinks on a single occasion at least once per week in the past year (10)]. Additionally, chronic alcohol users often have health complications associated with alcoholic hepatitis and its treatment, such as invasive aspergillosis (11) and infections of the lower respiratory and urinary tracts (12). Mouse models have similarly shown that excessive ethanol exposure is linked to deleterious effects on immunity; these include decreased responsiveness to Toll-like receptor (TLR) 2, 4, and 9 agonists (13), diminished phagocytic capacity (14, 15), impaired respiratory function (16), and increased airway neutrophils following acute lipopolysaccharide-induced lung injury (17). Neutrophil function is also compromised due to excessive ethanol consumption. For example, chronic ethanol exposure is associated with impaired neutrophil chemotaxis to the airways following pulmonary *Aspergillus fumigatus* infection, along with attenuated phagocytosis, fungal killing, and reactive oxygen species production in *A. fumigatus*-challenged neutrophils from ethanol-fed mice (18). Others have demonstrated that acute ethanol treatment (6 g/kg) decreases neutrophil infiltration into the peritoneal cavity following cecal ligation and puncture, accompanied by diminished production of neutrophil extracellular traps and bacterial killing (19).

Excessive alcohol use has been linked to increased susceptibility to infectious diseases such as pneumonia, with the most common bacterial cause being *Streptococcus pneumoniae* (20). The estimated annual incidence of pneumonia in the United States is 24.8 cases per 10,000 adults (21), and approximately 3.5% of pneumonia patients had an AUD at diagnosis (22). In fact, meta-analyses have found a dose-dependent, linear relationship between alcohol consumption and relative risk for contracting pneumonia (23, 24). In addition, patients with alcohol use disorder are more likely to have severe invasive disease that requires hospitalization (25) and adults who drink excessively (> 60 grams per day) are 4 times more likely to die within 30 days of infection (26).

Innate immune recognition of *S. pneumoniae* by tissue-resident alveolar macrophages or epithelial cells stimulates the production of pro-inflammatory C-X-C motif chemokine ligand 1 (CXCL1) and CXCL2, which recruit and activate cells, such as monocytes, macrophages, and neutrophils to the site of infection (27–29). Additionally, in the context of pulmonary injury, CXCL12 promotes neutrophil migration and retention in the lung (30, 31). Important chemokines for the production and mobilization of granulocytes from the bone marrow are granulocyte colony stimulating factor (G-CSF) and granulocyte macrophage colony stimulating factor (GM-CSF). Following an inflammatory stimuli such as infection, G-CSF and GM-CSF are rapidly produced and secreted by monocytes, macrophages, fibroblasts, and endothelial cells and this corresponds with an increase in neutrophil differentiation and production in the bone marrow (32–34). Indeed, mice lacking G-CSF or its receptor have reduced neutrophil counts in the blood and bronchoalveolar lavage (BAL) fluid following *Pseudomonas aeruginosa* lung infection (35). While the importance of innate

immune cells in the response to *S. pneumoniae* has long been appreciated (36–38), excessive accumulation of these cells can be deleterious to host tissue if the inflammatory response is not properly controlled. For example, increased neutrophil recruitment to the lungs following influenza-induced pneumonia in mice is associated with alveolar damage, pulmonary edema, and development of a phenotype similar to that seen in critically ill humans with acute respiratory distress syndrome (39).

Our current knowledge regarding the effects of acute alcohol intoxication on lung immunity is largely based on animal studies using supra-physiologic doses of alcohol (3-5 g/kg) (40, 41), sometimes high enough to raise blood alcohol concentration to 350-550 mg/dL (42, 43). Here, we sought to determine the effect of a 3 day lower-dose alcohol regimen (1.5 g/kg; target BAC of ~80 mg/dL) on the pulmonary response to a clinically relevant intranasal *S. pneumoniae* infection (44).

MATERIAL AND METHODS

Mice

Female BALB/cBy mice (Jackson Laboratory) were housed at the University of Colorado Anschutz Medical Campus in specific pathogen-free conditions for at least 2 weeks prior to the start of studies. Animals used in experiments were 3-5 months of age and weighed at least 20 grams. All animal experiments were performed under a protocol approved by the Institutional Animal Care and Use Committee at the University of Colorado Anschutz Medical Campus (protocol number 00087). Animals were housed in a temperature- (72°F ± 2°) and humidity- (35%) controlled room with a 14-hour light cycle (6am-8pm) and 10-hour dark cycle (8pm-6am), and provided with a nestlet for environmental enrichment. Experiments were performed between the hours of 8 and 10 am to minimize confounding effects of circadian variation in corticosterone and other hormones which can influence inflammatory and immune responses (45). For these studies, 3-6 mice comprised each control or treatment group and results are combined from 2-3 individual experiments as indicated in the figure legends.

Oral Gavage and Measurement of BAC

Mice were orally gavaged with a 20% v/v ethanol solution (1.5 g/kg based on body weight) or vehicle (sterile water) once daily for 3 consecutive days (46). BAC levels were confirmed in each experiment by obtaining blood *via* tail snip at 30 minutes post-gavage and analyzing ethanol levels in a 1:50 dilution of serum using a commercially available kit (BioVision K620). Animals were gavaged between 8 and 9 am to mimic human drinking patterns.

Bacterial Growth and Infection

Previously frozen glycerol stocks (1 ml) of *Streptococcus pneumoniae* serotype 3 (ATCC 6303) were quickly thawed at 37°C, added to 4 ml of tryptic soy broth (BD 211825), and incubated statically at 37°C/5% CO_2 until the culture reached mid-log phase (47). Bacteria were washed twice in sterile phosphate buffered saline (PBS), resuspended in an appropriate volume to yield approximately 10^4 colony forming units (CFU) in 50 µl, and kept on ice until inoculation. One hour after the final gavage, mice were anesthetized with an intraperitoneal injection of 12.5 mg/kg of ketamine and 1.25 mg/kg of xylazine (Webster Veterinary, Sterling, MA), and 50 ul of the prepared inoculum or sterile PBS (Gibco 14190-144) for sham animals was instilled trans-nasally. Mice were held vertically for 1 minute to assist inoculum draining into the lungs. Any mice losing more than 15% of their body weight were humanely euthanized and excluded from analysis. The exact dose of inoculum was quantified in each experiment by serial dilution of the bacterial suspension and plating on tryptic soy agar containing 5% sheep's blood (Remel R01200).

Plethysmography

Respiratory function was measured in conscious mice using unrestrained whole-body barometric plethysmography (Buxco Research Systems) as described (16, 48). Briefly, mice were allowed to acclimate in the sealed chamber for 5 minutes and respiratory parameters were measured and recorded for 10 minutes by the manufacturer's software (Buxco FinePointe). Mean values for each parameter per mouse were used for analysis.

Lung Bacterial Burden

Whole lungs were removed at 24 hours after infection, placed in 1 ml cold PBS, and homogenized using a Tissue Tearor (Dremel 985370). 100 µl of serially diluted sample was plated on tryptic soy agar containing 5% sheep's blood (Remel R01200), and CFU were counted after overnight incubation at 37°C/5% CO_2.

Lung Macrophage and Neutrophil Quantification by Flow Cytometry

Whole lungs were removed at 24 hours post-infection and dissociated into a single cell suspension per manufacturer's protocol (Miltenyi 130-095-927). Briefly, separated lung lobes were placed in a C tube (Miltenyi 130-096-334) containing 2.4 ml 1X Buffer S, 100 µl enzyme D, and 15 µl enzyme A. Samples were mechanically disrupted using a GentleMACS instrument (Miltenyi), filtered, and red blood cells were lysed by incubation in Ammonium-Chloride-Potassium (ACK) buffer (Gibco A10492-01) (16). 10^6 cells per sample were stained in PBS (Gibco) + 1% BSA (Quality Biological Inc K719500ML) with the following antibody cocktail: CD45-FITC (clone 30-F11, Biolegend 103108), CD11b-BV650 (clone M1/70, Biolegend 101259), CD11c-BV605 (clone N418, Biolegend 117334), F4/80-PerCP-Cy5.5 (clone BM8, Biolegend 123128), SiglecF-BV421 (clone E50-2440, BD Horizon 562681), and Ly6G-APC-Cy7 (clone 1A8, Biolegend 127624). Samples were resuspended in stabilizing fixative (BD 338036), run on an LSRII flow cytometer (BD Biosciences), and data were analyzed using FlowJo software v10.7.1 (BD Life Sciences).

Quantitative Real-Time PCR

RNA was extracted from homogenized lung tissue using the RNeasy Mini kit (Qiagen 74106) and reverse transcribed to

cDNA (BioRad 1708891) following the manufacturers' protocols (49). Equal quantities of cDNA were added to a Taqman master mix (Life Technologies 4304437) containing either *Cxcl1* (ThermoFisher Mm04207460_m1), *Cxcl2* (ThermoFisher Mm00436450_m1), *Cxcl12* (ThermoFisher Mm00445553_m1), *Ly6g* (ThermoFisher Mm04934123_m1), *Csf2* (ThermoFisher Mm01290062_m1) or *Csf3* (Mm00438334_m1), and *Gapdh* as endogenous control (Thermo Fisher 4352339E). Real-time quantitative PCR was performed using the QuantStudio 3 Real-Time PCR System (ThermoFisher Scientific) and analyzed using the ΔΔCt algorithm (50).

Enzyme-Linked Immunosorbent Assay (ELISA)

Blood was collected from mice *via* cardiac puncture immediately following euthanasia and allowed to coagulate for 30 minutes before serum separation by centrifugation. Granulocyte-colony stimulating factor (G-CSF) was measured in serum samples according to manufacturer's protocol (R&D Systems DY414).

Lung Histology and Immunohistochemistry (IHC)

The left lung lobe was inflated with 10% formalin (Fisher SF98-4), fixed overnight, and kept in 70% ethanol until processing. Paraffin-embedded tissue was sectioned (5 μm) and stained using hematoxylin and eosin (H&E) or IHC antibodies and scored in a blinded fashion by an experimental pathologist. IHC was performed using primary antibodies against Ly6G (1:250, BD Biosciences 551459) and *S. pneumoniae* (1:1000; Novus Biologicals NB100-64502), and detected using ImmPress polymer reagents (Vector Laboratories). Antigen expression was visualized with 3,3'Diaminobenzidine and alkaline phosphatase according to manufacturer's protocol (Vector Laboratories). Sections were counterstained with Hematoxylin QS and slides were coverslipped using VectaMount medium (Vector Laboratories).

Quantification of H&E- and IHC-Stained Lung Sections

Semi-quantitative assessment of the following injury criteria in the H&E-stained sections was performed: gross accumulations of inflammatory cells in the lung parenchyma (0-6), presence of leukocytes in the airways (0-2), peri-vascular inflammatory cell accumulation (0-2) or edema (0-2), and proteinaceous material in the alveolar space (0-2). Analysis of IHC staining intensity was achieved by capturing histologic images [enough 40x images per animal to completely cover the whole IHC-stained lung cross-section (5-8 per animal)] on an Olympus BX51 (Waltham, MA) microscope equipped with a 4 megapixel Macrofire digital camera using the PictureFrame Application 2.3 (Optronics, Goleta, CA). Images were then imported into Slidebook (3I, Denver, CO) for quantification. Data are expressed as percent IHC positive pixels (51). Phagocytosis of *S. pneumoniae* was measured by capturing stitched images with a light microscope equipped with a motorized XY-stage at 400x magnification (Olympus IX83) and CellSens software (version 1.16, Olympus Life Sciences). Manual quantification of 8-9 non-overlapping 400x images per animal was performed and phagocytosis was calculated as the number of cells with internalized *S. pneumoniae* relative to total nucleated cells. Average percentage phagocytosis per group is presented.

Statistical Analysis

Data were analyzed with Graph Pad Prism software for Windows version 9.2.0 (GraphPad Software, San Diego, California USA) using an unpaired two-tailed t test with Welch's correction or one-way ANOVA as appropriate and indicated in figure legends. p value < 0.05 was considered to represent a significant difference between treatment groups.

RESULTS

Ethanol-Exposed Mice Have Increased Lung Bacterial Burden After *S. pneumoniae* Infection Compared to Vehicle-Exposed Animals

To test our hypothesis that ethanol exposure impairs clearance of *S. pneumoniae* from the lungs, we gavaged mice with vehicle (water) or ethanol (1.5 g/kg) and intra-nasally instilled *S. pneumoniae* or PBS (**Figure 1A**). This dose of ethanol raised serum BAC to approximately 80 mg/dL at 30 minutes post-gavage (**Figure 1B**). Our results indicate that ethanol-exposed infected mice had significantly higher average *S. pneumoniae* CFU in whole lung homogenates at 24 hours post-infection (**Figure 1C**). Importantly, since we are introducing 10^4 CFU *S. pneumoniae via* an intra-nasal route (vs. direct administration of bacteria to the lungs *via* an intra-tracheal infection), our results confirm that the bacteria are able to withstand the initial immune response in the upper respiratory tract to reach the lungs, establish an infection, and begin to replicate.

Ethanol-Exposed Mice Have Impaired Respiratory Function After *S. pneumoniae* Infection Compared to Vehicle-Exposed Animals

To determine the effect of ethanol consumption on respiratory function in our infected animals, we performed unrestrained whole-body plethysmography prior to infection and up to 7 days after infection. Here, we report respiratory rate [breaths per minute (bpm)], enhanced pause ratio (penh) – a dimensionless index of airflow patterns as a mouse breathes (43), expiration time (Te), and Rpef – the time required to reach peak expiratory flow relative to Te (44). Before infection, all parameters were similar between our vehicle- and ethanol-exposed groups; therefore, we used vehicle-exposed uninfected animals as our control group throughout the 7-day time course (**Figure 2A–D**). When comparing respiratory parameters between infected groups, we noted a significantly higher penh value in our ethanol- compared to vehicle-exposed infected mice from days 1-4 post-infection (**Figure 2A**), decreased breathing frequency in the ethanol-exposed infected animals at 24 hours (**Figure 2B**),

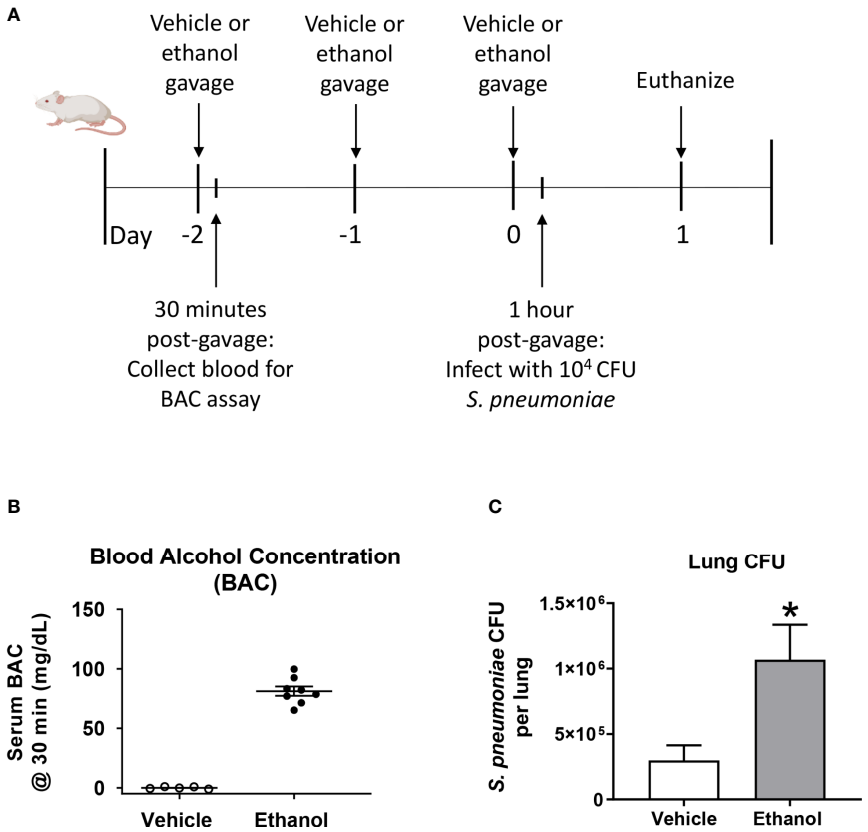

FIGURE 1 | Effect of ethanol exposure on blood alcohol concentration (BAC) and *S. pneumoniae* burden in the lung. **(A)** Schematic diagram of ethanol exposure and *S. pneumoniae* infection. **(B)** Representative BAC measurements from serum at 30 minutes post-gavage. Each dot represents the value from a single animal from one experiment. The line for each group represents average value ± SEM. **(C)** Whole lungs were collected at 24 hours post-infection, homogenized, and plated on agar. *S. pneumoniae* colony forming units (CFU) were enumerated and data are presented as mean ± SEM. n = 4-6 mice per group per experiment and data are combined from 3 individual experiments. *p < 0.05 by unpaired t test.

increased expiratory time in ethanol-exposed animals at 24 hours (**Figure 2C**), and a lower Rpef value in ethanol- compared to vehicle-exposed infected mice at 24 hours (**Figure 2D**). Notably, penh values in the vehicle-exposed infected mice did not differ from the uninfected mice through 7 days of infection (**Figure 2A**).

Ethanol-Exposed Mice Have Increased Numbers of Neutrophils, but Similar Numbers of Macrophages, in the Lung 24 Hours After Infection Compared to Vehicle-Exposed Mice

Since our initial results showed that ethanol administration is associated with increased pulmonary bacterial burden and impaired respiratory function at 24 hours, we wondered if this was due to ineffective trafficking of immune cells to the infection site at this time point. To test this, we used flow cytometry to quantify neutrophils and macrophages, important early responders to *S. pneumoniae* infection, in single cell suspensions of whole lung homogenates. We identified neutrophils as $CD45^+CD11b^+Ly6G^{hi}$, and distinguished tissue-resident alveolar macrophages from infiltrating macrophages based on SiglecF and CD11b expression (**Figure 3A**). Alveolar macrophages are designated as $CD45^+F4/80^+SiglecF^+CD11b^{neg/dim}$, while infiltrating macrophages are $CD45^+F4/80^+SiglecF^{neg/dim}CD11b^+$ (45). The number of cells in these subsets did not differ in our uninfected mice based on vehicle or ethanol treatment (**Figure 3B**). However, we found increased numbers of neutrophils in both infected groups relative to uninfected animals at 24 hours (**Figure 3B**), indicative of an innate immune response to the infection. When comparing vehicle-exposed infected animals to their ethanol-exposed counterparts, we found that ethanol exposure resulted in 1.8-fold more neutrophils in the lungs of infected animals at 24 hours but noted no difference in the number of alveolar or infiltrating macrophages (**Figure 3B**). Finally, to complement our result of increased neutrophils in the lungs of ethanol-exposed animals after infection, we performed quantitative PCR on whole lung homogenates for *Ly6g* expression. We observed 5.0- and 2.7-fold higher *Ly6g* transcript in lung homogenates of ethanol-exposed infected animals compared to uninfected animals or vehicle-exposed infected animals, respectively (**Figure 3C**).

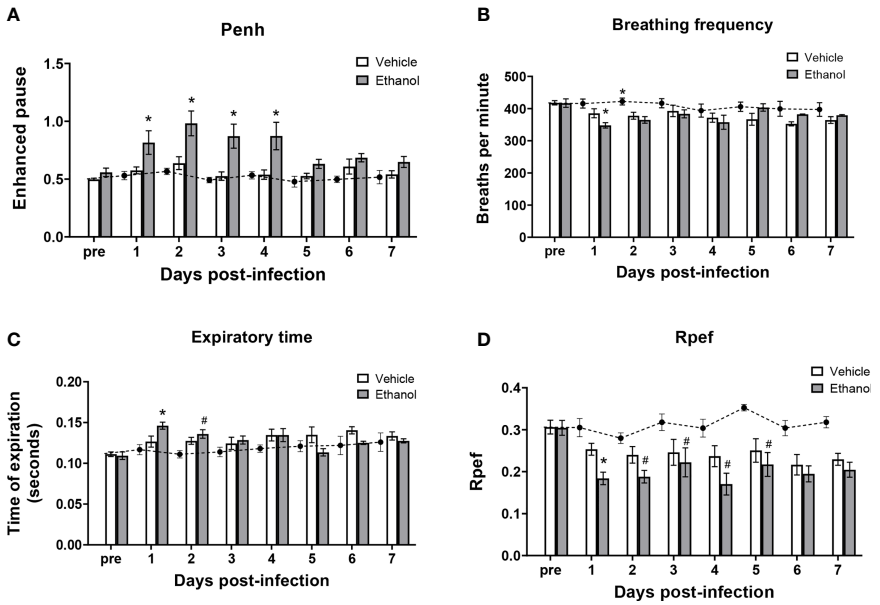

FIGURE 2 | Effect of ethanol consumption on respiratory function following infection. Enhanced pause (penh) **(A)**, breathing frequency **(B)**, time of respiratory expiration (Te) **(C)**, and Rpef (time to peak expiratory flow as a fraction of Te) **(D)** were measured by unrestrained whole-body plethysmography before infection and daily for 7 days post-infection. Black circles with dashed line represents values from vehicle-treated uninfected mice; solid bars represent values from infected animals (except for the "pre" values, which were obtained in vehicle- and ethanol-exposed mice prior to infection). Data are presented as mean ± SEM. n = 3-6 mice per group per experiment and data are combined from 3 individual experiments. *p < 0.05 compared to vehicle-exposed infected animals, #p < 0.05 compared to uninfected animals by one-way ANOVA.

Ethanol Exposure Prior to *S. pneumoniae* Infection Leads to Increased Pulmonary Expression of Pro-Inflammatory Cytokines and Chemokines, and Increased G-CSF in the Serum

Based on our results showing an increased number of lung neutrophils in ethanol-exposed infected animals observed by flow cytometry, we evaluated pulmonary expression of the chemokine genes *Cxcl1*, *Cxcl2*, and *Cxcl12*, important neutrophil chemoattractants and activators produced during the inflammatory response to infection (26, 46). Additionally, we measured pulmonary expression of *Csf2* and *Csf3*, the genes encoding for granulocyte macrophage-colony stimulating factor (GM-CSF) and granulocyte colony-stimulating factor (G-CSF), respectively, important cytokines for inducing granulopoiesis and the release of granulocytes from the bone marrow (47), along with serum levels of G-CSF. Our data show that, compared to vehicle-exposed infected animals, the ethanol-exposed infected mice had significantly higher expression of *Cxcl1* (3.0-fold) and *Cxcl2* (3.7-fold), and no difference in *Cxcl12*, in lung homogenates at 24 hours (**Figure 4A**). Further, we found no difference in *Csf2* expression, but rather elevated levels of *Csf3* transcript in the lung and G-CSF in the serum (17.2-fold and 3.0-fold higher, respectively), in ethanol- compared to vehicle-exposed infected animals (**Figures 4B, C**). We noted no difference in pulmonary gene expression or serum G-CSF levels between our vehicle- or ethanol-exposed uninfected groups (**Figure 4**).

Ethanol Exposure Alters Leukocyte and *S. pneumoniae* Localization in the Lung at 24 Hours Following Infection

Due to the increased number of neutrophils in the lungs of ethanol-exposed infected animals detected by flow cytometry at 24 hours, we analyzed histological markers of inflammation and injury in H&E-stained lung sections. We found that ethanol-exposed infected animals had significantly increased peri-vascular cell accumulation at 24 hours and a trend toward more leukocytes in the lumen of the larger airways compared to vehicle-exposed infected animals (**Figures 5A, B**). We failed to observe a difference in the other individual scoring criteria—gross accumulation of inflammatory cells in the lung parenchyma, peri-vascular edema, or proteinaceous material in the alveolar space (data not shown).

Next, since we noted altered leukocyte localization in the lungs by H&E and a difference in neutrophil numbers and transcript by flow cytometry and qPCR, respectively, we evaluated neutrophil and bacterial localization after infection utilizing IHC staining. Quantification of staining (as assessed by percent positive pixels) showed a great deal of variation between animals within groups, and thus, no statistical difference was observed in the levels of Ly6G or *S. pneumoniae* antigen in lung sections from our vehicle- and ethanol-exposed infected animals (**Supplementary Figure 1**).

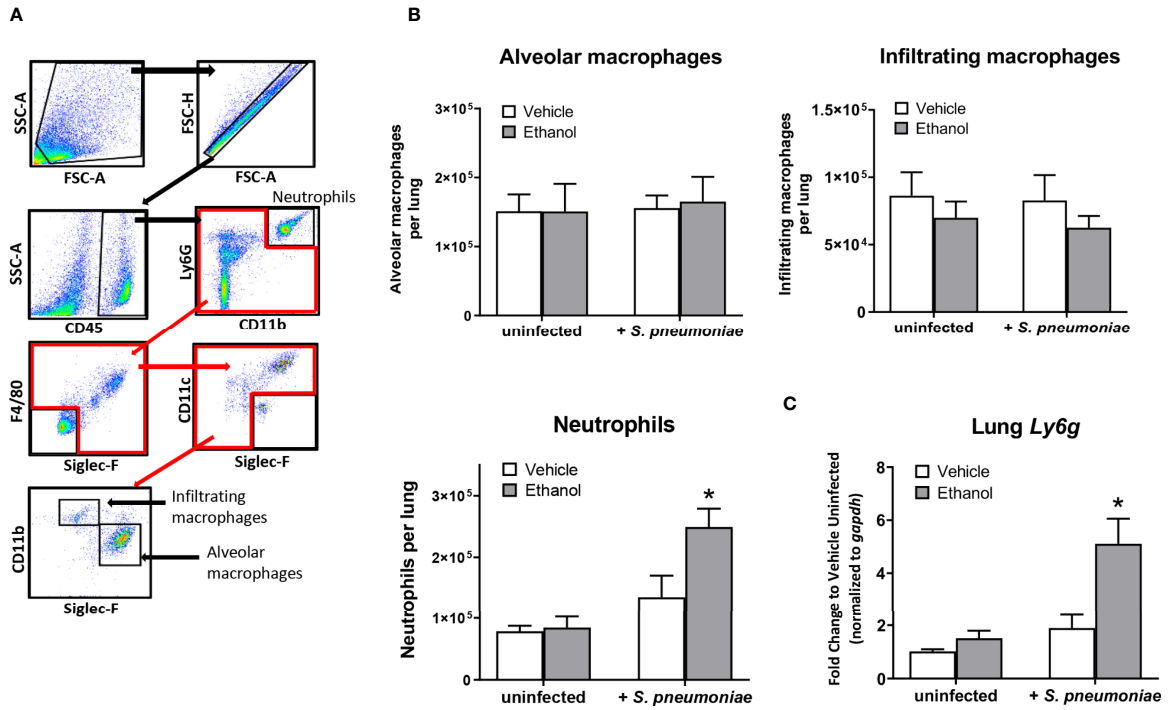

FIGURE 3 | Effect of ethanol consumption on macrophage and neutrophil numbers in the lung following infection. **(A)** Flow cytometry gating strategy to identify neutrophils, alveolar macrophages, and infiltrating macrophages in lung homogenates. **(B)** Average number of pulmonary cell subsets in lung homogenate at 24 hours post-infection. **(C)** RNA from lung homogenates was isolated at 24 hours post-infection and cDNA was analyzed by quantitative PCR for expression of *Ly6g*; target gene expression is normalized to *gapd*h and presented as fold change to vehicle-treated uninfected mice. Data are presented as mean ± SEM. n = 3-6 mice per group per experiment and data are combined from 2 individual experiments. *p < 0.05 compared to all other groups by one-way ANOVA.

We noted an increased presence of neutrophils in the infected groups compared to vehicle-exposed uninfected animals (**Supplementary Figure 1**), with neutrophil localization near *S. pneumoniae* in both infected groups (**Figure 6**). Additionally, we observed a 4.6-fold higher percentage of internalized *S. pneumoniae* in macrophages of vehicle- compared to ethanol-exposed infected animals (**Figure 6**).

DISCUSSION

Excessive alcohol consumption weakens the ability of the immune system to effectively respond to pathogens (52). Here, we describe those 3 consecutive days of a more moderate ethanol exposure than what is typically used in the literature (**Figures 1A, B**) can significantly alter the early pulmonary response to *Streptococcus pneumoniae*. Although the peak BAC in our studies is approximately 80 mg/dL, considered the "legal limit" for driving in humans, it is likely that the BAC levels for intoxication in mice are comparably lower due to increased metabolism of ethanol in rodents compared to humans (53). Nonetheless, we found that ethanol exposure increases bacterial burden in the lung and decreases respiratory function within 24 hours after *S. pneumoniae* infection (**Figures 1C**, **2**). Our results showing increased bacterial burden in the lungs of ethanol-exposed mice (**Figure 1C**) is in line with previous studies utilizing pathogens such as *S. pneumoniae* (54), *Klebsiella pneumoniae* (55, 56), and *Escherichia coli* (57). However, the animal models in these studies use supra-physiological levels of acute ethanol (often enough to raise BAC well above 350 mg/dL) or binge-on-chronic ethanol feeding [Lieber-DeCarli diet (58) for a total of 10 days with a 4 g/kg ethanol gavage on days 5 and 10 (55, 56)] before infection, making it challenging to directly compare results. Even so, our work expands upon previous findings by showing a similar response of increased bacterial burden in animals exposed to a much lower and shorter three-day ethanol exposure regimen (1.5 g/kg) and infected with a lower *S. pneumoniae* inoculum (10^4 CFU). We believe that our model better recapitulates how humans who drink alcohol may acquire bacterial pneumonia *via* respiratory droplets, as our mice are given an oral gavage of ethanol at a more moderate level and then infected intranasally. Furthermore, humans tend to drink alcohol for social motives (59) putting them in close proximity to others who may be infected, or more commonly, those who are asymptomatic carriers of *S. pneumoniae* (60).

Previous studies have found that respiratory disease is associated with impaired lung function using whole body plethysmography, including pneumococcal (61) and SARS-CoV2 infection (62), and bleomycin-induced lung injury (63). Further, our group has shown that multi-day ethanol exposure

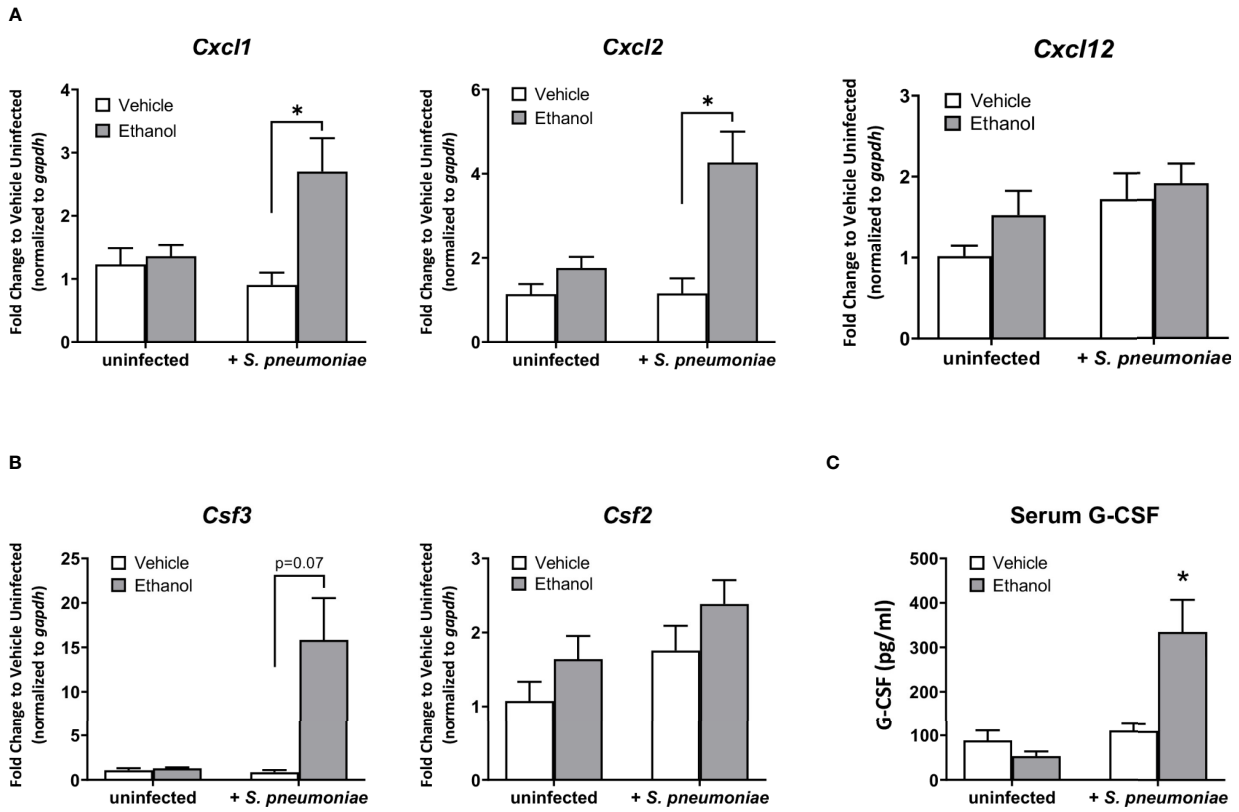

FIGURE 4 | Effect of ethanol exposure on chemokine gene expression in the lung and serum granulocyte-colony stimulating factor (G-CSF) levels after infection. **(A, B)** Gene expression as indicated in graph titles was measured as described in **Figure 3**. Target gene expression is normalized to *gapd*h and presented as fold change to vehicle-treated uninfected mice. **(C)** Serum concentration of G-CSF at 24 hours post-infection as measured by ELISA. Data are presented as mean ± SEM. n = 3-5 per group per experiment and represent averages from 3 individual experiments. *p < 0.05 by one-way ANOVA.

leads to respiratory dysfunction following traumatic injury, such as a cutaneous scald (16, 64). The increased penh values suggest altered airflow patterns in response to airway inflammation (65, 66), while the higher expiratory time and corresponding decreased Rpef values suggest airway narrowing/obstruction (67, 68) and airway collapse with increased airflow resistance (69, 70) in ethanol- compared to vehicle-exposed infected mice. Increased leukocyte accumulation, pulmonary edema, and alveolar wall thickening observed histologically (**Figure 5A**; **Supplementary Figure 2**) likely contribute to the impaired respiratory function observed by plethysmography. One caveat to our lung function data is that we observed mortality during the studies so respiratory parameters are representative of surviving animals only. On day 4, 6% and 14% of the vehicle- and ethanol-exposed infected animals, respectively, died. An additional 12% and 8%, respectively, of the remaining animals died on day 5; we did not observe any further mortality through day 7 post-infection (data not shown). Nevertheless, our study is the first to our knowledge that demonstrates an effect of multi-day lower-dose ethanol exposure on respiratory parameters following *S. pneumoniae* infection.

Neutrophils are critical early responders to respiratory pathogens, but their presence and activity at infection sites can be detrimental if not properly controlled. Using several different pathogens, animal studies have demonstrated that the host is more susceptible to severe pneumonia and death when neutrophils are depleted or otherwise unable to reach the lung (36, 71), but also when excessive neutrophil accumulation and their ineffective clearance leads to tissue damage (72–75). Our results show that ethanol-exposed mice had a higher pulmonary bacterial burden at 24 hours after infection (**Figure 1C**) despite increased numbers of pulmonary neutrophils (**Figure 3B**) and correspondingly higher expression of chemokines involved in neutrophil recruitment, such as *Cxcl1* and *Cxcl2* (**Figure 4A**). Likewise, the upregulation of *Csf3* in the lungs and increased levels of G-CSF in the serum of ethanol-exposed infected mice (**Figures 4B, C**) further suggests an immune response geared toward granulopoiesis and neutrophil homing to the lung. Indeed, others have shown that G-CSF mRNA levels are markedly increased in lung tissue from animals challenged intratracheally with *E. coli* but did not observe appreciable levels of G-CSF mRNA in spleen, liver, or kidney tissue from

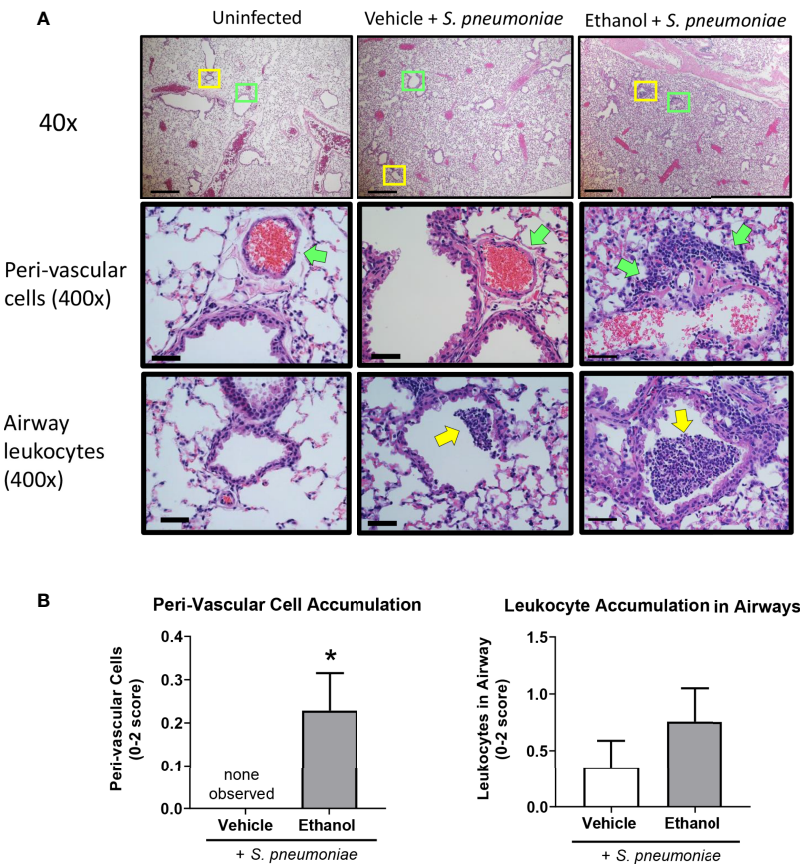

FIGURE 5 | Effect of ethanol exposure on lung inflammation following *S. pneumoniae* infection. **(A)** Representative images of lungs from uninfected and infected mice at 24 hours. Top panel = 40x magnification, scale bar = 500 μm. Boxes denote the magnified areas in the middle and bottom panels. Middle and bottom panels = 400x magnification, scale bar = 50 μm; green arrows denote peri-vascular cells and yellow arrows denote airway leukocytes. **(B)** Quantitative score for criterion of peri-vascular and airway cell accumulation (0-2 score). Data are presented as mean ± SEM. n = 3-6 mice per group per experiment and data are combined from 2 individual experiments. *p < 0.05 by unpaired t test.

the same animals (76). This suggests that the lung is a primary source of G-CSF production early after pulmonary infection.

Previous work from our lab has shown that prior ethanol exposure leads to excessive accumulation of neutrophils (77, 78) and apoptotic cells (78) in the lungs of mice up to 24 hours following burn injury, compared to vehicle-treated injured mice. Although not directly tested in these studies, others have shown that ethanol exposure decreases phagocytic capacity in both alveolar macrophages (14, 15, 79–81) and neutrophils (82–84), along with decreased efferocytosis by alveolar macrophages (17). Our results showing increased bacterial burden in the lung despite higher numbers of neutrophils may suggest that either the tissue-resident alveolar macrophages or the infiltrating neutrophils are less efficient at properly phagocytosing and/or breaking down *S. pneumoniae* within the first 24 hours after infection. Our IHC staining of infected lung tissue would suggest the former (**Figure 6**), although we cannot rule out that the recruited neutrophils are also functionally impaired. Additionally, the presence of Ly6G-negative airway cells could indicate apoptotic macrophages that were not detected by flow cytometry. It is also possible that ethanol treatment in our mice indirectly alters neutrophil apoptosis due to the hyper-inflammatory lung microenvironment following infection (85) and/or impairs efferocytosis of apoptotic neutrophils by alveolar macrophages or infiltrating macrophages; this question merits further evaluation and clarification. Indeed, others have reported delayed neutrophil apoptosis after acute ethanol exposure followed by a "second hit" to the immune system (86, 87). It has been shown that blood neutrophils from ethanol-exposed burned animals had decreased expression of pro-apoptotic proteins such as caspase-3 and Bax, and correspondingly decreased apoptosis as measured by histone-associated DNA fragments (86). Further, delayed neutrophil death appears to be a common characteristic of human inflammatory lung diseases such as cystic fibrosis, pneumonia, and idiopathic fibrosis, as well as in cancer with associated neutrophilia (87). Importantly, in our model, if recruited pulmonary neutrophils are not able to properly die *via* apoptosis and be cleared by alveolar

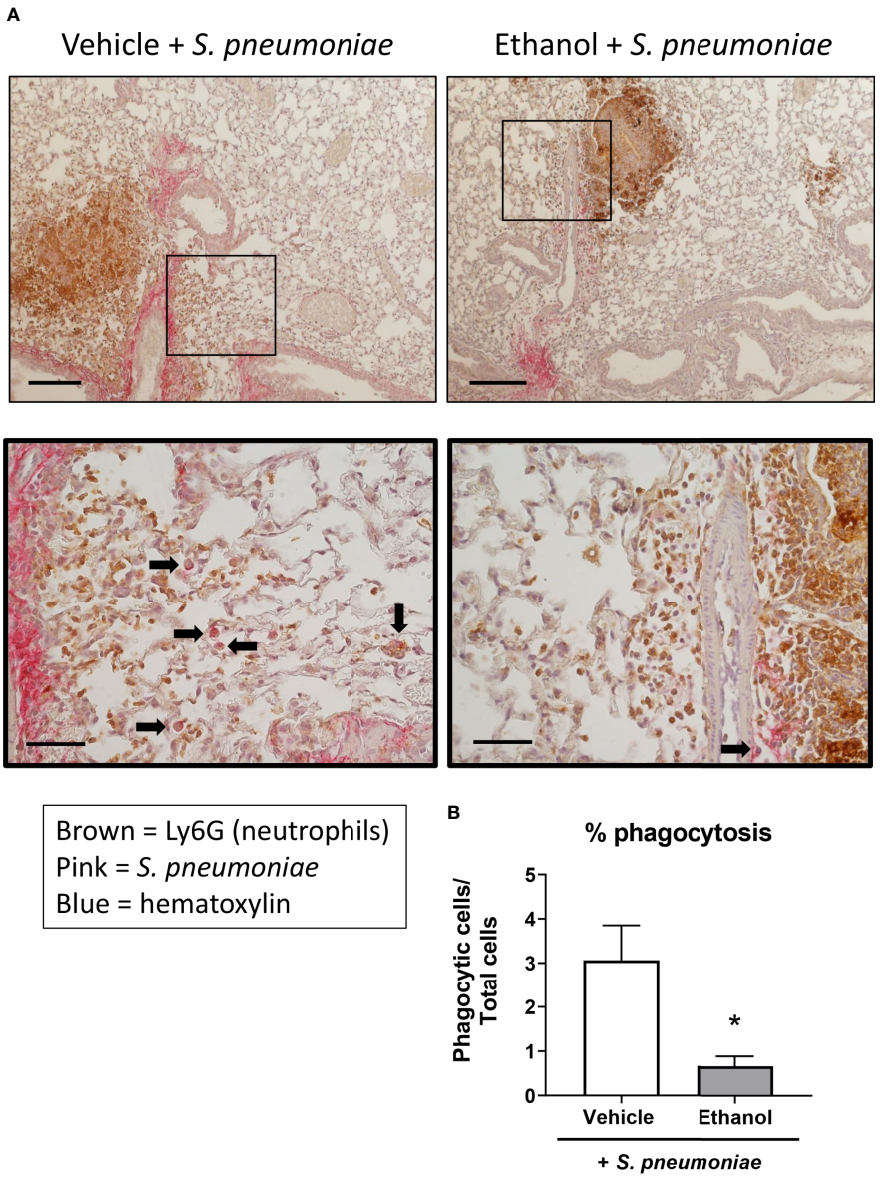

FIGURE 6 | Effect of ethanol exposure on neutrophil and S. pneumoniae localization and bacterial phagocytosis after infection. **(A)** IHC staining was performed onformalin-fixed lung sections with antibodies against Ly6G for neutrophils (brown) and *S. pneumoniae* (pink) and counterstained with hematoxylin. Representative images are at 100x magnification for the top panel (scale bar = 200μm) and 400x magnification for the bottom panel (scale bar = 50 μm). **(B)** Percent phagocytosis of *S. pneumoniae* as measured by the ratio of cells with internalized bacteria to total nucleated cells. Black arrows denote cells with internalized S. pneumoniae. Data are presented as mean ± SEM. n = 3-4 mice per group per experiment and are representative of 2 individual experiments. *p < 0.05 by unpaired t test.

macrophages, they may undergo secondary necrosis, releasing toxic mediators such as elastase and reactive oxygen species, and inducing lung damage in our ethanol-exposed animals (88, 89).

Inflammation is a necessary process to restore homeostasis after infection. Resident immune cells in the upper and lower respiratory tract detect pathogen associated molecular patterns on invading microorganisms and initiate a signaling cascade leading to mobilization and migration of leukocytes to the site of infection. The lungs of our infected animals showed an early accumulation of peri-vascular and airway leukocytes in animals with prior ethanol exposure (**Figures 4A, B**). This suggests that recruited immune cells are able to reach the lungs but appear to be less efficient at clearance of *S. pneumoniae* as noted by CFU counts at 24 hours post-infection in our ethanol-exposed mice (**Figure 1C**). While we failed to see differences in the number of alveolar or infiltrating macrophages in lung homogenates by flow cytometry (**Figure 3**), it is possible that ethanol exposure impairs monocyte trafficking to the lung, as others have previously shown (90).

Immunohistochemistry staining of lung sections provided valuable insight into the effect of ethanol on neutrophil and bacterial antigen localization, as well as bacterial internalization, following *S. pneumoniae* infection. We did not observe any gross difference in neutrophil proximity to *S. pneumoniae*, suggesting that neutrophils are able to migrate toward the infection site at 24 hours post-infection in our model. However, it is possible that neutrophil chemotaxis is impaired at earlier or later time points post-infection, or in other areas of the lung. Further, there was no significant difference in neutrophil or bacterial antigen staining intensity (**Supplementary Figure 1**), however, we are careful not to rely solely on this result since the quantification is from a single tissue section from each animal. Additionally, the *S. pneumoniae* antibody used for IHC is a whole cell serotype blend and will therefore bind to viable and non-viable bacteria and also closely related bacterial species; therefore, quantification of *S. pneumoniae* antigen by IHC may not directly relate to CFU counts of viable bacteria from lung homogenates.

The results presented here require further clarification in future studies. A strength of this work is the demonstration of increased neutrophils and *S. pneumoniae* in whole lung homogenates of ethanol-exposed infected animals at 24 hours, and visualization of the localization of each within the lung. In future experiments, we will characterize the number and functional capacity of neutrophil and macrophage populations in the airways following infection by isolation of these cells from BAL fluid (91). Advanced flow cytometry analysis of blood, BAL fluid, and whole lung homogenates will identify the changing inflammatory cell populations and discriminate cell death (apoptosis or necrosis) in each. Additionally, it would be useful to determine which subset of pulmonary cells are expressing *Cxcl1*, *Cxcl2* and *Csf3*, as this may yield a focused therapeutic target to improve health outcomes in alcohol consumers with pneumococcal pneumonia. Finally, because *S. pneumoniae* was still present in the lungs at 24 hours post-infection, it is imperative to examine the later innate and subsequent adaptive immune response in our model and determine whether complete resolution of the infection is altered due to ethanol exposure.

In summary, we show here that ethanol exposure—at a dose relevant to human consumption—results in higher lung bacterial burden despite an increased presence of pulmonary neutrophils following intranasal *S. pneumoniae* infection. An accumulation of leukocytes was visualized in the airways and peri-vascular space, and likely contributes to the respiratory dysfunction seen in our infected animals. Additionally, we noted differences in *S. pneumoniae* internalization in macrophages from our ethanol-exposed infected animals, which likely contributes to the increased inflammation noted in our mice and could lead to delayed resolution of the infection. Taken together, these findings contribute to our knowledge of how short-term ethanol consumption at physiological doses can alter pulmonary immunity to respiratory infection. Future studies aimed at understanding the mechanisms underlying this exacerbated neutrophilic response could improve health outcomes in pneumonia patients who drink alcohol.

DATA AVAILABILITY STATEMENT

The raw data supporting the conclusions of this article will be made available by the authors, without undue reservation.

ETHICS STATEMENT

The animal study was reviewed and approved by IACUC University of Colorado Anschutz Medical Campus.

AUTHOR CONTRIBUTIONS

HH and KN designed and carried out the experiments. HH analyzed the data and wrote the manuscript. RM provided guidance on study design, and analyzing and interpreting flow cytometry data. DB provided critical input on experimental strategy and panel design for the flow cytometry experiments. DO blindly scored the H&E sections and provided interpretation of the lung histology. EK supervised the project. All authors provided feedback on results and critically reviewed the manuscript. All authors contributed to the article and approved the submitted version.

FUNDING

This work was supported in part by NIH F31 AA027687 (HH), R21 AA026295 (EK), R01 AG018859 (EK), R35 GM131831 (EK), and VA 1 I01 BX004335 (EK).

ACKNOWLEDGMENTS

The authors are grateful to Juliet Mullen and Madison Paul for their technical assistance in performing experiments and collecting tissue samples.

SUPPLEMENTARY MATERIAL

The Supplementary Material for this article can be found online at: https://www.frontiersin.org/articles/10.3389/fimmu.2022.884719/full#supplementary-material

Supplementary Figure 1 | Effect of ethanol exposure on Ly6G and *S. pneumoniae* antigen levels. IHC staining was performed on formalin-fixed lung sections with antibodies against Ly6G for neutrophils (brown) and *S. pneumoniae* (pink) and counterstained with hematoxylin. **(A)** Representative images of lung sections from vehicle-exposed uninfected animals; scale bars = 500 μm for 40x magnification and 50 μm for 400x magnification. **(B)** Quantification of staining intensity as measured by percent positive pixels per lung. Images are representative of 3-6 mice per group per experiment from 2 individual experiments.

Supplementary Figure 2 | Effect of ethanol exposure on alveolar wall thickening and edema. Representative images at 200x of lungs from uninfected and infected mice at 24 hours. Scale bar = 100 μm; black arrows denote areas of alveolar wall thickening and edema, green arrows denote cellular accumulation and airway obstruction. Images are representative of 3-6 mice per group per experiment from 2 individual experiments.

REFERENCES

1. *Substance Abuse and Mental Health Services Administration. 2020 NSDUH Detailed Tables 2021*. Available at: https://www.samhsa.gov/data/report/2020-nsduh-detailed-tables.
2. *National Institute on Alcohol Abuse and Alcoholism. Alcohol Sales During the COVID-19 Pandemic 2021*. Available at: https://pubs.niaaa.nih.gov/publications/surveillance-covid-19/COVSALES.htm.
3. White AM, Castle I-JP, Powell PA, Hingson RW, Koob GF. Alcohol-Related Deaths During the COVID-19 Pandemic. *JAMA* (2022). doi: 10.1001/jama.2022.4308
4. *Centers for Disease Control and Prevention. Alcohol and Public Health: Alcohol Use Basics 2019*. Available at: https://www.cdc.gov/alcohol/fact-sheets.htm.
5. *National Institute on Alcohol Abuse and Alcoholism. Drinking Levels Defined 2020*. Available at: https://www.niaaa.nih.gov/alcohol-health/overview-alcohol-consumption/moderate-binge-drinking.
6. *National Institute on Alcohol Abuse and Alcoholism. Understanding Alcohol Use Disorder 2021*. Available at: https://www.niaaa.nih.gov/publications/brochures-and-fact-sheets/understanding-alcohol-use-disorder.
7. Booyse FM, Parks DA. Moderate Wine and Alcohol Consumption: Beneficial Effects on Cardiovascular Disease. *Thromb Haemost* (2001) 86(2):517–28. doi: 10.1055/s-0037-1616080
8. Wang JJ, Tung TH, Yin WH, Huang CM, Jen HL, Wei J, et al. Effects of Moderate Alcohol Consumption on Inflammatory Biomarkers. *Acta Cardiol* (2008) 63(1):65–72. doi: 10.2143/AC.63.1.2025334
9. Xi B, Veeranki SP, Zhao M, Ma C, Yan Y, Mi J. Relationship of Alcohol Consumption to All-Cause, Cardiovascular, and Cancer-Related Mortality in U.S. Adults. *J Am Coll Cardiol* (2017) 70(8):913–22. doi: 10.1016/j.jacc.2017.06.054
10. Plunk AD, Syed-Mohammed H, Cavazos-Rehg P, Bierut LJ, Grucza RA. Alcohol Consumption, Heavy Drinking, and Mortality: Rethinking the J-Shaped Curve. *Alcohol Clin Exp Res* (2014) 38(2):471–8. doi: 10.1111/acer.12250
11. Gustot T, Maillart E, Bocci M, Surin R, Trépo E, Degré D, et al. Invasive Aspergillosis in Patients With Severe Alcoholic Hepatitis. *J Hepatol* (2014) 60(2):267–74. doi: 10.1016/j.jhep.2013.09.011
12. Vergis N, Atkinson SR, Knapp S, Maurice J, Allison M, Austin A, et al. In Patients With Severe Alcoholic Hepatitis, Prednisolone Increases Susceptibility to Infection and Infection-Related Mortality, and Is Associated With High Circulating Levels of Bacterial DNA. *Gastroenterology* (2017) 152(5):1068–77.e4. doi: 10.1053/j.gastro.2016.12.019
13. Goral J, Kovacs EJ. *In Vivo* Ethanol Exposure Down-Regulates TLR2-, TLR4-, and TLR9-Mediated Macrophage Inflammatory Response by Limiting P38 and ERK1/2 Activation. *J Immunol* (2005) 174(1):456–63. doi: 10.4049/jimmunol.174.1.456
14. Karavitis J, Murdoch EL, Deburghgraeve C, Ramirez L, Kovacs EJ. Ethanol Suppresses Phagosomal Adhesion Maturation, Rac Activation, and Subsequent Actin Polymerization During Fcγr-Mediated Phagocytosis. *Cell Immunol* (2012) 274(1-2):61–71. doi: 10.1016/j.cellimm.2012.02.002
15. Karavitis J, Murdoch EL, Gomez CR, Ramirez L, Kovacs EJ. Acute Ethanol Exposure Attenuates Pattern Recognition Receptor Activated Macrophage Functions. *J Interferon Cytokine Res* (2008) 28(7):413–22. doi: 10.1089/jir.2007.0111
16. Shults JA, Curtis BJ, Chen MM, O'Halloran EB, Ramirez L, Kovacs EJ. Impaired Respiratory Function and Heightened Pulmonary Inflammation in Episodic Binge Ethanol Intoxication and Burn Injury. *Alcohol* (2015) 49(7):713–20. doi: 10.1016/j.alcohol.2015.06.006
17. Boé DM, Richens TR, Horstmann SA, Burnham EL, Janssen WJ, Henson PM, et al. Acute and Chronic Alcohol Exposure Impair the Phagocytosis of Apoptotic Cells and Enhance the Pulmonary Inflammatory Response. *Alcohol Clin Exp Res* (2010) 34(10):1723–32. doi: 10.1111/j.1530-0277.2010.01259.x
18. Malacco N, Souza JAM, Martins FRB, Rachid MA, Simplicio JA, Tirapelli CR, et al. Chronic Ethanol Consumption Compromises Neutrophil Function in Acute Pulmonary Aspergillus Fumigatus Infection. *Elife* (2020) 9. doi: 10.7554/eLife.58855
19. Jin L, Batra S, Jeyaseelan S. Diminished Neutrophil Extracellular Trap (NET) Formation is a Novel Innate Immune Deficiency Induced by Acute Ethanol Exposure in Polymicrobial Sepsis, Which can be Rescued by CXCL1. *PloS Pathogens* (2017) 13(9):e1006637. doi: 10.1371/journal.ppat.1006637
20. Simet SM, Sisson JH. Alcohol's Effects on Lung Health and Immunity. *Alcohol Res* (2015) 37(2):199–208.
21. H R YO. *Community-Acquired Pneumonia*. Treasure Island, FL: StatPearls Publishing (2022). Available at: https://www.ncbi.nlm.nih.gov/books/NBK430749/.
22. Gupta NM, Lindenauer PK, Yu P-C, Imrey PB, Haessler S, Deshpande A, et al. Association Between Alcohol Use Disorders and Outcomes of Patients Hospitalized With Community-Acquired Pneumonia. *JAMA Netw Open* (2019) 2(6):e195172–e. doi: 10.1001/jamanetworkopen.2019.5172
23. Samokhvalov AV, Irving HM, Rehm J. Alcohol Consumption as a Risk Factor for Pneumonia: A Systematic Review and Meta-Analysis. *Epidemiol Infect* (2010) 138(12):1789–95. doi: 10.1017/S0950268810000774
24. Simou E, Britton J, Leonardi-Bee J. Alcohol and the Risk of Pneumonia: A Systematic Review and Meta-Analysis. *BMJ Open* (2018) 8(8):e022344. doi: 10.1136/bmjopen-2018-022344
25. de Roux A, Cavalcanti M, Marcos MA, Garcia E, Ewig S, Mensa J, et al. Impact of Alcohol Abuse in the Etiology and Severity of Community-Acquired Pneumonia. *Chest* (2006) 129(5):1219–25. doi: 10.1378/chest.129.5.1219
26. Luján M, Gallego M, Belmonte Y, Fontanals D, Vallès J, Lisboa T, et al. Influence of Pneumococcal Serotype Group on Outcome in Adults With Bacteraemic Pneumonia. *Eur Respir J* (2010) 36(5):1073–9. doi: 10.1183/09031936.00176309
27. Opitz B, van Laak V, Eitel J, Suttorp N. Innate Immune Recognition in Infectious and Noninfectious Diseases of the Lung. *Am J Respir Crit Care Med* (2010) 181(12):1294–309. doi: 10.1164/rccm.200909-1427SO
28. Koppe U, Suttorp N, Opitz B. Recognition of Streptococcus Pneumoniae by the Innate Immune System. *Cell Microbiol* (2012) 14(4):460–6. doi: 10.1111/j.1462-5822.2011.01746.x
29. Maus UA, Waelsch K, Kuziel WA, Delbeck T, Mack M, Blackwell TS, et al. Monocytes are Potent Facilitators of Alveolar Neutrophil Emigration During Lung Inflammation: Role of the CCL2-CCR2 Axis. *J Immunol* (2003) 170(6):3273–8. doi: 10.4049/jimmunol.170.6.3273
30. Xu J, Mora A, Shim H, Stecenko A, Brigham KL, Rojas M. Role of the SDF-1/CXCR4 Axis in the Pathogenesis of Lung Injury and Fibrosis. *Am J Respir Cell Mol Biol* (2007) 37(3):291–9. doi: 10.1165/rcmb.2006-0187OC
31. Isles HM, Herman KD, Robertson AL, Loynes CA, Prince LR, Elks PM, et al. The CXCL12/CXCR4 Signaling Axis Retains Neutrophils at Inflammatory Sites in Zebrafish. *Front Immunol* (2019) 10. doi: 10.3389/fimmu.2019.01784
32. Lee KMC, Achuthan AA, Hamilton JA. GM-CSF: A Promising Target in Inflammation and Autoimmunity. *Immunotarg Ther* (2020) 9:225–40. doi: 10.2147/ITT.S262566
33. Roberts AW. G-CSF: A Key Regulator of Neutrophil Production, But That's Not All! *Growth Factors* (2005) 23(1):33–41. doi: 10.1080/08977190500055836
34. Hübel K, Dale DC, Liles WC. Therapeutic Use of Cytokines to Modulate Phagocyte Function for the Treatment of Infectious Diseases: Current Status of Granulocyte Colony-Stimulating Factor, Granulocyte-Macrophage Colony-Stimulating Factor, Macrophage Colony-Stimulating Factor, and Interferon-γ. *J Infect Dis* (2002) 185(10):1490–501. doi: 10.1086/340221
35. Gregory AD, Hogue LA, Ferkol TW, Link DC. Regulation of Systemic and Local Neutrophil Responses by G-CSF During Pulmonary Pseudomonas Aeruginosa Infection. *Blood* (2006) 109(8):3235–43. doi: 10.1182/blood-2005-01-015081
36. Garvy BA, Harmsen AG. The Importance of Neutrophils in Resistance to Pneumococcal Pneumonia in Adult and Neonatal Mice. *Inflammation* (1996) 20(5):499–512. doi: 10.1007/BF01487042
37. Taut K, Winter C, Briles DE, Paton JC, Christman JW, Maus R, et al. Macrophage Turnover Kinetics in the Lungs of Mice Infected With Streptococcus Pneumoniae. *Am J Respir Cell Mol Biol* (2008) 38(1):105–13. doi: 10.1165/rcmb.2007-0132OC
38. Goto Y, Hogg JC, Whalen B, Shih CH, Ishii H, Van Eeden SF. Monocyte Recruitment Into the Lungs in Pneumococcal Pneumonia. *Am J Respir Cell Mol Biol* (2004) 30(5):620–6. doi: 10.1165/rcmb.2003-0312OC
39. Narasaraju T, Yang E, Samy RP, Ng HH, Poh WP, Liew A-A, et al. Excessive Neutrophils and Neutrophil Extracellular Traps Contribute to Acute Lung Injury of Influenza Pneumonitis. *Am J Pathol* (2011) 179(1):199–210. doi: 10.1016/j.ajpath.2011.03.013

40. Happel KI, Odden AR, Zhang P, Shellito JE, Bagby GJ, Nelson S. Acute Alcohol Intoxication Suppresses the Interleukin 23 Response to Klebsiella Pneumoniae Infection. *Alcohol Clin Exp Res* (2006) 30(7):1200–7. doi: 10.1111/j.1530-0277.2006.00144.x
41. Happel KI, Rudner X, Quinton LJ, Movassaghi JL, Clark C, Odden AR, et al. Acute Alcohol Intoxication Suppresses the Pulmonary ELR-Negative CXC Chemokine Response to Lipopolysaccharide. *Alcohol* (2007) 41(5):325–33. doi: 10.1016/j.alcohol.2007.06.002
42. Boé DM, Nelson S, Zhang P, Bagby GJ. Acute Ethanol Intoxication Suppresses Lung Chemokine Production Following Infection With Streptococcus Pneumoniae. *J Infect Dis* (2001) 184(9):1134–42. doi: 10.1086/323661
43. Raasch CE, Zhang P, Siggins RW2nd, LaMotte LR, Nelson S, Bagby GJ. Acute Alcohol Intoxication Impairs the Hematopoietic Precursor Cell Response to Pneumococcal Pneumonia. *Alcohol Clin Exp Res* (2010) 34(12):2035–43. doi: 10.1111/j.1530-0277.2010.01291.x
44. Johansson N, Kalin M, Tiveljung-Lindell A, Giske CG, Hedlund J. Etiology of Community-Acquired Pneumonia: Increased Microbiological Yield With New Diagnostic Methods. *Clin Infect Dis* (2010) 50(2):202–9. doi: 10.1086/648678
45. Mohawk JA, Pargament JM, Lee TM. Circadian Dependence of Corticosterone Release to Light Exposure in the Rat. *Physiol Behav* (2007) 92(5):800–6. doi: 10.1016/j.physbeh.2007.06.009
46. Chen MM, Palmer JL, Ippolito JA, Curtis BJ, Choudhry MA, Kovacs EJ. Intoxication by Intraperitoneal Injection or Oral Gavage Equally Potentiates Postburn Organ Damage and Inflammation. *Mediators Inflamm* (2013) 2013:971481. doi: 10.1155/2013/971481
47. Puchta A, Verschoor CP, Thurn T, Bowdish DM. Characterization of Inflammatory Responses During Intranasal Colonization With Streptococcus Pneumoniae. *J Vis Exp* 2014(83):e50490. doi: 10.3791/50490
48. Lim R, Zavou MJ, Milton PL, Chan ST, Tan JL, Dickinson H, et al. Measuring Respiratory Function in Mice Using Unrestrained Whole-Body Plethysmography. *J Vis Exp* 2014(90):e51755. doi: 10.3791/51755
49. Curtis BJ, Shults JA, Boe DM, Ramirez L, Kovacs EJ. Mesenchymal Stem Cell Treatment Attenuates Liver and Lung Inflammation After Ethanol Intoxication and Burn Injury. *Alcohol* (2019) 80:139–48. doi: 10.1016/j.alcohol.2018.09.001
50. Schmittgen TD, Livak KJ. Analyzing Real-Time PCR Data by the Comparative CT Method. *Nat Protoc* (2008) 3(6):1101–8. doi: 10.1038/nprot.2008.73
51. Assiri MA, Roy SR, Harris PS, Ali H, Liang Y, Shearn CT, et al. Chronic Ethanol Metabolism Inhibits Hepatic Mitochondrial Superoxide Dismutase *via* Lysine Acetylation. *Alcohol Clin Exp Res* (2017) 41(10):1705–14. doi: 10.1111/acer.13473
52. Molina PE, Happel KI, Zhang P, Kolls JK, Nelson S. Focus on: Alcohol and the Immune System. *Alcohol Res Health* (2010) 33(1-2):97–108.
53. Livy DJ, Parnell SE, West JR. Blood Ethanol Concentration Profiles: A Comparison Between Rats and Mice. *Alcohol* (2003) 29(3):165–71. doi: 10.1016/S0741-8329(03)00025-9
54. Trevejo-Nunez G, Chen K, Dufour JP, Bagby GJ, Horne WT, Nelson S, et al. Ethanol Impairs Mucosal Immunity Against Streptococcus Pneumoniae Infection by Disrupting Interleukin 17 Gene Expression. *Infect Immun* (2015) 83(5):2082–8. doi: 10.1128/IAI.02869-14
55. Samuelson DR, Shellito JE, Maffei VJ, Tague ED, Campagna SR, Blanchard EE, et al. Alcohol-Associated Intestinal Dysbiosis Impairs Pulmonary Host Defense Against Klebsiella Pneumoniae. *PloS Pathogens* (2017) 13(6): e1006426. doi: 10.1371/journal.ppat.1006426
56. Samuelson DR, Gu M, Shellito JE, Molina PE, Taylor CM, Luo M, et al. Pulmonary Immune Cell Trafficking Promotes Host Defense Against Alcohol-Associated Klebsiella Pneumonia. *Commun Biol* (2021) 4(1):997. doi: 10.1038/s42003-021-02524-0
57. Bagby GJ, Zhang P, Stoltz DA, Nelson S. Suppression of the Granulocyte Colony-Stimulating Factor Response to Escherichia Coli Challenge by Alcohol Intoxication. *Alcohol Clin Exp Res* (1998) 22(8):1740–5. doi: 10.1111/j.1530-0277.1998.tb03974.x
58. Guo F, Zheng K, Benedé-Ubieto R, Cubero FJ, Nevzorova YA. The Lieber-DeCarli Diet-A Flagship Model for Experimental Alcoholic Liver Disease. *Alcohol Clin Exp Res* (2018) 42(10):1828–40. doi: 10.1111/acer.13840
59. Kuntsche E, Knibbe R, Gmel G, Engels R. Why do Young People Drink? A Review of Drinking Motives. *Clin Psychol Rev* (2005) 25(7):841–61. doi: 10.1016/j.cpr.2005.06.002
60. Donkor ES. Understanding the Pneumococcus: Transmission and Evolution. *Front Cell Infect Microbiol* (2013) 3:7. doi: 10.3389/fcimb.2013.00007
61. de Hennezel L, Debarre S, Ramisse F, Delamanche S, Harf A, Alonso JM, et al. Plethysmography for the Assessment of Pneumococcal Pneumonia and Passive Immunotherapy in a Mouse Model. *Eur Respir J* (2001) 17(1):94–9. doi: 10.1183/09031936.01.17100940
62. Menachery VD, Gralinski LE, Baric RS, Ferris MT. New Metrics for Evaluating Viral Respiratory Pathogenesis. *PloS One* (2015) 10(6):e0131451. doi: 10.1371/journal.pone.0131451
63. Milton PL, Dickinson H, Jenkin G, Lim R. Assessment of Respiratory Physiology of C57BL/6 Mice Following Bleomycin Administration Using Barometric Plethysmography. *Respiration* (2012) 83(3):253–66. doi: 10.1159/000330586
64. Curtis BJ, Boe DM, Shults JA, Ramirez L, Kovacs EJ. Effects of Multiday Ethanol Intoxication on Postburn Inflammation, Lung Function, and Alveolar Macrophage Phenotype. *Shock* (2019) 51(5):625–33. doi: 10.1097/SHK.0000000000001188
65. Mitzner W, Tankersley C. Noninvasive Measurement of Airway Responsiveness in Allergic Mice Using Barometric Plethysmography. *Am J Respir Crit Care Med* (1998) 158(1):340–1. doi: 10.1164/ajrccm.158.1.let1
66. Verheijden KAT, Henricks PAJ, Redegeld FA, Garssen J, Folkerts G. Measurement of Airway Function Using Invasive and Non-Invasive Methods in Mild and Severe Models for Allergic Airway Inflammation in Mice. *Front Pharmacol* (2014) 5. doi: 10.3389/fphar.2014.00190
67. Skloot GS, O'Connor-Chapman KL, Schechter CB, Markley DJ, Bates JHT. Forced Expiratory Time: A Composite of Airway Narrowing and Airway Closure. *J Appl Physiol (1985)* (2021) 130(1):80–6. doi: 10.1152/japplphysiol.00556.2020
68. Aggarwal A, Das S, Agarwal R, Singh N. Role of Forced Expiratory Time in Identifying Airway Obstruction and Systematic Review of English Literature. *Chest* (2017) 152(4):A956. doi: 10.1016/j.chest.2017.08.991
69. Fukushi M, Ito T, Oka T, Kitazawa T, Miyoshi-Akiyama T, Kirikae T, et al. Serial Histopathological Examination of the Lungs of Mice Infected With Influenza A Virus PR8 Strain. *PloS One* (2011) 6(6):e21207. doi: 10.1371/journal.pone.0021207
70. Hardy RD, Jafri HS, Olsen K, Wordemann M, Hatfield J, Rogers BB, et al. Elevated Cytokine and Chemokine Levels and Prolonged Pulmonary Airflow Resistance in a Murine Mycoplasma Pneumoniae Pneumonia Model: A Microbiologic, Histologic, Immunologic, and Respiratory Plethysmographic Profile. *Infect Immun* (2001) 69(6):3869–76. doi: 10.1128/IAI.69.6.3869-3876.2001
71. Tateda K, Moore TA, Newstead MW, Tsai WC, Zeng X, Deng JC, et al. Chemokine-Dependent Neutrophil Recruitment in a Murine Model of Legionella Pneumonia: Potential Role of Neutrophils as Immunoregulatory Cells. *Infect Immun* (2001) 69(4):2017–24. doi: 10.1128/IAI.69.4.2017-2024.2001
72. Bou Ghanem EN, Clark S, Roggensack SE, McIver SR, Alcaide P, Haydon PG, et al. Extracellular Adenosine Protects Against Streptococcus Pneumoniae Lung Infection by Regulating Pulmonary Neutrophil Recruitment. *PloS Pathog* (2015) 11(8):e1005126. doi: 10.1371/journal.ppat.1005126
73. Jeyaseelan S, Young SK, Yamamoto M, Arndt PG, Akira S, Kolls JK, et al. Toll/IL-1R Domain-Containing Adaptor Protein (TIRAP) Is a Critical Mediator of Antibacterial Defense In the Lung Against Klebsiella Pneumoniae But Not Pseudomonas Aeruginosa. *J Immunol* (2006) 177(1):538–47. doi: 10.4049/jimmunol.177.1.538
74. Grommes J, Soehnlein O. Contribution of Neutrophils to Acute Lung Injury. *Mol Med* (2011) 17(3-4):293–307. doi: 10.2119/molmed.2010.00138
75. Bordon J, Aliberti S, Fernandez-Botran R, Uriarte SM, Rane MJ, Duvvuri P, et al. Understanding the Roles of Cytokines and Neutrophil Activity and Neutrophil Apoptosis in the Protective Versus Deleterious Inflammatory Response in Pneumonia. *Int J Infect Dis* (2013) 17(2):e76–83. doi: 10.1016/j.ijid.2012.06.006
76. Quinton LJ, Nelson S, Boé DM, Zhang P, Zhong Q, Kolls JK, et al. The Granulocyte Colony-Stimulating Factor Response After Intrapulmonary and Systemic Bacterial Challenges. *J Infect Dis* (2002) 185(10):1476–82. doi: 10.1086/340504
77. Patel PJ, Faunce DE, Gregory MS, Duffner LA, Kovacs EJ. Elevation in Pulmonary Neutrophils and Prolonged Production of Pulmonary Macrophage Inflammatory Protein-2 After Burn Injury With Prior Alcohol Exposure. *Am J Respir Cell Mol Biol* (1999) 20(6):1229–37. doi: 10.1165/ajrcmb.20.6.3491

78. Shults JA, Curtis BJ, Boe DM, Ramirez L, Kovacs EJ. Ethanol Intoxication Prolongs Post-Burn Pulmonary Inflammation: Role of Alveolar Macrophages. *J Leukocyte Biol* (2016) 100(5):1037–45. doi: 10.1189/jlb.3MA0316-111R
79. Joshi PC, Applewhite L, Ritzenthaler JD, Roman J, Fernandez AL, Eaton DC, et al. Chronic Ethanol Ingestion in Rats Decreases Granulocyte-Macrophage Colony-Stimulating Factor Receptor Expression and Downstream Signaling in the Alveolar Macrophage. *J Immunol* (2005) 175(10):6837–45. doi: 10.4049/jimmunol.175.10.6837
80. Mehta AJ, Yeligar SM, Elon L, Brown LA, Guidot DM. Alcoholism Causes Alveolar Macrophage Zinc Deficiency and Immune Dysfunction. *Am J Respir Crit Care Med* (2013) 188(6):716–23. doi: 10.1164/rccm.201301-0061OC
81. Karavitis J, Kovacs EJ. Macrophage Phagocytosis: Effects of Environmental Pollutants, Alcohol, Cigarette Smoke, and Other External Factors. *J Leukocyte Biol* (2011) 90(6):1065–78. doi: 10.1189/jlb.0311114
82. Zhang P, Bagby GJ, Xie M, Stoltz DA, Summer WR, Nelson S. Acute Ethanol Intoxication Inhibits Neutrophil β2-Integrin Expression in Rats During Endotoxemia. *Alcoholism: Clin Exp Res* (1998) 22(1):135–41. doi: 10.1111/j.1530-0277.1998.tb03629.x
83. Zhang P, Nelson S, Summer WR, Spitzer JA. Acute Ethanol Intoxication Suppresses the Pulmonary Inflammatory Response in Rats Challenged With Intrapulmonary Endotoxin. *Alcoholism: Clin Exp Res* (1997) 21(5):773–8. doi: 10.1111/j.1530-0277.1997.tb03838.x
84. Gandhi JA, Ekhar VV, Asplund MB, Abdulkareem AF, Ahmadi M, Coelho C, et al. Alcohol Enhances Acinetobacter Baumannii-Associated Pneumonia and Systemic Dissemination by Impairing Neutrophil Antimicrobial Activity in a Murine Model of Infection. *PloS One* (2014) 9(4):e95707. doi: 10.1371/journal.pone.0095707
85. Fox S, Leitch AE, Duffin R, Haslett C, Rossi AG. Neutrophil Apoptosis: Relevance to the Innate Immune Response and Inflammatory Disease. *J Innate Immun* (2010) 2(3):216–27. doi: 10.1159/000284367
86. Akhtar S, Li X, Kovacs EJ, Gamelli RL, Choudhry MA. Interleukin-18 Delays Neutrophil Apoptosis Following Alcohol Intoxication and Burn Injury. *Mol Med* (2011) 17(1-2):88–94. doi: 10.2119/molmed.2010.00080
87. Dibbert B, Weber M, Nikolaizik WH, Vogt P, Schöni MH, Blaser K, et al. Cytokine-Mediated Bax Deficiency and Consequent Delayed Neutrophil Apoptosis: A General Mechanism to Accumulate Effector Cells in Inflammation. *Proc Natl Acad Sci USA* (1999) 96(23):13330–5. doi: 10.1073/pnas.96.23.13330
88. Rydell-Törmänen K, Uller L, Erjefält JS. Direct Evidence of Secondary Necrosis of Neutrophils During Intense Lung Inflammation. *Eur Respir J* (2006) 28(2):268–74. doi: 10.1183/09031936.06.00126905
89. Sahoo M, Del Barrio L, Miller MA, Re F. Neutrophil Elastase Causes Tissue Damage That Decreases Host Tolerance to Lung Infection With Burkholderia Species. *PloS Pathog* (2014) 10(8):e1004327. doi: 10.1371/journal.ppat.1004327
90. Imhof A, Blagieva R, Marx N, Koenig W. Drinking Modulates Monocyte Migration in Healthy Subjects: A Randomised Intervention Study of Water, Ethanol, Red Wine and Beer With or Without Alcohol. *Diabetes Vasc Dis Res* (2008) 5(1):48–53. doi: 10.3132/dvdr.2008.009
91. Chen MM, Palmer JL, Plackett TP, Deburghgraeve CR, Kovacs EJ. Age-Related Differences in the Neutrophil Response to Pulmonary Pseudomonas Infection. *Exp Gerontol* (2014) 54:42–6. doi: 10.1016/j.exger.2013.12.010

Conflict of Interest: The authors declare that the research was conducted in the absence of any commercial or financial relationships that could be construed as a potential conflict of interest.

frontiers | Frontiers in Immunology

ORIGINAL RESEARCH
published: 11 May 2022
doi: 10.3389/fimmu.2022.865492

Alcohol-Induced Glycolytic Shift in Alveolar Macrophages Is Mediated by Hypoxia-Inducible Factor-1 Alpha

Niya L. Morris[1,2], *David N. Michael*[1,2], *Kathryn M. Crotty*[1,2], *Sarah S. Chang*[1,2] *and Samantha M. Yeligar*[1,2]*

[1] Department of Medicine, Division of Pulmonary, Allergy, Critical Care and Sleep Medicine, Emory University, Atlanta, GA, United States, [2] Atlanta Veterans Affairs Health Care System, Decatur, GA, United States

Excessive alcohol use increases the risk of developing respiratory infections partially due to impaired alveolar macrophage (AM) phagocytic capacity. Previously, we showed that chronic ethanol (EtOH) exposure led to mitochondrial derangements and diminished oxidative phosphorylation in AM. Since oxidative phosphorylation is needed to meet the energy demands of phagocytosis, EtOH mediated decreases in oxidative phosphorylation likely contribute to impaired AM phagocytosis. Treatment with the peroxisome proliferator-activated receptor gamma (PPARγ) ligand, pioglitazone (PIO), improved EtOH-mediated decreases in oxidative phosphorylation. In other models, hypoxia-inducible factor-1 alpha (HIF-1α) has been shown to mediate the switch from oxidative phosphorylation to glycolysis; however, the role of HIF-1α in chronic EtOH mediated derangements in AM has not been explored. We hypothesize that AM undergo a metabolic shift from oxidative phosphorylation to a glycolytic phenotype in response to chronic EtOH exposure. Further, we speculate that HIF-1α is a critical mediator of this metabolic switch. To test these hypotheses, primary mouse AM (mAM) were isolated from a mouse model of chronic EtOH consumption and a mouse AM cell line (MH-S) were exposed to EtOH *in vitro.* Expression of HIF-1α, glucose transporters (Glut1 and 4), and components of the glycolytic pathway (Pfkfb3 and PKM2), were measured by qRT-PCR and western blot. Lactate levels (lactate assay), cell energy phenotype (extracellular flux analyzer), glycolysis stress tests (extracellular flux analyzer), and phagocytic function (fluorescent microscopy) were conducted. EtOH exposure increased expression of HIF-1α, Glut1, Glut4, Pfkfb3, and PKM2 and shifted AM to a glycolytic phenotype. Pharmacological stabilization of HIF-1α *via* cobalt chloride treatment *in vitro* mimicked EtOH-induced AM derangements (increased glycolysis and diminished phagocytic capacity). Further, PIO treatment diminished HIF-1α levels and reversed glycolytic shift following EtOH exposure. These studies support a critical role for HIF-1α in mediating the glycolytic shift in energy metabolism of AM during excessive alcohol use.

Keywords: ethanol, hypoxia-inducible factor-1 alpha, alveolar macrophage, energy metabolism, glycolysis

OPEN ACCESS

Edited by:
Guochang Hu,
University of Illinois at Chicago, United States

Reviewed by:
Rui Li,
Shaanxi Provincial People's Hospital, China
Zhongjie Fu,
Boston Children's Hospital and Harvard Medical School, United States

***Correspondence:**
Samantha M. Yeligar
syeliga@emory.edu

Specialty section:
This article was submitted to Nutritional Immunology, a section of the journal Frontiers in Immunology

Received: *29 January 2022*
Accepted: *15 April 2022*
Published: *11 May 2022*

Citation:
Morris NL, Michael DN, Crotty KM, Chang SS and Yeligar SM (2022) Alcohol-Induced Glycolytic Shift in Alveolar Macrophages Is Mediated by Hypoxia-Inducible Factor-1 Alpha. Front. Immunol. 13:865492. doi: 10.3389/fimmu.2022.865492

INTRODUCTION

Over 15 million people in the United States have been diagnosed with alcohol use disorders (1). Excessive alcohol use increases morbidity and mortality (2) and increases risk of developing respiratory infections (3), which is largely linked to immune dysfunction in alveolar macrophages (AM) (4–7). AM initiate the immune response to pathogens in the lower airway (8), but excessive alcohol use impairs AM phagocytic capacity and bacterial clearance (5, 9). Phagocytosis requires high energy demands, and mitochondrial-dependent oxidative phosphorylation is the most efficient method of generating cellular ATP. Our laboratory has established that chronic alcohol exposure results in AM mitochondrial dysfunction (e.g., mitochondrial fragmentation, morphological alteration, and derangements in mitochondrial bioenergetics) (10). Further, treatment with the peroxisome proliferator-activated receptor gamma (PPARγ) ligand, pioglitazone (PIO), improved AM phagocytic dysfunction (7, 11) and oxidative phosphorylation (10) during ethanol (EtOH) exposure.

One mechanism employed by cells to meet their energy demands in the absence of oxidative phosphorylation is glycolysis (12). Glycolysis is a metabolic pathway that converts glucose into pyruvate utilizing enzymatic proteins, such as 6-phosphofructo-2-kinase/fructose-2,6-bisphosphatase 3 (Pfkfb3) and pyruvate kinase M2 (PKM2), to generate energy (12, 13). Blocking key glycolytic proteins such as Pfkb3 and PKM2 has been shown to mitigate acute lung injury (14, 15). The effect of EtOH on these glycolytic proteins in AM has not been explored.

Stabilization of hypoxia-inducible factor (HIF)-1α and subsequent formation of HIF-1 (comprised of the inducible HIF-1α and constitutive HIF-1β) increases the transcription of numerous genes including those in the glycolytic pathway, such as glucose transporters (GLUT) 1 and 4 and pyruvate dehydrogenase kinase 1 (PDK-1) (16–19). Mounting evidence suggests that HIF-1α may act as a "metabolic switch", shifting cells from relying on oxidative phosphorylation towards glycolysis instead (17–19). The availability of glucose needed for glycolysis is in part regulated by glucose transporters which transport glucose into the cell (12). HIF-1α (with GLUT and PDK-1) have been shown in other models to contribute to lung injury (20–22). Further, numerous studies have shown a direct relationship between HIF-1α and EtOH-mediated pathologies in the brain (23), adipose tissue (24), and liver (25). The findings from these studies showed that EtOH-induced HIF-1α can occur during oxidative stress or elevated inflammation.

The relationship between HIF-1α and these metabolic derangements in the context of chronic EtOH-induced AM phagocytic dysfunction, however, have not been examined and are the focus of the current study. Our data demonstrate that HIF-1α is a critical mediator of EtOH-mediated energy derangements in AM, suggesting a key role of HIF-1α in EtOH-mediated lung pathobiology. Further, PIO attenuated EtOH-induced HIF-1α, which could provide a novel therapeutic strategy in the treatment of alcohol use disorders in the lung and decrease susceptibility to respiratory infections.

MATERIALS AND METHODS

Mouse Model of Chronic Ethanol Ingestion

Animal studies were carried out in accordance with the National Institutes of Health guidelines as outlined in the *Guide for the Care and Use of Laboratory Animals*. Additionally, all protocols were reviewed and approved by the Atlanta VA Health Care System Institutional Animal Care and Use Committee. 8- to 10-week-old male C57BL/6J mice purchased from Jackson Laboratory (Bar Harbor, Maine, United States) were fed standard laboratory chow *ad libitum*. Mice were randomly divided into two groups (control and EtOH). EtOH fed mice received increases of EtOH (5% w/v) in their drinking water for 2 weeks until the EtOH concentration reached 20% w/v and this concentration was maintained for 10 weeks, resulting in a 0.12% blood alcohol level (6, 7, 26). During the last week of ethanol ingestion, mice were administered PIO (10 mg/kg/day in 100-μL methylcellulose vehicle) or vehicle alone *via* oral gavage (7). Following euthanasia, tracheas were cannulated, and a tracheotomy was performed to collect bronchoalveolar lavage fluid. Bronchoalveolar lavage fluid was centrifuged at 8000 RPM for 5 minutes to isolate mouse alveolar macrophages (mAM). Isolated mAM were resuspended in RPMI-1640 culture medium (2% fetal bovine serum and 1% penicillin/streptomycin) for 24 hours for further experimentation (6, 7). Lung tissue was harvested and homogenized for RNA isolation.

In Vitro Ethanol Exposure of MH-S Cells

The mouse alveolar macrophage cell line (MH-S) was purchased from American Type Culture Collection (Manassas, VA, United States). MH-S cells were cultured in RPMI-1640 medium (10% fetal bovine serum, 1% penicillin/streptomycin, 11.9 mM sodium bicarbonate, gentamicin (40mg/ml) and 0.05 mM 2-mercaptoethanol) in the presence or absence of 0.08% EtOH for 72 hours (media changed daily) at 37°C in a humidified incubator in 5% CO_2 (5, 6). In a subset of experiments, MH-S were treated with PIO (10 μM; last 24 hours of EtOH exposure) (Cayman Chemicals, Ann Arbor, Michigan, United States).

Cell Energy Phenotype Test

Cell energy phenotype tests were performed to evaluate the metabolic phenotypes of mAM and MH-S using either an XFe96 (Catalog number: 103325-100) or an XFp extracellular flux analyzer (Catalog number: 103275-100) (Agilent Seahorse Bioscience Inc.; Billerica, MA, United States). Oxygen consumption rate (OCR) and extracellular acidification rate (ECAR) were measured in mAM and MH-S over time in XF Base Medium supplemented with 1 mM of sodium pyruvate, 10 mM glucose, and 2 mM of L-glutamine followed by a single injection of 2 μM oligomycin (ATP synthase inhibitor) + 0.5 μM carbonilcyanide p-triflouromethoxyphenylhydrazone (FCCP; a mitochondrial uncoupling agent). XFp plates were precoated with collagen (~4 hours) and washed with PBS and media prior to addition of mAM cells to promote mAM adherence to the plates. Raw OCR and ECAR were determined using the XF Wave 2.1 software. OCR and ECAR values were calculated, normalized to cell protein concentration in the same sample, and were

expressed as mean of biological replicates ± standard error of the mean (SEM).

Glycolysis Stress Test

Glycolysis stress tests were performed using either an XFe96 or an XFp extracellular flux analyzer (Agilent Seahorse Bioscience Inc.) to evaluate the parameters of glycolytic flux. ECAR was measured in mAM and MH-S over time in XF Base Medium supplemented with 2 mM L-glutamine followed by sequential injections of 10 mM glucose (saturating concentration of glucose to promote glycolysis), 2 μM oligomycin (ATP synthase inhibitor), and 50 mM 2-deoxy-glucose (2-DG; a glucose analog that inhibits glycolysis). To maximize mAM adherence to XFp microculture plates, wells were precoated with collagen (~4 hours) and were subsequently washed with PBS and media before addition of cells. Glycolysis, glycolytic capacity, glycolytic reserve, and non-glycolytic acidification were determined using the XF Wave 2.1 software. Raw ECAR was determined using the XF Wave 2.1 software. Glycolysis, glycolytic capacity, glycolytic reserve, and non-glycolytic acidification ECAR values were calculated, normalized to cell protein concentration in the same sample, and were expressed as mean of biological replicates ± SEM.

RNA Isolation and Quantitative RT-PCR (qRT-PCR)

TRIzol reagent (Catalog number:15596026, Invitrogen, Waltham, MA, United States) was used to isolate total RNA. Primer sequences outlined in **Table 1** were used to measure and quantify target mRNA levels by qRT-PCR with iTaq Universal SYBR Green One-Step kit (Catalog number: 1725151, Bio-Rad, Hercules, CA, United States) using the Applied Biosystems ABI Prism 7500 version 2.0.4 sequence detection system (6, 7). Target mRNA values were normalized to 9S or glyceraldehyde 3-phosphate dehydrogenase (GAPDH). mRNA levels were expressed as fold-change of mean ± SEM, relative to control samples.

Cytoimmunostaining and Phagocytosis by Fluorescent Microscopy

HIF-1α protein was measured in mAM isolated from control- and EtOH-fed mice. mAM were fixed with 4% paraformaldehyde and incubated with a HIF-1α rabbit monoclonal antibody (1:500, Cell Signaling Technology, Danvers, MA, United States) for 1 hour, washed, and incubated with fluorescent-labeled anti-rabbit secondary antibody (1:1000) for 1 hour. Protein values were normalized to DAPI nuclear stain.

In vitro phagocytic capacity in MH-S was determined using pHrodo *Staphylococcus aureus* BioParticles conjugate (Catalog number: A10010, Invitrogen). MH-S (1.2×10^5 cells) were incubated with 1×10^6 particles of pH-sensitive fluorescent-labeled *S. aureus* for 2 hours. Following the incubation, cells were fixed with 4% paraformaldehyde. Cells with internalized *S. aureus* were considered positive for phagocytosis. Phagocytic capacity was quantified as phagocytic index: cells positive for internalized bacteria is multiplied by the relative fluorescent units (RFU) of *S. aureus* per cell. Phagocytic index is expressed as fold-change of mean ± SEM, relative to control samples (7, 11).

Fluorescence for HIF-1α cytoimmunostaining and phagocytosis of *S. aureus* was measured using FluoView (Olympus, Melville, New York, United States) and are expressed as fold-change of mean relative fluorescent units RFU per cell ± SEM, relative to control samples. RFU were evaluated in at least 10 cells per field, with 10 fields per experimental condition. Gain and gamma microscope settings were constant for each field and experimental condition. ImageJ was used to deconvolute and analyze images (10, 27).

Western Blot

Proteins were isolated from MH-S using SESSA lysis buffer and quantified using the Pierce bicinchoninic acid (BCA) Protein Assay Kit (Catalog number for Pierce bicinchoninic acid (BCA) Protein Assay Reagent A: 23228 and Catalog number for Pierce bicinchoninic acid (BCA) Protein Assay Reagent B: 23224, Thermofisher, Waltham, Massachusetts, United States). Equal amounts of protein from cell lysates were loaded on NuPAGE Novex 10% Bis-Tris Protein Gels (Catalog number: NP0301BOX, Fisher Scientific, Hampton, NH, United States) subsequent to being transferred onto nitrocellulose membranes. The membranes were blocked in 5% non-fat milk and TBST for 1 hour and then incubated with primary antibodies for HIF-1α rabbit monoclonal antibody (Catalog number: 14179S, 1:500, Cell Signaling Technology) or glyceraldehyde 3-phosphate dehydrogenase rabbit polyclonal antibody (Catalog number: G9545-100UL, 1:20,000, GAPDH, Sigma-Aldrich, St. Louis, MO, United States) overnight at 4°C. Following this incubation, the membranes were washed and incubated with 1:10,000 anti-rabbit IRDye800CW Secondary Antibodies

TABLE 1 | Primer sequences to measure mRNA levels using qRT-PCR.

	Gene	Forward Sequence (5' → 3')	Reverse Sequence (5' → 3')
Mouse	GAPDH	GGATTTGGTCGTATTGGG	GGAAGATGGTGATGGGATT
Mouse	Glut1	CTCCTGCCCTGTTGTGTATAG	AAGGCCACAAAGCCAAAGAT-
Mouse	Glut4	AAAAGTGCCTGAAACCAGAG	TCACCTCCTGCTCTAAAAGG
Mouse	HIF-1α	CTCAAAGTCGGACAG	CCCTGCAGTAGGTTT
Mouse	Pfkfb3	TCTAGAGGAGGTGAGATCAG	CCTGCCACTCTTATCTTCTG
Mouse	Pkm2	GAGGCCTCCTTCAAGTGCT	CCAGACTTGGTGAGGACGAT
Mouse	9S	ATCCGCCAGCGCCATA	TCGATGTGCTTCTGGGAATCC

GAPDH; glyceraldehyde 3-phosphate dehydrogenase, Glut1; glucose transporter 1, Glut4; glucose transporter 4, HIF-1α; hypoxia-inducible factor-1 alpha, Pfkfb3; 6-phosphofructo-2-kinase/fructose-2,6-bisphosphatase 3, PKM2; pyruvate kinase M2.

(Catalog number: 926-32211, Li-COR Biosciences, Lincoln, NE, United States) for 1 hour at room temperature. Odyssey Infrared Imaging System (LI-COR Biosciences) was used to image the membranes. Image J software (NIH, Bethesda, MD, United States) was used to measure densitometry. HIF-1α protein values were normalized to GAPDH and expressed as fold-change of mean ± SEM, relative to control samples.

Lactate Assay

Lactate levels in MH-S were determined using a lactate assay kit (Catalog number: MAK064, Sigma Aldrich) according to the manufacturer's instructions. Lactate values were normalized to protein concentration in the same sample and were expressed as fold-change of mean ± SEM, relative to control samples.

Cobalt Chloride Treatment of MH-S

MH-S were treated with the HIF-1α stabilizer cobalt (II) chloride hexahydrate (Catalog number: C8661-25g, 25 μM, $CoCl_2$, Sigma-Aldrich) in PBS vehicle or PBS alone for 4 hours. $CoCl_2$ increases HIF-1α expression (28) and stabilizes HIF-1α by inhibiting the binding of von Hippel Lindau E3 ubiquitin ligase, preventing HIF-1α ubiquitination and subsequent degradation (29).

Transient Transfection of MH-S

HIF-1α was silenced in MH-S using transient transfection of a HIF-1α siRNA (Catalog number: sc-35562, Santa Cruz, Dallas, TX, United States), and HIF-1α was induced in MH-S using transient transfection of HIF-1α lysate (Catalog number: sc-120778, Santa Cruz). MH-S were resuspended in 100 μL of Amaxa Mouse Macrophage Nucleofector Kit solution (Catalog number: VPA-1009, Lonza, Alpharetta, GA, United States) containing 100 nM of control scrambled (Catalog number: sc-37007, control-scr, Santa Cruz), siRNA for HIF-1α (siHIF-1α), or HIF-1α lysate (HIF-1α) followed by nucleofection according to the manufacturer's protocol using program Y-001. Following transfection, MH-S were washed with media and cultured with or without 0.08% EtOH for 3 days (media changed daily).

Statistical Analysis

Data are presented as mean ± SEM. A Student's t-test was used in studies with two groups. In studies, with more than two groups, statistical significance was calculated using one-way analysis of variance (ANOVA) followed by Tukey-Kramer *post hoc* (GraphPad Prism version 9, San Diego, CA). In the event that the data was not normally distributed, a non-parametric statistical analysis using Kruskal-Wallis test was used. $p<0.05$ was considered significant.

RESULTS

Ethanol Shifted AM to a Glycolytic Metabolic Phenotype

Previously, we have shown that EtOH exposure altered mitochondrial morphology and negatively impacted mitochondrial bioenergetics (10). To assess whether EtOH exposure increased glycolysis, we evaluated the cell energy phenotype of mAM isolated from control and EtOH-fed mice. mAM from EtOH-fed mice shifted to a glycolytic phenotype in response to the oligomycin +FCCP stressors (**Figure 1A**). To provide further evidence that EtOH resulted in glycolytic shift, we performed a glycolysis stress test on mAM from control and EtOH fed mice. Compared with mAM from control mice, mAM from EtOH fed mice exhibited increased glycolytic profiling (**Figure 1B**), glycolysis (**Figure 1C**), glycolytic capacity (**Figure 1D**), glycolytic reserve (**Figure 1E**), and non-glycolytic acidification (**Figure 1F**). Similar to our *in vivo* studies, glycolytic bioenergetics were elevated in EtOH-treated MH-S (**Figure 2**) compared to control. Assessment of the cell energy phenotype of EtOH treated MH-S exhibited a glycolytic shift compared to control (**Figure 2A**). Additionally, EtOH treated MH-S displayed increased glycolytic profiling compared to control (**Figure 2B**). Finally, glycolysis (**Figure 2C**), and glycolytic capacity (**Figure 2D**) were also elevated in EtOH-treated MH-S compared to controls. We did not observe any differences in glycolytic reserve (**Figure 2E**) or non-glycolytic acidification (**Figure 2F**) between the groups. Collectively, these data illustrate that AM exhibit a glycolytic energy phenotype in response to EtOH.

Ethanol Increased Glycolytic Proteins in Mouse Lungs and MH-S

As we observed increases in glycolytic flux following EtOH exposure in AM, we assessed expression of the glucose transporters, Glut1 and Glut4, and key enzymes of the glycolytic pathway, Pfkfb3 and PKM2. mRNA levels of Glut1, Glut4, Pfkfb3, and PKM2 were increased in response to EtOH (**Figure 3A**). Additionally, EtOH induced mRNA expression of Glut1 in mouse lung homogenates (**Supplementary Figure 1**). Since lactate levels correlate with generation of ECAR during glycolysis (30), we investigated the effect of EtOH on AM lactate levels. Lactate was elevated in response to EtOH in MH-S (**Figure 3B**). These results further suggest that EtOH induces glycolysis in mouse lungs and AM.

Ethanol-Induced HIF-1α in mAM and MH-S

We sought to investigate the mechanism by which EtOH increased parameters of glycolytic flux in AM. HIF-1α, a component of the transcription factor HIF-1, can act as a "metabolic switch". HIF-1 increases the transcription of some genes in the glycolytic pathway and has been shown in other models to be increased by EtOH exposure (23–25, 31). Here, we examined how EtOH affected hypoxia-inducible factor (HIF)-1α in AM. mRNA and protein levels of HIF-1α were measured in control and EtOH mAM. EtOH feeding elevated mAM HIF-1α mRNA (**Figure 4A**) and protein (**Figure 4B**) expression. Similarly, we observed increases in HIF-1α mRNA (**Figure 4C**) and protein (**Figure 4D**) in MH-S exposed to EtOH compared to control. Collectively, these data show that EtOH induces HIF-1α in AM.

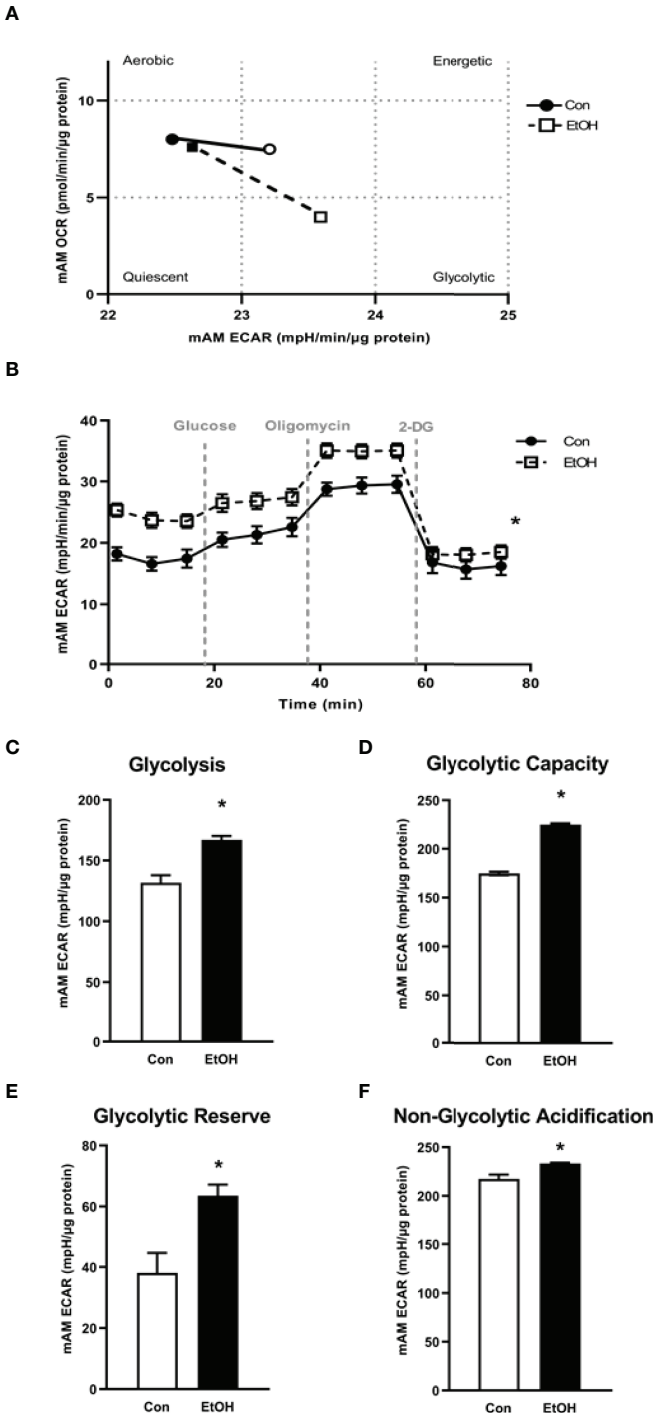

FIGURE 1 | EtOH induces glycolysis in mAM. Mouse alveolar macrophages (mAM) were isolated from mice fed either control (Con) or ethanol (EtOH; 20% v/w in drinking water, 12 weeks). **(A)** Oxygen consumption rates (OCR) and extracellular acidification rates (ECAR) were measured in response to an injection mixture of oligomycin (oligo; mitochondrial complex V inhibitor) and carbonilcyanide p-triflouromethoxyphenylhydrazone (FCCP; ATP synthase inhibitor and proton uncoupler) using an extracellular flux analyzer. Cell energy phenotype was measured, normalized to protein levels, and are expressed as mean ± SEM (n = 4-5). ECAR were measured in response to sequential injections of glucose (saturating concentration of glucose to promote glycolysis), oligomycin (ATP synthase inhibitor), and 2-deoxy-glucose (2-DG; a glucose analog that inhibits glycolysis) using an extracellular flux analyzer. OCR measures are pmol over time and ECAR measures are mpH over time, normalized to total protein in the same sample well, and are expressed as mean ± SEM. Parameters of glycolytic function **(B)**, glycolysis **(C)**, glycolytic capacity **(D)**, glycolytic reserve **(E)**, and non-glycolytic acidification **(F)** are expressed as mean ± SEM, relative to control (n = 12-14). *$p < 0.05$ verses control.

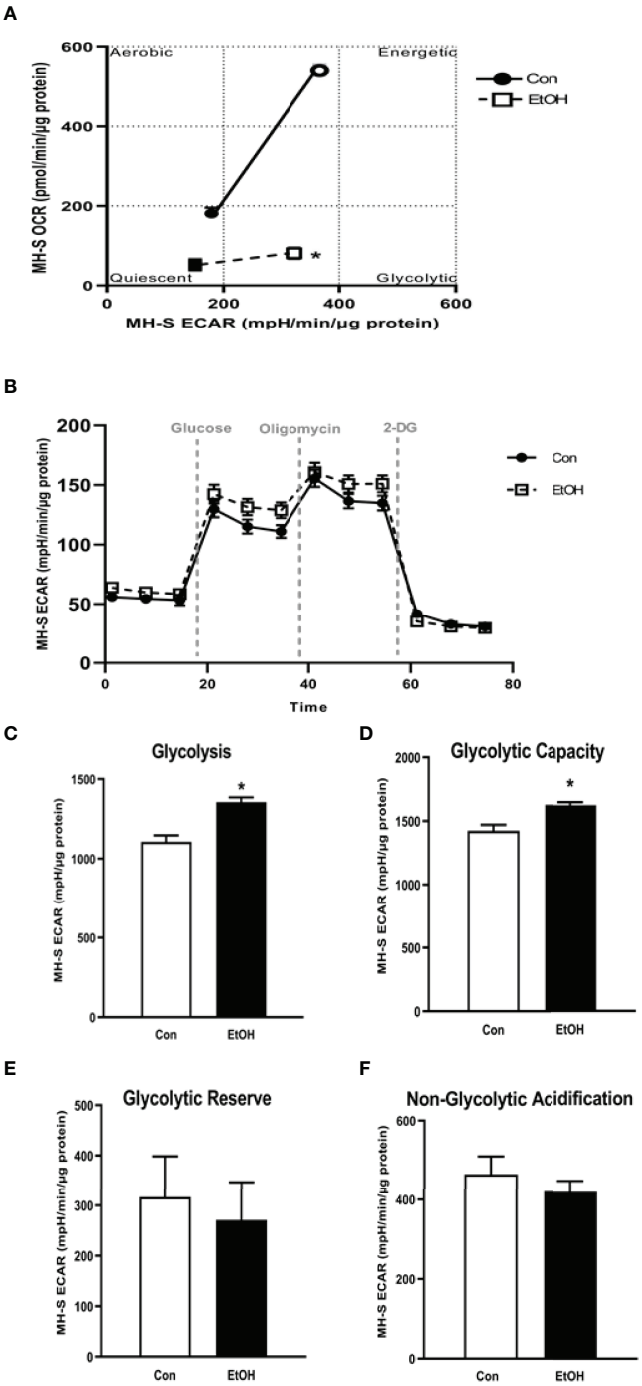

FIGURE 2 | EtOH induces glycolysis in MH-S cells. MH-S were exposed to either control (Con) or ethanol (EtOH; 0.08%) for 72 hours. **(A)** Oxygen consumption rates (OCR) and extracellular acidification rates (ECAR) were measured in response to an injection mixture of oligomycin (oligo; mitochondrial complex V inhibitor), carbonilcyanide p-triflouromethoxyphenylhydrazone (FCCP; ATP synthase inhibitor and proton uncoupler) using an extracellular flux analyzer. Cell energy phenotype was measured, normalized to protein levels, and are expressed as mean ± SEM (n = 3). ECAR were measured in response to sequential injections of glucose (saturating concentration of glucose to promote glycolysis), oligomycin (ATP synthase inhibitor), and 2-deoxy-glucose (2-DG; a glucose analog that inhibits glycolysis) using an extracellular flux analyzer. OCR measures are pmol over time and ECAR measures are mpH over time, normalized to total protein in the same sample well, and are expressed as mean ± SEM. Parameters of glycolytic function **(B)**, glycolysis **(C)**, glycolytic capacity **(D)**, glycolytic reserve **(E)**, and non-glycolytic acidification **(F)** are expressed as mean ± SEM, relative to control (n = 6). *$p < 0.05$ verses control.

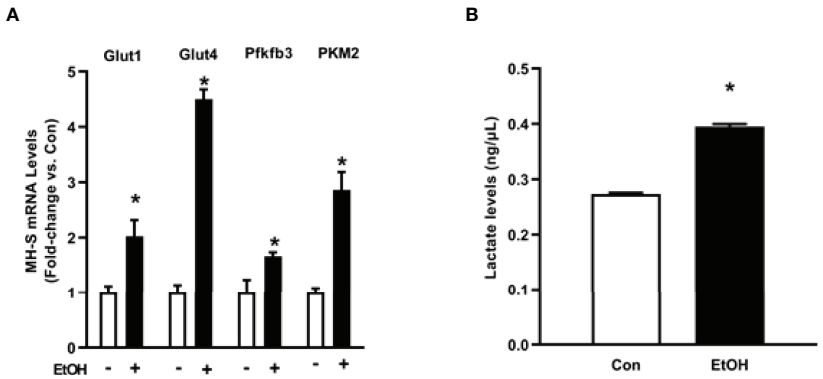

FIGURE 3 | Ethanol increases expression of glycolytic proteins and lactate levels in MH-S. MH-S were exposed to either control (Con) or ethanol (EtOH; 0.08%) for 72 hours. **(A)** mRNA levels of glucose transporter (Glut)1, Glut4, 6-phosphofructo-2-kinase/fructose-2,6-bisphosphatase 3 (Pfkfb3), and pyruvate kinase 2 (PKM2) were measured by qRT-PCR, in duplicate, normalized to GAPDH, and are expressed as mean ± SEM, relative to control. **(B)** Protein isolated from MH-S cells was used to evaluate lactate levels *via* lactate assay kit and are expressed as mean ± SEM, relative to control (n = 4-6). *$p < 0.05$ versus control.

Ethanol-Induced Derangements in AM Glycolytic Shift Is Mediated by HIF-1α in MH-S

To establish whether HIF-1α is implicated in EtOH-mediated glycolytic shift in AM, control MH-S were treated with cobalt chloride, a HIF-1α stabilizer. Treatment of MH-S with cobalt chloride mimicked the increase in HIF-1α mRNA (**Supplementary Figure 2A**) and protein (**Supplementary Figure 2B**) seen in AM exposed to EtOH (**Figure 4**). Cobalt chloride exposed MH-S exhibited increases in components of glycolytic profiling (**Figure 5A**), glycolysis (**Figure 5B**), and glycolytic capacity (**Figure 5C**) similar to our EtOH studies of AM (**Figures 1**, **2**). Similar to our *in vitro* studies (**Figure 2**), we did not observe changes in glycolytic reserve (**Figure 5D**) and non-glycolytic capacity (**Figure 5E**) with cobalt chloride treatment. Concomitantly, treatment of MH-S with HIF-1α lysate increased glycolytic profiling (**Supplementary Figure 3A**), glycolysis (**Supplementary Figure 3B**), glycolytic capacity (**Supplementary**

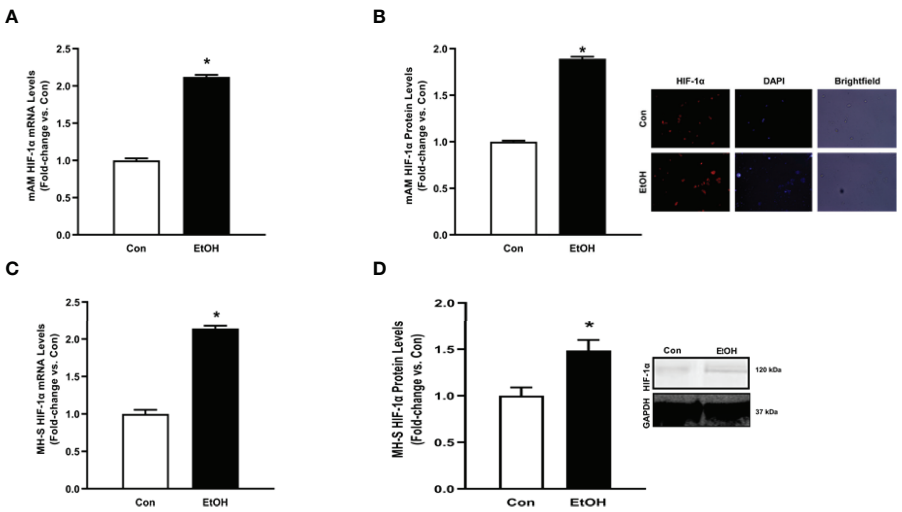

FIGURE 4 | Ethanol induces HIF-1α in mAM and MH-S. **(A, B)** Mouse alveolar macrophages (mAM) were isolated from mice fed either control (Con) or ethanol (EtOH; 20% v/w in drinking water, 12 weeks). **(A)** HIF-1α mRNA levels were measured by qRT-PCR, in duplicate, normalized to 9S, and expressed as mean ± SEM, relative to control. **(B)** HIF-1α protein levels were measured by fluorescence microscopy (10 fields/condition), normalized to DAPI, and are expressed as mean RFU ± SEM, relative to control. Representative microscopy images have been provided. **(C, D)** MH-S were exposed to either control (Con) or ethanol (EtOH; 0.08%) for 72 hours. **(C)** HIF-1α and were measured by qRT-PCR, in duplicate, normalized to GAPDH, and expressed as mean ± SEM, relative to control (n = 6). **(D)** HIF-1α protein levels were evaluated *via* western blot, normalized to GAPDH protein, and densitometry is expressed as mean ± SEM, relative to control (n = 4). Representative western blot images have been provided. *$p < 0.05$ versus control.

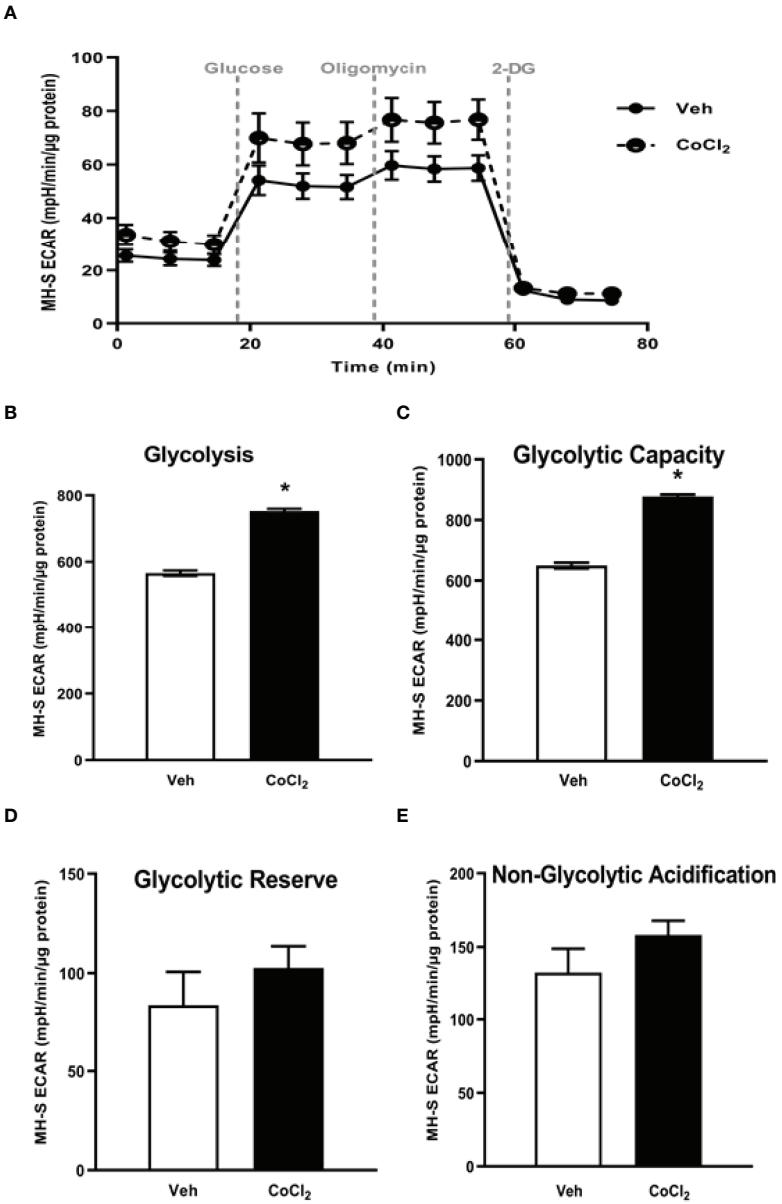

FIGURE 5 | Stabilization of HIF-1α *in vitro via* cobalt chloride mimics EtOH-mediated derangements in MH-S. MH-S were exposed to either vehicle (Veh) or cobalt chloride ($CoCl_2$, 25 μM) for 4 hours. Extracellular acidification rates (ECAR) were measured in response to sequential injections of glucose (saturating concentration of glucose to promote glycolysis), oligomycin (ATP synthase inhibitor), and 2-deoxy-glucose (2-DG; a glucose analog that inhibits glycolysis) using an extracellular flux analyzer. ECAR from glycolytic profiling, normalized to protein levels, and are expressed as mean ± SEM **(A)**, glycolysis **(B)**, glycolytic capacity **(C)**, glycolytic reserve **(D)**, and non-glycolytic acidification **(E)** are expressed as mean ± SEM, relative to vehicle (n = 6). *$p < 0.05$ versus vehicle.

Figure 3C), and glycolytic reserve (**Supplementary Figure 3D**). Glut4, Pfkfb3, and PKM2 (**Figure 6A**) mRNA levels and lactate levels (**Figure 6B**) were increased in response to cobalt chloride, similar EtOH-treated MH-S (**Figure 3**). As cobalt chloride is a mimetic for HIF-1α, these data suggest that EtOH-induced HIF-1α mediates the glycolytic shift observed in AM. Further, similar to our EtOH studies (7, 11), treatment with cobalt chloride led to AM phagocytic dysfunction (**Figure 6C**).

HIF-1α Modulates EtOH-Induced Glycolysis and Phagocytic Function in MH-S

To further implicate HIF-1α in modulating EtOH-induced glycolysis, we knocked down HIF-1α in the presence and absence of EtOH. We determined that knockdown of HIF-1α prevented EtOH-mediated glycolytic shift (**Figure 7A**). Further, these improvements coincided with improved phagocytic index in MH-S lacking HIF-1α in the presence of EtOH (**Figure 7B**).

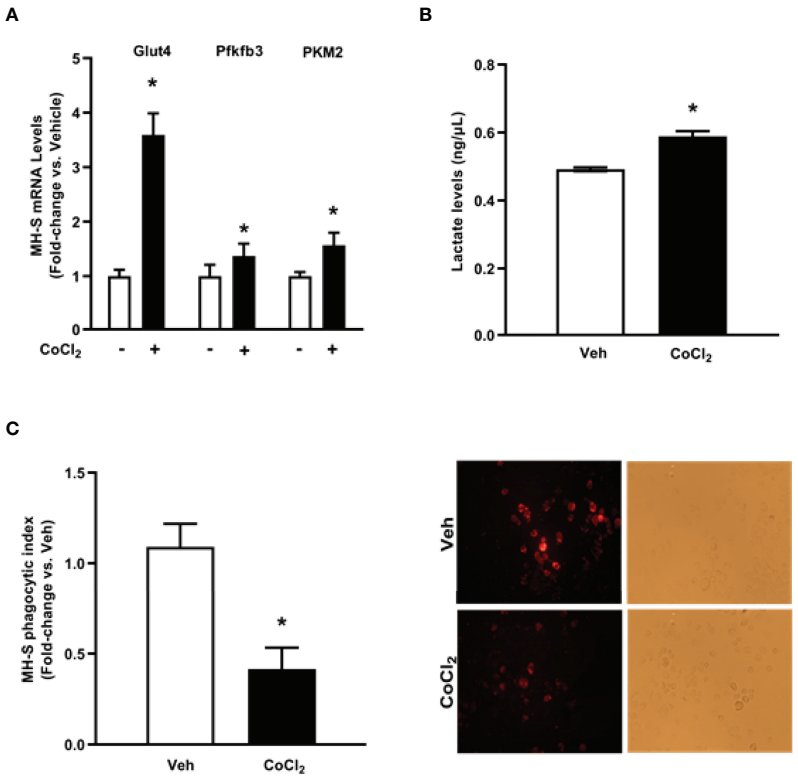

FIGURE 6 | Cobalt chloride induces expression of glycolytic proteins and lactate levels and causes phagocytic dysfunction in MH-S. MH-S were exposed to either vehicle (Veh) or cobalt chloride ($CoCl_2$, 25 μM) for 4 hours. **(A)** mRNA levels of glucose transporter (Glut)4, 6-phosphofructo-2-kinase/fructose-2,6-bisphosphatase 3 (Pfkfb3), and pyruvate kinase 2 (PKM2) were measured by qRT-PCR, in duplicate, normalized to GAPDH, and are expressed as mean ± SEM, relative to control (n = 4-6). **(B)** Protein isolated from MH-S was used to evaluate lactate levels *via* lactate assay kit and are expressed as mean ± SEM, relative to vehicle (n = 6). *$p < 0.05$ versus vehicle. **(C)** Phagocytic index was calculated from the percentage of cells positive for bacterial uptake multiplied by the RFU of *S. aureus* per cell. Values are expressed as mean ± SEM relative to vehicle (n = 5). Representative fluorescent and brightfield images have been provided. *$p < 0.05$ versus vehicle.

Collectively, these data show that HIF-1α plays a key role in EtOH-mediated increases in AM glycolysis and impaired phagocytic capacity.

Pioglitazone Treatment Reverses Ethanol-Induced HIF-1α

The PPARγ ligand, PIO, has been previously reported to improve EtOH-mediated mitochondrial derangements (10), and phagocytic dysfunction (7, 11). As such, we sought to delineate whether PIO may affect EtOH-induced AM HIF-1α. PIO treatment diminished HIF-1α mRNA (**Figure 8A**) and protein (**Figure 8B**) levels. Collectively, these data identify PIO as a therapeutic strategy to mitigate EtOH-induced HIF-1α in AM.

Pioglitazone Treatment Reverses EtOH-Induced Glycolysis

As treatment with PIO improved mitochondrial derangements due to EtOH exposure (10), here we sought to determine if PIO affected glycolysis in MH-S in the presence of EtOH. As demonstrated previously, EtOH induced a glycolytic shift in response to oligomycin+FCCP stressors however, PIO treatment prevented the EtOH-induced glycolytic shift in MH-S (**Figure 9A**). Treatment with PIO also reversed EtOH-induced increases in the MH-S glycolytic bioenergetics parameters, glycolytic profiling (**Figure 9B**), glycolysis (**Figure 9C**), glycolytic capacity (**Figure 9D**), glycolytic reserve (**Figure 9E**), and non-glycolytic acidification (**Figure 9F**). Similarly, PIO treatment prevented the glycolytic shift in mAM isolated from EtOH-fed mice (**Figure 10A**). Treatment with PIO also reversed EtOH-induced increases in the mAM glycolytic bioenergetics parameters, glycolytic profiling (**Figure 10B**), glycolysis (**Figure 10C**), glycolytic capacity (**Figure 10D**), glycolytic reserve (**Figure 10E**), and non-glycolytic acidification (**Figure 10F**). Collectively, these data show that AM glycolytic energy phenotype in response to EtOH is reversed with PIO treatment.

DISCUSSION

One of the hallmark immune functions of AM is to phagocytose invading pathogens in the lower respiratory tract (8). In order to meet the high energy demands of phagocytosis, oxidative

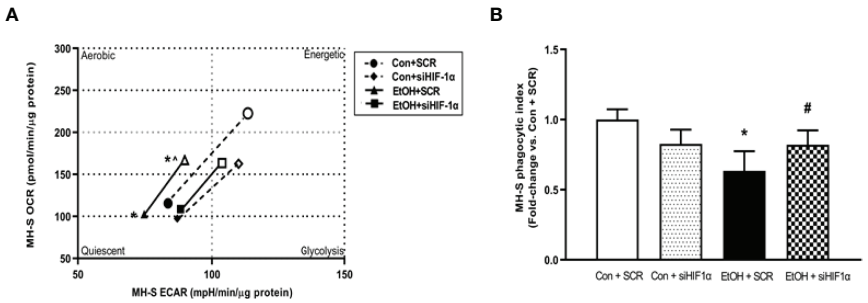

FIGURE 7 | HIF-1α modulates EtOH-induced glycolysis and phagocytic function in MH-S. MH-S transiently transfected with control scramble (SCR) or siRNA against HIF-1α (siHIF1α) were exposed to either Con or EtOH (0.08%) for 72 hours. **(A)** Oxygen consumption rates (OCR) and extracellular acidification rates (ECAR) were measured in response to an injection mixture of oligomycin (oligo; mitochondrial complex V inhibitor) and carbonilcyanide p-triflouromethoxyphenylhydrazone (FCCP; ATP synthase inhibitor and proton uncoupler) using an extracellular flux analyzer. Cell energy phenotype was measured, normalized to protein levels, and are expressed as mean ± SEM (n = 5). ECAR were measured in response to sequential injections of glucose (saturating concentration of glucose to promote glycolysis), oligomycin (ATP synthase inhibitor), and 2-deoxy-glucose (2-DG; a glucose analog that inhibits glycolysis) using an extracellular flux analyzer. OCR measures are pmol over time and ECAR measures are mpH over time, normalized to total protein in the same sample well, and are expressed as mean ± SEM. **(B)** Phagocytic index was calculated from the percentage of cells positive for bacterial uptake multiplied by the RFU of *S. aureus* per cell. Values are expressed as mean ± SEM relative to vehicle (n = 6). *$p < 0.05$ versus control; #$p < 0.05$ versus ethanol.

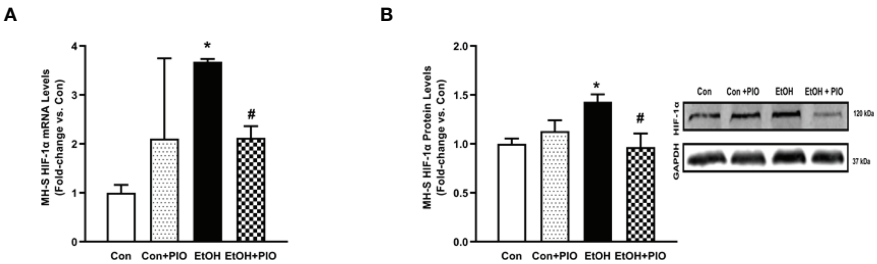

FIGURE 8 | Pioglitazone treatment reverses EtOH-induced HIF-1α levels. MH-S exposed to either control (Con) or ethanol (EtOH; 0.08%) for 72 hours ± pioglitazone (PIO; 10 μM, last 24 hours of EtOH exposure). **(A)** HIF-1α mRNA levels were measured by qRT-PCR, in triplicate, normalized to GAPDH, and expressed as mean ± SEM, relative to control (n = 3). *$p < 0.05$ versus control; #$p < 0.05$ versus EtOH. **(B)** HIF-1α protein levels were evaluated *via* western blot, normalized to GAPDH protein, and densitometry is expressed as mean ± SEM, relative to control (n = 3). Representative western blot images have been provided. *p < 0.05 versus control; #$p < 0.05$ versus ethanol.

phosphorylation is the most efficient process utilized for cellular ATP generation. Previously, we have demonstrated that EtOH exposure severely diminishes the ability of AM to phagocytose and clear pathogens (4–7). Further, we have shown that EtOH altered mitochondria morphology and diminished oxidative phosphorylation in MH-S. Additionally, we demonstrated that the PPARγ ligand, PIO, partially reversed EtOH-induced AM mitochondrial derangements (10) and improved EtOH-induced AM phagocytic dysfunction (11). However, the mechanisms by which EtOH alters AM metabolism have not been fully elucidated. This study aimed to evaluate whether HIF-1α has a role in EtOH-mediated energy derangements in AM. Our findings provide evidence that EtOH shifts AM to a glycolytic metabolic phenotype, which is mediated by EtOH-induced HIF-1α. Also, PIO treatment diminishes EtOH-induced HIF-1α, providing HIF-1α as a molecular mechanism by which PIO improves AM phagocytic function. This study establishes HIF-1α as a critical modulator of chronic EtOH-mediated metabolic derangements in AM.

This study provides a mechanistic understanding of our previous study (10) by showing that EtOH-mediated decreases in oxidative phosphorylation is due to a glycolytic shift. One method of meeting the metabolic requirements of the cell in the absence of oxidative phosphorylation is glycolysis. Glucose transporters transport glucose into the cell, providing some of the glucose needed for glycolysis (12). Glycolysis is a multistep process which utilizes proteins such as Pfkfb3 and PKM2 (12, 13). Our findings herein show that EtOH increases glycolysis (**Figures 1**, **2**). The variance in EtOH-induced alterations in ECAR in mAM (**Figure 1B**) versus MH-S (**Figure 2B**) may be due to the difference in duration of EtOH exposure (mAM isolated from mice fed EtOH for 12 weeks versus MH-S exposed to 0.08% EtOH *in vitro* for 72 hours) and systemic, physiological effects of EtOH. However, the glycolysis

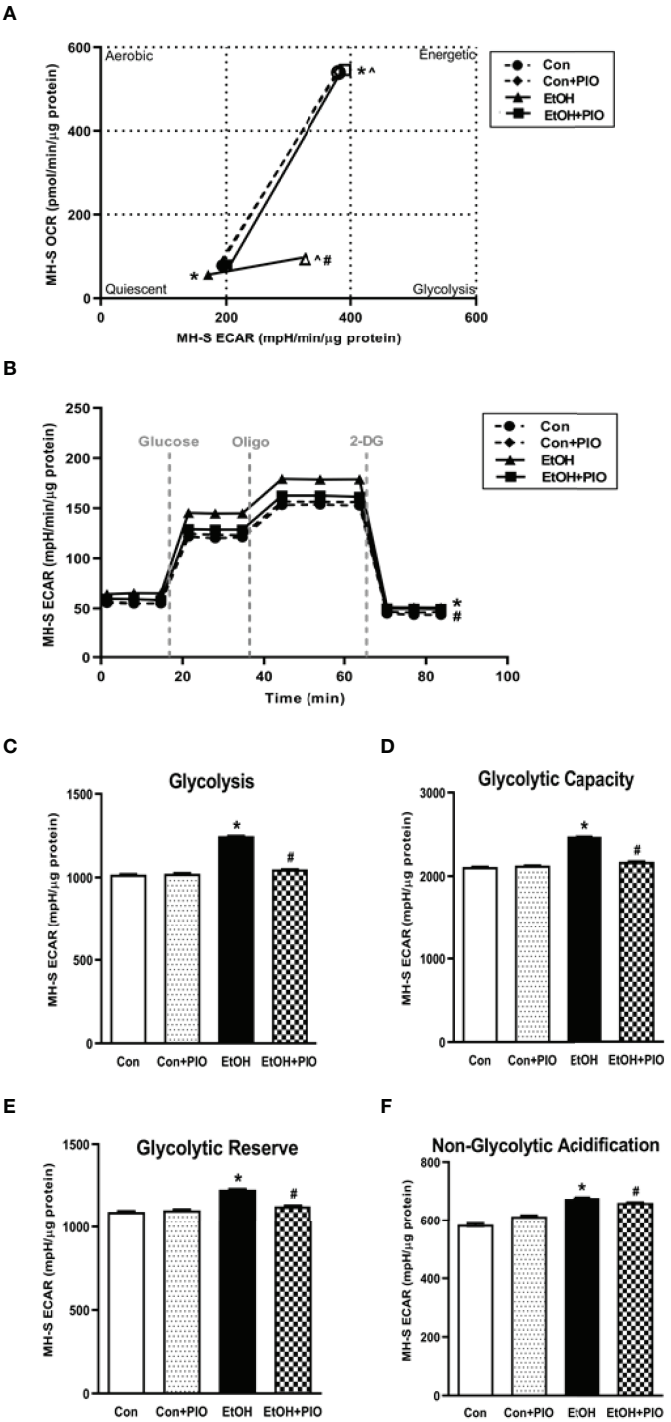

FIGURE 9 | Pioglitazone treatment reverses EtOH-induced glycolysis in MH-S. MH-S were exposed to either control (Con) or ethanol (EtOH; 0.08%; 72 hours) ± pioglitazone (PIO, last day of ethanol). **(A)** Oxygen consumption rates (OCR) and extracellular acidification rates (ECAR) were measured in response to an injection mixture of oligomycin (oligo; mitochondrial complex V inhibitor), carbonilcyanide p-triflouromethoxyphenylhydrazone (FCCP; ATP synthase inhibitor and proton uncoupler) using an extracellular flux analyzer. Cell energy phenotype was measured, normalized to protein levels, and are expressed as mean ± SEM (n = 15). ECAR were measured in response to sequential injections of glucose (saturating concentration of glucose to promote glycolysis), oligomycin (ATP synthase inhibitor), and 2-deoxy-glucose (2-DG; a glucose analog that inhibits glycolysis) using an extracellular flux analyzer. OCR measures are pmol over time and ECAR measures are mpH over time, normalized to total protein in the same sample well, and are expressed as mean ± SEM. Parameters of glycolytic function **(B)**, glycolysis **(C)**, glycolytic capacity **(D)**, glycolytic reserve **(E)**, and non-glycolytic acidification **(F)** are expressed as mean ± SEM, relative to control (n = 15). $^{*}p < 0.05$ verses control; $^{\#}p < 0.05$ versus ethanol; $^{\wedge}p < 0.05$ versus control stressed.

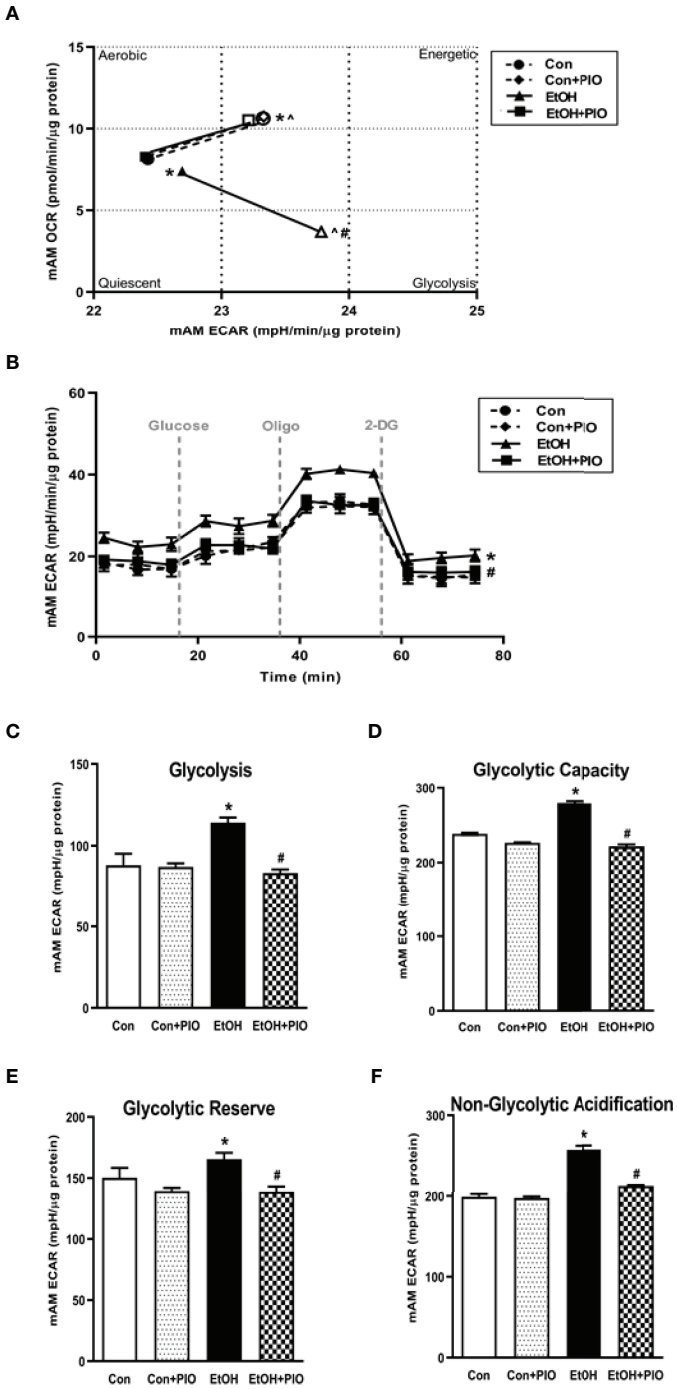

FIGURE 10 | Pioglitazone treatment reverses EtOH-induced glycolysis in mAM. Mouse alveolar macrophages (mAM) were isolated from mice fed either control (Con) or ethanol (EtOH; 20% v/w in drinking water) ± oral pioglitazone (PIO, last 7 days of ethanol). **(A)** Oxygen consumption rates (OCR) and extracellular acidification rates (ECAR) were measured in response to an injection mixture of oligomycin (oligo; mitochondrial complex V inhibitor) and carbonilcyanide p-triflouromethoxyphenylhydrazone (FCCP; ATP synthase inhibitor and proton uncoupler) using an extracellular flux analyzer. Cell energy phenotype was measured, normalized to protein levels, and are expressed as mean ± SEM (n = 10-12). ECAR were measured in response to sequential injections of glucose (saturating concentration of glucose to promote glycolysis), oligomycin (ATP synthase inhibitor), and 2-deoxy-glucose (2-DG; a glucose analog that inhibits glycolysis) using an extracellular flux analyzer. OCR measures are pmol over time and ECAR measures are mpH over time, normalized to total protein in the same sample well, and are expressed as mean ± SEM. Parameters of glycolytic function **(B)**, glycolysis **(C)**, glycolytic capacity **(D)**, glycolytic reserve **(E)**, and non-glycolytic acidification **(F)** are expressed as mean ± SEM, relative to control (n = 11-14). $^{*}p < 0.05$ versus control; $^{\#}p < 0.05$ versus ethanol; $^{\wedge}p < 0.05$ versus control stressed.

bioenergetics profiles for glycolysis and glycolytic capacity were comparable between these mAM *in vivo* (**Figures 1C, D**) and MH-S *in vitro* (**Figures 2C, D**) models. Further, we observed mRNA levels of glucose transporters (GLUT1 and GLUT 4) were elevated following EtOH exposure (**Figure 3**). Further, EtOH induced Pfkfb3, PKM2, and lactate in AM (**Figure 3**). Together, these data demonstrate that EtOH shifts AM to a glycolytic phenotype.

Other studies have described a direct relationship between HIF-1α and EtOH-mediated pathologies (23–25, 31). These studies have demonstrated that EtOH-induced HIF-1α occurs under conditions of elevated inflammation or oxidative stress. Other models have investigated the role of HIF-1α in chronic lung injury (20, 21). HIF-1α was activated *in vitro* in human pulmonary artery smooth muscle cells, demonstrating a role of HIF-1α in pulmonary hypertension pathogenesis (20). HIF-1α has been branded a "metabolic switch", shifting cells from utilizing oxidative phosphorylation to glycolysis (17–19). However, the relationship between HIF-1α and metabolic derangements in the context of chronic EtOH-induced AM phagocytic dysfunction have not been established until now and are supported by the data presented herein. This study illustrates that chronic EtOH exposure increases HIF-1α expression (**Figure 4**). Further, as shown in **Figures 5**, **6**, treatment with the HIF-1α mimetic, cobalt chloride, causes AM derangements similar to EtOH. Knockdown of HIF-1α in the presence of EtOH prevented EtOH induced glycolytic shift and glycolytic profiling (**Figures 7A, B**). Taken together, these data suggest that HIF-1α is a critical modulator of EtOH-induced glycolytic phenotype in AM. Interestingly, Kang et al. showed that EtOH did not alter glycolysis in bone marrow derived macrophages. The group did, however, conclude that EtOH increased glycolytic capacity, glycolytic reserve, and non-glycolytic acidification. HIF-1α expression and activity was also increased due to EtOH exposure (32). The slight variance in results between our studies could be due to the differences in experimental models using bone marrow-derived macrophages to model the AM phenotype. AM may be tissue-resident or recruited cells with key differential functions in host defense (33). However, the current study provides evidence of the critical role for HIF-1α in mediating the glycolytic shift in AM due to EtOH exposure using an AM cell line and AM isolated from *in vivo* EtOH-fed mice. As HIF-1α is a component of the transcription factor HIF-1; elevated levels could have effects not related to glycolysis. One limitation of the current study is that it does not explore non glycolytic effects of HIF-1α. As described above, previous reports have shown that HIF-1α is elevated as a response to inflammation or oxidative stress (23–25, 31), and our lab has shown that oxidative stress contributes to AM phagocytic impairments (7, 10, 11). Modulation of HIF-1α could be alleviating EtOH-mediated oxidative stress, thus improving phagocytic dysfunction.

Since HIF-1 is a transcription factor with numerous targets, other targets may be of future interest. For example, the HIF-1 target PDK-1 can repress mitochondrial function and oxygen consumption. PDK-1-mediated phosphorylation inhibits pyruvate dehydrogenase, preventing the use of pyruvate in oxidative phosphorylation and resulting in decreased mitochondrial oxygen consumption (34). Additionally, other mechanisms, such as fatty acid oxidation, may be involved in meeting the energy demands of the cell due to EtOH exposure. However, studies in the liver suggest that chronic alcohol exposure promotes hepatic injury but does not increase the rate of fatty acid β-oxidation through inhibition of mitochondrial β-oxidation (35–37).

Previously, our lab has shown that alcohol-mediated decreases in peroxisome proliferator-activated receptor gamma (PPARγ) cause AM dysfunction (7). PPARγ is activated by synthetic ligands, such as PIO. This results in heterodimerization of PPARγ with a retinoid receptor and subsequent binding to the PPAR response element in the promoter region of its target genes. The response to this binding is dependent on whether the heterodimerization results in recruitment of coactivators (increases gene expression) or corepressors (decreases gene expression) (38). Our lab has shown that treatment with PPARγ ligands diminished oxidative stress following chronic EtOH exposure (7, 10, 11). Interestingly, decreased expression of PPARγ impaired AM phagocytic capacity following chronic EtOH exposure (7). However, the mechanism by which PPARγ mediates these effects is not known. Other models which generate reactive oxygen species (ROS) have determined that there is an inverse relationship between PPARγ and HIF-1α and that PPARγ ligand treatment decreased hypoxia-induced HIF-1α expression (20, 39). Here, we show that treatment PIO attenuated EtOH-induced HIF-1α (**Figure 8**). It is unclear however, if PPARγ mediates its action on HIF-1α in a direct (binding to HIF-1α promoter) or indirect (reduction of ROS) manner. As shown in **Figures 5**, **6**, the HIF-1α mimetic, cobalt chloride produced results similar to EtOH-induced metabolic derangements. Collectively, these data demonstrated that EtOH-mediated phagocytic dysfunction is in part linked to increased HIF-1α levels, which is mitigated with PIO treatment. Further, PIO treatment reversed EtOH-induced glycolytic bioenergetics (**Figures 9**, **10**).

The current study fills a gap in knowledge by providing a mechanistic understanding to earlier studies which demonstrate that chronic EtOH exposure results in phagocytic dysfunction (4–7, 10) and decreases oxidative phosphorylation (10) in AM. Together, our previous studies suggest that AM has diminished phagocytic capacity due to an inability to meet the energy requirements for phagocytosis. Using both *in vitro* and *in vivo* approaches, we identified HIF-1α as a critical mediator of EtOH-mediated metabolic derangements in AM. These studies establish HIF-1α as a potential therapeutic target for PIO (approved for clinical use in the treatment of type 2 diabetes), which could mitigate the risk of developing respiratory infections in people with a history of alcohol use disorders.

DATA AVAILABILITY STATEMENT

The original contributions presented in the study are included in the article/**Supplementary Material**. Further inquiries can be directed to the corresponding author.

ETHICS STATEMENT

The animal study was reviewed and approved by Atlanta Veterans Affairs Health Care System Institutional Animal Care and Use Committee.

AUTHOR CONTRIBUTIONS

NLM designed experiments, obtained samples from animal experiments, analyzed experiments, and prepared the manuscript; DNM, KMC, and SSC obtained samples from animal experiments and analyzed experiments; SMY designed and analyzed experiments and prepared the manuscript. All authors contributed to the article and approved the submitted version.

FUNDING

This work was supported in part by grants from the National Institute on Alcohol Abuse and Alcoholism (R01AA026086) to SMY (ORCID ID: 0000-0001-9309-0233) and the National Heart, Lung, and Blood Institute (T32HL116271) to David M. Guidot, Lou Ann S. Brown, and C. Michael Hart. The contents of this report do not represent the views of the Department of Veterans Affairs or the US Government.

SUPPLEMENTARY MATERIAL

The Supplementary Material for this article can be found online at: https://www.frontiersin.org/articles/10.3389/fimmu.2022.865492/full#supplementary-material

REFERENCES

1. Alcohol Facts and Statistics. In: *National Institute of Alcohol Abuse and Alcoholism*. Bethesda, MD: NIAAA. Available at: https://www.niaaa.nih.gov/alcohol-health/overview-alcohol-consumption/alcohol-facts-and-statistics.
2. Moss M. Epidemiology of Sepsis: Race, Sex, and Chronic Alcohol Abuse. *Clin Infect Dis* (2005) 41 Suppl 7:S490–7. doi: 10.1086/432003
3. Mehta AJ, Guidot DM. Alcohol Abuse, the Alveolar Macrophage and Pneumonia. *Am J Med Sci* (2012) 343(3):244–7. doi: 10.1097/MAJ.0b013e31823ede77
4. Mehta AJ, Yeligar SM, Elon L, Brown LA, Guidot DM. Alcoholism Causes Alveolar Macrophage Zinc Deficiency and Immune Dysfunction. *Am J Respir Crit Care Med* (2013) 188(6):716–23. doi: 10.1164/rccm.201301-0061OC
5. Yeligar SM, Harris FL, Hart CM, Brown LA. Glutathione Attenuates Ethanol-Induced Alveolar Macrophage Oxidative Stress and Dysfunction by Downregulating NADPH Oxidases. *Am J Physiol Lung Cell Mol Physiol* (2014) 306(5):L429–41. doi: 10.1152/ajplung.00159.2013
6. Yeligar SM, Harris FL, Hart CM, Brown LA. Ethanol Induces Oxidative Stress in Alveolar Macrophages *via* Upregulation of NADPH Oxidases. *J Immunol* (2012) 188(8):3648–57. doi: 10.4049/jimmunol.1101278
7. Yeligar SM, Mehta AJ, Harris FL, Brown LA, Hart CM. Peroxisome Proliferator-Activated Receptor Gamma Regulates Chronic Alcohol-Induced Alveolar Macrophage Dysfunction. *Am J Respir Cell Mol Biol* (2016) 55(1):35–46. doi: 10.1165/rcmb.2015-0077OC
8. Aderem A, Underhill DM. Mechanisms of Phagocytosis in Macrophages. *Annu Rev Immunol* (1999) 17:593–623. doi: 10.1146/annurev.immunol.17.1.593
9. Brown LA, Harris FL, Ping XD, Gauthier TW. Chronic Ethanol Ingestion and the Risk of Acute Lung Injury: A Role for Glutathione Availability? *Alcohol* (2004) 33(3):191–7. doi: 10.1016/j.alcohol.2004.08.002
10. Morris NL, Harris FL, Brown LAS, Yeligar SM. Alcohol Induces Mitochondrial Derangements in Alveolar Macrophages by Upregulating NADPH Oxidase 4. *Alcohol* (2021) 90:27–38. doi: 10.1016/j.alcohol.2020.11.004
11. Yeligar SM, Mehta AJ, Harris FL, Brown LAS, Hart CM. Pioglitazone Reverses Alcohol-Induced Alveolar Macrophage Phagocytic Dysfunction. *J Immunol* (2021) 207(2):483–92. doi: 10.4049/jimmunol.2000565
12. Chaudhry R, Varacallo M. *Biochemistry, Glycolysis*. Treasure Island (FL: StatPearls (2021).
13. Ros S, Schulze A. Balancing Glycolytic Flux: The Role of 6-Phosphofructo-2-Kinase/Fructose 2,6-Bisphosphatases in Cancer Metabolism. *Cancer Metab* (2013) 1(1):8. doi: 10.1186/2049-3002-1-8
14. Gong Y, Lan H, Yu Z, Wang M, Wang S, Chen Y, et al. Blockage of Glycolysis by Targeting PFKFB3 Alleviates Sepsis-Related Acute Lung Injury *via* Suppressing Inflammation and Apoptosis of Alveolar Epithelial Cells. *Biochem Biophys Res Commun* (2017) 491(2):522–9. doi: 10.1016/j.bbrc.2017.05.173
15. Hu K, Yang Y, Lin L, Ai Q, Dai J, Fan K, et al. Caloric Restriction Mimetic 2-Deoxyglucose Alleviated Inflammatory Lung Injury *via* Suppressing Nuclear Pyruvate Kinase M2-Signal Transducer and Activator of Transcription 3 Pathway. *Front Immunol* (2018) 9:426. doi: 10.3389/fimmu.2018.00426
16. Liu W, Shen SM, Zhao XY, Chen GQ. Targeted Genes and Interacting Proteins of Hypoxia Inducible Factor-1. *Int J Biochem Mol Biol* (2012) 3(2):165–78.
17. Miska J, Lee-Chang C, Rashidi A, Muroski ME, Chang AL, Lopez-Rosas A, et al. HIF-1alpha Is a Metabolic Switch Between Glycolytic-Driven Migration and Oxidative Phosphorylation-Driven Immunosuppression of Tregs in Glioblastoma. *Cell Rep* (2019) 27(1):226–37 e4. doi: 10.1016/j.celrep.2019.03.029
18. Wang T, Liu H, Lian G, Zhang SY, Wang X, Jiang C. HIF1alpha-Induced Glycolysis Metabolism Is Essential to the Activation of Inflammatory Macrophages. *Mediators Inflamm* (2017) 2017:9029327. doi: 10.1155/2017/9029327
19. Del Rey MJ, Valin A, Usategui A, Garcia-Herrero CM, Sanchez-Arago M, Cuezva JM, et al. HIF-1alpha Knockdown Reduces Glycolytic Metabolism and Induces Cell Death of Human Synovial Fibroblasts Under Normoxic Conditions. *Sci Rep* (2017) 7(1):3644. doi: 10.1038/s41598-017-03921-4
20. Blum JI, Bijli KM, Murphy TC, Kleinhenz JM, Hart CM. Time-Dependent PPARgamma Modulation of HIF-1alpha Signaling in Hypoxic Pulmonary Artery Smooth Muscle Cells. *Am J Med Sci* (2016) 352(1):71–9. doi: 10.1016/j.amjms.2016.03.019
21. Wu G, Xu G, Chen DW, Gao WX, Xiong JQ, Shen HY, et al. Hypoxia Exacerbates Inflammatory Acute Lung Injury *via* the Toll-Like Receptor 4 Signaling Pathway. *Front Immunol* (2018) 9:1667. doi: 10.3389/fimmu.2018.01667
22. Cho SJ, Moon JS, Lee CM, Choi AM, Stout-Delgado HW. Glucose Transporter 1-Dependent Glycolysis Is Increased During Aging-Related Lung Fibrosis, and Phloretin Inhibits Lung Fibrosis. *Am J Respir Cell Mol Biol* (2017) 56(4):521–31. doi: 10.1165/rcmb.2016-0225OC
23. Katada R, Nishitani Y, Honmou O, Mizuo K, Okazaki S, Tateda K, et al. Expression of Aquaporin-4 Augments Cytotoxic Brain Edema After Traumatic Brain Injury During Acute Ethanol Exposure. *Am J pathology* (2012) 180(1):17–23. doi: 10.1016/j.ajpath.2011.09.011
24. He Z, Li M, Zheng D, Chen Q, Liu W, Feng L. Adipose Tissue Hypoxia and Low-Grade Inflammation: A Possible Mechanism for Ethanol-Related Glucose Intolerance? *Br J Nutr* (2015) 113(9):1355–64. doi: 10.1017/S000711451500077X
25. Yun JW, Son MJ, Abdelmegeed MA, Banerjee A, Morgan TR, Yoo SH, et al. Binge Alcohol Promotes Hypoxic Liver Injury Through a CYP2E1-HIF-1alpha-Dependent Apoptosis Pathway in Mice and Humans. *Free Radical Biol Med* (2014) 77:183–94. doi: 10.1016/j.freeradbiomed.2014.08.030
26. Wagner MC, Yeligar SM, Brown LA, Michael Hart C. PPARgamma Ligands Regulate NADPH Oxidase, eNOS, and Barrier Function in the Lung Following Chronic Alcohol Ingestion. *Alcohol Clin Exp Res* (2012) 36(2):197–206. doi: 10.1111/j.1530-0277.2011.01599.x

27. Yeligar SM, Kang BY, Bijli KM, Kleinhenz JM, Murphy TC, Torres G, et al. PPARgamma Regulates Mitochondrial Structure and Function and Human Pulmonary Artery Smooth Muscle Cell Proliferation. *Am J Respir Cell Mol Biol* (2018) 58(5):648–57. doi: 10.1165/rcmb.2016-0293OC
28. Nag S, Resnick A. Stabilization of Hypoxia Inducible Factor by Cobalt Chloride can Alter Renal Epithelial Transport. *Physiol Rep* (2017) 5(24): e13531. doi: 10.14814/phy2.13531
29. Yuan Y, Hilliard G, Ferguson T, Millhorn DE. Cobalt Inhibits the Interaction Between Hypoxia-Inducible Factor-Alpha and Von Hippel-Lindau Protein by Direct Binding to Hypoxia-Inducible Factor-Alpha. *J Biol Chem* (2003) 278 (18):15911–6. doi: 10.1074/jbc.M300463200
30. Woods PS, Kimmig LM, Meliton AY, Sun KA, Tian Y, O'Leary EM, et al. Tissue-Resident Alveolar Macrophages Do Not Rely on Glycolysis for LPS-Induced Inflammation. *Am J Respir Cell Mol Biol* (2020) 62(2):243–55. doi: 10.1165/rcmb.2019-0244OC
31. Yeligar SM, Machida K, Kalra VK. Ethanol-Induced HO-1 and NQO1 are Differentially Regulated by HIF-1alpha and Nrf2 to Attenuate Inflammatory Cytokine Expression. *J Biol Chem* (2010) 285(46):35359–73. doi: 10.1074/jbc.M110.138636
32. Kang H, Park YK, Lee JY. Nicotinamide Riboside, an NAD(+) Precursor, Attenuates Inflammation and Oxidative Stress by Activating Sirtuin 1 in Alcohol-Stimulated Macrophages. *Lab Invest* (2021) 101(9):1225–37. doi: 10.1038/s41374-021-00599-1
33. Herold S, Mayer K, Lohmeyer J. Acute Lung Injury: How Macrophages Orchestrate Resolution of Inflammation and Tissue Repair. *Front Immunol* (2011) 2:65. doi: 10.3389/fimmu.2011.00065
34. Papandreou I, Cairns RA, Fontana L, Lim AL, Denko NC. HIF-1 Mediates Adaptation to Hypoxia by Actively Downregulating Mitochondrial Oxygen Consumption. *Cell Metab* (2006) 3(3):187–97. doi: 10.1016/j.cmet.2006.01.012
35. Fischer M, You M, Matsumoto M, Crabb DW. Peroxisome Proliferator-Activated Receptor Alpha (PPARalpha) Agonist Treatment Reverses PPARalpha Dysfunction and Abnormalities in Hepatic Lipid Metabolism in Ethanol-Fed Mice. *J Biol Chem* (2003) 278(30):27997–8004. doi: 10.1074/jbc.M302140200
36. Blomstrand R, Kager L, Lantto O. Studies on the Ethanol-Induced Decrease of Fatty Acid Oxidation in Rat and Human Liver Slices. *Life Sci* (1973) 13 (8):1131–41. doi: 10.1016/0024-3205(73)90380-9
37. Correnti JM, Gottshall L, Lin A, Williams B, Oranu A, Beck J, et al. Ethanol and C2 Ceramide Activate Fatty Acid Oxidation in Human Hepatoma Cells. *Sci Rep* (2018) 8(1):12923. doi: 10.1038/s41598-018-31025-0
38. Sutliff RL, Kang BY, Hart CM. PPARgamma as a Potential Therapeutic Target in Pulmonary Hypertension. *Ther Adv Respir Dis* (2010) 4(3):143–60. doi: 10.1177/1753465809369619
39. Lee KS, Kim SR, Park SJ, Park HS, Min KH, Jin SM, et al. Peroxisome Proliferator Activated Receptor-Gamma Modulates Reactive Oxygen Species Generation and Activation of Nuclear factor-kappaB and Hypoxia-Inducible Factor 1alpha in Allergic Airway Disease of Mice. *J Allergy Clin Immunol* (2006) 118(1):120–7. doi: 10.1016/j.jaci.2006.03.021

Conflict of Interest: The authors declare that the research was conducted in the absence of any commercial or financial relationships that could be construed as a potential conflict of interest.

Publisher's Note: All claims expressed in this article are solely those of the authors and do not necessarily represent those of their affiliated organizations, or those of the publisher, the editors and the reviewers. Any product that may be evaluated in this article, or claim that may be made by its manufacturer, is not guaranteed or endorsed by the publisher.

frontiers | Frontiers in Immunology

ORIGINAL RESEARCH
published: 12 May 2022
doi: 10.3389/fimmu.2022.839390

Alcohol Impairs Immunometabolism and Promotes Naïve T Cell Differentiation to Pro-Inflammatory Th1 CD4$^+$ T Cells

Patrick M. McTernan[1,2], *Danielle E. Levitt*[1,2], *David A. Welsh*[2,3], *Liz Simon*[1,2], *Robert W. Siggins*[1,2] *and Patricia E. Molina*[1,2]*

[1] Department of Physiology, Louisiana State University Health Sciences Center, New Orleans, LA, United States, [2] Comprehensive Alcohol-HIV/AIDS Research Center, Louisiana State University Health Sciences Center, New Orleans, LA, United States, [3] Department of Medicine, Section of Pulmonary/Critical Care Medicine, Louisiana State University Health Sciences Center, New Orleans, LA, United States

OPEN ACCESS

Edited by:
Suhas Sureshchandra, University of California, Irvine, United States

Reviewed by:
Antonio Riva, Foundation for Liver Research, United Kingdom
Wendy Dankers, Amsterdam UMC, Netherlands

***Correspondence:**
Patricia E. Molina
PMolin@lsuhsc.edu

Specialty section:
This article was submitted to Nutritional Immunology, a section of the journal Frontiers in Immunology

Received: 19 December 2021
Accepted: 19 April 2022
Published: 12 May 2022

Citation:
McTernan PM, Levitt DE, Welsh DA, Simon L, Siggins RW and Molina PE (2022) Alcohol Impairs Immunometabolism and Promotes Naïve T Cell Differentiation to Pro-Inflammatory Th1 CD4$^+$ T Cells. Front. Immunol. 13:839390. doi: 10.3389/fimmu.2022.839390

CD4$^+$ T cell differentiation to pro-inflammatory and immunosuppressive subsets depends on immunometabolism. Pro-inflammatory CD4$^+$ subsets rely on glycolysis, while immunosuppressive Treg cells require functional mitochondria for their differentiation and function. Previous pre-clinical studies have shown that ethanol (EtOH) administration increases pro-inflammatory CD4$^+$ T cell subsets; whether this shift in immunophenotype is linked to alterations in CD4$^+$ T cell metabolism had not been previously examined. The objective of this study was to determine whether ethanol alters CD4$^+$ immunometabolism, and whether this affects CD4$^+$ T cell differentiation. Naïve human CD4$^+$ T cells were plated on anti-CD3 coated plates with soluble anti-CD28, and differentiated with IL-12 in the presence of ethanol (0 and 50 mM) for 3 days. Both Tbet-expressing (Th1) and FOXP3-expressing (Treg) CD4$^+$ T cells increased after differentiation. Ethanol dysregulated CD4$^+$ T cell differentiation by increasing Th1 and decreasing Treg CD4$^+$ T cell subsets. Ethanol increased glycolysis and impaired oxidative phosphorylation in differentiated CD4$^+$ T cells. Moreover, the glycolytic inhibitor 2-deoxyglucose (2-DG) prevented the ethanol-mediated increase in Tbet-expressing CD4$^+$ T cells but did not attenuate the decrease in FOXP3 expression in differentiated CD4$^+$ T cells. Ethanol increased Treg mitochondrial volume and altered expression of genes implicated in mitophagy and autophagosome formation (*PINK1* and *ATG7*). These results suggest that ethanol impairs CD4$^+$ T cell immunometabolism and disrupts mitochondrial repair processes as it promotes CD4$^+$ T cell differentiation to a pro-inflammatory phenotype.

Keywords: immunometabolism, alcohol, differentiation, mitochondria, glycolysis, CD4$^+$ T cell

INTRODUCTION

At-risk alcohol use is the most common and costly form of substance use in the United States (US), and approximately 29% of the US adult population meets diagnostic criteria for alcohol use disorder (AUD) (1–4). At-risk alcohol use increases persistent systemic inflammation, which is one of the major mechanisms linked to alcohol-associated end-organ injury (5). Clinical studies show that alcohol-induced systemic inflammation leads to increased susceptibility to infections, impaired bacterial clearance and increased disease burden (5–9). Preclinical studies have shown that chronic ethanol administration increases activated, proliferating $CD4^+$ T cells, and dysregulates effector cell differentiation by increasing pro-inflammatory Th17 $CD4^+$ T cells in the gut while increasing the ratio of T-Box Expressed in T cells (Tbet)-expressing (Th1) to Forkhead Box P3 (FOXP3)-expressing (Treg) $CD4^+$ T cells in the colon (10–16). These changes to immune cell activation and differentiation promote a pro-inflammatory environment that can increase the risk of developing autoimmune disorders (17) and susceptibility to infections, including human immunodeficiency virus (HIV), which targets activated $CD4^+$ T cells (18, 19).

The adaptive immune system is critical for immunological memory and a sustained immune response to antigenic and inflammatory signals, and T cells are important in this process. T cells are classified as $CD4^+$ and $CD8^+$ based on the expression of an accessory glycoprotein co-receptor, which is responsible for their interaction with major histocompatibility complex (MHC) class II or class I molecules, respectively (20, 21). While $CD8^+$ T cells are important in attacking infected or malignant cells, $CD4^+$ T cells are responsible for the recruitment of cytotoxic T cells to sites of infection, mediating the humoral antibody response, and regulating innate and acquired immune cell activation and proliferation.

Chronic ethanol administration impairs normal metabolism in tissues, such as the liver, including glycolysis and mitochondrial electron transport chain (ETC) complexes (22–24). This impairment of glycolysis within the liver occurs, in part, due to an increase in the $NADH/NAD^+$ ratio, which depletes free NAD^+ cofactor availability for glycolytic enzymes, such as glyceraldehyde 3-phosphate dehydrogenase (25). Ethanol also decreases myoblast (muscle stem cells) glycolytic function and leads to decreased differentiation (26). Further, ethanol increases reactive oxygen species (ROS) formation in mitochondria, which can damage mitochondrial DNA and ETC proteins, leading to impaired mitochondrial function and cell death (24, 27). Though the ethanol-mediated changes to tissue metabolism are well characterized, ethanol changes to immunometabolism have not been previously investigated.

$CD4^+$ T cells rely on both glycolysis and oxidative phosphorylation to support energy requirements of immune responses (28). Naïve $CD4^+$ T cells exist in a quiescent state and rely on fatty acid oxidation as their primary energy source. Upon binding of the T cell receptor (TCR), T cells are activated, and metabolism shifts from fatty acid oxidation to aerobic glycolysis, a process necessary to meet the energetic demands of the proliferating, activated T cells (28). After activation of naïve $CD4^+$ T cells, transcription factor networks direct differentiation, and the expression of these networks depends on distinct metabolic pathways (29–31). Expression of master transcription factors *Tbet* (Th1), GATA Binding Protein 3 (*GATA3*; Th2), and Retinoic Acid-Related Orphan Receptor Gamma T (*RORγt*; Th17) all depend on glycolytic pathway activation, specifically Mammalian Target of Rapamycin Complex 1 (MTORC1), MTORC2, and Hypoxia Inducible Factor 1 subunit alpha (HIF-1α) signaling, respectively, for their expression. *FOXP3* (Treg) expression relies on oxidative phosphorylation and adenosine monophosphate-activated protein kinase (AMPK) inhibition, which is important for the promotion of mitochondrial biogenesis (32). Impairment of either of these bioenergetic pathways can dysregulate normal $CD4^+$ T cell differentiation. Studies using 2-deoxyglucose (2-DG), an inhibitor of glycolysis, or rapamycin, an inhibitor of mTOR, shifted $CD4^+$ differentiation from Th1, Th2, and Th17, towards a Treg phenotype (33–35). Moreover, activating $mTOR^{-/-}$ T cells only generates Treg cells and no other effector T cells (36). On the other hand, Treg differentiation can be impaired by using etomoxir, an inhibitor of complex I in the electron transport chain (ETC) (37).

Mitochondria play a crucial role in cellular energy metabolism and Treg differentiation (29, 32). Both preclinical and clinical studies have demonstrated that ethanol alters mitochondrial function by impairing mitochondrial biogenesis, increasing mitochondrial DNA damage, and increasing oxidative stress (38–40). Further, ethanol dysregulates gene expression implicated in mitohormesis, a response to stress to restore health and viability of mitochondria, and induces mitochondrial DNA (mtDNA) damage within alveolar macrophages (41, 42). Myoblasts isolated from persons living with HIV (PLWH) with high alcohol use disorder identification test (AUDIT) scores showed increased mitochondrial content and decreased bioenergetic health index compared to PLWH with low AUDIT scores (43). This mitochondrial dysfunction is speculated to be due to ethanol-mediated mitochondrial damage and defective mitophagy (44) as shown in previous studies where ethanol decreased expression of genes important to mitophagy, including *PINK1* and *PARKIN* (44). These ethanol-mediated impairments of mitochondrial homeostatic processes could significantly impact the capacity for Treg differentiation.

This study tested the hypothesis that ethanol impairs bioenergetics of $CD4^+$ T cells and dysregulates differentiation. Our results indicate that ethanol promoted differentiation of pro-inflammatory Th1 $CD4^+$ T cells by increasing glycolysis, and decreased immunosuppressive Treg $CD4^+$ T cell differentiation by impairing mitochondrial function. To date, this is the first report to investigate how ethanol regulates T cell immunometabolism and alter the fate of cell differentiation.

MATERIALS AND METHODS

In Vitro Activation and Differentiation of $CD4^+$ T Cells and Ethanol Treatments

Peripheral blood mononuclear cells (PBMCs) were isolated from blood bank donor buffy coats using a Ficoll-Paque gradient (Cytiva, Marlborough, MA) and frozen in 10% DMSO

(ThermoFisher, Waltham, MA) in fetal bovine serum (FBS) at -80° C (45). PBMCs were thawed and washed twice using growth media [RPMI 1640 supplemented with 10% FBS, 3 mM L-glutamine, and 100 U/ml penicillin/streptomycin (Gibco, Waltham, MA)] and cultured overnight at 37°C, 5% CO_2 and 100% relative humidity. Naïve $CD4^+$ T cells were sorted using the human Naïve $CD4^+$ T cell Isolation Kit II and LS MACS sorting columns (Miltenyi Biotec, Auburn, CA) following the manufacturer's protocol. Naïve $CD4^+$ T cells were then activated and differentiated by plating at a density of 2 x 10^5 cells in 100 ul (2x10^6/ml) per well on coated anti-CD3 (5 μg/ml; catalog # 16-0037-81; ThermoFisher) 96 well flat-bottom plates (Costar, Washington DC, MD) in the presence of soluble anti-CD28 (2.5 μg/ml; catalog # 16-0289-81; ThermoFisher) and IL-12 (25 ng/ml; catalog #573002; Biolegend, San Diego, CA) for 3 days in 37°C incubators with 5% CO_2 with and without 50 mM ethanol. IL-12 was added to growth media (ThermoFisher) to promote both Th1 and Treg differentiation (DIFF). There was no difference in promotion of FOXP3 expression with either IL-12 or TGF-beta and IL-2 stimulated $CD4^+$ T cells (**Supplementary Figure 1**). Growth media with no IL-12, was referred to as control media (Act). Naïve $CD4^+$ T cells that were not activated and differentiated were plated (density of 2x10^6/ml per well) in growth media without anti-CD3 and anti-CD28. Water pans containing 75 mM ethanol were changed daily to maintain the 50 mM ethanol concentration in the incubator atmosphere as previously described (26). Both 25 mM and 50 mM ethanol were used in preliminary studies, but 25 mM had no significant effect on $CD4^+$ T cell differentiation (data not shown), hence all subsequent experiments were performed with 50 mM. Experimental groups for this study are defined as:

- Naïve – naïve $CD4^+$ T cells that are not activated and differentiated or treated with ethanol.
- EtOH – naïve $CD4^+$ T cells that are not activated and differentiated but are treated with 50 mM ethanol.
- DIFF – naïve $CD4^+$ T cells that are activated, using anti-CD3 and anti-CD28, and differentiated, using IL-12, and not treated with 50 mM ethanol.
- DIFF + EtOH – naïve $CD4^+$ T cells that are activated, using anti-CD3 and anti-CD28, and differentiated, using IL-12, and treated with 50 mM ethanol.

Flow Cytometry

$CD4^+$ T cells were immunostained with antibodies purchased from Biolegend unless otherwise specified using the following panel ($CD4^+$ differentiation panel): CD4-APC (clone: A161A1), CD45RA-BV570 (clone: HI100), CD38-AF700 (clone: HIT2), CD25-BV650 (clone: BC96), CD3-PE-Cy7 (clone: OKT3), CD28-BV605 (clone: CD28.2), FOXP3-PE-CY5 (clone: PCH101) (ThermoFisher, MA, USA), Tbet-PE (clone: 4B10), GATA3-BV421 (clone: 16E10A23), RORγt -PE-CF594 (clone: Q31-378) (BD Biosciences, Franklin Lake, NJ), Live/Dead – eFluor780 (Invitrogen, Waltham, MA). The staining was performed in two steps. The gating strategy for the CD4 differentiation panel is shown as **Supplementary Figure 2**. Cells were incubated with antibodies (1 μg) targeting CD4, CD45RA, CD38, CD25, and Live/Dead at 4°C for 30 minutes. Cells were then fixed for 30 minutes at room temperature in the dark using the Foxp3/Transcription Factor Staining Buffer Set (catalog #: 00-5523-00; ThermoFisher) according to the manufacturer's protocol. Following permeabilization, cells were stained with antibodies targeting CD3, CD28, FOXP3, Tbet, GATA3, and RORγt at 4°C overnight for 16-18 hours. GLUT1 expression was assessed using a separate panel, and included CD3, CD4, Tbet, and FOXP3 from the $CD4^+$ differentiation panel. GLUT1 (R&D Systems; clone: MAB1418) was conjugated with FITC in the laboratory using the Lighting-Link FITC conjugation kit (catalog #: 707-0010; Novus Biologicals, CO, USA). Samples were analyzed using an 18-color BD LSRII flow cytometer and FACSDiva software (ver. 8.0.1, Becton, Dickinson, Franklin Lakes, NJ). Flow cytometry gates were defined based on fluorescence minus one (FMO) controls.

Sorting of $CD25^+$-Expressing $CD4^+$ T Cells

The differentiated $CD4^+$ T cells were sorted to Tbet- and FOXP3-enriched $CD4^+$ T cell subsets using the human $CD4^+CD25^+$ regulatory T cell isolation kit (catalog #: 130-091-301; Miltenyi Biotec, Auburn, CA). After sorting, flow cytometry, using the CD4 Differentiation Panel, confirmed that 29% of $CD4^+CD25^+$ T cells expressed FOXP3 and 21% expressed Tbet. Flow through containing $CD4^+CD25^-$ $CD4^+$ T cells were enriched in Tbet-expressing $CD4^+$ T cells (18% Tbet and 4% FOXP3; **Supplementary Figure 3**). These sorted populations were defined as either CD4+CD25+ "Enriched Treg" or CD4+CD25- "Enriched Th1".

Mitochondrial Function

Mitochondrial oxygen consumption rate (OCR) was measured using a Mito Stress Test (31) and Seahorse XFe96 technology (Agilent Technologies, Santa Clara, CA). Naïve and IL-12-differentiated $CD4^+$ T cells were seeded on Cell-Tak (Corning, Corning, NY)-coated 96-well Seahorse plates in triplicate at a density of 3 x 10^5 cells/well within 200 ul, at a concentration of 1.5 million cells/ml, and maintained under standard cell culture conditions (5% CO_2, 37^0C). Cells were incubated in XF Assay Medium (pH 7.4) with sodium pyruvate (1 mM), L-glutamine (2 mM), and glucose (10 mM) at 37°C without CO_2 for 1 hr before measuring T cell OCR with an XFe96 Extracellular Flux Analyzer (Agilent Technologies, Santa Clara, CA) according to manufacturer's instructions. Respiratory parameters were assessed by the sequential addition of oligomycin (1 μM), carbonyl cyanide-p-trifluoromethoxyphenylhydrazone (FCCP; 2 μM), and rotenone/antimycin A (0.5 μM). OCR measurements were normalized to cell count obtained by staining nuclei with Hoescht dye (2 μM; ThermoFisher Scientific) and visualizing on a BioTek Cytation 1 cell imaging multi-mode reader (BioTek, Winooski, VT).

Glycolytic Function

A Glycolysis Stress Test (31) was performed in naïve and IL-12-differentiated $CD4^+$ T cells seeded as described above. Cells were incubated at 37°C without CO_2 for 1 hr in glucose-free XF Assay

Medium (pH 7.4) with L-glutamine (2 mM) before measuring $CD4^+$ T cell extracellular acidification rate (ECAR) at baseline and after the sequential addition of glucose (10 mM), oligomycin (1 μM), and 2-deoxyglucose (2-DG; 50 mM). ECAR measurements were normalized to cell count as described for the Mito Stress Test.

Mitochondrial Content

T cell mitochondrial content was quantified with MitoTracker Deep Red FM probes (Thermofisher) (46, 47). Naïve and IL-12-differentiated $CD4^+$ T cells were incubated in growth media containing MitoTracker Deep Red FM (17 nM) under standard cell culture conditions for one hour. An unstained control sample was simultaneously incubated in growth media without MitoTracker. Cells were pelleted, washed with phosphate-buffered saline (PBS; Gibco) and fixed for flow cytometry using the PerFix-nc Kit (Beckman Coulter, Brea, CA) according to manufacturer instructions. Samples were analyzed on a BD FACSCanto II flow cytometer (Becton, Dickinson and Company). The gating strategy for the Mitotracker Deep Red assay is shown as **Supplementary Figure 4**. Mean fluorescent intensities (MFI) were calculated using BD FACSDiva software (ver 8.0.1).

Glucose Uptake

Glucose uptake was measured with 2-Deoxy-2-[(7-nitro-2,1,3-benzoxadiazol-4-yl) amino]-D-glucose (2-NBDG) (Sigma-Aldrich, St. Louis USA). Briefly, $CD4^+$ T cells were washed with PBS and incubated in glucose-free RPMI 1640 supplemented with 10% FBS, 3 mM L-glutamine, and 100 U/ml penicillin/streptomycin (Gibco, Waltham, MA) for 1 hour. After incubation, 2-NBDG was added to culture wells to a final concentration of 150 μM for 30 minutes at 37°C and 5% CO_2. $CD4^+$ T cells were washed twice with PBS and analyzed using the 533 nm wavelength channel on a BD FACSCanto II flow cytometer (Becton, Dickinson and Company). The gating strategy for the 2-NBDG uptake assay is shown as **Supplementary Figure 5**. Mean fluorescent intensities (MFI) were calculated using BD DIVA software (ver 8.0.1).

2-Deoxyglucose Treatment

Naïve $CD4^+$ T cells were activated and allowed to differentiate using the *in vitro* differentiation protocol above, and on day 2 of the 3-day culture, 2-DG (0.5 mM) was added for 24 h. After incubation with 2-DG, cells were stained and assessed by flow cytometry using the $CD4^+$ differentiation panel as described above.

Expression of Genes Implicated in Mitochondrial Function

Total RNA was extracted from naïve and IL-12-differentiated $CD4^+$ T cells after 3 days in the presence and absence of 50 mM ethanol using the miRNeasy Mini Kit (Qiagen, Valencia, CA) according to manufacturer's instructions. cDNA was synthesized using the Qiagen RT^2 First Strand synthesis kit (Qiagen, Valencia, CA) and qPCR performed using custom RT^2 qPCR profiler arrays (Qiagen: CAPA9632-12:CLAH42284). qPCR reactions were carried out in duplicate using a CFX96 thermal cycler (Bio-Rad, Hercules, CA) with Beta-2-Microglobulin (*B2M*) as the endogenous control. Data were then analyzed using the $2^{-\Delta\Delta Ct}$ method. All genes analyzed are summarized in **Table 1**.

Statistical Analysis

Data were checked for assumption of normality using the Shapiro-Wilk test. The alpha level set for all statistical analysis was a p value < 0.05. $CD4^+$ differentiation, glycolysis, MitoTracker, and RT^2 profiler array data were analyzed using a 2 (differentiation) x 2 (ethanol) analysis of variance (ANOVA) with repeated measures on both factors. 2-DG data were analyzed using a 2 (differentiation) x 2 (ethanol) x 2 (2-DG) ANOVA with repeated measures on all factors. When appropriate, *post hoc* pairwise comparisons were conducted and p-values adjusted using Tukey's HSD for 2-way ANOVA and Sidak for 3-way ANOVA. To analyze the effect of IL-12 on $CD4^+$ differentiation, and of ethanol on Tbet-FOXP3-expressing $CD4^+$ T cells, paired T tests were performed. Paired T tests were also performed to assess the effect of ethanol on $CD4^+$ T cell mitochondrial function and to analyze the MitoTracker data within Treg and Th1 $CD4^+$ subsets. The Treg OCR-linked proton leak data did not pass normality or lognormality tests and therefore a Wilcoxon test was used to analyze significance. All analyses except 3-way ANOVA were performed using GraphPad prism 9.2.0 (San Diego, CA). 3-way ANOVA analyses were conducted using SPSS (Version 25, IBM Corporation, Armonk, NY).

RESULTS

IL-12 Promotes $CD4^+$ T Cell Expression of Tbet

IL-12 was used to direct differentiation of $CD4^+$ T cells. IL-12 preferentially directed differentiation of Tbet- (Th1; p = 0.006; **Figures 1A, B**) and had no effect on FOXP3- (Treg; **Figures 1C, D**) expressing $CD4^+$ T cells, while decreasing the expression of

TABLE 1 | List of gene targets analyzed by RT^2 qPCR profiler arrays.

Gene Symbol	Gene Targets
Mitochondrial Maintenance and Mitophagy Related Genes	
PRKN & *PINK1*	Parkin & PTEN-induced Kinase 1
ATG5, ATG7, & *ATG13*	Autophagy Related 5, 7, and 13
MFN1 & *MFN2*	Mitofusin 1 & 2
BNIP3L & *ULK1*	NIX & Autophagy Activating Kinase 1
TFAM	Transcription Factor A, mitochondrial
PPARGC1A & *PPARGC1B*	PPAR-γ Co-activator α & β
MAP1LC3B	Microtubule Associated Protein 1 Light Chain 3 Beta
BECN1	Beclin 1
USP30	Ubiquitin Specific Peptidase 30
OPA1	OPA1 Mitochondrial Dynamin Like GTPase
House Keeping Genes	
B2M	Beta-2-microglobulin
RPLPO	Ribosomal Protein Lateral Stalk Subunit P0

GATA3 (Th2; $p < 0.001$; **Figures 1E, F**) and RORγt (Th17; $p < 0.01$; **Figures 1G, H**).

Alcohol Promotes CD4+ T Cell Differentiation Towards a Pro-Inflammatory Phenotype

To test the impact of alcohol on CD4+ T cell differentiation, naïve CD4+ T cells were differentiated in the presence of 50 mM ethanol under Th1-promoting conditions. There was a significant interaction observed between DIFF and EtOH on both Tbet ($p < 0.05$) and FOXP3-expressing ($p < 0.01$) CD4+ T cells. *Post hoc* pairwise comparisons indicated that differentiation of CD4+ T cells significantly increased Tbet-expressing CD4+ T cells compared to undifferentiated naïve CD4+ T cells ($p < 0.0001$) and ethanol increased expression of Tbet within differentiated CD4+ T cells ($p = 0.001$; **Figures 2A, B**). Also, *post hoc* pairwise comparisons indicated that differentiation significantly increased FOXP3-expressing CD4+ T cells compared to undifferentiated naïve CD4+ T cells ($p < 0.0001$) and ethanol decreased expression of FOXP3 in differentiated CD4+ T cells ($p = 0.001$; **Figures 2C, D**). Ethanol increased the Tbet : FOXP3 ratio ($p = 0.004$; **Figure 2E**) in differentiated CD4+ T cells. No significant differences were detected between undifferentiated Naïve and EtOH-treated groups.

Alcohol Increases Glycolysis and Glycolytic Capacity in Differentiating CD4+ T Cells

Glycolysis was assessed to understand if metabolism played a role in the ethanol-mediated increase of Tbet-expressing CD4+ T cells. There was a significant interaction observed between DIFF and EtOH on CD4+ T cell GLUT1 expression ($p < 0.01$), 2-NBDG uptake ($p < 0.05$), glycolysis ($p < 0.0001$) and glycolytic capacity ($p < 0.0001$). *Post hoc* pairwise comparisons indicated that differentiation of CD4+ T cells significantly increased GLUT1 expression ($p < 0.0001$; **Figures 3A, B**), glucose uptake (2-NBDG; $p = 0.0002$; **Figures 3C, D**), glycolysis ($p < 0.0001$; **Figures 3E, F**) and glycolytic capacity ($p < 0.0001$; **Figure 3G**) compared to undifferentiated naïve CD4+ T cells. Also, *post hoc* pairwise comparisons indicated that ethanol increased GLUT1 expression ($p = 0.005$; **Figure 3B**), glucose uptake ($p = 0.014$; **Figure 3D**), glycolysis ($p = 0.005$; **Figure 3F**) and glycolytic capacity ($p < 0.0001$; **Figure 3G**) within differentiated CD4+ T cells. No significant differences were detected between undifferentiated naïve and naïve EtOH groups.

Inhibition of Glycolysis With 2-Deoxyglucose (2-DG) Prevents the Alcohol-Mediated Increase in CD4+ T Cell Tbet-Expression

To further understand the importance of glycolysis on the ethanol-mediated increase of Tbet-expressing CD4+ T cells, CD4+ T cells were exposed with ethanol in the presence of the glycolytic inhibitor 2-deoxyglucose (2-DG). The was a significant interaction observed between DIFF, EtOH, and 2-DG on Tbet-expressing CD4+ T cells ($p < 0.05$) and a significant interaction observed between DIFF and EtOH on FOXP3-expressing CD4+ T cells ($p < 0.05$). *Post hoc* pairwise comparisons indicated that differentiation increased Tbet ($p < 0.0001$; **Figures 4A, B**) and FOXP3-expressing ($p < 0.0001$; **Figures 4C, D**) CD4+ T cells

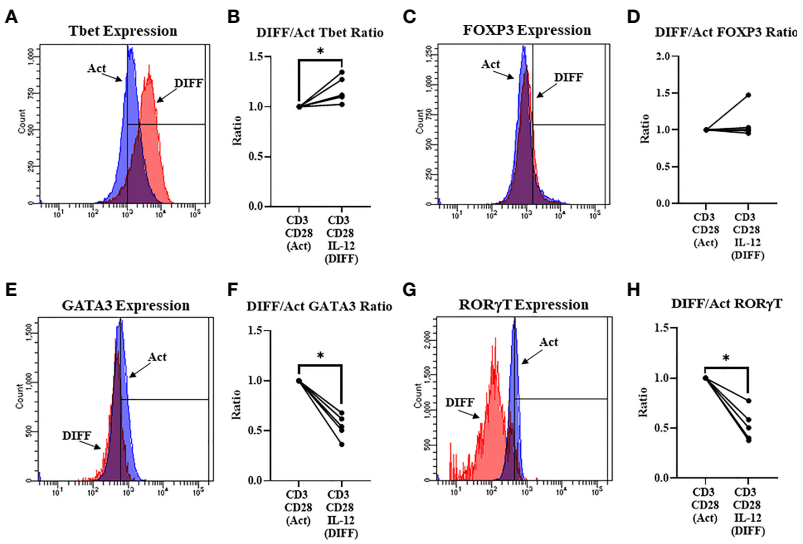

FIGURE 1 | Differentiation (Anti-CD3, Anti-CD28, & IL-12) of naïve CD4+ T cells. **(A)** Representative FACS histograms of Tbet expression in Act and DIFF CD4+ T cells **(B)** IL-12 increased the ratio of CD4+ T cells expressing Tbet. **(C)** Representative FACS histograms of FOXP3 expression in Act and DIFF CD4+ T cells. **(D)** IL-12 had no effect on CD4+ T cells expressing FOXP3. **(E)** Representative FACS histograms of GATA3 expression in Act and DIFF CD4+ T cells. **(F)** IL-12 decreased the ratio of CD4+ T cells expressing GATA3. **(G)** Representative FACS histograms of RORgT expression in Act and DIFF CD4+ T cells. **(H)** IL-12 decreased the ratio of CD4+ T cells expressing RORgT. Act, Activation; DIFF, Differentiation. Data are average values for 3 independent experiments using CD4+ T cells from 5 donors. Significant differences ($p<0.05$) were detected using a paired T-test. *$p \leq 0.05$.

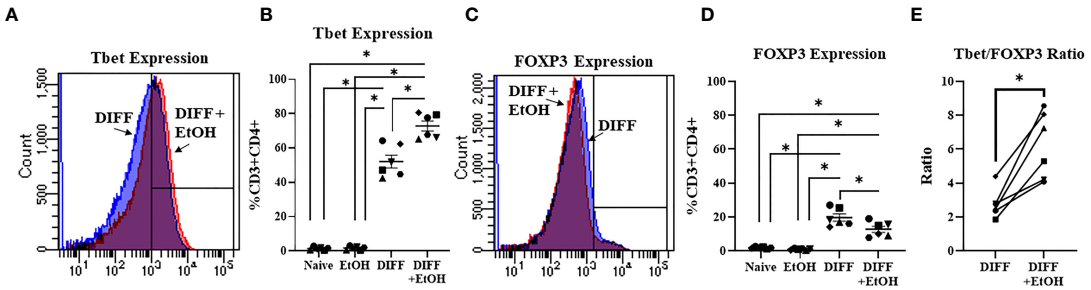

FIGURE 2 | Effect of ethanol on CD4+ T cell differentiation. **(A)** Representative FACS histograms of Tbet expression in DIFF and DIFF + EtOH CD4+ T cells. **(B)** Ethanol increased percent of CD4+ Tbet-expressing cells. **(C)** Representative FACS histograms of FOXP3 expression in DIFF and DIFF + EtOH CD4+ T cells. **(D)** Ethanol decreased percent expression of FOXP3 in CD4+ T cells. **(E)** Ethanol increased the Tbet/FOXP3 ratio in differentiated CD4+ T cells. Naïve = undifferentiated and no ethanol treatment, EtOH = undifferentiated and ethanol-treated, DIFF = differentiated and no ethanol treatment, and DIFF + EtOH = differentiated and ethanol-treated. Data are average values for 3 independent experiments using CD4+ T cells from 6 donors expressed as mean ± SEM. Significant differences ($p<0.05$) were determined by repeated measures 2-way ANOVA (Panels **B, D**) and paired T-tests (Panel **E**).*$p \leq 0.05$.

compared to undifferentiated naïve CD4+ T cells. Ethanol increased Tbet-expression within differentiated CD4+ T cells ($p = 0.002$; **Figures 4A,B**). 2-DG prevented the ethanol-induced increase in Tbet-expression in differentiated CD4+ T cells (**Figures 4A, B**). Ethanol decreased CD4+ T cell FOXP3 expression within differentiated CD4+ T cells ($p = 0.024$; **Figures 4C, D**) irrespective of 2-DG treatment ($p = 0.012$; **Figures 4C, D**). No significant differences were detected between undifferentiated naïve and naïve EtOH groups.

Alcohol Impaired Differentiated CD4+ T Cell Mitochondrial Function

In order to understand the ethanol-mediated decrease in FOXP3-expressing CD4+ T cells, mitochondrial parameters were assessed using the Mitostress test. Ethanol decreased maximal respiration ($p = 0.049$; **Figures 5A, B**) and increased OCR-linked proton leak within the differentiated CD4+ T cells ($p = 0.022$; **Figure 5C**). Ethanol decreased coupling efficiency ($p = 0.036$; **Figure 5D**), and OCR-linked ATP production

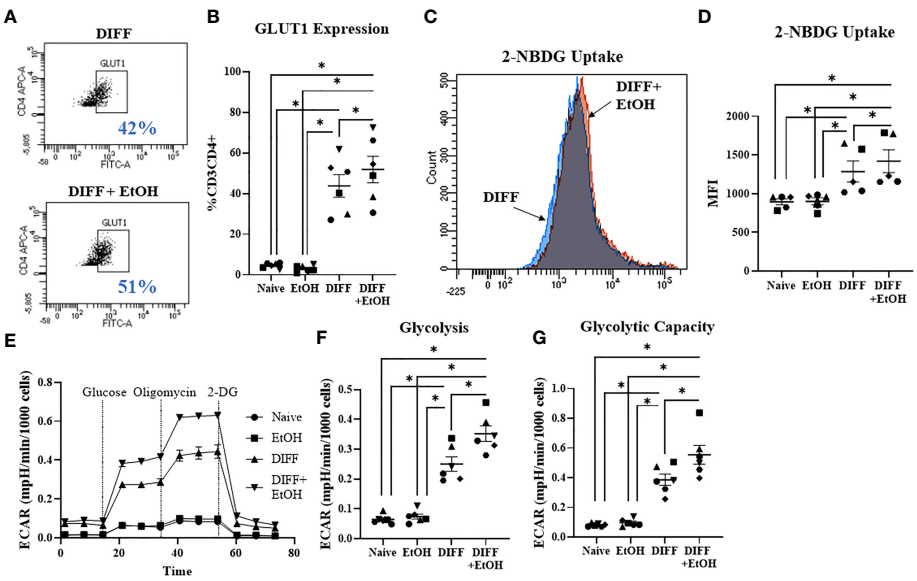

FIGURE 3 | Effect of ethanol on CD4+ T cell glucose metabolism. **(A)** Representative FACS plots of GLUT1 expression in DIFF and DIFF + EtOH CD4+ T cells. **(B)** Ethanol increased CD4+ T cell GLUT1 expression. **(C)** Representative FACS histograms of 2-NBDG uptake in DIFF and DIFF + EtOH CD4+ T cells. **(D)** Ethanol increased glucose uptake within differentiated CD4+ T cells. **(E)** All experimental groups were analyzed using the Glycolytic Stress test. Ethanol increased glycolysis **(F)** and glycolytic capacity **(G)** within differentiated groups. MFI = mean fluorescent intensity, 2-NBDG = 2-Deoxy-2-[(7-nitro-2,1,3-benzoxadiazol-4-yl)amino]-D-glucose, ECAR = extracellular acidification rate, Naïve = undifferentiated and no ethanol treatment, EtOH = undifferentiated and ethanol-treated, DIFF = differentiated and no ethanol treatment, and DIFF + EtOH = differentiated and ethanol-treated. Data represents average values using CD4+ T cells from 6 donors expressed as mean ± SEM. Significant differences ($p<0.05$) were determined by repeated measures 2-way ANOVA. *$p \leq 0.05$.

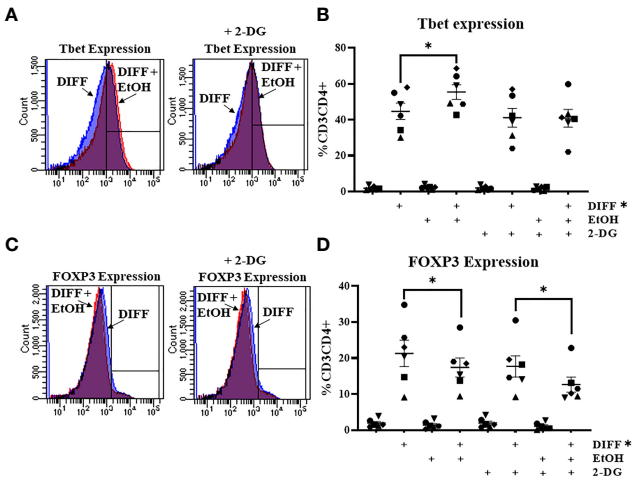

FIGURE 4 | Effect of 2-deoxyglucose (2-DG) on CD4+ T cells. **(A)** Representative FACS histograms plots of Tbet expression in DIFF, DIFF + EtOH, and DIFF+ EtOH + 2-DG CD4+ T cells. **(B)** The addition of 0.5 mM 2-deoxyglucose (2-DG) prevents the ethanol-mediated increase of Tbet-expressing CD4+ T cells. **(C)** Representative FACS histograms plots of FOXP3 expression in DIFF, DIFF + EtOH, and DIFF+ EtOH + 2-DG CD4+ T cells. **(D)** The addition of 0.5 mM 2-deoxyglucose (2-DG) did not alter the ethanol-mediated decrease of FOXP3-expressing CD4+ T cells. Naïve = undifferentiated and no ethanol treatment, EtOH = undifferentiated and ethanol-treated, DIFF = differentiated and no ethanol treatment, and DIFF + EtOH = differentiated and ethanol-treated. Data represents average values using CD4+ T cells from 6 donors expressed as mean ± SEM. Significant differences ($p<0.05$) were determined by repeated measures 3-way ANOVA. *Post-hoc* analysis was done using Sidaks multiple comparison test. *$p \leq 0.05$.

($p = 0.014$; **Figure 5E**) within the differentiated CD4+ T cells. Ethanol decreased Bioenergetic Health Index (BHI; $p = 0.04$; **Figure 5F**) and decreased the OCR/ECAR ratio ($p = 0.01$; **Figure 5G**) within differentiated CD4+ T cells.

Alcohol Impaired CD4+CD25+ T Cell Mitochondrial Function

To further understand the ethanol-mediated decrease in mitochondrial function within CD4+ T cells, cells were sorted with the human CD4+CD25+ regulatory T cell isolation kit to enrich Treg (CD4+CD25+ T cells) and negatively select CD4+CD25- Th1-enriched T cells. Ethanol increased OCR-linked proton leak in enriched Treg cells ($p = 0.0313$; **Figures 6A, B**). Ethanol decreased coupling efficiency ($p = 0.0031$; **Figure 6C**) and OCR-linked ATP production ($p = 0.044$; **Figure 6D**) in enriched Treg cells. There were no observed significant effects of ethanol on mitochondrial parameters within enriched Th1 cells. There were no differences for BHI or OCR/ECAR ratio observed between the enriched populations (**Supplementary Figure 6**)

Alcohol Increased CD4+ T Cell Mitochondrial Volume

Since mitochondrial function was impaired within ethanol-treated CD4+ T cells, mitochondrial content was assessed to determine any further potential ethanol-mediated dysfunction. There was a significant interaction observed between DIFF and EtOH on CD4+ T cell mitochondrial content ($p < 0.01$). *Post hoc* pairwise comparisons indicated that differentiation increased mean fluorescence intensity (MFI) of MitoTracker Deep Red within CD4+ T cells compared to undifferentiated naïve cells ($p < 0.0001$; **Figures 7A, B**) and ethanol increased MitoTracker MFI within differentiated CD4+ T cells ($p = 0.004$; **Figures 7A, B**). To determine if both Th1 and Treg cells are contributing to this ethanol-mediated increase in mitochondrial content, enriched CD4+ subsets were stained. Ethanol increased MitoTracker MFI in enriched Treg cells ($p = 0.038$; **Figures 7C, D**), with no observed significant increase in enriched Th1 cells ($p = 0.062$; **Figures 7E, F**).

Alcohol and Differentiation Altered CD4+ T Cell Mitochondrial Gene Expression

Gene expression important for mitochondrial repair and mitophagy were assessed to determine the potential impact of ethanol on CD4+ T cell mitochondrial homeostasis. There was a main effect of DIFF to increase gene expression important for autophagosome formation (*ATG5*, $p = 0.01$; *ATG13*, $p = 0.04$; *MAP1LC3B*, $p = 0.01$; *BECN1*, $p = 0.01$; *BNIP3L*, $p = 0.05$; *ULK1*, $p = 0.002$; **Figure 8**), mitochondrial biogenesis (*TFAM*, $p = 0.03$; **Figure 8**), and mitochondrial fission (*MFF*, $p = 0.02$; **Figure 8**), and decrease *PPARGC1B* ($p = 0.005$; **Figure 8**) expression. There was a main effect of DIFF and a main effect of EtOH to increase gene expression important for mitochondrial fusion (*MFN2*, DIFF: $p = 0.001$, EtOH: $p = 0.01$; *OPA1*: DIFF: $p = 0.003$, EtOH: $p = 0.03$; **Figure 8**). There was a main effect of EtOH to increase gene expression important for mitophagy (*PINK1*, $p = 0.01$; **Figure 8**) and decrease expression important for autophagosome formation (*ATG7*, $p = 0.04$; **Figure 8**). (Summarized in **Figure 9**). No significant interaction effects were observed.

DISCUSSION

At-risk alcohol use promotes systemic inflammation by increasing differentiation of pro-inflammatory immune cells, such as Th1 and Th17 CD4+ T cells. These studies sought to determine whether ethanol-mediated changes in CD4+ T cell immunometabolism regulate differentiation. Results indicate that 50 mM ethanol, observed in high-risk drinkers and translates to a blood alcohol concentration (BAC) of 0.23 g/dl, shifts differentiation of activated naïve CD4+ T cells toward pro-inflammatory Th1 and away from immunosuppressive Treg cells. This shift in phenotype appears to be dependent on ethanol-mediated impaired bioenergetics that is associated with increased Treg mitochondrial content and dysregulation of genes implicated in mitochondrial maintenance and mitophagy.

Functional bioenergetics are crucial for CD4+ T cell differentiation. Numerous studies have demonstrated that dysregulation of either glycolysis or oxidative phosphorylation impairs CD4+ T cell differentiation (32–37). In this study, the *in*

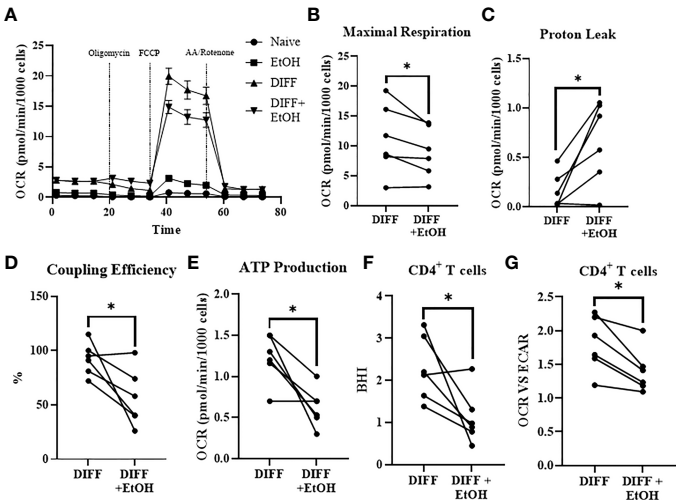

FIGURE 5 | Impact of ethanol on CD4+ T cell mitochondrial function. **(A)** All experimental groups were analyzed using the Mitostress test. **(B)** Ethanol decreased maximal respiration. **(C)** Ethanol increased mitochondrial proton leak. **(D)** Ethanol decreased coupling efficiency and **(E)** ATP production. Ethanol decreased **(F)** BHI and **(G)** OCR/ECAR ratio in differentiated CD4+ T cells. OCR= oxygen consumption rate; FCCP, Carbonyl cyanide-p-trifluoromethoxyphenylhydrazone; AA, Antimycin; BHI, Bioenergetic Health Index; DIFF, differentiated and no ethanol treatment, and DIFF + EtOH, differentiated and ethanol-treated. Data represents CD4+ T cells from 6 donors with lines connecting values of same donors. Significance differences ($p \leq 0.05$) were determined by paired T-tests. *$p \leq 0.05$.

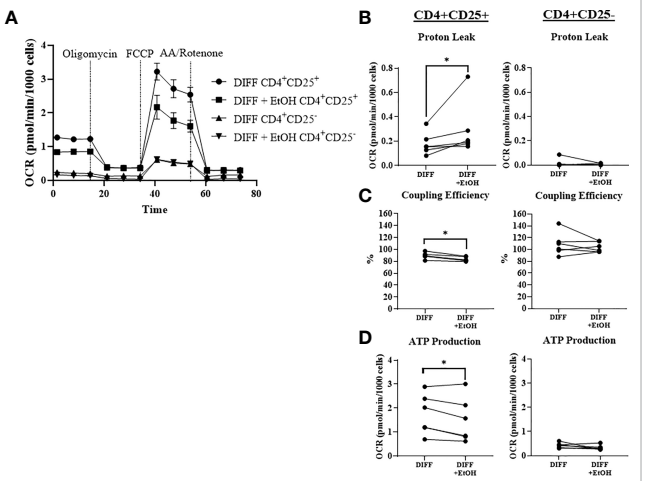

FIGURE 6 | Mitochondrial function within CD4+ CD25+ (enriched Treg) and CD4+ CD25- (enriched Th1) CD4+ subsets. **(A)** Enriched Treg and Th1 cells from DIFF and DIFF + EtOH groups were analyzed using Mitostress test. **(B)** Ethanol increased proton leak in enriched Treg, but not enriched Th1 cells. **(C)** Ethanol decreased coupling efficiency in enriched Treg, but not enriched Th1. **(D)** Ethanol decreased ATP production in enriched Treg, but not enriched Th1 cells. OCR= oxygen consumption rate. FCCP = Carbonyl cyanide-p-trifluoromethoxyphenylhydrazone. AA = Antimycin **(A)** DIFF = differentiated cells and no ethanol treatment, and DIFF + EtOH = differentiated and ethanol-treated. Data represents CD4+ T cells from 6 donors with lines connecting values of same donors. Significance differences ($p \leq 0.05$) were determined by paired T-tests and Wilcoxin test (Treg – proton leak). *$p \leq 0.05$.

vitro ethanol-mediated dysregulation of CD4+ T cell differentiation under Th1-promoting conditions, by increasing Tbet-expressing and decreasing FOXP3-expressing CD4+ T cells, recapitulated previously reported literature that *Tbet : FOXP3* ratio was higher in CD4+ T cells isolated from the colon of ethanol-administered mice (16). Treg CD4+ T cells produce anti-inflammatory cytokines IL-10, IL-35, and TGF-β (48). Decreased IL-10 production promotes Th1 differentiation, as IL-10 is a critical negative regulator of Th1 differentiation (49). Thus, an ethanol-mediated decrease in Treg differentiation could potentially result in decreased anti-inflammatory T cells, anti-inflammatory cytokine production, and promote proinflammatory Th1 differentiation.

Ethanol increased CD4+ T cell GLUT1 expression, glucose uptake, and glycolytic rate. GLUT1 is the main glucose transporter expressed by T cells (50). It has been shown that increased GLUT1 expression on activated T cells correlates with increased effector function and IFN-γ production, one of the predominant Th1 cytokines (50). Further, high glycolytic rates are associated with increased permissiveness of HIV viral infection of CD4+ T cells (51, 52). This highlights a possible consequence of ethanol-mediated increases in GLUT1-expressing Th1 cells to increase HIV replication in viral reservoirs, and could potentially contribute to the observed increase in viral replication that was observed in SIV-infected chronic binge alcohol (CBA)-administered rhesus macaques (10–13). Our results indicate that inhibition of glycolysis with 2-DG, prevented the ethanol-mediated increase in Th1 differentiation without altering FOXP3-expressing CD4+ T cells. These findings agree with previous reports that Tregs do not rely on glycolysis for their differentiation and function (28–30). Thus, our results indicate that ethanol increases Th1 differentiation by promoting glycolysis in differentiated CD4+ T cells.

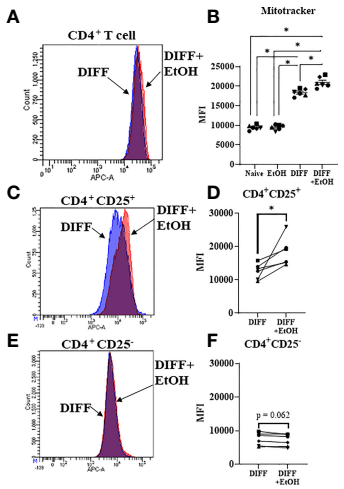

FIGURE 7 | Mitochondrial volume of CD4+ T cells. **(A)** Representative FACS histogram of Mitotracker Deep Red staining of DIFF and DIFF + EtOH CD4+ T cells. **(B)** Ethanol increased the MFI of Mitotracker Deep Red in differentiated CD4+ T cells. **(C)** Representative FACS histogram of Mitotracker Deep Red staining of DIFF and DIFF + EtOH CD4+ CD25+ (enriched Treg) cells. **(D)** Ethanol increased the MFI of Mitotracker Deep Red in enriched Treg cells. **(E)** Representative FACS histogram of Mitotracker Deep Red staining of DIFF and DIFF + EtOH CD4+ CD25- (enriched Th1) cells. **(F)** There were no significant differences in MFI of enriched Th1 cells. MFI = mean fluorescent intensity, Naïve = undifferentiated and no ethanol treatment, EtOH = undifferentiated and ethanol-treated, DIFF = differentiated cells and no ethanol treatment, and DIFF + EtOH = differentiated and ethanol-treated. Data represents average values using PBMCS from 6 donors expressed as mean ± SEM. Significant differences ($p<0.05$) were determined by repeated measures 2-way ANOVA (Panel **B**)and paired T-tests (Panels **D, F**). *$p \leq 0.05$.

We observed that ethanol decreased CD4+ T cell maximal respiration, coupling efficiency, ATP production, and increased proton leak, indicative of impaired mitochondrial function. These changes in mitochondrial respiration were observed in enriched Treg T cells. Treg differentiation is dependent on mitochondrial function, and the ethanol-mediated impairment of oxidative phosphorylation could partially be responsible for the decrease in Treg CD4+ T cells caused by ethanol. Ethanol increased mitochondrial volume in enriched Treg cells, without significantly altering Th1 cell mitochondrial content. An increase in mitochondrial content has been associated with an inability to repair dysfunctional mitochondria by autophagy/mitophagy and an increase in cell death (41, 43, 53–55). Also, mitochondrial swelling due to ethanol-induced endoplasmic reticulum stress could be responsible for an increase in mitochondrial volume (56). Based on previous literature (41) and results from this study, we postulate that the increase in mitochondrial volume is due to dysfunctional mitochondrial repair and

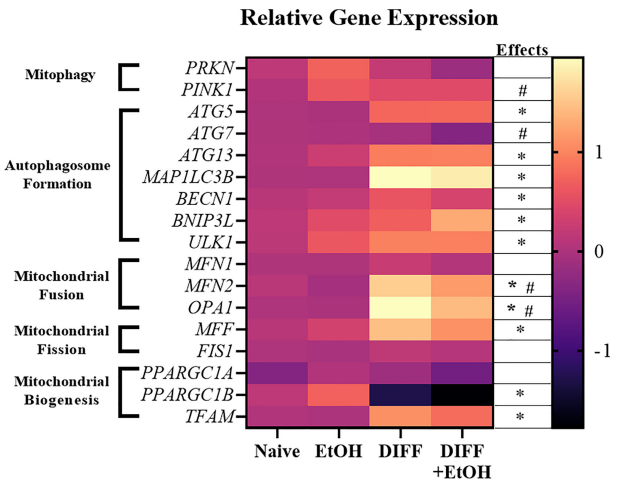

FIGURE 8 | Heat map showing increased and decreased gene expression in response to ethanol or differentiation. Data are normalized as fold change to naïve CD4+ T cell gene expression and represents data using PBMCs from 6 matched donors. Naïve = undifferentiated and no ethanol treatment, EtOH = undifferentiated and ethanol-treated, DIFF = differentiated cells and no ethanol treatment, and DIFF + EtOH = differentiated and ethanol-treated. * differentiation main effect ($p \leq 0.05$). # ethanol main effect ($p \leq 0.05$) as determined by repeated measures 2-way ANOVA.

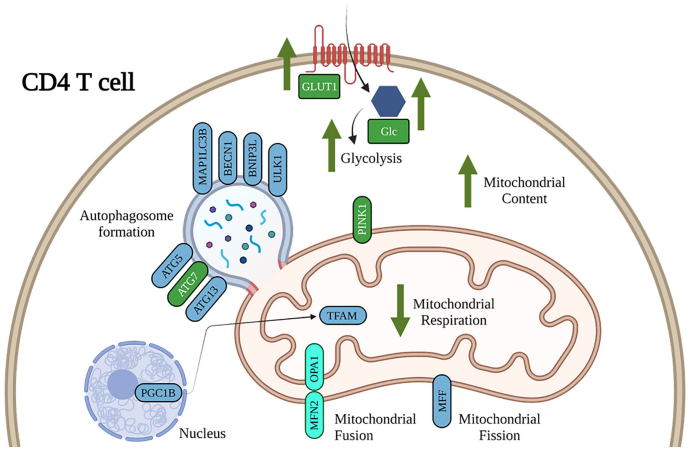

FIGURE 9 | Working model of the impact of ethanol on CD4+ T cell energy metabolism and mitochondrial dynamics. Our results show that ethanol increases CD4+ T cell glycolytic processes, decreases mitochondrial respiration, and dysregulates gene expression important for CD4+ T cell mitochondrial maintenance and mitophagy. Blue denotes gene expression affected by DIFF and green denote gene expression affected by EtOH. Cyan denotes gene expression affected by both DIFF and EtOH.

mitophagy, suggesting an inability to properly eliminate dysfunctional mitochondria.

To explore potential mechanisms underlying increased mitochondrial content, CD4+ T cell expression of genes involved in mitophagy was assessed. Ethanol increased expression of *PINK1*, important for mitophagy, and decreased expression of *ATG7*, important for autophagosome formation, within differentiated CD4+ T cells. ATG7 is critical for both the survival and development of T cells (57). Further, it was shown that ATG7-deficient T cells had increased mitochondrial content, ROS production, and an imbalanced expression of pro- and anti-apoptotic proteins leading to increased T cell death. We propose that these changes in mitochondrial gene expression may indicate that the ethanol-mediated impairments in mitophagy, specifically autophagosome formation, potentially leads to Treg cell death.

This study has some limitations, as it was performed using immune cells from blood bank donors to identify ethanol's potential impact on CD4+ T cell immunometabolism and differentiation, which no study to date has addressed. Future studies are warranted to translate these findings to people with at-risk alcohol use. This study used only naïve CD4+ T cells rather than PBMCs, and has not assessed functional measures including CD4+ T cell cytokine production to complement the transcription factor expression. MACS sorting was used to examine CD4+ subsets, which only moderately enriched for Tregs and Th1 CD4+ subsets, and it was not feasible to obtain homogenous Treg and Th1 populations. Ongoing studies will determine the functional implications of the observed results and whether it mechanistically contributes to increased HIV viral replication. Further, there is a gap in the literature on whether alcohol dysregulates mTOR or AMPK pathways in T cells. mTOR in the absence of alcohol is involved in differentiation of more pro-inflammatory CD4+ T cell subsets and AMPK inhibition promotes Treg differentiation (29–32). Our group and others have shown that alcohol-administration impairs mTOR signaling in skeletal muscle and heart (58–60) and AMPK signaling in human alveolar macrophages and heart (61, 62). If alcohol impairs mTOR or AMPK signaling in T cells to the same extent as observed in other tissues, we would expect to see impaired Th1 and Treg differentiation, but currently we only see decreased FOXP3-expressing CD4+ T cells (Treg) within our acute *in vitro* ethanol model. Further understanding of these ethanol-related impairments, as well as addressing the limitations of the study outlined above will be addressed in future studies.

Our findings advance our understanding of the mechanisms underlying ethanol-mediated disruption of differentiation of pro- and anti-inflammatory T cells (**Figure 9**). Our study is the first to show that alcohol-mediated shifts in T cell subsets were associated with changes in immune cell bioenergetics. We also show that the observed mitochondrial dysfunction in Tregs was associated with increased mitochondrial content and dysregulated expression of genes implicated in mitophagy and autophagosome formation. Future studies are warranted to systematically investigate whether strategies to maintain immunometabolic homeostasis can ameliorate alcohol-mediated proinflammatory shifts of CD4+ T cells. This will provide evidence for potential lifestyle or therapeutic interventions to improve T cell immunometabolism and alleviate risk and progression of autoimmune or viral diseases in people with at-risk alcohol use (63).

DATA AVAILABILITY STATEMENT

The original contributions presented in the study are included in the article/**Supplementary Material**. Further inquiries can be directed to the corresponding author.

AUTHOR CONTRIBUTIONS

PMM performed the experiments; PMM, DL, DW, LS, RS, and PEM provided intellectual discussion. PMM, LS, RS, and PEM designed the experiments. PMM, LS, and RS wrote the manuscript. All authors critically revised and approved the manuscript.

FUNDING

This research was supported by the National Institute for Health T32AA007577 and P60AA009803.

ACKNOWLEDGMENTS

The authors would like to thank the research staff at the LSUHSC Comprehensive Alcohol-HIV/AIDS Research Center for technical assistance (Connie Porretta, BS, Bryant Autin, MS; Jessica Miller, MS). We thank the Cellular Immunology and Immune Metabolism Core at the Louisiana Cancer Research Center (Grant 5P30GM114732-05 NIH/NIGMS) for access to the Seahorse XFe96 equipment, and Dorota Wyczechowska, PhD, for outstanding technical support. **Figure 9** was created using BioRender.com.

SUPPLEMENTARY MATERIAL

The Supplementary Material for this article can be found online at: https://www.frontiersin.org/articles/10.3389/fimmu.2022.839390/full#supplementary-material

Supplementary Figure 1 | IL-12 promotes FOXP3 expression similar to TGF-beta + IL-2 in CD3/CD28 stimulated CD4+ T cells.

Supplementary Figure 2 | Gating strategy used for assessment of master transcription factor expression in CD4+ T cells.

Supplementary Figure 3 | Moderate enrichment of CD25+FOXP3+ and CD25-Tbet+ CD4 T cells by MACS sorting. **(A)** CD4+CD25+ T cells were enriched with FOXP3+ Cells. **(B)** CD4+CD25- T cells were enriched with Tbet+ Cells.

Supplementary Figure 4 | Gating strategy used for assessment of 2-NBDG uptake in CD4+ T cells.

Supplementary Figure 5 | Gating strategy used for assessment of Mitotracker Deep Red mitochondrial stain in CD4+ T cells.

Supplementary Figure 6 | Bioenergetic Health Index (BHI) and Oxygen Consumption Rate (OCR)/Extracellular Acidification Rate (ECAR) of enriched Treg and Th1 subsets. **(A)** There were no significant differences observed in BHI between DIFF and DIFF + EtOH of enriched Treg or Th1 subsets. **(B)** There were no significant differences observed in OCR/ECAR between DIFF and DIFF + EtOH of enriched Treg of Th1 subsets. Paired T test.

REFERENCES

1. Durvasula R, Miller TR. Substance Abuse Treatment in Persons With HIV/AIDS: Challenges in Managing Triple Diagnosis. *Behav Med* (2014) 40(2):43–52. doi: 10.1080/08964289.2013.866540
2. Molina PE, Simon L, Amedee AM, Welsh DA, Ferguson TF. Impact of Alcohol on HIV Disease Pathogenesis, Comorbidities and Aging: Integrating Preclinical and Clinical Findings. *Alcohol and Alcoholism* (2018) 53(4):439–47. doi: 10.1093/alcalc/agy016
3. Williams EC, Hahn JA, Saitz R, Bryant K, Lira MC, Samet JH. Alcohol Use and Human Immunodeficiency Virus (HIV) Infection: Current Knowledge, Implications, and Future Directions. *Alcohol Clin Exp Res* (2016) 40 (10):2056–72. doi: 10.1111/acer.13204
4. Grant BF, Goldstein RB, Saha TD, Chou SP, Jung J, Zhang H, et al. Epidemiology of *DSM-5* Alcohol Use Disorder: Results From the National Epidemiologic Survey on Alcohol and Related Conditions III. *JAMA Psychiatry* (2015) 72(8):757–66. doi: 10.1001/jamapsychiatry.2015.0584
5. Wang HJ, Zakhari S, Jung MK. Alcohol, Inflammation, and Gut-Liver-Brain Interactions in Tissue Damage and Disease Development. *World J Gastroenterol* (2010) 16(11):1304–13. doi: 10.3748/wjg.v16.i11.1304
6. Caslin B, Mohler K, Thiagarajan S, Melamed E. Alcohol as Friend or Foe in Autoimmune Diseases: A Role for Gut Microbiome? *Gut Microbes* (2021) 13 (1):1916278. doi: 10.1080/19490976.2021.1916278
7. Gurung P, Young BM, Coleman RA, Wiechert S, Turner LE, Ray NB, et al. Chronic Ethanol Induces Inhibition of Antigen Specific CD8+ But Not CD4+ Immunodominant T Cell Responses FollowingInoculation. *J Leukoc Biol* (2009) 85:34–43. doi: 10.1189/jlb.0208101
8. Meyerholz DK, Edsen-Moore M, McGill J, Coleman RA, Cook RT, Legge KL. Chronic Alcohol Consumption Increases the Severity of Murine Influenza Virus Infections. *J Immunol* (2008) 181:641–8. doi: 10.4049/jimmunol.181.1.641
9. Mason CM, Dobard E, Zhang P, Nelson S. Alcohol Exacerbates Murine Pulmonary Tuberculosis. *Infect Immun* (2004) 72:2556–63. doi: 10.1128/IAI.72.5.2556-2563.2004
10. Bagby GJ, Stoltz DA, Zhang P, Kolls JK, Brown J, Bohm RPJr, et al. The Effect of Chronic Binge Ethanol Consumption on the Primary Stage of SIV Infection in Rhesus Macaques. *Alcohol Clin Exp Res* (2003) 27(3):495–502. doi: 10.1097/01.ALC.0000057947.57330.BE
11. Bagby GJ, Zhang P, Purcell JE, Didier PJ, Nelson S. Chronic Binge Ethanol Consumption Accelerates Progression of Simian Immunodeficiency Virus Disease. *Alcohol Clin Exp Res* (2006) 30(10):1781–90. doi: 10.1111/j.1530-0277.2006.00211.x
12. Poonia B, Nelson S, Bagby GJ, Veazey RS. Intestinal Lymphocyte Subsets and Turnover Are Affected by Chronic Alcohol Consumption: Implications for SIV/HIV Infection. *J Acquir Immune Defic Syndr* (2006) 41(5):537–47. doi: 10.1097/01.qai.0000209907.43244.ee
13. Veazey RS, Amedee A, Wang X, Kaack BM, Porretta C, Dufour J, et al. Chronic Binge Alcohol Administration Increases Intestinal T-Cell Proliferation and Turnover in Rhesus Macaques. *Alcohol Clin Exp Res* (2015) 39:1373–9. doi: 10.1111/acer.12784
14. Azizov V, Dietel K, Steffen F, Dürholz K, Meidenbauer J, Lucas S, et al. Ethanol Consumption Inhibits T_{FH} Cell Responses and the Development of Autoimmune Arthritis. *Nat Commun* (2020) 11(1):1998. doi: 10.1038/s41467-020-15855-z
15. Neveu WA, Staitieh BS, Mills ST, Guidot DM, Sueblinvong V. Alcohol-Induced Interleukin-17 Expression Causes Murine Lung Fibroblast-To-Myofibroblast Transdifferentiation *via* Thy-1 Down-Regulation. *Alcohol Clin Exp Re* (2019) 43:1427–38. doi: 10.1111/acer.14110
16. Grumish EL, Armstrong AR, Voigt RM, Forsyth CB, Bishehsari F. Alcohol-Induced Immune Dysregulation in the Colon Is Diurnally Variable. *Visc Med* (2020) 36(3):212–9. doi: 10.1159/000507124
17. Pakpoor J, Goldacre R, Disanto G, Giovannoni G , Goldacre MJ. Alcohol Misuse Disorders and Multiple Sclerosis Risk. *JAMA Neurol* (2014) 71 (9):1188–9. doi: 10.1001/jamaneurol.2014.1795
18. Trkola A, Dragic T, Arthos J, Binley BM, Olson WC, Allaway GP, et al. CD4-Dependent, Antibody-Sensitive Interactions Between HIV-1 and Its Co-Receptor CCR-5. *Nature* (1996) 384:184–7. doi: 10.1038/384184a0
19. Endres MJ, Clapham PR, Marsh M, Ahuja A, Turner JD, McKnight A, et al. CD4-Independent Infection by HIV-2 Is Mediated by Fusin/Cxcr4. *Cell* (1996) 87(4):745–56. doi: 10.1016/S0092-8674(00)81393-8
20. Kumar B, Connors T, Farber D. Human T Cell Development, Localization, Function Throughout Life. *Immunity* (2018) 48(2):202–13. doi: 10.1016/j.immuni.2018.01.007

21. Zloza A, Al-Harthi L. Multiple Populations of T Lymphocytes are Distinguished by the Level of CD4 and CD8 Coexpression and Require Individual Consideration. *J Leukoc Biol* (2006) 79:4–6. doi: 10.1189/jlb.0805455
22. Cederbaum A. Alcohol Metabolism. *Clin Liver Dis* (2012) 16(4):667–85. doi: 10.1016/j.cld.2012.08.002
23. Zakhari S. Overview: How Is Alcohol Metabolized by the Body? *Alcohol Res Health* (2006) 29(4):245–54. doi: 10.1159/000095013
24. Hoek JB, Cahill A, Pastorino JG. Alcohol and Mitochondria: A Dysfunctional Relationship. *Gastroenterology* (2002) 122(7):2049–63. doi: 10.1053/gast.2002.33613
25. Abdulla A.-B. B. A. Review of the Effects of Alcohol on Carbohydrate Metabolism. *Alcohol and Alcoholism* (1977) 12(3):120–36. doi: 10.1093/oxfordjournals.alcalc.a044072
26. Levitt DE, Chalapati N, Prendergast MJ, Simon L, Molina PE. Ethanol-Impaired Myogenic Differentiation Is Associated With Decreased Myoblast Glycolytic Function. *Alcohol Clin Exp Res* (2020) 44(11):2166–76. doi: 10.1111/acer.14453
27. Bailey SM. A Review of the Role of Reactive Oxygen and Nitrogen Species in Alcohol-Induced Mitochondrial Dysfunction. *Free Radic Res* (2003) 37 (6):585–96. doi: 10.1080/1071576031000091711
28. Pearce EL, Poffenberger MC, Chang CH, Jones RG. Fueling Immunity: Insights Into Metabolism and Lymphocyte Function. *Science* (2013) 342 (6155):1242454. doi: 10.1126/science.1242454
29. MacIver NJ, Michalek RD, Rathmell JC. Metabolic Regulation of T Lymphocytes. *Annu Rev Immunol* (2013) 31:259–83. doi: 10.1146/annurev-immunol-032712-095956
30. Palmer C, Ostrowski M, Balderson B, Christian N, Crowe S. Glucose Metabolism Regulates T Cell Activation, Differentiation, and Functions. *Front Immunol* (2015) 6:1–6. doi: 10.3389/fimmu.2015.00001
31. Jones N, Cronin J, Dolton G, Panetti S, Schauenburg A, Galloway S, et al. Metabolic Adaptation of Human CD4+ and CD8+ T-Cells to T-Cell Receptor-Mediated Stimulation. *Front Immunol* (2017) 8:1516. doi: 10.3389/fimmu.2017.01516
32. Herzig S, Shaw RJ. AMPK: Guardian of Metabolism and Mitochondrial Homeostasis. *Nat Rev Mol Cell Biol* (2018) 19(2):121–35. doi: 10.1038/nrm.2017.95
33. Liu RT, Zhang M, Yang CL, Zhang P, Zhang N, Du T, et al. Enhanced Glycolysis Contributes to the Pathogenesis of Experimental Autoimmune Neuritis. *J Neuroinflammation* (2018) 15(1):51. doi: 10.1186/s12974-018-1095-7
34. Zheng Y, Collins SL, Lutz MA, Allen AN, Kole TP, Zarek PE, et al. A Role for Mammalian Target of Rapamycin in Regulating T Cell Activation Versus Anergy. *J Immunol* (2007) 178(4):2163–70. doi: 10.4049/jimmunol.178.4.2163
35. Kopf H, de la Rosa GM, Howard OM, Chen X. Rapamycin Inhibits Differentiation of Th17 Cells and Promotes Generation of FoxP3+ T Regulatory Cells. *Int Immunopharmacol* (2007) 7(13):1819–24. doi: 10.1016/j.intimp.2007.08.027
36. Delgoffe GM, Kole TP, Zheng Y, Zarek PE, Matthews KL, Xiao B, et al. The mTOR Kinase Differentially Regulates Effector and Regulatory T Cell Lineage Commitment. *Immunity* (2009) 30(6):832–44. doi: 10.1016/j.immuni.2009.04.014
37. Michalek RD, Gerriets VA, Jacobs SR, Macintyre AN, MacIver NJ, Mason EF, et al. Cutting Edge: Distinct Glycolytic and Lipid Oxidative Metabolic Programs Are Essential for Effector and Regulatory CD4+ T Cell Subsets. *J Immunol* (2011) 186(6):3299–303. doi: 10.4049/jimmunol.1003613
38. Abdallah MA, Singal AK. Mitochondrial Dysfunction and Alcohol-Associated Liver Disease: A Novel Pathway and Therapeutic Target. *Sig Transduct Target Ther* (2020) 5:26. doi: 10.1038/s41392-020-0128-8
39. Singal AK, Jampana SC, Weinman SA. Antioxidants as Therapeutic Agents for Liver Disease. *Liver Int* (2011) 31(10):1432–48. doi: 10.1111/j.1478-3231.2011.02604.x
40. Mansouri A, Gaou I, De Kerguenec C, Amsellem S, Haouzi D, Berson A, et al. An Alcoholic Binge Causes Massive Degradation of Hepatic Mitochondrial DNA in Mice. *Gastroenterology* (1999) 117(1):181–90. doi: 10.1016/s0016-5085(99)70566-4
41. Duplanty AA, Simon L, Molina PE. Chronic Binge Alcohol-Induced Dysregulation of Mitochondrial-Related Genes in Skeletal Muscle of Simian Immunodeficiency Virus-Infected Rhesus Macaques at End-Stage Disease. *Alcohol and Alcoholism* (2017) 52(3):298–304. doi: 10.1093/alcalc/agw107
42. Sadikot RT, Bedi B, Li J, Yeligar SM. Alcohol-Induced Mitochondrial DNA Damage Promotes Injurious Crosstalk Between Alveolar Epithelial Cells and Alveolar Macrophages. *Alcohol* (2019) 80:65–72. doi: 10.1016/j.alcohol.2018.08.006
43. Levitt DE, Ferguson TF, Primeaux SD, Zavala JA, Ahmed J, Marshall RH, et al. Skeletal Muscle Bioenergetic Health and Function in People Living With HIV: Association With Glucose Tolerance and Alcohol Use. *Am J Physiol Regul Integr Comp Physiol* (2021) 321(5):R781–90. doi: 10.1152/ajpregu.00197.2021
44. Bingol B, Sheng M. Mechanisms of Mitophagy: PINK1, Parkin, USP30 and Beyond. *Free Radic Biol Med* (2016) 100:210–22. doi: 10.1016/j.freeradbiomed.2016.04.015
45. Pahar B, Amedee AM, Thomas J, Dufour JP, Zhang P, Nelson S, et al. Effects of Alcohol Consumption on Antigen-Specific Cellular and Humoral Immune Responses to SIV in Rhesus Macaques. *J Acquir Immune Defic Syndr* (2013) 64 (4):332–41. doi: 10.1097/QAI.0b013e31829f6dca
46. Xiao B, Deng X, Zhou W, Tan EK. Flow Cytometry-Based Assessment of Mitophagy Using MitoTracker. *Front Cell Neurosci* (2016) 10:76. doi: 10.3389/fncel.2016.00076
47. Gautam N, Sankaran S, Yason JA, Tan KSW, Gascoigne NRJ. A High Content Imaging Flow Cytometry Approach to Study Mitochondria in T Cells: MitoTracker Green FM Dye Concentration Optimization. *Methods* (2018) 134(135):11–9. doi: 10.1016/j.ymeth.2017.11.015
48. Romano M, Fanelli G, Albany CJ, Giganti G, Lombardi G. Past, Present, and Future of Regulatory T Cell Therapy in Transplantation and Autoimmunity. *Front Immunol* (2019) 10:43. doi: 10.3389/fimmu.2019.00043
49. O'Garra A, Vieira P. T(H)1 Cells Control Themselves by Producing Interleukin-10. *Nat Rev Immunol* (2007) 7(6):425–8. doi: 10.1038/nri2097
50. Cretenet G, Clerc I, Matias M, Loisel S, Craveiro M, Oburoglu L, et al. Cell Surface Glut1 Levels Distinguish Human CD4 and CD8 T Lymphocyte Subsets With Distinct Effector Functions. *Sci Rep* (2016) 6:24129. doi: 10.1038/srep24129
51. Loisel-Meyer S, Swainson L, Craveiro M, Oburoglu L, Mongellaz C, Costa C, et al. Glut1-Mediated Glucose Transport Regulates HIV Infection. *Proc Natl Acad Sci USA* (2012) 109(7):2549–54. doi: 10.1073/pnas.1121427109
52. Kang S, Tang H. HIV-1 Infection and Glucose Metabolism Reprogramming of T Cells: Another Approach Toward Functional Cure and Reservoir Eradication. *Front Immunol* (2020) 11:572677. doi: 10.3389/fimmu.2020.572677
53. Scheibye-Knudsen M, Ramamoorthy M, Sykora P, Maynard S, Lin PC, Minor RK, et al. Cockayne Syndrome Group B Protein Prevents the Accumulation of Damaged Mitochondria by Promoting Mitochondrial Autophagy. *J Exp Med* (2012) 209(4):855–69. doi: 10.1084/jem.20111721
54. De Gaetano A, Gibellini L, Zanini G, Nasi M, Cossarizza A, Pinti M. Mitophagy and Oxidative Stress: The Role of Aging. *Antioxidants (Basel)* (2021) 10(5):794. doi: 10.3390/antiox10050794
55. Twig G, Shirihai OS. The Interplay Between Mitochondrial Dynamics and Mitophagy. *Antioxid Redox Signal* (2011) 14(10):1939–51. doi: 10.1089/ars.2010.3779
56. Ma L, Dong JX, Wu C, Li XY, Chen J, Zhang H, et al. Spectroscopic, Polarographic, and Microcalorimetric Studies on Mitochondrial Dysfunction Induced by Ethanol. *J Membr Biol* (2017) 250(2):195–204. doi: 10.1007/s00232-017-9947-0
57. Pua HH, Guo J, Komatsu M, He YW. Autophagy Is Essential for Mitochondrial Clearance in Mature T Lymphocytes. *J Immunol* (2009) 182 (7):4046–55. doi: 10.4049/jimmunol.0801143
58. Simon L, Jolley SE, Molina PE. Alcoholic Myopathy: Pathophysiologic Mechanisms and Clinical Implications. *Alcohol Res* (2017) 38(2):207–17.
59. Steiner JL, Lang CH. Alcohol Impairs Skeletal Muscle Protein Synthesis and mTOR Signaling in a Time-Dependent Manner Following Electrically Stimulated Muscle Contraction. *J Appl Physiol* (1985) 117(10):1170–9. doi: 10.1152/japplphysiol.00180.2014
60. Vary TC, Deiter G, Lantry R. Chronic Alcohol Feeding Impairs mTOR(Ser 2448) Phosphorylation in Rat Hearts. *Alcohol Clin Exp Res* (2008) 32(1):43–51. doi: 10.1111/j.1530-0277.2007.00544.x
61. Kaphalia L, Srinivasan MP, Kakumanu RD, Kaphalia BS, Calhoun WJ. Ethanol Exposure Impairs AMPK Signaling and Phagocytosis in Human

Alveolar Macrophages: Role of Ethanol Metabolism. *Alcohol Clin Exp Res* (2019) 43(8):1682–94. doi: 10.1111/acer.14131
62. Chen L, Wang F, Sun X, Zhou J, Gao L, Jiao Y, et al. Chronic Ethanol Feeding Impairs AMPK and MEF2 Expression and Is Associated With GLUT4 Decrease in Rat Myocardium. *Exp Mol Med* (2010) 42(3):205–15. doi: 10.3858/emm.2010.42.3.021
63. Pizzorno J. Mitochondria-Fundamental to Life and Health. *Integr Med (Encinitas)* (2014) 13(2):8–15.

Conflict of Interest: The authors declare that the research was conducted in the absence of any commercial or financial relationships that could be construed as a potential conflict of interest.

Publisher's Note: All claims expressed in this article are solely those of the authors and do not necessarily represent those of their affiliated organizations, or those of the publisher, the editors and the reviewers. Any product that may be evaluated in this article, or claim that may be made by its manufacturer, is not guaranteed or endorsed by the publisher.

frontiers | Frontiers in Immunology

MINI REVIEW
published: 12 May 2022
doi: 10.3389/fimmu.2022.865522

Hyaladherins May be Implicated in Alcohol-Induced Susceptibility to Bacterial Pneumonia

Kathryn M. Crotty[1,2†] *and Samantha M. Yeligar*[1,2*†]

[1] Department of Medicine, Division of Pulmonary, Allergy, Critical Care and Sleep Medicine, Emory University, Atlanta, GA, United States, [2] Atlanta Veterans Affairs Health Care System, Decatur, GA, United States

Although the epidemiology of bacterial pneumonia and excessive alcohol use is well established, the mechanisms by which alcohol induces risk of pneumonia are less clear. Patterns of alcohol misuse, termed alcohol use disorders (AUD), affect about 15 million people in the United States. Compared to otherwise healthy individuals, AUD increase the risk of respiratory infections and acute respiratory distress syndrome (ARDS) by 2-4-fold. Levels and fragmentation of hyaluronic acid (HA), an extracellular glycosaminoglycan of variable molecular weight, are increased in chronic respiratory diseases, including ARDS. HA is largely involved in immune-assisted wound repair and cell migration. Levels of fragmented, low molecular weight HA are increased during inflammation and decrease concomitant with leukocyte levels following injury. In chronic respiratory diseases, levels of fragmented HA and leukocytes remain elevated, inflammation persists, and respiratory infections are not cleared efficiently, suggesting a possible pathological mechanism for prolonged bacterial pneumonia. However, the role of HA in alcohol-induced immune dysfunction is largely unknown. This mini literature review provides insights into understanding the role of HA signaling in host immune defense following excessive alcohol use. Potential therapeutic strategies to mitigate alcohol-induced immune suppression in bacterial pneumonia and HA dysregulation are also discussed.

Keywords: hyaluronan, alcohol use disorder, pneumonia, hyaladherin, immunity

OPEN ACCESS

Edited by:
Jean-Michel Constantin, Hôpital Pitié-Salpêtrière, France

Reviewed by:
Gavin Arteel, University of Pittsburgh, United States

***Correspondence:**
Samantha M. Yeligar
syeliga@emory.edu

***ORCID:**
Kathryn M. Crotty
orcid.org/0000-0002-9461-4032
Samantha M. Yeligar
orcid.org/0000-0001-9309-0233

Specialty section:
This article was submitted to Nutritional Immunology, a section of the journal Frontiers in Immunology

Received: *30 January 2022*
Accepted: *15 April 2022*
Published: *12 May 2022*

Citation:
Crotty KM and Yeligar SM (2022) Hyaladherins May be Implicated in Alcohol-Induced Susceptibility to Bacterial Pneumonia. Front. Immunol. 13:865522. doi: 10.3389/fimmu.2022.865522

INTRODUCTION

Excessive alcohol use associated with alcohol use disorders (AUD) (1) is linked to over 5 million annual deaths globally (2), in part due to an increased risk of respiratory infections (3) and acute respiratory distress syndrome (ARDS) (4). Pneumonia is a serious respiratory infection that is caused by at least one of several opportunistic bacteria, viruses, or fungi. Nearly 44,000 people die

Abbreviations: AUD, alcohol use disorder; ARDS, acute respiratory distress syndrome; HA, hyaluronic acid; EtOH, ethanol; CD44, Cluster of differentiation 44; GM-CSF, Granulocyte-macrophage colony stimulating factor; PPARγ, peroxisome proliferator activating receptor gamma; CHI3L1, chitinase-3 like-protein-1; TSG-6, Tumor necrosis factor-stimulated gene-6; PTX3, pentatraxin 3; TLR, Toll-like receptor; IαI, inter-α-trypsin-inhibitor; LPS, lipopolysaccharide; TNFα, tumor necrosis factor α; RHAMM, Receptor for HA mediated motility; HABP, hyaluronic acid binding protein; TGFβ, transforming growth factor beta; NFκB, nuclear factor kappa B; PAR, protease-activated receptors; LYVE-1, lymphatic vessel endothelial cell receptor 1.

annually due to pneumonia in the United States, while another 1.5 million are hospitalized for pneumonia as a primary diagnosis (5). Ethanol (EtOH) impairs mucociliary clearance in the upper airway (6, 7) and diminishes innate immune defense in the lower airway by impairing the ability of alveolar macrophages (AM) to phagocytose pathogens (8–11), such as bacterial pneumonia (11, 12). Upon pneumonia-associated microbial evasion of host immune defense mechanisms in the upper airway, microbial culture in the lower airways causes pneumonia. This mini review focuses on molecular mechanisms, such as that of hyaluronic acid (HA), that may be implicated in increased susceptibility to bacterial pneumonia during acute and chronic EtOH use. Modulation of HA metabolism, signaling, and intracellular communication that impact cellular immune functions during bacterial pneumonia may pave the way for future investigations on how alterations in the extracellular matrix may be exacerbated by excessive alcohol use.

EXTRACELLULAR MATRIX IN THE LUNG

The extracellular matrix is a dynamic environment, rich with proteins, carbohydrates, and other significant structural molecules. In diseased states, additional matrix deposition results in diminished intracellular communication and progression to fibrosis. AUD-associated risk of pneumonia and ARDS (3, 4) precedes pulmonary fibrosis and loss of function if unresolved (13).

Hyaluronic acid (HA), an extracellular matrix glycosaminoglycan, is essential for maintaining tissue structure, promoting cell survival, and regulating inflammation and leukocyte motility after pulmonary injury (14–19). Further, accumulation of HA fragments is associated with chronic pulmonary inflammation mediated by innate immune cells (20–27). Increased HA synthesis and fragmentation is commonly involved in pulmonary disease pathology including fibrotic diseases (27–30), excessive remodeling (14, 18, 31, 32), and inflammation (15, 24, 33–37). In non-pathologic conditions, HA is expressed at very low concentrations in bronchoalveolar lavage fluid (38, 39) but is increased during pulmonary inflammation and pneumonia infections from *Klebsiella pneumoniae (*40*)* and *Escherichia coli* (41, 42).

Bacterial pneumonia clearance depends on dynamic, but regulated, HA metabolism and HA binding protein signaling (36, 40–44). Regulation of HA size and signaling through cell surface immune receptors is necessary to mobilize leukocytes, including alveolar macrophages, for recognition and destruction of infectious pathogens in those with AUD. Remodeling after respiratory infections is crucial and involves a restoration of HA dynamics coinciding with decreases in bacterial colonization, inflammation, and leukocyte recruitment.

HA SIGNALING: HYALADHERINS AND HA-PROTEIN INTERACTIONS

Hyaladherins are HA binding proteins that transmit changes in the extracellular matrix to cell signals for altered intra- or inter-immune cell function (14) through intermediate proteoglycans (45, 46) or by ionic HA binding to membrane proteins (47, 48). Although alcohol diminishes the ability of alveolar macrophages to recognize and clear pathogens, the role of HA on bacterial recognition during excessive alcohol use is largely unknown.

CD44 and CHI3L1

Cluster of differentiation 44 (CD44) is a hyaladherin that spans the cellular membrane, binds HA, and internalizes HA for lysosomal degradation by hyaluronidase enzymes (49, 50). CD44 is the primary cell surface receptor for HA binding in lymphocytes (51–53) and forms an anti-apoptotic coat of HA around alveolar macrophages (54). Therefore, CD44 is crucial for HA metabolism and signaling in leukocytes. Granulocyte-macrophage colony stimulating factor (GM-CSF) and peroxisome proliferator-activated receptor gamma (PPARγ) agonism induce expression of CD44 in monocytes that do not readily bind HA (54). However, chronic alcohol diminishes GM-CSF and PPARγ (11, 55) in primary alveolar macrophages, potentially decreasing their ability to form an anti-apoptotic HA coat for signaling with other hyaladherins.

Patients with eosinophilic pneumonia have high concentrations of CD44, HA, and interleukin-5 in their bronchoalveolar fluid. In contrast, CD44 deficient mice show decreased HA content after *Streptococcus pneumoniae* but increased HA in response to *E. coli* infection (41), suggesting that bacterial strains differentially influence host HA matrices. Yet, these studies do not address altered HA binding or signaling as mechanisms for worsened bacterial pneumonia. While altered CD44 expression following alcohol use may be one mechanism of bacterial pneumonia pathogenesis, altered HA molecular weight or indirect HA signaling may also impact inflammatory signaling and the innate immune response in leukocytes.

For indirect immune cell signaling, chitinase-3 like-protein-1 (CHI3L1) forms an intermediate bond between CD44 and HA (56). Through HA binding to CHI3L1 (57, 58), lysosomal degradation of HA by CD44 internalization is inhibited. Thus, CHI3L1 indirectly inhibits HA uptake and degradation through CD44 mediated internalization, suggesting CHI3L1 as an important regulator of HA metabolism. CHI3L1 is expressed in macrophages, neutrophils and endothelial cells and is necessary for antigen response, oxidant injury response, inflammation, and macrophage phenotype in the lung (59). Alcohol and high CHI3L1 levels have been linked to the progression of liver injury and fibrosis (60–62), but not yet in alcohol and bacterial pneumonia.

In bacterial pneumonia, CHI3L1 activity promotes innate immune defenses by sensing oxidant stress, cytokines, growth factors and miRNAs in the extracellular environment. Patients hospitalized with pneumonia have increased levels of CHI3L1 in serum (44, 63, 64). Additionally, *S. pneumoniae* induces CHI3L1 expression, but mice lacking CHI3L1 have reduced bacterial clearance and enhanced mortality following *S. pneumoniae* infection (43). These studies suggest CD44 and CHI3L1 as important regulators of innate immunity in the lung during bacterial pneumonia. Further, these studies provide CD44 and

CHI3L1 as targetable mechanisms for treating bacterial pneumonia in those with AUD.

HA Heavy Chain Formation

Tumor necrosis factor-stimulated gene-6 (TSG-6) is secreted by immune cells (65) and catalyzes inter-α-trypsin-inhibitor (IαI)-heavy chain complex to HA through pentatraxin 3 (PTX3) (66). Together, these molecular components generate a heavy chain HA matrix involved in airway inflammation (67), hyperresponsiveness (68–71) and toll-like receptor 4 (TLR4)-mediated lung injury (35, 69), possibly through PTX3 stimulation by TLR signaling (72). IαI attenuates lung injury in a porcine model of lipopolysaccharide (LPS)-induced sepsis (73), and PTX3 deficiency worsens LPS-induced lung injury. TSG-6 expression in cultured U-937 monocytes is enhanced by *Staphylococcus aureus* and *Chlamydia pneumoniae (*74*)*, suggesting enhanced expression in some strains of bacterial pneumonia. Further, PTX3 is involved in microbial recognition and innate immunity through recruitment of leukocytes and binding to *K. pneumoniae, Pseudomonas aeruginosa, Salmonella enterica, S. aureus, Neisseria meningitidis*, and *S. pneumoniae (*75–77*)*. Altogether, there is sufficient evidence for the role of heavy chain HA matrices in bacterial pneumonia, but further studies are needed to elucidate if PTX3 involvement in heavy chain HA formation is due to production by host or pathogen.

Little is known about heavy chain HA formation during excessive alcohol use. If heavy chain HA formation is involved in lung injury amelioration during bacterial pneumonia, disruptions in this process may lead to further lung injury and possibly sepsis. The risk of developing sepsis from pneumonia increases from 35% to 60% in people with AUD (4). EtOH feeding to C57BL/6 mice significantly diminished survival rates and lung PTX3 expression in a model of sepsis, and delayed tumor necrosis factor α (TNFα) level increases in plasma (78). Similarly, in a binge drinking mouse model of gram-negative bacterial lung infection, plasma TNFα was suppressed even while bacterial colonization was increased (79). Overall, these studies suggest that sepsis after excessive alcohol use not due to lack of inflammatory TNFα signaling. Rather, alterations in PTX3 disrupt HA heavy matrix formation and may be a mechanism for deranged immune function in those with AUD.

Versican and TLRs

Lecticans are HA-binding proteoglycans, containing chondroitin sulfate side chains, that ionically bind to HA through clusters of positively charged amino acids forming the link domain (48, 53). Little is known about how lecticans are impacted in bacterial pneumonia; however, levels of hyaluronan and the lectican, versican, increase during lung injury (38, 80, 81), perhaps by HA synthase regulation (82, 83). Although rats exposed to fetal alcohol showed a decrease in synaptic versican (84), the role of versican in alcohol-induced lung derangements continue to be an active area of investigation.

TLRs bind to hyaladherins and are known mediators of the inflammatory response during bacterial pneumonia. Like HA, versican can act as a danger associated molecular pattern for TLR signaling in alveolar macrophages (85, 86). Versican is augmented in the lungs of adult mice exposed to *P. aeruginosa* and upon TLR agonism (87). Comparatively, conditional versican deficiency in myeloid cells reduced inflammatory cell recruitment to the lungs (88). LPS stimulation of the TLR4/Trif pathway increases HA and versican levels in bone marrow derived macrophages *in vitro* and in murine alveolar macrophages (42, 88), but there is a lack of similar studies with gram positive bacteria.

Defects in TLR signaling predispose an individual to immunodeficiency that can result in severe bacterial pneumonia (89). Further, the versican receptors TLR2 and TLR4 are affected by excessive alcohol use. TLR2 and TLR4 do not bind HA but have been hypothesized to interact with HA through clustering of other matrix or membrane proteins and proteoglycans, like versican. Individuals with alcohol use disorders showed significant increases in TLR2; those with AUD and cannabis use exhibited significant increases in TLR6 (90). No experimental groups had increased TLR4 expression in that study, but another study showed that alcohol exposure induced TLR4 endocytosis in alveolar macrophages, limiting TLR4 activity for the recognition of pathogens (11). These results suggest that TLR expression or signaling may compensate for impaired bacterial recognition in those who have an AUD and bacterial pneumonia. Other membrane hyaladherins can also bind HA simultaneously to influence leukocyte phenotype (91) and affect pro- or anti-inflammatory signaling depending on the binding protein. While it is not known if hyaluronan or any binding partners interact with the other TLRs, these studies identified multiple targets for therapeutic intervention.

RHAMM, HABP1 and HABP2

Receptor for HA mediated motility (RHAMM), and HA binding protein 1 and 2 (HABP1, HABP2) are expressed ubiquitously and have multiple binding partners, including HA (92, 93). RHAMM contains putative binding domains for HA (94), but RHAMM is mainly expressed intracellularly (93, 95–97) to participate in signaling excluding HA. However, it is possible that HA binds to hyaladherins within the cell membrane because several hyaladherins are expressed intracellularly. Upon HA interaction with RHAMM, cell migration is promoted, influencing tissue remodeling or immune cell trafficking (98). In mice, there is increased membrane expression of RHAMM following lung injury (99). Further, RHAMM can compensate for CD44 through increased HA binding without increased RHAMM expression, indicating convergence of HA signaling pathways (100).

RHAMM is implicated in acute lung injury (101), and alcohol use exacerbates acute lung injury (4, 8, 13, 102, 103). However, it is not yet known how alcohol consumption directly affects RHAMM in any organ system. Past work has shown that RHAMM and transforming growth factor beta (TGFβ) work collectively to promote cell motility (104). Alcohol use inhibits inflammatory cytokines while stimulating TGFβ, which acts as an inhibitory cytokine in human monocytes exposed to bacterial stimuli (105). In contrast, some studies show that alcohol induces lung injury through proinflammatory pathways and promote

fibrosis by stimulating TGFβ1 activity (106, 107). In alveolar macrophages, alcohol-induced oxidative stress through TGFβ1 regulation of NADPH oxidases diminished alveolar macrophage function (108). Altogether, TGFβ1 is clearly involved in immune dysfunction following alcohol use, but more information is necessary to conclude that changes in TGFβ1 contribute to alterations in RHAMM signaling.

HABP1, also known as p32 or gClqR, can be found at the cell surface with higher affinity for HA corresponding to ionic strength and acidic environments (109), and HA binding to HABP1 can inhibit HA degradation by *S. pneumoniae* hyaluronidases (110). Bacteria express hyaluronidase proteins that degrade host HA matrices to allow for greater bacterial movement; thus, HABP1 activity is an endogenous antibacterial host defense. In humans, HABP1 assists in the regulation of HA metabolism in non-diseased states. While there is little known about HABP1 involvement in bacterial pneumonia, HABP1 activity is well described in cancer and mitochondrial biology. Alcohol exposure impairs alveolar macrophage ability to phagocytose pathogens (8–11) via increased cellular oxidative stress (111), mitochondrial redox imbalance (112, 113), and impaired mitochondrial bioenergetics (114). Mitochondrial HABP1 regulates oxidative phosphorylation (115, 116) by maintaining mitochondrial protein translation (117), and cleavage of HABP1 by caspase-1 shifts cancer cell phenotype toward glycolysis (118). In human lung cancers, HABP1 is highly expressed, leading to altered nuclear factor kappa B (NFκB) activity and cell proliferation (119), revealing a role for HABP1 in the lung microenvironment.

HABP2, also known as factor VII activating protease or plasma hyaluronan binding protein, is extracellular. High molecular weight HA inhibits HABP2's activity to maintain barrier integrity while low molecular weight HA prevents a leaky barrier (120, 121). Normal barrier function prevents bacterial spread into the vasculature during bacterial pneumonia that would otherwise result in sepsis. Further, alcohol impairs pulmonary barrier function (122, 123). In the lung, HABP2 may be involved in LPS-induced lung injury (121) and ARDS (124) primarily through its role in modulating lung barrier integrity. In patients with ARDS, HABP2 levels and activity are increased in alveolar macrophage, epithelial, and endothelial cells (124), and chronic alcohol use elevates the risk for ARDS (4).

In vivo HABP2 silencing by small interfering RNA attenuated LPS-mediated lung injury and hyperpermeability, indicating a possible therapeutic strategy for bacterial pneumonia in those with AUD-induced barrier dysfunction. Additionally, HABP2 primarily binds to cell surface protease-activated receptors (PAR) (125), and silencing of PAR1 and PAR3 can attenuate LPS-mediated barrier dysfunction (121). Mice with PAR2 genetic deletions exhibited severe lung inflammation, neutrophil accumulation, and diminished macrophage and neutrophil bacterial phagocytosis in a model of *P. aeruginosa*. These alterations were attenuated by PAR2 activation (126), indicating a possible role for HABP2 in bacterial pneumonia clearance. Other studies show similar roles for PARs in bacterial pneumonia pathology (126–128); however, this mechanism needs to be further elucidated since HABP1 and the PARs each have multiple binding partners.

DISCUSSION

This mini review addresses modulation of HA signaling by alcohol and bacterial pneumonia. CD44 and RHAMM are involved in HA metabolism, signaling, and intracellular communication. CHI3L1, IαI, TSG-6, PTX3, and versican all act as intermediates between HA and membrane signaling proteins, like CD44 and TLRs. Herein we also review how HA modulates cellular energy metabolism through HABP2 and intracellular signaling. Another hyaladherin, lymphatic vessel endothelial cell receptor 1 (LYVE-1), binds HA for immune cell motility and HA metabolism but was not discussed in detail due to its low expression in the lungs. Nevertheless, CD44 and LYVE-1 jointly assist in immune cell migration within the lymphatic system (129–131) to traffic cells to the lungs during bacterial pneumonia. HA-hyaladherin interactions additionally assist with leukocyte motility. In summary, changes in the extracellular matrix impact cellular signaling in bacterial pneumonia that can be exacerbated by excessive alcohol use but there is much to learn still. Nevertheless, targeting hyaladherins may be a potential therapeutic strategy for mitigating lung injury in those with alcohol use disorders. These pathways have been summarized in **Figure 1**.

Controversies in the HA Field

Is increased HA production during lung disease pathological and does it need to be "fixed?" HA concentration increases, but average molecular weight decreases, in multiple pulmonary diseases involving immune dysfunction and inflammation. However, the mechanisms of HA signaling based on variations in molecular weight remain controversial in the field. Increased HA production appears to decrease leukocyte mobility and bacterial spread in pneumonia due to higher viscosity. However, increased HA production may aid in leukocyte motility through endogenous hyaladherins while preventing bacterial spread because of their lack of the same receptors.

Further, fragmented HA is thought to be pro-inflammatory while endogenous high molecular weight HA is anti-inflammatory (25, 34, 132). It is also clear that bacteria contain hyaluronidases to degrade host HA matrices, and fragmented HA can act as a danger associated molecular pattern for immune cell release of key immune factors. Our group has hypothesized that alcohol increases high molecular weight HA synthesis, thereby decreasing necessary pro-inflammatory signaling from fragmented HA. However, size classifications remain controversial in the field since "fragmented HA" or "low molecular weight HA" could range from HA chains of a few polysaccharides to 500 kD. Future studies should be done to clarify the immune response of leukocytes to different sized HA polymers to confirm past results.

Therapeutic Potential

Although the risk AUD individuals for getting sepsis and ARDS from pneumonia is approximately double that of non-AUD individuals (4), treatment strategies are comparable between AUD

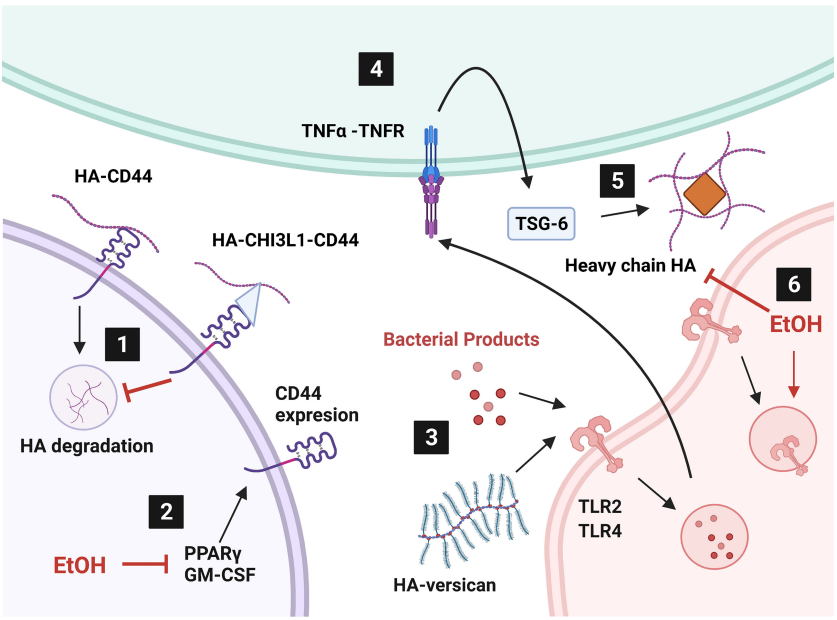

FIGURE 1 | Alcohol affects hyaladherin signaling in the lung. 1) Internalization and degradation of hyaluronic acid (HA) is inhibited by overproduction of chitinase-3 like-protein-1 (CHI3L1). 2) Ethanol (EtOH) diminishes peroxisome proliferator activated receptor gamma (PPARγ) and granulocyte-macrophage colony stimulating factor (GM-CSF) levels. 3) HA-versican competes with bacterial products for toll-like receptor (TLR) signaling. 4) TLR signaling induces tumor necrosis factor alpha (TNFα) production. TNFα stimulates TNFα-stimulated gene-6 (TSG-6) expression. 5) TSG-6 catalyzes heavy chain HA matrix formation through pentatraxin 3 (PTX3, orange diamond). 6) EtOH induces TLR4 internalization and heavy chain formation by decreasing TNFα. Created with BioRender.com.

and non-AUD individuals. There are several FDA approved modulators of HA or HA binding proteins that are available by prescription or as a clinical treatment; however, additional studies on HA modulation in bacterial pneumonia and alcohol are needed before therapeutic targeting of these pathways in people with AUD can take place. Targeting bacterial protein influence in host HA matrices and barrier dysfunction go hand-in-hand. As bacteria spread and host lung cell apoptosis persists, cellular barriers are broken down. Use of current small molecule inhibitors of bacterial hyaluronidases are insufficient as a therapeutic strategy because they have low specificity and potency. Bacteria contain some hyaluronidases that are different than those in humans. Therefore, upregulation of host defenses against bacterial hyaluronidases, like HABP1, may work as an alternative treatment to prevent uncontrolled bacterial proliferation.

Proposed mechanisms of EtOH-induced oxidative stress in alveolar macrophage include loss of PPARγ activity (8, 11, 111), which is diminished following alcohol exposure (11, 55, 111). Rosiglitazone and pioglitazone, PPARγ agonists, improve EtOH-induced alveolar macrophage oxidative stress (9), mitochondrial-derived ROS (114), and dysfunctional phagocytosis and clearance of *K. pneumoniae* (11). Further, pioglitazone, reversed alcohol-induced derangements phagocytosis in alveolar macrophages (11, 55, 111). Because mitochondrial derived ATP is necessary for high energy processes, like phagocytosis, impaired mitochondrial function is one explanation for why alcohol impairs alveolar macrophage phagocytic ability. Identifying alcohol-induced mechanisms that impair HA signaling could further elucidate underlying mitochondrial dysfunction in alveolar macrophages.

In conclusion, AUDs increase the risk of respiratory infections and levels of the extracellular matrix component, HA, are increased in chronic respiratory diseases. HA signaling through hyaladherins are affected by alcohol use, which could modify inflammation and immune cell activity during bacterial pneumonia. The role of hyaladherins in alcohol-induced immune dysfunction is still largely unknown. This mini review highlights the necessity for future studies to provide insight into understanding the role of HA and its binding partners in host immune defense following excessive alcohol use.

AUTHOR CONTRIBUTIONS

KMC outlined and prepared the manuscript; SMY outlined and prepared the manuscript. All authors contributed to the article and approved the submitted version.

FUNDING

This work was supported in part by grants from: the National Institute on Alcohol Abuse and Alcoholism (F31AA029938) to KMC (ORCID ID: 0000-0002-9461-4032) and (R01AA026086)

to SMY (ORCID ID: 0000-0001-9309-0233) as well as the National Institute of General Medical Sciences (T32GM008602) to Randy A. Hall. The contents of this report do not represent the views of the Department of Veterans Affairs or the US Government.

ACKNOWLEDGMENTS

The authors would like to acknowledge the Emory University Molecular and Systems Pharmacology Program and the Atlanta VA Health Care System for their continued support.

REFERENCES

1. Association, A. P. *Diagnostic and Statistical Manual of Mental Disorders. 5th ed*. Arlington, VA: American Psychiatric Association (2013).
2. Organization, W. H. *Global Status Report on Alcohol and Health*. Geneva: World Health Organization (2018).
3. Baker RC, Jerrells TR. Recent Developments in Alcoholism: Immunological Aspects. *Recent Dev Alcohol* (1993) 11:249–71. doi: 10.1007/978-1-4899-1742-3_15
4. Moss M, Parsons PE, Steinberg KP, Hudson LD, Guidot DM, Burnham EL, et al. Chronic Alcohol Abuse is Associated With an Increased Incidence of Acute Respiratory Distress Syndrome and Severity of Multiple Organ Dysfunction in Patients With Septic Shock. *Crit Care Med* (2003) 31:869–77. doi: 10.1097/01.CCM.0000055389.64497.11
5. *Centers for Disease Control and Prevention, Released in 2020. Data are From the Multiple Cause of Death Files, 1999-2019, as Compiled From Data Provided by the 57 Vital Statistics Jurisdictions Through the Vital Statistics Cooperative Program* (2021). Available at: http://wonder.cdc.gov/ucd-icd10.html.
6. Price ME, Gerald CL, Pavlik JA, Schlichte SL, Zimmerman MC, DeVasure JM, et al. Loss of cAMP-Dependent Stimulation of Isolated Cilia Motility by Alcohol Exposure is Oxidant-Dependent. *Alcohol* (2019) 80:91–8. doi: 10.1016/j.alcohol.2018.09.010
7. Wyatt TA, Gentry-Nielsen MJ, Pavlik JA, Sisson JH. Desensitization of PKA-Stimulated Ciliary Beat Frequency in an Ethanol-Fed Rat Model of Cigarette Smoke Exposure. *Alcoholism Clin Exp Res* (2004) 28:998–1004. doi: 10.1097/01.ALC.0000130805.75641.F4
8. Yeligar SM, Chen MM, Kovacs EJ, Sisson JH, Burnham EL, Brown LA. Alcohol and Lung Injury and Immunity. *Alcohol* (2016) 55:51–9. doi: 10.1016/j.alcohol.2016.08.005
9. Baughman RP, Roselle GA. Surfactant Deficiency With Decreased Opsonic Activity in a Guinea Pig Model of Alcoholism. *Alcohol Clin Exp Res* (1987) 11:261–4. doi: 10.1111/j.1530-0277.1987.tb01303.x
10. Greenberg SS, Zhao X, Hua L, Wang JF, Nelson S, Ouyang J. Ethanol Inhibits Lung Clearance of Pseudomonas Aeruginosa by a Neutrophil and Nitric Oxide-Dependent Mechanism, In Vivo. *Alcohol Clin Exp Res* (1999) 23:735–44. doi: 10.1111/j.1530-0277.1999.tb04177.x
11. Yeligar SM, Mehta AJ, Harris FL, Brown LA, Hart CM. Peroxisome Proliferator-Activated Receptor Gamma Regulates Chronic Alcohol-Induced Alveolar Macrophage Dysfunction. *Am J Respir Cell Mol Biol* (2016) 55:35–46. doi: 10.1165/rcmb.2015-0077OC
12. Yeligar SM, Harris FL, Hart CM, Brown LA. Glutathione Attenuates Ethanol-Induced Alveolar Macrophage Oxidative Stress and Dysfunction by Downregulating NADPH Oxidases. *Am J Physiol Lung Cell Mol Physiol* (2014) 306:L429–441. doi: 10.1152/ajplung.00159.2013
13. Sueblinvong V, Kerchberger VE, Saghafi R, Mills ST, Fan X, Guidot DM. Chronic Alcohol Ingestion Primes the Lung for Bleomycin-Induced Fibrosis in Mice. *Alcohol Clin Exp Res* (2014) 38:336–43. doi: 10.1111/acer.12232
14. Johnson P, Arif AA, Lee-Sayer SSM, Dong Y. Hyaluronan and Its Interactions With Immune Cells in the Healthy and Inflamed Lung. *Front Immunol* (2018) 9:2787. doi: 10.3389/fimmu.2018.02787
15. Noble PW, Jiang D. Matrix Regulation of Lung Injury, Inflammation, and Repair: The Role of Innate Immunity. *Proc Am Thorac Soc* (2006) 3:401–4. doi: 10.1513/pats.200604-097AW
16. Jiang D, Liang J, Fan J, Yu S, Luo Y, Chen S, et al. Regulation of Lung Injury and Repair by Toll-Like Receptors and Hyaluronan. *Nat Med* (2005) 11:1173–9. doi: 10.1038/nm1315
17. Jiang D, Liang J, Noble PW. Hyaluronan as an Immune Regulator in Human Diseases. *Physiol Rev* (2011) 91:221–64. doi: 10.1152/physrev.00052.2009
18. Jiang D, Liang J, Noble PW. Hyaluronan in Tissue Injury and Repair. *Annu Rev Cell Dev Biol* (2007) 23:435–61. doi: 10.1146/annurev.cellbio.23.090506.123337
19. Teder P, Vandivier RW, Jiang D, Liang J, Cohn L, Pure E, et al. Resolution of Lung Inflammation by CD44. *Science* (2002) 296:155–8. doi: 10.1126/science.1069659
20. Cantin AM, Larivee P, Begin RO. Extracellular Glutathione Suppresses Human Lung Fibroblast Proliferation. *Am J Respir Cell Mol Biol* (1990) 3:79–85. doi: 10.1165/ajrcmb/3.1.79
21. Cantor J, Ma S, Turino G. A Pilot Clinical Trial to Determine the Safety and Efficacy of Aerosolized Hyaluronan as a Treatment for COPD. *Int J Chron Obstruct Pulmon Dis* (2017) 12:2747–52. doi: 10.2147/COPD.S142156
22. Gebe JA, Yadava K, Ruppert SM, Marshall P, Hill P, Falk BA, et al. Modified High-Molecular-Weight Hyaluronan Promotes Allergen-Specific Immune Tolerance. *Am J Respir Cell Mol Biol* (2017) 56:109–20. doi: 10.1165/rcmb.2016-0111OC
23. Haserodt S, Aytekin M, Dweik RA. A Comparison of the Sensitivity, Specificity, and Molecular Weight Accuracy of Three Different Commercially Available Hyaluronan ELISA-Like Assays. *Glycobiology* (2011) 21:175–83. doi: 10.1093/glycob/cwq145
24. Papakonstantinou E, Roth M, Klagas I, Karakiulakis G, Tamm M, Stolz D. COPD Exacerbations Are Associated With Proinflammatory Degradation of Hyaluronic Acid. *Chest* (2015) 148:1497–507. doi: 10.1378/chest.15-0153
25. Sokolowska M, Chen LY, Eberlein M, Martinez-Anton A, Liu Y, Alsaaty S, et al. Low Molecular Weight Hyaluronan Activates Cytosolic Phospholipase A2alpha and Eicosanoid Production in Monocytes and Macrophages. *J Biol Chem* (2014) 289:4470–88. doi: 10.1074/jbc.M113.515106
26. Stern R, Asari AA, Sugahara KN. Hyaluronan Fragments: An Information-Rich System. *Eur J Cell Biol* (2006) 85:699–715. doi: 10.1016/j.ejcb.2006.05.009
27. Vistejnova L, Safrankova B, Nesporova K, Slavkovsky R, Hermannova M, Hosek P, et al. Low Molecular Weight Hyaluronan Mediated CD44 Dependent Induction of IL-6 and Chemokines in Human Dermal Fibroblasts Potentiates Innate Immune Response. *Cytokine* (2014) 70:97–103. doi: 10.1016/j.cyto.2014.07.006
28. Buonpensiero P, De Gregorio F, Sepe A, Di Pasqua A, Ferri P, Siano M, et al. Hyaluronic Acid Improves "Pleasantness" and Tolerability of Nebulized Hypertonic Saline in a Cohort of Patients With Cystic Fibrosis. *Adv Ther* (2010) 27:870–8. doi: 10.1007/s12325-010-0076-8
29. Liang J, Zhang Y, Xie T, Liu N, Chen H, Geng Y, et al. Hyaluronan and TLR4 Promote Surfactant-Protein-C-Positive Alveolar Progenitor Cell Renewal and Prevent Severe Pulmonary Fibrosis in Mice. *Nat Med* (2016) 22:1285–93. doi: 10.1038/nm.4192
30. Savani RC, Hou G, Liu P, Wang C, Simons E, Grimm PC, et al. A Role for Hyaluronan in Macrophage Accumulation and Collagen Deposition After Bleomycin-Induced Lung Injury. *Am J Respir Cell Mol Biol* (2000) 23:475–84. doi: 10.1165/ajrcmb.23.4.3944
31. Tseng V, Ni K, Allawzi A, Prohaska C, Hernandez-Lagunas L, Elajaili H, et al. Extracellular Superoxide Dismutase Regulates Early Vascular Hyaluronan Remodeling in Hypoxic Pulmonary Hypertension. *Sci Rep* (2020) 10:280. doi: 10.1038/s41598-019-57147-7
32. Vaday GG, Franitza S, Schor H, Hecht I, Brill A, Cahalon L, et al. Combinatorial Signals by Inflammatory Cytokines and Chemokines Mediate Leukocyte Interactions With Extracellular Matrix. *J Leukoc Biol* (2001) 69:885–92. doi: 10.1189/jlb.69.6.885
33. Bollyky PL, Lord JD, Masewicz SA, Evanko SP, Buckner JH, Wight TN, et al. Cutting Edge: High Molecular Weight Hyaluronan Promotes the Suppressive Effects of CD4+CD25+ Regulatory T Cells. *J Immunol* (2007) 179:744–7. doi: 10.4049/jimmunol.179.2.744
34. Johnson CG, Stober VP, Cyphert-Daly JM, Trempus CS, Flake GP, Cali V, et al. High Molecular Weight Hyaluronan Ameliorates Allergic Inflammation and Airway Hyperresponsiveness in the Mouse. *Am J*

Physiol Lung Cell Mol Physiol (2018) 315:L787–98. doi: 10.1152/ajplung.00009.2018
35. Li Z, Potts-Kant EN, Garantziotis S, Foster WM, Hollingsworth JW. Hyaluronan Signaling During Ozone-Induced Lung Injury Requires TLR4, MyD88, and TIRAP. *PloS One* (2011) 6:e27137. doi: 10.1371/journal.pone.0027137
36. McKallip RJ, Ban H, Uchakina ON. Treatment With the Hyaluronic Acid Synthesis Inhibitor 4-Methylumbelliferone Suppresses LPS-Induced Lung Inflammation. *Inflammation* (2015) 38:1250–9. doi: 10.1007/s10753-014-0092-y
37. Wight TN, Frevert CW, Debley JS, Reeves SR, Parks WC, Ziegler SF. Interplay of Extracellular Matrix and Leukocytes in Lung Inflammation. *Cell Immunol* (2017) 312:1–14. doi: 10.1016/j.cellimm.2016.12.003
38. Nettelbladt O, Hallgren R. Hyaluronan (Hyaluronic Acid) in Bronchoalveolar Lavage Fluid During the Development of Bleomycin-Induced Alveolitis in the Rat. *Am Rev Respir Dis* (1989) 140:1028–32. doi: 10.1164/ajrccm/140.4.1028
39. Underhill CB, Nguyen HA, Shizari M, Culty M. CD44 Positive Macrophages Take Up Hyaluronan During Lung Development. *Dev Biol* (1993) 155:324–36. doi: 10.1006/dbio.1993.1032
40. Wang Q, Teder P, Judd NP, Noble PW, Doerschuk CM. CD44 Deficiency Is Associated With Increased Bacterial Clearance But Enhanced Lung Inflammation During Gram-Negative Pneumonia. *Am J Pathol* (2010) 177:2483–94. doi: 10.2353/ajpath.2010.100562
41. Wang Q, Teder P, Judd NP, Noble PW, Doerschuk CM. CD44 Deficiency Leads to Enhanced Neutrophil Migration and Lung Injury in Escherichia Coli Pneumonia in Mice. *Am J Pathol* (2002) 161:2219–28. doi: 10.1016/S0002-9440(10)64498-7
42. Chang MY, Tanino Y, Vidova V, Kinsella MG, Chan CK, Johnson PY, et al. A Rapid Increase in Macrophage-Derived Versican and Hyaluronan in Infectious Lung Disease. *Matrix Biol* (2014) 34:1–12. doi: 10.1016/j.matbio.2014.01.011
43. Dela Cruz CS, Liu W, He CH, Jacoby A, Gornitzky A, Ma B, et al. Chitinase 3-Like-1 Promotes Streptococcus Pneumoniae Killing and Augments Host Tolerance to Lung Antibacterial Responses. *Cell Host Microbe* (2012) 12:34–46. doi: 10.1016/j.chom.2012.05.017
44. Nordenbaek C, Johansen JS, Junker P, Borregaard N, Sorensen O, Price PA. YKL-40, a Matrix Protein of Specific Granules in Neutrophils, is Elevated in Serum of Patients With Community-Acquired Pneumonia Requiring Hospitalization. *J Infect Dis* (1999) 180:1722–6. doi: 10.1086/315050
45. Neame PJ, Christner JE, Baker JR. Cartilage Proteoglycan Aggregates. The Link Protein and Proteoglycan Amino-Terminal Globular Domains Have Similar Structures. *J Biol Chem* (1987) 262:17768–78. doi: 10.1016/S0021-9258(18)45445-2
46. Zimmermann DR, Ruoslahti E. Multiple Domains of the Large Fibroblast Proteoglycan, Versican. *EMBO J* (1989) 8:2975–81. doi: 10.1002/j.1460-2075.1989.tb08447.x
47. Goldstein LA, Zhou DF, Picker LJ, Minty CN, Bargatze RF, Ding JF, et al. A Human Lymphocyte Homing Receptor, the Hermes Antigen, is Related to Cartilage Proteoglycan Core and Link Proteins. *Cell* (1989) 56:1063–72. doi: 10.1016/0092-8674(89)90639-9
48. Kohda D, Morton CJ, Parkar AA, Hatanaka H, Inagaki FM, Campbell ID, et al. Solution Structure of the Link Module: A Hyaluronan-Binding Domain Involved in Extracellular Matrix Stability and Cell Migration. *Cell* (1996) 86:767–75. doi: 10.1016/s0092-8674(00)80151-8
49. Culty M, Nguyen HA, Underhill CB. The Hyaluronan Receptor (CD44) Participates in the Uptake and Degradation of Hyaluronan. *J Cell Biol* (1992) 116:1055–62. doi: 10.1083/jcb.116.4.1055
50. Culty M, O'Mara TE, Underhill CB, Yeager HJr., Swartz RP. Hyaluronan Receptor (CD44) Expression and Function in Human Peripheral Blood Monocytes and Alveolar Macrophages. *J Leukoc Biol* (1994) 56:605–11. doi: 10.1002/jlb.56.5.605
51. Aruffo A, Stamenkovic I, Melnick M, Underhill CB, Seed B. CD44 is the Principal Cell Surface Receptor for Hyaluronate. *Cell* (1990) 61:1303–13. doi: 10.1016/0092-8674(90)90694-a
52. Miyake K, Underhill CB, Lesley J, Kincade PW. Hyaluronate can Function as a Cell Adhesion Molecule and CD44 Participates in Hyaluronate Recognition. *J Exp Med* (1990) 172:69–75. doi: 10.1084/jem.172.1.69
53. Toole BP. Hyaluronan and its Binding Proteins, the Hyaladherins. *Curr Opin Cell Biol* (1990) 2:839–44. doi: 10.1016/0955-0674(90)90081-o
54. Dong Y, Poon GFT, Arif AA, Lee-Sayer SSM, Dosanjh M, Johnson P. The Survival of Fetal and Bone Marrow Monocyte-Derived Alveolar Macrophages is Promoted by CD44 and its Interaction With Hyaluronan. *Mucosal Immunol* (2018) 11:601–14. doi: 10.1038/mi.2017.83
55. Yeligar SM, Mehta AJ, Harris FL, Brown LAS, Hart CM. Pioglitazone Reverses Alcohol-Induced Alveolar Macrophage Phagocytic Dysfunction. *J Immunol* (2021) 207:483–92. doi: 10.4049/jimmunol.2000565
56. Geng B, Pan J, Zhao T, Ji J, Zhang C, Che Y, et al. Chitinase 3-Like 1-CD44 Interaction Promotes Metastasis and Epithelial-to-Mesenchymal Transition Through Beta-Catenin/Erk/Akt Signaling in Gastric Cancer. *J Exp Clin Cancer Res* (2018) 37:208. doi: 10.1186/s13046-018-0876-2
57. Malinda KM, Ponce L, Kleinman HK, Shackelton LM, Millis AJ. Gp38k, a Protein Synthesized by Vascular Smooth Muscle Cells, Stimulates Directional Migration of Human Umbilical Vein Endothelial Cells. *Exp Cell Res* (1999) 250:168–73. doi: 10.1006/excr.1999.4511
58. Nishikawa KC, Millis AJ. Gp38k (CHI3L1) is a Novel Adhesion and Migration Factor for Vascular Cells. *Exp Cell Res* (2003) 287:79–87. doi: 10.1016/s0014-4827(03)00069-7
59. Zhao T, Su Z, Li Y, Zhang X, You Q. Chitinase-3 Like-Protein-1 Function and its Role in Diseases. *Signal Transduct Target Ther* (2020) 5:201. doi: 10.1038/s41392-020-00303-7
60. Lee DH, Han JH, Lee YS, Jung YS, Roh YS, Yun JS, et al. Chitinase-3-Like-1 Deficiency Attenuates Ethanol-Induced Liver Injury by Inhibition of Sterol Regulatory Element Binding Protein 1-Dependent Triglyceride Synthesis. *Metabolism* (2019) 95:46–56. doi: 10.1016/j.metabol.2019.03.010
61. Nojgaard C, Johansen JS, Christensen E, Skovgaard LT, Price PA, Becker U, et al. Serum Levels of YKL-40 and PIIINP as Prognostic Markers in Patients With Alcoholic Liver Disease. *J Hepatol* (2003) 39:179–86. doi: 10.1016/s0168-8278(03)00184-3
62. Johansen JS, Christoffersen P, Moller S, Price PA, Henriksen JH, Garbarsch C, et al. Serum YKL-40 is Increased in Patients With Hepatic Fibrosis. *J Hepatol* (2000) 32:911–20. doi: 10.1016/s0168-8278(00)80095-1
63. Kronborg G, Ostergaard C, Weis N, Nielsen H, Obel N, Pedersen SS, et al. Serum Level of YKL-40 is Elevated in Patients With Streptococcus Pneumoniae Bacteremia and is Associated With the Outcome of the Disease. *Scand J Infect Dis* (2002) 34:323–6. doi: 10.1080/00365540110080233
64. Ostergaard C, Johansen JS, Benfield T, Price PA, Lundgren JD. YKL-40 is Elevated in Cerebrospinal Fluid From Patients With Purulent Meningitis. *Clin Diagn Lab Immunol* (2002) 9:598–604. doi: 10.1128/cdli.9.3.598-604.2002
65. Milner CM, Tongsoongnoen W, Rugg MS, Day AJ. The Molecular Basis of Inter-Alpha-Inhibitor Heavy Chain Transfer on to Hyaluronan. *Biochem Soc Trans* (2007) 35:672–6. doi: 10.1042/BST0350672
66. Salustri A, Garlanda C, Hirsch E, De Acetis M, Maccagno A, Bottazzi B, et al. PTX3 Plays a Key Role in the Organization of the Cumulus Oophorus Extracellular Matrix and in. *Vivo fertilization Dev* (2004) 131:1577–86. doi: 10.1242/dev.01056
67. Stober VP, Johnson CG, Majors A, Lauer ME, Cali V, Midura RJ, et al. TNF-Stimulated Gene 6 Promotes Formation of Hyaluronan-Inter-Alpha-Inhibitor Heavy Chain Complexes Necessary for Ozone-Induced Airway Hyperresponsiveness. *J Biol Chem* (2017) 292:20845–58. doi: 10.1074/jbc.M116.756627
68. Garantziotis S, Li Z, Potts EN, Kimata K, Zhuo L, Morgan DL, et al. Hyaluronan Mediates Ozone-Induced Airway Hyperresponsiveness in Mice. *J Biol Chem* (2009) 284:11309–17. doi: 10.1074/jbc.M802400200
69. Garantziotis S, Li Z, Potts EN, Lindsey JY, Stober VP, Polosukhin VV, et al. TLR4 is Necessary for Hyaluronan-Mediated Airway Hyperresponsiveness After Ozone Inhalation. *Am J Respir Crit Care Med* (2010) 181:666–75. doi: 10.1164/rccm.200903-0381OC
70. Lazrak A, Creighton J, Yu Z, Komarova S, Doran SF, Aggarwal S, et al. Hyaluronan Mediates Airway Hyperresponsiveness in Oxidative Lung Injury. *Am J Physiol Lung Cell Mol Physiol* (2015) 308:L891–903. doi: 10.1152/ajplung.00377.2014
71. Swaidani S, Cheng G, Lauer ME, Sharma M, Mikecz K, Hascall VC, et al. TSG-6 Protein is Crucial for the Development of Pulmonary Hyaluronan

Deposition, Eosinophilia, and Airway Hyperresponsiveness in a Murine Model of Asthma. *J Biol Chem* (2013) 288:412–22. doi: 10.1074/jbc.M112.389874
72. Balhara J, Koussih L, Mohammed A, Shan L, Lamkhioued B, Gounni AS. PTX3 Deficiency Promotes Enhanced Accumulation and Function of CD11c (+)CD11b(+) DCs in a Murine Model of Allergic Inflammation. *Front Immunol* (2021) 12:641311. doi: 10.3389/fimmu.2021.641311
73. Jourdain M, Tournoys A, Leroy X, Mangalaboyi J, Fourrier F, Goudemand J, et al. Effects of N Omega-Nitro-L-Arginine Methyl Ester on the Endotoxin-Induced Disseminated Intravascular Coagulation in Porcine Septic Shock. *Crit Care Med* (1997) 25:452–9. doi: 10.1097/00003246-199703000-00014
74. Mandi Y, Endresz V, Mosolygo T, Burian K, Lantos I, Fulop F, et al. The Opposite Effects of Kynurenic Acid and Different Kynurenic Acid Analogs on Tumor Necrosis Factor-Alpha (TNF-Alpha) Production and Tumor Necrosis Factor-Stimulated Gene-6 (TSG-6) Expression. *Front Immunol* (2019) 10:1406. doi: 10.3389/fimmu.2019.01406
75. Bottazzi B, Bastone A, Doni A, Garlanda C, Valentino S, Deban L, et al. The Long Pentraxin PTX3 as a Link Among Innate Immunity, Inflammation, and Female Fertility. *J Leukoc Biol* (2006) 79:909–12. doi: 10.1189/jlb.1005557
76. Presta M, Camozzi M, Salvatori G, Rusnati M. Role of the Soluble Pattern Recognition Receptor PTX3 in Vascular Biology. *J Cell Mol Med* (2007) 11:723–38. doi: 10.1111/j.1582-4934.2007.00061.x
77. Deban L, Jaillon S, Garlanda C, Bottazzi B, Mantovani A. Pentraxins in Innate Immunity: Lessons From PTX3. *Cell Tissue Res* (2011) 343:237–49. doi: 10.1007/s00441-010-1018-0
78. Kasuda S, Kudo R, Yuui K, Sakurai Y, Hatake K. Acute Ethanol Intoxication Suppresses Pentraxin 3 Expression in a Mouse Sepsis Model Involving Cecal Ligation and Puncture. *Alcohol* (2017) 64:1–9. doi: 10.1016/j.alcohol.2017.04.003
79. Jimenez VMJr., Settles EW, Currie BJ, Keim PS, Monroy FP. Persistence of Burkholderia Thailandensis E264 in Lung Tissue After a Single Binge Alcohol Episode. *PloS One* (2019) 14:e0218147. doi: 10.1371/journal.pone.0218147
80. Hallgren R, Samuelsson T, Laurent TC, Modig J. Accumulation of Hyaluronan (Hyaluronic Acid) in the Lung in Adult Respiratory Distress Syndrome. *Am Rev Respir Dis* (1989) 139:682–7. doi: 10.1164/ajrccm/139.3.682
81. Hallgren O, Nihlberg K, Dahlback M, Bjermer L, Eriksson LT, Erjefalt JS, et al. Altered Fibroblast Proteoglycan Production in COPD. *Respir Res* (2010) 11:55. doi: 10.1186/1465-9921-11-55
82. Evanko SP, Potter-Perigo S, Johnson PY, Wight TN. Organization of Hyaluronan and Versican in the Extracellular Matrix of Human Fibroblasts Treated With the Viral Mimetic Poly I:C. *J Histochem Cytochem* (2009) 57:1041–60. doi: 10.1369/jhc.2009.953802
83. Chang MY, Kang I, Gale M Jr, Manicone AM, Kinsella MG, Braun KR, et al. Versican is Produced by Trif- and Type I Interferon-Dependent Signaling in Macrophages and Contributes to Fine Control of Innate Immunity in Lungs. *Am J Physiol Lung Cell Mol Physiol* (2017) 313:L1069–86. doi: 10.1152/ajplung.00353.2017
84. Elibol B, Beker M, Jakubowska-Dogru E, Kilic U. Fetal Alcohol and Maternal Stress Modify the Expression of Proteins Controlling Postnatal Development of the Male Rat Hippocampus. *Am J Drug Alcohol Abuse* (2020) 46:718–30. doi: 10.1080/00952990.2020.1780601
85. Wang W, Xu GL, Jia WD, Ma JL, Li JS, Ge YS, et al. Ligation of TLR2 by Versican: A Link Between Inflammation and Metastasis. *Arch Med Res* (2009) 40:321–3. doi: 10.1016/j.arcmed.2009.04.005
86. Zhang Z, Miao L, Wang L. Inflammation Amplification by Versican: The First Mediator. *Int J Mol Sci* (2012) 13:6873–82. doi: 10.3390/ijms13066873
87. Snyder JM, Washington IM, Birkland T, Chang MY, Frevert CW. Correlation of Versican Expression, Accumulation, and Degradation During Embryonic Development by Quantitative Immunohistochemistry. *J Histochem Cytochem* (2015) 63:952–67. doi: 10.1369/0022155415610383
88. Kang I, Harten IA, Chang MY, Braun KR, Sheih A, Nivison MP, et al. Versican Deficiency Significantly Reduces Lung Inflammatory Response Induced by Polyinosine-Polycytidylic Acid Stimulation. *J Biol Chem* (2017) 292:51–63. doi: 10.1074/jbc.M116.753186
89. Currie AJ, Davidson DJ, Reid GS, Bharya S, MacDonald KL, Devon RS, et al. Primary Immunodeficiency to Pneumococcal Infection Due to a Defect in Toll-Like Receptor Signaling. *J Pediatr* (2004) 144:512–8. doi: 10.1016/j.jpeds.2003.10.034
90. Bailey KL, Wyatt TA, Katafiasz DM, Taylor KW, Heires AJ, Sisson JH, et al. Alcohol and Cannabis Use Alter Pulmonary Innate Immunity. *Alcohol* (2019) 80:131–8. doi: 10.1016/j.alcohol.2018.11.002
91. Wight TN, Kang I, Merrilees MJ. Versican and the Control of Inflammation. *Matrix Biol* (2014) 35:152–61. doi: 10.1016/j.matbio.2014.01.015
92. D'Souza M, Datta K. Evidence for Naturally Occurring Hyaluronic Acid Binding Protein in Rat Liver. *Biochem Int* (1985) 10:43–51.
93. Turley EA, Noble PW, Bourguignon LY. Signaling Properties of Hyaluronan Receptors. *J Biol Chem* (2002) 277:4589–92. doi: 10.1074/jbc.R100038200
94. Yang B, Zhang L, Turley EA. Identification of Two Hyaluronan-Binding Domains in the Hyaluronan Receptor RHAMM. *J Biol Chem* (1993) 268:8617–23. doi: 10.1016/S0021-9258(18)52919-7
95. Assmann V, Jenkinson D, Marshall JF, Hart IR. The Intracellular Hyaluronan Receptor RHAMM/IHABP Interacts With Microtubules and Actin Filaments. *J Cell Sci 112 (Pt* (1999) 22):3943–54. doi: 10.1242/jcs.112.22.3943
96. Entwistle J, Hall CL, Turley EA. HA Receptors: Regulators of Signalling to the Cytoskeleton. *J Cell Biochem* (1996) 61:569–77. doi: 10.1002/(sici)1097-4644(19960616)61:4<569::aid-jcb10>3.0.co;2-b
97. Lynn BD, Turley EA, Nagy JI. Subcellular Distribution, Calmodulin Interaction, and Mitochondrial Association of the Hyaluronan-Binding Protein RHAMM in Rat Brain. *J Neurosci Res* (2001) 65:6–16. doi: 10.1002/jnr.1122
98. Sherman L, Sleeman J, Herrlich P, Ponta H. Hyaluronate Receptors: Key Players in Growth, Differentiation, Migration and Tumor Progression. *Curr Opin Cell Biol* (1994) 6:726–33. doi: 10.1016/0955-0674(94)90100-7
99. Zaman A, Cui Z, Foley JP, Zhao H, Grimm PC, Delisser HM, et al. Expression and Role of the Hyaluronan Receptor RHAMM in Inflammation After Bleomycin Injury. *Am J Respir Cell Mol Biol* (2005) 33:447–54. doi: 10.1165/rcmb.2004-0333OC
100. Nedvetzki S, Gonen E, Assayag N, Reich R, Williams RO, Thurmond RL, et al. RHAMM, a Receptor for Hyaluronan-Mediated Motility, Compensates for CD44 in Inflamed CD44-Knockout Mice: A Different Interpretation of Redundancy. *Proc Natl Acad Sci U.S.A.* (2004) 101:18081–6. doi: 10.1073/pnas.0407378102
101. Liang J, Jiang D, Jung Y, Xie T, Ingram J, Church T, et al. Role of Hyaluronan and Hyaluronan-Binding Proteins in Human Asthma. *J Allergy Clin Immunol* (2011) 128:403–411 e403. doi: 10.1016/j.jaci.2011.04.006
102. Esposito AJ, Bhatraju PK, Stapleton RD, Wurfel MM, Mikacenic C. Hyaluronic Acid is Associated With Organ Dysfunction in Acute Respiratory Distress Syndrome. *Crit Care* (2017) 21:304. doi: 10.1186/s13054-017-1895-7
103. Liang Y, Yeligar SM, Brown LA. Chronic-Alcohol-Abuse-Induced Oxidative Stress in the Development of Acute Respiratory Distress Syndrome. *ScientificWorldJournal* (2012) 2012:740308. doi: 10.1100/2012/740308
104. Samuel SK, Hurta RA, Spearman MA, Wright JA, Turley EA, Greenberg AH, et al. TGF-Beta 1 Stimulation of Cell Locomotion Utilizes the Hyaluronan Receptor RHAMM and Hyaluronan. *J Cell Biol* (1993) 123:749–58. doi: 10.1083/jcb.123.3.749
105. Szabo G, Mandrekar P, Girouard L, Catalano D. Regulation of Human Monocyte Functions by Acute Ethanol Treatment: Decreased Tumor Necrosis Factor-Alpha, Interleukin-1 Beta and Elevated Interleukin-10, and Transforming Growth Factor-Beta Production. *Alcohol Clin Exp Res* (1996) 20:900–7. doi: 10.1111/j.1530-0277.1996.tb05269.x
106. Sueblinvong V, Tseng V, Smith T, Saghafi R, Mills ST, Neujahr DC, et al. TGFbeta1 Mediates Alcohol-Induced Nrf2 Suppression in Lung Fibroblasts. *Alcoholism Clin Exp Res* (2014) 38:2731–42. doi: 10.1111/acer.12563
107. Kaphalia L, Calhoun WJ. Alcoholic Lung Injury: Metabolic, Biochemical and Immunological Aspects. *Toxicol Lett* (2013) 222:171–9. doi: 10.1016/j.toxlet.2013.07.016
108. Brown SD, Brown LA. Ethanol (EtOH)-Induced TGF-Beta1 and Reactive Oxygen Species Production are Necessary for EtOH-Induced Alveolar Macrophage Dysfunction and Induction of Alternative Activation.

Alcoholism Clin Exp Res (2012) 36:1952–62. doi: 10.1111/j.1530-0277.2012.01825.x
109. Jha BK, Mitra N, Rana R, Surolia A, Salunke DM, Datta K. pH and Cation-Induced Thermodynamic Stability of Human Hyaluronan Binding Protein 1 Regulates its Hyaluronan Affinity. *J Biol Chem* (2004) 279:23061–72. doi: 10.1074/jbc.M310676200
110. Yadav G, Prasad RL, Jha BK, Rai V, Bhakuni V, Datta K. Evidence for Inhibitory Interaction of Hyaluronan-Binding Protein 1 (HABP1/p32/gC1qR) With Streptococcus Pneumoniae Hyaluronidase. *J Biol Chem* (2009) 284:3897–905. doi: 10.1074/jbc.M804246200
111. Wagner MC, Yeligar SM, Brown LA, Michael Hart C. PPARgamma Ligands Regulate NADPH Oxidase, eNOS, and Barrier Function in the Lung Following Chronic Alcohol Ingestion. *Alcohol Clin Exp Res* (2012) 36:197–206. doi: 10.1111/j.1530-0277.2011.01599.x
112. Liang Y, Harris FL, Jones DP, Brown LAS. Alcohol Induces Mitochondrial Redox Imbalance in Alveolar Macrophages. *Free Radic Biol Med* (2013) 65:1427–34. doi: 10.1016/j.freeradbiomed.2013.10.010
113. Liang Y, Harris FL, Brown LA. Alcohol Induced Mitochondrial Oxidative Stress and Alveolar Macrophage Dysfunction. *BioMed Res Int* (2014) 2014:371593. doi: 10.1155/2014/371593
114. Morris NL, Harris FL, Brown LAS, Yeligar SM. Alcohol Induces Mitochondrial Derangements in Alveolar Macrophages by Upregulating NADPH Oxidase 4. *Alcohol* (2021) 90:27–38. doi: 10.1016/j.alcohol.2020.11.004
115. Fogal V, Richardson AD, Karmali PP, Scheffler IE, Smith JW, Ruoslahti E. Mitochondrial P32 Protein is a Critical Regulator of Tumor Metabolism via Maintenance of Oxidative Phosphorylation. *Mol Cell Biol* (2010) 30:1303–18. doi: 10.1128/MCB.01101-09
116. Muta T, Kang D, Kitajima S, Fujiwara T, Hamasaki N. P32 Protein, a Splicing Factor 2-Associated Protein, is Localized in Mitochondrial Matrix and is Functionally Important in Maintaining Oxidative Phosphorylation. *J Biol Chem* (1997) 272:24363–70. doi: 10.1074/jbc.272.39.24363
117. Yagi M, Uchiumi T, Takazaki S, Okuno B, Nomura M, Yoshida S, et al. P32/Gc1qr is Indispensable for Fetal Development and Mitochondrial Translation: Importance of its RNA-Binding Ability. *Nucleic Acids Res* (2012) 40:9717–37. doi: 10.1093/nar/gks774
118. Sunderhauf A, Raschdorf A, Hicken M, Schlichting H, Fetzer F, Brethack AK, et al. GC1qR Cleavage by Caspase-1 Drives Aerobic Glycolysis in Tumor Cells. *Front Oncol* (2020) 10:575854. doi: 10.3389/fonc.2020.575854
119. Sun YJ, Shi GH, Zhao WW, Zheng SY. HABP1 Promotes Proliferation and Invasion of Lung Adenocarcinoma Cells Through NFkappaB Pathway. *Neoplasma* (2021) 69:155–64. doi: 10.4149/neo_2021_210904N1271
120. Sumiya J, Asakawa S, Tobe T, Hashimoto K, Saguchi K, Choi-Miura NH, et al. Isolation and Characterization of the Plasma Hyaluronan-Binding Protein (PHBP) Gene (HABP2). *J Biochem* (1997) 122:983–90. doi: 10.1093/oxfordjournals.jbchem.a021861
121. Mambetsariev N, Mirzapoiazova T, Mambetsariev B, Sammani S, Lennon FE, Garcia JG, et al. Hyaluronic Acid Binding Protein 2 Is a Novel Regulator of Vascular Integrity. *Arterioscler Thromb Vasc Biol* (2010) 30:483–90. doi: 10.1161/ATVBAHA.109.200451
122. Burnham EL, Brown LA, Halls L, Moss M. Effects of Chronic Alcohol Abuse on Alveolar Epithelial Barrier Function and Glutathione Homeostasis. *Alcoholism Clin Exp Res* (2003) 27:1167–72. doi: 10.1097/01.ALC.0000075821.34270.98
123. Pelaez A, Bechara RI, Joshi PC, Brown LA, Guidot DM. Granulocyte/macrophage Colony-Stimulating Factor Treatment Improves Alveolar Epithelial Barrier Function in Alcoholic Rat Lung. *Am J Physiol Lung Cell Mol Physiol* (2004) 286:L106–111. doi: 10.1152/ajplung.00148.2003
124. Wygrecka M, Markart P, Fink L, Guenther A, Preissner KT. Raised Protein Levels and Altered Cellular Expression of Factor VII Activating Protease (FSAP) in the Lungs of Patients With Acute Respiratory Distress Syndrome (ARDS). *Thorax* (2007) 62:880–8. doi: 10.1136/thx.2006.069658
125. Byskov K, Etscheid M, Kanse SM. Cellular Effects of Factor VII Activating Protease (FSAP). *Thromb Res* (2020) 188:74–8. doi: 10.1016/j.thromres.2020.02.010
126. Moraes TJ, Martin R, Plumb JD, Vachon E, Cameron CM, Danesh A, et al. Role of PAR2 in Murine Pulmonary Pseudomonal Infection. *Am J Physiol Lung Cell Mol Physiol* (2008) 294:L368–377. doi: 10.1152/ajplung.00036.2007
127. Kager LM, Schouten M, Wiersinga WJ, de Boer JD, Lattenist LC, Roelofs JJ, et al. Overexpression of the Endothelial Protein C Receptor is Detrimental During Pneumonia-Derived Gram-Negative Sepsis (Melioidosis). *PloS Negl Trop Dis* (2013) 7:e2306. doi: 10.1371/journal.pntd.0002306
128. Schouten M, van't Veer C, Roelofs JJ, Levi M, van der Poll T. Protease-Activated Receptor-1 Impairs Host Defense in Murine Pneumococcal Pneumonia: A Controlled Laboratory Study. *Crit Care* (2012) 16:R238. doi: 10.1186/cc11910
129. Johnson LA, Banerji S, Lawrance W, Gileadi U, Prota G, Holder KA, et al. Dendritic Cells Enter Lymph Vessels by Hyaluronan-Mediated Docking to the Endothelial Receptor LYVE-1. *Nat Immunol* (2017) 18:762–70. doi: 10.1038/ni.3750
130. Banerji S, Ni J, Wang SX, Clasper S, Su J, Tammi R, et al. LYVE-1, a New Homologue of the CD44 Glycoprotein, is a Lymph-Specific Receptor for Hyaluronan. *J Cell Biol* (1999) 144:789–801. doi: 10.1083/jcb.144.4.789
131. Jackson DG. Leucocyte Trafficking via the Lymphatic Vasculature-Mechanisms and Consequences. *Front Immunol* (2019) 10:471. doi: 10.3389/fimmu.2019.00471
132. Petrey AC, de la Motte CA. Hyaluronan, a Crucial Regulator of Inflammation. *Front Immunol* (2014) 5:101. doi: 10.3389/fimmu.2014.00101

Conflict of Interest: The authors declare that the research was conducted in the absence of any commercial or financial relationships that could be construed as a potential conflict of interest.

frontiers | Frontiers in Immunology

ORIGINAL RESEARCH
published: 13 May 2022
doi: 10.3389/fimmu.2022.866073

Ethanol Induces Secretion of Proinflammatory Extracellular Vesicles That Inhibit Adult Hippocampal Neurogenesis Through G9a/GLP-Epigenetic Signaling

Jian Zou[1], *T. Jordan Walter*[1], *Alexandra Barnett*[1], *Aaron Rohlman*[1], *Fulton T. Crews*[1,2,3] *and Leon G. Coleman Jr*[1,2]*

[1] Bowles Center for Alcohol Studies, University of North Carolina at Chapel Hill School of Medicine, Chapel Hill, NC, United States, [2] Department of Pharmacology, University of North Carolina at Chapel Hill School of Medicine, Chapel Hill, NC, United States, [3] Department of Psychiatry, University of North Carolina at Chapel Hill School of Medicine, Chapel Hill, NC, United States

OPEN ACCESS

Edited by:
Samantha Yeligar, Emory University, United States

Reviewed by:
Fabia Filipello, Washington University in St. Louis, United States
Angeles Vinuesa, Instituto de Biología y Medicina Experimental (IBYME) (CONICET), Argentina

***Correspondence:**
Leon G. Coleman Jr.
leon_coleman@med.unc.edu

Specialty section:
This article was submitted to Nutritional Immunology, a section of the journal Frontiers in Immunology

Received: *30 January 2022*
Accepted: *07 April 2022*
Published: *13 May 2022*

Citation:
Zou J, Walter T J, Barnett A, Rohlman A, Crews FT and Coleman LG Jr (2022) Ethanol Induces Secretion of Proinflammatory Extracellular Vesicles That Inhibit Adult Hippocampal Neurogenesis Through G9a/GLP-Epigenetic Signaling. Front. Immunol. 13:866073. doi: 10.3389/fimmu.2022.866073

Adult hippocampal neurogenesis (AHN) is involved in learning and memory as well as regulation of mood. Binge ethanol reduces AHN, though the mechanism is unknown. Microglia in the neurogenic niche are important regulators of AHN, and ethanol promotes proinflammatory microglia activation. We recently reported that extracellular vesicles (EVs) mediate ethanol-induced inflammatory signaling in microglia. Therefore, we investigated the role of EVs in ethanol-induced loss of adult hippocampal neurogenesis. At rest, microglia promoted neurogenesis through the secretion of pro-neurogenic extracellular vesicles (pn-EVs). Depletion of microglia using colony-stimulating factor 1 receptor (CSFR1) inhibition *in vivo* or using *ex vivo* organotypic brain slice cultures (OBSCs) caused a 30% and 56% loss of neurogenesis in the dentate, respectively, as measured by immunohistochemistry for doublecortin (DCX). Likewise, chemogenetic inhibition of microglia using a CD68.hM4di construct caused a 77% loss in OBSC, indicating a pro-neurogenic resting microglial phenotype. EVs from control OBSC were pro-neurogenic (pn-EVs), enhancing neurogenesis when transferred to other naive OBSC and restoring neurogenesis in microglia-depleted cultures. Ethanol inhibited neurogenesis and caused secretion of proinflammatory EVs (EtOH-EVs). EtOH-EVs reduced hippocampal neurogenesis in naïve OBSC by levels similar to ethanol. Neurogenesis involves complex regulation of chromatin structure that could involve EV signaling. Accordingly, EtOH-EVs were found to be enriched with mRNA for the euchromatin histone lysine methyltransferase (Ehm2t/G9a), an enzyme that reduces chromatin accessibility through histone-3 lysine-9 di-methylation (H3K9me2). EtOH-EVs induced G9a and H3K9me2 by 2-fold relative to pn-EVs in naïve OBSCs. Pharmacological inhibition of G9a with either BIX-01294 or UNC0642 prevented loss of neurogenesis caused by both EtOH and EtOH-EVs. Thus, this work finds that proinflammatory EtOH-EVs promote the loss of adult hippocampal neurogenesis through G9a-mediated epigenetic modification of chromatin structure.

Keywords: alcohol, inflammation, neurogenesis, microglia, epigenetics, G9a

1 INTRODUCTION

Heavy alcohol use and alcohol use disorder (AUD) are significant causes of morbidity worldwide. Chronic alcohol (i.e., ethanol) abuse causes dysfunction of key behaviors that contribute to ongoing misuse and age-related functional decline such as depressed mood, cognitive decline, and deficits in learning and memory plasticity. Adult hippocampal neurogenesis (AHN) occurs in the dentate gyrus and plays an important role in each of these functions (1–3). Chronic binge alcohol intake causes a loss of AHN with corresponding behavioral deficits (4–8). However, the underlying cause of the ethanol-induced loss of AHN is unknown.

AHN requires cooperation of multiple cell types and epigenetic regulation of specific transcriptomic cassettes (9–12). Proinflammatory activation of microglia, the resident monocyte/macrophage in brain, blunts AHN in infection or stress models (13–17). However, recently, resting microglia have been found to promote AHN through their secretome (18–20). Therefore, insults that modulate microglial activation state can regulate neurogenesis. Binge levels of ethanol promote proinflammatory microglial activation (21–23). Interventions that reduce induction of proinflammatory cytokines in brain, such as indomethacin and exercise, protect against ethanol inhibition of AHN (24). Therefore, we hypothesized that loss of AHN caused by ethanol involves secretion of anti-neurogenic factors from proinflammatory microglia. However, it is unknown how secreted factors from microglia alter transcriptional profiles in neuro-progenitors, to result in loss of AHN. In both embryonic and adult stages, epigenetic modifications of histone chromatin structure (e.g., acetylation and methylation) regulate neurogenesis (10–12, 25–28). Several enzymes are capable of remodeling chromatin structure. Several enzymes are capable of remodeling chromatin structure. We focused on the euchromatin histone-methyl transferase (EHMT2/G9a) since it has been implicated in facilitating changes in neuronal phenotype in response to ethanol (29, 30). G9a forms an enzymatic complex with a highly homologous protein G9a-like protein (GLP) to promote monomethylation and dimethylation of the histone 3 lysine 9 locus (H3K9me and H3K9me2 respectively), to play key roles in neurodevelopment (12). G9a is increased by ethanol, and alters neuron-specific genes in the basal forebrain (29, 30). Further, H3K9 methylation status is thought to regulate to neural cell proliferation (28). Therefore, we hypothesized that the regulation of AHN by ethanol and microglia involves secretion of EVs capable of regulating G9a/GLP-mediated epigenetic modifications of chromatin structure.

We recently reported that ethanol induction of proinflammatory signaling in brain involves the secretion of extracellular vesicles (EVs) from microglia (31). EVs are small, lipid-bilayer particles released from virtually all cell types that can affect the function of target cells (32). These proinflammatory EtOH-EVs were produced by microglia and reproduced the induction of proinflammatory cytokines caused by ethanol, and blocking their secretion prevented cytokine induction caused by ethanol. EVs have emerged as key mediators of disease pathology across organ systems (32–34). EVs facilitate the transfer of diverse cargo (i.e., protein, lipid, mRNA, miRNA, lncRNA, DNA) to target cells and/or elicit responses through interaction with cell surface receptors. EVs may cause epigenetic modifications to chromatin and DNA (35). In the context of ethanol exposure, EVs may participate in mediating transgenerational epigenetic inheritance (36) and regulating fetal neural stem cell development (37). Therefore, we hypothesized that proinflammatory EVs secreted in response to ethanol regulate AHN through epigenetic mechanisms. To study mechanisms regulating AHN we used both *in vivo* and *ex vivo* primary organotypic brain slice (OBSC) experiments. OBSC has all the brain cellular components and extracellular matrix of the adult hippocampal neurogenic niche and matures *ex vivo* to a neurological phenotype consistent with young adulthood with mature synapses and ongoing AHN (38–42). The use of OBSCs allows for EV transfer experiments to specifically identify the role of EVs. We found that resting microglia promote AHN through the secretion of pro-neurogenic (pn) EVs. EVs secreted by ethanol (EtOH-EVs) were proinflammatory and blunted AHN through a euchromatic histone-methyl transferase (EHMT2/G9a) epigenetic mechanism.

2 MATERIALS AND METHODS

2.1 Animals

Adult C57BL/6 mice were obtained from Jackson Laboratory. Pregnant Sprague Dawley rat mothers from Charles River (Raleigh, NC, USA) were used for all slice culture preparation. All protocols followed in this study were approved by the Institutional Animal Care and Use Committee at the University of North Carolina at Chapel Hill (protocols 20-231.0 and 21-224.0) and were in accordance with National Institutes of Health regulations for the care and use of animals in research.

2.2 Materials

The CSF1R inhibitor PLX-3397 was obtained from MCE (Monmouth Junction, NJ, USA). PLX-5622 was provided by Plexxikon (Berkeley, CA, USA). Antibodies were purchased from the following vendors: DCX (Santa Cruz, sc-271390, USA), Ki67 (abcam, ab16667, Boston, USA), G9a (abcam, ab185050, Boston, USA), H3K9me (abcam, ab32521, Boston, MA, USA), beta actin (abcam, ab8229). The G9a inhibitor BIX-01294 was purchased from Selleckchem (Houston, TX, USA) and UNC0642 is from Santa Cruz (Santa Cruz, CA, USA).

2.3 Microglial Depletion *In Vivo*

Microglia were depleted brain-wide using the colony stimulating factor 1 receptor (CSF1R) antagonist PLX-5622 supplemented in chow (1200 ppm) as described previously (43). Briefly, mice were given PLX-supplemented or normal chow for three weeks. Mice were sacrificed by intracardial perfusion with paraformaldehyde, and brains processed for immunohistochemistry (IHC) as we have reported previously (43, 44).

2.4 Primary Organotypic Brain Slice Culture (OBSC)

Primary organotypic brain slice cultures (OBSCs) were prepared from the hippocampal-entorhinal cortex formation of postnatal

day (P)7 pups using previously established techniques of Stoppini and colleagues (45) with modifications as we have described previously (31, 46, 47). Briefly, a Sprague Dawley rat mother with a litter of 12 pups on P6 were obtained from Charles River (Raleigh, NC, USA) and housed overnight in the animal facility. All neonates at P7 were decapitated, the brains were removed, and hippocampal-entorhinal complex dissected in Gey's buffer (Sigma-Aldrich, St. Louis, MO, USA). Slices (~25/pup) were transversely cut with a McIlwain tissue chopper at a thickness of 375 μm and placed onto a 30 mm diameter Millicell low height culture insert (Millipore, PICMORG50), 10-13 slices/tissue insert. Slices from both sexes were pooled together. Slices were cultured with MEM containing 25 mM HEPES and Hank's salts, supplemented with 25% horse serum (HS) + 5.5 g/L glucose + 2 mM L-glutamine in a humidified 5% CO2 incubator at 36.5°C for 7 days *in vitro* (DIV), followed by 4DIV in MEM + 12% HS, and then slices were cultured with MEM + 6% HS until the end of experiments. Two replicates were performed for each experimental condition, with each experiment repeated at least twice. Serum-free N2-supplemented MEM was used to mix with MEM containing 25% HS throughout experiments. OBSC slices were incubated for a total of 14 days prior to treatment as described by Stoppini et al. to allow for functional maturation of synapses (45). OBSC slices are long-lived with undetectable cell death up to 42 days in culture in our previous report (21).

For transfection of the hM4di DREADD in microglia, OBSCs were treated with either control AAV9.EGFP or AAV9.CD68.hm4Di.mCherry (VectorBuilder) for 24 h prior to administration of the hM4di agonist CNO for 4 days.

2.5 Microglial Depletion in OBSC

For microglial depletion in OBSC, slices at 4DIV were treated with the CSF1R inhibitor PLX-3397 (1μM), chosen for solubility in media, for 7 days in regular culture medium (MEM containing 25% HS), followed by 3DIV in MEM + 12% HS to deplete microglia. We used 1μM PLX-3397 since we have previously reported that this successfully depletes >90% of microglia in our *ex vivo* slice culture model (21). At the end of PLX3397 treatment, slices were either immediately removed for analysis or followed by microglial repopulation protocol in MEM + 6% HS without PLX-3397 (21).

2.6 Immunohistochemistry (IHC) and Quantification *In Vivo* and in OBSC

2.6.1 *In Vivo*:

IHC was performed on PFA-perfused mice as we have reported previously (43). Briefly, perfused brains were dehydrated in 30% sucrose. Brains were then sliced at 40μM thickness using a freezing microtome. Free-floating sections were washed in 0.1M PBS, endogenous peroxidases neutralized by incubation in 0.3% H_2O_2 for 30 min, washed again in PBS, and permeabilized and blocked for 1 h in 0.25% Triton-X100/5% normal serum at room temperature (RT). Sections were then incubated overnight at 4°C in primary antibody in blocking solution. The next day sections were washed in PBS and incubated in biotinylated secondary antibody (1:200; Vector Laboratories, Burlingame, CA, USA) for 1 h at RT. After washes sections were incubated in avidin–biotin complex solution (Vectastain ABC Kit, Vector Laboratories, Burlingame, CA, Cat. # PK6100) for 1 h at RT. Immunoreactivity was visualized using nickel-enhanced diaminobenzidine (Sigma-Aldrich, St. Louis, MO, USA, Cat. # D5637). Tissue was mounted onto slides, dehydrated, and coverslips placed. At least three sections per mouse were quantified for immunoreactivity (+IR)

2.6.2 *OBSC:*

At the end of each experiment, OBSC slices were quickly washed in cold PBS and fixed with 4% paraformaldehyde in 0.1M PBS for 24 h at 4°C. Floating OBSC slices were washed with PBS and incubated with 0.6% H_2O_2 to inhibit endogenous peroxidase. After further washing with PBS, slices were blocked with 3% rabbit serum containing 0.25% Triton X100 for 1 h at RT and then incubated with mouse anti-DCX or anti-H3K9me2 for 48 h at 4°C. DCX+IR was detected using an ABC kit and followed by the DAB method. For quantification of DCX IR, DCX+ cell and processes in DG region of the hippocampus were imaged live at 8x magnification, background corrected, and DCX IR measured with the Keynce BZ-H4XF imaging software (*in vivo*) or ImageJ (OBSC).

2.7 EV Isolation and Assessment by Nanoparticle Tracking Analysis and Transmission Electron Microscopy (TEM)

2.7.1 EV Isolation:

EVs were isolated by sequential centrifugation from OBSC media as we have reported previously (31, 48). Briefly, media were centrifuged at 300 g for 10 min and followed by 6000g for 10 min to remove cellular debris. The supernatant was then centrifuged at 21,000g for 96 min at 4°C to pellet EVs. This method isolates primarily microvesicles (MVs, 0.05-1.0μm diameter) and larger exosomes (0.05-0.1μm diameter) (32). EVs were resuspended in fresh MEM media.

2.7.2 *TEM Negative Stain*:

EVs were visualized by negative-stain transmission electron microscopy (TEM) in the UNC Microscopy Services Laboratory. Briefly, this involved floating a glow-discharged formvar/carbon-coated 400 mesh copper grid (Ted Pella, Inc., Redding, CA, USA) on a 20μl droplet of the sample suspension for 12 min. This was transferred quickly to 2 drops of deionized water followed by addition of a droplet of 2% aqueous uranyl acetate stain for 1 minute. The grid was blotted with filter paper and airdried. Samples were then visualized at 80kV using a JEOL JEM-1230 transmission electron microscope operating (JEOL USA INC., Peabody, MA, USA). Images were taken using a Gatan Orius SC1000 CCD camera with Gatan Microscopy Suite version 3.10.1002.0 software (Gatan, Inc., Pleasanton, CA, USA).

2.7.3 *Nanoparticle Tracking Analysis (NTA)*:

Media samples were diluted in 0.02 μm filtered PBS and assessed by NTA on the ParticleMetrix ZetaView® PMX-420 Video Microscope in the Nanomedicines Characterization Core Facility at UNC as we have reported previously (31, 49–51).

2.8 Ethanol Treatment and Conditioned EV Transfers in OBSC

All ethanol treatments with the indicated concentrations occurred in a desiccator containing 300ml water plus ethanol at the same concentration present in the culture media as we have reported previously (31, 52, 53). OBSC slices at 14DIV were exposed to ethanol (100mM) for 4 days in the absence or presence of G9a inhibitor BIX-01294. We have previously found this concentration *ex vivo* causes induction of immune genes that is similar to findings *in vivo* and in postmortem human AUD brain (48, 53). Though this is a high concentration of alcohol for non-dependent individuals, patients with AUD reach these blood alcohol concentrations while being conscious and functional (54). At the end of experiments, slices were removed for further analysis.

For conditioned EV transfer experiments, pelleted EVs from control or ethanol-treated groups were resuspended in MEM + 6% horse serum. This media and serum concentration has been optimized in our previous studies for the assessment of neurogenesis in the OBSC (42). To account for potential effects of EVs in the media, all experiments include unconditioned media controls as recommended by the International Society for Extracellular Vesicles (ISEV) guidelines in situations when the use of exosome-depleted media is not desirable (55). We also perform EV supernatant controls (described below). We have reported that this technique recovers ~30% of total media MVs, thus a ratio of EVs pelleted from 2 slice culture wells to 1 new slice culture well is transferred (31). EVs were isolated from 1 mL of culture media. Each culture well had 10-13 hippocampal slices (300μm thickness). $1.4x10^{10}$ EVs were added to each recipient culture which is ~20% of the total slice media EVs at baseline, similar to our previous studies (31, 49, 50). At the end of EV treatment, slices were removed for either mRNA analysis by RT-PCR or immunostaining for measurement of neurogenesis. To determine if remaining proteins in the EV preparations mediate the effects of EVs two methods were employed. First, supernatant (SUPN) from the final spin of EV isolation was transferred to naïve OBSC as we had done previously (31) to determine if soluble components in media mediate the effects as recommended by the ISEV guidelines (55). Briefly, SUPN from the final spin was diluted 1:1 with fresh media to ensure adequate nutrition and was then added to naive OBSC. Further, we also performed digestion of remaining proteins in the EV preparation using proteinase K as described previously (56). Briefly, pelleted EVs were resuspended in PBS and incubated with 20μg/mL of Proteinase K (Prot K, Invitrogen) at 37°C for 1 hour. Prot K activity was quenched by adding 5mM phenylmethylsulfonyl fluoride (10 min at RT). EVs were then re-pelleted (21,000g, 96 minutes) and resuspended in fresh MEM, then added to naïve OBSC.

2.9 Measurement of mRNAs and Protein in EVs and OBSC Tissue

2.9.1 RNA Isolation *and Reverse Transcription*:

Total RNA was isolated either from the pelleted EVs or OBSC slice tissue using miRNAeasy Kit (Qiagen Inc., CA, USA) according to manufacturer's protocol. Briefly, the pelleted EVs from 2-3 culture media or 10-13 pooled tissue slices/per group were dissolved in total of 700ul Trizol lysis buffer as we have previously reported (21, 31). After centrifugation at 12,000g for 15 min, supernatant was removed for total RNA purification. The total amount of RNA was quantified by Nanodrop™. For reverse transcription, either 200ng of RNA from EVs or 2 μg of RNA from slices was used to synthesize the first strand of cDNA using random primers (Invitrogen) and reverse transcriptase Moloney murine leukemia virus (Invitrogen). After a 1:2 dilution with water, 2 μl of the first strand cDNA solution was used for RT-PCR.

2.9.2 *RT-PCR*:

The primer sequences for real time RT-PCR were as follows: TNFα-F: AGCCCTGGTATGAGCCCATGTA, R:CCGGACTCCGTGA TGTCTAAG; IL-1β-F:TTGTGCAAG TGTCTGAAGCA, R: TGTCAGCCTCAAAGAACAGG; G9a-F:CTCCGGTCCC TTGTCTCC, R:CT ATGAGAGGTGTCCCCCAA; β-Actin-F: CTACAATGAGCTGCGTGTGGC, R: CAGGTCCAGAC GCAGGATGGC; 18S-F: CGGGGAATCAGGGTTCGATT, R: TCGGGAGTGGGTAATTTGCG. Primer sequences were validated using the NCBI Primer-BLAST, with only primers that targeted the desired mRNA and had single-peak melt curves (showing amplification of a single product) being used. SYBER Green Supermix (AB system, UK) was used as a RT-PCR solution. The real time RT-PCR was run with initial activation for 10 min at 95° C and followed by either 48 cycles (EV mRNA) or 40 cycles (tissue mRNA) of denaturation (95°C, 40 s), annealing (58°C, 45 s) and extension (72°C, 40 s). The threshold cycle (C_T) of each target product was determined and normalized to a reference housekeeping gene. For all analyses in OBSC tissue, β-actin was used as the housekeeping gene. For measurement of mRNAs in EVs, 18S was used as the housekeeping gene since actin mRNA was not detected in the vesicles. Difference in C_T values (ΔC_T) of two genes was calculated $\left[\text{difference} = 2^{-(C_T \text{ of target genes} - C_T \text{ of } \beta-\text{actin})} = 2_T^{-\Delta C}\right.$ and the result was expressed as the percentage compared to control.

2.9.3 *Western Blot*:

OBSC sections (4-6) were pooled and lysed with Tris buffer and centrifuged at 21,000g to remove the nuclear fraction as we previously reported (48). Protein concentrations were measured using a Pierce BCA assay kit with the manufacturer's instructions (ThermoFisher Scientific). Samples were diluted in RIPA and DTT containing reducing buffer (Pierce TM Cat. # 39000) to a final amount of 40 μg protein per well. Protein samples were separated on a 4–15% Ready Gel Tris-HCL gel (BioRad) and transferred onto PVDF membranes (BioRad). PVDF membranes were incubated at 4°C overnight with primary antibody. The following day, secondary antibody incubation (Li-Cor IRDye® 680 or 800) was performed, and membranes visualized using the LiCor Odyssey™ imaging system. Values for proteins of interest were normalized to beta-actin expression for each sample.

2.10 Statistical Analyses

For experiments when only two groups were compared, *t*-tests were performed. Statistical analyses for experiments with

multiple treatment groups were performed using One-way ANOVAs, with Sidak's *post hoc* tests for multiple comparisons. Differences were considered statistically significant if $p < 0.05$.

3 RESULTS

3.1 Microglia Promote Neurogenesis Through the Secretion of Pro-Neurogenic Extracellular Vesicles (pn-EVs)

Microglia have been found to promote adult hippocampal neurogenesis through their secretome (18–20). EVs are a key aspect of the microglial secretome (31); therefore we assessed their role in neurogenesis. First, we determined the impact of microglial depletion on neurogenesis both *in vivo* and *ex vivo*. Microglia were depleted using the CSF1R antagonist PLX-5622 as reported previously (43). PLX5622 effectively removed Iba1+ microglia in the hippocampus with ~96% depletion of microglia (**Figures 1A, B**). We then assessed hippocampal neurogenesis in the dentate gyrus using immunohistochemistry (IHC) for doublecortin (DCX). DCX is a cytoskeleton marker of neuroprogenitors expressed during maturation of dendrites and other neuronal structures. DCX was reduced by 30% in microglia-depleted mice (**Figures 1C, D**, $*p<0.05$). Likewise, a 24% reduction in Ki67, a marker of proliferation, was found (**Figures 1E, F**). The role of microglia in neurogenesis was then assessed in OBSC, where PLX depletion of microglia caused a 56% reduction in DCX in the dentate gyrus (**Figures 1G, H**). To confirm that the loss of microglial activity underlies the loss of neurogenesis rather than factors released by dying microglia or off-target effects of CSF1R-inhibition, we next inhibited microglial activation using a chemogenetic approach. Microglial activity was inhibited by transfection with the hM4di inhibitory designer receptor exclusively activated by designer drugs (DREADD) using a viral construct (AAV9.CD68.hm4di) as we have reported previously (21). In the presence of microglial hM4di expression, a significant treatment effect across groups was found (ANOVA $F_{5,61} = 7.148$, $****p<0.0001$) with the hM4di agonist CNO causing a 77% reduction in neurogenesis in the dentate gyrus as measured by DCX staining (**Figures 1I, J**, $***p<0.001$, Sidak's post-test). Neither hM4di transfection alone nor CNO alone significantly altered neurogenesis. Thus, microglia in healthy mouse dentate gyrus and OBSC brain slice culture promote hippocampal neurogenesis both *in vivo* and *ex vivo*. Since the microglial secretome has been implicated in hippocampal neuroprogenitor survival, we next studied the role of secreted extracellular vesicles.

To determine the effect of OBSC EVs on neurogenesis, we used EV transfer experiments using our previously established protocols (31). EVs were transferred from either normal or

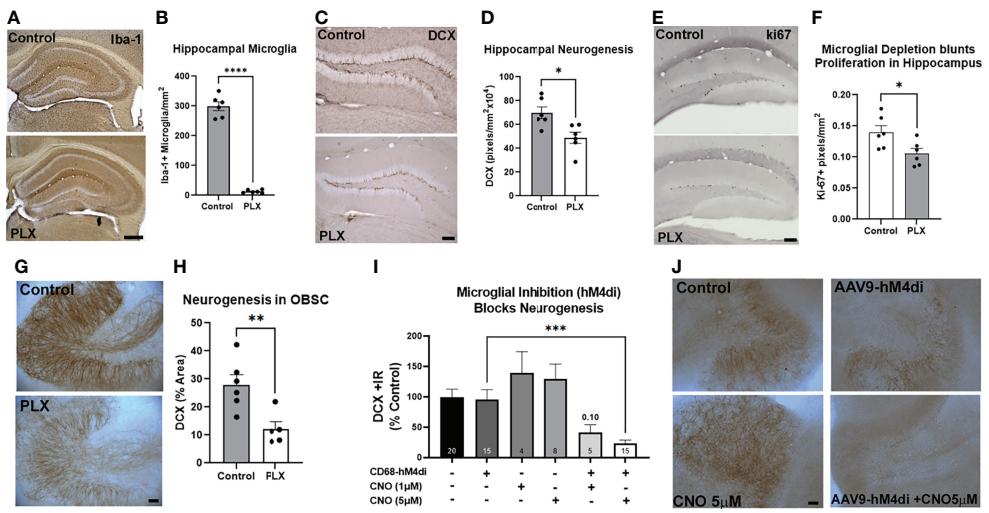

FIGURE 1 | Microglia at rest promote adult hippocampal neurogenesis. **(A-F)** Adult mice were given either normal or PLX-5622-supplemented chow for 3 weeks to deplete microglia. **(A)** PLX chow caused robust depletion of microglia as measured by Iba-1 IHC. **(B)** Quantification of Iba-1 staining in hippocampus found ~96% depletion of microglia. $****p <$ 0.0001, *t*-test vs. control. Scale bar: 500μm **(C)** Representative images of DCX staining in hippocampal dentate gyrus showing loss of neurogenesis with microglial depletion. Scale bar 100 μm. **(D)** Quantification found a ~30% reduction in DCX immunoreactivity. $*p <$ 0.05, *t*-test vs. control. **(E)** Representative images of ki67 immunostaining after EtOH in dentate regions of the hippocampus in control and microglia depleted (PLX) mice. **(F)** Ethanol caused a 24% reduction in ki67. $*p < 0.05$, *t*-test. **(G, H)** OBSC were treated with PLX-3397 (1μM) for 10 days to deplete microglia and determine its effect on neurogenesis. **(G)** Representative images of DCX in hippocampal region of OBSC showing loss of neurogenesis with microglial depletion. Scale bar: 100μm. **(H)** Quantification found a 56% reduction in DCX staining with microglial depletion. $**p < 0.01$, *t*-test vs. control. **(I, J)** Microglial inhibition reduces neurogenesis. OBSC were treated with either AAV9.CD68.hM4di or AAV9.EGFP control for 24 hours prior to treatment with CNO (1μM or 5μM) or vehicle for 4 days, followed by IHC for DCX. **(I)** Quantification of DCX found that neither viral transfection alone nor CNO alone significantly altered neurogenesis. Addition of CNO to microglial hM4di-transfected slices caused a 77% reduction in DCX with 5μM CNO. 1-Way ANOVA, $F_{5,61} = 7.148$, $p <$ 0.0001. $***p < 0.001$, Sidak's *post-hoc* test vs. AAV9.CD68.hM4di alone **(J)** Representative images of DCX +/- CNO and AAV9 transfection. Scale bar: 100μm.

microglia-depleted OBSC donors to either normal (microglia +) or microglia-depleted OBSC recipient cultures (**Figure 2A**). A significant treatment effect was found across the groups ($F_{5,39}$ = 9.705, p<0.0001). As above, microglial depletion with PLX alone caused a robust reduction in neurogenesis as measured by DCX (62%, **Figure 2C**, *p<0.05 vs. Control, Sidak's post-test) that was clearly visible (**Figure 2D**, top panel). EVs transferred from normal microglia-containing cultures were pro-neurogenic (pn-EVs), increasing levels of neurogenesis in normal slices by 56% (**Figures 2C, D** middle panel, *p<0.05 vs. Control, Sidak's post-test). pn-EVs also increased the expression of the pro-neurogeneic cytokine IL-4 (57). IL-4 was increased by 82% (**Supplementary Figure 1A**, *p<0.05, Sidak's post-test). Further, pn-EVs restored the loss of DCX in PLX microglia-depleted slices, increasing DCX by 290% relative to vehicle PLX slices (***p=0.001, vs. PLX alone, Sidak's post-test) EVs isolated from microglia-depleted-cultures, however (**Figures 2C, D** lower panel), did not increase DCX in neither control (p=0.43 vs. control alone) nor microglia-depleted (p=0.78, vs. PLX alone) recipient OBSCs. This indicates that microglial EVs at baseline promote neurogenesis through the generation of pn-EVs.

3.2 Ethanol Induces Secretion of Proinflammatory EVs (EtOH-EVs) That Inhibit Hippocampal Neurogenesis

We recently reported that EVs play a key role in proinflammatory induction caused by ethanol, reproducing the effects of ethanol treatment (31). Though EtOH did not increase the number of EVs released as measured by nanoparticle tracking analysis, it altered EV contents and function (31). Proinflammatory stimuli such as binge ethanol are known to blunt neurogenesis (13, 15, 58), with the microglial secretome playing an important role in this regulation (18–20). Therefore, we investigated the role of EtOH-induced EVs on hippocampal neurogenesis. EVs were isolated from OBSC media with control or EtOH treatment as we have previously reported (31). NTA analysis confirmed EVs in the 50-300nm diameter size range in both control/pn-EVs and EtOH-EVs (**Figure 3A**). The phenotype of EVs was then assessed by TEM negative staining. TEM confirmed the presence of EVs with the expected morphology (**Figure 3B**). Western blot further confirmed the presence of EVs with positive expression of the MV marker Annexin A1, the exosomal marker CD63, and the shared MV/exosomal marker CD81 (**Figure 3C**). EtOH-

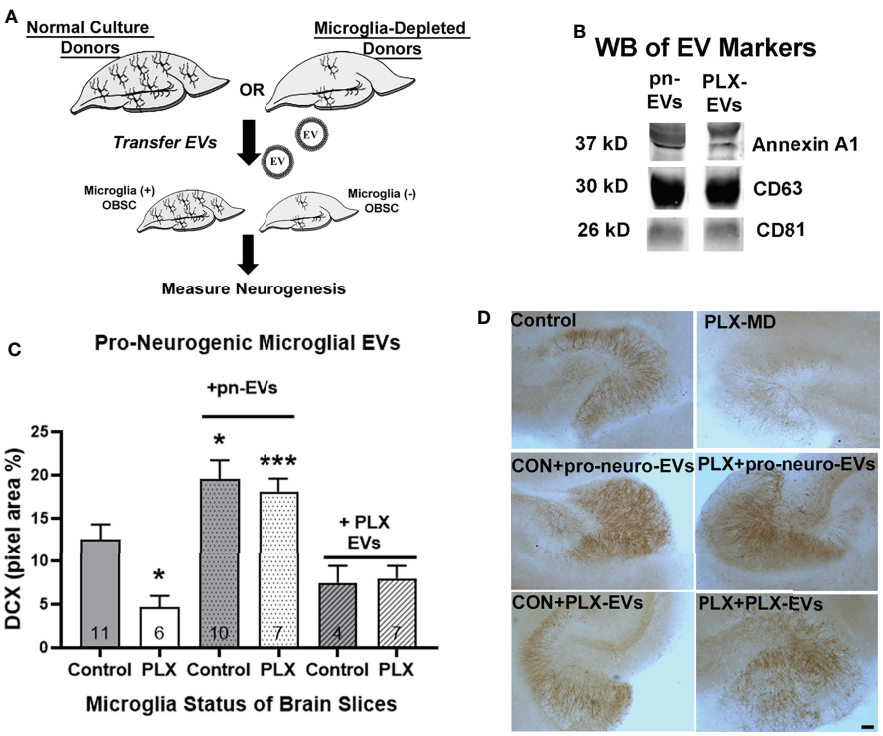

FIGURE 2 | EVs from microglia-containing cultures are pro-neurogenic. **(A)** Experimental design for EV transfer experiments from normal microglia-containing and PLX microglia-depleted OBSCs. EVs from each donor condition were transferred to either microglia-containing (Control) or microglia-depleted (PLX) OBSC recipients. **(B)** Western blot analysis shows expression of EV markers Annexin A1, CD63 and CD81 in pn-EVs and PLX-EVs. **(C)** Quantification of treatment effect on DCX immunostaining (One-way ANOVA, $F_{5,39}$ = 9.705, p < 0.0001). Microglial depletion with PLX-3397 (1μM, 10 days) caused a 62% reduction in DCX in the dentate region of the OBSC (*p < 0.05 vs. control, Sidak's post-test). EVs from control OBSC (pn-EVs) increased basal levels of DCX by 55% (gray bar with dots, *p < 0.05 vs. Control, Sidak's post-test) and increased DCX in microglia-depleted recipient OBSCs by 290% (white bar with dots, ***p < 0.001 vs. PLX alone, Sidak's post-test). EVs from microglia-depleted OBSC donors (PLX-EVs), however, did not significantly change DCX levels in control (p=0.43 vs. control alone, Sidak's post-test) or microglia-depleted OBSC slices (p=0.78, vs. PLX alone, Sidak's post-test) N for each group is included within each bar. **(D)** Representative images of DCX IHC in OBSC treatment groups. Scale bar 100 μm.

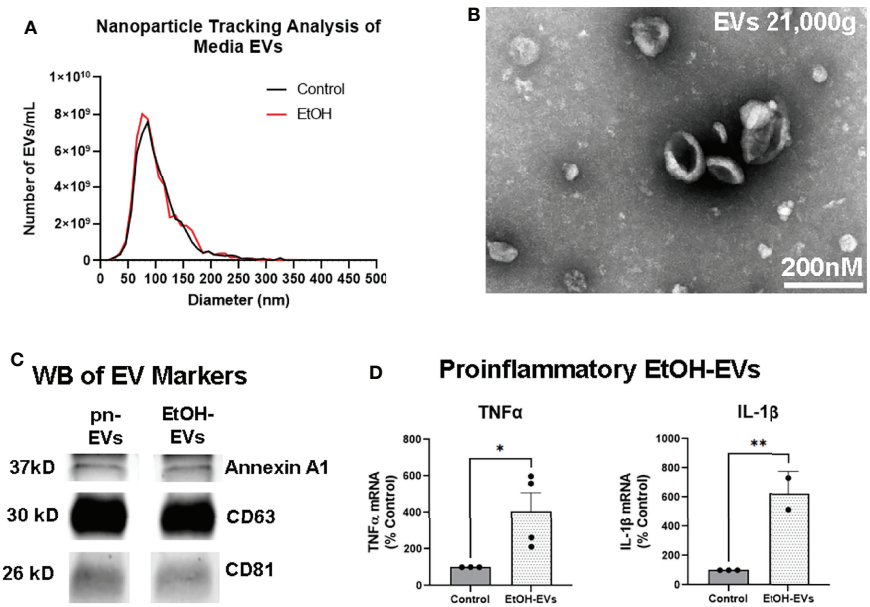

FIGURE 3 | EVs secreted by ethanol are proinflammatory. EVs were isolated from OBSC media after either ethanol (EtOH-EVs) or vehicle control (pro-neurogenic, pn-EVs). **(A)** NTA assessment of OBSC media showed similar size distributions between Control/pn-EVs and EtOH-EVs, mostly between 50-300nm in diameter. Averaged distributions from 3 samples per group depicted. **(B)** Transmitting electron microscopy confirmed the presence EVs with the expected size and cup-shaped morphology. **(C)** Western blot (WB) analysis of EV markers found Annexin A1, CD63, and CD81 in both pn-EVs and EtOH-EVs. **(D)** EtOH-EVs were transferred to naïve OBSC slices, and levels of proinflammatory cytokines in slices measured by RT-PCR. A significant main effect of treatment was found (One-way ANOVA $F_{3,8} = 9.211$, $p=0.0055$). EtOH-EVs caused robust inductions of TNFα (4-fold) and IL-1β (6-fold), $^{*}p < 0.05$, $^{**}p < 0.01$ Sidak's post-tests.

conditioned EVs were proinflammatory, with adoptive transfer to naïve slices causing a significant treatment effect (**Figure 3D**, $F_{3,8} = 9.211$, $p=0.0055$). *Post-hoc* analyses confirmed a 4-fold increase in gene expression of TNFα ($^{*}p<0.05$, Sidak's post-test) and a 6-fold increase in IL-1β ($^{**}p<0.01$ Sidak's post-test) consistent with our previous work (31).

Next, we assessed the effect of EtOH and EtOH-EVs on neurogenesis. A significant main effect of treatment was found on neurogenesis as measured by DCX (**Figures 4A, B**, $F_{5,\ 58} = 20.9$, $p<0.0001$) and ki67 (**Figures 4C, D**, $F_{3,\ 22} = 18.25$, $p<0.0001$). Ethanol reduced DCX expression by 48% compared to control (**Figures 4A, B**, $^{***}p<0.001$, Sidak's post-test), consistent with previous findings *in vivo* and *ex vivo* (6, 24, 59). EVs from control OBSC were pro-neurogenic (pn) with a 67% increase in DCX ($^{****}p<0.0001$ vs. Control, Sidak's post-test). However, EVs from EtOH-treated OBSC reduced DCX staining by ~52% compared to controls ($^{***}p<0.001$) similar to the effects of ethanol. There was no significant difference between EtOH treated and EtOH-EV treated EVs ($p=0.998$). Likewise, reductions in ki67 were seen caused by ethanol (**Figure 4D**, 77%, $^{**}p<0.01$ vs. control) and EtOH-EVs (**Figure 4D**, 62% vs. pn-EVs, $^{****}p<0.0001$). In order to determine if remaining media proteins in the EV preparations mediate this effect, we also assessed the effects of the EV supernatant on AHN, as recommended by the ISEV guidelines (55). This experiment is needed in order to attribute biological effects to EVs rather than a soluble component, and avoids the confounding of effects of components from size exclusion columns on biological function of recipient cells (55). We previously reported that EVs, but not EV depleted supernatant cause proinflammatory gene induction in brain slices (31). Likewise, we found that neither supernatant (SUPN) from control/pn-EV preparations, nor SUPN from EtOH-EV preparations had any effect on DCX (**Figure 4B**). Further, proteinase K digestion of EtOH-EV preparations to degrade all protein species outside of the EV membrane had no impact on the loss of DCX (**Figure 4B**) or ki67 (**Figure 4D**) caused by EtOH-EVs. This indicates that the observed effects of EtOH-EVs are not due to remaining protein in the isolated EVs. Thus, EVs secreted in response to ethanol are proinflammatory and anti-neurogenic, phenocopying the effects of ethanol. Since neurogenesis involves complex changes in chromatin accessibility to allow lineage specific gene transcription, we sought to investigate if EtOH-EV inhibition of neurogenesis involved an epigenetic mechanism.

3.3 EtOH-EVs Are Enriched With Euchromatin Histone Lysine Methyltransferase (Ehmt2)/G9a mRNA and Increase Histone-3 Lysine-9 Di-Methylation (H3K9me2)

Neurogenesis involves a complex orchestration of differential transcriptional programs that are regulated by chromatin modifications (10–12). EVs contain complex cargo including

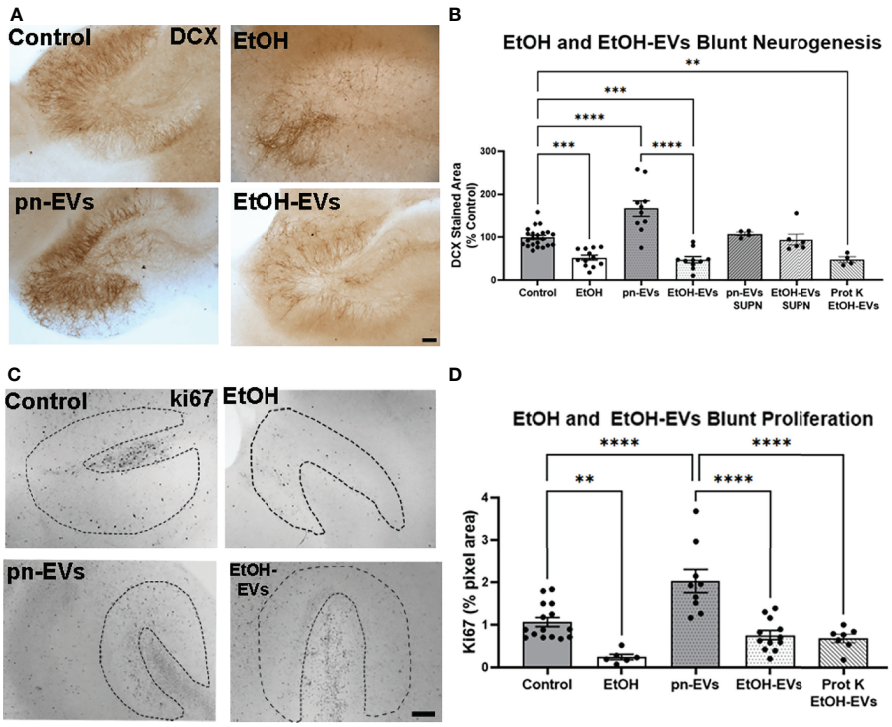

FIGURE 4 | EVs secreted by ethanol blunt neurogenesis. OBSCs were treated for 4 days with either vehicle, ethanol, pn-EVs, EtOH-EVs, supernatant (SUPN) from EV preparations, or EtOH-EVs treated with proteinase K (Prot K) to degrade free proteins. Neurogenesis measured by IHC for DCX. **(A)** Representative images showing enhancement of neurogenesis by pn-EVs and a clear reduction of neurogenesis by EtOH and EtOH-EVs. Scale bar 100 µm. **(B)** Quantification of DCX staining found a significant main effect of treatment ($F_{5, 58}$ = 20.9, p < 0.0001). A 48% reduction in DCX was caused by EtOH, a 67% increase by pn-EVs relative to control. EtOH-EVs caused a 52% reduction compared to pn-EVs. SUPN isolated from pn-EV and EtOH-EV preparations had no effect on DCX. Prot K digestion of free proteins had no effect on reduction of DCX caused by EtOH-EVs. **(C)** Representative images of ki67 immunostaining in OBSC in control, EtOH, control/pn-EVs and EtOH-EVs. The neurogenic niche in the OBSC is outlined by the dashed lines. **(D)** Quantification of ki67 found a main effect of treatment (one-way ANOVA, $F_{3,41}$ = 21.75, $p < 0.0001$.) Ethanol-EVs caused a 45% reduction in 60% reduction in ki67 staining compared to pn-EVs. Prot K digestion free proteins had no impack on loss of Ki67 caused by EtOH-EVs.**$p < 0.01$, ***$p < 0.001$, ****$p < 0.00001$ Sidak's post-test. Each dot represents an individual culture slice.

mRNAs, non-coding RNAs, miRNAs, and proteins that could potentially regulate epigenetic chromatin modifications that could regulate neurogenesis (33, 60). Therefore, we investigated whether EVs alter epigenetic modifications that regulate neurogenesis. The euchromatin histone lysine methyltransferase (Ehmt2/G9a) facilitates di-methylation of the lysine 9 residue on histone 3 (H3K9me2) to repress gene expression. G9a is involved in lineage specification during embryonic neurogenesis (12), and G9a-associated epigenetic marks are reduced by environmental enrichment-enhanced neurogenesis (11). G9a mRNA was increased by 2.5-fold (***p<0.001, **Figure 5A**) in microglia-depleted slices, consistent with an association between its induction and a loss of neurogenesis. In EtOH-EVs, we found that G9a mRNA was increased by more than 3-fold relative to control pn-EVs (**Figure 5B**, *p<0.05). In OBSC tissue, a main effect of treatment was found on G9a mRNA after treatment with either ethanol or EtOH-EVs (**Figure 5C**, One-way ANOVA, $F_{3,17}$ = 12.90, p=0.0001). Both ethanol and EtOH-EVs increased expression of G9a mRNA by 3-fold (****p<0.0001, Sidak's post-test) and 2-fold (*p<0.05, Sidak's), respectively, compared to controls with no effect of pn-EVs (**Figure 5C**). Since G9a mRNA was increased in OBSC by ethanol, we assessed if its associated H3K9me2 mark was also increased. IHC revealed H3K9me2 staining primarily in the neuronal granular region of the dentate and at the neurogenic niche (**Figure 5D**, dashed line). Ethanol increased H3K9me2 in the neuronal granular region of the dentate by 30% (**Figure 5D**). We then assessed the effect of EtOH-EV treatment of OBSCs on both G9a and H3K9me2 by western blot to confirm RT-PCR and IHC findings. EtOH-EVs caused a ~2-fold increase in both G9a protein (**Figure 5E**, **p<0.01) and H3K9me2 (**Figure 5F**, **p<0.01) in OBSC tissue. Since we found induction of G9a and H3K9me2, we next investigated if pharmacological inhibition of the G9a/GLP complex could prevent the loss of neurogenesis caused by ethanol and EtOH-EVs.

3.4 Pharmacological Inhibition of G9a/GLP Prevents Loss of Neurogenesis by EtOH and EtOH-EVs

Since we found that ethanol and EtOH-EVs block adult hippocampal neurogenesis and increase expression of G9a, we

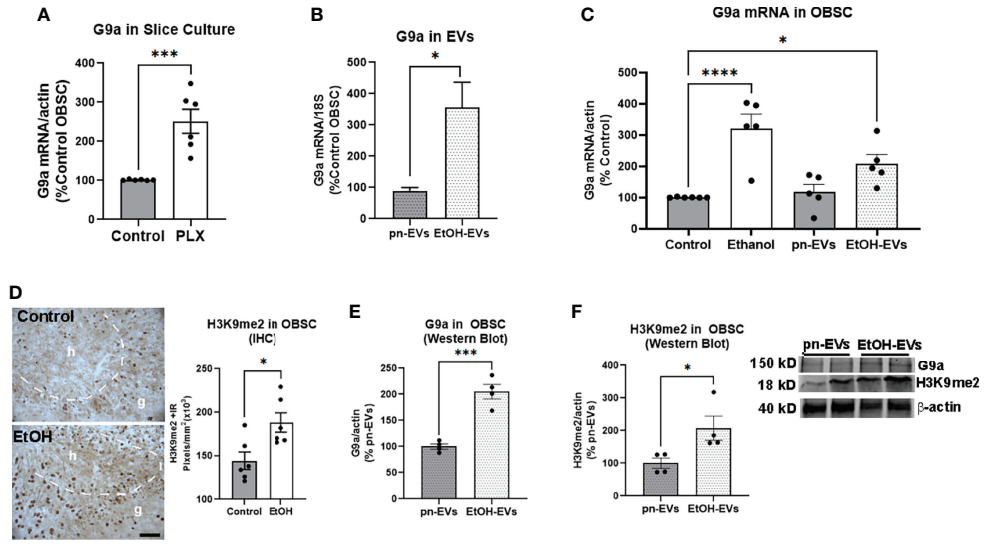

FIGURE 5 | Microglia depletion and ethanol-EVs increase G9a in OBSC. **(A)** G9a mRNA was measured in control or PLX-microglial depleted OBSC. PLX resulted in a 2.5-fold increase in G9a relative to controls. N = 6 experimental replicates. ***$p < 0.001$, *t*-test **(B)** EVs were isolated from OBSC media after either ethanol (EtOH-EVs) or vehicle control (pn-EVs). RT-PCR of mRNA isolated from EVs found a 3.5-fold increase of G9a mRNA in EtOH-EVs. N = 2 experimental replicates/group. **(C)** G9a mRNA was increased in OBSC slice tissue after treatment with either ethanol (3-fold) or EtOH-EVs (2-fold). *$p < 0.05$, ****$p < 0.0001$, Sidak's post-test. **(D)** IHC found EtOH increased the number of H3K9me2 immunoreactive (+IR) pixels/mm^2 in the dentate granular (g) cell region of OBSC by 30%. The dashed white line marks the border of the hilus (h), which is the neurogenic region. Each dot represents an OBSC slice. *$p < 0.05$, *t*-test Scale bar 100 µm. **(E, F)** OBSCs were treated with either control (pn-EVs) or EtOH-EVs. Western blot found that EtOH EVs increased of levels of **(E)** G9a protein (2-fold) and **(F)** H3K9me2 (2.1-fold). Each dot represents 4-6 pool OBSC slices. *$p < 0.05$, ***$p < 0.001$, *t*-test. Insert with representative western blot images of G9a, H3K9me2 and actin.

next determined if inhibition of G9a signaling would prevent the loss of neurogenesis. We first measured G9a expression levels in OBSC after microglial depletion with PLX, which blunts neurogenesis (**Figures 1** and **2**). G9a methyl-transferase activity was then blocked using pharmacological inhibitors of the G9a/GLP complex – BIX-01294 (BIX), and UNC0642 (UNC) (61, 62). A main effect of treatment was observed (**Figure 6A**, One-way ANOVA $F_{13,68} = 6.8$, ****p<0.0001). As above, ethanol robustly inhibited hippocampal neurogenesis in OBSC (74% reduction, **Figures 6A, B**, ****p<0.0001 vs. control Sidak's post-test). Neither BIX (500nM) nor UNC (1µM) alone impacted DCX levels in control OBSC (**Figure 5A**). However, both UNC (**Figures 6A, B**) and BIX (**Figures 6C, D**) prevented the ethanol-induced loss of neurogenesis, returning DCX to control levels (##p<0.01, ###p<0.001 vs. EtOH, Sidak's post-test). Regarding the effects of EVs, EtOH-EVs again reduced DCX (**Figure 6C**, *p<0.01 vs. pn-EVs, Sidak's post-test). Further, like the effects of G9a inhibition on ethanol-treated OBSCs, BIX prevented the loss of neurogenesis caused by EtOH-EVs (**Figures 6C, D**, ##p<0.01 vs. EtOH-EVs) while UNC showed a trend toward a reversal (p=0.18). In order to confirm that BIX and UNC effectively inhibit G9a/GLP complex activity at these concentrations, we measured H3K9me2 in EtOH-EV-treated OBSC +/- these inhibitors by IHC. A main effect of treatment was found ($F_{2,12} = 22.9$, p<0.0001) with both UNC (****p<0.0001, Sidak's post-test) and BIX (***p<0.001) reducing H3K9me2 levels by 49% and 46% respectively (**Supplementary Figure 1B**), consistent with predictions from prior studies (61, 62). Thus, G9a/GLP complex activity facilitates the loss of hippocampal neurogenesis caused by EtOH and EtOH-EVs.

4 DISCUSSION

Adult hippocampal neurogenesis is an important neurological process that is inhibited by ethanol (5, 63). Chronic ethanol abuse causes dysfunction in hippocampal behaviors linked with AHN such as learning plasticity, memory, and mood (1–4, 64, 65). Thus, strategies that ameliorate the loss of AHN caused by alcohol could have a therapeutic benefit for behavioral dysfunction caused by alcohol abuse. Here, we report that extracellular vesicles from resting microglia promote adult hippocampal neurogenesis. However, EVs secreted in response to ethanol cause deficits in neurogenesis through a G9a/GLP-mediated mechanism (**Figure 7**). EtOH-EVs mimicked the effects of ethanol on neurogenesis and were enriched with G9a mRNA. Both ethanol and EtOH-EVs increased G9a levels in recipient cultures, and G9a inhibitors prevented the ethanol- and EtOH-EV-induced loss of hippocampal neurogenesis. This identifies a novel EV-epigenetic signaling system that could be targeted to improve cognitive and behavioral deficits associated with ethanol.

Both stressful and proinflammatory stimuli cause reductions in adult hippocampal neurogenesis (15–17). Microglia have

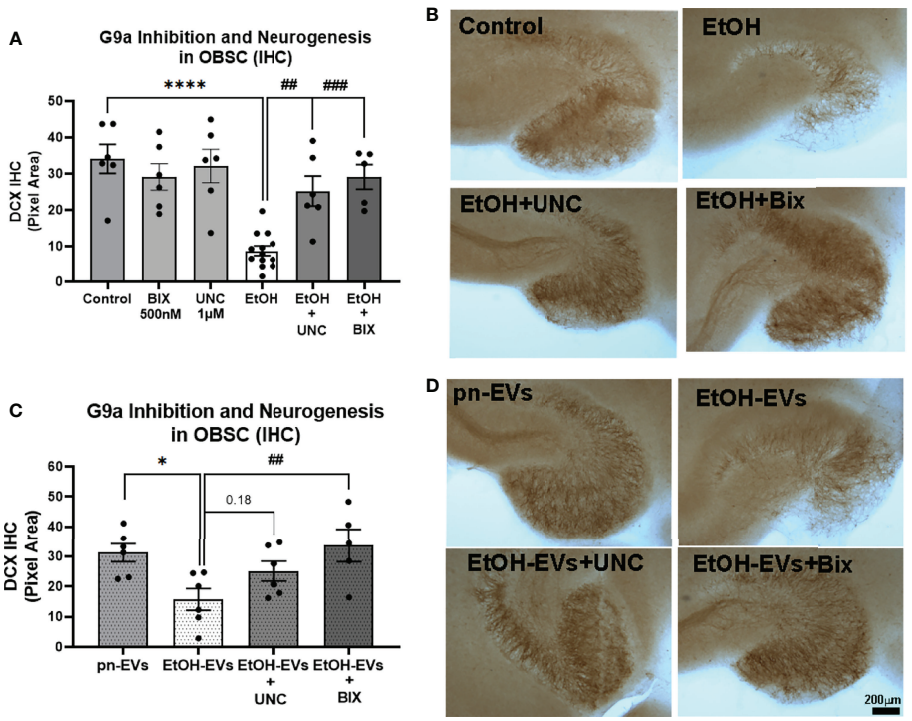

FIGURE 6 | Pharmacological inhibition of G9a prevents loss of neurogenesis caused by ethanol and EtOH-EVs. OBSCs were treated with either EtOH or EtOH-EVs +/- G9a inhibitors BIX-01294 (BIX) or UNC0642 (UNC). Neurogenesis was measured by IHC for DCX. **(A)** EtOH caused a 74% reduction of DCX that was prevented by UNC (1μM) and BIX (500nM). 1-Way ANOVA, $F_{13,68} = 6.8$, $^{****}p < 0.0001$ vs. control, $^{\#\#}p < 0.01$ and $^{\#\#\#}p < 0.001$ vs. EtOH, Sidak's *post-hoc* multiple comparison's test. **(B)** Representative images show loss of neurogenesis with EtOH that was prevented by G9a inhibitors. **(C)** pn-EVs increased DCX by 37%, while EtOH-EVs caused a 50% reduction in DCX relative to control pn-EVs. One-way ANOVA, $F_{4,23} = 4.05$, $^{*}p < 0.01$ vs. pn-EVs, $^{\#\#}p < 0.01$ vs. EtOH-EVs, Sidak's post-test. **(D)** Images showing G9a inhibitors blocked the loss of neurogenesis caused by EtOH-EVs.

recently been identified as regulators of AHN, with their phagocytic secretome increasing AHN (18, 19). In our previous report, we found that microglia induce EtOH-EVs that further promote the proinflammatory effects of ethanol (31). Here we find that resting microglia promote AHN through production of pro-neurogenic EVs. However, in the presence of ethanol, EtOH-EVs inhibit AHN through G9a. Here we find that G9a inhibitors blocked the EtOH- and EtOH-EV-induced loss of neurogenesis. Previously we reported the proinflammatory activity of EtOH-EVs was blocked by the anti-inflammatory inhibitor of HMGB1, GLY (31). However, GLY had no effect on G9a or H3K9me2 levels in these studies (not shown). This suggests that G9a-epigenetic signaling is either upstream or required in parallel with HMGB1 for proinflammatory gene activation to occur. Regarding adult hippocampal neurogenesis, a role of G9a/Ehmt2 has not been reported previously. However, other studies are consistent with this work, suggesting histone methylation represses AHN (66). A loss of the histone lysine-specific demethylase 1 (LSD1), which demethylates H3K9 (27) (resulting in increased methylation), was found to reduce neural stem cell proliferation (28), consistent with our finding. Global increases in H3K9 acetylation, the "opposing" epigenetic mark of H3K9me2, were found to increase differentiation of adult progenitors into neurons (10). Further, pro-neurogenic environmental enrichment reduced H3K9 methylation at the promoter of the neurogenesis promoting growth factor BDNF, increasing its expression (11). Thus, methylation of H3K9 in adulthood seems to inhibit AHN, though details regarding this regulation need to be explored further in future work. Though little is known about G9a regulation of adult hippocampal neuronal proliferation and differentiation, this "anti-neurogenic" role in adulthood seems to differ from its actions during embryonic development.

During embryogenesis, G9a promotes neuronal differentiation and suppresses expression of non-neuronal genes (12, 25, 26). However, evidence in adults suggests that H3K9me2 silences neuron lineage-specific genes in fully differentiated cholinergic neurons to promote a loss of the cholinergic phenotype after ethanol (30). Thus, the role of G9a appears to differ during embryonic and adult stages. This study is the first report to our knowledge that investigates the role of G9a in adult hippocampal neurogenesis. The impact of G9a on differentiation of other cell types in the adult hippocampus, however, remains unknown. It is possible that EtOH- or EtOH-EV-induced increases in G9a could promote differentiation of progenitors into other cell types, resulting in less neurogenesis. Further studies are needed to fully define the specific roles of G9a in proliferation and differentiation across cell types in the adult brain. It is important to note that the

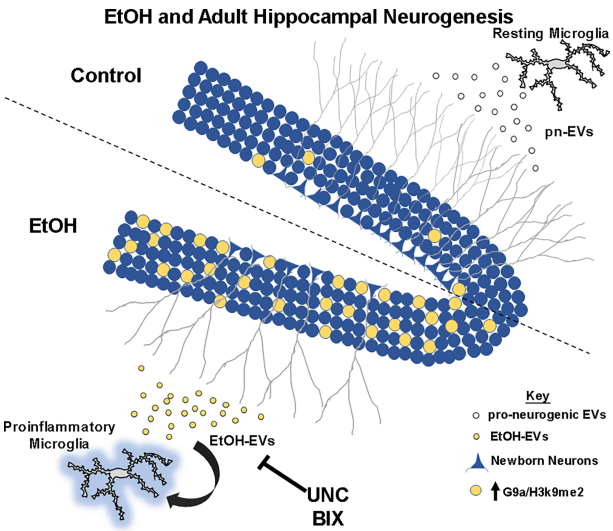

FIGURE 7 | Summary of findings. At rest, microglia secrete pro-neurogenic EVs (pn-EVs) to promote neurogenesis (gray branches). Ethanol causes proinflammatory activation of microglia, with secretion of proinflammatory EtOH-EVs (Crews et al., 2021) now found to be enriched with G9a mRNA. EtOH induces G9a and H3K9me2 (yellow) in the neurogenic niche of the dentate gyrus to blunt neurogenesis (gray branches). Inhibition of G9a activity with UNC and BIX prevent loss of neurogenesis caused by EtOH and EtOH-EVs.

inhibitors of G9a signaling inhibit the G9a/GLP complex, also acting on GLP. Thus, the observed effects could be due to G9a or GLP. Our goal here is not to differentiate specifically between the roles GLP and G9a, rather to identify epigenetic mechanisms ex-vivo that can be moved *in vivo* in future work, with well-established inhibitors.

Though we found increased G9a mRNA in EtOH-EVs and induction of G9a in naïve OBSC by EtOH-EVs, it is unclear whether EtOH-EVs cause this increase through transfer of their mRNA. EVs can exert their influence in a variety of ways, many of which involve activation of immune pathways (67, 68). This can include transfer of contents to recipient cells (e.g., mRNAs, miRNAs), delivery of their contents to cell surface receptors (e.g., cytokines), or delivery of bioactive lipid species or damage-associated molecular pattern molecules (DAMPs, e.g., HMGB1). Recent studies have found that EVs play key roles in mediating multiple alcohol-related pathologies. In the periphery, this includes modulation of peripheral monocyte activity (69), promoting induction of monocyte chemoattractant protein-1 in hepatocytes (70), and induction of fibrotic genes in hepatic stellate cells through miRNA delivery (71). In the brain, microglial EVs promote hypothalamic neuronal death caused by ethanol during the embryonic period through delivery of the complement protein C1q (72) as well as neuronal death in adulthood through delivery of the miRNA let-7b (48). Astrocytes can also, in response to ethanol, secrete EVs that damage neurons involving a TLR4 neuro-immune pathway (73). An unexpected finding was that EVs from microglial-depleted cultures showed a trend toward a reduction of DCX in control OBSCs. It is possible that a loss of trophic factors in PLX-EVs or the presence of neurotoxic factors secreted in PLX-EVs mediate this, though future studies are needed to determine this. Nonetheless, EVs promote central and peripheral ethanol pathology, often through immune mechanisms. Consistent with this, we recently reported that EtOH-EVs induced by microglia seem to drive proinflammatory gene induction caused by ethanol (31). In that previous report, our studies suggested that MVs rather than exosomes mediate the pro-inflammatory signaling caused by EtOH-EVs. Here, we did not distinguish between the effects of MVs versus exosomes on AHN. Both MVs and exosomes are critical EVs, capable of modulating responses in recipient cells. Several factors known to regulate AHN have been found in exosomes (74), and MVs derived from mesenchymal stem cells are also able to promote neurogenesis (75). Thus, both MVs and exosomes could be involved in our observation, and should be investigated further in future work. This current work now implicates a role for EV modulation of epigenetic modifications to chromatin structure in both the induction of proinflammatory gene induction and loss of AHN caused by ethanol.

In summary, we found that microglia promote neurogenesis through secretion of pn-EVs and that EtOH-EVs inhibit adult hippocampal neurogenesis. The G9a/GLP complex is implicated in the loss of neurogenesis caused by ethanol and EtOH-EVs. In future work, we plan to investigate the ability of pn-EVs to reverse loss of AHN *in vivo*. The use of EVs as therapeutic agents could represent a promising biological medicine approach (76). Future studies will also investigate the gene targets of G9a in different cell types in brain, both *ex vivo* and *in vitro*, as well as the ability of G9a inhibitors to alter alcohol effects *in vivo*. Elucidating the targets of G9a and its function *in vivo* will determine if targeting this epigenetic pathway could be a beneficial therapeutic approach for mood and cognitive dysfunction in AUD.

DATA AVAILABILITY STATEMENT

The original contributions presented in the study are included in the article/**Supplementary Material**, further inquiries can be directed to the corresponding author.

ETHICS STATEMENT

The animal study was reviewed and approved by UNC Institutional Animal Care and Use Committee (IACUC).

AUTHOR CONTRIBUTIONS

JZ and LGC drafted the text and figures. All authors contributed to the article and approved the submitted version.

FUNDING

This research was funded by NIH, grant numbers: AA024829, AA028924, AA028599, AA020024, and The Bowles Center for Alcohol Studies.

ACKNOWLEDGMENTS

The Microscopy Services Laboratory, Department of Pathology and Laboratory Medicine, is supported in part by P30 CA016086 Cancer Center Core Support Grant to the UNC Lineberger Comprehensive Cancer Center.

SUPPLEMENTARY MATERIAL

The Supplementary Material for this article can be found online at: https://www.frontiersin.org/articles/10.3389/fimmu.2022.866073/full#supplementary-material

Supplementary Figure 1 | EtOH-EVs blunt IL-4 and UNC and BIX Inhibit G9a/GLP activity. **(A)** OBSCs were treated with either pn-EVs, or EtOH-EVs for 96 hours. pn-EVs caused an 82% increase in IL-4 gene expression (one-way ANOVA, $F_{2,6} = 7.98$, $p < 0.0001$). $^{*}p < 0.05$, $^{**}p < 0.01$, $^{****}p < 0.0001$, Sidak's post-test. **(B)** OBSCs were treated with EtOH-EVs for 96 hours +/- UNC (1μM) or BIX (500nM). H3K9me2 was measured in slices by IHC. A main effect of treatment was found (One-way ANOVA, $F_{2,12} = 22.9$, $p<0.0001$) with UNC and BIX reducing H3K9me2 levels by 49% and 47% respectively, $^{***}p < 0.001$ $^{****}p < 0.0001$, Sidak's post-test.

REFERENCES

1. Anacker C, Hen R. Adult Hippocampal Neurogenesis and Cognitive Flexibility - Linking Memory and Mood. *Nat Rev Neurosci* (2017) 18 (6):335–46. doi: 10.1038/nrn.2017.45
2. Jessberger S, Clark RE, Broadbent NJ, Clemenson GD Jr, Consiglio A, Lie DC, et al. Dentate Gyrus-Specific Knockdown of Adult Neurogenesis Impairs Spatial and Object Recognition Memory in Adult Rats. *Learn Mem* (2009) 16 (2):147–54. doi: 10.1101/lm.1172609
3. Suarez-Pereira I, Canals S, Carrion AM. Adult Newborn Neurons are Involved in Learning Acquisition and Long-Term Memory Formation: The Distinct Demands on Temporal Neurogenesis of Different Cognitive Tasks. *Hippocampus* (2015) 25(1):51–61. doi: 10.1002/hipo.22349
4. Vetreno RP, Crews FT. Binge Ethanol Exposure During Adolescence Leads to a Persistent Loss of Neurogenesis in the Dorsal and Ventral Hippocampus That Is Associated With Impaired Adult Cognitive Functioning. *Front Neurosci* (2015) 9:35. doi: 10.3389/fnins.2015.00035
5. Crews FT, Nixon K. Mechanisms of Neurodegeneration and Regeneration in Alcoholism. *Alcohol Alcohol* (2009) 44(2):115–27. doi: 10.1093/alcalc/agn079
6. Broadwater MA, Liu W, Crews FT, Spear LP. Persistent Loss of Hippocampal Neurogenesis and Increased Cell Death Following Adolescent, But Not Adult, Chronic Ethanol Exposure. *Dev Neurosci* (2014) 36(3-4):297–305. doi: 10.1159/000362874
7. Sakharkar AJ, Vetreno RP, Zhang H, Kokare DM, Crews FT, Pandey SC. A Role for Histone Acetylation Mechanisms in Adolescent Alcohol Exposure-Induced Deficits in Hippocampal Brain-Derived Neurotrophic Factor Expression and Neurogenesis Markers in Adulthood. *Brain Struct Funct* (2016) 221(9):4691–703. doi: 10.1007/s00429-016-1196-y
8. Swartzwelder HS, Healey KL, Liu W, Dubester K, Miller KM, Crews FT. Changes in Neuroimmune and Neuronal Death Markers After Adolescent Alcohol Exposure in Rats are Reversed by Donepezil. *Sci Rep* (2019) 9 (1):12110. doi: 10.1038/s41598-019-47039-1
9. Vicidomini C, Guo N, Sahay A. Communication, Cross Talk, and Signal Integration in the Adult Hippocampal Neurogenic Niche. *Neuron* (2020) 105 (2):220–35. doi: 10.1016/j.neuron.2019.11.029
10. Hsieh J, Nakashima K, Kuwabara T, Mejia E, Gage FH. (2004). Histone Deacetylase Inhibition-Mediated Neuronal Differentiation of Multipotent Adult Neural Progenitor Cells. *Proc Natl Acad Sci USA* (2004) 101 (47):16659–64. doi: 10.1073/pnas.0407643101
11. Kuzumaki N, Ikegami D, Tamura R, Hareyama N, Imai S, Narita M, et al. Hippocampal Epigenetic Modification at the Brain-Derived Neurotrophic Factor Gene Induced by an Enriched Environment. *Hippocampus* (2011) 21 (2):127–32. doi: 10.1002/hipo.20775
12. Deimling SJ, Olsen JB, Tropepe V. The Expanding Role of the Ehmt2/G9a Complex in Neurodevelopment. *Neurogen (Austin)* (2017) 4(1):e1316888. doi: 10.1080/23262133.2017.1316888
13. Ekdahl CT, Claasen JH, Bonde S, Kokaia Z, Lindvall O. Inflammation Is Detrimental for Neurogenesis in Adult Brain. *Proc Natl Acad Sci USA* (2003) 100(23):13632–7. doi: 10.1073/pnas.2234031100
14. Monje ML, Toda H, Palmer TD. Inflammatory Blockade Restores Adult Hippocampal Neurogenesis. *Science* (2003) 302(5651):1760–5. doi: 10.1126/science.1088417
15. Borsini A, Cattaneo A, Malpighi C, Thuret S, Harrison NA, Consortium MRCI, et al. Interferon-Alpha Reduces Human Hippocampal Neurogenesis and Increases Apoptosis via Activation of Distinct STAT1-Dependent Mechanisms. *Int J Neuropsychopharmacol* (2017) 21(2):187–200. doi: 10.1093/ijnp/pyx083
16. Snyder JS, Soumier A, Brewer M, Pickel J, Cameron HA. Adult Hippocampal Neurogenesis Buffers Stress Responses and Depressive Behaviour. *Nature* (2011) 476(7361):458–61. doi: 10.1038/nature10287
17. Goshen I, Kreisel T, Ben-Menachem-Zidon O, Licht T, Weidenfeld J, Ben-Hur T, et al. Brain Interleukin-1 Mediates Chronic Stress-Induced Depression in Mice *via* Adrenocortical Activation and Hippocampal Neurogenesis Suppression. *Mol Psychiatry* (2008) 13(7):717–28. doi: 10.1038/sj.mp.4002055
18. Diaz-Aparicio I, Paris I, Sierra-Torre V, Plaza-Zabala A, Rodriguez-Iglesias N, Marquez-Ropero M, et al. Microglia Actively Remodel Adult Hippocampal Neurogenesis Through the Phagocytosis Secretome. *J Neurosci* (2020) 40 (7):1453–82. doi: 10.1523/JNEUROSCI.0993-19.2019
19. Osman AM, Rodhe J, Shen X, Dominguez CA, Joseph B, Blomgren K. The Secretome of Microglia Regulate Neural Stem Cell Function. *Neuroscience* (2019) 405:92–102. doi: 10.1016/j.neuroscience.2017.10.034
20. Kreisel T, Wolf B, Keshet E, Licht T. Unique Role for Dentate Gyrus Microglia in Neuroblast Survival and in VEGF-Induced Activation. *Glia* (2019) 67 (4):594–618. doi: 10.1002/glia.23505
21. Coleman LG Jr, Zou J, Crews FT. Microglial Depletion and Repopulation in Brain Slice Culture Normalizes Sensitized Proinflammatory Signaling. *J Neuroinflam* (2020) 17(1):27. doi: 10.1186/s12974-019-1678-y
22. Fernandez-Lizarbe S, Montesinos J, Guerri C. Ethanol Induces TLR4/TLR2 Association, Triggering an Inflammatory Response in Microglial Cells. *J Neurochem* (2013) 126(2):261–73. doi: 10.1111/jnc.12276

23. He J, Crews FT. Increased MCP-1 and Microglia in Various Regions of the Human Alcoholic Brain. *Exp Neurol* (2008) 210(2):349–58. doi: 10.1016/j.expneurol.2007.11.017
24. Vetreno RP, Lawrimore CJ, Rowsey PJ, Crews FT. Persistent Adult Neuroimmune Activation and Loss of Hippocampal Neurogenesis Following Adolescent Ethanol Exposure: Blockade by Exercise and the Anti-Inflammatory Drug Indomethacin. *Front Neurosci* (2018) 12:200. doi: 10.3389/fnins.2018.00200
25. Fiszbein A, Kornblihtt AR. Histone Methylation, Alternative Splicing and Neuronal Differentiation. *Neurogen (Austin).* (2016) 3(1):e1204844. doi: 10.1080/23262133.2016.1204844
26. Olsen JB, Wong L, Deimling S, Miles A, Guo H, Li Y, et al. G9a and ZNF644 Physically Associate to Suppress Progenitor Gene Expression During Neurogenesis. *Stem Cell Rep* (2016) 7(3):454–70. doi: 10.1016/j.stemcr.2016.06.012
27. Metzger E, Wissmann M, Yin N, Muller JM, Schneider R, Peters AH, et al. LSD1 Demethylates Repressive Histone Marks to Promote Androgen-Receptor-Dependent Transcription. *Nature* (2005) 437(7057):436–9. doi: 10.1038/nature04020
28. Sun G, Alzayady K, Stewart R, Ye P, Yang S, Li W, et al. Histone Demethylase LSD1 Regulates Neural Stem Cell Proliferation. *Mol Cell Biol* (2010) 30 (8):1997–2005. doi: 10.1128/MCB.01116-09
29. Crews FT, Fisher R, Deason C, Vetreno RP. Loss of Basal Forebrain Cholinergic Neurons Following Adolescent Binge Ethanol Exposure: Recovery With the Cholinesterase Inhibitor Galantamine. *Front Behav Neurosci* (2021) 15:652494. doi: 10.3389/fnbeh.2021.652494
30. Vetreno RP, Bohnsack JP, Kusumo H, Liu W, Pandey SC, Crews FT. Neuroimmune and Epigenetic Involvement in Adolescent Binge Ethanol-Induced Loss of Basal Forebrain Cholinergic Neurons: Restoration With Voluntary Exercise. *Addict Biol* (2020) 25(2):e12731. doi: 10.1111/adb.12731
31. Crews FT, Zou J, Coleman LG Jr. Extracellular Microvesicles Promote Microglia-Mediated Pro-Inflammatory Responses to Ethanol. *J Neurosci Res* (2021) 99(8):1940–56. doi: 10.1002/jnr.24813
32. van Niel G, D'Angelo G, Raposo G. Shedding Light on the Cell Biology of Extracellular Vesicles. *Nat Rev Mol Cell Biol* (2018) 19(4):213–28. doi: 10.1038/nrm.2017.125
33. Vassileff N, Cheng L, Hill AF. Extracellular Vesicles - Propagators of Neuropathology and Sources of Potential Biomarkers and Therapeutics for Neurodegenerative Diseases. *J Cell Sci* (2020) 133(23):1–15. doi: 10.1242/jcs.243139
34. Jeppesen DK, Fenix AM, Franklin JL, Higginbotham JN, Zhang Q, Zimmerman LJ, et al. Reassessment of Exosome Composition. *Cell* (2019) 177(2):428–45.e18. doi: 10.1016/j.cell.2019.02.029
35. Di Liegro CM, Schiera G, Di Liegro I. Extracellular Vesicle-Associated RNA as a Carrier of Epigenetic Information. *Genes (Basel)* (2017) 8(10):1–23. doi: 10.3390/genes8100240
36. Rompala GR, Ferguson C, Homanics GE. Coincubation of Sperm With Epididymal Extracellular Vesicle Preparations From Chronic Intermittent Ethanol-Treated Mice is Sufficient to Impart Anxiety-Like and Ethanol-Induced Behaviors to Adult Progeny. *Alcohol* (2020) 87:111–20. doi: 10.1016/j.alcohol.2020.05.001
37. Tseng AM, Chung DD, Pinson MR, Salem NA, Eaves SE, Miranda RC. Ethanol Exposure Increases miR-140 in Extracellular Vesicles: Implications for Fetal Neural Stem Cell Proliferation and Maturation. *Alcoholism Clin Exp Res* (2019) 43(7):1414–26. doi: 10.1111/acer.14066
38. Raineteau O, Rietschin L, Gradwohl G, Guillemot F, Gahwiler BH. Neurogenesis in Hippocampal Slice Cultures. *Mol Cell Neurosci* (2004) 26 (2):241–50. doi: 10.1016/j.mcn.2004.01.003
39. Noraberg J, Poulsen FR, Blaabjerg M, Kristensen BW, Bonde C, Montero M, et al. Organotypic Hippocampal Slice Cultures for Studies of Brain Damage, Neuroprotection and Neurorepair. *Curr Drug Targets CNS Neurol Disord* (2005) 4(4):435–52. doi: 10.2174/1568007054546108
40. Bonhoeffer T, Yuste R. Spine Motility. Phenomenology, Mechanisms, and Function. *Neuron* (2002) 35(6):1019–27. doi: 10.1016/S0896-6273(02)00906-6
41. Weinhard L, di Bartolomei G, Bolasco G, Machado P, Schieber NL, Neniskyte U, et al. Microglia Remodel Synapses by Presynaptic Trogocytosis and Spine Head Filopodia Induction. *Nat Commun* (2018) 9(1):1228. doi: 10.1038/s41467-018-03566-5
42. Zou J, Crews FT. Inflammasome-IL-1beta Signaling Mediates Ethanol Inhibition of Hippocampal Neurogenesis. *Front Neurosci* (2012) 6:77. doi: 10.3389/fnins.2012.00077
43. Walter TJ, Crews FT. Microglial Depletion Alters the Brain Neuroimmune Response to Acute Binge Ethanol Withdrawal. *J Neuroinflam* (2017) 14(1):86. doi: 10.1186/s12974-017-0856-z
44. Qin L, Zou J, Barnett A, Vetreno RP, Crews FT, Coleman LG. TRAIL Mediates Neuronal Death in AUD: A Link Between Neuroinflammation and Neurodegeneration. *Int J Mol Sci* (2021) 22(5):2547. doi: 10.3390/ijms22052547
45. Stoppini L, Buchs PA, Muller D. A Simple Method for Organotypic Cultures of Nervous Tissue. *J Neurosci Methods* (1991) 37(2):173–82. doi: 10.1016/0165-0270(91)90128-M
46. Zou JY, Crews FT. TNF Alpha Potentiates Glutamate Neurotoxicity by Inhibiting Glutamate Uptake in Organotypic Brain Slice Cultures: Neuroprotection by NF Kappa B Inhibition. *Brain Res* (2005) 1034(1-2):11–24. doi: 10.1016/j.brainres.2004.11.014
47. Zou J, Crews F. CREB and NF-kappaB Transcription Factors Regulate Sensitivity to Excitotoxic and Oxidative Stress Induced Neuronal Cell Death. *Cell Mol Neurobiol* (2006) 26(4-6):385–405. doi: 10.1007/s10571-006-9045-9
48. Coleman LG Jr, Zou J, Crews FT. Microglial-Derived miRNA Let-7 and HMGB1 Contribute to Ethanol-Induced Neurotoxicity *via* TLR7. *J Neuroinflam* (2017) 14(1):22. doi: 10.1186/s12974-017-0799-4
49. Willis ML, Mahung C, Wallet SM, Barnett A, Cairns BA, Coleman LG Jr, et al. Plasma Extracellular Vesicles Released After Severe Burn Injury Modulate Macrophage Phenotype and Function. *J Leukocyte Biol* (2021) 111:33–49. doi: 10.1002/JLB.3MIA0321-150RR
50. Maile R, Willis M, Herring LE, Prevatte A, Mahung C, Cairns B, et al. Burn Injury Induces Proinflammatory Plasma Extracellular Vesicles That Associate With Length of Hospital Stay in Women: CRP and SAA1 as Potential Prognostic Indicators. *Int J Mol Sci* (2021) 22(18):1–19. doi: 10.3390/ijms221810083
51. Desai CS, Khan A, Bellio MA, Willis ML, Mahung C, Ma X, et al. Characterization of Extracellular Vesicle miRNA Identified in Peripheral Blood of Chronic Pancreatitis Patients. *Mol Cell Biochem* (2021) 476:4331–41. doi: 10.1007/s11010-021-04248-5
52. Zou JY, Crews FT. Release of Neuronal HMGB1 by Ethanol Through Decreased HDAC Activity Activates Brain Neuroimmune Signaling. *PloS One* (2014) 9(2):e87915. doi: 10.1371/journal.pone.0087915
53. Crews FT, Qin L, Sheedy D, Vetreno RP, Zou J. High Mobility Group Box 1/Toll-Like Receptor Danger Signaling Increases Brain Neuroimmune Activation in Alcohol Dependence. *Biol Psychiatry* (2013) 73(7):602–12. doi: 10.1016/j.biopsych.2012.09.030
54. Olson KN, Smith SW, Kloss JS, Ho JD, Apple FS. Relationship Between Blood Alcohol Concentration and Observable Symptoms of Intoxication in Patients Presenting to an Emergency Department. *Alcohol Alcohol* (2013) 48(4):386–9. doi: 10.1093/alcalc/agt042
55. Thery C, Witwer KW, Aikawa E, Alcaraz MJ, Anderson JD, Andriantsitohaina R, et al. Minimal Information for Studies of Extracellular Vesicles 2018 (MISEV2018): A Position Statement of the International Society for Extracellular Vesicles and Update of the MISEV2014 Guidelines. *J Extracel Vesicle.* (2018) 7(1):1535750. doi: 10.1080/20013078.2018.1535750
56. Cvjetkovic A, Jang SC, Konecna B, Hoog JL, Sihlbom C, Lasser C, et al. Detailed Analysis of Protein Topology of Extracellular Vesicles-Evidence of Unconventional Membrane Protein Orientation. *Sci Rep* (2016) 6:36338. doi: 10.1038/srep36338
57. Zhang J, Rong P, Zhang L, He H, Zhou T, Fan Y, et al. IL4-Driven Microglia Modulate Stress Resilience Through BDNF-Dependent Neurogenesis. *Sci Adv* (2021) 7(12):1–14. doi: 10.1126/sciadv.abb9888
58. Macht V, Crews FT, Vetreno RP. Neuroimmune and Epigenetic Mechanisms Underlying Persistent Loss of Hippocampal Neurogenesis Following Adolescent Intermittent Ethanol Exposure. *Curr Opin Pharmacol* (2020) 50:9–16. doi: 10.1016/j.coph.2019.10.007
59. Nixon K, Crews FT. Binge Ethanol Exposure Decreases Neurogenesis in Adult Rat Hippocampus. *J Neurochem* (2002) 83(5):1087–93. doi: 10.1046/j.1471-4159.2002.01214.x
60. Ting K, Aitken KJ, Penna F, Samiei AN, Sidler M, Jiang JX, et al. Uropathogenic E. Coli (UPEC) Infection Induces Proliferation Through

Enhancer of Zeste Homologue 2 (Ezh2). *PloS One* (2016) 11(3):e0149118. doi: 10.1371/journal.pone.0149118
61. Vedadi M, Barsyte-Lovejoy D, Liu F, Rival-Gervier S, Allali-Hassani A, Labrie V, et al. A Chemical Probe Selectively Inhibits G9a and GLP Methyltransferase Activity in Cells. *Nat Chem Biol* (2011) 7(8):566–74. doi: 10.1038/nchembio.599
62. Chang Y, Zhang X, Horton JR, Upadhyay AK, Spannhoff A, Liu J, et al. Structural Basis for G9a-Like Protein Lysine Methyltransferase Inhibition by BIX-01294. *Nat Struct Mol Biol* (2009) 16(3):312–7. doi: 10.1038/nsmb.1560
63. Richardson HN, Chan SH, Crawford EF, Lee YK, Funk CK, Koob GF, et al. Permanent Impairment of Birth and Survival of Cortical and Hippocampal Proliferating Cells Following Excessive Drinking During Alcohol Dependence. *Neurobiol Dis* (2009) 36(1):1–10. doi: 10.1016/j.nbd.2009.05.021
64. Geil CR, Hayes DM, McClain JA, Liput DJ, Marshall SA, Chen KY, et al. Alcohol and Adult Hippocampal Neurogenesis: Promiscuous Drug, Wanton Effects. *Prog Neuropsychopharmacol Biol Psychiatry* (2014) 54:103–13. doi: 10.1016/j.pnpbp.2014.05.003
65. Canales JJ. Deficient Plasticity in the Hippocampus and the Spiral of Addiction: Focus on Adult Neurogenesis. *Curr Top Behav Neurosci* (2013) 15:293–312. doi: 10.1007/7854_2012_230
66. Sheehy RN, Quintanilla LJ, Song J. Epigenetic Regulation in the Neurogenic Niche of the Adult Dentate Gyrus. *Neurosci Lett* (2022) 766:136343. doi: 10.1016/j.neulet.2021.136343
67. Rahman MA, Patters BJ, Kodidela S, Kumar S. Extracellular Vesicles: Intercellular Mediators in Alcohol-Induced Pathologies. *J Neuroimmune Pharmacol* (2020) 15(3):409–21. doi: 10.1007/s11481-019-09848-z
68. Tetta C, Ghigo E, Silengo L, Deregibus MC, Camussi G. Extracellular Vesicles as an Emerging Mechanism of Cell-to-Cell Communication. *Endocrine* (2013) 44(1):11–9. doi: 10.1007/s12020-012-9839-0
69. Saha B, Momen-Heravi F, Kodys K, Szabo G. MicroRNA Cargo of Extracellular Vesicles From Alcohol-Exposed Monocytes Signals Naive Monocytes to Differentiate Into M2 Macrophages. *J Biol Chem* (2016) 291 (1):149–59. doi: 10.1074/jbc.M115.694133
70. Saha B, Momen-Heravi F, Furi I, Kodys K, Catalano D, Gangopadhyay A, et al. Extracellular Vesicles From Mice With Alcoholic Liver Disease Carry a Distinct Protein Cargo and Induce Macrophage Activation Through Heat Shock Protein 90. *Hepatology* (2018) 67(5):1986–2000. doi: 10.1002/hep.29732
71. Brandon-Warner E, Feilen NA, Culberson CR, Field CO, deLemos AS, Russo MW, et al. Processing of Mir17-92 Cluster in Hepatic Stellate Cells Promotes Hepatic Fibrogenesis During Alcohol-Induced Injury. *Alcoholism Clin Exp Res* (2016) 40(7):1430–42. doi: 10.1111/acer.13116
72. Mukherjee S, Cabrera MA, Boyadjieva NI, Berger G, Rousseau B, Sarkar DK. Alcohol Increases Exosome Release From Microglia to Promote Complement C1q Induced Cellular Death of Proopiomelanocortin Neurons in the Hypothalamus in a Rat Model of Fetal Alcohol Spectrum Disorders. *J Neurosci* (2020) 40:7965–79. doi: 10.1523/JNEUROSCI.0284-20.2020
73. Ibanez F, Montesinos J, Urena-Peralta JR, Guerri C, Pascual M. TLR4 Participates in the Transmission of Ethanol-Induced Neuroinflammation *via* Astrocyte-Derived Extracellular Vesicles. *J Neuroinflam* (2019) 16 (1):136. doi: 10.1186/s12974-019-1529-x
74. Zhang Y, Xu C. Effects of Exosomes on Adult Hippocampal Neurogenesis and Neuropsychiatric Disorders. *Mol Biol Rep* (2022). doi: 10.1007/s11033-022-07313-4
75. Lee JY, Kim E, Choi SM, Kim DW, Kim KP, Lee I, et al. Microvesicles From Brain-Extract-Treated Mesenchymal Stem Cells Improve Neurological Functions in a Rat Model of Ischemic Stroke. *Sci Rep* (2016) 6:33038. doi: 10.1038/srep33038
76. Coleman LG. The Emerging World of Subcellular Biological Medicine: Extracellular Vesicles as Novel Biomarkers, Targets, and Therapeutics. *Neural Regener Res* (2022) 17(5):1020–2. doi: 10.4103/1673-5374.324846

Conflict of Interest: The authors declare that the research was conducted in the absence of any commercial or financial relationships that could be construed as a potential conflict of interest.

Publisher's Note: All claims expressed in this article are solely those of the authors and do not necessarily represent those of their affiliated organizations, or those of the publisher, the editors and the reviewers. Any product that may be evaluated in this article, or claim that may be made by its manufacturer, is not guaranteed or endorsed by the publisher.

frontiers | Frontiers in Immunology

ORIGINAL RESEARCH
published: 18 May 2022
doi: 10.3389/fimmu.2022.866925

Acute Intoxication With Alcohol Reduces Trauma-Induced Proinflammatory Response and Barrier Breakdown in the Lung *via* the Wnt/β-Catenin Signaling Pathway

Laurens Noack[1], Katrin Bundkirchen[2], Baolin Xu[1,2], Severin Gylstorff[1], Yuzhuo Zhou[1,2], Kernt Köhler[3], Phatcharida Jantaree[4], Claudia Neunaber[2], Aleksander J. Nowak[1†] and Borna Relja[1†]*

[1] Department of Radiology and Nuclear Medicine, Experimental Radiology, Otto-von-Guericke University, Magdeburg, Germany, [2] Trauma Department, Hannover Medical School, Hannover, Germany, [3] Institute of Veterinary Pathology, Justus Liebig University Giessen, Giessen, Germany, [4] Institute of Experimental Internal Medicine, Otto-von-Guericke University, Magdeburg, Germany

OPEN ACCESS

Edited by:
Derrick Richard Samuelson, University of Nebraska Medical Center, United States

Reviewed by:
Todd A. Wyatt, University of Nebraska Medical Center, United States
Martin Ronis, Louisiana State University, United States

***Correspondence:**
Borna Relja
info@bornarelja.com

[†]These authors have contributed equally to this work

Specialty section:
This article was submitted to Nutritional Immunology, a section of the journal Frontiers in Immunology

Received: 31 January 2022
Accepted: 07 April 2022
Published: 18 May 2022

Citation:
Noack L, Bundkirchen K, Xu B, Gylstorff S, Zhou Y, Köhler K, Jantaree P, Neunaber C, Nowak AJ and Relja B (2022) Acute Intoxication With Alcohol Reduces Trauma-Induced Proinflammatory Response and Barrier Breakdown in the Lung via the Wnt/β-Catenin Signaling Pathway. Front. Immunol. 13:866925. doi: 10.3389/fimmu.2022.866925

Background: Trauma is the third leading cause of mortality worldwide. Upon admission, up to 50% of traumatized patients are acutely intoxicated with alcohol, which might lead to aberrant immune responses. An excessive and uncontrolled inflammatory response to injury is associated with damage to trauma-distant organs. We hypothesize that, along with inflammation-induced apoptosis, the activation of the Wnt/β-catenin signaling pathway would cause breakdown of the lung barrier and the development of lung injury after trauma. It remains unclear whether ethanol intoxication (EI) prior to trauma and hemorrhagic shock will attenuate inflammation and organ injury.

Methods: In this study, 14 male C57BL/6J mice were randomly assigned to two groups and exposed either to EtOH or to NaCl as a control by an oral gavage before receiving a femur fracture (Fx) and hemorrhagic shock, followed by resuscitation (THFx). Fourteen sham animals received either EtOH or NaCl and underwent surgical procedures without THFx induction. After 24 h, oil red O staining of fatty vacuoles in the liver was performed. Histological lung injury score (LIS) was assessed to analyze the trauma-induced RLI. Gene expression of *Cxcl1*, *Il-1β*, *Muc5ac*, *Tnf*, and *Tnfrsf10b* as well as CXCL1, IL-1β, and TNF protein levels in the lung tissue and bronchoalveolar lavage fluid were determined by RT-qPCR, ELISA, and immunohistological analyses. Infiltrating polymorphonuclear leukocytes (PMNLs) were examined *via* immunostaining. Apoptosis was detected by activated caspase-3 expression in the lung tissue. To confirm active Wnt signaling after trauma, gene expression of *Wnt3a* and its inhibitor sclerostin (*Sost*) was determined. Protein expression of A20 and RIPK4 as possible modulators of the Wnt signaling pathway was analyzed *via* immunofluorescence.

Results: Significant fatty changes in the liver confirmed the acute EI. Histopathology and decreased *Muc5ac* expression revealed an increased lung barrier breakdown and

concomitant lung injury after THFx versus sham. EI prior trauma decreased lung injury. THFx increased not only the gene expression of pro-inflammatory markers but also the pulmonary infiltration with PMNL and apoptosis versus sham, while EI prior to THFx reduced those changes significantly. EI increased the THFx-reduced gene expression of *Sost* and reduced the THFx-induced expression of *Wnt3a*. While A20, RIPK4, and membranous β-catenin were significantly reduced after trauma, they were enhanced upon EI.

Conclusion: These findings suggest that acute EI alleviates the uncontrolled inflammatory response and lung barrier breakdown after trauma by suppressing the Wnt/β-catenin signaling pathway.

Keywords: femur fracture, hemorrhagic shock, inflammation, pulmonary, ethanol

INTRODUCTION

Traumatic injury is one of the leading causes of worldwide mortality (1). Femur fracture accompanied by hemorrhage is associated with high morbidity and mortality rates (2). Notably, hemorrhagic shock (HS) is characterized by marked early inflammatory response and concomitant activation of immune cells, leading to organ damage and significant mortality (3). Femur fracture in particular can induce remote organ complications, especially in the lungs (4). Lung and remote lung injury (RLI), a common complication after surgical procedures post-trauma, have also been shown in the combinatory model of femur fracture accompanied by hemorrhage (THFx) in mice (5, 6). Many inflammatory pathways and mediators including cytokines and other damage-associated molecular patterns were found to be important triggers for the development of lung injury. Studies have shown that proinflammatory cytokines, among the systemically distributed interleukins (IL)-1β, IL-6, IL-8, and tumor necrosis factor (TNF)-α, were associated with the activation of caspase-3, leading to pulmonary apoptosis and alveolar–capillary barrier dysfunction with the subsequent development of lung injury after trauma (5).

Wnt signaling with its main mediator protein β-catenin is essential in a variety of biological responses, including bone formation and remodeling, organ development and repair, as well as embryogenesis and carcinogenesis (7, 8). The hallmark of the canonical Wnt pathway is to control the β-catenin dynamics and, thus, the activation of β-catenin-mediated transcriptional activity. The cytoplasmic level of β-catenin is tightly regulated *via* its phosphorylation by the "destruction complex", consisting of the tumor suppressor adenomatous polyposis coli (APC), the scaffold protein AXIN, glycogen synthase kinase (GSK)3β, and casein kinase (CK)1α (7, 9). CKI and GSK3β initiate the phosphorylation of β-catenin, allowing the beta-transducin repeat-containing protein to promote ubiquitination and, thus, the degradation of β-catenin (9). A Wnt member protein (e.g., WNT3A) binding to its receptor inhibits the destruction complex activities, leading to stabilization and accumulation of the cytoplasmic β-catenin, eventually allowing its translocation into the nucleus (7, 9, 10). In the absence of a Wnt stimulus, the majority of β-catenin is located at the cytoplasmic side of the cell membrane in complexes with E-cadherin and α-catenin, preventing β-catenin from degradation (9, 10). β-catenin–E-cadherin-based maintenance and stabilization of adherens junctions promote cell-to-cell adhesion (10). Tumor necrosis factor, alpha-induced protein 3 (TNFAIP3, also known as A20) is indispensable for regulating vascular E-cadherin expression in adherens junctions to maintain and repair damaged endothelial functions after pulmonary vascular injury by lipopolysaccharide (11). Interestingly, there is also an evidence of A20 presumed involvement to Wnt signaling *via* the receptor interacting protein kinase (RIPK)4, which is a positive modulator of the Wnt pathway (12). Over the past decades, significant progress has been made in therapeutics targeting the Wnt/β-catenin signaling pathway in bone regeneration settings, focusing on agents that neutralize or inhibit the negative regulators of Wnt signaling, such as sclerostin, among others (13).

Approximately one-third of trauma-related deaths are accompanied by a positive blood alcohol concentration (BAC), and up to 50% of hospital admissions after trauma involve alcohol/ethanol intoxication (EI) (14, 15). Studies have shown the beneficial effects of an acute EI in experimental trauma *via* reduced systemic and local inflammation, while current data indicate that EI might lead to a higher susceptibility to infections (e.g., sepsis and pneumonia) (3, 16). The overall impact of an acute EI on the trauma/hemorrhage-induced Wnt/β-catenin signaling pathway and subsequent lung barrier breakdown as well as organ damage is unknown. Interestingly, a previous study has shown that alcohol exposure had a negative impact on fracture-associated Wnt signaling required for normal bone fracture repair. Here, the phosphorylation of β-catenin was promoted, targeting the protein for degradation and reducing total β-catenin in the fracture callus (17).

Based on this background, the goal of this study was to investigate the following: (1) the role of the canonical Wnt signaling pathway in the trauma-induced lung injury, and (2) the effects of an acute EI on the lung inflammation and barrier breakdown after THFx. We hypothesize that an acute EI would alleviate the uncontrolled inflammatory response and lung

barrier breakdown after trauma by suppressing the Wnt/β-catenin signaling pathway.

MATERIALS AND METHODS

Animal Husbandry

This study was authorized by the local institutional animal care and research advisory committee and permitted by the local government of Lower Saxony, Germany (approval number: 33.12-42502-04-17/2491). Male C57BL/6J mice (17–26 weeks, Janvier Labs, Le Genest-Saint-Isle, France) were used for the experiments and were handled only by persons who had a certificate of the Federation of European Laboratory Animal Science Associations. The animals were kept under standardized conditions in the Central Animal Laboratory of the Hannover Medical School and housed in individual cages with an area of 530 cm^2 (type IIL cage). Standard softwood granules (Altromin GmbH, Lage, Germany) for laboratory animals were used as litter material. Once per week, the cages, bedding, and the drinking water bottles were changed.

Group Allocation

Animals were randomly assigned to one of four groups. Mice were gavaged with either sodium chloride (NaCl, ctrl) or ethanol (EtOH) as described in the experimental model. Animals in sham groups (sham ctrl: $n = 7$; sham EtOH: $n = 7$) received an external fixator and catheterization of the femoral artery, but no osteotomy or blood loss was induced. Mice in trauma groups (THFx ctrl: $n = 7$, THFx EtOH: $n = 7$) received the external fixator followed by osteotomy of the femur and HS was induced and maintained by blood withdrawal *via* the catheterized femoral artery.

Experimental Model

Depending on group assignment, mice received an intragastric gavage of either 0.9% sodium chloride (NaCl, ctrl, 12.66 µl/g body weight) or 35% ethanol (EtOH, >99.5% ethanol diluted in 0.9% sodium chloride, 12.66 µl/g body weight resulting in a 3.5 g EtOH/kg body weight) *via* a rigid blunt cannula 2 h before surgery. An alcohol concentration of 35% was selected to simulate acute EI prior to subsequent procedures. In previous studies, such acute EI generated fatty changes in the liver that confirmed the induced EI (18). In total, the animals received two gavages. In the first gavage, 50% of the total volume (NaCl or EtOH) was administered. After 15 min, the remaining volume was administered *via* the second gavage. The animals were observed for activity, general health condition, posture, signs of pain, and lameness. To achieve a high blood alcohol level in the mice, surgery was started 2 h after gavage. We measured the alcohol concentration in the blood in the Clinical Chemistry Department of the MHH in six mice. They had an alcohol concentration 1.54‰ at 2 h after intoxication. This time point was chosen according to a previous study (19).

All surgical procedures were performed under deep inhalation anesthesia using isoflurane (Baxter Deutschland GmbH, Unterschleißheim, Germany) as described before (20, 21). Interdigital reflexes were proofed regularly and the surgery began when this reflex was negative. During the surgical procedure, mice were warmed using heating pads. An intraoperative analgesia with 5 mg/kg body weight carprofen (Rimadyl®, Zoetis Deutschland GmbH, Berlin, Germany) and 1 mg/kg body weight butorphanol (Torbugesic®, Zoetis Deutschland GmbH, Berlin, Germany) was injected subcutaneously. Local anesthesia with prilocaine hydrochloride was applied into the sites of the operation. For postoperative analgesia, 200 mg/kg body weight metamizole was added to the drinking water. After the surgery, the animals were kept warm and under red light until full awakening and housed individually in cages to avoid aggressive behavior between male mice and littermates reopening the surgical wound. Postoperative controls of the animals were conducted regularly, and the general health status of the animals as well as activity and possible lameness were controlled.

All surgical procedures were conducted as described before (20, 21). The placement of an external fixator (MouseExFix simple L 100%, RISystem, Davos, Switzerland) to the right femoral bone was performed in the sham and trauma group. In brief, the fixator was implanted according to the manufactuter's manual and afterwards a diaphyseal osteotomy was performed centrally between the two middle pins using a wire saw with a diameter of 0.44 mm (Gigli wire saw, RISystem). Sham animals (sham ctrl; sham EtOH) only received the external fixator, but no osteotomy was performed. Animals in the trauma groups (THFx ctrl; THFx EtOH) underwent a subsequent pressure-controlled HS. Briefly, a catheter was installed into the femoral artery and blood was collected until a mean arterial blood pressure with a target value of 35 ± 5 mmHg was reached. The shock state of hypovolemia was maintained for 90 min in total. After 90 min, four times the amount of the withdrawn blood (maximum 2.4 ml) was reperfused with body-warm Ringer's solution over a period of 30 min and the catheter was removed after reinfusion. In the sham animals, only catheterization was performed, but no blood loss was induced. Wounds were closed by suturing with Prolene 6-0 (Ethicon, Cincinnati, USA) and the animals were allowed to move freely immediately after the experimental procedure.

Harvesting Procedures

Twenty-four hours after surgery, the animals were sacrificed. Mice were anesthetized with 75 mg/kg body weight ketamine and 1 mg/kg body weight medetomidine *via* intraperitoneal injection. After confirming a negative interdigital and tail pinch reflexes, the sacrifice was initiated. The heart was punctured with a heparinized sharp 25-gauge syringe (BD, Franklin Lakes, USA) and followed by cardiac exsanguination for blood collection. Then, mice were killed by cervical dislocation. Abdominal cavity was opened and the incision was extended over the chest wall until the trachea was visible. The trachea was first punctured with a 25-gauge needle (BD, Franklin Lakes, USA) and then a 19-gauge syringe (BD, Franklin Lakes, USA) containing 1.1 ml of phosphate-buffered saline (PBS) was inserted. Lungs were flushed with 1.1 ml of PBS, followed by collection of at least

800 µl of bronchoalveolar lavage fluid (BALF). The BALF was centrifuged at 1,164 × *g* for 5 min at 4°C and the cell-free supernatant was frozen at −80°C for subsequent analyses. The hole in the trachea was closed with a blunt clamp, and perfusion of the entire animal with 20 ml of PBS *via* a 21-gauge blunt syringe (BD, Franklin Lakes, USA) through the heart (apex) began. The left lung was ligated, removed, snap frozen using liquid nitrogen, and stored at −80°C for later analyses. Mice were subsequently perfused with 10 ml of 4% buffered Zn-Formalin (Thermo Fisher Scientific, Waltham, USA) *via* the heart with a 21-gauge syringe (BD, Franklin Lakes, USA). The right liver lobe and right lung were removed for overnight fixation and further histo(morpho)logical analyses.

Examination of EtOH-Induced Hepatic Fat Accumulation

The evaluation of the fatty vacuoles (oil red O staining) in the liver after 24 h post-trauma confirms an acute EI, which was established and proofed in previous studies (3). Hepatic sections (3 µm) were fixed with 10% buffered Zn-formalin. Lipids were stained for 50–60 min with an oil red O working solution (0.35 g oil red O dissolved in 25 ml of 100% methanol mixed with 10 ml of 1 M NaOH) and counterstained with hematoxylin (5 g/L) for 10 min. The images were captured by using the Zeiss Axio Observer Z1 microscope (40× objective, Zeiss, Göttingen, Germany).

Examination of Lung Injury

Specimens were fixated in 4% buffered Zn-formalin overnight and embedded in paraffin. For subsequent staining with hematoxylin-eosin (HE), sectioning of 3-µm samples was performed. Lung sections were deparaffinized, rehydrated, and stained with hemalum solution according to Mayer (Carl Roth, Karlsruhe, Germany) for 10 min. After blue annealing in rinsing water (10 min), the tissue was counterstained with eosin (Carl Roth, Karlsruhe, Germany) for 3 min. This was followed by differentiation, dehydration using an ascending alcohol series, and xylene-based mounting medium (Mountex, Medite Medical GmbH, Burgdorf, Germany). An independent examiner determined the histological tissue damage of HE-stained sections of the various experimental groups in a blinded manner. To quantify the histopathological lung injury, sections of lungs were examined for desquamation, dystelectasis/atelectasis, emphysema, congestion, interstitial thickness/infiltration with inflammatory cells, and bronchial exudate by an independent examiner. The orientation for scoring is provided by Matute-Bello et al. (22). The findings from the sham ctrl group were used for normalization as 100%.

Quantification of Protein Expression Levels in BALF

To assess the extent of lung damage and loss of pulmonary barrier integrity, levels of proinflammatory mediators in the BALF were determined. Lungs of the anesthetized mice were subjected to BAL, and the BALF was processed as described above. Supernatants were stored at −80°C for later analyses of the protein concentration of CXCL1, IL-1β, and IFN-gamma using mouse-specific ELISA kits (R&D Systems, Minneapolis, USA) according to the manufacturer's instructions. ELISA was performed using the Infinite M200 microplate reader (Tecan, Männedorf, Switzerland).

Ribonucleic Acid Isolation and Reverse Transcription-Quantitative Polymerase Chain Reaction Analysis

The tissue was homogenized using the Precellys 24 Homogenizer (Bertin Technologies, Montigny-le-Bretonneux, France) according to the manufacturer's instructions. RNA was then isolated from the homogenate using the RNeasy assay (Qiagen, Hilden, Germany) following the manufacturer's protocol. To remove residual DNA, the RNase-free DNase kit (Qiagen, Hilden, Germany) was used. The quantity and quality of RNA were determined using the Spark M10 Microplate Reader with the Tecan's NanoQuant Plate (Tecan, Männedorf, Switzerland). The iScript™ cDNA Synthesis Kit (BioRad, Hercules, USA) was used according to the manufacturer's instructions for cDNA synthesis. Gene expressions of *Cxcl1* (qMnuCED0047655), *Il-1β* (qMnuCED0045755), *Tnf* (qMnuCED0004141), tnfrsf10b (qMnuCED0046132), *Muc5ac* (qMnuCED0061472), *Wnt3a* (qMnuCID0005162), and *Sost* (qMnuCED0045167) were quantified by using a specific primer for mouse and *Gapdh* (qMnuCED0027467, all PrimePCR SYBR Green Assay, BioRad, Hercules, USA) as housekeeping gene (control). The total volume of the PCR reaction was 25 µl with SYBR green qPCR Master Mix (BioRad) according to the manufacturer's instructions. The PCR reaction was performed on a C1000 Touch Thermal Cycler with the CFX96 Touch Real-Time PCR Detection System (BioRad, Hercules, USA) and consists of an initial denaturation step at 95°C for 10 min, followed by 40 cycles of denaturation at 95°C for 15 s, and annealing/extension at 60°C for 60 s. The relative gene expression of each target gene normalized to *GAPDH* was calculated by using the $2^{-\Delta\Delta CT}$ method [comparative threshold-cycle (CT) method].

Immunohistology Staining of CXCL1, Neutrophile Elastase, and Active Caspase-3

Lung tissue sections (3 µm) were deparaffinized using Roti Histol (Carl Roth, Karlsruhe, Germany) and rehydrated using a descending alcohol series. Heat-induced epitope retrieval (HIER) was performed by using R-Universal epitope recovery buffer (Aptum, Kassel, Germany) in the 2100-Retriever (Prestige Medical, Blackburn, England) for 60 min at 121°C. Blocking of endogenous peroxidase was performed *via* hydrogen peroxide (Peroxidase UltraVision Block, Thermo Fisher Scientific, Waltham, USA) for 20 min. Primary antibodies for CXCL1 (abcam, USA, rabbit anti-mouse, 1:300), neutrophil elastase (Bioss, USA, rabbit anti-mouse, 1:200), and active caspase-3 [Cell Signaling Technology, USA, anti-cleaved caspase-3 (Asp175), #9661, rabbit anti-mouse] were diluted as suggested by the manufacturer in Antibody Dilution Buffer (Dako Cytomation) and incubated for 1 h at room temperature.

Subsequently, the secondary antibody conjugated with horseradish peroxidase (HRP) [Histofine Simple Stain Mouse MAX PO (R), Nichirei Biosciences Inc.] was applied for 30 min at room temperature and 3-amino-9-ethylcarbazol (AEC, DCS Innovative Diagnostik-Systeme, Hamburg) was used to detect specific binding. Slides were counterstained with hematoxylin (Carl Roth, Karlsruhe, Germany) and mounted (Medite Medical GmbH, Burgdorf, Germany). Imaging was performed using the Zeiss Axio Observer Z1 microscope (40× objective, Zeiss, Göttingen, Germany). The evaluation was done *via* ImageJ software. For CXCL1, mean intensity values were measured for all groups, whereas for neutrophil elastase and active caspase-3, positive-counted cells were measured in 25 high-power fields (HPF) at 400× magnification.

Immunofluorescent Staining of A20, β-Catenin, E-Cadherin, RIPK4, and CD4 T Cells

Paraffin-embedded lung tissue sections (3 µm) were deparaffinized with Roti Histol (Carl Roth, Karlsruhe, Germany) (2× 5 min) and rehydrated with a descending alcohol series. HIER was performed using R-Universal Epitope Recovery Buffer (Aptum, Kassel, Germany) for 10 min at 90°C in a preheated water bath. Slides were then cooled to room temperature in distilled water for 30 min and washed in distilled water (3× 5 min) and DPBS (Thermo Fisher Scientific, USA) (1× 5 min). Permeabilization was performed with 0.1% Tween 20 (Merck, Darmstadt, Germany) in DPBS (Thermo Fisher Scientific, USA) for 10 min at RT followed by washing in DPBS (1× 5 min and 2× 3 min) (Thermo Fisher Scientific, USA). Permeabilization was followed by blocking the slides with BSA (1%, Merck, Darmstadt, Germany) in PBST (PBS with 0.1% Tween 20) for 30 min at RT in a humidified incubation chamber. After blocking, slides were washed again in distilled water (1× 5 min) and DPBS (1× 5 min and 2× 3 min) (Thermo Fisher Scientific, USA). Lung sections were incubated with primary antibodies against A20 (abcam, USA, rabbit anti-mouse, 1:500, cat. ab92324), β-catenin (antibodies-online GmbH, Aachen, Germany, rabbit anti-mouse, 1:500, cat. ABIN2855042), CD4 (BD, rat anti-mouse, 1:50, cat. 550278), E-cadherin (Purified mouse anti-E-cadherin, BD Biosciences, 1:500, 610182), and RIPK4 [Santa Cruz, USA, mouse anti-mouse, RIP4 Antibody (E-7) Alexa Fluor® 647, 1:200, cat. sc-377368 AF647] overnight at 4°C in a humidified incubation chamber, which were diluted in blocking buffer (1% BSA in PBST) according to the manufacturer's instructions. Incubation of primary antibodies was followed by washing according to the washing steps after blocking. The next steps were performed in the dark. The secondary antibodies (Thermo Fisher Scientific, USA Alexa Fluor® 488, donkey anti-rabbit, Alexa Fluor 568 donkey anti-Mouse IgG, and goat anti-rat Alexa Fluor® 647, 1:1,000) were diluted in blocking buffer according to the manufacturer's instructions and applied to the A20 and β-catenin slides, where it was stained for 60 min at RT in a humidified incubation chamber. This was followed by another wash in DPBS (3× 5 min) (Thermo Fisher Scientific, USA). RIPK4 primary antibody was conjugated with Alexa Fluor® 647 (Molecular Probes, Inc., Oregon, USA). Tissue slides were counterstained with DAPI (Cambrex Bioscience, USA, 1:10,000) for 10 min with subsequent washing in DPBS (4× 5 min) (Thermo Fisher Scientific, USA) and mounted using Gold Antifade Mountant (Invitrogen™-ProLong™). The slides were sealed with nail polish after mounting. Imaging was performed using the Zeiss Axio Observer Z1 microscope (40× objective, Zeiss, Göttingen, Germany). Pictures at 400× magnification were evaluated with the FIJI (ImageJ) software. Mean intensity values were measured, and means were calculated for each group. Colocalization analysis of β-catenin–E-cadherin complexes was performed on fluorescent sections using ZEN Pro-software 3.2. The images for analysis were obtained using a ZEISS Axio Observer fluorescent microscope and the Zeiss digital camera ZEISS Axiocam (705 mono) with ×63 objective. Each analyzed image was individually evaluated for validation of the pattern of the staining used before processing. The images were opened in the ZEN Pro colocalization module, and the region of interest (ROI) for colocalization was defined by allowing fluorescence channels to concentrate on the relevant parts of the image. A colocalized channel was created; and channel statistics were calculated.

Statistical Analysis

Statistical analysis was performed using GraphPad Prism 6 (GraphPad Software, Inc., San Diego, CA). Based on the histogram and Shapiro–Wilk test, the non-parametric Kruskal–Wallis test, which does not assume a normal distribution of the residuals, followed by Dunn's *post hoc* test for the correction of multiple comparisons was applied. Results were expressed as mean and standard error of the mean. A p-value of less than 0.05 was considered to be statistically significant.

RESULTS

Impact of Acute EI on Lung Damage After THFx

Animals received a gavage of either NaCl or EtOH 2 h before the procedures as shown in **Figure 1A**. Mice receiving EtOH showed a clear accumulation of fatty vacuoles in liver 24 h after the procedure compared to animals receiving sodium chloride, confirming successfully induced acute EI as displayed in **Figure 1B**.

Lung organ damage caused by systemic inflammation following THFx was measured by assessing the relative lung injury and compared to the sham ctrl. The histomorphological differences between the groups in the lung after HE staining are demonstrated in **Figure 1C**. A significantly increased histopathological lung injury, e.g., thickening of the alveolar walls/loss of alveolar space, is found in the THFx ctrl group vs. all other groups ($p < 0.05$, **Figures 1C, G**). THFx EtOH exerts a significantly lower relative lung injury vs. THFx ctrl ($p < 0.05$).

The association of the proinflammatory changes with apoptosis induction is shown in **Figure 1D** as representative staining of active caspase-3 (red arrows). Quantification of cells that are positive for active caspase-3 as a direct indicator of apoptosis indicates significantly increased apoptosis in the THFx ctrl group vs. all groups ($p < 0.05$, **Figure 1E**). However, acute EI in the THFx significantly decreased caspase-3-positive cells vs. THFx ctrl ($p < 0.05$).

Furthermore, the gene expression of *Muc5ac* coding for its lung protective protein in homogenized lung tissue was investigated (23). Both sham groups had significantly higher

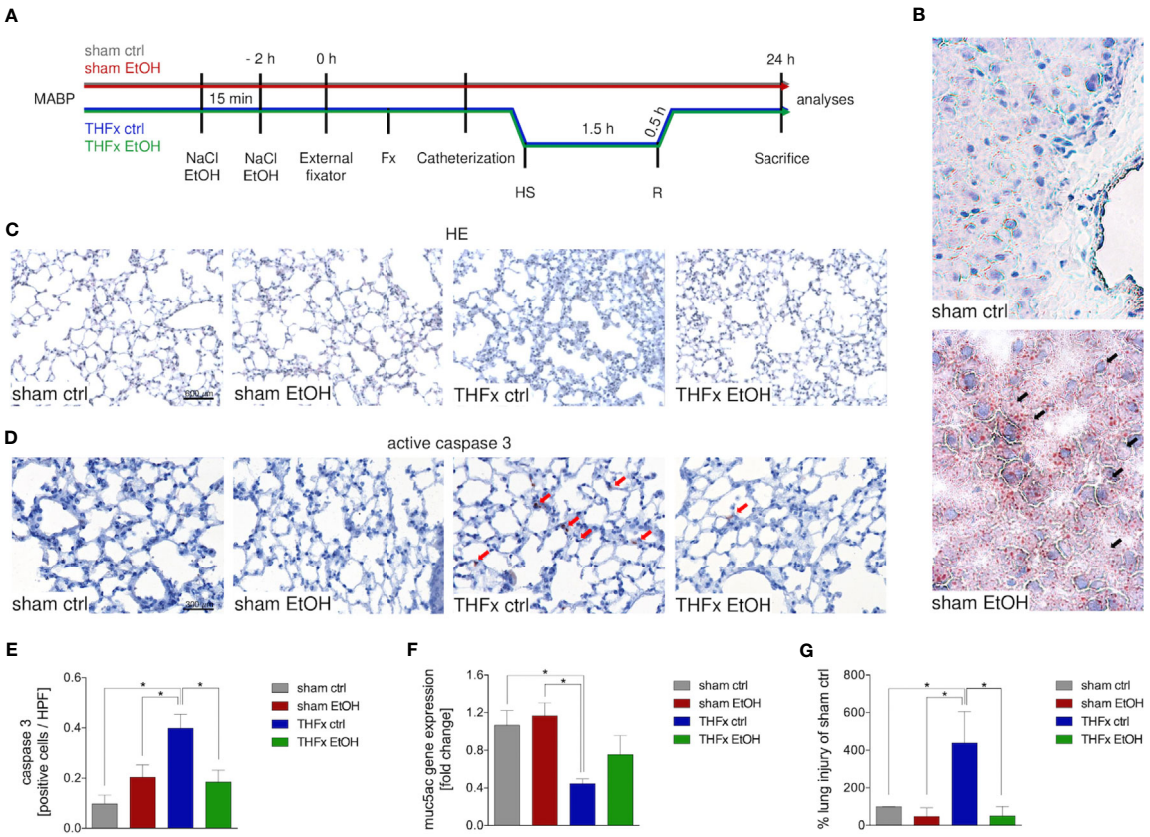

FIGURE 1 | Impact of acute ethanol intoxication (EI) on lung damage after femoral fracture (Fx) and hemorrhagic shock (HS). **(A)** Experimental design is shown. Two hours before the initiation of experiments, the animals received an intragastric gavage of either sodium chloride (NaCl, ctrl, $n = 14$) or ethanol (EtOH, $n = 14$) to simulate an acute intoxication with alcohol. Trauma groups underwent Fx (*via* osteotomy after the placement of an external fixator) and a pressure-controlled HS with subsequent resuscitation (R) with Ringer's solution (TH) *via* catheterized femoral artery ($n = 14$). Sham groups underwent catheterization and received an external fixator, but THFx was not induced ($n = 14$). Twenty-four hours after the end of the experiment, mice were euthanized, and sampling was performed. MABP: mean arterial blood pressure. **(B)** Representative oil red O staining of fatty vacuoles in hepatic tissue of mice undergoing sham procedure. Fatty vacuoles are colored red (black arrow). **(C)** Representative lung sections upon hematoxylin/eosin (HE) staining of the sham ctrl, sham EtOH, THFx ctrl, and THFx EtOH groups are shown. **(D)** Representative lung sections upon the staining of activated caspase-3 in the sham ctrl, sham EtOH, THFx ctrl, and THFx EtOH groups are shown. Exemplary caspase-3-positively stained cells are marked with red arrows. **(E)** Quantification of caspase 3-positively stained cells per high-power field (HPF) is shown. **(F)** RT-qPCR with homogenized lung tissue was performed. Relative gene expression of Muc5ac normalized to Gapdh in lung tissue was calculated by using the comparative threshold-cycle $2^{-\Delta\Delta CT}$ method. **(G)** Quantification of the histopathological lung injury. The findings from the sham ctrl group were used for normalization as 100%. **(E, F)** Data are presented as mean ± standard error of the mean; $n = 7$ in all groups, $^*p < 0.05$ between indicated groups.

relative gene expression compared to THFx ctrl ($p < 0.05$, **Figure 1F**). THFx EtOH does not significantly differ from the sham groups. There was a tendency to upregulate *Muc5ac* gene expression in the THFx EtOH group vs. THFx ctrl (**Figure 1F**).

Impact of Acute EI on CXCL1 Expression and Neutrophilic Infiltration After THFx

Both protein and gene expression of CXCL1 in homogenized lung tissue and CXCL1 protein concentration in the BALF were assessed.

Representative immunostaining of CXCL1 is shown in **Figure 2A**, and the mean intensity values are demonstrated in **Figure 2B**. Comparison of the mean intensity values between the four groups showed the same pattern as observed regarding the protein expression of CXCL1 in the lungs and CXCL concentration in the BALF. The marked local remote proinflammatory response to trauma is confirmed by the significantly increased CXCL1 expression in the lung in THFx ctrl vs. sham ctrl and also sham EtOH ($p < 0.05$, **Figures 2A, B**). CXCL1 expression in the THFx EtOH group is significantly reduced vs. the THFx ctrl group ($p < 0.05$, **Figure 2B**).

Protein expression of CXCL1 in lung tissue is significantly increased in THFx ctrl vs. all other groups ($p < 0.05$, **Figure 2C**). Trauma animals undergoing EI have significantly decreased protein expression vs. THFx ctrl ($p < 0.05$, **Figure 2C**).

CXCL1 protein expression in the BALF was significantly increased in THFx ctrl vs. all other groups ($p < 0.05$, **Figure 2D**), comparable to results that were observed for CXCL1 protein concentration in the lung tissue homogenates. In THFx EtOH, CXCL1 protein expression is significantly lower vs. THFx ctrl ($p < 0.05$, **Figure 2D**).

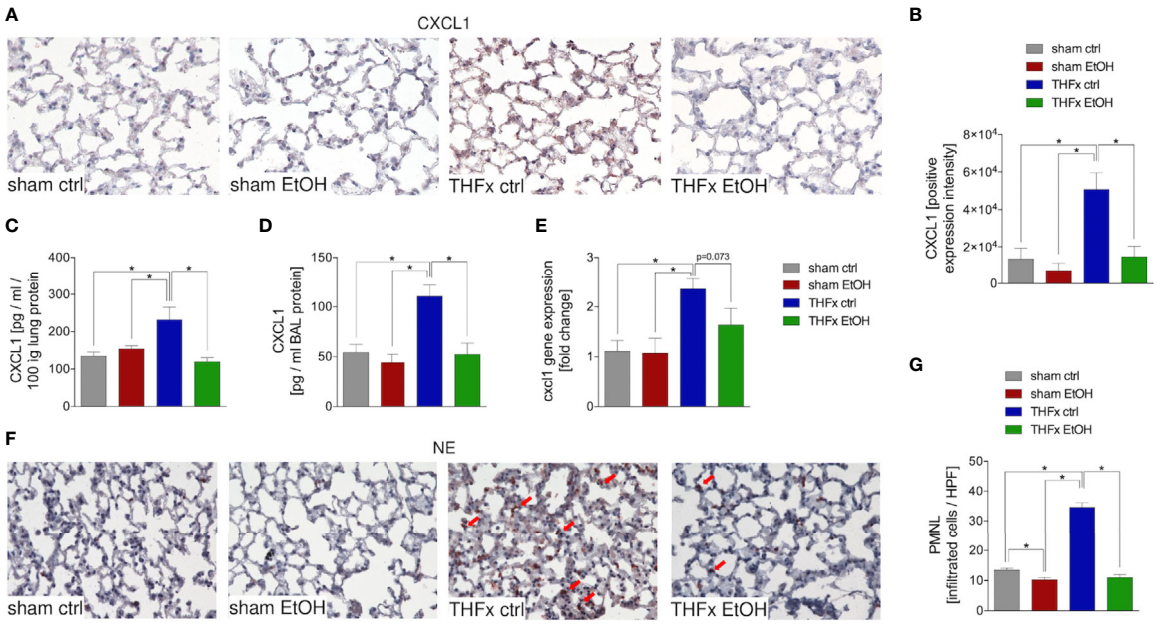

FIGURE 2 | Impact of acute ethanol intoxication (EI) on Cxcl1 gene and CXCL1 protein expression and neutrophilic infiltration after femoral fracture (Fx) and hemorrhagic shock (HS). The animals received an intragastric gavage of either sodium chloride (ctrl, $n = 14$) or ethanol (EtOH, $n = 14$) to simulate an acute intoxication with alcohol. Two hours before the initiation of experiments, the animals in trauma groups underwent an Fx (*via* osteotomy after the placement of an external fixator) and a pressure-controlled HS with subsequent resuscitation with Ringer's solution (THFx) *via* catheterized femoral artery ($n = 14$). Sham groups underwent catheterization and received an external fixator, but THFx was not induced ($n = 14$). Twenty-four hours after the end of the experiment, mice were euthanized, and sampling was performed. **(A)** Representative lung sections upon the staining of CXCL1 in the sham ctrl, sham EtOH, THFx ctrl, and THFx EtOH groups are shown. **(B)** Quantification of CXCL1-positively stained cells per high-power field (HPF) is shown. **(C)** Quantification of CXCL1 protein concentration in lung tissue homogenates using mouse-specific ELISA kits is shown. **(D)** Quantification of CXCL1 protein concentration in bronchoalveolar lavage (BAL) fluid is represented. Briefly, to obtain BAL, *via* trachea, lungs were flushed with 1.1 ml of phosphate buffered saline and then 800 µl was withdrawn for the determination of total protein concentration. **(E)** RT-qPCR with homogenized lung tissue for Cxcl1 gene expression analyses is depicted. The relative gene expression of Cxcl1 normalized to Gapdh was calculated by using the comparative threshold-cycle $2^{-\Delta\Delta CT}$ method. **(F)** Representative immune histological staining of neutrophil elastase (NE) as a marker of polymorphonuclear leukocytes (PMNLs) in lung sections is represented. Red arrows indicate NE-positively stained cells. **(G)** Quantification of NE-positively stained cells per high-power field (HPF) is shown. Data are presented as mean ± standard error of the mean; $n = 7$ in all groups, $^*p < 0.05$ between indicated groups.

Relative gene expression of *Cxcl1* does not significantly differ between sham ctrl and sham EtOH (**Figure 2E**). Significantly higher relative gene expression of *Cxcl1* in THFx ctrl vs. both sham groups is observed ($p < 0.05$, **Figure 2E**). However, there is a trend to decreased relative gene expression in THFx EtOH vs. THFx ctrl ($p = 0.073$, **Figure 2E**).

As CXCL1 plays an important role in attracting neutrophils, we investigated neutrophil recruitment to the lungs (24). Neutrophil infiltration of lung tissue was assessed by immunohistology staining (**Figure 2F**) and quantified by counting the positively stained cells (**Figure 2G**). Neutrophil infiltration is significantly increased in THFx ctrl vs. all other groups ($p < 0.05$). Compared to THFx ctrl, in THFx EtOH, a significantly reduced neutrophil infiltration is shown ($p < 0.05$, **Figure 2G**). In sham EtOH, a significantly lower neutrophil invasion vs. sham ctrl is observed ($p < 0.05$, **Figure 2G**).

Impact of Acute EI on IL-1β and TNF as Well as Tnfrs10b After THFx

Similar to CXCL1, we investigated Il-1β gene expression and IL-1β protein expression in homogenized lung tissue as well as protein concentration in the BALF. The relative gene expression of Il-1β was significantly higher in THFx ctrl vs. all other groups ($p < 0.05$, **Figure 3A**). Il-1β gene expression is significantly reduced in THFx EtOH vs. THFx ctrl ($p < 0.05$, **Figure 3A**).

IL-1β concentration in the lung tissue protein homogenates was significantly increased in THFx ctrl vs. all other groups ($p < 0.05$, **Figure 3B**). IL-1β concentration was significantly reduced in THFx EtOH vs. THFx ctrl ($p < 0.05$, **Figure 3B**). There are no differences between the sham groups.

IL-1β concentration in the BALF was significantly enhanced in THFx ctrl vs. all other groups ($p < 0.05$, **Figure 3C**). In THFx EtOH, IL-1β levels were significantly reduced vs. THFx ctrl ($p < 0.05$). Sham animals did not differ significantly.

There was a significantly higher relative gene expression of Tnf in THFx ctrl vs. all other groups ($p < 0.05$, **Figure 3D**). Tnf gene expression was significantly decreased in THFx EtOH vs. THFx ctrl ($p < 0.05$, **Figure 3D**). However, Tnf gene expression in THFx ETOH was significantly increased vs. sham EtOH ($p < 0.05$, **Figure 3D**).

Compared with the significant differences that are observed regarding the *Tnf* gene expression, only a tendency regarding the

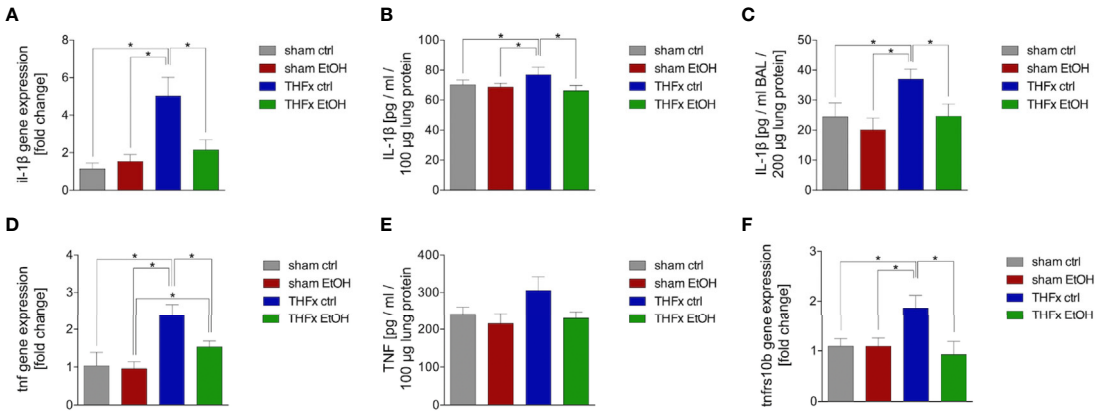

FIGURE 3 | Impact of acute ethanol intoxication (EI) on IL-1β and TNF as well as Tnfrs10b after femoral fracture (Fx) and hemorrhagic shock (HS, THFx respectively). The animals received an intragastric gavage of either sodium chloride (ctrl, $n = 14$) or ethanol (EtOH, $n = 14$) to simulate an acute intoxication with alcohol. Two hours before the initiation of experiments, the animals in trauma groups underwent an Fx (*via* osteotomy after the placement of an external fixator) and a pressure-controlled HS with subsequent resuscitation with Ringer's solution (THFx) *via* catheterized femoral artery ($n = 14$). Sham groups underwent catheterization and received an external fixator, but THFx was not induced ($n = 14$). Twenty-four hours after the end of the experiment, mice were euthanized, and sampling was performed. **(A)** RT-qPCR of homogenized lung tissue has been performed. The relative gene expression of Il-1β normalized to Gapdh was calculated by using the $2^{-\Delta\Delta CT}$ method. **(B)** Quantification of IL-1β protein concentration in total lung tissue protein homogenates using mouse-specific ELISA kits is shown. **(C)** Quantification of IL-1β protein concentration in bronchoalveolar lavage fluid (BALF) is represented. Briefly, to obtain BALF, *via* trachea, lungs were flushed with 1.1 ml of phosphate buffered saline and then 800 µl was withdrawn for the determination of total protein concentration and IL-1β levels. **(D)** The relative gene expression of Tnf normalized to Gapdh after RT-qPCR was calculated by using the comparative threshold-cycle $2^{-\Delta\Delta CT}$ method. **(E)** Quantification of TNF protein concentration in total lung tissue protein homogenates using mouse-specific ELISA kits is shown. **(F)** The relative gene expression of Tnfrs10b normalized to Gapdh was assessed *via* RT-qPCR and calculated by using the comparative threshold-cycle $2^{-\Delta\Delta CT}$ method. Data are presented as mean ± standard error of the mean; $n = 7$ in all groups, $^*p < 0.05$ between indicated groups.

TNF protein expression in lung tissue among the respective groups was observed (**Figure 3E**). Between all groups, the highest protein expression was shown in THFx ctrl.

The relative gene expression of *Tnfrsf10b* did not differ between both sham groups (**Figure 3F**). In THFx ctrl, a significantly increased relative *Tnfrsf10b* gene expression vs. all other groups was detected ($p < 0.05$, **Figure 3F**). A significantly decreased relative gene expression of Tnfrsf10b in THFx EtOH vs. THFx ctrl was shown ($p < 0.05$, **Figure 3F**).

Impact of Acute EI on Wnt Signaling, β-Catenin–E-Cadherin Co-Expression, and A20 After THFx

The relative gene expression of *Sost* was examined. The THFx ctrl group had a significantly reduced *Sost* gene expression vs. all other groups ($p < 0.05$, **Figure 4A**). In THFx EtOH, a significantly increased *Sost* gene expression vs. THFx ctrl was detected ($p < 0.05$, **Figure 4A**). Sham groups did not differ significantly.

Among all groups, the highest and most significant increase in relative *Wnt3a* gene expression in THFx ctrl vs. all other groups was detected ($p < 0.05$, **Figure 4B**). Relative *Wnt3a* gene expression was significantly reduced in THFx EtOH vs. THFx ctrl ($p < 0.05$, **Figure 4B**).

The protein expression of A20 was investigated *via* quantification of the mean intensity values in IF. Representative pictures are demonstrated in **Figure 4C**. A20 expression was significantly reduced in THFx ctrl vs. both sham groups ($p < 0.05$, **Figure 4D**). A20 expression in THFx EtOH did not statistically differ from sham ctrl. However, A20 was significantly reduced in THFx EtOH vs. sham EtOH ($p < 0.05$, **Figure 4D**). Sham EtOH showed a significantly higher A20 expression vs. the sham ctrl group ($p < 0.05$, **Figure 4D**). This increase upon EI was also observed after THFx; however, this tendency was not significant vs. THFx ctrl (**Figure 4D**).

We also examined the association of A20 to RIPK4 in lung tissue by IF, which is representatively shown in **Figure 4C** and quantified in **Figure 4E**. RIPK4 expression in lung tissue showed a significant increase in sham EtOH vs. all other groups ($p < 0.05$, **Figure 4E**). No significant differences among the other groups were found. RIPK4 expression increased in THFx EtOH compared with THFx ctrl; however, this tendency was not significant (**Figure 4E**).

In IF, the expression and distribution of β-catenin protein was determined and compared to the mean intensity values among the groups. The β-catenin levels were significantly enhanced in sham EtOH vs. sham ctrl and against both trauma groups ($p < 0.05$, **Figure 4F**). The expression levels of β-catenin were significantly decreased in THFx ctrl vs. all other groups ($p < 0.05$, **Figure 4F**). EI prior to trauma significantly increased the β-catenin levels vs. THFx ctrl ($p < 0.05$, **Figure 4F**). In both trauma groups, the β-catenin expression was significantly reduced compared to the corresponding control groups, respectively ($p < 0.05$, **Figure 4F**).

Stratifying the localization of the β-catenin and E-cadherin expression (**Figure 5A**) has shown that the colocalization of β-catenin–E-cadherin complexes was significantly higher in THFx vs. all other groups ($p < 0.05$, **Figure 5B**). However, expression of β-catenin was significantly increased in all groups vs. the THFx ctrl group, both membranous ($p < 0.05$, **Figure 5C**) and cytosolic expression ($p < 0.05$, **Figure 5D**). Membranous E-cadherin expression was significantly enhanced in both EtOH groups vs.

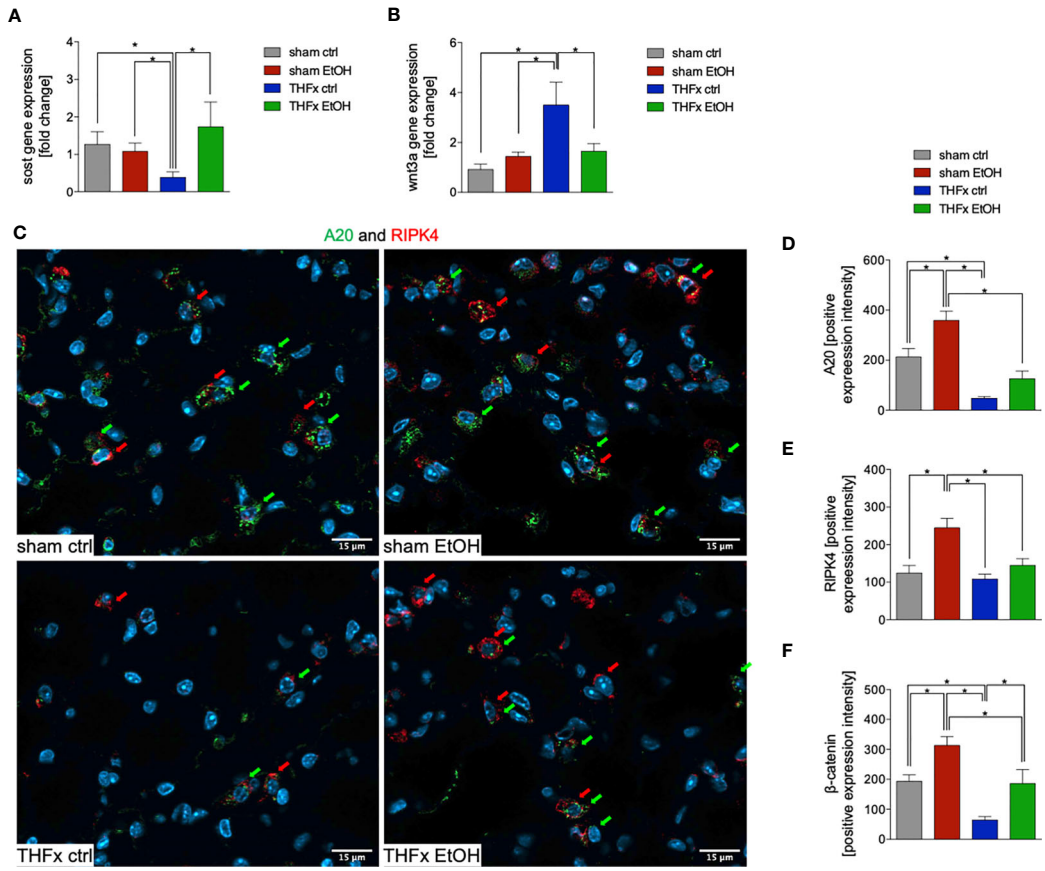

FIGURE 4 | Impact of acute ethanol intoxication (EI) on Wnt signaling and A20 after femoral fracture (Fx) and hemorrhagic shock (HS, THFx respectively). The animals received an intragastric gavage of either sodium chloride (ctrl, $n = 14$) or ethanol (EtOH, $n = 14$) to simulate an acute intoxication with alcohol. Two hours before the initiation of experiments, the animals in trauma groups underwent an Fx (*via* osteotomy after the placement of an external fixator) and a pressure-controlled HS with subsequent resuscitation with Ringer's solution (THFx) *via* catheterized femoral artery ($n = 14$). Sham groups underwent catheterization and received an external fixator, but THFx was not induced ($n = 14$). Twenty-four hours after the end of the experiment, mice were euthanized, and sampling was performed. Wnt3a and its inhibitor sclerostin (Sost) were determined. **(A)** RT-qPCR of homogenized lung tissue was performed. The relative gene expression of Sost, an Wnt inhibitor, normalized to Gapdh was calculated by using the comparative threshold-cycle $2^{-\Delta\Delta CT}$ method. **(B)** RT-qPCR of Wnt3a is shown after Wnt3a relative gene expression normalization to Gapdh by using the comparative threshold-cycle $2^{-\Delta\Delta CT}$ method. **(C)** Representative immunofluorescent staining of A20 in green (green arrows, Alexa Fluor 488) and receptor interacting protein kinase 4 in red (RIPK4, red arrows, Alexa Fluor 647) are represented. **(D)** Quantification of A20-positively stained cells per high-power field (HPF) is shown. **(E)** Quantification of RIPK-4 positively stained cells per HPF is shown. **(F)** Immunofluorescence staining of the β-catenin as the key mediator of the Wnt/β-catenin signaling pathway in lung sections of mice was performed, and quantification of the positively stained area per HPF is depicted. Data are presented as mean ± standard error of the mean; $n = 7$ in all groups, $^*p < 0.05$ between indicated groups.

the corresponding ctrl groups ($p < 0.05$, **Figure 5E**), while THFx showed significantly less E-cadherin presence at the membrane vs. all other groups ($p < 0.05$, **Figure 5E**). The significantly reduced E-cadherin presence in THFx vs. all other groups is also observed in the cytosol ($p < 0.05$, **Figure 5F**).

Impact of Acute EI on CD4 T Cell Infiltration After THFx

Representative immunostaining of CD4 is shown in **Figure 6A**, and the quantification of counted CD4-positive cells is shown in **Figure 6B**. The marked local proinflammatory response to trauma is confirmed by the significantly increased CD4 T cell infiltration in the lung in THFx ctrl vs. sham ctrl and also sham EtOH ($p < 0.05$, **Figures 6A, B**). Infiltration with CD4-positive cells in the THFx EtOH group is also significantly increased vs. sham ctrl as well as vs. sham EtOH ($p < 0.05$, **Figures 6A, B**).

IFN-gamma protein expression in the BALF was significantly increased in THFx ctrl vs. all other groups ($p < 0.05$, **Figure 6C**), comparable to results that were observed for CXCL1 gene and protein expression.

The proposed, presumed mechanism of action is demonstrated in **Figure 7**.

DISCUSSION

In this work, we aimed to analyze the basic mechanisms of lung barrier disruption and organ damage after THFx with and

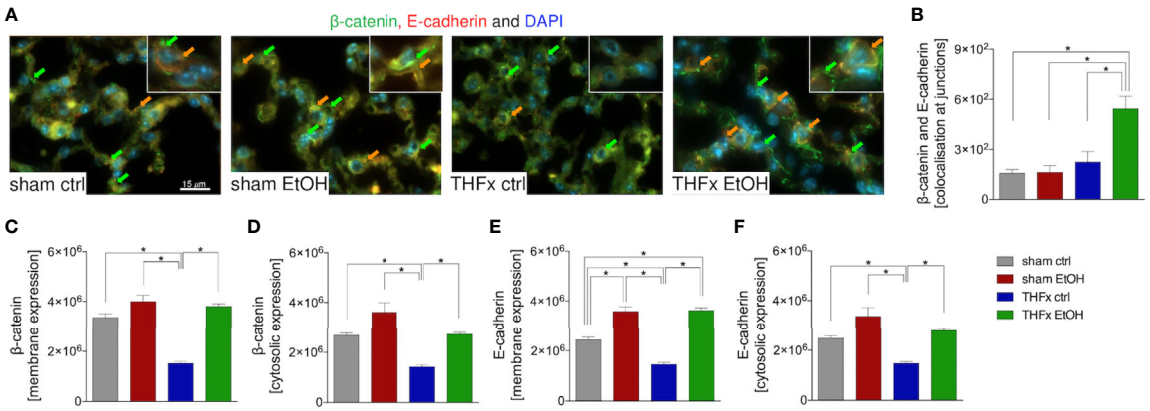

FIGURE 5 | Impact of acute ethanol intoxication (EI) on the β-catenin–E-cadherin co-expression after femoral fracture (Fx) and hemorrhagic shock (HS, THFx respectively). The animals received an intragastric gavage of either sodium chloride (ctrl, $n = 14$) or ethanol (EtOH, $n = 14$) to simulate an acute intoxication with alcohol. Two hours before the initiation of experiments, the animals in trauma groups underwent an Fx (*via* osteotomy after the placement of an external fixator) and a pressure-controlled HS with subsequent resuscitation with Ringer's solution (THFx) *via* catheterized femoral artery ($n = 14$). Sham groups underwent catheterization and received an external fixator, but THFx was not induced ($n = 14$). Twenty-four hours after the end of the experiment, mice were euthanized, and sampling was performed. Expression of β-catenin and E-cadherin as well as their co-localization were determined. **(A)** Representative immunofluorescent staining of β-catenin in green (green arrows, Alexa Fluor 488) and E-cadherin in red (Alexa Fluor 568), and overlay (orange arrows) are represented. **(B)** Quantification of the β-catenin–E-cadherin co-expression at junctions is shown. **(C)** Quantification of β-catenin expression at the membrane, **(D)** β-catenin expression in the cytosol, **(E)** E-cadherin at the membrane, and **(F)** E-cadherin in the cytosol in lung sections of mice is depicted. Data are presented as mean ± standard error of the mean; $n = 7$ in all groups, $^*p < 0.05$ between indicated groups.

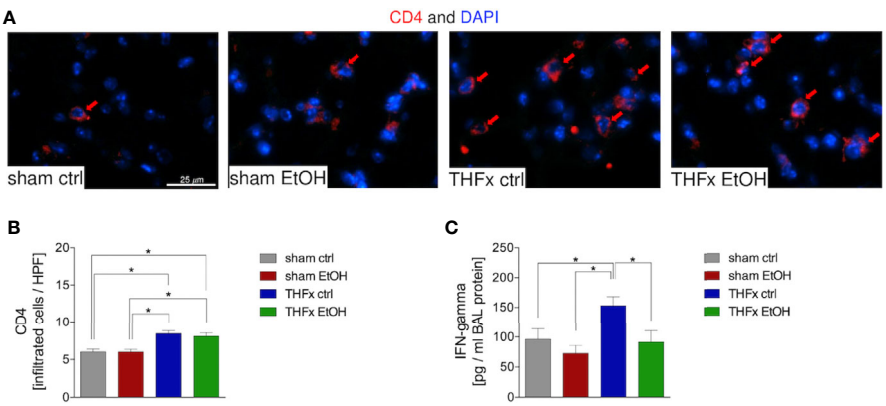

FIGURE 6 | Impact of acute ethanol intoxication (EI) on CD4 T-cell infiltration after femoral fracture (Fx) and hemorrhagic shock (HS, THFx respectively). The animals received an intragastric gavage of either sodium chloride (ctrl, $n = 14$) or ethanol (EtOH, $n = 14$) to simulate an acute intoxication with alcohol. Two hours before the initiation of experiments, the animals in trauma groups underwent an Fx (*via* osteotomy after the placement of an external fixator) and a pressure-controlled HS with subsequent resuscitation with Ringer's solution (THFx) *via* catheterized femoral artery ($n = 14$). Sham groups underwent catheterization and received an external fixator, but THFx was not induced ($n = 14$). Twenty-four hours after the end of the experiment, mice were euthanized, and sampling was performed. **(A)** Immunofluorescence staining of CD4 in red (red arrows, Alexa Fluor 647) in lung sections of mice was performed, and **(B)** quantification of the positively stained cells per HPF is depicted. **(C)** Quantification of interferon (IFN)-gamma protein concentration in bronchoalveolar lavage (BAL) fluid is represented. Data are presented as mean ± standard error of the mean; $n = 7$ in all groups, $^*p < 0.05$ between indicated groups.

without EI. Acute alcohol abuse resulting in EI has been implicated as a major risk factor not only for traumatic injury itself but also for post-traumatic immune regulation and recovery. The results thus far have been equivocal. This is of particular importance, as it is estimated that up to 50% of trauma patients present acutely intoxicated (25, 26). Thus, there is a significant need for understanding the influence of acute EI on the inflammatory response and lung injury after trauma. In particular, this study examined the involvement of the canonical Wnt/β-catenin signaling pathway after trauma.

Our results demonstrate that THFx triggered lung injury in mice, which developed from an uncontrolled inflammatory

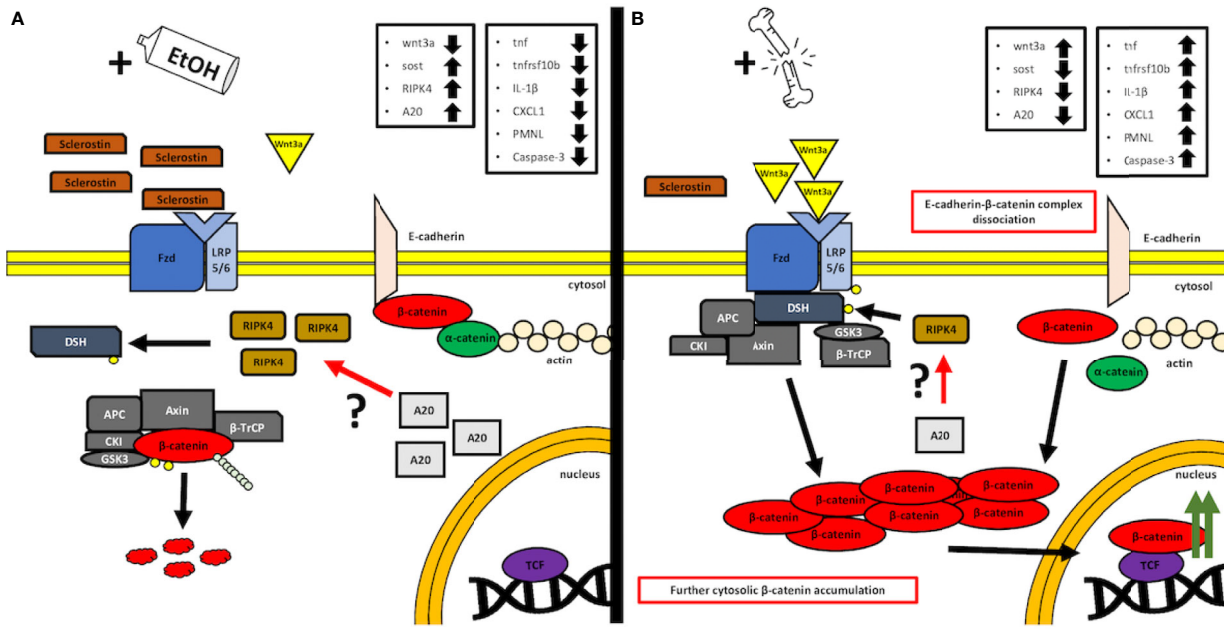

FIGURE 7 | A simplified, graphical depiction of the regulation mechanism of the Wnt/β-catenin signaling by the acute ethanol intoxication (EI) **(A)** and with the major trauma injury **(B)**. **(A)** Suspected mechanism of the EI influence over the activity of the canonical Wnt/β-catenin. According to our findings, we observed that acute alcohol intake leads to the elevated levels of Sost gene expression, whose product, sclerostin, acts as a natural competitor inhibitor for Wnt receptors. Additionally, we noticed increased expression levels of both receptor-interacting protein kinase 4 (RIPK4) and A20 protein in the same EI setting. Interestingly, it was reported before that RIPK4 appears to be a positive regulator of canonical Wnt/β-catenin signaling, while A20 protein seems to be the natural inhibitor of RIPK4 activity and presumably regulates the Wnt/β-catenin signaling through this kinase (12). In our findings, the upregulated levels appear to be contradictory to these results; however, both levels of A20 and RIPK4 seem to compensate each other, and thus, one may suspect an interaction between those, which cancels the RIPK4-upregulating activity, as the Wnt/β-catenin-driven trauma-induced inflammation is suppressed compared to the ctrl group. However, further investigation is required, especially on the field of the base protein expression and gene transcription and the involvement of the alcohol as a potential regulator of A20–RIPK4 interplay. **(B)** Trauma-based breakdown of the lung barrier through the positive regulation of Wnt/β-catenin signaling in the presence of alcohol. The major trauma injury affects the internal sclerostin and wnt3a ligand competition of the Fzd and LRP-5/6 receptor by favoring the expression of the latter, thus stimulating the destruction complex disruption and β-catenin release to the cytosol. In addition, β-catenin appears to dissociate from E-cadherin-based AJ (adherens junction) complexes, thus disrupting the cell–cell interactions of epithelial cells. At the same time, the expression levels of A20 and RIPK4 seem to decrease; however, it is unknown if this downregulation influences the withdrawal of the destruction complex from the cytosol or maybe it is a time-dependent interaction that requires kinetics-based observations, so that the fold change in time of both molecules during the transition between off and on states can be followed. APC: adenomatous polyposis coli, AXIN: the axis inhibition protein scaffold protein, βTrCP: the beta-transducin repeat containing protein, CKI: casein kinase, Fzd: frizzled protein, GSK3β: glycogen synthase kinase 3β, LRP 5/6: low-density lipoprotein receptor-related protein 5/6.

response, e.g., increased expression of TNF-α, IL-1β, CXCL1, and lung infiltration with PMNL, as well as apoptosis, which promotes lung injury. The current investigation explored whether the canonical Wnt/β-catenin signaling pathway, which plays a key role in repair mechanisms and cell-to-cell adhesion, will contribute to the breakdown of the lung barrier after trauma (27, 28). Our findings demonstrate THFx-induced activation of the canonical Wnt *via* inhibition of the destruction complex, since expression of *Wnt3a* increased and that of *Sost* decreased, altogether leading to the stabilization and accumulation of the cytoplasmic β-catenin levels, allowing its translocation into the nucleus. Furthermore, reduced levels of β-catenin, which ultimately lead to the absence of β-catenin in the E-cadherin–β-catenin complexes at the cytoplasmic side of the cell membrane, suggest loss of cell-to-cell adherence and lung barrier breakdown after THFx. In this study, we found that acute EI alleviated the uncontrolled inflammatory response and lung barrier breakdown *via* the canonical Wnt/β-catenin signaling pathway.

Prior studies have shown that severe trauma causes damage to trauma-remote organs such as lungs or liver, mainly by an uncontrolled systemic and local proinflammatory response (4–6). Zhang et al. found increased inflammation and lung damage as also shown by the LIS after hip fracture in rats (29). These results are in line with our findings. We have shown that reduction of the lung-protective *Muc5ac* (23) is associated with enhanced lung injury after THFx. It is well known that mediators of inflammation correlate with the magnitude of the injury and subsequent organ failure in trauma (30). Zhang et al. found increased circulating levels of TNF-α and IL-1β 24 h after traumatic fracture and surgery (29), while Xu et al. also demonstrated increased IL-1β levels in the BALF after HS in mice (31). Here, we demonstrate that lung injury is associated with significantly increased local TNF-α and IL-1β in lungs after THFx. Furthermore, we found THFx-induced *Cxcl1* gene as well as CXCL1 protein expression in the lungs and BALF. As CXCL1 is an important neutrophil chemoattractant (32), the observed increase

in PMNL lung infiltration after THFx was expected. These observations are supported by other experimental trauma studies, showing increased CXCL1 and infiltration of inflammatory cells into lungs after experimental multiple trauma models/polytrauma (6, 33). An uncontrolled inflammatory response with excessive cytokine production and leukocyte recruitment can lead to cellular apoptosis/necrosis, tissue damage, hemodynamic changes, and organ failure (34–36). However, the cell counts of neutrophils in the BALF have not been performed. Given the excessive inflammatory mediator release and lung injury after THFx, apoptosis in which caspase activation plays a central role was analyzed. In agreement with Zhang et al., who assessed increased levels of active caspase-3 in lung tissue 24 h after traumatic fracture induction (29), we found markedly increased caspase-3 activation after THFx, indicating lung barrier disruption.

Given the fact that increased apoptosis is associated with increased lung barrier disruption and pulmonary permeability (5), and furthermore, Wnt/β-catenin signaling pathway plays a key role in repair mechanisms and cell-to-cell adhesion (27, 28), we examined this pathway. It is well known that Wnt (e.g., WNT3A) binding to its receptor inhibits the destruction complex, leading to accumulation of the cytoplasmic β-catenin, allowing its translocation into the nucleus (7, 9, 10). Furthermore, in the absence of Wnt stimulus, the majority of β-catenin is located at the cytoplasmic side of the cell membrane in adherens junction-stabilizing complexes with E-cadherin and α-catenin, preventing β-catenin from degradation (9, 10). Activation of the Wnt/β-catenin signaling pathway leads to the release of β-catenin from complexes with E-cadherin (7, 9, 37), and thereby might contribute to the breakdown of the lung barrier. β-catenin signaling is tightly regulated in the early phases of fracture healing, and alterations to β-catenin signaling can play a disparate role in fracture healing (38). Although the Wnt/β-catenin signaling pathway plays a pivotal role in fracture healing, its role in remote organ damage after trauma is still largely unknown. Sawant et al. demonstrated caspase-3 activity, microvascular permeability, and an active canonical Wnt signaling pathway in rat lung microvascular endothelial cells after HS (37). Furthermore, specific inhibition of β-catenin phosphorylation and, thus, inhibition of the trauma-induced Wnt/β-catenin signaling protected from caspase-3 enzyme activity and against microvascular hyperpermeability following HS (37). In the current study, THFx-induced expression of *Wnt3a*, a major trigger for the active canonical Wnt/β-catenin signaling pathway (37), and THFx-reduced expression sclerostin, an inhibitor of the Wnt signaling pathway (13), demonstrate that THFx also induces the Wnt/β-catenin signaling pathway. Therefore, we hypothesize that enhanced canonical Wnt/β-catenin signaling pathways and loss of β-catenin from the membranous complexes as confirmed by the IF cause lung barrier breakdown and lung injury after THFx.

In this study, we focused on acute EI to elaborate its effects on the lung inflammation and barrier breakdown after THFx. Therefore, no unambiguous conclusions can be drawn regarding subacute or chronic EI. The current data regarding the impact of an acute EI on the inflammatory response and organ damage after trauma are conflicting (3, 18, 39, 40). In this study, we found that EI reduced lung damage after THFx. In agreement with our previous findings in experimental traumatic brain injury (18), we found that acute EI decreased the proinflammatory mediators that were released and activated after THFx. EI-reduced expression of *Tnf* and *Il-1β* after THFx in this study is supported by Xu et al. demonstrating reduced expressions of *Tnf-α* and *Il-1β* in the lungs in a combined model of traumatic brain injury model with acute EI (18). Similar results were confirmed in the liver as well, under the influence of an acute EI after HS in rats (3). In contrast to the anti-inflammatory effects of an acute EI, Hu et al. showed in their rat model of HS that an acute EI increased circulatory TNF-α levels and histopathological damage of the lung (39). The reports must be carefully interpreted since, e.g., Hu et al. administered EtOH intravenously (39), which is a physiologically absolutely different approach. Regarding the TNF-α levels in the serum, which we did not assess here, it is already well-reported that alcohol can induce the TNF-α release from the liver macrophages, the Kupffer cells, due to the LPS-driven NF-κB signaling pathway (41). Additionally, ethanol sensitizes the TNF receptor 1 (TNFR1) to the TNF, strengthening the inflammatory response and the recruitment of leukocytes (42), and thus contributing to local hepatic inflammation, as well as systemic inflammation. This could be a prevalent factor contributing to the circulating TNF-α levels; however it is worth mentioning that the macrophages' general capability to express TNF-α is relatively low according to the gene/protein expression data from the Human Protein Atlas (ID: ENSG00000232810-TNF). Moreover, soluble TNF-α cytokine lifespan is rather short (43), which always brings difficulties as we have also observed in our study measuring the total circulating level of this cytokine and reflecting its importance more as a local mediator/attractant. Regarding the lung tissue response and production of TNF-α, ethanol brings mixed conclusions regarding its influence on cytokine production, impairing the LPS-driven TNF-α release and contributing to the expression of anti-inflammatory cytokines (44). We have observed this trend in our studies involving the sera derived from traumatic patients and co-incubated with human immortalized epithelial lung cells prior to the exposure to ethanol, which concluded in decreased activation of the NF-κB pathway and the desensitization of neutrophils (45). It is difficult to clearly affirm or denounce the elevated levels of circulating TNF-α coming from the Kupffer cells' activation in the liver due to alcohol activity, while facing the difficulties described above; however, it is certain that the TNF-α gene expression levels change locally in the lung along the applied conditions. On the other hand, regarding the TNF-α levels, the disintegrin and metalloprotease 17, known also as ADAM-17 or TACE, is an enzyme capable of proteolytic cleavage of the TNF-α precursor protein, a membrane-anchored pro-protein, thus releasing the outer domain (known as ectodomain) into the mature, soluble TNF-α cytokine in the process known as "shedding" (46). This strongly indicates the role of ADAM-17 and other potentially "shedding" proteins in the regulation of expression levels of the final extracellular concentration of active TNF-α cytokine, as the target gene expression levels do not

indicate the final levels of protein after translation, especially with secondary post-translational regulators such as ADAM-17, required for the maturation step of the protein. In our experimental setting, it is obviously a relevant factor for consideration, as it was shown by DeBerge et al. that the inhibition of ADAM-17 yields a decreased ratio of TNF-α processing in the animal model of lung injury and thus decreased levels of active cytokine and attenuated severity of lung injury and increased survival of mice (47). Moreover, what is especially relevant in our study is the observation that acute ethanol exposure is capable of regulating the expression of ADAM17 and thus downregulating the maturation of soluble TNF-α and its release (48, 49). However, downregulation of ADAM17 by ethanol does not exclude the negative influence of ethanol on the TNF-α gene expression, which appears to be the prevalent mechanism of action. Further comparisons were used to experimentally validate our present study. Acute EI reduced THFx-induced CXCL1 as well as PMNL presence in the lungs after THFx, which supports our previous reports obtained from the liver analyses upon an acute EI in HS (3). However, Sears et al. demonstrated an enhanced inflammatory response concomitant with increased leukocyte infiltration in lungs 24 h after acute EI and bilateral femur fracture in rats (40). These paradoxical observations might be explained in part by the differences in basic methodology. In contrast to our THFx (osteotomy) model with intragastric EtOH application, Sears et al. applied a blunt guillotine to induce femur fractures and injected EtOH intraperitoneally. In our scenario, acute EI significantly reduced uncontrolled lung inflammatory response and apoptosis after THFx. Acute EI had a marked impact on the Wnt/β-catenin signaling pathway by reducing THFx-induced *Wnt3a*, increasing sclerostin levels, and increasing β-catenin as demonstrated by the IF. Further studies are necessary to determine if increased sclerostin inhibits the active Wnt/β-catenin signaling pathway, ultimately increasing β-catenin in membranous complexes, and thus promoting the stability of adherens junctions after THFx as postulated here. To the best of our knowledge, there are no currently published studies that examine the influence of an acute EI on Wnt/β-catenin signaling pathway in the context of lung barrier breakdown after THFx. However, Dogget and Breslin investigated the impact of an acute EI on microvascular leakage in rats and found an increase in mesenteric microcirculation permeability caused by disrupted VE-cadherin organization at junctions (50). While our data indicate lung barrier stabilization, alcohol-induced endothelial barrier dysfunction was proposed by Dogget and Breslin (50). The ubiquitin-binding protein A20 was indispensable for regulating vascular E-cadherin expression in adherens junctions to maintain and repair damaged endothelial functions after pulmonary vascular injury by lipopolysaccharide (LPS) (11). According to Nakamura et al., it is presumed that A20 interacts with a proximal signaling protein RIPK4 of the Wnt signaling pathway through its natural affinity towards RIPK family proteins, and the regulation of Wnt signaling by A20 occurs *via* RIPK4, which interestingly enough acts by itself as a positive regulator of Wnt/β-catenin canonical signaling through its kinase activity of the Dsh protein (12). It is known that A20 negatively regulates the transcription factor of the nuclear factor kappa-light-chain-enhancer of activated B cells (NF-κB), i.e., through interacting with RIPK proteins, and it was shown that A20 is capable of suppressing the activation of the NF-κB in the experimental setting of the murine traumatic bone injury model, challenged with LPS as a stimulus (51). However, the data on A20 and its modulatory involvement in trauma with/without EI are still missing to a large extent. What we have observed in our study is presumably a potential correlation between those two factors, as both A20 and RIPK4 levels seem to change in a similar manner simultaneously, which may or may not imply a potential complexing interaction or molecular connection, which could be in line with the observations considering the role of A20 in interacting with RIPK proteins. We noticed that increased levels of both A20 and RIPK4 are connected to suppressed activity of Wnt/β-catenin signaling, while its downregulation by trauma injury only seems to induce the further release of β-catenin. This initial observation is thus contradictory to the data from Nakamura et al., as diminished levels of RIPK4 negatively impact the Wnt/β-catenin signaling, as it prohibits sequestration of the destruction complex (12). This may underline the role of A20 as a negative inhibitor of RIPK4, and it is A20 that is one of the targets of EI and trauma stimulation. We illustrate the potential interaction in **Figure 7**; however, it is clearly too early to draw any significant conclusions based only on those data. This aspect requires more insight and deep experimental investigations, especially on the protein–protein interaction plane with huge emphasis on studying the expression patterns.

Here, we show that acute EI prior to THFx downregulated the THFx-induced increase in Wnt3a gene expression, which correlated with an increased β-catenin expression in the lung. Thus, we hypothesize that the data indicate an inhibitory effect of acute EI on Wnt signaling in the lung after trauma. It appears that this effect either is organ-specific or depends on the type of alcohol intoxication (acute vs. chronic EI). Considering the effects of chronic alcohol abuse on Wnt signaling in, e.g., liver, there are several studies that report an opposite and, thus, enhancing impact of alcohol on Wnt signaling. The consequence of such impact is often enhanced development or progression of alcoholic liver disease (ALD), which can ultimately lead to hepatitis, fibrosis, cirrhosis, or hepatocellular carcinoma (52–54). Mercer et al. examined the effects of chronic alcohol abuse (16 weeks) on the development of diethylnitrosamine (DEN)-induced hepatic tumors in a mouse model (52). In tumor-free liver tissue from EtOH+DEN-treated mice, they found significantly increased β-catenin expression in the membrane and cytosol, and enhanced accumulation in the nucleus. Moreover, induction of alcohol-induced liver disease in rats resulted in increased expression of cytosolic and nuclear β-catenin, phosphorylated GSK3β, and significantly increased gene expression of Wnt2, Wnt7a, and β-catenin target genes (52). The consequence of increased Wnt signaling was a significantly increased incidence of liver tumors in the EtOH+DEN group compared to the controls (52). Similar effects were observed by Warner et al., who investigated the role of specific dietary fatty acids (n3-PUFA) in Wnt signaling and the development of ALD

in mice (53). Wild type (WT) and fat-1 transgenic mice underwent chronic EI (6 weeks) with a single final LPS challenge. Chronic EI resulted in increased gene expression of Wnt5a and Wnt4 and significantly reduced gene expression of the negative feedback regulator of Wnt signaling Axin2 in WT mice compared with control animals without long-term alcohol consumption (53). The reported data contrast with our observed effects of acute EI on Wnt signaling in the lung, although it should be noted that our work involved acute EI and not long-term alcohol abuse, and that the influence of trauma was not examined in the above-mentioned studies. Additionally, it should be noted that studies on the influence of alcohol on Wnt signaling in the liver are inconclusive. Several studies exist that describe an inhibitory influence of chronic alcohol abuse on Wnt signaling. Huang et al. investigated the influence of pharmacological activation of Wnt signaling on ALD development and progression in a rat model (54). Rats were subjected to 8 weeks of alcohol consumption. The impact of a 3-week treatment with Wnt agonists in parallel to chronic EI was additionally investigated. They found decreased cytosolic and nuclear β-catenin expression in the liver of animals with chronic alcohol abuse compared with controls (54). Pharmacological activation of the Wnt signaling pathway resulted in decreased ALD progression (54). Similar effects were demonstrated in the work of Xu et al. who examined the crosstalk of chronic alcohol abuse and both the insulin/IGF and Wnt pathways on liver regeneration. After 8 weeks of alcohol administration, rat liver tissue showed decreased gene expression of Wnt1, Wnt7a, and Fzd3 compared to control animals without alcohol administration (55). These data also suggest inhibition of Wnt signaling by chronic alcohol abuse.

Despite the fact that the data suggest the Wnt signaling pathway being involved in the observed changes, there are definitely other involved mechanisms of the widely spoken multicellular impact of ethanol, independent of Wnt signaling, as ethanol influence is exceptionally broad and affects a magnitude of several dependent and independent physiological aspects (56–58), with many of them already settled down in our scientific interests (59, 60). In the study of Samuelson et al., the authors have shown an interesting result derived from an experimental model of the recolonization of microbiota from the alcohol-fed mice donors, followed up by the evaluation of lung inflammation severity and intestinal integrity upon *Klebsiella pneumoniae* infection (61). The study underlines the role of alcohol-induced dysbiosis in the pathogenesis of inflammation and the importance of gastrointestinal tract homeostatic microbiota in supporting the host defense capabilities, showing increased susceptibility to pneumonia severity in the alcohol-affected microbiota (61). The nature of *K. pneumoniae* infection is a key factor here, considering that as an opportunistic, Gram-negative bacteria species, *K. pneumoniae* releases LPS (endotoxin) to its environment, which leads to the activation of Toll-like receptors (TLRs), and thus transduction of proinflammatory transcription factors and the recruitment of inflammatory cells in the end (62). Moreover, there are lines of evidences that the LPS induction of TLR4 can activate the canonical Wnt/β-catenin signaling pathway (63), which further strengthens the significance of this pathway in ethanol-mediated mechanism of action. In regard to the work of Samuelson et al. once more, we had investigated the influence of alcohol on the integrity of intestinal barrier and observed in samples derived from the healthy volunteers after acute alcohol consumption early increased levels of circulating fatty acid binding protein (FABP-I), which acts as a biomarker for intestinal damage (64). This only further underlines the role and mechanisms of malfunctioning microbiota homeostasis in contributing to the pathogenesis of inflammation. Additionally, in this study, we observed the decreased levels of proinflammatory cytokines from trauma alcohol-fed mice, which stands in opposite to the data from severely affected and overgrown microbiota due to binge-on-chronic alcohol intake, where the proinflammatory cytokine levels were increased due to alcohol dysbiosis, further showing its effect on the enhanced inflammation (61). As indicated in **Figure 6**, the infiltration with other inflammatory cells such as CD4-positive T cells with the trauma-induced interferon-gamma also increases, and its decrease upon acute EI after trauma underlines the importance of other immune cells and pathways in the alcohol-modulated inflammation. In summary, there are definitely other mechanisms of ethanol action, where it displays its nature from both pro-inflammatory and anti-inflammatory capabilities, especially interplaying with traumatic injury and alcohol consumption. In this study, our focus was to investigate the DAMP-induced activation of immune response; however we are absolutely aware of the PAMP and gut–liver axis importance in the pathomechanism of damage, and we consider GI tract integrity as an important inflammatory benefactor during traumatic injury.

In our work, we observed that animals with acute EI before THFx exerted less lung injury. In contrast to the acute EI we studied, chronic EI is known to have adverse effects on the lung barrier. When alcohol consumption shifts from moderate or binge drinking to chronic alcohol consumption, increased permeability of the cellular lung barrier has been observed in numerous studies. Fan et al. found a significantly increased permeability of the alveolar epithelial barrier caused by increased disruption of tight junctions upon chronic EI (65). A mechanistic study by Otis et al. on the development of ARDS in prior chronic EI showed increased permeability of the alveolar epithelia with enhanced incidence of pulmonary edema in mice (66). In contrast to the effects of acute EI as observed also in the present study, Smith et al. identified chronic EI as a risk factor for the development of ARDS in sepsis (67). The observed effects of chronic alcohol consumption on the lung barrier not only have been demonstrated *in vivo* but also have been part of human studies. Burnham et al. examined pulmonary permeability in subjects with chronic EI showing that even in the absence of symptoms, individuals with a history of chronic EI had increased baseline lung permeability compared with controls, which could prime for a severe course of ARDS in the setting of sepsis (68). The negative effects of chronic EI in the context of ARDS have also been described by Berkowitz et al., demonstrating that patients with chronic EI also had a threefold increased risk of developing pulmonary edema (69). In general, it remains important to understand the mechanistically different effects of acute versus

chronic EI, yet in regard to the public health context, alcohol consumption is one of the leading causes of accidents and, according to several clinical studies, the percentage of alcoholized polytrauma patients is over 25% (70). Alcohol consumption leads to increased financial, time, and personnel burden, requiring additional routine and specific laboratory controls, with clinical imaging mostly of the head due to the reduced vigilance, difficult anamnesis, and compliance of the patients admitted to hospitals (71).

The present study has its limitations. Most notably, we only used young male mice in our experiments. Thus, the conclusions can only be drawn for a younger patient cohort. Further research will be required to determine if the differences in age or gender correlate to the observed results. Additionally, some of the variability in the dataset may be caused by the sample size of mice. While the clinical scenario implies first fracture and then its stabilization, in this experimental model, an external fixator is provided first, and then the osteotomy. Femur fracture is frequently accompanied by hemorrhage, which underlines the importance of this model; however, the impact of isolated fracture on remote organ injury cannot be assessed by this model. To ensure comparability, we performed a controlled HS, which would not occur in a real trauma situation of uncontrolled bleeding. During the experiment, the animals were not ventilated using intubation, which might also influence the dataset. Interindividual differences regarding the absorption rate of EtOH may have an impact on the BAC; thus, intravenous administration of EtOH might improve the inter-group comparisons, as it was done in other studies (39). However, the intravenous EtOH application does not mimic real-life conditions, and reproducing the findings in the future using an alcohol feeding model, which may prove to have different exposure parameters due to the definition of "acute", should be considered in translational models of EI. No conclusions can be drawn regarding the influence of subacute or chronic EI from this dataset. Also, in our work, we assessed the CXCL1 gene expression and protein expression in lung and BALF, and based on known data, and because of this, a subsequent increase in neutrophil invasion into lung tissue after THFx is observed. Together with known data, our results clearly indicate a CXCL1-mediated recruitment of neutrophils to lungs after trauma; however, in future studies, neutrophil counts in the BALF should be analyzed. Finally, the results of all the analyses are at a single time point in the complex process of THFx. Having multiple post-trauma time points would have allowed for a temporal analysis of EI-induced effects and mechanisms.

In summary, the current work adds novel information about the effects of canonical Wnt/β-catenin signaling pathway in trauma-induced uncontrolled local inflammatory response and lung injury. An acute EI alleviates the uncontrolled inflammatory response and lung barrier breakdown after trauma by suppressing the Wnt/β-catenin signaling pathway. Future studies should explore the association between acute EI and other upstream and downstream factors involved in Wnt/β-catenin signal transduction after trauma to provide interventional targets.

DATA AVAILABILITY STATEMENT

The data can be obtained upon a reasonable request from the corresponding author.

ETHICS STATEMENT

This study was authorized by the local institutional animal care and research advisory committee and permitted by the local government of Lower Saxony, Germany (approval number: 33.12-42502-04-17/2491).

AUTHOR CONTRIBUTIONS

Conceptualization: CN and BR. Methodology: LN, BX, KB, YZ, and KK. Validation: AJN, LN, and BR. Formal analysis: LN and BR. Investigation: LN, BX, KB, SG, and AJN. Resources: CN and BR. Data curation: LN, BX, YZ, and BR. Writing—original draft preparation: LN, AJN, and BR. Writing—review and editing: KB, YZ, PJ, and CN. Visualization: BR. Supervision: CN, AJN, and BR. Funding acquisition: CN and BR. All authors contributed to the article and approved the submitted version.

FUNDING

This research was funded by the German Research Foundation DFG with grant numbers DFG RE 3304/9-1, NE 1932/1-3, and 361210922/RTG 2408.

REFERENCES

1. Sakran JV, Greer SE, Werlin E, McCunn M. Care of the Injured Worldwide: Trauma Still the Neglected Disease of Modern Society. *Scand J Trauma Resusc Emerg Med* (2012) 20:64. doi: 10.1186/1757-7241-20-64
2. Lichte P, Kobbe P, Pfeifer R, Campbell GC, Beckmann R, Tohidnezhad M. Impaired Fracture Healing After Hemorrhagic Shock. *Mediators Inflamm* (2015) 2015:132451. doi: 10.1155/2015/132451
3. Relja B, Höhn C, Bormann F, Seyboth K, Henrich D, Marzi I. Acute Alcohol Intoxication Reduces Mortality, Inflammatory Responses and Hepatic Injury After Haemorrhage and Resuscitation *In Vivo*: Acute Alcohol After Haemorrhagic Shock. *Br J Pharmacol* (2012) 165(4b):1188–99. doi: 10.1111/j.1476-5381.2011.01595.x
4. Lefaivre KA, Starr AJ, Stahel PF, Elliot AC, Smith WR. Prediction of Pulmonary Morbidity and Mortality in Patients With Femur Fracture. *J Trauma* (2010) 69(6):1527–36. doi: 10.1097/TA.0b013e3181f8fa3b
5. Chen L, Zhao H, Alam A, Mi E, Eguchi S, Yao S. Postoperative Remote Lung Injury and Its Impact on Surgical Outcome. *BMC Anesthesiol* (2019) 19(1):30. doi: 10.1186/s12871-019-0698-6
6. Relja B, Yang B, Bundkirchen K, Xu B, Köhler K, Neunaber C. Different Experimental Multiple Trauma Models Induce Comparable Inflammation and Organ Injury. *Sci Rep* (2020) 10(1):20185. doi: 10.1038/s41598-020-76499-z

7. Secreto FJ, Hoeppner LH, Westendorf JJ. Wnt Signaling During Fracture Repair. *Curr Osteoporos Rep* (2009) 7(2):64–9. doi: 10.1007/s11914-009-0012-5
8. Moon RT, Bowerman B, Boutros M, Perrimon N. The Promise and Perils of Wnt Signaling Through Beta-Catenin. *Science* (2002) 296(5573):1644–6. doi: 10.1126/science.1071549
9. Brembeck FH, Rosário M, Birchmeier W. Balancing Cell Adhesion and Wnt Signaling, the Key Role of β-Catenin. *Curr Opin Genet Dev* (2006) 16(1):51–9. doi: 10.1016/j.gde.2005.12.007
10. Valenta T, Hausmann G, Basler K. The Many Faces and Functions of β-Catenin: β-Catenin: A Life by, Beyond, and Against the Wnt Canon. *EMBO J* (2012) 31(12):2714–36. doi: 10.1038/emboj.2012.150
11. Soni D, Wang D-M, Regmi SC, Mittal M, Vogel SM, Schlüter D. Deubiquitinase Function of A20 Maintains and Repairs Endothelial Barrier After Lung Vascular Injury. *Cell Death Discov* (2018) 4(1):60. doi: 10.1038/s41420-018-0056-3
12. Nakamura BN, Glazier A, Kattah MG, Duong B, Jia Y, Campo D. A20 Regulates Canonical Wnt-Signaling Through an Interaction With RIPK4. *PloS One* (2018) 13(5):e0195893. doi: 10.1371/journal.pone.0195893
13. Kim J, Han W, Park T, Kim EJ, Bang I, Lee HS. Sclerostin Inhibits Wnt Signaling Through Tandem Interaction With Two LRP6 Ectodomains. *Nat Commun* (2020) 11(1):5357. doi: 10.1038/s41467-020-19155-4
14. Rivara FP, Jurkovich GJ, Gurney JG, Seguin D, Fligner CL, Ries R. The Magnitude of Acute and Chronic Alcohol Abuse in Trauma Patients. *Arch Surg Chic Ill 1960* (1993) 128(8):907–12; discussion 912-913. doi: 10.1001archsurg.1993.01420200081015
15. Howard BM, Kornblith LZ, Redick BJ, Conroy AS, Nelson MF, Calfee CS. Exposing the Bidirectional Effects of Alcohol on Coagulation in Trauma: Impaired Clot Formation and Decreased Fibrinolysis in Rotational Thromboelastometry. *J Trauma Acute Care Surg* (2018) 84(1):97–103. doi: 10.1097/TA.0000000000001716
16. Nelson S, Kolls JK. Alcohol, Host Defence and Society. *Nat Rev Immunol* (2002) 2(3):205–9. doi: 10.1038/nri744
17. Kapania EM, Reif TJ, Tsumura A, Eby JM, Callaci JJ. Alcohol-Induced Wnt Signaling Inhibition During Bone Fracture Healing Is Normalized by Intermittent Parathyroid Hormone Treatment. *Anim Models Exp Med* (2020) 3(2):200–7. doi: 10.1002/ame2.12116
18. Xu B, Chandrasekar A, olde Heuvel F, Powerski M, Nowak A, Noack L. Ethanol Intoxication Alleviates the Inflammatory Response of Remote Organs to Experimental Traumatic Brain Injury. *Int J Mol Sci* (2020) 21(21):8181. doi: 10.3390/ijms21218181
19. Wagner N, Dieteren S, Franz N, Khler K, Perl M, Marzi I. Alcohol–Induced Attenuation of Post–Traumatic Inflammation Is Not Necessarily Liver –Protective Following Trauma/Hemorrhage. *Int J Mol Med* (2019) 27:1127–38. doi: 10.3892/ijmm.2019.4259
20. Bundkirchen K, Macke C, Reifenrath J, Schäck LM, Noack S, Relja B. Severe Hemorrhagic Shock Leads to a Delayed Fracture Healing and Decreased Bone Callus Strength in a Mouse Model. *Clin Orthop* (2017) 475(11):2783–94. doi: 10.1007/s11999-017-5473-8
21. Bundkirchen K, Macke C, Angrisani N, Schäck LM, Noack S, Fehr M. Hemorrhagic Shock Alters Fracture Callus Composition and Activates the IL6 and RANKL/OPG Pathway in Mice. *J Trauma Acute Care Surg* (2018) 85(2):359–66. doi: 10.1097/TA.0000000000001952
22. Matute-Bello G, Downey G, Moore BB, Groshong SD, Matthay MA, Slutsky AS. An Official American Thoracic Society Workshop Report: Features and Measurements of Experimental Acute Lung Injury in Animals. *Am J Respir Cell Mol Biol* (2011) 44(5):725–38. doi: 10.1165/rcmb.2009-0210ST
23. Ehre C, Worthington EN, Liesman RM, Grubb BR, Barbier D, O'Neal WK. Overexpressing Mouse Model Demonstrates the Protective Role of Muc5ac in the Lungs. *Proc Natl Acad Sci USA* (2012) 109(41):16528–33. doi: 10.1073/pnas.1206552109
24. Sawant KV, Poluri KM, Dutta AK, Sepuru KM, Troshkina A, Garofalo RP. Chemokine CXCL1 Mediated Neutrophil Recruitment: Role of Glycosaminoglycan Interactions. *Sci Rep* (2016) 6(1):33123. doi: 10.1038/srep33123
25. Levy RS, Hebert CK, Munn BG, Barrack RL. Drug and Alcohol Use in Orthopedic Trauma Patients: A Prospective Study. *J Orthop Trauma* (1996) 10(1):21–7. doi: 10.1097/00005131-199601000-00004
26. Savola O, Niemelä O, Hillbom M. Alcohol Intake and the Pattern of Trauma in Young Adults and Working Aged People Admitted After Trauma. *Alcohol Alcohol Oxf Oxfs* (2005) 40(4):269–73. doi: 10.1093/alcalc/agh159
27. Brembeck FH, Rosário M, Birchmeier W. Balancing Cell Adhesion and Wnt Signaling, the Key Role of Beta-Catenin. *Curr Opin Genet Dev* (2006) 16(1):51–9. doi: 10.1016/j.gde.2005.12.007
28. Valenta T, Hausmann G, Basler K. The Many Faces and Functions of β-Catenin. *EMBO J* (2012) 31(12):2714–36. doi: 10.1038/emboj.2012.150
29. Zhang H, Sun T, Liu Z, Zhang J, Wang X, Liu J. Systemic Inflammatory Responses and Lung Injury Following Hip Fracture Surgery Increases Susceptibility to Infection in Aged Rats. *Mediators Inflamm* (2013) 2013:1–9. doi: 10.1155/2013/536435
30. Relja B, Land WG. Damage-Associated Molecular Patterns in Trauma. *Eur J Trauma Emerg Surg Off Publ Eur Trauma Soc* (2020) 46(4):751–75. doi: 10.1007/s00068-019-01235-w
31. Xu P, Wen Z, Shi X, Li Y, Fan L, Xiang M. Hemorrhagic Shock Augments Nlrp3 Inflammasome Activation in the Lung Through Impaired Pyrin Induction. *J Immunol* (2013) 190(10):5247–55. doi: 10.4049/jimmunol.1203182
32. Papayannopoulos V. Neutrophils Stepping Through (to the Other Side). *Immunity* (2018) 49(6):992–4. doi: 10.1016/j.immuni.2018.12.006
33. Störmann P, Auner B, Schimunek L, Serve R, Horst K, Simon T-P. Leukotriene B4 Indicates Lung Injury and on-Going Inflammatory Changes After Severe Trauma in a Porcine Long-Term Model. *Prostaglandins Leukot Essent Fatty Acids* (2017) 127:25–31. doi: 10.1016/j.plefa.2017.09.014
34. Chertov O, Yang D, Howard OM, Oppenheim JJ. Leukocyte Granule Proteins Mobilize Innate Host Defenses and Adaptive Immune Responses. *Immunol Rev* (2000) 177:68–78. doi: 10.1034/j.1600-065X.2000.17702.x
35. Czaja AJ. Hepatic Inflammation and Progressive Liver Fibrosis in Chronic Liver Disease. *World J Gastroenterol* (2014) 20(10):2515–32. doi: 10.3748/wjg.v20.i10.2515
36. Liu Z, Wang Y, Wang Y, Ning Q, Zhang Y, Gong C. Dexmedetomidine Attenuates Inflammatory Reaction in the Lung Tissues of Septic Mice by Activating Cholinergic Anti-Inflammatory Pathway. *Int Immunopharmacol* (2016) 35:210–6. doi: 10.1016/j.intimp.2016.04.003
37. Sawant DA, Tharakan B, Hunter FA, Childs EW. Glycogen Synthase Kinase 3 Inhibitor Protects Against Microvascular Hyperpermeability Following Hemorrhagic Shock. *J Trauma Acute Care Surg* (2015) 79(4):609–16. doi: 10.1097/TA.0000000000000807
38. Chen Y, Whetstone HC, Lin AC, Nadesan P, Wei Q, Poon R. Beta-Catenin Signaling Plays a Disparate Role in Different Phases of Fracture Repair: Implications for Therapy to Improve Bone Healing. *PloS Med* (2007) 4(7):e249. doi: 10.1371/journal.pmed.0040249
39. Hu T-M, Lee R-P, Lee C-J, Subeq Y-M, Lin N-T, Hsu B-G. Heavy Ethanol Intoxication Increases Proinflammatory Cytokines and Aggravates Hemorrhagic Shock-Induced Organ Damage in Rats. *Mediators Inflamm* (2013) 2013:1–9. doi: 10.1155/2013/121786
40. Sears BW, Volkmer D, Yong S, Himes RD, Lauing K, Morgan M. Binge Alcohol Exposure Modulates Rodent Expression of Biomarkers of the Immunoinflammatory Response to Orthopaedic Trauma. *J Bone Jt Surg* (2011) 93(8):739–49. doi: 10.2106/JBJS.J.00318
41. Marasliogl M, Oppermann E, Blattner C, Weber R, Henrich D, Jobin C. Chronic Ethanol Feeding Modulates Inflammatory Mediators, Activation of Nuclear Factor-κb, and Responsiveness to Endotoxin in Murine Kupffer Cells and Circulating Leukocytes. *Mediators Inflamm* (2014) 2014:808695. doi: 10.1155/2014/808695
42. Rodriguez DA, Moncada C, Núñez MT, Lavandero S, Ponnappa BC, Israel Y. Ethanol Increases Tumor Necrosis Factor-Alpha Receptor-1 (TNF-R1) Levels in Hepatic, Intestinal, and Cardiac Cells. *Alcohol Fayettev N* (2004) 33(1):9–15. doi: 10.1016/S0741-8329(04)00056-4
43. Ma Y, Zhao S, Shen S, Fang S, Ye Z, Shi Z. A Novel Recombinant Slow-Release TNF α-Derived Peptide Effectively Inhibits Tumor Growth and Angiogensis. *Sci Rep* (2015) 5:13595. doi: 10.1038/srep13595
44. D'Souza El-Guindy NB, de Villiers WJ, Doherty DE. Acute Alcohol Intake Impairs Lung Inflammation by Changing Pro- and Anti-Inflammatory Mediator Balance. *Alcohol Fayettev N* (2007) 41(5):335–45. doi: 10.1016/j.alcohol.2007.07.002
45. Mörs K, Hörauf J-A, Kany S, Wagner N, Sturm R, Woschek M. Ethanol Decreases Inflammatory Response in Human Lung Epithelial Cells by

Inhibiting the Canonical NF-kB-Pathway. *Cell Physiol Biochem Int J Exp Cell Physiol Biochem Pharmacol* (2017) 43(1):17–30. doi: 10.1159/000480313
46. Hiraoka Y, Yoshida K, Ohno M, Matsuoka T, Kita T, Nishi E. Ectodomain Shedding of TNF-Alpha Is Enhanced by Nardilysin *via* Activation of ADAM Proteases. *Biochem Biophys Res Commun* (2008) 370(1):154–8. doi: 10.1016/j.bbrc.2008.03.050
47. DeBerge MP, Ely KH, Cheng G-S, Enelow RI. ADAM17-Mediated Processing of TNF-α Expressed by Antiviral Effector CD8+ T Cells Is Required for Severe T-Cell-Mediated Lung Injury. *PloS One* (2013) 8(11):e79340. doi: 10.1371/journal.pone.0079340
48. Taïeb J, Delarche C, Ethuin F, Selloum S, Poynard T, Gougerot-Pocidalo M-A. Ethanol-Induced Inhibition of Cytokine Release and Protein Degranulation in Human Neutrophils. *J Leukoc Biol* (2002) 72(6):1142–7.
49. von Maltzan K, Tan W, Pruett SB. Investigation of the Role of TNF-α Converting Enzyme (TACE) in the Inhibition of Cell Surface and Soluble TNF-α Production by Acute Ethanol Exposure. *PloS One* (2012) 7(2):e29890. doi: 10.1371/journal.pone.0029890
50. Doggett TM, Breslin JW. Acute Alcohol Intoxication-Induced Microvascular Leakage. *Alcohol Clin Exp Res* (2014) 38(9):2414–26. doi: 10.1111/acer.12525
51. Liu B, Jiang D, Ou Y, Hu Z, Jiang J, Lei X. An Anti-Inflammatory Role of A20 Zinc Finger Protein During Trauma Combined With Endotoxin Challenge. *J Surg Res* (2013) 185(2):717–25. doi: 10.1016/j.jss.2013.06.031
52. Mercer KE, Hennings L, Sharma N, Lai K, Cleves MA, Wynne RA. Alcohol Consumption Promotes Diethylnitrosamine-Induced Hepatocarcinogenesis in Male Mice Through Activation of the Wnt/β-Catenin Signaling Pathway. *Cancer Prev Res Phila Pa* (2014) 7(7):675–85. doi: 10.1158/1940-6207.CAPR-13-0444-T
53. Warner DR, Warner JB, Hardesty JE, Song YL, Chen C-Y, Chen Z. Beneficial Effects of an Endogenous Enrichment in N3-PUFAs on Wnt Signaling are Associated With Attenuation of Alcohol-Mediated Liver Disease in Mice. *FASEB J Off Publ Fed Am Soc Exp Biol* (2021) 35(2):e21377. doi: 10.1096/fj.202001202R
54. Huang C-K, Yu T, de la Monte SM, Wands JR, Derdak Z, Kim M. Restoration of Wnt/β-Catenin Signaling Attenuates Alcoholic Liver Disease Progression in a Rat Model. *J Hepatol* (2015) 63(1):191–8. doi: 10.1016/j.jhep.2015.02.030
55. Xu CQ, de la Monte SM, Tong M, Huang C-K, Kim M. Chronic Ethanol-Induced Impairment of Wnt/β-Catenin Signaling is Attenuated by PPAR-δ Agonist. *Alcohol Clin Exp Res* (2015) 39(6):969–79. doi: 10.1111/acer.12727
56. Ron D, Messing RO. Signaling Pathways Mediating Alcohol Effects. *Curr Top Behav Neurosci* (2013) 13:87–126. doi: 10.1007/978-3-642-28720-6_161
57. Wand G, Levine M, Zweifel L, Schwindinger W, Abel T. The cAMP-Protein Kinase A Signal Transduction Pathway Modulates Ethanol Consumption and Sedative Effects of Ethanol. *J Neurosci Off J Soc Neurosci* (2001) 21(14):5297–303. doi: 10.1523/JNEUROSCI.21-14-05297.2001
58. Wilson DF, Matschinsky FM. Ethanol Metabolism: The Good, the Bad, and the Ugly. *Med Hypotheses* (2020) 140:109638. doi: 10.1016/j.mehy.2020.109638
59. Nowak AJ, Relja B. The Impact of Acute or Chronic Alcohol Intake on the NF-κb Signaling Pathway in Alcohol-Related Liver Disease. *Int J Mol Sci* (2020) 21(24):E9407. doi: 10.3390/ijms21249407
60. Mörs K, Sturm R, Hörauf J-A, Kany S, Cavalli P, Omari J. Anti-Inflammatory Effects of Alcohol Are Associated With JNK-STAT3 Downregulation in an *In Vitro* Inflammation Model in HepG2 Cells. *Dis Markers* (2021) 2021:6622701. doi: 10.1155/2021/6622701
61. Samuelson DR, Shellito JE, Maffei VJ, Tague ED, Campagna SR, Blanchard EE. Alcohol-Associated Intestinal Dysbiosis Impairs Pulmonary Host Defense Against Klebsiella Pneumoniae. *PloS Pathog* (2017) 13(6):e1006426. doi: 10.1371/journal.ppat.1006426
62. Lu Y-C, Yeh W-C, Ohashi PS. LPS/TLR4 Signal Transduction Pathway. *Cytokine* (2008) 42(2):145–51. doi: 10.1016/j.cyto.2008.01.006
63. Santaolalla R, Sussman DA, Ruiz JR, Davies JM, Pastorini C, España CL. TLR4 Activates the β-Catenin Pathway to Cause Intestinal Neoplasia. *PloS One* (2013) 8(5):e63298. doi: 10.1371/journal.pone.0063298
64. Sturm R, Haag F, Janicova A, Xu B, Vollrath JT, Bundkirchen K. Acute Alcohol Consumption Increases Systemic Endotoxin Bioactivity for Days in Healthy Volunteers-With Reduced Intestinal Barrier Loss in Female. *Eur J Trauma Emerg Surg Off Publ Eur Trauma Soc* (2021) 11. doi: 10.1007/s00068-021-01666-4
65. Fan X, Joshi PC, Koval M, Guidot DM. Chronic Alcohol Ingestion Exacerbates Lung Epithelial Barrier Dysfunction in HIV-1 Transgenic Rats. *Alcohol Clin Exp Res* (2011) 35(10):1866–75. doi: 10.1111/j.1530-0277.2011.01531.x
66. Otis JS, Mitchell PO, Kershaw CD, Joshi PC, Guidot DM. Na,K-ATPase Expression Is Increased in the Lungs of Alcohol-Fed Rats. *Alcohol Clin Exp Res* (2008) 32(4):699–705. doi: 10.1111/j.1530-0277.2008.00626.x
67. Smith P, Jeffers LA, Koval M. Effects of Different Routes of Endotoxin Injury on Barrier Function in Alcoholic Lung Syndrome. *Alcohol Fayettev N* (2019) 80:81–9. doi: 10.1016/j.alcohol.2018.08.007
68. Burnham EL, Halkar R, Burks M, Moss M. The Effects of Alcohol Abuse on Pulmonary Alveolar-Capillary Barrier Function in Humans. *Alcohol Alcohol Oxf Oxfs* (2009) 44(1):8–12. doi: 10.1093/alcalc/agn051
69. Berkowitz DM, Danai PA, Eaton S, Moss M, Martin GS. Alcohol Abuse Enhances Pulmonary Edema in Acute Respiratory Distress Syndrome. *Alcohol Clin Exp Res* (2009) 33(10):1690–6. doi: 10.1111/j.1530-0277.2009.01005.x
70. Relja B, Menke J, Wagner N, Auner B, Voth M, Nau C. Effects of Positive Blood Alcohol Concentration on Outcome and Systemic Interleukin-6 in Major Trauma Patients. *Injury* (2016) 47(3):640–5. doi: 10.1016/j.injury.2016.01.016
71. O'Keeffe T, Shafi S, Sperry JL, Gentilello LM. The Implications of Alcohol Intoxication and the Uniform Policy Provision Law on Trauma Centers; a National Trauma Data Bank Analysis of Minimally Injured Patients. *J Trauma* (2009) 66(2):495–8. doi: 10.1097/TA.0b013e31818234bf

Conflict of Interest: The authors declare that the research was conducted in the absence of any commercial or financial relationships that could be construed as a potential conflict of interest.

frontiers | Frontiers in Immunology

ORIGINAL RESEARCH
published: 20 May 2022
doi: 10.3389/fimmu.2022.866795

Malondialdehyde Acetaldehyde-Adduction Changes Surfactant Protein D Structure and Function

*Claire G. Nissen[1], Deanna D. Mosley[2], Kusum K. Kharbanda[2,3], Dawn M. Katafiasz[2], Kristina L. Bailey[2,3] and Todd A. Wyatt[1,2,3]**

[1] Department of Environmental, Agricultural and Occupational Health, College of Public Health, University of Nebraska Medical Center, Omaha, NE, United States, [2] Department of Internal Medicine, College of Medicine, University of Nebraska Medical Center, Omaha, NE, United States, [3] Research Service Veterans Affairs Nebraska-Western Iowa Health Care System, Omaha, NE, United States

OPEN ACCESS

Edited by:
Suhas Sureshchandra, University of California, Irvine, United States

Reviewed by:
Kenneth Reid, University of Oxford, United Kingdom
Jens Madsen, University College London, United Kingdom

***Correspondence:**
Todd A. Wyatt
twyatt@unmc.edu

Specialty section:
This article was submitted to Nutritional Immunology, a section of the journal Frontiers in Immunology

Received: 31 January 2022
Accepted: 13 April 2022
Published: 20 May 2022

Citation:
Nissen CG, Mosley DD, Kharbanda KK, Katafiasz DM, Bailey KL and Wyatt TA (2022) Malondialdehyde Acetaldehyde-Adduction Changes Surfactant Protein D Structure and Function. Front. Immunol. 13:866795. doi: 10.3389/fimmu.2022.866795

Alcohol consumption with concurrent cigarette smoking produces malondialdehyde acetaldehyde (MAA)-adducted lung proteins. Lung surfactant protein D (SPD) supports innate immunity *via* bacterial aggregation and lysis, as well as by enhancing macrophage-binding and phagocytosis. MAA-adducted SPD (SPD-MAA) has negative effects on lung cilia beating, macrophage function, and epithelial cell injury repair. Because changes in SPD multimer structure are known to impact SPD function, we hypothesized that MAA-adduction changes both SPD structure and function. Purified human SPD and SPD-MAA (1 mg/mL) were resolved by gel filtration using Sephadex G-200 and protein concentration of each fraction determined by Bradford assay. Fractions were immobilized onto nitrocellulose by slot blot and assayed by Western blot using antibodies to SPD and to MAA. Binding of SPD and SPD-MAA was determined fluorometrically using GFP-labeled *Streptococcus pneumoniae* (GFP-SP). Anti-bacterial aggregation of GFP-SP and macrophage bacterial phagocytosis were assayed by microscopy and permeability determined by bacterial phosphatase release. Viral injury was measured as LDH release in RSV-treated airway epithelial cells. Three sizes of SPD were resolved by gel chromatography as monomeric, trimeric, and multimeric forms. SPD multimer was the most prevalent, while the majority of SPD-MAA eluted as trimer and monomer. SPD dose-dependently bound to GFP-SP, but SPD-MAA binding to bacteria was significantly reduced. SPD enhanced, but MAA adduction of SPD prevented, both aggregation and macrophage phagocytosis of GFP-SP. Likewise, SPD increased bacterial permeability while SPD-MAA did not. In the presence of RSV, BEAS-2B cell viability was enhanced by SPD, but not protected by SPD-MAA. Our results demonstrate that MAA adduction changes the quaternary structure of SPD from multimer to trimer and monomer leading to a decrease in the native anti-microbial function of SPD. These findings suggest one mechanism for increased pneumonia observed in alcohol use disorders.

Keywords: alcohol, lung, pneumonia, surfactant, aldehydes, adduction

INTRODUCTION

Alcohol misuse causes injury to the respiratory system as well as impeding lung repair and normal immune function (1). Alcohol use desensitizes ciliated upper airway epithelium resulting in diminished clearance of inhaled pathogens (2). In the lower airways, alcohol abuse causes failure to phagocytose and clear pathogens, induction of inflammatory cytokine release, upregulation and recruitment of inflammatory T cells, and up-regulation of pro-inflammatory transcription factors and pathways (1). Chronic alcohol use is associated with elevated cytokine levels resulting from increased oxidative injury in the lungs (3). Such oxidative inflammatory injury also results in the generation of reactive aldehydes such as malondialdehyde (MDA) (4). Acetaldehyde is another reactive aldehyde found in the lungs, not only in response to alcohol metabolism, but also because of smoking, where more than 0.5 mg/cigarette is inhaled (5). Cigarette and alcohol polysubstance use can adversely impact the respiratory system by depleting lung antioxidant levels, leading to chronic inflammation and increased susceptibility to bacterial infections (6, 7).

To minimize infection injury, the lungs have several innate defense mechanisms including the anti-microbial collectin, surfactant protein D (SPD). Secreted by alveolar type II cells and Club cells, SPD is a Ca^{+2} dependent lectin, preferring to bind to simple carbohydrates like glucose, mannose, and inositol (8, 9). SPD aggregates bacteria to enhance mucociliary transport in the upper airway and mediates macrophage phagocytosis of pathogens in the lower airways (8). In an environment not exposed to cigarette smoke or alcohol consumption, SPD is known to exist in several structures with varying functions. While monomers of SPD appear to have little function, large multimeric forms of SPD (such as dodecamers and even higher order structures) are strongly antimicrobial (10). Conversely, the trimeric form of SPD shows little antimicrobial characteristics and can even be pro-inflammatory (9).

We previously observed that the lungs of individuals who smoked cigarettes and were heavy alcohol drinkers formed MAA-adducted protein in response to the elevated amounts of lung acetaldehyde and malondialdehyde (11). Furthermore, we identified SPD to be one of these MAA-adducted proteins in mice (12). *In vitro* experiments demonstrated an adverse effect of SPD-MAA on lung epithelial cells and macrophages (7, 13). Therefore, we hypothesized that MAA adduction changes the structure of SPD from multimer to trimer/monomer and, in doing so, reduces the anti-microbial characteristics of SPD. Such a decrease in this important innate defensin through the covalent modification by reactive aldehydes would represent one of the injury mechanisms caused by alcohol and cigarette smoke to help explain the pathogenesis of increased pneumonia observed in alcohol misuse.

METHODS

Purification and MAA-Adduction of Surfactant Protein D (SPD)

SPD was purified and adducted as previously described (7). Lung SPD was purified from human pulmonary alveolar proteinosis fluid (14). SPD was MAA-adducted by incubating 1-2 mg of SPD with a 2:1 ratio solution of malondialdehyde and acetaldehyde (SigmaAldrich, St. Louis, MO) for 3 d at 37°C in sealed polypropylene tubes as reported (15). Approximately 1–1.5 mg/mL of SPD was incubated with 1.0 mM acetaldehyde and 2.0 mM MDA in pyrogen-free 20 mM Tris buffer pH 7.4 containing 10 mM EDTA, 2 mM diethylenetriaminepentaacetic acid, and 2 mM Phytic acid in a sealed polypropylene vessel. The reaction was performed under sterile and non-oxidizing conditions in the dark for 72 h. At the end of incubation, the reaction mixture was exhaustively dialyzed under aseptic conditions against pyrogen-free phosphate buffered saline solution for 24 h at 4°C. As a handling control, mock-treated SPD was treated in the same manner in the absence of aldehydes.

The fluorescent 2:1 adduct formed during MAA adduct generation was quantified using a luminescence spectrophotometer excitation at 398 nm and emission maximum at 460 nm (Perkin Elmer, Norwalk, CT) and expressed as nanomole of fluorescent MAA equivalents per milligram protein.

Gel Filtration Chromatography

Purified SPD and SPD-MAA were filtered using size-exclusion chromatography. An FPLC column (1.5 x 12 cm) (SigmaAldrich) was packed with 20 mL of Sephadex G-200 (Pharmacia Fine Chemicals, New York, NY) and equilibrated with 0.05 M $HNaPO_4$ and 0.15 M NaCl (pH 7, 0.45 μm filtered). Purified SPD and SPD-MAA (1.5 mg/mL) were loaded onto separate columns and eluted into 12 x 1 mL fractions under isocratic conditions. Protein concentration of each fraction of SPD and SPD-MAA was quantified using a Bradford assay (16). Aliquots (10 μL) of each fraction and bovine serum albumin (BSA) standards (0, 0.125, 0.25, 0.5, 1, and 2 mg/mL) were diluted in 500 μL of Coomassie Blue (Bio-Rad, Hercules, CA) and absorption measured at 595 nm by visible spectrophotometry (Bio-Tek, Winsooki, VT).

Western Blot

Eluted fractions were immobilized by slot blot (Bio-Rad Bio-Dot SF, Hercules, CA). Bio-Dot SF filter paper (Bio-Rad) and 1 sheet of 0.2 μm nitrocellulose membrane (Bio-Rad) were soaked in Western blocking buffer (0.05 M Tris, 0.15 M NaCl, pH 7.5) for 10 min. Samples were diluted 1:1000 in Western blocking buffer and 200 μL loaded into each slot. Nitrocellulose membranes were incubated in Western blocking buffer with 3% BSA (MilliporeSigma, Allentown, PA) overnight at 4°C. After a brief rinse in Western blocking buffer, primary antibody solution was added to the blot and rocked for 1 h at room temperature. Primary antibodies of goat-anti SPD (R&D Systems, Minneapolis, MN) and rabbit anti-MAA (17) were diluted 1:10,000 in Western blot buffer with 3% BSA. Blots were rinsed with blocking buffer for 20 min at room temperature with rocking, rinsed again with blocking buffer containing 0.02% NP-40 (SigmaAldrich) for 20 min with rocking, and lastly repeat washing with blocking buffer. Secondary antibodies for SPD (HRP-conjugated rabbit-anti Goat; Invitrogen, Carlsbad, CA) and SPD-MAA (HRP-goat anti-rabbit; Rockland, Limerick, PA) were diluted 1:15,000 in Western blocking buffer with 3% BSA and incubated for 1 h at

room temperature. After repeat rinsing as described for primary antibodies, blots were incubated with ECL Western Blotting Substrate and Developer (ThermoFisher). Blots were exposed to X-ray film (PDC Healthcare, Valencia, CA) for 30 sec within 10 min after adding the developer to the nitrocellulose.

Bacterial Preparation

Streptococcus pneumoniae expressing green fluorescent protein (GFP-SP) was a generous gift from the lab of Jan-Willem Veening in the Netherlands. *S. pneumoniae* were grown in Remel Mueller Hinton Broth with cations (calcium and magnesium), and laked horse blood (LHB) (ThermoFisher; Waltham, MA) until they reached log phase growth. The strep suspension was centrifuged at 1000 × *g* for 10 min and resuspended in 10% neutral buffered formalin for 10 min. The bacteria were subsequently washed three times in phosphate-buffered saline (PBS) and resuspended in PBS for further use.

GFP-SP-SPD Binding Assay

SPD and SPD-MAA were biotinylated using a previously described method (18). Biotinylation of proteins was carried out by incubating with Immunopure NHS-LC-Biotin (Pierce, Rockford, IL) at a ratio of 2:1 of biotin to collectin by weight for 2 h at room temperature in the dark. Unbound biotin was removed by overnight dialysis. SPD and SPD-MAA binding to bacteria was tested by ELISA where *S. pneumoniae* (1 μg/ml) was dried onto 96-well plates (Falcon, Glendale, AZ) and fixed with methanol (MilliporeSigma) as described (19). Non-specific binding was blocked using BSA (MilliporeSigma) and gelatin (Bio-Rad) before incubation with biotinylated SPD. MAA-adducted BSA (BSA-MAA) was used as a control against any non-specific MAA adduct artifact. Bound biotinylated protein was detected with streptavidin conjugated to horseradish peroxidase followed by TMB substrate (Bio-Rad). Reactions were halted with 1 N H_2SO_4 and optical density measured with an ELISA plate reader using visible photospectroscopy (Bio-Tek).

Cell Culture

BEAS-2B bronchial epithelial cells and Raw 264.7 macrophages were purchased from American Type Cell Culture (ATCC, Rockville, MD) and cultured in Dulbecco's modified Eagle's medium (DMEM) (Gibco, Grand Island, NY) supplemented with 10% fetal bovine serum (FBS, Atlantis Biosciences, Singapore) and 1% penicillin/streptomycin (Gibco) and maintained at 37°C in a humidified CO_2 incubator (Panasonic, Wood Dale, IL).

Aggregation Assay

The aggregation assay was performed as previously described (18, 20) in the presence or absence of 5 mM calcium. PBS was used to acquire a final volume of 50 μL. A Zeiss Axio inverted fluorescence microscope (Zeiss, Oberkochen, Germany) was used to visualize aggregation. An average of 10 fields of view were examined per slide. Suspensions (50 μl) of GFP-SP were incubated with SPD (10 μg/ml) for 90 min at 37°C in the presence or absence of 5 mM $CaCl_2$. Samples were placed on slides and examined by phase-contrast and fluorescence microscopy (magnification, 50X). Ten fields of view were counted per slide, and the average area and number of clumps of aggregated bacteria per field of view was determined.

Phagocytosis Assay

Phagocytosis of GFP-SP was performed as previously described (21). RAW 264.7 cells were incubated overnight in media onto coverslips in a 12-well plate. RAW cells were then incubated for 30 min in a final 500 μL suspension of SPD or MAA-SPD in PBS with or without 5 mM calcium. Cells were then incubated with 100 μL of bacterial suspension for 60 min, quenched with 1 mL Trypan Blue (Gibco)/well for 3 min, washed 2X with PBS, fixed with 0.5% formalin (ThermoFisher) for 10 min, and then washed again. Coverslips were mounted onto slides and fluorescence was visualized by fluorescence microscopy.

Permeability Assay

The permeabilizing effects of SPD and SPD-MAA on *S. pneumoniae* were assayed as a function of bacterial phosphatase release using a commercial endogenous phosphatase detector kit (Thermo Fisher).

Anti-Viral Protection Assay

BEAS-2B (2 x 10^5 cells/mL) were cultured in 24-well tissue culture plates for 2 d, until approximately 85% confluent. Respiratory syncytial virus (RSV-2A; Advanced Biotechnologies; Eldersburg, MD) was diluted to 0.1 MOI in DMEM without serum or antibiotics in the presence of 0, 10, and 100 μg/mL SPD or SPD-MAA in a total volume of 0.5 mL and incubated for 1 h at 4°C. Cells were washed in PBS to remove serum and antibiotics and 200 μL per well of each RSV treatment condition was added to a well for 2 h at 37°C. After 2 h, an additional 200 μL of DMEM with penicillin/streptomycin was added (post-inoculation) and cells incubated for 48 h at 37°C. Cell supernates were then collected, dead cells pelleted at 200 g for 10 min, and media decanted. Pelleted cells and remaining cells attached in wells were assayed for total protein by Bradford. As previously reported for RSV-infected BEAS-2B (22), lactate dehydrogenase (LDH) activity was measured in the supernatant media using the LDH Activity Assay Kit (Sigma-Aldrich) according to the manufacturer's instructions. Cell homogenates were added to the LDH assay buffer and LDH substrate mix. Absorbances were measured at 595 nm by visible spectrophotometry (Bio-Tek). Each sample was standardized by total protein.

Statistical Analysis

All experiments were performed a minimum of 5 times (n=5). Each data point graphically presented represents the standard deviation of those experiments. Data were analyzed using Graph Pad Prism (v9.2.0 for Mac, GraphPad Software, San Diego CA). Data were analyzed for statistical significance using a non-parametric Kruskal-Wallis test. Significance was accepted at the 95% confidence interval.

RESULTS

MAA Adduction Changes the Structure of SPD

Purified SPD and SPD-MAA (1.5 mg/mL) were each resolved by size exclusion chromatography and measurable protein detected by Bradford assay in eluted fractions 3, 7, and 9 (**Figure 1**). Three fractions corresponding to multimer (>589 kDa), trimer (55 kDa), and monomer (18 kDa) were collected from SPD with multimeric protein eluting out of the column first in fraction 3. Only two SPD-MAA fractions containing protein were eluted as fraction 7 and 9, corresponding to trimer and monomer. Western blot using goat anti-SPD revealed the presence of SPD protein in all 3 fractions for purified SPD, but only fractions 7 and 9 for purified SPD-MAA. Western blot using rabbit anti-MAA detected MAA-adducted protein in fractions 7 and 9 for SPD-MAA. No reactivity for anti-MAA was observed in the fractions eluted from non-adducted, purified SPD. As expected, these data confirm that purified non-adducted SPD predominately exists as multimer, trimer, and monomer, but most of the SPD-MAA elutes as trimer and monomer with no detection of the multimeric form.

MAA Adduction Decreases SPD Binding to Bacteria

SPD exhibits loss of bacterial binding in trimeric form as compared to the native multimeric form [Arroyo 2020]. To determine whether SPD-MAA exhibits reduced bacterial binding compared to SPD, we conducted binding assays using *S. pneumoniae* and biotinylated surfactant proteins. SPD bound to bacteria in a dose-dependent manner with maximum binding between 10-20 μg/mL SPD (**Figure 2**). In contrast, SPD-MAA showed no significant binding to *S. pneumoniae* except at the highest concentration (20 μg/mL) tested. At this concentration, SPD bound significantly higher ($p<0.01$) than SPD-MAA. No bacterial binding was detected with BSA or BSA-MAA. These data reveal a functional difference in SPD bacterial binding when the protein is MAA-adducted.

MAA Adduction Decreases SPD Aggregation of Bacteria

As the term collectin suggests, SPD aggregates bacteria to enhance opsonization and phagocytosis. Using GFP-SP in the absence of any cells, we observed a diffuse punctate dispersal of bacteria by fluorescence microscopy (**Figure 3**). Upon the addition of 5 mM calcium, *S. pneumonia* can form small clumps in culture. In the presence of 10 μg/mL SPD, large aggregates of GFP-SP were readily evident. However, at the same concentration, SPD-MAA failed to aggregate bacteria and produced no additional clumping beyond that observed with calcium alone. These data identify a functional difference in bacterial aggregation between SPD and SPD-MAA that is consistent with the reported difference between SPD multimer vs. trimer forms.

MAA Adduction Decreases SPD Enhancement of Phagocytosis

Phagocytosis of *S. pneumoniae* is enhanced by the binding and aggregation of SPD to bacteria. We evaluated the impact of MAA adduction on the SPD-mediated *S. pneumoniae* phagocytosis by macrophages in an *in vitro* assay. RAW 264.7 macrophages were incubated with GFP-SP in the presence or absence of 10 μg/mL SPD or SPD-MAA. Cultures were then washed, and Trypan blue was used to quench non-internalized GFP-SP fluorescence allowing for visualization of only internalized GFP-SP by fluorescence microscopy. GFP-SP was phagocytosed by 25-50% of the

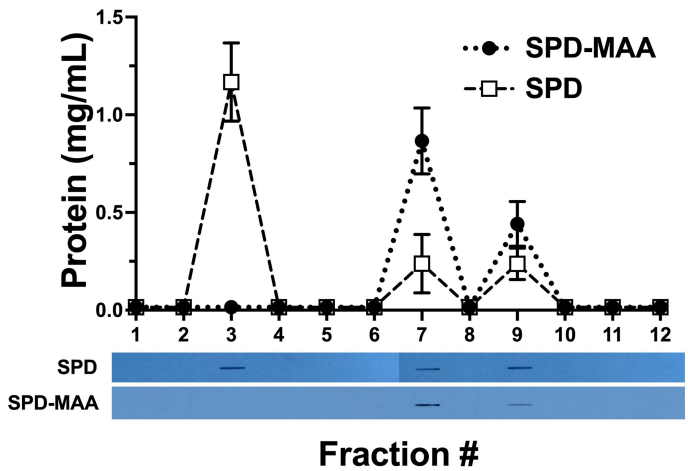

FIGURE 1 | Bradford protein assay with corresponding bands from the Western blot. Column fraction protein concentrations were quantified using a Bradford assay. Protein was detected in 3 fractions eluted by gel filtration. In SPD, most of the protein (multimer) was collected in Fraction 3. In SPD-MAA, almost no multimer eluted while trimer (Fraction 7) and monomer (Fraction 9) were collected. Western blots for each slot blotted fraction were probed for SPD and SPD-MAA. The SPD column fractions showed the presence of SPD in 3 fractions. SPD-MAA column fractions only contained SPD in Fractions 7 and 9. Blots probed with anti-MAA detected protein from SPD-MAA column fractions 7 and 9 (not shown).

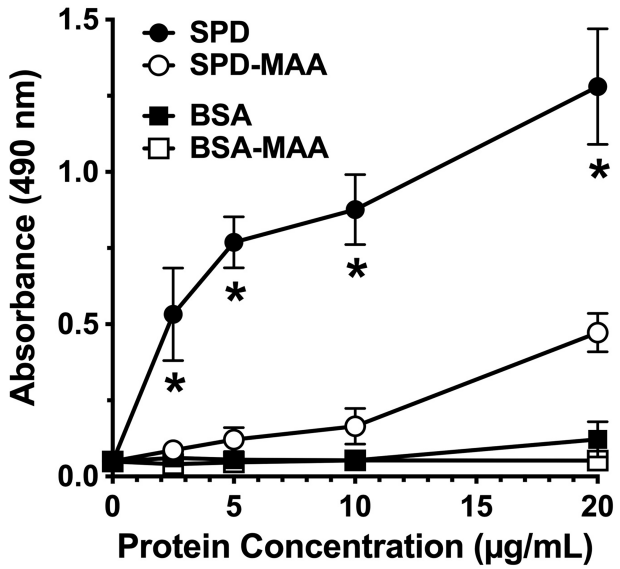

FIGURE 2 | Surfactant protein binding to *S. pneumoniae*. Plates were coated with bacteria and incubated with 0-20 µg/mL SPD, SPD-MAA, BSA (negative control), or BSA-MAA. Bound SPD was detected with antibodies by ELISA. Absorbance at 450 nm of bound SPD at the different concentrations was determined (n = 5), non-parametric Kruskal-Wallis test was performed, differences between SPD and SPD-MAA were significant at all concentrations (*p< 0.01). The data are the averages +/- SD of five experiments. The only significant difference between SPD-MAA and the BSA negative control was observed at 20 µg/mL. No binding was observed for BSA-MAA.

RAW 264.7 cells per each field of view (**Figure 4**). The addition of 10 µg/mL SPD enhanced the average number of cells phagocytosing GFP-SP. However, SPD-MAA had no significant enhancement effect on bacterial uptake by the macrophages. A significantly different level of phagocytosis was observed between SPD and SPD-MAA ($p<0.0004$). These data suggest that MAA adduction of SPD prevents surfactant protein enhancement of phagocytosis.

MAA Adduction Decreases SPD Enhancement of Bacterial Permeability

Surfactant can engage in direct anti-microbial action through increasing bacterial membrane permeability. To determine the effect of MAA adduction on SPD anti-bacterial killing, we assayed membrane permeability as a function of endogenous phosphatase release in cell-free *in vitro* suspensions of *S. pneumoniae* and surfactant. After 30 min of incubation with 10 µg/mL SPD, we detected a significant increase ($p<0.01$) in endogenous phosphate release vs. no SPD (**Figure 5**). However, the ability of SPD-MAA to permeabilize bacteria was significantly ($p<0.05$) decreased compared to that of SPD. These data support that MAA adduction reduces anti-bacterial killing.

MAA Adduction Decreases SPD Anti-Viral Protection

The anti-microbial innate defense by SPD extends to anti-viral protection. RSV is a pathogen that specifically infects the airway epithelium resulting in cell detachment and death. To determine if surfactant protein protection from RSV is impacted by MAA adduction, we infected bronchial epithelial BEAS-2B cells with RSV in the presence or absence of 10-100 µg/mL SPD or SPD-MAA and measured LDH as a marker for cell viability. RSV caused a decrease in cell viability, but the addition of 10 or 100 µg/mL SPD significantly ($p<0.0002$) decreased the amount of LDH detected (**Figure 6**). In contrast, SPD-MAA produced no protection from cell death, as increased LDH remained after treatment with 10 µg/mL ($p<0.01$) and 100 µg/mL ($p<0.006$) SPD.

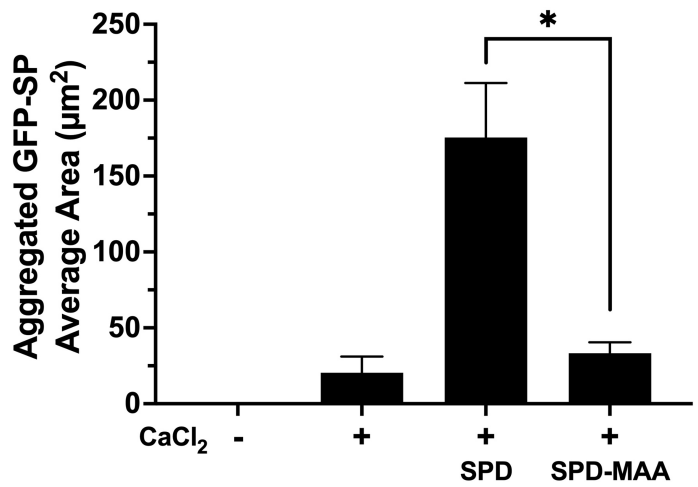

FIGURE 3 | Aggregation of *S. pneumoniae* in the presence of surfactant protein. GFP-SP were incubated with 10 µg/ml SPD or SPD-MAA for 90 min in the presence of calcium (5 mM) and visualized by fluorescence microscopy (X 500). The average area of aggregated clumps of bacteria was measured per field of view. The data are the averages +/- SD of five experiments. In the presence of calcium, SPD significantly increased aggregation compared to SPD-MAA, *p<0.0003. No clumping or aggregation of pneumococci was observed in the absence of calcium.

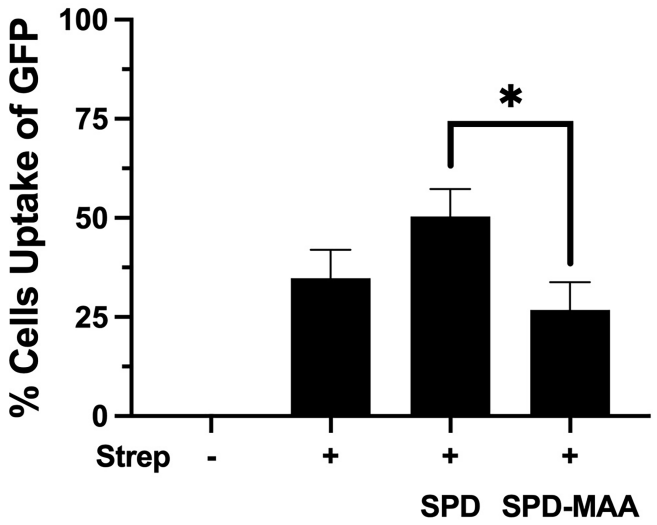

FIGURE 4 | MAA adduction of SPD decreases phagocytosis of *S. pneumoniae*. GFP-*S. pneumoniae* were incubated with the murine macrophage cell line RAW264.7. The percent of RAW264.7 cells containing internalized bacterial cells per field was determined using fluorescence microscopy (X 500) after quenching non-internalized GFP-SP with Trypan blue. The image results are a representative of 5 independent experiments summarized by graph. Bars represent averages +/- SD, *p<0.0004.

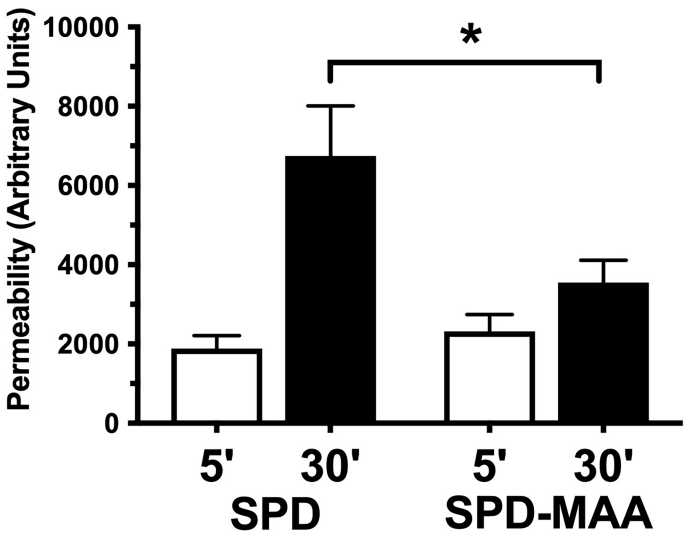

FIGURE 5 | SPD-induced anti-bacterial permeability is decreased by MAA adduction. *S. pneumoniae* was incubated in the presence of either 10 μg/mL SPD or SPD-MAA for up to 30 min and supernatant media phosphatase release measured as a function of bacterial permeability. A significant reduction in permeability (*p<0.05) was observed between SPD and SPD-MAA. Bars represent averages +/- SD, n=5 experiments.

DISCUSSION

Chronic alcohol use predisposes an individual to a plethora of maladies including chronic liver disease, chronic kidney disease, cancer, and respiratory disease (23). Alcohol is particularly important in pulmonology as alcohol misuse is associated with increased risk of acquiring pneumonia, developing antibiotic resistant pneumonia, and pneumonia severity compared to individuals who do not abuse alcohol (24). Alcohol abuse has been shown to leave an individual more at risk of contracting respiratory illness from *S. pneumonia, L. pneumophila*, and gram-negative enteric bacilli (24).

In 2019, an estimated 14.5 million Americans over the age of 12 were impacted by alcohol use disorder (AUD) (25). Already classified as one of the top 3 lifestyle-related causes of death in the United States (26), alcohol misuse is expected to rise due to

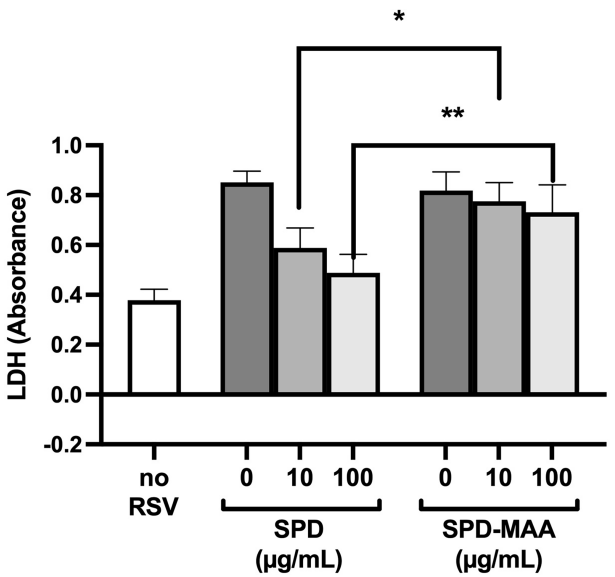

FIGURE 6 | MAA adduction of SPD decreases cell viability in response to respiratory syncytial virus (RSV). Infection of BEAS-2B with RSV increases LDH release compared to control media (no RSV). SPD (10-100 µg/mL) significantly ($p<0.0002$) decreases RSV-induced LDH release vs. the absence of SPD. No such decrease is observed with either 10 µg/mL (*$p<0.01$) or 100 µg/mL (**$p<0.006$) SPD-MAA vs. equal amounts of SPD. Bars represent averages +/- SD, n=5 experiments.

COVID-19 (27), thus underscoring the importance of understanding alcohol effects on tissue injury.

As with alcohol, cigarette smoking is the leading cause of preventable death and disease in America (28). Cigarette smoking is an established cause of several health ailments, including impairing the respiratory system's ability to function, protect, and repair itself (29). With 34.1 million active Americans adult smokers in 2019, the burden that cigarettes place on individual and public health results in nearly $300 billion dollars of smoking-related costs each year (28). Cigarette smokers incur up to a fourfold increased risk ratio of developing pneumonia than non-smokers (29). Cigarette smokers have increased white blood cell counts, specifically with regard to $CD4^+$ and $CD8^+$ lymphocytes, cytokines (IL-1, IL-8, TNF alpha, and granulocyte-macrophage colony-stimulating factor), and decreased phagocyte activity (29).

The combined use of alcohol and cigarettes introduces a new set of potential risk factors to respiratory disease and immune function. Most individuals with an AUD also use cigarettes (6). Evidence suggests that individuals consuming nicotine are more likely to overconsume alcohol (30). It is known that co-exposure to cigarette smoke and alcohol use is uniquely negative to the respiratory system. The proposed mechanism for this damage is through reactive aldehydes generated during the metabolism of both cigarette smoke and alcohol (11). Cigarette smoke contains acetaldehyde (AA) and several reactive oxidative species (ROS), and when inhaled cause oxidative stress (31). ROS can cause lipid peroxidation in the liver leading to the synthesis of malondialdehyde (MDA) (15, 31). Alcohol metabolism similarly leads to the AA formation through CYP2E1 and alcohol dehydrogenase (12). CYP2E1 also generates ROS, leading to lipid peroxidation in the liver which forms MDA (12). ROS can lead to inflammation and cytokine release, activating neutrophils and monocytes (4). Chronic inflammation from this can lead to DNA damage, cancer, and inhibition of apoptosis, leading to illnesses like chronic obstructive pulmonary disorder (COPD) (4). AA can form adducts to proteins and DNA, which can lead to robust inflammatory responses (12). AA and MDA can react through a Schiff base intermediate to generate hybrid malondialdehyde-acetaldehyde adducts, or MAA adducts (32). MAA adducts are stable and can covalently bond to proteins at lysine residues (15, 33).

One of the first lines of defense the body has is innate defense mechanisms; in the respiratory system this includes SPD. The simplest unit of SPD is the monomer, which lacks discernable function on its own (10). SPD monomer structure consists of 355 amino acids (43 kDa) arranged into 4 subunits: a short N-terminal domain, a long collagen region, alpha-helical coiled neck domain, and a C-terminus with a carbohydrate recognizing domain (8, 9). The neck and head region of SPD are stabilized by 2 Ca^{+2} ions and 2 disulfide bonds (9). The carbohydrate recognizing domain is located at amino acids Glu 321 and Asn 323, in order to bind to carbohydrates a glycoprotein is required (9).. The long collagen region is a repeating sequence of Gly-X-Y, a region thought to be responsible for oligomerization of SPD and interacting with scavenger receptor A (SRA). SRA is the hypothesized macrophage receptor that interacts with SPD to generate its immune functions (9). The short N-terminus is composed of 2 Cys located in aa15 and aa20 allowing for an interchain disulfide crosslinking to form which stabilized SPDs trimer structure (9). Three monomers can oligomerize to a trimer through the assembly of the collagen regions into triple helices and a coiled bundle made of alpha-helical neck regions (8). Trimers lack the protective immune functions of high order structures but can still bind to 2-3 glycoconjugates due to the spacing of the heads (9, 10). High level of trimerized SPD could inhibit higher order oligomer functions, such as bacterial aggregation and phagocytosis, but encourage inflammation (9). Two trimers can form a hexamer, the next higher order structure of SPD found *in vivo*. Hexamers are a structural intermediate, found as either V-shaped or rod-shaped forms, and bind and aggregate 50-60% of available bacteria (8, 10). Four trimers make up a dodecomer structure, which is the most abundant structure *in vivo* (8). Dodecamers and other higher order structures (fuzzy balls) have shown to be strongly antimicrobial (10). The formation and distribution of SPD structures was largely facilitated by the immediate environment's pH (8). Dodecamers and other higher order oligomers are associated through the N-terminus of trimer subunits (9).

Inactivation of SPD through N-terminus modifications can occur through several known modifications including nitrosylation of the cysteine-residues, which also results in a change in the structure from an oligomeric form to a trimeric form (34). While by no means the only means of SPD structural

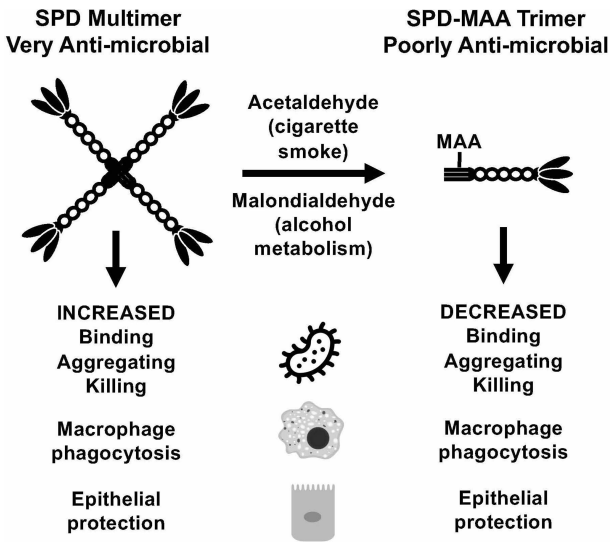

FIGURE 7 | Summary model. Covalent modification of surfactant protein D (SPD) by malondialdehyde-acetaldehyde (MAA) adduction changes the structure of the protein from multimeric form to trimeric form and reduces anti-microbial innate defense.

change, MAA adduction occurs primarily on lysine residues. At the N-terminus of SPD, which governs quaternary structure, is a lysine-containing target for possible adduction. It is the N-terminal region of each SPD subunit that is responsible for the formation of multimeric structures (9). When MAA adducts to SPD to form SPD-MAA, it forms a stable intermediate (**Figure 7**) that is not easily degraded and leads to altered immune effects (12). SPD-MAA adducted proteins bind to scavenger receptor A (CD204) before being internalized to trigger an inflammatory response (31). SRA is found on immune cells such as macrophages, epithelial cells, dendritic cells, and the endothelium (31). Ligand-bound SRA activates PKC_ϵ to recruit more neutrophils, keratinocyte chemoattractant (KC), and release inflammatory signal molecules and chemokines including: TNFα, IL-6, IL-8, IL-12 (12, 35, 36). Due to the decreased protective functions of SPD once it has been MAA adducted, we observed that SPD-MAA functionally resembles the SPD trimer structure that lacks the innate immune properties of higher order oligomers such as the dodecomer (**Figure 7**). Our size exclusion results confirmed that native SPD predominately exists in multimeric form while SPD-MAA exists as trimer and monomer structures. Our findings provide a potential mechanism for the previous study where a reactive aldehyde contained in cigarette smoke, acrolein, also resulted in decreased SPD function (37). This shift in SPD structure from multimer to trimer due to MAA adduction replicates the previously reported decreases in SPD binding, aggregation, and killing of bacteria (10). In addition, macrophage phagocytosis of *S. pneumoniae* was no longer enhanced when SPD was MAA adducted. As well as being antibacterial, SPD is an endogenously produced antiviral protein (9). We observed that bronchial epithelial cell death due to RSV infection was significantly reduced in the presence of SPD. This protection was lost when SPD was MAA adducted. Because SPD is the key surfactant in the lungs that binds to the S-protein of SARS-CoV-2 (38, 39), decreased SPD protection against COVID-19 may be similar to that of RSV. Loss of innate defense at the level of SPD in alcohol misuse may explain one of the mechanisms for alcohol comorbidities observed in the COVID-19 pandemic (10, 40).

DATA AVAILABILITY STATEMENT

The raw data supporting the conclusions of this article will be made available by the authors, without undue reservation.

AUTHOR CONTRIBUTIONS

CN wrote the manuscript and conducted experiments. DM and KB conducted experiments and edited the manuscript. KK prepared SPD-MAA and edited the manuscript. TW designed, analyzed data, wrote, and edited the manuscript. All authors contributed to the article and approved the submitted version.

FUNDING

Support was obtained from Central States Center for Agricultural Safety and Health (CS-CASH; U54 OH010162 to TW), VA Merit (I01 BX003635 to TW and I01 BX005413 to TW and KB), and National Institute on Aging (R01 AG0535553 to KB). TW is the recipient of a Research Career Scientist Award (IK6 BX003781) from the Department of Veterans Affairs.

ACKNOWLEDGMENTS

The authors wish to acknowledge Lisa Chudomelka for expert editorial assistance in the preparation of this manuscript.

REFERENCES

1. Yeligar SM, Chen MM, Kovacs EJ, Sisson JH, Burnham EL, Brown LA. Alcohol and Lung Injury and Immunity. *Alcohol* (2016) 55:51–9. doi: 10.1016/j.alcohol.2016.08.005
2. Price ME, Case AJ, Pavlik JA, DeVasure JM, Wyatt TA, Zimmerman MC, et al. S-Nitrosation of Protein Phosphatase 1 Mediates Alcohol-Induced Ciliary Dysfunction. *Sci Rep* (2018) 8(1):9701. doi: 10.1038/s41598-018-27924-x
3. Wu D, Cederbaum AI. Alcohol, Oxidative Stress, and Free Radical Damage. *Alcohol Res Health* (2003) 27(4):277–84.
4. Sapkota M, Wyatt TA. Alcohol, Aldehydes, Adducts and Airways. *Biomolecules* (2015) 5(4):2987–3008. doi: 10.3390/biom5042987
5. Seeman JI, Dixon M, Haussmann HJ. Acetaldehyde in Mainstream Tobacco Smoke: Formation and Occurrence in Smoke and Bioavailability in the Smoker. *Chem Res Toxocol* (2002) 15:1331–50. doi: 10.1021/tx020069f

6. Burnham EL, McNally A, Gaydos J, Brown LA. The Relationship Between Airway Antioxidant Levels, Alcohol Use Disorders, and Cigarette Smoking. *Alcohol Clin Exp Res* (2016) 40(10):2147–60. doi: 10.1111/acer.13201
7. Wyatt TA, Kharbanda KK, McCaskill ML, Tuma DJ, Yanov D, DeVasure J, et al. Malondialdehyde-Acetaldehyde-Adducted Protein Inhalation Causes Lung Injury. *Alcohol* (2012) 46(1):51–9. doi: 10.1016/j.alcohol.2011.09.001
8. Arroyo R, Martin-Gonzalez A, Echaide M, Jain A, Brondyk WH, Rosenbaum J, et al. Supramolecular Assembly of Human Pulmonary Surfactant Protein SP-D. *J Mol Biol* (2018) 430(10):1495–509. doi: 10.1016/j.jmb.2018.03.027
9. Crouch EC. Surfactant Protein-D and Pulmonary Host Defense. *Respir Res* (2000) 1(2):93–108. doi: 10.1186/rr19
10. Arroyo R, Echaide M, Moreno-Herrero F, Perez-Gil J, Kingma PS. Functional Characterization of the Different Oligomeric Forms of Human Surfactant Protein SP-D. *Biochim Biophys Acta Proteins Proteom* (2020) 1868(8):140436. doi: 10.1016/j.bbapap.2020.140436
11. Sapkota M, Burnham EL, DeVasure JM, Sweeter JM, Hunter CD, Duryee MJ, et al. Malondialdehyde-Acetaldehyde (MAA) Protein Adducts Are Found Exclusively in the Lungs of Smokers With Alcohol Use Disorders and Are Associated With Systemic Anti-MAA Antibodies. *Alcohol Clin Exp Res* (2017) 41(12):2093–9. doi: 10.1111/acer.13509
12. McCaskill ML, Kharbanda KK, Tuma DJ, Reynolds JD, DeVasure JM, Sisson JH, et al. Hybrid Malondialdehyde and Acetaldehyde Protein Adducts Form in the Lungs of Mice Exposed to Alcohol and Cigarette Smoke. *Alcohol Clin Exp Res* (2011) 35(6):1106–13. doi: 10.1111/j.1530-0277.2011.01443.x
13. Wyatt TA, Warren KJ, Wetzel TJ, Suwondo T, Rensch GP, DeVasure JM, et al. Malondialdehyde-Acetaldehyde Adduct Formation Decreases Immunoglobulin A Transport Across Airway Epithelium in Smokers Who Abuse Alcohol. *Am J Pathol* (2021) 191(10):1732–42. doi: 10.1016/j.ajpath.2021.06.007
14. Strong P, Kishore U, Morgan C, Lopez Bernal A, Singh M, Reid KB. A Novel Method of Purifying Lung Surfactant Proteins A and D From the Lung Lavage of Alveolar Proteinosis Patients and From Pooled Amniotic Fluid. *J Immunol Methods* (1998) 220(1-2):139–49. doi: 10.1016/S0022-1759(98)00160-4
15. Tuma DJ, Thiele GM, Xu D, Klassen LW, Sorrell MF. Acetaldehyde and Malondialdehyde React Together to Generate Distinct Protein Adducts in the Liver During Long-Term Ethanol Administration. *Hepatology* (1996) 23 (4):872–80. doi: 10.1002/hep.510230431
16. Bradford MM. A Rapid and Sensitive Method for the Quantitation of Microgram Quantities of Protein Utilizing the Principle of Protein-Dye Binding. *Anal Biochem* (1976) 72:248–54. doi: 10.1016/0003-2697(76)90527-3
17. Wyatt TA, Kharbanda KK, Tuma DJ, Sisson JH, Spurzem JR. Malondialdehyde-Acetaldehyde Adducts Decrease Bronchial Epithelial Wound Repair. *Alcohol* (2005) 36(1):31–40. doi: 10.1016/j.alcohol.2005.06.002
18. Hartshorn KL, Crouch E, White MR, Colamussi ML, Kakkanatt A, Tauber B, et al. Pulmonary Surfactant Proteins A and D Enhance Neutrophil Uptake of Bacteria. *Am J Physiol* (1998) ;274(6):L958–69. doi: 10.1152/ajplung.1998.274.6.L958
19. Barka N, Tomasi JP, Stadtsbaeder S. Use of Whole Streptococcus Pneumoniae Cells as a Solid Phase Sorbent for C-Reactive Protein Measurement by ELISA. *J Immunol Methods* (1985) 82(1):57–63. doi: 10.1016/0022-1759(85)90224-8
20. Jounblat R, Kadioglu A, Iannelli F, Pozzi G, Eggleton P, Andrew PW. Binding and Agglutination of Streptococcus Pneumoniae by Human Surfactant Protein D (SP-D) Vary Between Strains, But SP-D Fails to Enhance Killing by Neutrophils. *Infect Immun* (2004) 72(2):709–16. doi: 10.1128/IAI.72.2.709-716.2004
21. Kjos M, Aprianto R, Fernandes VE, Andrew PW, van Strijp JA, Nijland R, et al. Bright Fluorescent Streptococcus Pneumoniae for Live-Cell Imaging of Host-Pathogen Interactions. *J Bacteriol* (2015) 197(5):807–18. doi: 10.1128/JB.02221-14
22. Huang YC, Li Z, Hyseni X, Schmitt M, Devlin RB, Karoly ED, et al. Identification of Gene Biomarkers for Respiratory Syncytial Virus Infection in a Bronchial Epithelial Cell Line. *Genom Med* (2008) 2(3-4):113–25. doi: 10.1007/s11568-009-9080-y
23. CDC. *Alcohol Use and Your Health*. Atlanta, GA, USA: Centers for Disease Conrol and Prevention (2021).
24. de Roux A, Cavalcanti M, Marcos MA, Garcia E, Ewig S, Mensa J, et al. Impact of Alcohol Abuse in the Etiology and Severity of Community-Acquired Pneumonia. *Chest* (2006) 129(5):1219–25. doi: 10.1378/chest.129.5.1219
25. Alcoholism NIoAAa. *Alcohol Facts and Statistics*. Bethesda, MD, USA: National Institute on Alcohol Abuse and Alcoholism (2021).
26. Danaei G, Ding EL, Mozaffarian D, Taylor B, Rehm J, Murray CJ, et al. The Preventable Causes of Death in the United States: Comparative Risk Assessment of Dietary, Lifestyle, and Metabolic Risk Factors. *PLoS Med* (2009) 6(4):e1000058. doi: 10.1371/journal.pmed.1000058
27. Steffen J, Schlichtiger J, Huber BC, Brunner S. Altered Alcohol Consumption During COVID-19 Pandemic Lockdown. *Nutr J* (2021) 20(1):44. doi: 10.1186/s12937-021-00699-0
28. CDC. *Current Cigarette Smoking Among U.S. Adults Aged 18 Years and Older*. Atlanta, GA, USA: Centers for Disease Conrol and Prevention (2021).
29. Arcavi L, Benowitz NL. Cigarette Smoking and Infection. *Arch Intern Med* (2004) 164(20):2206–16. doi: 10.1001/archinte.164.20.2206
30. Doyon WM, Dong Y, Ostroumov A, Thomas AM, Zhang TA, Dani JA. Nicotine Decreases Ethanol-Induced Dopamine Signaling and Increases Self-Administration *via* Stress Hormones. *Neuron* (2013) 79(3):530–40. doi: 10.1016/j.neuron.2013.06.006
31. Berger JP, Simet SM, DeVasure JM, Boten JA, Sweeter JM, Kharbanda KK, et al. Malondialdehyde-Acetaldehyde (MAA) Adducted Proteins Bind to Scavenger Receptor A in Airway Epithelial Cells. *Alcohol* (2014) 48(5):493–500. doi: 10.1016/j.alcohol.2014.02.005
32. Thiele GM, Worrall S, Tuma DJ, Klassen LW, Wyatt TA, Nagata N. The Chemistry and Biological Effects of Malondialdehyde-Acetaldehyde Adducts. *Alcohol Clin Exp Res* (2001) 25(5 Suppl ISBRA):218S–24S. doi: 10.1111/j.1530-0277.2001.tb02399.x
33. Freeman TL, Haver A, Duryee MJ, Tuma DJ, Klassen LW, Hamel FG, et al. Aldehydes in Cigarette Smoke React With the Lipid Peroxidation Product Malonaldehyde to Form Fluorescent Protein Adducts on Lysines. *Chem Res Toxicol* (2005) 18(5):817–24. doi: 10.1021/tx0500676
34. Guo CJ, Atochina-Vasserman EN, Abramova E, Foley JP, Zaman A, Crouch E, et al. S-Nitrosylation of Surfactant Protein-D Controls Inflammatory Function. *PLoS Biol* (2008) 6(11):e266. doi: 10.1371/journal.pbio.0060266
35. Sapkota M, Kharbanda KK, Wyatt TA. Malondialdehyde-Acetaldehyde-Adducted Surfactant Protein Alters Macrophage Functions Through Scavenger Receptor a. *Alcohol Clin Exp Res* (2016) 40(12):2563–72. doi: 10.1111/acer.13248
36. Sapkota M, DeVasure JM, Kharbanda KK, Wyatt TA. Malondialdehyde-Acetaldehyde (MAA) Adducted Surfactant Protein Induced Lung Inflammation is Mediated Through Scavenger Receptor a (SR-A1). *Respir Res* (2017) 18(1):36. doi: 10.1186/s12931-017-0517-x
37. Takamiya R, Takahashi M, Maeno T, Saito A, Kato M, Shibata T, et al. Acrolein in Cigarette Smoke Attenuates the Innate Immune Responses Mediated by Surfactant Protein D. *Biochim Biophys Acta Gen Subj* (2020) 1864(11):129699. doi: 10.1016/j.bbagen.2020.129699
38. Leth-Larsen R, Zhong F, Chow VT, Holmskov U, Lu J. The SARS Coronavirus Spike Glycoprotein is Selectively Recognized by Lung Surfactant Protein D and Activates Macrophages. *Immunobiology* (2007) 212(3):201–11. doi: 10.1016/j.imbio.2006.12.001
39. Hsieh MH, Beirag N, Murugaiah V, Chou YC, Kuo WS, Kao HF, et al. Human Surfactant Protein D Binds Spike Protein and Acts as an Entry Inhibitor of SARS-CoV-2 Pseudotyped Viral Particles. *Front Immunol* (2021) 12:641360. doi: 10.3389/fimmu.2021.641360
40. Bailey KL, Samuelson DR, Wyatt TA. Alcohol Use Disorder: A Pre-Existing Condition for COVID-19? *Alcohol* (2021) 90:11–7. doi: 10.1016/j.alcohol.2020.10.003

Conflict of Interest: The authors declare that the research was conducted in the absence of any commercial or financial relationships that could be construed as a potential conflict of interest.

Publisher's Note: All claims expressed in this article are solely those of the authors and do not necessarily represent those of their affiliated organizations, or those of the publisher, the editors and the reviewers. Any product that may be evaluated in this article, or claim that may be made by its manufacturer, is not guaranteed or endorsed by the publisher.

frontiers | Frontiers in Immunology

REVIEW
published: 29 June 2022
doi: 10.3389/fimmu.2022.911951

Transcriptional and Epigenetic Regulation of Monocyte and Macrophage Dysfunction by Chronic Alcohol Consumption

*Delphine C. Malherbe and Ilhem Messaoudi**

Department of Microbiology, Immunology and Molecular Genetics, College of Medicine, University of Kentucky, Lexington, KY, United States

Drinking alcohol, even in moderation, can affect the immune system. Studies have shown disproportionate effects of alcohol on circulating and tissue-resident myeloid cells (granulocytes, monocytes, macrophages, dendritic cells). These cells orchestrate the body's first line of defense against microbial challenges as well as maintain tissue homeostasis and repair. Alcohol's effects on these cells are dependent on exposure pattern, with acute drinking dampening but chronic drinking enhancing production of inflammatory mediators. Although chronic drinking is associated with heightened systemic inflammation, studies on tissue resident macrophage populations in several organs including the spleen, liver, brain, and lung have also shown compromised functional and metabolic capacities of these cells. Many of these effects are thought to be mediated by oxidative stress caused by alcohol and its metabolites which can directly impact the cellular epigenetic landscapes. In addition, since myeloid cells are relatively short-lived in circulation and are under constant repopulation from the bone marrow compartment, alcohol's effects on bone marrow progenitors and hematopoiesis are important for understanding the impact of alcohol systemically on these myeloid populations. Alcohol-induced disruption of progenitor, circulating, and tissue resident myeloid populations contribute to the increased susceptibility of patients with alcohol use disorders to viral and bacterial infections. In this review, we provide an overview of the impact of chronic alcohol consumption on the function of monocytes and macrophages in host defense, tissue repair and inflammation. We then summarize our current understanding of the mechanisms underlying alcohol-induced disruption and examine changes in transcriptome and epigenome of monocytes and mcrophages. Overall, chronic alcohol consumption leads to hyper-inflammation concomitant with decreased microbial and wound healing responses by monocytes/macrophages due to a rewiring of the epigentic and transcriptional landscape. However, in advanced alcoholic liver disease, myeloid cells become immunosuppressed as a response to the surrounding hyper-inflammatory milieu. Therefore, the effect of chronic alcohol on the inflammatory response depends on disease state and the immune cell population.

Keywords: monocytes/macrophages, epigenetics, transcriptome (RNA-seq), inflammation, alcohol

OPEN ACCESS

Edited by:
Pinyi Lu,
National Cancer Institute at Frederick (NIH), United States

Reviewed by:
Jingbo Pang,
University of Illinois at Chicago, United States
Thierry Gustot,
Free University of Brussels, Belgium

***Correspondence:**
Ilhem Messaoudi,
Ilhem.Messaoudi@uky.edu

Specialty section:
This article was submitted to Nutritional Immunology, a section of the journal Frontiers in Immunology

Received: *03 April 2022*
Accepted: *27 May 2022*
Published: *29 June 2022*

Citation:
Malherbe DC and Messaoudi I (2022) Transcriptional and Epigenetic Regulation of Monocyte and Macrophage Dysfunction by Chronic Alcohol Consumption. Front. Immunol. 13:911951. doi: 10.3389/fimmu.2022.911951

INTRODUCTION

Burden of Alcohol Use Disorder

Per the National Institute on Alcohol Abuse and Alcoholism (NIAAA), alcohol use disorder (AUD) is "a medical condition characterized by an impaired ability to stop or control alcohol use despite adverse social, occupational, or health consequences" ranging from mild to severe. Lasting changes in the brain caused by alcohol misuse perpetuate AUD and make individuals vulnerable to relapse (1). AUD exerts a heavy burden on people's health and the economy. According to the 2020 National Survey on Drug Use and Health (NSDUH), alcohol consumption is widespread in the USA with 138.5 million people 12 and older reporting drinking alcohol in 2020 and 50% of them drinking alcohol in the month preceding the survey. While a majority of individuals are considered moderate drinkers defined as consuming 2 alcoholic drinks/day or less for men and 1 drink/day for women, 6.4% of people reported engaging in heavy alcohol use in the month preceding the survey. Heavy alcohol use is defined as binge drinking on 5 or more days in the past 30 days with binge drinking defined as consuming ≥5 or more drinks in one sitting for men and ≥4 drinks in one sitting for women. Furthermore, it is estimated that 10.2% of American age 12 and older and 2.8% of adolescents ages 12–17 met the diagnosis of AUD in 2020 (2).

In the United States (U.S.), alcohol is the third-leading preventable cause of death, with an estimated annual death toll of 95,000 people (3). Furthermore, the economic cost of alcohol misuse was estimated to be $249.0 billion in 2010 (4). Adverse outcomes associated with heavy drinking are not limited to the U.S. In 2016, 5.3% of all global deaths, were attributable to alcohol drinking and alcohol abuse was the seventh-leading risk factor for premature death and disability worldwide. Of alcohol-related deaths in 2016, 21.3% were due to digestive diseases (liver cirrhosis, pancreatitis), 19% to cardiovascular diseases, and 12.9% to infectious diseases (including tuberculosis, pneumonia, and HIV/AIDS) (3). These data suggest dysregulated anti-microbial and inflammatory responses with chronic alcohol consumption.

Importance of Myeloid Cells for Innate Immune Functions

During infection or inflammation, macrophages and monocytes are recruited rapidly to the affected tissues where they play a crucial role in the antimicrobial immune response *via* phagocytosis and secretion of immune mediators (cytokines, chemokines, and growth factors). Furthermore, monocytes and macrophages coordinate the recruitment of additional immune cell populations including lymphocytes (5, 6). Monocytes and macrophages play a critical role in tissue repair and wound healing by participating in the initial inflammatory response, clearance of injured tissue and invading pathogens, and the resolution phase (7).

Myeloid cell embryonic development occurs in three distinct waves in humans and in mice, involving first the yolk sac then the fetal liver, and finally the fetal bone marrow (5, 8). Yolk-sac derived macrophages seed multiple tissues where they persist for the life of the organism (9). In the adult bone marrow, monocytes develop from hematopoietic progenitor stem cells (HPSC) *via* progressively restricted lineage-committed progenitors (10, 11). Monopoeisis is well characterized in adult humans and mice, where two independent developmental pathways exist from common myeloid progenitors (CMP): *via* granulocyte-monocyte progenitors (GMP) to monocyte progenitors (MP) or *via* monocyte-DC progenitors (MDP) to common monocyte progenitors (cMoP). Mature monocytes develop from the MP and cMoP progenitor populations into the three well-defined subsets of classical, intermediate, and non-classical monocytes (8) based on their expression of CD14 and CD16. The three subsets have distinct yet sometimes overlapping functions. Classical monocytes ($CD14^{++}$ $CD16^{-}$) are involved in phagocytosis, innate sensing/immune responses, and migration. Intermediate monocytes ($CD14^{++}$ $CD16^{+}$) main functions are antigen presentation, cytokine secretion (TNF-α, IL-1β, and IL-6, following TLR stimulation), differentiation, and regulation of apoptosis. Non-classical monocytes ($CD14^{dim}$ $CD16^{++}$) are involved in anti-viral responses, complement and Fcγ-mediated phagocytosis, and adhesion (6).

While monocytes are relatively short-lived blood circulating phagocytes, macrophages are longer-lived cells that reside in tissues, including the brain, lung, liver, and intestine, where they perform a central role in antimicrobial responses as well as in tissue homeostasis and repair. Microglia are the tissue-resident macrophages in the brain where they comprise approximately 5-15% of cells (12). Microglia originate from yolk-sac progenitor cells and are maintained in adulthood by self-replenishment without the involvement of progenitor cells from the bone marrow (13, 14). Microglia have two main functions: immune defense of the central nervous system (CNS) *via* phagocytosis and mediator production as well as CNS maintenance *via* their control of neuronal proliferation (15). Lung macrophages are the most abundant immune cell population in the healthy lung and are composed of alveolar macrophages in the lumen and interstitial macrophages in the tissue (16, 17). Alveolar macrophages arise from fetal liver-derived monocytes and populate alveoli after birth. They are maintained by self-renewal without the contribution of bone marrow (16, 17). Alveolar macrophages participate in lung host defense and in gas exchange (16, 17). Kupffer cells are the liver tissue-resident macrophages and also are self-renewing populations originating from fetal-liver precursors (18). Other tissue-resident macrophage populations, including in the intestine (where they reside primarily in the lamina propria) (19) and the dermis (20), develop *via* fetal liver monocyte intermediates and are replenished in adulthood by monocyte-derived macrophages.

While chronic moderate alcohol consumption and acute alcohol exposure affect multiple cell populations and their functions, this review will focus on the impact of chronic heavy alcohol use on circulating monocytes and macrophages that reside within the brain, liver, intestine, and lung since a rich body of literature indicates that heavy alcohol consumption disproportionally impacts their phenotype and function (21, 22).

MODELS CURRENTLY AVAILABLE TO STUDY THE IMPACT OF CHRONIC ALCOHOL CONSUMPTION ON MONOCYTES AND MACROPHAGES

Findings from clinical studies are confounded by the presence of organ damage, smoking, use of recreational or illicit drugs, nutritional deficiencies, and by self-reported alcohol intake. To address these limitations, different experimental models have been developed to study the effects of alcohol on cell function in more defined settings. The main model systems are described below and listed in **Table 1**.

In Vitro Systems

To model ethanol consumption, primary and immortalized cells/cell lines are exposed *in vitro* to ethanol at different concentrations and for various durations (23, 24). Due to their ease of manipulation, several macrophage cell lines have been used to study the *in vitro* effect of alcohol exposure on cellular processes. Some notable examples include cell lines to model lung alveolar macrophages [mouse AM cell line MH-S cells (25), rat alveolar macrophage cell line NR8383 cells (26), and mouse macrophage cell line RAW264.7 (27)]; Kupffer cells [HepG2 human liver hepatocellular carcinoma (28), Huh7 human hepatoma cells (29), rat Kupffer cell line 1 (RKC1) (30), human macrophage cell lines MonoMac6 (31), and mouse J774.1 cell line (32)]; microglia [mouse BV2 cell line (33)], rat cell line Microglia-SV40 (34)). In addition, THP-1 human cells differentiated into macrophages have been extensively used (35). Primary cells, including alveolar macrophages, hepatocytes and peripheral blood mononuclear cells (PBMCs) obtained from control and alcohol-exposed animals and humans have also been used (24).

However, transformed cell lines respond differently to immunological challenges compared to primary cells (36) and *in vitro* exposure to ethanol does not accurately recapitulate the complexity of *in vivo* alcohol consumption such as the generation of ethanol metabolites (37). To address some of these challenges, organoid models have been developed, offering new opportunities to explore the impact of chronic ethanol exposure using three-dimensional (3D) *in vitro* structures that better replicate the cellular complexity as well as the morphological and functional features of *in vivo* tissues compared to cells grown in a monolayer (38). Organoid models for organs heavily impacted by alcohol consumption (including liver, brain, intestine, colon, lung) are now available (39–45). A recent liver organoid model replicates alcoholic liver disease (ALD)-associated pathophysiologic changes upon ethanol treatment, including oxidative stress response, steatosis, inflammatory mediators release, and fibrosis in hepatocytes (39). Brain organoids (40) were recently used to assess the effect of alcohol binge drinking on neurons and astrocytes (46). Alcohol-mediated neurotoxicity was unveiled at the structural, functional, and transcriptional levels, revealing that alcohol-induced dose-dependent apoptosis was more severe in neurons than in astrocytes (46). Gut organoids have also been developed including a colon organoid based on a normal colon epithelium (41, 42). Jejunum and colon organoids showed that alcohol's effects mainly targeted colon cells leading to gut leakiness (43) in line with findings showing that ALD patients with the worse intestinal dysbiosis exhibit the greatest gut leakiness (47). While alcohol's effect on epithelial and endothelial cells was assessed in these various organoids, the role of macrophages in alcohol-mediated disease was not investigated even though they are a prominent cell subset in the colon, brain, and liver (18).

Rodent Models

Mice and rats are the animal models most commonly used to study the impact of chronic alcohol consumption on several organ systems. Depending on the model, ethanol is administered *via* different modalities (liquid diet, ethanol in water, gavage, or injection) in combination with dietary, chemical, or genetic manipulations (48, 49). Two prominent mouse models are the Lieber–DeCarli liquid diet (LD) and the Meadows-Cook diet (MC) of *ad libitum* ethanol feeding (50, 51). The LD model, designed to enhance the alcoholic liver injury phenotype in mice (50, 52), is based on an isocaloric liquid diet with alcohol concentration usually increased from 0% to 3.395% w/v for a period of 25 days to 8 weeks, with a 4-week duration most commonly used. In contrast, in the MC diet where alcohol is delivered in the water, exposure to alcohol consists of a 2-week ramping up phase from 0% to 20% ethanol followed by a maintenance phase of 4–16 weeks with a 12-week duration most commonly used (51). Some cellular immunological changes are model-dependent and limited common shared alcohol-

TABLE 1 | Animal models of chronic alcohol exposure.

Model	Species	Alcohol administration	Characteristics
Meadows-Cook (MC)	Rodent	Ad libitum alcohol-drinking water	Mild steatosis
Lieber-DeCarli (LD)	Rodent	Ad libitum liquid diet	Mild inflammation Marked steatosis
Tsukamoto-French	Rodent	Enteral feeding	Mild inflammation Severe steatosis Fibrosis
2nd hit models	Rodent	Ethanol exposure combined with LPS or high/fat diet	Fibrosis High mortality rate
Voluntary drinking	Nonhuman primate	Self-administration (22h/day)	Animals stratified based on blood ethanol concentration No overt liver damage after 12 months Fatty liver disease after 19 months
Gastric infusion	Nonhuman primate	Intragastric catheter (5h/4days or 0.5h/day for 3 months)	

induced transcriptional abnormalities are observed between LD and MC models (53). In addition, these mouse models of chronic alcohol consumption are characterized by minimal liver inflammation (52). Thus, both MC and LD mouse models are models of early alcoholic liver injury (steatosis) and not models of more advanced liver diseases such as fibrosis, cirrhosis, or alcoholic hepatitis. Moreover, the aversion to self-administration of ethanol in some mouse strains (BALB/c resistance vs C57BL/6) as well rodents' higher alcohol catabolism rate compared to humans, make the analysis of organ damage challenging in a self-administration setting (54, 55).

To address these limitations, models delivering ethanol *via* oral gavage or intragastric injection were established, including the Tsukamoto-French enteral feeding model that results in moderate liver inflammation and steatosis (55). To model more advanced ALD while using the oral delivery route and drinking patterns closer to those observed in humans, second-hit models were developed that combine ethanol exposure with a secondary stimulus including genetic knockout/overexpression, LPS stimulation, or high-fat diet (49). Furthermore, additional mouse models were established to study specific aspects of AUD such as binge drinking with the drinking in the dark model (56); a voluntary escalation in consumption with the chronic two-bottle choice drinking (57); and development of dependence with the chronic intermittent vapor model (58). In addition to mouse models, rat models of ethanol drinking have also been developed, including the alcohol-preferring (P) and the high-alcohol-drink (HAD) rat models which prefer an alcohol solution containing 10% ethanol over water (59).

Nonhuman Primate Models

Nonhuman primate (NHP) models are the gold standard to study human diseases due to their genetic proximity to humans; therefore different NHP models of ethanol delivery were developed to mimic human alcohol consumption. Models of oral ethanol self-administration include some with stress triggers including shock avoidance, food and water deprivation, or social stressors (60–62) as well as those with positive reinforcement triggers (63). In one of the models of voluntary ethanol self-administration using a positive reinforcement trigger, rhesus macaques are first induced to freely consume increasing daily doses of ethanol, ranging from 0.5 g/kg/day to 1.5 g/kg/day over a 3-month phase followed by "open access" to a 4% w/v ethanol solution for 22 h/day. This approach establishes consistent ethanol self-administration, and thus represents a true model of alcohol addiction in rhesus and cynomolgus macaques (64, 65) with animals being categorized as low drinkers (average ethanol intake less than 2 g/kg), binge drinkers (average intake of 2.4 g/kg), heavy drinkers (average intake of 2.8 g/kg) or very heavy drinkers (intake higher than 3 g/kg) (66). While this experimental model does not induce any overt liver damage over a 12-month period, signs of fatty liver disease were observed in cynomolgus macaques exposed to an open access period of 6 months followed by 12 months of abstinence that was followed by another open access period of up to 19 months (67). This rhesus macaque model was used to define the impact of chronic drinking on circulating and tissue-resident immune cells showing that the circulating innate immune cells bear the largest burden of chronic heavy drinking (21, 22, 68–73). However due to the inherent variation in alcohol consumed in the voluntary drinking models, a model of gastric infusion of alcohol was developed in order to deliver a consistent alcohol dose in treated rhesus macaques, where animals are infused with 30% ethanol in water (w/v) *via* an intragastric catheter either 4 days per week or 7 days per week during 3 months resulting in blood alcohol levels of 2.3 g/kg (74–76). This model has been used to study the impact of alcohol consumption on simian immunodeficiency virus (SIV) infection (74–76).

IMPACT OF ALCOHOL CONSUMPTION ON SUSCEPTIBILITY TO INFECTION AND WOUND HEALING

Infection

Chronic alcohol consumption weakens antimicrobial responses by impairing the immune system's responses and by affecting the integrity of the mucosal barrier resulting in increased susceptibility to bacterial and viral infections (77–80). In particular, chronic alcohol consumption is a predisposing factor for severe respiratory infections, such as bacterial pneumonia, respiratory syncytial virus and SARS-CoV-2 infections (81–86). Several mechanisms contribute to increased disease severity, including alcohol-induced impairment of the innate immune response, chronic oxidative stress, and alcohol-induced organ damage due to excessive inflammation (82). In addition, chronic alcohol consumption affects lung physiology by desensitizing lung airway cilia and compromising the mucociliary escalator, and leading to impaired clearance of invading pathogens (82).

Community-acquired pneumonia is a leading cause of death in the USA and patients who suffer from AUD experience more severe pneumonia than non-AUD patients (77, 81, 83, 87). Streptococcus pneumoniae, usually a commensal bacterium in the upper respiratory tract, is the prevalent infectious agent of community-acquired pneumonia (81) but alcohol abuse is also associated with an increased incidence of pneumonia from gastric aspiration of Klebsiella pneumoniae (82, 83). Moreover, alcohol abuse is a risk factor for active tuberculosis (TB) with a three-fold risk increase of active TB associated with heavy drinking (80, 88) as well as reactivation of latent tuberculosis (80, 88, 89). AUD patients are also at a higher risk of viral infections, notably respiratory syncytial virus (RSV) (84) and SARS-CoV-2 (85, 86). Increased severity of COVID-19 is believed to be additionally mediated by increased prevalence of cardiovascular diseases and chronic respiratory diseases with alcohol abuse (85, 86). Finally, chronic alcohol consumption is an independent risk factor to develop acute respiratory distress syndrome (ARDS) (90). ARDS is characterized by endothelial and alveolar epithelial barrier dysfunction, severe inflammation, and pulmonary surfactant dysfunction leading to impaired gas exchange in the lung and insufficient oxygen levels in the blood and tissues resulting in organ failure (82).

Infectious diseases affecting the liver are also more prevalent in AUD patients as alcohol metabolism takes place in the liver (91). Specifically, the prevalence of hepatitis C virus (HCV) infection is up to 30-fold higher in AUD patients compared with the general population (92), with a 4.6% to 55.5% rate in AUD patients (93). Moreover, chronic alcohol has been reported to enhance the replication of hepatitis B virus and possibly HCV (93). The increased susceptibility is also mediated by an alcohol-induced increase in oxidative stress and impaired antiviral immune responses in the liver (91, 94). In addition to respiratory and liver diseases, alcohol abuse is also positively associated with HIV incidence and progression towards AIDS in part due to antiretroviral therapy failure (95). Moreover, alcohol increases the risk of multiple AIDS comorbidities including hepatic fibrosis, hepatic cirrhosis, neurocognitive impairment, and AIDS-related dementia (96).

Wound Healing

Wound healing is a dynamic and tightly coordinated process defined by three interconnected phases: inflammation, proliferation, and remodeling. Studies have revealed the critical role played by myeloid cells at several steps of this process. Inflammation is the first phase where neutrophils and macrophages are recruited to the injury site to protect it from infection by phagocytosing invading pathogens and by producing reactive oxygen species (ROS) and pro-inflammatory cytokines and chemokines. These mediators are produced both by local tissue-resident macrophages and by circulating monocytes being recruited from bone marrow to differentiate into macrophages at the site of injury (7). After this initial pro-inflammatory response, macrophages switch to an anti-inflammatory phenotype and participate in wound resolution *via* their contribution to angiogenesis and formation of fibrous tissue (97). During the proliferative second phase, cell migration and proliferation are upregulated to repopulate the injured tissue with fibroblasts, endothelial and epithelial cells. Tissue reorganization takes place last during the remodeling phase so that the injured tissue can regain its functionality (98).

Alcohol abuse impairs wound healing by affecting each step of the repair process (97–99) resulting in AUD patients recovering poorly from surgeries and traumas. AUD patients with a burn injury require longer hospitalizations with more aggressive antibiotic treatments (100), exhibit higher rates of secondary bacterial infections, and are more likely to die compared to non-AUD burn patients (101, 102) even from smaller burn injuries (100). In case of other types of trauma, findings are conflicting with some studies showing that acute rather than chronic alcohol consumption accounts for septic complications after abdominal penetrating trauma while others found that chronic but not acute alcohol consumption influences the outcome from trauma (103). Alcohol consumption is associated with an increased risk for *Staphylococcus aureus* infection of the skin, further compromising the response to wound healing (82). Chronic alcohol exposure may impair wound healing by preventing macrophages from switching to a regulatory phenotype, a critical step to enable the subsequent resolution phase of the healing process (104). Indeed, alcohol exposure induces alterations in transcription and chromatin accessibility in alveolar macrophages indicative of decreased capability for tissue repair (105). In addition, alcohol-exposed macrophages have a reduced phagocytic capacity (26, 105) and this could further impair the wound healing process by reducing the clearance of invading pathogens (104).

IMPACT OF CHRONIC ETHANOL CONSUMPTION ON THE FUNCTIONAL AND TRANSCRIPTIONAL LANDSCAPE OF MONOCYTES AND MACROPHAGES

Altered Inflammatory Response

The effect of chronic alcohol on the inflammatory response depends on the disease phase (early vs late) and the cell populations affected (tissue macrophages vs circulating monocytes). A pro-inflammatory cytokine profile (**Figure 1**) is observed in AUD patients, with elevated plasma levels of TNF-α, IL-1β, and IL-6 (106). Similarly, chronic alcohol results in a systemic pro-inflammatory response in ethanol-fed mice with increased circulating protein levels of TNF-α, IL-6 and MCP-1 (107). This heightened inflammatory state has been associated with multi-organ damage affecting the liver, intestine, lung, and brain (108–111). Prolonged *in vitro* exposure to ethanol upregulates TNF-α gene expression in human monocytes (112). Hyper-inflammation and heightened cell activation have also been observed in HIV patients suffering from AUD with increased plasma levels of soluble CD40 and TGF-β as well as upregulation of CD16, CD163 and TLR4 expression on monocytes (113). In addition, chronic alcohol consumption increases human monocyte sensitivity to LPS as indicated by elevated secretion of pro-inflammatory mediator TNF-α in part *via* downregulation of IRAK-M and enhanced activation of NF-κB and ERK kinases (23, 114).

Inflammatory responses are imbalanced in alcoholic hepatitis (AH) and acute-on-chronic liver failure (ACLF), two severe conditions with substantial mortality and morbidity observed in patients with significant AUD. While AH was initially associated with a proinflammatory phenotype due to higher circulating cytokines levels (115–117), recent studies revealed that AH leads to monocyte immuneparesis characterized by a downregulation of HLA-DR, TNF-α, Il-1β and IL-6; upregulation of regulatory IL-10, PPARγ and MERTK that were accompanied by a decrease in non-classical monocytes and increase in intermediate monocytes (118). Indeed, at the transcription level, monocytes from patients with severe AH display a phenotype characterized by immunosuppressive features including reduced expression of genes related to immune pathways (innate immune responses, cytokines, response to IFNs, antigenic presentation, phagocytosis) (118). Similarly, immuneparesis was also observed in ACLF monocytes with downregulation of HLA-DR and CD86; and upregulation of regulatory IL-10 and MERTK while classical monocyte populations decreased and intermediate monocytes increased (119, 120). The seemingly contradiction of a systemic pro-inflammatory milieu and immunosuppressed cells could be due to an environment with heightened release of soluble

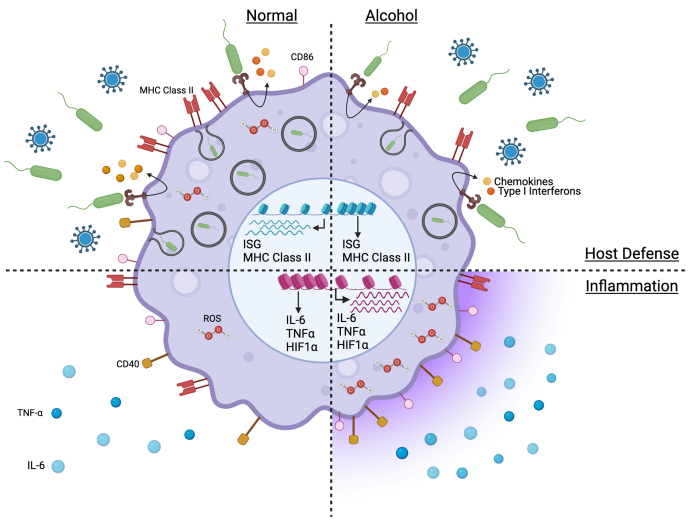

FIGURE 1 | Model capturing the impact of chronic alcohol consumption on the phenotype and function of monocytes and macrophages in absence of severe alcoholic liver disease. Figure created with BioRender.com.

proinflammatory mediators by alcohol-injured tissues leading to expansion of mononuclear $CD14^{+}HLA\text{-}DR^{-}$ myeloid-derived suppressor cells resulting in immunosuppression of monocytes in an attempt to reduce the inflammation (121–123). This immuneparesis extended to peritoneal and mesenteric lymph node macrophages and Kupffer cells in ACLF patients (119).

Furthermore, single-cell transcriptome analyses performed at rest revealed an unsuspected level of heterogeneity in classical monocyte subsets of AH patients with three distinct classical monocyte clusters (124). These three classical clusters differentially expressed markers including CD14, MHC class II, TLR8, and CD86 (124). Interestingly, this high level of heterogeneity in classical monocytes was also observed in alcohol-fed NHPs with the identification of seven classical monocyte clusters by single cell RNA sequencing analysis (68). Two of these clusters were exclusively composed of cells from chronic heavy drinking macaques: *HIF1A*^{hi} and *SOD2*^{hi}. Marker genes of these clusters enriched to gene ontology terms related to myeloid cell differentiation, cytokine signaling, and response to alcohol. Trajectory analysis showed that chronic heavy drinking was associated with a specific lineage that culminated in the *HIF1A*^{hi} cluster, indicating that heavy drinking dysregulates monocyte differentiation states thereby affecting monocyte response to inflammation (68). In addition, chronic heavy drinking was associated with downregulated expression of MHC class II genes but upregulated expression of IFN-inducible genes and activation of NF-κB signaling pathway in classical monocytes (68).

In alcohol-fed animal models, chronic drinking also results in pro-inflammatory responses by Kupffer cells, microglia, splenic and lung alveolar macrophages (22, 82, 107, 125–129). Ethanol-fed mice upregulate the expression of *Tlr1*, *2*, *4*, *6-9* genes leading to an increase in *Tnf* gene expression (130). Furthermore, alcohol-fed mice deficient in TLR4, CD14, TNF-α or LPS-binding proteins (LBP) have reduced liver inflammation and do not develop liver injury (131–133). Anti-TNF-α antibody treatment prevented liver inflammation in alcohol-fed rats (134). Chronic heavy drinking in rhesus macaques is associated with higher gene expression of pattern recognition receptors (*TLR4, FPR3, TLR2*), chemokine receptors (*CCR1, CCR5*), differentiation and activation markers (*CD163*) in splenic macrophages (22). This effect is mediated by alcohol-induced enhanced chromatin accessibility of stress-responsive transcription factors that regulate genes involved in macrophage phagocytosis (*GATA-2*), activation (*CEBPA*), hypoxia (*HIF-1α*), polarization (*GATA-3, NFAT5*) and pro-inflammatory cytokine production (*GATA-2, NRF-1, NFAT5*) (22). In addition, chronic alcohol enhances chromatin accessibility of promoters that regulate genes involved in pro-inflammatory responses, including *TLR4* and *CCL2* genes (22). Chronic alcohol exposure also increases access to transcription factors that regulate expression of inflammatory genes in alveolar macrophages, including AP-1, IRF8, and NF-κB. In the lung, chronic alcohol also upregulates genes involved in granulocyte activation and degranulation (*CTSG, SNAP25, MYO3A*); and downregulates genes involved in anti-inflammation (*CLEC1B*) (105). At the single cell level, chronic alcohol increased the expression of genes involved in oxidative stress (*LCN2*), *HIF-1α*, and cytokine signaling (105).

Alcohol consumption also elicits functional and transcriptial changes in the microglia, with high expression of *TLR2* gene in alcoholic human brains (135). Moreover, alcohol treatment of mice upregulates expression of *Tlr3* in the cortex where microglia are found (136) and chronic intermittent ethanol vapor exposure leads to upregulation of type I interferon-stimulated genes in the prefrontal cortex of mice (137). Additionally, gene ontology analysis identified "toll-like receptor signaling pathway" and "activation of innate immune response" as the main processes in microglia affected by alcohol exposure (137, 138). Chronic alcohol induces transcription of pro-inflammatory IL-6, IL-1β, TNF-α, and

MCP-1 in mouse brain tissue, cortex, and isolated microglial cells *via* NF-κB activation (136, 138). In addition, levels of anti-inflammatory IL-10 were decreased in a mouse model of chronic alcohol-induced neuroinflammation (139).

LPS stimulation of alcohol-exposed monocytes and tissue macrophages further enhances the alcohol-induced hyper-inflammatory response. Upon LPS stimulation, monocytes of alcohol-fed NHPs upregulate genes associated with myeloid inflammatory pathways (*TNFSF21*, *TLR2*). These transcriptional pro-inflammatory changes were confirmed at the protein level with the increased production of pro-inflammatory mediators TNF-α, IL-6, IL-15, and CCL4 in LPS-stimulated monocytes (68). In splenic macrophages isolated from male macaques classified as chronic heavy drinkers, LPS stimulation induced greater production of TNF-α, MIP-1α, MIP-1β, IL-1β, IL-6, IL-8, and GM-CSF (22). From a transcriptional standpoint, LPS-responsive transcription factors NF-KB, p65, STAT1, SMAD1, and HIF-1 were upregulated along with genes associated with "innate immune response", "TGF-β signaling" and "response to LPS" including *CD80, NFKB1, JUN, IL6ST, IFNG, TNFRSF8* and *TNFRSF10B* and *SOCS1* (22).

Alcohol-induced altered inflammatory state following LPS stimulation is not limited to circulating monocytes or macrophages from lymphoid tissues. Chronic heavy ethanol consumption for 12 months leads to a hyper-inflammatory response to LPS stimulation by NHP alveolar macrophages with increased production of IL-6, TNF-α, CXCL8, CXCL10, CCL2, and CCL4 (105). Similarly, chronic alcohol consumption increased protein levels of IFN-α and IFN-β in bronchoalveolar lavage (BAL) of mice. In addition, alveolar macrophages from alcohol-fed mice infected with RSV secrete higher levels of MCP-1 and TNF-α (84). In mice, chronic alcohol also leads to increased expression of pro-inflammatory mediators IL-6, TNF-α, CXCL-1 and MMP-9 by liver-resident Kupffer cells (107). Alcohol-induced liver inflammation in mice and rats is mediated by Kupffer cells, as suggested by upregulation of cell surface expression of CD14 and increased production of pro-inflammatory mediators TNFα, MCP-1, and reactive oxygen species (ROS) (140–145). Both alcohol-induced ROS and increased Kupffer-cell sensitization to endotoxin further exacerbate proinflammatory responses and are major drivers of ALD (91, 144). Intestinal macrophages from alcohol-exposed mice express higher levels of pro-inflammatory genes both at rest and following LPS-induced systemic inflammation, including *Lcn2*, *Tnf*, *Il1b* and *Csf1* (146). *Lcn2* gene encodes Lipocalin-2 which plays a pro-inflammatory role in metabolic diseases (147). *Csf1* plays a role in the maintenance of intestinal macrophage populations (148), thus suggesting that alcohol-induced inflammation may increase the number of resident intestinal macrophages (147). In addition, LPS stimulation of alcohol-fed mice increases the expression of pro-inflammatory chemokine gene *Cxcl1* (neutrophil recruitment) and cytokine signaling gene *Il1a* and its receptor *Il1r* in the ileum (146).

One of the potential drivers of the heightened inflammatory response following chronic alcohol exposure is microbial translocation and leakage of endotoxin in the portal circulation driven by impaired intestinal barrier function and increased gut permeability (149, 150). Additionally, alcohol abuse leads to bacterial overgrowth (151) and altered microbiome composition in the gut of alcoholic patients and alcohol-fed mice (152–154). Fecal transplants from alcohol-fed mice into germ-free mice induced intestinal inflammation, leaky gut, and liver injury (155), thus highlighting the role of dysbiosis in alcohol-induced inflammation. These effects are mediated by bacterial toxins including cytolysin as demonstrated by inhibition of alcohol-induced liver injury in humanized mice by bacteriophage treatment targeting cytolysin-producing *E.faecalis* (156). In addition, plasma endotoxin levels correlated with liver inflammation in alcohol-fed rats (157). While endotoxin leakage has been observed in some mouse models of chronic alcohol consumption (152, 158, 159), there is no consistent increase in endotoxin levels in plasma or in antibody-bound endotoxin levels in NHPs after 12 month of chronic ethanol consumption suggesting that a longer duration may be necessary to detect significant dysbiosis and translocation of microbial products in this model (68, 153).

Defects in Phagocytosis and Antiviral Responses

Defects in anti-microbial functions of monocytes and macrophages (**Figure 1**) have been reported to play a critical role in the observed increased vulnerability to infectious diseases due to chronic drinking resulting in reduced phagocytic activity and pathogen-fighting function in Kupffer cells, microglia, alveolar and splenic macrophages (22, 107, 125–128). Under homeostatic conditions, chronic alcohol leads to a transcriptional downregulation of genes associated with immune and anti-viral responses (MHC class II, antigen processing and presentation, and IFNγ signaling pathways) in non-classical monocytes of alcohol-fed NHPs (68). In contrast to the hyper-inflammatory response to LPS generated by monocytes/macrophages from heavy drinking humans or animals, chronic alcohol exposure leads to a dampened production of immune mediators by macaque monocytes stimulated with *E.coli* bacteria, including reduced production of IL-1β, IL-5, IL-6, IL-15, CCL4 and CXCL11 (68). In addition, genes associated with adaptive immune activation (*IL21R, CD40, MHC class II*) are downregulated in LPS-stimulated monocytes from heavy drinking NHPs (68). Similarly, in splenic macrophages, LPS stimulation leads to downregulation of genes associated with "type I interferon signaling", "defense response to virus" (22). Furthermore, monocytes from AH patients upregulate SOCS1 (160), a negative regulator of the JAK/STAT pathway (161), leading to impaired IFNγ signaling and impaired intracellular killing of phagocytosed bacteria in a subset of patients and is associated with poor survival outcomes (160). Chronic alcohol also led to reduced immune response to vaccination in NHPs and downregulation of several innate immune genes predicted to be highly expressed by myeloid cells including genes involved in antigen presentation (MHC class II genes), defense responses (type I IFN) as well as microbial sensors (*CD14, TLR4, TLR5*) (71).

In addition to impairing antimicrobial functions of monocytes and macrophages of lymphoid organs, chronic alcohol also alters the function of tissue-resident macrophage populations, notably alveolar macrophages, Kupffer cells, and microglia, resulting in increased disease severity (94). Patients with AUD are more susceptible to respiratory infections (81–86) and alcohol-fed mice

infected with Mycobacterium tuberculosis have a higher lung bacterial load and a dampened IFN-γ production (162). In addition, chronic alcohol exposure impairs phagocytosis of bacteria by alveolar macrophages, such as *E.coli* by rat macrophages and *S.aureus* by NHP macrophages (26, 105). Chronic alcohol consumption also leads to blunted induction of interferon-stimulated genes (ISGs) by alveolar macrophages in response to RSV in NHPs suggesting disrupted anti-viral responses (105). Similarly, in a mouse model of chronic ethanol consumption, RSV infection resulted in increased viral loads in the lung and reduced IFNγ protein levels in bronchoalveolar lavage (84). Influenza infection of alcohol-fed mice leads to increased lung viral loads and disease severity (163). In addition, alcohol-fed mice infected with *Mycobacterium avium* have higher bacterial burden in the liver, spleen, and blood (164); and chronic alcohol has been shown to reduce *E.coli* phagocytosis by rat Kupffer cells and microglia (165, 166). Therefore, chronic alcohol dampens microbe phagocytosis by multiple tissue-resident macrophage populations, leading to defects in antimicrobial responses in rodents and NHPs exposed to chronic alcohol.

Alcohol and Increased Oxidative Stress Response

ROS are important mediators in cell signaling and apoptosis (167) and play a critical role in the pathogenesis of various diseases including respiratory infections. ROS are produced by NADPH oxidases (Noxes) (167, 168). Chronic drinking upregulates Nox expression resulting in elevated ROS production leading to heightened oxidative stress in Kupffer cells, microglia and brain cortex, alveolar and splenic macrophages (22, 107, 125–128, 136, 169). One proposed mechanism is *via* alcohol-mediated downregulation of PPARγ. This downregulation of PPARγ in alveolar macrophages following chronic alcohol exposure results in upregulation of Nox and an increase in oxidative stress response leading to heightened intracellular ROS levels (105). In addition, ROS increases the expression of transcription factors HIF-1α and HIF-2α which have important roles in the response to hypoxia in several tissues including mouse liver and rat brain cortex (170, 171). Furthermore, chronic alcohol elicits upregulation of genes enriched in the HIF-1α signaling pathway in alveolar and splenic macrophages as well as monocytes of ethanol-fed NHPs (22, 68, 105). Under homeostatic conditions, chronic alcohol also leads to increased differentiation of classical monocytes expressing high levels of HIF-1α (68). Alcohol's effect on HIF-1α expression in the intestine is more complex with an increased HIF-1α expression in mice exposed to chronic alcohol for 28 days but a decreased expression when alcohol exposure is prolonged to 42 days (159). Therefore, overall chronic alcohol increases tissue hypoxia but its effect can be organ- and exposure-dependent.

MECHANISMS UNDERLYING ALCOHOL-INDUCED DISRUPTION OF MONOCYTE AND MACROPHAGE FUNCTION

The functional effects of alcohol on myeloid cells are dictated by changes at the epigenome level that affect gene transcription (172). Regulation of gene expression can be mediated by epigenetic changes resulting in DNA modification that does not alter the genome sequence. The main epigenetic modifications are provided by noncoding RNAs, DNA methylation, and modifications of histones. MicroRNA molecules (miRNA) are short (19-25 nt), highly conserved, single-stranded non-coding RNAs that modulate target proteins by regulating mRNA expression through decreased transcription or by post-transcriptionally induced mRNA decay (173). In addition to having an autocrine effect, miRNAs can have a paracrine effect *via* exosomal delivery (174). DNA methylation is an epigenetic mark that targets cytosine residues of cytosine-guanine dinucleotide repeats and is regulated by DNA methyltransferases (DNMT) and ten-eleven translocation (TET) enzymes. Hyper-methylation in promoter gene regions leads to transcriptional repression and down-regulation of protein production (175). Histone proteins play key structural and regulatory roles by enabling the formation of nucleosomes. Histone modifications (methylation, phosphorylation, acetylation, and deacetylation as well as ubiquitination) impact chromatin packing thereby modulating gene expression (176). Histone acetyltransferases (HAT) increase chromatin accessibility and promote transcription, whereas histone deacetylases (HDAC) decrease chromatin accessibility and inhibit transcription. In contrast, the result of histone methylation is more complex and depends on several factors including the degree of methylation, the histone and lysine residue targeted, the level of chromatin condensation as well as the function of the genome region targeted (i.e. promoter, enhancer). H3K4, H3K9, and H3K27 are some of the most prominent lysine residues targeted. Studies have reported that alcohol can interfere with the fundamental processes of epigenetic regulation in several cell types including monocytes and macrophages in a dose-, duration-, and time-dependent manner (176).

Role of MicroRNAs in Alcohol-Mediated Disruption of Monocyte and Macrophage Function

miRNAs play a critical role in regulating the function of macrophages and inflammatory pathways in alcoholic steatohepatitis (174). Indeed, several miRNAs modulate the alcohol-induced hyper-inflammatory response by inhibiting negative regulators of TLR signaling pathways (177) in multiple tissue-resident macrophages populations including Kupffer cells, microglia and alveolar macrophages. Alcohol exposure upregulates miR-155 and miR-132 in murine Kupffer cells (178–180) and microglia (181). miR-155 inhibits negative regulators of the TLR4 pathway, including IRAK-M, SHIP1, and PU.1, resulting in increased sensitization to LPS and increased production of pro-inflammatory TNF-α (179) in liver and TNF-α and MCP1 (CCL2) by microglia (181). In addition, miR-155 downregulates STAT3 and SOCS1 in murine Kupffer cells resulting in upregulation of pro-inflammatory cytokines TNF-α and IL-1β and downregulation of anti-inflammatory cytokine IL-10 (161, 179, 182). On the other hand, miR-132 regulates expression of TGF-β, IL-1β, and MCP-1 in Kupffer cells as well as TNF-α and MCP1 in the cerebellum (180, 181). Increased

levels of TGF-β are key for the development of fibrogenesis in the liver, while increased levels of inflammatory mediators (IL-1β, TNF-α, MCP-1) contribute to increased hepatic inflammation and development of steatosis in alcohol-fed mice (183). Indeed, miR-132 is elevated in the liver of AUD patients with fibrosis/cirrhosis (180). Other alcohol-induced miRNAs contribute to dysregulation of monocyte/macrophage cytokine responses including miR-217 which also regulates TGF-β expression in Kupffer cells of alcohol-fed mice (184), as well as miR291b and miR-181b-3b both of which are negative regulators of the TLR signaling pathway (185, 186).

In addition to their effect on the production of cytokines and chemokines, alcohol-induced miRNAs affect other monocyte/macrophage cell functions including oxidative stress and phagocytosis. Chronic drinking downregulates miR-92a and upregulates miR-130a and miR-301a in mouse alveolar macrophages leading to increased oxidative stress and reduced bacterial phagocytosis (25, 187). Downregulation of miR-92a leads to upregulation of Nox4 (25) while upregulation of miR-130a and miR-301a reduces PPARγ expression leading to increased gene expression of Noxes 1, 2, and 4 (187). Nox upregulation results in increased oxidative stress response and increased production of TGF-β as well as decreased phagocytosis (25, 187, 188). ROS production by Kupffer cells is also upregulated by alcohol-induced miR-217 (184).

Alcohol-induced changes in miRNA expression can modulate macrophage polarization balance. LPS-stimulated Kupffer cells from alcohol-exposed rats show enrichment of miR-125a-5p (189), which inhibits TLR4-dependent signaling pathway and mediator production leading to anti-inflammatory polarization (189). Moreover, miR-27a, which regulates macrophage polarization towards a regulatory profile *via* IL-10, is downregulated in PBMCs of ethanol-fed NHPs (21) suggesting an alcohol-induced rewiring towards a pro-inflammatory profile.

In addition to regulating gene expression within the cells in which they are generated, miRNAs can be transferred into other target cells *via* exosomes, thus regulating the function of other cell populations including monocytes and macrophages in a paracrine manner (174, 190, 191). Of note, increased miR-122 levels have been measured in circulating exosomes of chronic alcohol-fed mice (140) and binge-drinking humans (191). miR-122 is liver-specific and is associated with lipid metabolism, stress response, and hepatitis C virus replication (192). *In vitro*, horizontal transfer of miRNA-122 from ethanol-treated hepatocytes to monocytic cells *via* exosomes upregulates the production of pro-inflammatory cytokines TNF-α and IL-1β (191). In PBMCs isolated from heavy drinking NHPs, alcohol exposure had a differential effect on several extracellular vesicle (EV)-derived miRNAs that regulate genes with roles in myeloid cell activation and angiogenesis. Gene ontology analyses revealed enrichment of putative target genes to TGF-β receptor signaling, histone, and chromatin modification, response to ROS, and myeloid leukocyte activation. Over-expression of candidates miR-155, miR-154, miR-34c, miR-450a, and miR-204, which are upregulated in EV with alcohol drinking, led to a heightened inflammatory response in PBMCs after stimulation (190).

DNA Methylation

DNA methylation plays an important role in ethanol-mediated dysfunction. In Kupffer cells, alcohol treatment leads to abnormal DNA methylation patterns and upregulation of methyl-transferases DNMT1, DNMT3a, and DNMT3b (193) which in turn hyper-methylate anti-inflammatory mediators, *PSTPIP2*, *SOCS1*, and *ZSWIM3* leading to their inhibition and inhibition of downstream anti-inflammatory targets and promotion of a pro-inflammatory profile (193). Specifically, downregulation of *PSTPIP2* leads to activation of the STAT1 pathway *via* increased STAT1 phosphorylation. Downregulation of *PSTPIP2* also leads to activation of the NF-κB signaling pathway by affecting phosphorylation of p65 and IκBα as well as the nuclear transfer of p65. Activation of these pathways results in increased transcription of pro-inflammatory mediators IL-1β, TNF-α, IL-6, IL-17, and CCL2 and increased protein production of IL-1β, TNF-α, and IL-6. Thus, *PSTPIP2* plays a crucial role in macrophage-induced inflammatory responses by regulating the STAT1 and NF-κB signaling pathways (193). In the same chronic-plus-binge mouse model, alcohol exposure also reduces the expression of *ZSWIM3* in Kupffer cells due to DNMT3b-induced hypermethylation of *ZSWIM3* promoter. Downregulation of *ZSWIM3* leads to activation of adaptor protein TRAF2 which plays a crucial role in the activation of the NF-κB signaling pathway resulting in increased transcription of IL-1β, TNF-α, IL-6 and MCP-1 as well as increased protein production of IL-1β, TNF-α and IL-6 (194) thus eliciting a pro-inflammatory phenotype.

Histone Modifications

Chronic alcohol exposure leads to histone modifications that contribute to enhanced pro-inflammatory responses. Sirtuins are NAD+ dependent deacetylases that play a key role in inflammation and oxidative stress. Ethanol metabolism results in a decrease of NAD+ in the liver leading to sirtuin dysregulation. Additionally, alcohol consumption leads to the upregulation of miR-217 and miR-132 in Kupffer cells, which in turn leads to decreased levels of sirtuin SIRT1 (184, 195). Decreased SIRT1 gene and protein expression results in the downregulation of AMPK, an anti-inflammatory regulator, and the upregulation of NF-κB and NFATC4 through H3K9 acetylation. Activation of the NF-κB and NFATC4 signaling pathways results in increased production of pro-inflammatory IL-1β, TNF-α, IL-6 and MCP-1 (184). In addition to sirtuins, other classes of deacetylases have been involved in alcohol-induced effects. Histone deacetylase 11 (HDAC11) is induced in Kupffer cells in a mouse model of ALD *via* upregulation of miR-155 by alcohol metabolite acetaldehyde that leads to activation of the NF-κB signaling pathway, resulting in reduced expression of anti-inflammatory IL-10 (179). The mechanism of action of HDAC11 in macrophages has been elucidated. HDAC11 binds to the proximal site of the IL-10 promoter and modulates the recruitment of PU.1, Sp1, and STAT3 at late stages of LPS activation (196).

Histone methylation is also affected by alcohol consumption. H3K27me3, mediating epigenetic silencing, is enriched at the

TGF-β promoter but reduced at the TNF-α promoter location in Kupffer cells of ACLF patients. Enhancer of zeste homolog 2 (EZH2) catalyzes the methylation of H3K27 loci and increased EZH2 expression and enhanced H3K27me3 are observed in PBMCs of ACLF patients. In addition, in a murine model of liver failure induced by administration of D-galactosamine, upregulation of EZH2 and H3K27me3 in Kupffer cells correlates with upregulation of pro-inflammatory cytokine TNF-α, IL-1β, and IL-6 (197). Furthermore, in splenic macrophages of alcohol-fed NHPs, chronic alcohol affects increased tri-methylation of H3K4, an active promoter mark. In addition, changes in overlapping regions enriched for cis-regulatory inactive enhancer H3K4me1 and active enhancer H3K27Ac are associated with host defense processes including "Immune System Process" and "regulation of cytokine production" in alcohol-exposed splenic macrophages (22).

Chromatin Accessibility

Changes in histone modifications can lead to alterations in chromatin accessibility, resulting in changes in gene expression. Several studies have reported modulation of chromatin accessibility in monocytes and macrophages from alcoholic hepatitis (AH) patients and NHP chronically consuming ethanol leading to enhanced pro-inflammatory gene expression and reduced expression of genes involved in metabolic processes (22, 105, 118). In alveolar macrophages of alcohol-fed NHPs, these dysregulated responses are mediated by increased chromatin accessibility in intergenic regions that regulate inflammatory genes and binding motifs for transcription factors AP-1, IRF8, and NF-κB p-65 and reduced chromatin accessibility of promoters of genes important for endothelium development and cell junction assembly (105). In splenic macrophages of alcohol-fed NHPs, chronic alcohol increases chromatin accessibility of promoters and intergenic enhancer regions that regulate the expression of genes participating in immune activation, cytokine signaling pathways, myeloid cell activation (CD40), and cellular stress responses. Specifically, chronic alcohol increases accessibility in regions regulated by transcription factors involved in oxidative stress (NRF-1, AHR), hypoxia (HIF-1α), and inflammatory responses (NF-κB). Chronic alcohol is also associated with increased chromatin accessibility of genes engaged in inflammatory and immune responses including *TLR4*, *CCL2*, *C3AR1*, and *LAMP1* (22).

In addition to its effect on tissue macrophages, chronic heavy alcohol consumption also increases chromatin accessibility at promoter regions that regulate the expression of genes involved in cytokine production and myeloid activation in monocytes of ethanol-fed NHPs, including regions containing binding sites for transcription factors important for monocyte activation and differentiation such as FOS, JUNB and PU.1 (68). Furthermore, studies reported increased accessibility to binding sites for transcription factors CEBP and MAF as well as regions associated with immunoregulatory genes such as *PPARG* in monocytes isolated from patients with severe AH. In contrast to what has been described for monocytes of heavy drinkers in the absence of liver disease, binding sites for NF-κB, IRF, and STAT1 were less accessible in enhancer regions as was chromatin accessibility in regions associated with genes involved in innate immune response, antigen presentation and cytokine secretion in monocytes obtained from patients with AH (118).

IMPACT OF AUD ON BONE MARROW MYELOID PROGENITORS

Monocytes develop continuously in the bone marrow from CD34+ hematopoietic stem and progenitor cells *via* increasingly restricted lineage-committed progenitors (10, 11). Inflammation and infection can affect monocyte production and induce emergency monopoiesis in the bone marrow (10, 198). AUD patients suffer from blood cell disorders including lymphopenia, anemia, and thrombocytopenia (199–203). In addition, almost half of alcoholics have foamy macrophages due to the storage of alcohol-induced lipids in the cytoplasm (204). Hemostasis is also perturbed in ALD, due to alcohol's effects on the platelets leading to an increased risk of disseminated intravascular coagulation (205). These defects suggest that alcohol exposure impacts bone marrow progenitor cell populations and hematopoiesis in humans. Alcohol-induced effects on the myeloid progenitor compartment are wide-ranging, impacting hematopoietic precursor cell activation and differentiation as well as genes involved in inflammatory and metabolic responses. Multiple bone marrow precursor cell populations are affected by chronic alcohol, including erythrocytes and granulocytes where vacuolization is induced. This damage appears within a week of heavy drinking but is reversible (205).

Mice exposed to acute alcohol and infected with *E.coli* have a reduced number of bone marrow myeloid progenitor cells and alcohol treatment prevents switching to granulocyte phenotype. Furthermore, alcohol exposure increases the bacterial burden and mortality of E.coli-infected mice (206). In a chronic plus binge mouse model, alcohol administration triggers the release of granulocytes from the bone marrow compartment, resulting in a reduction of the granulocyte reserve in the marrow concomitant with an elevation of granulocytes in the circulation. This phenomenon is enhanced further following bacteremia, where alcohol impairs activation of granulopoietic precursor proliferation and response to LPS stimulation (207). These findings were confirmed in NHPs, where chronic alcohol exposure reduces the number of primitive hematopoietic stem and progenitor cells in the bone marrow and impairs their ability to proliferate and differentiate towards erythroid and granulocyte-monocyte cells (208). In addition, alcohol exposure leads to remodeling of the bone marrow niche and these alterations persisted after 1-month abstinence thus indicating that the effects of alcohol are long-lived (208) and may involve epigenetic rewiring of progenitor cells.

CONCLUSION

In summary, chronic alcohol consumption leads to a hyper-inflammatory response with heightened cytokine, chemokine, and ROS production concomitantly with decreased microbial

and wound healing responses in circulating monocytes and tissue-resident macrophages. This profile is due to alcohol's interference with the fundamental processes of epigenetic regulation at the transcriptome level.

AUTHOR CONTRIBUTIONS

All authors listed have made a substantial, direct, and intellectual contribution to the work and approved it for publication. IM secured funding for this work.

FUNDING

This work was funded by NIH Grant number R01 AA028735.

ACKNOWLEDGMENTS

We thank Dr. Suhas Sureshchandra for critical reading of the manuscript and Madison Blanton for help with **Figure 1**.

REFERENCES

1. Available at: https://www.niaaa.nih.gov/publications/brochures-and-fact-sheets/understanding-alcohol-use-disorder.
2. Available at: https://www.samhsa.gov/data/report/2020-nsduh-annual-national-report.
3. Available at: https://www.niaaa.nih.gov/publications/brochures-and-fact-sheets/alcohol-facts-and-statistics.
4. Sacks JJ, Gonzales KR, Bouchery EE, Tomedi LE, Brewer RD. 2010 National and State Costs of Excessive Alcohol Consumption. *Am J Prev Med* (2015) 49(5):e73–e9. doi: 10.1016/j.amepre.2015.05.031
5. Mass E. Delineating the Origins, Developmental Programs and Homeostatic Functions of Tissue-Resident Macrophages. *Int Immunol* (2018) 30 (11):493–501. doi: 10.1093/intimm/dxy044
6. Guilliams M, Mildner A, Yona S. Developmental and Functional Heterogeneity of Monocytes. *Immunity* (2018) 49(4):595–613. doi: 10.1016/j.immuni.2018.10.005
7. Snyder RJ, Lantis J, Kirsner RS, Shah V, Molyneaux M, Carter MJ. Macrophages: A Review of Their Role in Wound Healing and Their Therapeutic Use. *Wound Repair Regen* (2016) 24(4):613–29. doi: 10.1111/wrr.12444
8. Teh YC, Ding JL, Ng LG, Chong SZ. Capturing the Fantastic Voyage of Monocytes Through Time and Space. *Front Immunol* (2019) 10:834. doi: 10.3389/fimmu.2019.00834
9. Hoeffel G, Ginhoux F. Ontogeny of Tissue-Resident Macrophages. *Front Immunol* (2015) 6:486. doi: 10.3389/fimmu.2015.00486
10. Wolf AA, Yanez A, Barman PK, Goodridge HS. The Ontogeny of Monocyte Subsets. *Front Immunol* (2019) 10:1642. doi: 10.3389/fimmu.2019.01642
11. Kawamura S, Ohteki T. Monopoiesis in Humans and Mice. *Int Immunol* (2018) 30(11):503–9. doi: 10.1093/intimm/dxy063
12. Lawson LJ, Perry VH, Dri P, Gordon S. Heterogeneity in the Distribution and Morphology of Microglia in the Normal Adult Mouse Brain. *Neuroscience* (1990) 39(1):151–70. doi: 10.1016/0306-4522(90)90229-W
13. Zhang L, Cao Y, Zhang X, Gu X, Mao Y, Peng B. The Origin and Repopulation of Microglia. *Dev Neurobiol* (2022) 82(1):112–24. doi: 10.1002/dneu.22862
14. Huang Y, Xu Z, Xiong S, Sun F, Qin G, Hu G, et al. Repopulated Microglia are Solely Derived From the Proliferation of Residual Microglia After Acute Depletion. *Nat Neurosci* (2018) 21(4):530–40. doi: 10.1038/s41593-018-0090-8
15. Ginhoux F, Lim S, Hoeffel G, Low D, Huber T. Origin and Differentiation of Microglia. *Front Cell Neurosci* (2013) 7:45. doi: 10.3389/fncel.2013.00045
16. Liegeois M, Legrand C, Desmet CJ, Marichal T, Bureau F. The Interstitial Macrophage: A Long-Neglected Piece in the Puzzle of Lung Immunity. *Cell Immunol* (2018) 330:91–6. doi: 10.1016/j.cellimm.2018.02.001
17. Evren E, Ringqvist E, Willinger T. Origin and Ontogeny of Lung Macrophages: From Mice to Humans. *Immunology* (2020) 160(2):126–38. doi: 10.1111/imm.13154
18. Nobs SP, Kopf M. Tissue-Resident Macrophages: Guardians of Organ Homeostasis. *Trends Immunol* (2021) 42(6):495–507. doi: 10.1016/j.it.2021.04.007
19. Bain CC, Mowat AM. Macrophages in Intestinal Homeostasis and Inflammation. *Immunol Rev* (2014) 260(1):102–17. doi: 10.1111/imr.12192
20. Tamoutounour S, Guilliams M, Montanana Sanchis F, Liu H, Terhorst D, Malosse C, et al. Origins and Functional Specialization of Macrophages and of Conventional and Monocyte-Derived Dendritic Cells in Mouse Skin. *Immunity* (2013) 39(5):925–38. doi: 10.1016/j.immuni.2013.10.004
21. Sureshchandra S, Rais M, Stull C, Grant K, Messaoudi I. Transcriptome Profiling Reveals Disruption of Innate Immunity in Chronic Heavy Ethanol Consuming Female Rhesus Macaques. *PloS One* (2016) 11(7):e0159295. doi: 10.1371/journal.pone.0159295
22. Sureshchandra S, Stull C, Ligh BJK, Nguyen SB, Grant KA, Messaoudi I. Chronic Heavy Drinking Drives Distinct Transcriptional and Epigenetic Changes in Splenic Macrophages. *EBioMedicine* (2019) 43:594–606. doi: 10.1016/j.ebiom.2019.04.027
23. Mandrekar P, Bala S, Catalano D, Kodys K, Szabo G. The Opposite Effects of Acute and Chronic Alcohol on Lipopolysaccharide-Induced Inflammation Are Linked to IRAK-M in Human Monocytes. *J Immunol* (2009) 183 (2):1320–7. doi: 10.4049/jimmunol.0803206
24. Liangpunsakul S, Toh E, Ross RA, Heathers LE, Chandler K, Oshodi A, et al. Quantity of Alcohol Drinking Positively Correlates With Serum Levels of Endotoxin and Markers of Monocyte Activation. *Sci Rep* (2017) 7(1):4462. doi: 10.1038/s41598-017-04669-7
25. Morris NL, Harris FL, Brown LAS, Yeligar SM. Alcohol Induces Mitochondrial Derangements in Alveolar Macrophages by Upregulating NADPH Oxidase 4. *Alcohol* (2021) 90:27–38. doi: 10.1016/j.alcohol.2020.11.004
26. Staitieh BS, Egea EE, Fan X, Amah A, Guidot DM. Chronic Alcohol Ingestion Impairs Rat Alveolar Macrophage Phagocytosis *via* Disruption of RAGE Signaling. *Am J Med Sci* (2018) 355(5):497–505. doi: 10.1016/j.amjms.2017.12.013
27. Shi L, Kishore R, McMullen MR, Nagy LE. Chronic Ethanol Increases Lipopolysaccharide-Stimulated Egr-1 Expression in RAW 264.7 Macrophages: Contribution to Enhanced Tumor Necrosis Factor Alpha Production. *J Biol Chem* (2002) 277(17):14777–85. doi: 10.1074/jbc.M108967200
28. Pochareddy S, Edenberg HJ. Chronic Alcohol Exposure Alters Gene Expression in HepG2 Cells. *Alcohol Clin Exp Res* (2012) 36(6):1021–33. doi: 10.1111/j.1530-0277.2011.01677.x
29. Plumlee CR, Lazaro CA, Fausto N, Polyak SJ. Effect of Ethanol on Innate Antiviral Pathways and HCV Replication in Human Liver Cells. *Virol J* (2005) 2:89. doi: 10.1186/1743-422X-2-89
30. Shen Z, Ajmo JM, Rogers CQ, Liang X, Le L, Murr MM, et al. Role of SIRT1 in Regulation of LPS- or Two Ethanol Metabolites-Induced TNF-Alpha Production in Cultured Macrophage Cell Lines. *Am J Physiol Gastrointest Liver Physiol* (2009) 296(5):G1047–53. doi: 10.1152/ajpgi.00016.2009
31. Zhang Z, Bagby GJ, Stoltz D, Oliver P, Schwarzenberger PO, Kolls JK. Prolonged Ethanol Treatment Enhances Lipopolysaccharide/Phorbol Myristate Acetate-Induced Tumor Necrosis Factor-Alpha Production in Human Monocytic Cells. *Alcohol Clin Exp Res* (2001) 25(3):444–9. doi: 10.1111/j.1530-0277.2001.tb02233.x
32. Jung F, Lippmann T, Brandt A, Jin CJ, Engstler AJ, Baumann A. Moderate Consumption of Fermented Alcoholic Beverages Diminishes Diet-Induced Non-Alcoholic Fatty Liver Disease Through Mechanisms Involving Hepatic Adiponectin Signaling in Mice. *Eur J Nutr* (2020) 59(2):787–99. doi: 10.1007/s00394-019-01945-2
33. Correa F, De Laurentiis A, Franchi AM. Ethanol Downregulates N-Acyl Phosphatidylethanolamine-Phospholipase D Expression in BV2 Microglial Cells *via* Epigenetic Mechanisms. *Eur J Pharmacol* (2016) 786:224–33. doi: 10.1016/j.ejphar.2016.06.004

34. Chiavari M, Ciotti GMP, Navarra P, Lisi L. Pro-Inflammatory Activation of A New Immortalized Human Microglia Cell Line. *Brain Sci* (2019) 9(5):111. doi: 10.3390/brainsci9050111
35. Nurmi K, Virkanen J, Rajamaki K, Niemi K, Kovanen PT, Eklund KK. Ethanol Inhibits Activation of NLRP3 and AIM2 Inflammasomes in Human Macrophages–a Novel Anti-Inflammatory Action of Alcohol. *PloS One* (2013) 8(11):e78537. doi: 10.1371/journal.pone.0078537
36. Andreu N, Phelan J, de Sessions PF, Cliff JM, Clark TG, Hibberd ML. Primary Macrophages and J774 Cells Respond Differently to Infection With Mycobacterium Tuberculosis. *Sci Rep* (2017) 7:42225. doi: 10.1038/srep42225
37. Pruett SB, Fan R, Zheng Q, Schwab C. Differences in IL-10 and IL-12 Production Patterns and Differences in the Effects of Acute Ethanol Treatment on Macrophages *In Vivo* and *In Vitro*. *Alcohol* (2005) 37(1):1–8. doi: 10.1016/j.alcohol.2005.09.004
38. Heydari Z, Moeinvaziri F, Agarwal T, Pooyan P, Shpichka A, Maiti TK, et al. Organoids: A Novel Modality in Disease Modeling. *Biodes Manuf* (2021) 4 (4):689–716. doi: 10.1007/s42242-021-00150-7
39. Wang S, Wang X, Tan Z, Su Y, Liu J, Chang M, et al. Human ESC-Derived Expandable Hepatic Organoids Enable Therapeutic Liver Repopulation and Pathophysiological Modeling of Alcoholic Liver Injury. *Cell Res* (2019) 29 (12):1009–26. doi: 10.1038/s41422-019-0242-8
40. Adams JW, Cugola FR, Muotri AR. Brain Organoids as Tools for Modeling Human Neurodevelopmental Disorders. *Physiology (Bethesda)* (2019) 34 (5):365–75. doi: 10.1152/physiol.00005.2019
41. Devall M, Jennelle LT, Bryant J, Bien S, Peters U, Powell S, et al. Modeling the Effect of Prolonged Ethanol Exposure on Global Gene Expression and Chromatin Accessibility in Normal 3D Colon Organoids. *PloS One* (2020) 15(1):e0227116. doi: 10.1371/journal.pone.0227116
42. Devall M, Plummer SJ, Bryant J, Jennelle LT, Eaton S, Dampier CH, et al. Ethanol Exposure Drives Colon Location Specific Cell Composition Changes in a Normal Colon Crypt 3D Organoid Model. *Sci Rep* (2021) 11(1):432. doi: 10.1038/s41598-020-80240-1
43. Forsyth CB, Shaikh M, Bishehsari F, Swanson G, Voigt RM, Dodiya H, et al. Alcohol Feeding in Mice Promotes Colonic Hyperpermeability and Changes in Colonic Organoid Stem Cell Fate. *Alcohol Clin Exp Res* (2017) 41 (12):2100–13. doi: 10.1111/acer.13519
44. Drakhlis L, Devadas SB, Zweigerdt R. Generation of Heart-Forming Organoids From Human Pluripotent Stem Cells. *Nat Protoc* (2021) 16 (12):5652–72. doi: 10.1038/s41596-021-00629-8
45. Liberti DC, Morrisey EE. Organoid Models: Assessing Lung Cell Fate Decisions and Disease Responses. *Trends Mol Med* (2021) 27(12):1159–74. doi: 10.1016/j.molmed.2021.09.008
46. Arzua T, Yan Y, Jiang C, Logan S, Allison RL, Wells C, et al. Modeling Alcohol-Induced Neurotoxicity Using Human Induced Pluripotent Stem Cell-Derived Three-Dimensional Cerebral Organoids. *Transl Psychiatry* (2020) 10(1):347. doi: 10.1038/s41398-020-01029-4
47. Mutlu EA, Gillevet PM, Rangwala H, Sikaroodi M, Naqvi A, Engen PA, et al. Colonic Microbiome Is Altered in Alcoholism. *Am J Physiol Gastrointest Liver Physiol* (2012) 302(9):G966–78. doi: 10.1152/ajpgi.00380.2011
48. Bennett B, Downing C, Parker C, Johnson TE. Mouse Genetic Models in Alcohol Research. *Trends Genet* (2006) 22(7):367–74. doi: 10.1016/j.tig.2006.05.005
49. Ghosh Dastidar S, Warner JB, Warner DR, McClain CJ, Kirpich IA. Rodent Models of Alcoholic Liver Disease: Role of Binge Ethanol Administration. *Biomolecules* (2018) 8(1):3. doi: 10.3390/biom8010003
50. Lieber CS, DeCarli LM, Sorrell MF. Experimental Methods of Ethanol Administration. *Hepatology* (1989) 10(4):501–10. doi: 10.1002/hep.1840100417
51. Meadows GG, Wallendal M, Kosugi A, Wunderlich J, Singer DS. Ethanol Induces Marked Changes in Lymphocyte Populations and Natural Killer Cell Activity in Mice. *Alcohol Clin Exp Res* (1992) 16(3):474–9. doi: 10.1111/j.1530-0277.1992.tb01403.x
52. Nevzorova YA, Boyer-Diaz Z, Cubero FJ, Gracia-Sancho J. Animal Models for Liver Disease - A Practical Approach for Translational Research. *J Hepatol* (2020) 73(2):423–40. doi: 10.1016/j.jhep.2020.04.011
53. Vogle A, Qian T, Zhu S, Burnett E, Fey H, Zhu Z, et al. Restricted Immunological and Cellular Pathways Are Shared by Murine Models of Chronic Alcohol Consumption. *Sci Rep* (2020) 10(1):2451. doi: 10.1038/s41598-020-59188-9
54. Holmes RS, Duley JA, Algar EM, Mather PB, Rout UK. Biochemical and Genetic Studies on Enzymes of Alcohol Metabolism: The Mouse as a Model Organism for Human Studies. *Alcohol Alcohol* (1986) 21(1):41–56.
55. Mathews S, Xu M, Wang H, Bertola A, Gao B. Animals Models of Gastrointestinal and Liver Diseases. Animal Models of Alcohol-Induced Liver Disease: Pathophysiology, Translational Relevance, and Challenges. *Am J Physiol Gastrointest Liver Physiol* (2014) 306(10):G819–23. doi: 10.1152/ajpgi.00041.2014
56. Thiele TE, Navarro M. "Drinking in the Dark" (DID) Procedures: A Model of Binge-Like Ethanol Drinking in non-Dependent Mice. *Alcohol* (2014) 48 (3):235–41. doi: 10.1016/j.alcohol.2013.08.005
57. Osterndorff-Kahanek E, Ponomarev I, Blednov YA, Harris RA. Gene Expression in Brain and Liver Produced by Three Different Regimens of Alcohol Consumption in Mice: Comparison With Immune Activation. *PloS One* (2013) 8(3):e59870. doi: 10.1371/journal.pone.0059870
58. Becker HC, Lopez MF. Increased Ethanol Drinking After Repeated Chronic Ethanol Exposure and Withdrawal Experience in C57BL/6 Mice. *Alcohol Clin Exp Res* (2004) 28(12):1829–38. doi: 10.1097/01.ALC.0000149977.95306.3A
59. McBride WJ, Rodd ZA, Bell RL, Lumeng L, Li TK. The Alcohol-Preferring (P) and High-Alcohol-Drinking (HAD) Rats–Animal Models of Alcoholism. *Alcohol* (2014) 48(3):209–15. doi: 10.1016/j.alcohol.2013.09.044
60. Clark R, Polish E. Avoidance Conditioning and Alcohol Consumption in Rhesus Monkeys. *Science* (1960) 132(3421):223–4. doi: 10.1126/science.132.3421.223
61. Mello NK, Mendelson JH. Evaluation of a Polydipsia Technique to Induce Alcohol Consumption in Monkeys. *Physiol Behav* (1971) 7(6):827–36. doi: 10.1016/0031-9384(71)90047-3
62. Higley JD, Hasert MF, Suomi SJ, Linnoila M. Nonhuman Primate Model of Alcohol Abuse: Effects of Early Experience, Personality, and Stress on Alcohol Consumption. *Proc Natl Acad Sci USA* (1991) 88(16):7261–5. doi: 10.1073/pnas.88.16.7261
63. Grant KA, Johanson CE. The Nature of the Scheduled Reinforcer and Adjunctive Drinking in Nondeprived Rhesus Monkeys. *Pharmacol Biochem Behav* (1988) 29(2):295–301. doi: 10.1016/0091-3057(88)90159-1
64. Grant KA, Johanson CE. Oral Ethanol Self-Administration in Free-Feeding Rhesus Monkeys. *Alcohol Clin Exp Res* (1988) 12(6):780–4. doi: 10.1111/j.1530-0277.1988.tb01345.x
65. Vivian JA, Green HL, Young JE, Majerksy LS, Thomas BW, Shively CA, et al. Induction and Maintenance of Ethanol Self-Administration in Cynomolgus Monkeys (Macaca Fascicularis): Long-Term Characterization of Sex and Individual Differences. *Alcohol Clin Exp Res* (2001) 25(8):1087–97. doi: 10.1111/j.1530-0277.2001.tb02321.x
66. Baker EJ, Farro J, Gonzales S, Helms C, Grant KA. Chronic Alcohol Self-Administration in Monkeys Shows Long-Term Quantity/Frequency Categorical Stability. *Alcohol Clin Exp Res* (2014) 38(11):2835–43. doi: 10.1111/acer.12547
67. Ivester P, Roberts LJ2nd, Young T, Stafforini D, Vivian J, Lees C, et al. Ethanol Self-Administration and Alterations in the Livers of the Cynomolgus Monkey, Macaca Fascicularis. *Alcohol Clin Exp Res* (2007) 31 (1):144–55. doi: 10.1111/j.1530-0277.2006.00276.x
68. Lewis SA, Sureshchandra S, Doratt B, Jimenez VA, Stull C, Grant KA, et al. Transcriptional, Epigenetic, and Functional Reprogramming of Monocytes From Non-Human Primates Following Chronic Alcohol Drinking. *Front Immunol* (2021) 12:724015. doi: 10.3389/fimmu.2021.724015
69. Barr T, Lewis SA, Sureshchandra S, Doratt B, Grant KA, Messaoudi I. Chronic Ethanol Consumption Alters Lamina Propria Leukocyte Response to Stimulation in a Region-Dependent Manner. *FASEB J* (2019) 33(6):7767–77. doi: 10.1096/fj.201802780R
70. Sureshchandra S, Raus A, Jankeel A, Ligh BJK, Walter NAR, Newman N, et al. Dose-Dependent Effects of Chronic Alcohol Drinking on Peripheral Immune Responses. *Sci Rep* (2019) 9(1):7847. doi: 10.1038/s41598-019-44302-3
71. Barr T, Girke T, Sureshchandra S, Nguyen C, Grant K, Messaoudi I. Alcohol Consumption Modulates Host Defense in Rhesus Macaques by Altering Gene Expression in Circulating Leukocytes. *J Immunol* (2016) 196(1):182–95. doi: 10.4049/jimmunol.1501527

72. Asquith M, Pasala S, Engelmann F, Haberthur K, Meyer C, Park B, et al. Chronic Ethanol Consumption Modulates Growth Factor Release, Mucosal Cytokine Production, and microRNA Expression in Nonhuman Primates. *Alcohol Clin Exp Res* (2014) 38(4):980–93. doi: 10.1111/acer.12325
73. Messaoudi I, Asquith M, Engelmann F, Park B, Brown M, Rau A, et al. Moderate Alcohol Consumption Enhances Vaccine-Induced Responses in Rhesus Macaques. *Vaccine* (2013) 32(1):54–61. doi: 10.1016/j.vaccine.2013.10.076
74. Bagby GJ, Stoltz DA, Zhang P, Kolls JK, Brown J, Bohm RPJr., et al. The Effect of Chronic Binge Ethanol Consumption on the Primary Stage of SIV Infection in Rhesus Macaques. *Alcohol Clin Exp Res* (2003) 27(3):495–502. doi: 10.1097/01.ALC.0000057947.57330.BE
75. Winsauer PJ, Moerschbaecher JM, Brauner IN, Purcell JE, Lancaster JRJr., Bagby GJ, et al. Alcohol Unmasks Simian Immunodeficiency Virus-Induced Cognitive Impairments in Rhesus Monkeys. *Alcohol Clin Exp Res* (2002) 26 (12):1846–57. doi: 10.1111/j.1530-0277.2002.tb02492.x
76. Amedee AM, Nichols WA, Robichaux S, Bagby GJ, Nelson S. Chronic Alcohol Abuse and HIV Disease Progression: Studies With the Non-Human Primate Model. *Curr HIV Res* (2014) 12(4):243–53. doi: 10.2174/1570162X12666140721115717
77. Saitz R, Ghali WA, Moskowitz MA. The Impact of Alcohol-Related Diagnoses on Pneumonia Outcomes. *Arch Intern Med* (1997) 157 (13):1446–52. doi: 10.1001/archinte.1997.00440340078008
78. Baum MK, Rafie C, Lai S, Sales S, Page JB, Campa A. Alcohol Use Accelerates HIV Disease Progression. *AIDS Res Hum Retroviruses* (2010) 26(5):511–8. doi: 10.1089/aid.2009.0211
79. Bhattacharya R, Shuhart MC. Hepatitis C and Alcohol: Interactions, Outcomes, and Implications. *J Clin Gastroenterol* (2003) 36(3):242–52. doi: 10.1097/00004836-200303000-00012
80. Lonnroth K, Williams BG, Stadlin S, Jaramillo E, Dye C. Alcohol Use as a Risk Factor for Tuberculosis - A Systematic Review. *BMC Public Health* (2008) 8:289. doi: 10.1186/1471-2458-8-289
81. Bhatty M, Pruett SB, Swiatlo E, Nanduri B. Alcohol Abuse and Streptococcus Pneumoniae Infections: Consideration of Virulence Factors and Impaired Immune Responses. *Alcohol* (2011) 45(6):523–39. doi: 10.1016/j.alcohol.2011.02.305
82. Simet SM, Sisson JH. Alcohol's Effects on Lung Health and Immunity. *Alcohol Res* (2015) 37(2):199–208.
83. Jong GM, Hsiue TR, Chen CR, Chang HY, Chen CW. Rapidly Fatal Outcome of Bacteremic Klebsiella Pneumoniae Pneumonia in Alcoholics. *Chest* (1995) 107(1):214–7. doi: 10.1378/chest.107.1.214
84. Jerrells TR, Pavlik JA, DeVasure J, Vidlak D, Costello A, Strachota JM, et al. Association of Chronic Alcohol Consumption and Increased Susceptibility to and Pathogenic Effects of Pulmonary Infection With Respiratory Syncytial Virus in Mice. *Alcohol* (2007) 41(5):357–69. doi: 10.1016/j.alcohol.2007.07.001
85. Vallecillo G, Perello R, Guerri R, Fonseca F, Torrens M. Clinical Impact of COVID-19 on People With Substance Use Disorders. *J Public Health (Oxf)* (2021) 43(1):9–12. doi: 10.1093/pubmed/fdaa181
86. Ojo AS, Balogun SA, Williams OT, Ojo OS. Pulmonary Fibrosis in COVID-19 Survivors: Predictive Factors and Risk Reduction Strategies. *Pulm Med* (2020) 2020:6175964. doi: 10.1155/2020/6175964
87. Gupta NM, Lindenauer PK, Yu PC, Imrey PB, Haessler S, Deshpande A, et al. Association Between Alcohol Use Disorders and Outcomes of Patients Hospitalized With Community-Acquired Pneumonia. *JAMA Netw Open* (2019) 2(6):e195172. doi: 10.1001/jamanetworkopen.2019.5172
88. Narasimhan P, Wood J, Macintyre CR, Mathai D. Risk Factors for Tuberculosis. *Pulm Med* (2013) 2013:828939. doi: 10.1155/2013/828939
89. Rehm J, Samokhvalov AV, Neuman MG, Room R, Parry C, Lonnroth K, et al. The Association Between Alcohol Use, Alcohol Use Disorders and Tuberculosis (TB). A Systematic Review. *BMC Public Health* (2009) 9:450. doi: 10.1186/1471-2458-9-450
90. Moss M, Bucher B, Moore FA, Moore EE, Parsons PE. The Role of Chronic Alcohol Abuse in the Development of Acute Respiratory Distress Syndrome in Adults. *JAMA* (1996) 275(1):50–4. doi: 10.1001/jama.1996.03530250054027
91. Hyun J, Han J, Lee C, Yoon M, Jung Y. Pathophysiological Aspects of Alcohol Metabolism in the Liver. *Int J Mol Sci* (2021) 22(11):5717. doi: 10.3390/ijms22115717
92. Singal AK, Anand BS. Mechanisms of Synergy Between Alcohol and Hepatitis C Virus. *J Clin Gastroenterol* (2007) 41(8):761–72. doi: 10.1097/MCG.0b013e3180381584
93. Xu HQ, Wang CG, Zhou Q, Gao YH. Effects of Alcohol Consumption on Viral Hepatitis B and C. *World J Clin Cases* (2021) 9(33):10052–63. doi: 10.12998/wjcc.v9.i33.10052
94. Chan C, Levitsky J. Infection and Alcoholic Liver Disease. *Clin Liver Dis* (2016) 20(3):595–606. doi: 10.1016/j.cld.2016.02.014
95. Azar MM, Springer SA, Meyer JP, Altice FL. A Systematic Review of the Impact of Alcohol Use Disorders on HIV Treatment Outcomes, Adherence to Antiretroviral Therapy and Health Care Utilization. *Drug Alcohol Depend* (2010) 112(3):178–93. doi: 10.1016/j.drugalcdep.2010.06.014
96. Yan J, Ouyang J, Isnard S, Zhou X, Harypursat V, Routy JP, et al. Alcohol Use and Abuse Conspires With HIV Infection to Aggravate Intestinal Dysbiosis and Increase Microbial Translocation in People Living With HIV: A Review. *Front Immunol* (2021) 12:741658. doi: 10.3389/fimmu.2021.741658
97. Radek KA, Ranzer MJ, DiPietro LA. Brewing Complications: The Effect of Acute Ethanol Exposure on Wound Healing. *J Leukoc Biol* (2009) 86 (5):1125–34. doi: 10.1189/jlb.0209103
98. Jung MK, Callaci JJ, Lauing KL, Otis JS, Radek KA, Jones MK, et al. Alcohol Exposure and Mechanisms of Tissue Injury and Repair. *Alcohol Clin Exp Res* (2011) 35(3):392–9. doi: 10.1111/j.1530-0277.2010.01356.x
99. Benveniste K, Thut P. The Effect of Chronic Alcoholism on Wound Healing. *Proc Soc Exp Biol Med* (1981) 166(4):568–75. doi: 10.3181/00379727-166-41110
100. Jones JD, Barber B, Engrav L, Heimbach D. Alcohol Use and Burn Injury. *J Burn Care Rehabil* (1991) 12(2):148–52. doi: 10.1097/00004630-199103000-00012
101. Messingham KA, Faunce DE, Kovacs EJ. Alcohol, Injury, and Cellular Immunity. *Alcohol* (2002) 28(3):137–49. doi: 10.1016/S0741-8329(02)00278-1
102. Maier RV. Ethanol Abuse and the Trauma Patient. *Surg Infect (Larchmt)* (2001) 2(2):133–41; discussion 41-4. doi: 10.1089/109629601750469456
103. Jurkovich GJ, Rivara FP, Gurney JG, Fligner C, Ries R, Mueller BA, et al. The Effect of Acute Alcohol Intoxication and Chronic Alcohol Abuse on Outcome From Trauma. *JAMA* (1993) 270(1):51–6. doi: 10.1001/jama.1993.03510010057029
104. Guo S, Dipietro LA. Factors Affecting Wound Healing. *J Dent Res* (2010) 89 (3):219–29. doi: 10.1177/0022034509359125
105. Lewis SA, Doratt B, Sureshchandra S, Jankeel A, Newman N, Shen W, et al. Ethanol Consumption Induces Non-Specific Inflammation and Functional Defects in Alveolar Macrophages. *Am J Respir Cell Mol Biol* (2022). doi: 10.1165/rcmb.2021-0346OC
106. Szabo G, Saha B. Alcohol's Effect on Host Defense. *Alcohol Res* (2015) 37 (2):159–70.
107. Maraslioglu M, Oppermann E, Blattner C, Weber R, Henrich D, Jobin C, et al. Chronic Ethanol Feeding Modulates Inflammatory Mediators, Activation of Nuclear Factor-Kappab, and Responsiveness to Endotoxin in Murine Kupffer Cells and Circulating Leukocytes. *Mediators Inflamm* (2014) 2014:808695. doi: 10.1155/2014/808695
108. Bishehsari F, Magno E, Swanson G, Desai V, Voigt RM, Forsyth CB, et al. Alcohol and Gut-Derived Inflammation. *Alcohol Res* (2017) 38(2):163–71.
109. Mehta AJ, Guidot DM. Alcohol and the Lung. *Alcohol Res* (2017) 38(2):243–54.
110. Mukherjee S. Alcoholism and its Effects on the Central Nervous System. *Curr Neurovasc Res* (2013) 10(3):256–62. doi: 10.2174/15672026113109990004
111. Szabo G, Lippai D. Converging Actions of Alcohol on Liver and Brain Immune Signaling. *Int Rev Neurobiol* (2014) 118:359–80. doi: 10.1016/B978-0-12-801284-0.00011-7
112. Pang M, Bala S, Kodys K, Catalano D, Szabo G. Inhibition of TLR8- and TLR4-Induced Type I IFN Induction by Alcohol is Different From its Effects on Inflammatory Cytokine Production in Monocytes. *BMC Immunol* (2011) 12:55. doi: 10.1186/1471-2172-12-55
113. Underwood ML, Park B, Uebelhoer LS, Gu G, Kunkel LE, Korthuis PT, et al. Chronic Alcohol Exposure Among People Living With HIV Is Associated With Innate Immune Activation and Alterations in Monocyte Phenotype and Plasma Cytokine Profile. *Front Immunol* (2022) 13. doi: 10.3389/fimmu.2022.867937

114. Thakur V, McMullen MR, Pritchard MT, Nagy LE. Regulation of Macrophage Activation in Alcoholic Liver Disease. *J Gastroenterol Hepatol* (2007) 22 Suppl 1:S53–6. doi: 10.1111/j.1440-1746.2006.04650.x
115. Khoruts A, Stahnke L, McClain CJ, Logan G, Allen JI. Circulating Tumor Necrosis Factor, Interleukin-1 and Interleukin-6 Concentrations in Chronic Alcoholic Patients. *Hepatology* (1991) 13(2):267–76. doi: 10.1002/hep.1840130211
116. McClain CJ, Cohen DA. Increased Tumor Necrosis Factor Production by Monocytes in Alcoholic Hepatitis. *Hepatology* (1989) 9(3):349–51. doi: 10.1002/hep.1840090302
117. Bird GL, Sheron N, Goka AK, Alexander GJ, Williams RS. Increased Plasma Tumor Necrosis Factor in Severe Alcoholic Hepatitis. *Ann Intern Med* (1990) 112(12):917–20. doi: 10.7326/0003-4819-112-12-917
118. Weichselbaum L, Azouz A, Smolen KK, Das J, Splittgerber M, Lepida A, et al. Epigenetic Basis for Monocyte Dysfunction in Patients With Severe Alcoholic Hepatitis. *J Hepatol* (2020) 73(2):303–14. doi: 10.1016/j.jhep.2020.02.017
119. Bernsmeier C, Pop OT, Singanayagam A, Triantafyllou E, Patel VC, Weston CJ, et al. Patients With Acute-on-Chronic Liver Failure Have Increased Numbers of Regulatory Immune Cells Expressing the Receptor Tyrosine Kinase MERTK. *Gastroenterology* (2015) 148(3):603–15 e14. doi: 10.1053/j.gastro.2014.11.045
120. Korf H, du Plessis J, van Pelt J, De Groote S, Cassiman D, Verbeke L, et al. Inhibition of Glutamine Synthetase in Monocytes From Patients With Acute-on-Chronic Liver Failure Resuscitates Their Antibacterial and Inflammatory Capacity. *Gut* (2019) 68(10):1872–83. doi: 10.1136/gutjnl-2018-316888
121. Bernsmeier C, Triantafyllou E, Brenig R, Lebosse FJ, Singanayagam A, Patel VC, et al. CD14(+) CD15(-) HLA-DR(-) Myeloid-Derived Suppressor Cells Impair Antimicrobial Responses in Patients With Acute-on-Chronic Liver Failure. *Gut* (2018) 67(6):1155–67. doi: 10.1136/gutjnl-2017-314184
122. Casulleras M, Zhang IW, Lopez-Vicario C, Claria J. Leukocytes, Systemic Inflammation and Immunopathology in Acute-On-Chronic Liver Failure. *Cells* (2020) 9(12):2632. doi: 10.3390/cells9122632
123. Triantafyllou E, Woollard KJ, McPhail MJW, Antoniades CG, Possamai LA. The Role of Monocytes and Macrophages in Acute and Acute-On-Chronic Liver Failure. *Front Immunol* (2018) 9:2948. doi: 10.3389/fimmu.2018.02948
124. Kim A, Bellar A, McMullen MR, Li X, Nagy LE. Functionally Diverse Inflammatory Responses in Peripheral and Liver Monocytes in Alcohol-Associated Hepatitis. *Hepatol Commun* (2020) 4(10):1459–76. doi: 10.1002/hep4.1563
125. Coleman LGJr., Crews FT. Innate Immune Signaling and Alcohol Use Disorders. *Handb Exp Pharmacol* (2018) 248:369–96. doi: 10.1007/164_2018_92
126. O'Halloran EB, Curtis BJ, Afshar M, Chen MM, Kovacs EJ, Burnham EL. Alveolar Macrophage Inflammatory Mediator Expression Is Elevated in the Setting of Alcohol Use Disorders. *Alcohol* (2016) 50:43–50. doi: 10.1016/j.alcohol.2015.11.003
127. He J, Crews FT. Increased MCP-1 and Microglia in Various Regions of the Human Alcoholic Brain. *Exp Neurol* (2008) 210(2):349–58. doi: 10.1016/j.expneurol.2007.11.017
128. Zhu X, Coleman RA, Alber C, Ballas ZK, Waldschmidt TJ, Ray NB, et al. Chronic Ethanol Ingestion by Mice Increases Expression of CD80 and CD86 by Activated Macrophages. *Alcohol* (2004) 32(2):91–100. doi: 10.1016/j.alcohol.2004.01.004
129. D'Souza NB, Nelson S, Summer WR, Deaciuc IV. Alcohol Modulates Alveolar Macrophage Tumor Necrosis Factor-Alpha, Superoxide Anion, and Nitric Oxide Secretion in the Rat. *Alcohol Clin Exp Res* (1996) 20(1):156–63. doi: 10.1111/j.1530-0277.1996.tb01059.x
130. Gustot T, Lemmers A, Moreno C, Nagy N, Quertinmont E, Nicaise C, et al. Differential Liver Sensitization to Toll-Like Receptor Pathways in Mice With Alcoholic Fatty Liver. *Hepatology* (2006) 43(5):989–1000. doi: 10.1002/hep.21138
131. Yin M, Bradford BU, Wheeler MD, Uesugi T, Froh M, Goyert SM, et al. Reduced Early Alcohol-Induced Liver Injury in CD14-Deficient Mice. *J Immunol* (2001) 166(7):4737–42. doi: 10.4049/jimmunol.166.7.4737
132. Kawaratani H, Tsujimoto T, Douhara A, Takaya H, Moriya K, Namisaki T, et al. The Effect of Inflammatory Cytokines in Alcoholic Liver Disease. *Mediators Inflamm* (2013) 2013:495156. doi: 10.1155/2013/495156
133. Wang H, Mehal W, Nagy LE, Rotman Y. Immunological Mechanisms and Therapeutic Targets of Fatty Liver Diseases. *Cell Mol Immunol* (2021) 18 (1):73–91. doi: 10.1038/s41423-020-00579-3
134. Iimuro Y, Gallucci RM, Luster MI, Kono H, Thurman RG. Antibodies to Tumor Necrosis Factor Alfa Attenuate Hepatic Necrosis and Inflammation Caused by Chronic Exposure to Ethanol in the Rat. *Hepatology* (1997) 26 (6):1530–7. doi: 10.1002/hep.510260621
135. Brenner E, Tiwari GR, Kapoor M, Liu Y, Brock A, Mayfield RD. Single Cell Transcriptome Profiling of the Human Alcohol-Dependent Brain. *Hum Mol Genet* (2020) 29(7):1144–53. doi: 10.1093/hmg/ddaa038
136. Qin L, Crews FT. Chronic Ethanol Increases Systemic TLR3 Agonist-Induced Neuroinflammation and Neurodegeneration. *J Neuroinflammation* (2012) 9:130. doi: 10.1186/1742-2094-9-130
137. McCarthy GM, Farris SP, Blednov YA, Harris RA, Mayfield RD. Microglial-Specific Transcriptome Changes Following Chronic Alcohol Consumption. *Neuropharmacology* (2018) 128:416–24. doi: 10.1016/j.neuropharm.2017.10.035
138. Lippai D, Bala S, Petrasek J, Csak T, Levin I, Kurt-Jones EA, et al. Alcohol-Induced IL-1beta in the Brain is Mediated by NLRP3/ASC Inflammasome Activation That Amplifies Neuroinflammation. *J Leukoc Biol* (2013) 94 (1):171–82. doi: 10.1189/jlb.1212659
139. Qin L, He J, Hanes RN, Pluzarev O, Hong JS, Crews FT. Increased Systemic and Brain Cytokine Production and Neuroinflammation by Endotoxin Following Ethanol Treatment. *J Neuroinflammation* (2008) 5:10. doi: 10.1186/1742-2094-5-10
140. Bala S, Petrasek J, Mundkur S, Catalano D, Levin I, Ward J, et al. Circulating microRNAs in Exosomes Indicate Hepatocyte Injury and Inflammation in Alcoholic, Drug-Induced, and Inflammatory Liver Diseases. *Hepatology* (2012) 56(5):1946–57. doi: 10.1002/hep.25873
141. Mandrekar P, Ambade A, Lim A, Szabo G, Catalano D. An Essential Role for Monocyte Chemoattractant Protein-1 in Alcoholic Liver Injury: Regulation of Proinflammatory Cytokines and Hepatic Steatosis in Mice. *Hepatology* (2011) 54(6):2185–97. doi: 10.1002/hep.24599
142. Thakur V, Pritchard MT, McMullen MR, Wang Q, Nagy LE. Chronic Ethanol Feeding Increases Activation of NADPH Oxidase by Lipopolysaccharide in Rat Kupffer Cells: Role of Increased Reactive Oxygen in LPS-Stimulated ERK1/2 Activation and TNF-Alpha Production. *J Leukoc Biol* (2006) 79(6):1348–56. doi: 10.1189/jlb.1005613
143. Kono H, Wheeler MD, Rusyn I, Lin M, Seabra V, Rivera CA, et al. Gender Differences in Early Alcohol-Induced Liver Injury: Role of CD14, NF-Kappab, and TNF-Alpha. *Am J Physiol Gastrointest Liver Physiol* (2000) 278(4):G652–61. doi: 10.1152/ajpgi.2000.278.4.G652
144. Enomoto N, Ikejima K, Bradford BU, Rivera CA, Kono H, Goto M, et al. Role of Kupffer Cells and Gut-Derived Endotoxins in Alcoholic Liver Injury. *J Gastroenterol Hepatol* (2000) 15 Suppl:D20–5. doi: 10.1046/j.1440-1746.2000.02179.x
145. Nagy LE. Recent Insights Into the Role of the Innate Immune System in the Development of Alcoholic Liver Disease. *Exp Biol Med (Maywood)* (2003) 228(8):882–90. doi: 10.1177/153537020322800803
146. Hardesty JE, Warner JB, Song YL, Rouchka EC, McClain CJ, Warner DR, et al. Ileum Gene Expression in Response to Acute Systemic Inflammation in Mice Chronically Fed Ethanol: Beneficial Effects of Elevated Tissue N-3 PUFAs. *Int J Mol Sci* (2021) 22(4):1582. doi: 10.3390/ijms22041582
147. Moschen AR, Adolph TE, Gerner RR, Wieser V, Tilg H. Lipocalin-2: A Master Mediator of Intestinal and Metabolic Inflammation. *Trends Endocrinol Metab* (2017) 28(5):388–97. doi: 10.1016/j.tem.2017.01.003
148. Dai XM, Zong XH, Sylvestre V, Stanley ER. Incomplete Restoration of Colony-Stimulating Factor 1 (CSF-1) Function in CSF-1-Deficient Csf1op/Csf1op Mice by Transgenic Expression of Cell Surface CSF-1. *Blood* (2004) 103(3):1114–23. doi: 10.1182/blood-2003-08-2739
149. Tang Y, Banan A, Forsyth CB, Fields JZ, Lau CK, Zhang LJ, et al. Effect of Alcohol on miR-212 Expression in Intestinal Epithelial Cells and its Potential Role in Alcoholic Liver Disease. *Alcohol Clin Exp Res* (2008) 32(2):355–64. doi: 10.1111/j.1530-0277.2007.00584.x
150. Basuroy S, Sheth P, Mansbach CM, Rao RK. Acetaldehyde Disrupts Tight Junctions and Adherens Junctions in Human Colonic Mucosa: Protection by EGF and L-Glutamine. *Am J Physiol Gastrointest Liver Physiol* (2005) 289(2): G367–75. doi: 10.1152/ajpgi.00464.2004

151. Rao R. Endotoxemia and Gut Barrier Dysfunction in Alcoholic Liver Disease. *Hepatology* (2009) 50(2):638–44. doi: 10.1002/hep.23009
152. Bull-Otterson L, Feng W, Kirpich I, Wang Y, Qin X, Liu Y, et al. Metagenomic Analyses of Alcohol Induced Pathogenic Alterations in the Intestinal Microbiome and the Effect of Lactobacillus Rhamnosus GG Treatment. *PloS One* (2013) 8(1):e53028. doi: 10.1371/journal.pone.0053028
153. Barr T, Sureshchandra S, Ruegger P, Zhang J, Ma W, Borneman J, et al. Concurrent Gut Transcriptome and Microbiota Profiling Following Chronic Ethanol Consumption in Nonhuman Primates. *Gut Microbes* (2018) 9 (4):338–56. doi: 10.1080/19490976.2018.1441663
154. Chen P, Starkel P, Turner JR, Ho SB, Schnabl B. Dysbiosis-Induced Intestinal Inflammation Activates Tumor Necrosis Factor Receptor I and Mediates Alcoholic Liver Disease in Mice. *Hepatology* (2015) 61(3):883–94. doi: 10.1002/hep.27489
155. Canesso MCC, Lacernada NL, Ferreira CM, Goncalves JL, Almeida D, Gamba C, et al. Comparing the Effects of Acute Alcohol Consumption in Germ-Free and Conventional Mice: The Role of the Gut Microbiota. *BMC Microbiol* (2014) 14:240. doi: 10.1186/s12866-014-0240-4
156. Duan Y, Llorente C, Lang S, Brandl K, Chu H, Jiang L, et al. Bacteriophage Targeting of Gut Bacterium Attenuates Alcoholic Liver Disease. *Nature* (2019) 575(7783):505–11. doi: 10.1038/s41586-019-1742-x
157. Nanji AA, Khettry U, Sadrzadeh SM, Yamanaka T. Severity of Liver Injury in Experimental Alcoholic Liver Disease. Correlation With Plasma Endotoxin, Prostaglandin E2, Leukotriene B4, and Thromboxane B2. *Am J Pathol* (1993) 142(2):367–73.
158. Yan AW, Fouts DE, Brandl J, Starkel P, Torralba M, Schott E, et al. Enteric Dysbiosis Associated With a Mouse Model of Alcoholic Liver Disease. *Hepatology* (2011) 53(1):96–105. doi: 10.1002/hep.24018
159. Shao T, Zhao C, Li F, Gu Z, Liu L, Zhang L, et al. Intestinal HIF-1alpha Deletion Exacerbates Alcoholic Liver Disease by Inducing Intestinal Dysbiosis and Barrier Dysfunction. *J Hepatol* (2018) 69(4):886–95. doi: 10.1016/j.jhep.2018.05.021
160. Vergis N, Khamri W, Beale K, Sadiq F, Aletrari MO, Moore C, et al. Defective Monocyte Oxidative Burst Predicts Infection in Alcoholic Hepatitis and Is Associated With Reduced Expression of NADPH Oxidase. *Gut* (2017) 66 (3):519–29. doi: 10.1136/gutjnl-2015-310378
161. Norkina O, Dolganiuc A, Catalano D, Kodys K, Mandrekar P, Syed A, et al. Acute Alcohol Intake Induces SOCS1 and SOCS3 and Inhibits Cytokine-Induced STAT1 and STAT3 Signaling in Human Monocytes. *Alcohol Clin Exp Res* (2008) 32(9):1565–73. doi: 10.1111/j.1530-0277.2008.00726.x
162. Mason CM, Dobard E, Zhang P, Nelson S. Alcohol Exacerbates Murine Pulmonary Tuberculosis. *Infect Immun* (2004) 72(5):2556–63. doi: 10.1128/IAI.72.5.2556-2563.2004
163. Meyerholz DK, Edsen-Moore M, McGill J, Coleman RA, Cook RT, Legge KL. Chronic Alcohol Consumption Increases the Severity of Murine Influenza Virus Infections. *J Immunol* (2008) 181(1):641–8. doi: 10.4049/jimmunol.181.1.641
164. Bermudez LE, Young LS. Ethanol Augments Intracellular Survival of Mycobacterium Avium Complex and Impairs Macrophage Responses to Cytokines. *J Infect Dis* (1991) 163(6):1286–92. doi: 10.1093/infdis/163.6.1286
165. Bautista AP. Chronic Alcohol Intoxication Primes Kupffer Cells and Endothelial Cells for Enhanced CC-Chemokine Production and Concomitantly Suppresses Phagocytosis and Chemotaxis. *Front Biosci* (2002) 7:a117–25. doi: 10.2741/A746
166. Aroor AR, Baker RC. Ethanol Inhibition of Phagocytosis and Superoxide Anion Production by Microglia. *Alcohol* (1998) 15(4):277–80. doi: 10.1016/S0741-8329(97)00129-8
167. Forman HJ, Torres M. Reactive Oxygen Species and Cell Signaling: Respiratory Burst in Macrophage Signaling. *Am J Respir Crit Care Med* (2002) 166(12 Pt 2):S4–8. doi: 10.1164/rccm.2206007
168. Piotrowski WJ, Marczak J. Cellular Sources of Oxidants in the Lung. *Int J Occup Med Environ Health* (2000) 13(4):369–85.
169. Liang Y, Harris FL, Brown LA. Alcohol Induced Mitochondrial Oxidative Stress and Alveolar Macrophage Dysfunction. *BioMed Res Int* (2014) 2014:371593. doi: 10.1155/2014/371593
170. Morris NL, Yeligar SM. Role of HIF-1alpha in Alcohol-Mediated Multiple Organ Dysfunction. *Biomolecules* (2018) 8(4):170. doi: 10.3390/biom8040170
171. Nath B, Levin I, Csak T, Petrasek J, Mueller C, Kodys K, et al. Hepatocyte-Specific Hypoxia-Inducible Factor-1alpha is a Determinant of Lipid Accumulation and Liver Injury in Alcohol-Induced Steatosis in Mice. *Hepatology* (2011) 53(5):1526–37. doi: 10.1002/hep.24256
172. Curtis BJ, Zahs A, Kovacs EJ. Epigenetic Targets for Reversing Immune Defects Caused by Alcohol Exposure. *Alcohol Res* (2013) 35(1):97–113.
173. Bushati N, Cohen SM. microRNA Functions. *Annu Rev Cell Dev Biol* (2007) 23:175–205. doi: 10.1146/annurev.cellbio.23.090506.123406
174. Gao B, Ahmad MF, Nagy LE, Tsukamoto H. Inflammatory Pathways in Alcoholic Steatohepatitis. *J Hepatol* (2019) 70(2):249–59. doi: 10.1016/j.jhep.2018.10.023
175. Jones PA. Functions of DNA Methylation: Islands, Start Sites, Gene Bodies and Beyond. *Nat Rev Genet* (2012) 13(7):484–92. doi: 10.1038/nrg3230
176. Bannister AJ, Kouzarides T. Regulation of Chromatin by Histone Modifications. *Cell Res* (2011) 21(3):381–95. doi: 10.1038/cr.2011.22
177. Lai L, Song Y, Liu Y, Chen Q, Han Q, Chen W, et al. MicroRNA-92a Negatively Regulates Toll-Like Receptor (TLR)-Triggered Inflammatory Response in Macrophages by Targeting MKK4 Kinase. *J Biol Chem* (2013) 288(11):7956–67. doi: 10.1074/jbc.M112.445429
178. Bala S, Marcos M, Kodys K, Csak T, Catalano D, Mandrekar P, et al. Up-Regulation of microRNA-155 in Macrophages Contributes to Increased Tumor Necrosis Factor {Alpha} (TNF{alpha}) Production *via* Increased mRNA Half-Life in Alcoholic Liver Disease. *J Biol Chem* (2011) 286 (2):1436–44. doi: 10.1074/jbc.M110.145870
179. Bala S, Csak T, Kodys K, Catalano D, Ambade A, Furi I, et al. Alcohol-Induced miR-155 and HDAC11 Inhibit Negative Regulators of the TLR4 Pathway and Lead to Increased LPS Responsiveness of Kupffer Cells in Alcoholic Liver Disease. *J Leukoc Biol* (2017) 102(2):487–98. doi: 10.1189/jlb.3A0716-310R
180. Bala S, Szabo G. MicroRNA Signature in Alcoholic Liver Disease. *Int J Hepatol* (2012) 2012:498232. doi: 10.1155/2012/498232
181. Lippai D, Bala S, Csak T, Kurt-Jones EA, Szabo G. Chronic Alcohol-Induced microRNA-155 Contributes to Neuroinflammation in a TLR4-Dependent Manner in Mice. *PloS One* (2013) 8(8):e70945. doi: 10.1371/journal.pone.0070945
182. Bala S, Petrasek J, Csak T, Catalano D, Kodys K, Mundkur S, et al. MicroRNA-155 Regulates Inflammation in Alcoholic Liver Disease *via* Targeting SOCS1 and SHIP1. *J Immunol* (2012) 188(1):54.15.
183. Jager J, Aparicio-Vergara M, Aouadi M. Liver Innate Immune Cells and Insulin Resistance: The Multiple Facets of Kupffer Cells. *J Intern Med* (2016) 280(2):209–20. doi: 10.1111/joim.12483
184. Yin H, Liang X, Jogasuria A, Davidson NO, You M. miR-217 Regulates Ethanol-Induced Hepatic Inflammation by Disrupting Sirtuin 1-Lipin-1 Signaling. *Am J Pathol* (2015) 185(5):1286–96. doi: 10.1016/j.ajpath.2015.01.030
185. Saikia P, Roychowdhury S, Bellos D, Pollard KA, McMullen MR, McCullough RL, et al. Hyaluronic Acid 35 Normalizes TLR4 Signaling in Kupffer Cells From Ethanol-Fed Rats *via* Regulation of Microrna291b and its Target Tollip. *Sci Rep* (2017) 7(1):15671. doi: 10.1038/s41598-017-15760-4
186. Saikia P, Bellos D, McMullen MR, Pollard KA, de la Motte C, Nagy LE. MicroRNA 181b-3p and its Target Importin Alpha5 Regulate Toll-Like Receptor 4 Signaling in Kupffer Cells and Liver Injury in Mice in Response to Ethanol. *Hepatology* (2017) 66(2):602–15. doi: 10.1002/hep.29144
187. Yeligar SM, Mehta AJ, Harris FL, Brown LA, Hart CM. Peroxisome Proliferator-Activated Receptor Gamma Regulates Chronic Alcohol-Induced Alveolar Macrophage Dysfunction. *Am J Respir Cell Mol Biol* (2016) 55(1):35–46. doi: 10.1165/rcmb.2015-0077OC
188. Yeligar SM, Harris FL, Hart CM, Brown LA. Ethanol Induces Oxidative Stress in Alveolar Macrophages *via* Upregulation of NADPH Oxidases. *J Immunol* (2012) 188(8):3648–57. doi: 10.4049/jimmunol.1101278
189. Kim A, Saikia P, Nagy LE. miRNAs Involved in M1/M2 Hyperpolarization Are Clustered and Coordinately Expressed in Alcoholic Hepatitis. *Front Immunol* (2019) 10:1295. doi: 10.3389/fimmu.2019.01295
190. Lewis SA, Doratt B, Sureshchandra S, Pan T, Gonzales SW, Shen W, et al. Profiling of Extracellular Vesicle-Bound miRNA to Identify Candidate Biomarkers of Chronic Alcohol Drinking in Nonhuman Primates. *Alcohol Clin Exp Res* (2022) 46(2):221–31. doi: doi: 10.1111/acer.14760

191. Momen-Heravi F, Saha B, Kodys K, Catalano D, Satishchandran A, Szabo G. Increased Number of Circulating Exosomes and Their microRNA Cargos are Potential Novel Biomarkers in Alcoholic Hepatitis. *J Transl Med* (2015) 13:261. doi: 10.1186/s12967-015-0623-9
192. Hsu SH, Wang B, Kota J, Yu J, Costinean S, Kutay H, et al. Essential Metabolic, Anti-Inflammatory, and Anti-Tumorigenic Functions of miR-122 in Liver. *J Clin Invest* (2012) 122(8):2871–83. doi: 10.1172/JCI63539
193. Xu JJ, Zhu L, Li HD, Du XS, Li JJ, Yin NN, et al. DNMT3a-Mediated Methylation of PSTPIP2 Enhances Inflammation in Alcohol-Induced Liver Injury via Regulating STAT1 and NF-kappaB Pathway. *Pharmacol Res* (2022) 177:106125. doi: 10.1016/j.phrs.2022.106125
194. Li HD, Chen X, Xu JJ, Du XS, Yang Y, Li JJ, et al. DNMT3b-Mediated Methylation of ZSWIM3 Enhances Inflammation in Alcohol-Induced Liver Injury *via* Regulating TRAF2-Mediated NF-kappaB Pathway. *Clin Sci (Lond)* (2020) 134(14):1935–56. doi: 10.1042/CS20200031
195. Momen-Heravi F, Catalano D, Talis A, Szabo G, Bala S. Protective Effect of LNA-anti-miR-132 Therapy on Liver Fibrosis in Mice. *Mol Ther Nucleic Acids* (2021) 25:155–67. doi: 10.1016/j.omtn.2021.05.007
196. Villagra A, Cheng F, Wang HW, Suarez I, Glozak M, Maurin M, et al. The Histone Deacetylase HDAC11 Regulates the Expression of Interleukin 10 and Immune Tolerance. *Nat Immunol* (2009) 10(1):92–100. doi: 10.1038/ni.1673
197. Zhou T, Sun Y, Li M, Ding Y, Yin R, Li Z, et al. Enhancer of Zeste Homolog 2-Catalysed H3K27 Trimethylation Plays a Key Role in Acute-on-Chronic Liver Failure *via* TNF-Mediated Pathway. *Cell Death Dis* (2018) 9(6):590. doi: 10.1038/s41419-018-0670-2
198. Takizawa H, Boettcher S, Manz MG. Demand-Adapted Regulation of Early Hematopoiesis in Infection and Inflammation. *Blood* (2012) 119(13):2991–3002. doi: 10.1182/blood-2011-12-380113
199. Shi X, DeLucia AL, Bao J, Zhang P. Alcohol Abuse and Disorder of Granulopoiesis. *Pharmacol Ther* (2019) 198:206–19. doi: 10.1016/j.pharmthera.2019.03.001
200. Panasiuk A, Kemona A. Bone Marrow Failure and Hematological Abnormalities in Alcoholic Liver Cirrhosis. *Rocz Akad Med Bialymst* (2001) 46:100–5.
201. Latvala J, Parkkila S, Niemela O. Excess Alcohol Consumption is Common in Patients With Cytopenia: Studies in Blood and Bone Marrow Cells. *Alcohol Clin Exp Res* (2004) 28(4):619–24. doi: 10.1097/01.ALC.0000122766.54544.3B
202. Ballard HS. The Hematological Complications of Alcoholism. *Alcohol Health Res World* (1997) 21(1):42–52.
203. Smith C, Gasparetto M, Jordan C, Pollyea DA, Vasiliou V. The Effects of Alcohol and Aldehyde Dehydrogenases on Disorders of Hematopoiesis. *Adv Exp Med Biol* (2015) 815:349–59. doi: 10.1007/978-3-319-09614-8_20
204. Budde R, Hellerich U. Alcoholic Dyshaematopoiesis: Morphological Features of Alcohol-Induced Bone Marrow Damage in Biopsy Sections Compared With Aspiration Smears. *Acta Haematol* (1995) 94(2):74–7. doi: 10.1159/000203977
205. Heermans EH. Booze and Blood: The Effects of Acute and Chronic Alcohol Abuse on the Hematopoietic System. *Clin Lab Sci* (1998) 11(4):229–32.
206. Zhang P, Welsh DA, Siggins RW2nd, Bagby GJ, Raasch CE, Happel KI, et al. Acute Alcohol Intoxication Inhibits the Lineage- C-Kit+ Sca-1+ Cell Response to Escherichia Coli Bacteremia. *J Immunol* (2009) 182(3):1568–76. doi: 10.4049/jimmunol.182.3.1568
207. Shi X, Lin YP, Gao B, Zhang P. Impairment of Hematopoietic Precursor Cell Activation During the Granulopoietic Response to Bacteremia in Mice With Chronic-Plus-Binge Alcohol Administration. *Infect Immun* (2017) 85(11):e00369-17. doi: 10.1128/IAI.00369-17
208. Varlamov O, Bucher M, Myatt L, Newman N, Grant KA. Daily Ethanol Drinking Followed by an Abstinence Period Impairs Bone Marrow Niche and Mitochondrial Function of Hematopoietic Stem/Progenitor Cells in Rhesus Macaques. *Alcohol Clin Exp Res* (2020) 44(5):1088–98. doi: 10.1111/acer.14328

Conflict of Interest: The authors declare that the research was conducted in the absence of any commercial or financial relationships that could be construed as a potential conflict of interest.

Publisher's Note: All claims expressed in this article are solely those of the authors and do not necessarily represent those of their affiliated organizations, or those of the publisher, the editors and the reviewers. Any product that may be evaluated in this article, or claim that may be made by its manufacturer, is not guaranteed or endorsed by the publisher.

frontiers | Frontiers in Immunology

TYPE Review
PUBLISHED 29 August 2022
DOI 10.3389/fimmu.2022.934617

OPEN ACCESS

EDITED BY
Jochen Mattner,
University of Erlangen Nuremberg, Germany

REVIEWED BY
Luc Van Kaer,
Vanderbilt University Medical Center, United States
Barbara L Kee,
The University of Chicago, United States
Hui Peng,
University of Science and Technology of China, China

*CORRESPONDENCE
Derrick R. Samuelson
derrick.samuelson@unmc.edu

†These authors have contributed equally to this work

SPECIALTY SECTION
This article was submitted to Nutritional Immunology, a section of the journal Frontiers in Immunology

RECEIVED 02 May 2022
ACCEPTED 25 July 2022
PUBLISHED 29 August 2022

CITATION
Ruiz-Cortes K, Villageliu DN and Samuelson DR (2022) Innate lymphocytes: Role in alcohol-induced immune dysfunction.
Front. Immunol. 13:934617.
doi: 10.3389/fimmu.2022.934617

Innate lymphocytes: Role in alcohol-induced immune dysfunction

Karla Ruiz-Cortes†, Daniel N. Villageliu† and Derrick R. Samuelson*

College of Medicine, Department of Internal Medicine, Division of Pulmonary, Critical Care and Sleep, University of Nebraska Medical Center, Omaha, NE, United States

Alcohol use is known to alter the function of both innate and adaptive immune cells, such as neutrophils, macrophages, B cells, and T cells. Immune dysfunction has been associated with alcohol-induced end-organ damage. The role of innate lymphocytes in alcohol-associated pathogenesis has become a focus of research, as liver-resident natural killer (NK) cells were found to play an important role in alcohol-associated liver damage pathogenesis. Innate lymphocytes play a critical role in immunity and homeostasis; they are necessary for an optimal host response against insults including infections and cancer. However, the role of innate lymphocytes, including NK cells, natural killer T (NKT) cells, mucosal associated invariant T (MAIT) cells, gamma delta T cells, and innate lymphoid cells (ILCs) type 1–3, remains ill-defined in the context of alcohol-induced end-organ damage. Innate-like B lymphocytes including marginal zone B cells and B-1 cells have also been identified; however, this review will address the effects of alcohol misuse on innate T lymphocytes, as well as the consequences of innate T-lymphocyte dysfunction on alcohol-induced tissue damage.

KEYWORDS

pneumonia, bacteria, alcohol, innate immunity, innate lymphocytes

Introduction

A complete immune response requires optimal and timely responses from both tissue-resident and circulating immune cell populations. Innate immune cells are often found in peripheral tissues and respond to various infectious challenges, cancers, and allergens through the expression of toll-like receptors (TLRs) and limit tissue injury *via* the production of a wide variety of TLR-dependent effectors. However, there is a growing appreciation and understanding of the scope and diversity of tissue-resident lymphocytes in peripheral organs, which suggests that myeloid cells may not be the primary, or only, immune response prior to the initiation of classical adaptive immunity (1). Innate lymphocytes are broken into two distinct groups: innate lymphoid cells (ILCs) and innate-

like T lymphocytes. Innate lymphocytes have been shown to mediate normal host immune responses to various infectious challenges, cancers, and allergens, as well as provide immune regulatory and modulatory effects. Currently, ILCs are classified into five subsets within three major groups: natural killer (NK) cells, ILC1 (group 1), ILC2 (group 2), and ILC3 and LTi cells (group 3) (1). Innate-like T lymphocytes or unconventional T cells are typically classified as gamma delta (γδ) T cells, mucosal associated invariant T cells (MAIT), natural killer T cells (NKT), and invariant natural killer T cells (iNKT) and, similar to ILCs, mediate both immune responses and homeostasis (1). This review will address our current knowledge regarding the effects of alcohol misuse on these innate and innate-like lymphocytes (Figure 1), as well as the consequences of innate lymphocyte dysfunction on alcohol-induced end-organ damage.

Innate lymphocytes: Role and function in immune homeostasis

Innate lymphoid cells

ILCs utilize a variety of germline-encoded activating and inhibitory receptors, as opposed to conventional lymphocytes which express rearranged antigen receptors (2). ILCs are primarily located at epithelial barrier surfaces (i.e., intestine, lung, and skin) but can also be identified in lymphoid and other non-lymphoid tissues (3). ILCs are often classified based on their expression of transcription factors, cell surface markers, cytokines, and effector molecules. Following tissue injury due to infection or inflammation, as well as perturbation to the intestinal commensal microbiota, ILCs produce both proinflammatory and regulatory cytokines to combat the tissue insult (1, 3, 4). Nearly every organ has associated tissue-specific ILCs, which attests to their ability to support many critical functions necessary for immune homeostasis.

Group 1 ILCs

NK cells and type 1 ILCs (ILC1), which are defined based on the secretion of interferon (IFN)-γ, are the prototypical group 1 ILC. Group 1 ILCs are highly responsive to interleukin IL-15, IL-18, and IL-12 and are typically characterized by the expression of the surface receptors NKp46 and NK1.1 (mice) or CD56 (humans) (5). ILC1s are often considered to be more tissue specific/resident than NK cells and express higher levels of CD103, CD49a, and CD69, all of which are considered markers of tissue residency (1). Conversely, NK cells typically express surface markers that facilitate circulation, such as CCR7,

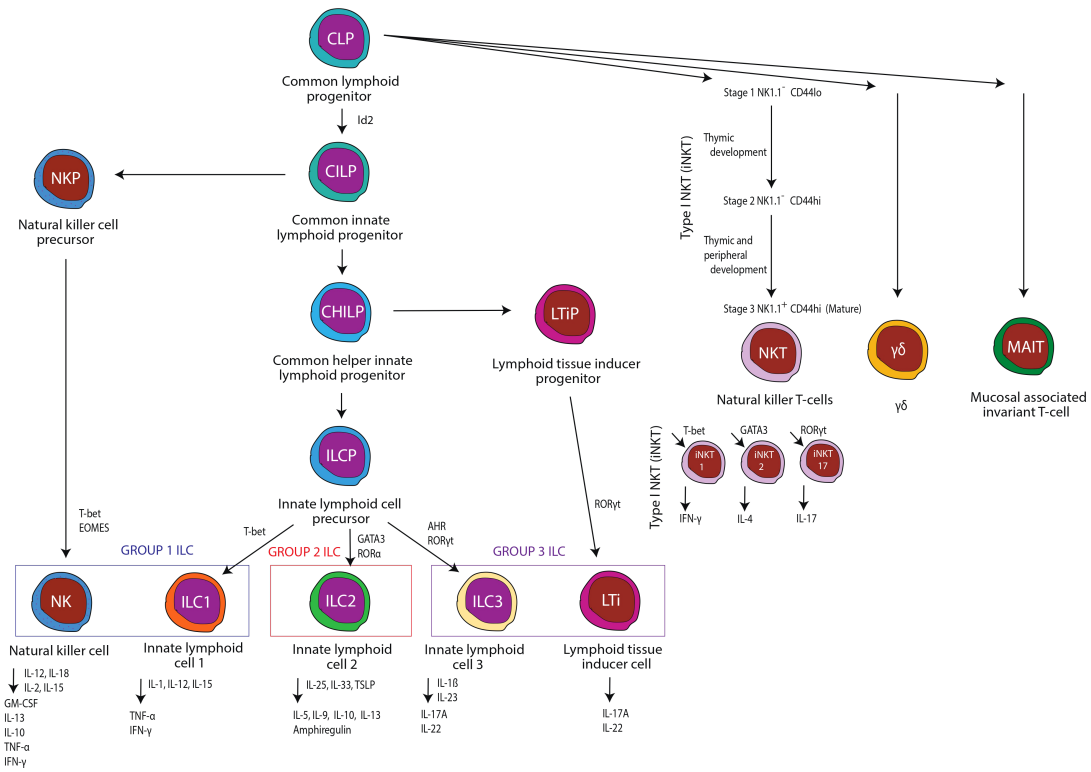

FIGURE 1
An overview of innate and innate-like immune cells examined in this review.

S1PR, and CD62L (6). Likewise, NK cells are more cytolytic than ILC1s, as they have a higher expression of both perforin and granzymes (7). However, ILC1s also have the potential to be cytolytic *via* the production of the tumor necrosis factor-related apoptosis-inducing ligand. Innate lymphoid cell precursor (ILCP) differentiation into ILC1 requires the transcription factors T-bet and Hobit (8, 9); conversely, differentiation of precursor NK cells into mature NK cells is dependent on the transcription factors Eomes and T-bet (10). While these transcription factors are widely accepted for cellular development in rodents, the transcriptional profile for human ILC1s and NK-cell development is less defined. Eome expression is found in intestinal intraepithelial ILC1s (11) but, until recently, was not believed to contribute to liver-resident NK cells (12). Interestingly, however, it has been shown in humans that a liver-resident $Eomes^{hi}$ NK-cell population does exist (13). In fact, it appears that Eomes expression in humans is a factor for NK retention. Cuff et al. examined liver transplants from donors which were HLA mismatched (HLA-A2 or HLA-A3 mismatches). This allowed them to distinguish between donor liver–derived and recipient-derived leucocytes *via* antibody staining for the specific donor-recipient HLA mismatch. They found that $Eomes^{lo}$ NK cells circulate freely whereas $Eomes^{hi}$ NK cells were only observed in the liver and not found in blood samples. Cuff et al. went to further establish that liver NK-cell replenishment from the circulation can occur, possibly *via* $Eomes^{lo}$ NK cells being induced to upregulate Eomes expression. These data suggest that $Eomes^{hi}$ expression may be a characteristic of mature liver NK cells; however, the role of Eomes expression in NK development remains clouded. For example, some authors have described Eomes expression as part of NK-cell development but have also argued that the $Eomes^{hi}$ state is associated with immature NK cells. They argue instead that mature NK cells are more associated with an abundance of T-bet (14). Whatever the case may be, NK cells and ILC1s are best known for their critical role in the normal immune responses to viral infection through secretion of IFN-γ.

Group 2 ILCs

The secretion of the classical type-2 cytokines amphiregulin, IL-13, IL-9, and IL-5 in response to IL-33, IL-25, and TSLP secreted by parenchymal cells is one key defining feature of group 2 ILCs (3, 4, 15). ILC2s are also classically defined by the expression of CRTH2, KLRG1, ST2, and CD25 (16, 17). Interestingly, the expression of CD44 and CD161 on ILC2 seems to differ between mice and humans, as mouse ILC2s are CD44+ CD161-, while human ILC2s are CD44- CD161+ (18). Differentiation from ILCPs into mature ILC2s depends on the transcription factors GATA3 (also required for effector function), RORα, and TCF-1 (19–23). Recently, ILC2s have been sub-characterized *via* their ability to respond to IL-33 (natural ILC2s) and IL-25 (inflammatory ILC2s), or their ability to secrete IL-10 ($ILC2_{10}$) (24–26). The ILC2-mediated secretion of IL-13 and amphiregulin is critical for the repair of tissue damage following helminth or viral infections. IL-13 is also important for host-mediated removal of helminths.

Group 3 ILCs

Group 3 ILCs (innate counterparts of Th17 T cells) typically produce IL-22 and IL-17A following activation by IL-1β and IL-23. Furthermore, ILC3 can also secrete TNF-α and GM-CSF in response to stimulation (27, 28). ILC3 development from ILCPs is primarily driven by three key transcription factors: 1) aryl hydrocarbon receptor (AhR), 2) promyelocytic leukemia zinc finger (PLZF), and 3) retinoid-related orphan receptor γt (RORγt) (29–31). Similarly, lymphoid tissue inducer (LTi) cells, a unique subtype of ILC3s, also require RORγt for differentiation and similarly produce the cytokines IL-22 and IL-17; however, PLZF in not necessary for development (30). Similarly, ILC3s are classified by their expression of NKp46, CD127, c-Kit, and CCR6. However, in mice $CCR6^{+}NKp46^{-}$ LTi cells as well as $CCR6^{-}NKp46^{-}$ and $CCR6^{-}NKp46^{+}$ ILC3 cells have also been described. ILC3 through the production of IL-22 play an integral role in immune homeostasis, by stimulating antimicrobial peptide production by epithelial cells and goblet cell mucus secretion, both of which support barrier integrity. Additionally, the ILC3 secretion of IL-17 and GM-CSF promotes granulopoiesis, the production of neutrophil chemoattractant (32), as well as the generation and survival of myeloid cells, and tolerogenic T cells (27).

Innate-like T lymphocytes

Alongside ILCs, innate-like T lymphocytes participate in host defense against tissue damage or pathogenic insult prior to the adaptive immune response. Unconventional T-cell subsets express restricted T-cell receptor (TCR) sequences. Consequently, unconventional T-cell stimulation occurs independent of the classical major histocompatibility complex (MHC) I and II-dependent presentation of microbial components and/or antigens (33). Like ILCs, the classification of unconventional T cells depends on cytokines, effector molecules, transcription factors, and surface markers (Table 1). Growing evidence supports an important role of unconventional T cells in the early immune response by providing an immediate cellular response and facilitating conventional T-cell responses (33).

Natural killer T cells and invariant natural killer T cells

Presentation of lipid antigens *via* CD1d is the major defining characteristic of NKT cells. NKT cells are classically subdivided into two distinct populations based on the expression of different TCR alpha chains (38–41). Type 1 NKT cells (iNKT cells)

10.3389/fimmu.2022.934617

TABLE 1 Innate-like immune cells: recognized surface markers, effectors, and transcription regulators.

Type of cell	Surface markers	Non-cytokine effectors	Key cytokines	Transcription factors	Citation
MAIT	*αβ* T-cell receptor with a semi-invariant TCR-α chain (usually Vα7.2–Jα33) associated with TCR-β chains *(Vβ2, Vβ13), CD161^{high}, CD3^{+}, CD8α^{+}, MR1*	Perforin, granzyme B	TNF-*α*, interleukin-17, IFN-γ, IL-4, IL-22	RAR-related orphan receptor γt (RORγt), promyelocytic leukemia zinc finger protein (PLZF), and eomesodermin (EOMES)	(34)
ILC-1	NKp46/NCR1, CD56, CD122, NK1.1/CD161, CD49a, CD103, Integrin α1, CXCR6, CXCR3, CD103, CD69, and CD39, CD127/IL-7 receptor α		IFN-γ	T-bet, Hobit	(1, 35)
ILC-2	CRTH2, KLRG1, ST2, CD25, variant CD44, and CD161 expression		IL-5, IL-9, IL-13, amphiregulin	GATA-3, ROR-α, TCF-1	(3, 4, 13, 14, 16, 20, 21)
ILC-3	Nkp44, CD127, c-Kit, and CCR6		IL-17A, IL-22, GM-CSF, TNF-*α*	RORγt, lymphoid tissue inducer (Lti), aryl hydrocarbon receptor (AhR), and promyelocytic leukemia zinc finger	(27, 28, 36, 37)
NKT/iNKT	Invariant TCRα (iNKT), restricted TCRβ chains (iNKT), greater diversity of TCRα and TCRβ chains (type 2 NKT)	Perforin, granzyme B	TNF-α, IFN-γ, IL-17, IL-4		(33, 38–43)

express an invariant TCRα chain and a limited TCRβ profile. Human iNKT cells typically express the TCRα chain Vα24-Jα18, while iNKT cells from mice expresses the TCRα chain Vα14-Jα18. NKT cells also possess cytotoxic capabilities due to the expression of perforin, CD95/CD95 L, and TNF (42). Conversely, type 2 NKT cells express an expanded TCRα and TCRβ profile (40, 43). Alpha-galactosylceramide (α-GalCer), a ceramide lipid attached to a polar galactose head, is a model CD1d antigen. iNKT cells react and expand rapidly in response to α-GalCer, which drives iNKT cells to a classical effector status characterized by the production of key immunoregulatory cytokines. Non-lipid antigen-specific responses in iNKT cells have also been reported; however, most iNKT cells drive innate and adaptive immune responses *via* tumor necrosis factor-α (TNF-α), IFN-γ, IL-17, and IL-4-mediated activation of antigen-presenting cells (APCs). Finally, iNKT cells can also be characterized based on specific cytokines and transcription factors unique to each subset. Specifically, iNKT cells are often subdivided into the following groups: 1) iNKT1 cells, which utilize T-bet and secrete IFN-γ, 2) iNKT2 cells, which are GATA-3 expressing and IL-4 secreting, and 3) iNKT17 cells, which are dependent of RORγt expression and produce IL-17 (44).

Mucosal associated invariant T cells

MAIT cells co-express a semi-invariant TCR alpha (α) and beta (β) chain and CD161. In humans, TCR Vα 7.2-Jα 33/12/20 and Vβ2/13 are the most common TCR αβ chains, while in mice TCR Vα 19-Jα 33 paired with Vβ6/20 classically defines MAIT cells (45, 46). Recognition of vitamin B (riboflavin and folic acid) metabolites *via* presentation through the highly conserved MHC class I-related molecule 1 (MR1) is widely viewed as one of the, if not the, main characteristic of MAIT cells. Upon stimulation, MAIT cells rapidly secrete IFN-γ, TNF-α, IL-2, and IL-17, as well as exhibit cytotoxic effects (45, 47–53). In addition to classical MAIT-cell activation *via* MR1 ligands, MAIT cells can be alternatively activated *via* IL-15, IL-18, and IL-12 without TCR engagement (54–56). RORγt and PLZF are the two key transcription factors for MAIT-cell development (57, 58). Interestingly, there appear to be tissue-specific populations of MAIT cells. For example, MAIT cells derived from the liver generally have higher levels of the tissue residency markers CD69 and CD103, as well as markers of cellular activation CD56, CD38, PD-1, and NKG2D, under normal physiological conditions (54, 55, 59). MAIT cells facilitate immune regulation both during normal physiological conditions and during pathogenic or antigenic insult.

Gamma delta T cells

γδ T cells represent a unique subset of unconventional T cells, as they exhibit characteristics of both innate and adaptive immune cells. For example, following insult γδ T cells respond rapidly and do not require clonal selection or TCR recognition-mediated differentiation (60). Additionally, γδ T cells can be further characterized into distinct populations based on their TCRδ chain expression. γδ T cells that express either the Vδ1 or Vδ2 TCR chain are the two most common populations. These γδ T-cell subsets seem to also display a tissue-specific tropic behavior. Vδ2+ γδ T cells are mainly located in the circulatory system, while Vδ1+ γδ T cells are primarily mucosal-associated (61). Vδ1+ γδ T cells are also long-lived cells that exhibit low levels of CD27 and high levels of granzyme B and CX3CR1 (62). In addition, Vδ1+ γδ T cells also retain their proliferative capacity and TCR sensitivity (62). Likewise, Vδ1+ γδ T cells

secrete IFN-γ and TNF-α, as well as perforin and granzyme B following TCR or CD1d stimulation (60, 62, 63). Recently, Vδ3+ γδ T cells have been described and were found to be enriched with hepatic tissues. These cells are activated by CD1d stimulation, which drives the production of Th1, Th2, and Th17 cytokines. These cells were also demonstrated to exhibit cytotoxic activity (64). γδ T cells play an important role in host defense, especially within mucosal-associated tissues.

Innate lymphocytes: The effects of alcohol misuse

Alcohol use is known to alter the number and function of immune cells, such as macrophages, neutrophils, and T cells. This also appears to be true for innate lymphocytes (Table 2). Immune dysfunction has been associated with alcohol-induced end-organ damage (Figure 2). However, the role of innate lymphocytes remains ill-defined in the context of alcohol-induced end-organ damage. Below, we will highlight our current understanding of the effects of alcohol on innate lymphocyte populations.

Innate lymphoid cells

Group 1 ILCs

Chronic alcohol consumption has been demonstrated to decrease the abundance and function of NK cells in the periphery (65). Zhang et al. demonstrated that following chronic alcohol exposure, NK cells are arrested in their development at the $CD27^{+}CD11b^{+}$ stage (Figure 3). Further, cytotoxic NK cells (cNK) appear to accumulate in the bone marrow with a corresponding drop in the number of cNK cells in tissues (i.e., the spleen, lung, liver, and lymph nodes). Given that cNK cells produce IFN-γ and the cytotoxic effector molecules perforin and granzyme B, it is likely that the impairment of cNK maturation alters the release of IFN-γ and cytotoxic effector molecules, which has further downstream effects/impairments in other components of the innate immune system. Importantly, treatment with IL-15 and IL-15Rα restores the alcohol-mediated impairment of cNK development and maturation. This finding implies that the deleterious effects of alcohol might be traced to an impairment of upstream cells/pathways critical for the secretion of IL-15. For example, IL-15-producing $CD11c^{hi}$ cells in the spleen are

TABLE 2 Innate-like immune cells: their function and known alcohol-related impairments.

Type of cell	General function	Alteration by alcohol	Citation
NK	Cytolytic effector lymphocytes which produce IFN-γ and act to control infection and tumor spread	Decreases the abundance and function of NK cells in the periphery, arrests development at the CD27+ CD11b+ stage, and impairs chemotaxis into inflamed/infected tissues. Alcohol also increases the number of IFN-γ-producing NK cells, while inhibiting the induction of perforin, granzyme A, and granzyme B following IL-2 stimulation.	(65–67)
ILC1	Production of proinflammatory and regulatory cytokines (particularly IFN-γ), maintenance of immune homeostasis. Usually tissue-specific residents.	ILC1 numbers are relatively unaffected by chronic alcohol administration, but ILC1 impairments in alcohol + infection murine models have been previously suggested. Understudied.	(65, 66, 68)
ILC2	Production of proinflammatory and regulatory cytokines (particularly type 2 cytokines). Critical to type 2 inflammation. Of particular importance to lung tissue homeostasis with influences on epithelial barrier integrity, mucus, and airway influence.	Likely dysregulated; however, we found no studies that evaluated the effects of alcohol on ILC2 cells in any tissue.	
ILC3	Production of proinflammatory and regulatory cytokines (particularly IL-22, IL-17A). In the gut, they serve as sentinels involved in maintaining homeostasis and tolerance to commensals while also functioning to prevent invasion by pathogens. The LTi subtype appears important for the long-term maintenance of memory CD4 T cells.	Ethanol impairs secretion of IL-22 from gut ILC3, which was correlated with alcohol-related changes in the composition of the intestinal microbiota and increased intestinal permeability.	(36, 69, 70)
NKT/iNKT	These cells are CD1d-restricted and react to lipid antigenic stimulation within minutes by secreting a wide variety of cytokines. This rapid response time makes these cells important in the early response to infection.	Alcohol increases proliferation and maturation of iNKT cells. These cells secrete IL-10 and IFN-γ which are both altered in alcohol use disorder.	(65, 71, 72)
γδ	Part of early rapid response to insult, these cells have characteristics of both innate and adaptive immune cells but do not require clonal selection or TCR recognition. Cytotoxic.	In a murine model, subsets of dermal γδ T cells (CD3hiVγ3+ and CD3intVγ3-) were diminished. Diminished IL-17 secretion.	(73, 74)
MAIT	MAIT cells react to key microbe-associated molecules (riboflavin) *via* a conserved TCR that recognizes MR1. Though they recognize a more restrictive subset of antigens than other conventional MHC-restricted T cells, their response is more rapid. These cells are a crucial part of the early infection response mounted in peripheral mucosal tissue like the lung and GI tract.	Chronically, alcohol depletes MAIT cells in the liver, GI, and lungs, as well as reduces their antibacterial activity. Alcohol also dysregulates cytokine production following infection in a tissue-specific manner.	(75, 76)

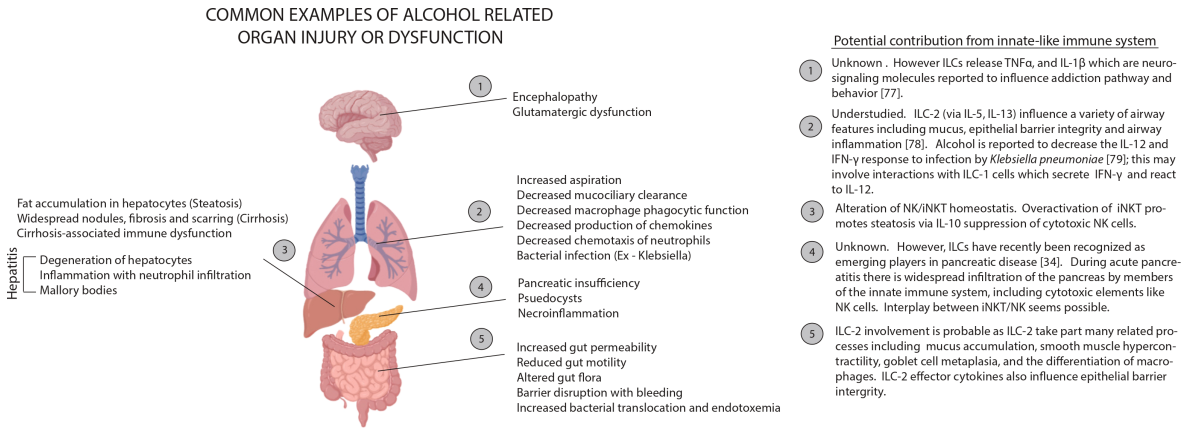

FIGURE 2
Examples of alcohol related organ injury with potential influences from the innate-like immune system. Many tissues rely on processes regulated by innate-like immune signaling to maintain homeostasis. Alcohol can perturb homeostasis by interfering with signal release (ex. decrease in IL-22 release by ILC-3 cells), by depleting or activating regulatory cells (ex. maturation of iNKT and inactivation of NK cells following alcohol exposure) or by interfering with effector cell function. Little has been rigorously established about how broad changes in the innate-like immune system result in tissue damage. However, we can make some informed inferences. Depletion of signals like IL-22 could facilitate injury in tissues like the lungs and small intestines (2, 5) because IL-22 is a fundamental mediator of inflammation, mucous production and tissue regeneration. During necrotic alcohol-associated tissue injuries (3, 4), there is often tissue infiltration by cytolytic elements including NK cells. In a healthy individual, the activity of these cytotoxic elements is kept in check by cytokine signaling by innate-like including iNKT cells. However, alcohol exposure can dysregulate this signaling and periods of hypo- and hyperactive cytolytic activity may result.

significantly decreased following chronic alcohol consumption. However, IL-15 can be produced from a variety of different cells including intestinal epithelial cells, thymic epithelial cells, keratinocytes, macrophages, and dendritic cells (80).

Mice depleted of NK cells by anti-AsGM1 antibody treatment displayed increased hepatic triglyceride levels and decreased serum alanine aminotransferase (ALT) levels following chronic ethanol exposure in mice, suggesting that NK cells mediate, in part, liver steatosis and injury. These data are also consistent with research that suggests that NK activation is beneficial in the short run, by increasing host defense against fibrosis and hepatic steatosis through selective cytotoxic activity. However, it is clear that chronic NK-cell activation contributes to liver damage (81). Cui et al. argued that the hepato-specific effects of NK cells were partially mediated by IFN-γ. IFN-γ downregulated the expression of several genes related to lipogenesis and fatty uptake including *Srebp-1*, *Fas*, *Acc*, *Gpat*, *Scd1*, and *Fat* (82). In addition, IFN-γ genetic knockout mice exhibited significantly more severe steatosis than WT mice. Finally, in recent work from our group we found that mice fed a binge-on-chronic ethanol diet exhibited reduced recruitment of NK cells and T cells to the lungs in response to bacterial pneumonia compared to control mice (83). Importantly, indole or probiotics supplementation restored pulmonary immune cell recruitment (NK cells and T cells) to the lungs of alcohol-fed mice and was dependent on AhR signaling, suggesting that alcohol-mediated intestinal dysbiosis and loss of specific microbial metabolites impairs recruitment of NK cells and T cells to the lungs to combat pathogenic insult (83). While NK-cell numbers and function are detrimentally affected by alcohol, it does not appear to affect the frequency of group I ILC.

In summary, alcohol arrests the development of NK cells in $CD27^{+}CD11b^{+}$ which could contribute to systemic dysregulation *via* interference with NK-driven IFN-γ signaling. Such dysregulation can contribute to the development of alcoholic liver disease, and studies on the depletion of cNK cells (*via* the anti-AsGM1 antibody) show increased steatohepatitis. Interestingly, NK-cell maturation can be rescued by the administration of IL-15 which suggests that IL-15 signaling is disrupted following alcohol administration. However, we have not rigorously identified which specific IL-15 producers are involved.

Group 2 ILCs

To our knowledge, there are no studies that have evaluated the effects of alcohol on ILC2 cells in any tissue. However, it is likely that ILC2s are affected by alcohol and contribute to alcohol-induced end-organ damage. ILC2 are critically important for type 2 inflammation and the regulation of normal host physiological responses, such as eosinophil and mast-cell recruitment, mucus accumulation, smooth-muscle hypercontractility, goblet-cell metaplasia, and the differentiation of macrophages toward an M2 phenotype. Alcohol is known to impair goblet-cell metaplasia and mucus accumulation (84–86), smooth-muscle hypercontractility (87), eosinophil and mast-cell recruitment (88–90), and alternative macrophage activation (91, 92). It follows that ILC2

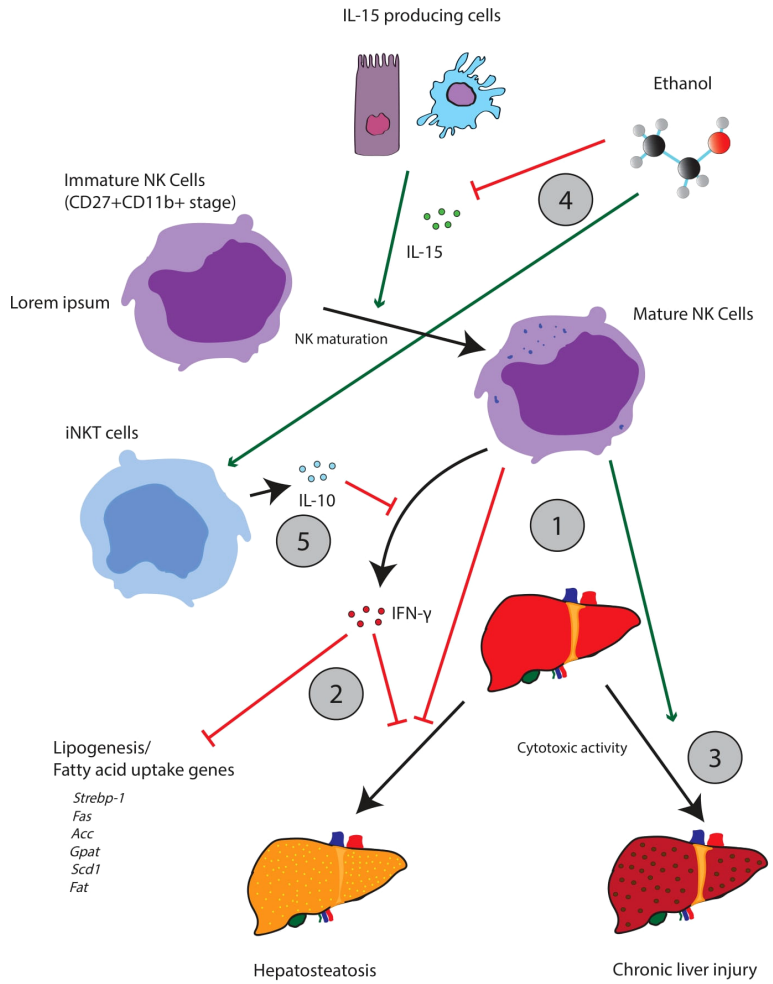

FIGURE 3
The interplay between iNKT cells and NK cells appears central to the pathogenesis of hepatic steatosis and other aspects of alcoholic liver disease. Mature NK cells appear to oppose hepatic steatosis, but also facilitate tissue injury through cytotoxic activity (1). Acutely, NK activity is thought to be beneficial; NK cells release IFN-γ which downregulates a variety of lipogenic and fatty uptake genes (2). NK cells can also promote beneficial remodeling and regeneration of the liver. Chronically however, over activation of NK cells may contribute to liver injury (3). Alcohol can perturb the iNKT/NK cell balance, favoring iNKT cell maturation while suppressing the maturation of NK cells (3). This change can be achieved through a variety of possible mechanisms. For example, ethanol impairs the release of IL-15 which promotes the maturation of NK cells (4). Ethanol can also promote the release of IL-10 from iNKT cells which will suppress NK activity (5).

dysregulation may contribute to alcohol-induced impairment of these processes. However, the role of ILC2 cells in these processes in the context of alcohol use is unknown and primed for future research.

Group 3 ILCs

While ILC3s have become a hot topic in immune research, little is known about the role of ILC3 in alcohol-induced end-organ damage. However, this is an ever-growing interest in the field. To date, only one study has examined the effects of alcohol on ILC3. Specifically, ethanol feeding was found to impair IL-22 production by ILC3s in the gastrointestinal tract (69). Loss of ILC3-mediated IL-22 production was driven by alcohol-associated dysbiosis and reduced levels of indole-3-acetic acid (I3AA). Noteworthily, supplementation of alcohol-fed mice with I3AA protected mice from steatohepatitis *via* increased expression of IL-22 and REG3G, as well as decreased bacterial translocation to the liver (69). Given that the importance of ILC3 in immune homeostasis is continually expanding, it is likely that ILC3 dysregulation may be a contributing factor during alcohol-induced end-organ damage. However, the role of ILC3 cells in the context of alcohol use is still understudied and primed for future research.

Innate-like T lymphocytes

NKT and iNKT cells

The effects of alcohol on traditional NK (discussed above), NKT, and iNKT cells are the most well studied of effects on innate lymphocyte populations. However, given the ever-growing role and understanding of innate lymphocytes, even our knowledge of the effects of alcohol on these cell types is most likely in its infancy. Further, there are differences in the effects of acute and chronic alcohol consumption and there are likely subtle differences in the effects of alcohol across specific iNKT subsets. Broadly speaking, alcohol appears to increase immature iNKT-cell proliferation and maturation in the thymus with a corresponding increase in IFN-γ-producing iNKT-1 cells (65). *In vivo*, this facilitates a Th1-dominant immune response. This activation is interesting as it contrasts strongly to the inhibitory effects that alcohol exhibits on NK cells (discussed above).

Some have hypothesized that NK and iNKT cells may be interlinked through a system of contra-regulation (71). A significant fraction of iNKT cells produce interleukin-10 (IL-10). IL-10 is an interleukin known to antagonize the action of NK cells (72). For example, in contrast to NK-cell activity, iNKT cells promote hepatic steatosis by inhibiting the accumulation of NK cells and the release of IFN-γ (71). In addition, Jα18$^{-/-}$ mice (a knockout model deficient in iNKT cells) demonstrated significantly higher levels of total NK-cell count and IFN-γ release following alcohol exposure, while WT mice exhibited a loss of total NK cells and IFN-γ. Likewise, iNKT-deficient Jα18$^{-/-}$ mice appeared relatively protected from hepatic steatosis, but if these mice were also depleted of their NK cells by using the anti-AsGM1 antibody, alcoholic liver injury steatosis was significantly aggravated. Further, hepatic IL-10 was significantly upregulated, but no changes in TGF-β or IL-4 were noted. As noted above, iNKT cells are known for generating IL-10, which can inhibit NK activation and recruitment. In support of this cross talk, steatosis and liver damage were also alleviated in IL-10 KO mice, presumably *via* the suppression of NK cells.

In summary, alcohol enhances the development of iNKT cells, which promotes a Th1-dominant immune response. The extent to which the altered abundance of iNKT alters host health is unclear. However, dysregulation of iNKT may account for reports of alcohol-related signaling dysfunction involving IL-10 and other iNKT-derived cytokines. There is also evidence that increased iNKT activity promotes alcohol steatosis.

MAIT cells

Alcohol consumption influences MAIT-cell numbers and function through a variety of mechanisms. For example, chronic alcohol use is associated with impaired intestinal transport of riboflavin, as well as other B vitamins (93), which likely contributes to MAIT-cell depletion following chronic alcohol consumption. Work done by Zhang et al. demonstrates that there is a decrease in the abundance of MAIT cells in subjects with chronic alcoholic liver disease (78). Changes in MAIT-cell numbers also appear to depend on chronic ethanol consumption, as changes in MAIT-cell numbers were not observed following short-term binge drinking or short-term abstinence. Furthermore, the levels of peripheral MAIT cells were decreased and exhibited reduced antibacterial activity in subjects with alcoholic cirrhosis or severe alcoholic hepatitis (79). The hepatic expressions of the key transcription factors RORγt, PLZF, and Eomes were all reduced in subjects with severe alcoholic hepatitis (79).

Although alcohol can directly affect immune cells, it is worth noting that alcohol-related effects on intestinal bacterial antigens and/or metabolites, independent of ethanol, can deplete MAIT cells (79), which suggests that impairment in hepatic and circulating MAIT cells in patients with severe alcoholic hepatis is more likely due to chronic exposure to bacteria than to alcohol. Recent studies from our group have found that the number of MAIT cells in the mucosal tissues was significantly decreased in mice following binge-on-chronic alcohol feeding (47). However, CD69 expression was increased following alcohol feeding. Interestingly, the expression levels of Th1-specific cytokines and transcription factors were tissue specific. Th1-specific responses were decreased in the intestinal tract but enhanced in the lung and liver (47). Like previous studies which found a critical association of the gut microbiota with MAIT cells, we found that transplantation of the fecal microbiota from alcohol-fed mice into alcohol-naïve mice resulted in a MAIT-cell profile similar to those seen in our alcohol-feeding model (47). Importantly, the differences observed between MAIT cells from alcohol- and control-fed mice were mitigated by antibiotic treatment. Further, in subjects with alcohol-associated liver disease, as well as in rodent ethanol-feeding models, there is increased intestinal permeability with systemic distribution of bacterial products, such as LPS and bacterially derived riboflavin (94, 95). Riboflavin is known to activate MAIT cells, at least in the short term; however, long-term exposure may lead to MAIT-cell exhaustion, which has been reported in chronic conditions like HIV (96, 97).

In summary, alcohol decreases the function and abundance of MAIT cells. However, these deficiencies are not caused solely by the direct effects of alcohol and its metabolites on the eukaryotic cells of the host. Rather, it appears that alcohol-related changes to the microbiota can produce MAIT-cell dysfunction independent and in addition to changes caused directly by alcohol.

γδ T cells

Like ILC3 cells, there is a paucity of data regarding the effects of alcohol on γδ T cells. Currently, the effects of alcohol on dermal immunological responses, particularly γδ T cells, are the most well

characterized. In a murine model, chronic EtOH feeding leads to a loss of specific subsets of dermal T cells, including Foxp3+ regulatory T cells and both $CD3^{hi}V\gamma3+$ and $CD3^{int}V\gamma3$-γδ T cells (73). EtOH was also correlated with an impaired functional capacity of dermal γδ T cells (the prototypical dermal cells that produce IL-17). Precisely, IL-17 production following anti-CD3 stimulation was significantly reduced in dermal γδ T cells (73). Further, lymph node-associated γδ T cells isolated from EtOH-fed mice also exhibited diminished IL-17 production following stimulation (73). In similar studies, hepatic IL-17A production was found to be cell type specific depending on alcohol exposure. In alcohol-naïve mice, IL-17 is produced primarily by hepatic γδ T cells. However, following acute-on-chronic EtOH consumption, the secretion of IL-17A was shifted to a more $CD4^+$ T-cell mediated response (74). Noteworthily, these results were not seen in TLR3 KO or Kupffer cell-depleted mice, which suggest that TLR3 activation in Kupffer cells leads to an elevated IL-1β expression, thus driving IL-17A secretion by γδ T cells early during alcohol-associated liver disease and increased CD4+ T-cell secretion of IL-17A during the end stage of alcohol-associated liver disease (74).

Discussion

Alcohol is known to impair immune function and perturb immune homeostasis. It follows that organ systems which rely on immune signaling for proper functioning are also impaired. Some systems, like the nervous system may be altered in subtle ways that alter behavior (75). In contrast, systems which directly encounter pathogens from the environment can become more susceptible to infection and injury (76, 77). However, our understanding of the mechanisms by which this occurs remains in its infancy. Multiple researchers have reported that alcohol use can deplete critical cell subpopulations, by impairing cell maturation and chemotaxis. The depletion of these cells can propagate multiple deleterious effects. For example, a depletion of NK cells (cytotoxic, IFN-γ secreting) would be expected to impair immune responses reliant on cytotoxicity; however, NK depletion would also be expected to impact tissue IFN-γ levels and thereby attenuate responses by the adaptive and innate arms of the immune system. Examples of cell depletion and signaling disruption have been reported for many types of innate immune cells. However, it is also worth recognizing that alcohol and alcohol-related metabolites can interact with a variety of lymphocytes in nuanced ways through mechanisms other than cellular depletion. Some cell types, such as MAIT cells, may be mediated through indirect pathways that involve the microbiota. This review was primarily concerned with innate-like T lymphocytes, and therefore, we emphasized examples like the observation that alcohol increases iNKT IL-10 secretion. Consider however that IL-10 signaling is also heavily utilized by innate-like B cells, a group important for IgM and as the first line of defense against infection (98). It would be worth exploring the effects of alcohol on these cells, both in their secretion of IL-10 and in their ability to repel infection. At the time of this review, we found little research discussing the effects of alcohol on innate-like B cells. Overall, research on the effect of alcohol on all innate-like lymphocytes remains underdeveloped.

Author contributions

DV, KR-C, and DS reviewed the literature and wrote the manuscript. All authors contributed to the article and approved the submitted version.

Funding

The work was supported by the National Institute on Alcohol Abuse and Alcoholism Grants: #K99-AA026336 and #R00-AA026336. The content is solely the responsibility of the authors and does not necessarily represent the official views of the National Institutes of Health. The funders had no role in study design, data collection and analysis, decision to publish, or preparation of manuscript.

Conflict of interest

The authors declare that the research was conducted in the absence of any commercial or financial relationships that could be construed as a potential conflict of interest.

Publisher's note

References

1. Vivier E, Artis M, Colonna A, Diefenbach JP, Di Santo G, Eberl S, et al. Innate lymphoid cells: 10 years on. *Cell* (2018) 174(5):1054–66. doi: 10.1016/j.cell.2018.07.017

2. Spits D, Artis M, Colonna A, Diefenbach JP, Di Santo G, Eberl S, et al. Innate lymphoid cells–a proposal for uniform nomenclature. *Nat Rev Immunol* (2013) 13 (2):145–9. doi: 10.1038/nri3365

3. Panda SK, Colonna M. Innate lymphoid cells in mucosal immunity. *Front Immunol* (2019) 10:861. doi: 10.3389/fimmu.2019.00861

4. Castellanos JG, Longman RS. Innate lymphoid cells link gut microbes with mucosal T cell immunity. *Gut Microbes* (2020) 11(2):231–6. doi: 10.1080/19490976.2019.1638725

5. Fuchs A, Vermi JS, Lee S, Lonardi S, Gilfillan RD, Newberry M, et al. Intraepithelial type 1 innate lymphoid cells are a unique subset of IL-12- and IL-15-responsive IFN-gamma-producing cells. *Immunity* (2013) 38(4):769–81. doi: 10.1016/j.immuni.2013.02.010

6. Cortez VS, Robinette ML, Colonna M. Innate lymphoid cells: new insights into function and development. *Curr Opin Immunol* (2015) 32:71–7. doi: 10.1016/j.coi.2015.01.004

7. Bernink JH, Peters CP, Munneke te Velde MAA, Meijer SL, te Velde AA, Weijer K, et al. Human type 1 innate lymphoid cells accumulate in inflamed mucosal tissues. *Nat Immunol* (2013) 14(3):221–9. doi: 10.1038/ni.2534

8. Klose CSN, Flach M, Mohle L., Rogell L, Hoyler T, Ebert K, et al. Differentiation of type 1 ILCs from a common progenitor to all helper-like innate lymphoid cell lineages. *Cell* (2014) 157(2):340–56. doi: 10.1016/j.cell.2014.03.030

9. Mackay LK, Minnich M., Kragten NA, Liao Y, Nota B, Seillet C, et al. Hobit and Blimp1 instruct a universal transcriptional program of tissue residency in lymphocytes. *Science* (2016) 352(6284):459–63. doi: 10.1126/science.aad2035

10. Gordon SM, Chaix J, Rupp LJ, Wu J, Madera S, Sun JC, et al. The transcription factors T-bet and eomes control key checkpoints of natural killer cell maturation. *Immunity* (2012) 36(1):55–67. doi: 10.1016/j.immuni.2011.11.016

11. Bernink JH, Krabbendam L, Germar K., de Jong E, Gronke K, Kofoed-Nielsen M, et al. Interleukin-12 and -23 control plasticity of CD127(+) group 1 and group 3 innate lymphoid cells in the intestinal lamina propria. *Immunity* (2015) 43 (1):146–60. doi: 10.1016/j.immuni.2015.06.019

12. Marquardt N, Beziat S, Nystrom J, Hengst MA, Ivarsson E, Kekalainen H, et al. Cutting edge: identification and characterization of human intrahepatic CD49a+ NK cells. *J Immunol* (2015) 194(6):2467–71. doi: 10.4049/jimmunol.1402756

13. Cuff AO, Robertson FP, Stegmann KA, Pallett LJ, Maini MK, Davidson BR, et al. Eomeshi NK cells in human liver are long-lived and do not recirculate but can be replenished from the circulation. *J Immunol* (2016) 197(11):4283–91. doi: 10.4049/jimmunol.1601424

14. Collins A, Rothman N, Liu K, Reiner SL. Eomesodermin and T-bet mark developmentally distinct human natural killer cells. *JCI Insight* (2017) 2(5):e90063. doi: 10.1172/jci.insight.90063

15. Zwirner NW, Fuertes MB, Domaica CI. Innate lymphoid cells. new players in tissue homeostasis and inflammatory responses. *Medicina (B Aires)* (2019) 79 (Spec 6/1):564–9.

16. Lim AI, Menegatti S, Bustamante J, Le Bourhis L, Allez M, Rogge L, et al. IL-12 drives functional plasticity of human group 2 innate lymphoid cells. *J Exp Med* (2016) 213(4):569–83. doi: 10.1084/jem.20151750

17. Mjosberg JM, Trifari S, Crellin NK, Peters CP, van Drunen CM, Piet Fokkens BWJ, et al. Human IL-25- and IL-33-responsive type 2 innate lymphoid cells are defined by expression of CRTH2 and CD161. *Nat Immunol* (2011) 12 (11):1055–62. doi: 10.1038/ni.2104

18. Hurrell BP, Shafiei Jahani P, Akbari O. Social networking of group two innate lymphoid cells in allergy and asthma. *Front Immunol* (2018) 9:2694. doi: 10.3389/fimmu.2018.02694

19. Halim TY, MacLaren A, Romanish MT, Gold MJ, McNagny KM, Takei F. Retinoic-acid-receptor-related orphan nuclear receptor alpha is required for natural helper cell development and allergic inflammation. *Immunity* (2012) 37 (3):463–74. doi: 10.1016/j.immuni.2012.06.012

20. Yang Q, Monticelli LA, Saenz SA, Chi AW, Sonnenberg GF, Tang J, et al. T Cell factor 1 is required for group 2 innate lymphoid cell generation. *Immunity* (2013) 38(4):694–704. doi: 10.1016/j.immuni.2012.12.003

21. Hoyler T, Klose CS, Souabni A, Turqueti-Neves A, Pfeifer D, Rawlins EL, et al. The transcription factor GATA-3 controls cell fate and maintenance of type 2 innate lymphoid cells. *Immunity* (2012) 37(4):634–48. doi: 10.1016/j.immuni.2012.06.020

22. Yagi R, Zhong C, Northrup DL, Yu F, Bouladoux N, Spencer S, et al. The transcription factor GATA3 is critical for the development of all IL-7Ralpha-expressing innate lymphoid cells. *Immunity* (2014) 40(3):378–88. doi: 10.1016/j.immuni.2014.01.012

23. Mjosberg J, et al. The transcription factor GATA3 is essential for the function of human type 2 innate lymphoid cells. *Immunity* (2012) 37(4):649–59. doi: 10.1016/j.immuni.2012.08.015

24. Seehus CR, et al. Alternative activation generates IL-10 producing type 2 innate lymphoid cells. *Nat Commun* (2017) 8(1):1900. doi: 10.1038/s41467-017-02023-z

25. Huang Y, et al. IL-25-responsive, lineage-negative KLRG1(hi) cells are multipotential 'inflammatory' type 2 innate lymphoid cells. *Nat Immunol* (2015) 16(2):161–9. doi: 10.1038/ni.3078

26. Huang Y, Paul WE. Inflammatory group 2 innate lymphoid cells. *Int Immunol* (2016) 28(1):23–8. doi: 10.1093/intimm/dxv044

27. Mortha A, Chudnovskiy A, Hashimoto D, Bogunovic M, Spencer SP, Belkaid Y, et al. Microbiota-dependent crosstalk between macrophages and ILC3 promotes intestinal homeostasis. *Science* (2014) 343(6178):1249288. doi: 10.1126/science.1249288

28. Cella M, Chudnovskiy A, Hashimoto D, Bogunovic M, Spencer SP, Belkaid Y, et al. A human natural killer cell subset provides an innate source of IL-22 for mucosal immunity. *Nature* (2009) 457(7230):722–5. doi: 10.1038/nature07537

29. Lee JS, Cella M, McDonald KG, Garlanda C, Kennedy GD, Nukaya M, et al. AHR drives the development of gut ILC22 cells and postnatal lymphoid tissues via pathways dependent on and independent of notch. *Nat Immunol* (2011) 13 (2):144–51. doi: 10.1038/ni.2187

30. van de Pavert SA. Lymphoid tissue inducer (LTi) cell ontogeny and functioning in embryo and adult. *BioMed J* (2021) 44(2):123–32. doi: 10.1016/j.bj.2020.12.003

31. Sanos SL, Bui VL, Mortha A, Oberle K, Heners C, Johner C, et al. RORgammat and commensal microflora are required for the differentiation of mucosal interleukin 22-producing NKp46+ cells. *Nat Immunol* (2009) 10(1):83–91. doi: 10.1038/ni.1684

32. Stark MA, Huo Y, Burcin TL, Morris MA, Olson TS, Ley K. Phagocytosis of apoptotic neutrophils regulates granulopoiesis via IL-23 and IL-17. *Immunity* (2005) 22(3):285–94. doi: 10.1016/j.immuni.2005.01.011

33. Godfrey DI, Le Nours J, Andrews DM, Uldrich AP, Rossjohn J. Unconventional T cell targets for cancer immunotherapy. *Immunity* (2018) 48 (3):453–73. doi: 10.1016/j.immuni.2018.03.009

34. Shi S, Ye L, Jin K, Xiao Z, and Yu X, Wu W. Innate lymphoid cells: Emerging players in pancreatic disease. *Int J Mol Sci* (2022) 23(7):3748. doi: 10.3390/ijms23073748

35. Lamichhane R, Schneider M, Harpe SM, Harrop TWR, Hannaway RF, Dearden PK, et al. TCR- or cytokine-activated CD8+ mucosal-associated invariant T cells are rapid polyfunctional effectors that can coordinate immune responses. *Cell Rep* (2019) 28(12):3061–76.e5. doi: 10.1016/j.celrep.2019.08.054

36. Jiao Y, Huntington ND, and Belz GT, Seillet C. Type 1 innate lymphoid cell biology: Lessons learnt from natural killer cells. *Front Immunol* (2016) 7:426–6. doi: 10.3389/fimmu.2016.00426

37. Sawa S, Lochner M, Satoh-Takayama N, Dulauroy S, Bérard M, Kleinschek M, et al. RORγt+ innate lymphoid cells regulate intestinal homeostasis by integrating negative signals from the symbiotic microbiota. *Nat Immunol* (2011) 12(4):320–6. doi: 10.1038/ni.2002

38. Nishioka Y, Masuda S, Tomaru U, Ishizu A. CD1d-restricted type II NKT cells reactive with endogenous hydrophobic peptides. *Front Immunol* (2018) 9:548. doi: 10.3389/fimmu.2018.00548

39. Ambrosino E, Terabe M, Halder RC, Peng J, Takaku S, Miyake S, et al. Cross-regulation between type I and type II NKT cells in regulating tumor immunity: a new immunoregulatory axis. *J Immunol* (2007) 179(8):5126–36. doi: 10.4049/jimmunol.179.8.5126

40. Weng X, He Y, Visvabharathy L, Liao CM, Tan X, Balakumar A, et al. Crosstalk between type II NKT cells and T cells leads to spontaneous chronic inflammatory liver disease. *J Hepatol* (2017) 67(4):791–800. doi: 10.1016/j.jhep.2017.05.024

41. Miko E, Barakonyi A, Meggyes M, Szereday L. The role of type I and type II NKT cells in materno-fetal immunity. *Biomedicines* (2021) 9(12):1901.

42. Berzins SP, Smyth MJ, Baxter AG. Presumed guilty: natural killer T cell defects and human disease. *Nat Rev Immunol* (2011) 11(2):131–42. doi: 10.3390/biomedicines9121901

43. Terabe M, Berzofsky JA. The immunoregulatory role of type I and type II NKT cells in cancer and other diseases. *Cancer Immunol Immunother* (2014) 63 (3):199–213. doi: 10.1007/s00262-013-1509-4

44. Gapin L. Development of invariant natural killer T cells. *Curr Opin Immunol* (2016) 39:68–74. doi: 10.1016/j.coi.2016.01.001

45. Rahimpour A, Koay H.F, Enders A, Clanchy R, Eckle SB, Meehan B, et al. Identification of phenotypically and functionally heterogeneous mouse mucosal-associated invariant T cells using MR1 tetramers. *J Exp Med* (2015) 212(7):1095–108. doi: 10.1084/jem.20142110

46. Martin E, Treiner E, Duban L, Guerri L, Laude H, Toly C, et al. Stepwise development of MAIT cells in mouse and human. *PloS Biol* (2009) 7(3):e54. doi: 10.1371/journal.pbio.1000054

47. Gu M, Samuelson DR, Taylor CM, Molina PE, Luo M, Siggins RW, et al. Alcohol-associated intestinal dysbiosis alters mucosal-associated invariant T-cell phenotype and function. *Alcohol Clin Exp Res* (2021) 45(5):934–47. doi: 10.1111/acer.14589

48. Kulicke C, Karamooz E, Lewinsohn D, Harriff M. Covering all the bases: Complementary MR1 antigen presentation pathways sample diverse antigens and intracellular compartments. *Front Immunol* (2020) 11:2034. doi: 10.3389/fimmu.2020.02034

49. Huang S, et al. Evidence for MR1 antigen presentation to mucosal-associated invariant T cells. *J Biol Chem* (2005) 280(22):21183–93. doi: 10.1074/jbc.M501087200

50. McWilliam HE, Eckle SB, Theodossis A, Liu L, Chen Z, Wubben JM, et al. The intracellular pathway for the presentation of vitamin b-related antigens by the antigen-presenting molecule MR1. *Nat Immunol* (2016) 17(5):531–7. doi: 10.1038/ni.3416

51. McWilliam HE, Villadangos JA. MR1 antigen presentation to MAIT cells: new ligands, diverse pathways? *Curr Opin Immunol* (2018) 52:108–13. doi: 10.1016/j.coi.2018.04.022

52. Huang S, Martin E, Kim S, Yu L, Soudais C, Fremont DH, et al. MR1 antigen presentation to mucosal-associated invariant T cells was highly conserved in evolution. *Proc Natl Acad Sci U.S.A.* (2009) 106(20):8290–5. doi: 10.1073/pnas.0903196106

53. Treiner E, Duban L, Bahram S, Radosavljevic M, Wanner V, Tilloy F, et al. Selection of evolutionarily conserved mucosal-associated invariant T cells by MR1. *Nature* (2003) 422(6928):164–9. doi: 10.1038/nature01433

54. Rha MS, Han JW, Kim JH, Koh JY, Park HJ, et al. Human liver CD8(+) MAIT cells exert TCR/MR1-independent innate-like cytotoxicity in response to IL-15. *J Hepatol* (2020) 73(3):640–50. doi: 10.1016/j.jhep.2020.03.033

55. Jo J, Tan AT, Ussher JE, Sandalova E, Tang XZ, Tan-Garcia A, et al. Toll-like receptor 8 agonist and bacteria trigger potent activation of innate immune cells in human liver. *PloS Pathog* (2014) 10(6):e1004210. doi: 10.1371/journal.ppat.1004210

56. Liu J, Brutkiewicz RR. The toll-like receptor 9 signalling pathway regulates MR1-mediated bacterial antigen presentation in b cells. *Immunology* (2017) 152 (2):232–42. doi: 10.1111/imm.12759

57. Savage AK, Constantinides MG, Han J, Picard D, Martin E, Li B, et al. The transcription factor PLZF directs the effector program of the NKT cell lineage. *Immunity* (2008) 29(3):391–403. doi: 10.1016/j.immuni.2008.07.011

58. Ivanov II, McKenzie BS, Zhou L, Tadokoro CE, Lepelley A, Lafaille JJ, et al. The orphan nuclear receptor RORgammat directs the differentiation program of proinflammatory IL-17+ T helper cells. *Cell* (2006) 126(6):1121–33. doi: 10.1016/j.cell.2006.07.035

59. Tang XZ, Jo J, Tan AT, Sandalova E, Chia A, Tan KC, et al. IL-7 licenses activation of human liver intrasinusoidal mucosal-associated invariant T cells. *J Immunol* (2013) 190(7):3142–52. doi: 10.4049/jimmunol.1203218

60. Bonneville M, O'Brien RL, Born WK. Gammadelta T cell effector functions: a blend of innate programming and acquired plasticity. *Nat Rev Immunol* (2010) 10 (7):467–78. doi: 10.1038/nri2781

61. Davey MS, Willcox CR, Hunter S, Kasatskaya SA, Remmerswaal EBM, Salim M, et al. The human Vdelta2(+) T-cell compartment comprises distinct innate-like Vgamma9(+) and adaptive Vgamma9(-) subsets. *Nat Commun* (2018) 9(1):1760. doi: 10.1038/s41467-018-04076-0

62. Davey MS, Willcox CR, Joyce SP, Ladell K, Kasatskaya SA, McLaren JE, et al. Clonal selection in the human Vdelta1 T cell repertoire indicates gammadelta TCR-dependent adaptive immune surveillance. *Nat Commun* (2017) 8:14760. doi: 10.1038/ncomms14760

63. Hunter S, Willcox CR, Davey MS, Kasatskaya SA, Jeffery HC, Chudakov DM, et al. Human liver infiltrating gammadelta T cells are composed of clonally expanded circulating and tissue-resident populations. *J Hepatol* (2018) 69(3):654–65. doi: 10.1016/j.jhep.2018.05.007

64. Mangan BA, Dunne MR, O'Reilly VP, Dunne PJ, Exley MA, O'Shea D, et al. Cutting edge: CD1d restriction and Th1/Th2/Th17 cytokine secretion by human Vdelta3 T cells. *J Immunol* (2013) 191(1):30–4. doi: 10.4049/jimmunol.1300121

65. Zhang H, Zhang F, Zhu Z, Luong D, Meadows GG. Chronic alcohol consumption enhances iNKT cell maturation and activation. *Toxicol Appl Pharmacol* (2015) 282(2):139–50. doi: 10.1016/j.taap.2014.11.013

66. Zhang F, Little A, Zhang H. Chronic alcohol consumption inhibits peripheral NK cell development and maturation by decreasing the availability of IL-15. *J Leukoc Biol* (2017) 101(4):1015–27. doi: 10.1189/jlb.1A0716-298RR

67. Spitzer JH, Meadows GG. Modulation of perforin, granzyme a, and granzyme b in murine natural killer (NK), IL2 stimulated NK, and lymphokine-activated killer cells by alcohol consumption. *Cell Immunol* (1999) 194(2):205–12. doi: 10.1006/cimm.1999.1511

68. Ito I, Asai A, McCalla CT, Kobayashi M, Suzuki F. A role of lamina propria ILC1 in the impaired host antibacterial resistance of chronic alcohol consuming mice. *J Immunol* (2016) 196(1 Supplement):131.5–5.

69. Hendrikx T, Duan Y, Wang Y, Oh JH, Alexander LM, Huang W, et al. Bacteria engineered to produce IL-22 in intestine induce expression of REG3G to reduce ethanol-induced liver disease in mice. *Gut* (2019) 68(8):1504–15. doi: 10.1136/gutjnl-2018-317232

70. Lane P, Gaspal F, McConnell F, Withers D, Anderson G. Lymphoid tissue inducer cells: Pivotal cells in the evolution of CD4 immunity and tolerance? *Front Immunol* (2012) 3. doi: 10.3389/fimmu.2012.00024

71. Cui K, Yan G, Zheng X, Bai L, Wei H, Sun R, et al. Suppression of natural killer cell activity by regulatory NKT10 cells aggravates alcoholic hepatosteatosis. *Front Immunol* (2017) 8. doi: 10.3389/fimmu.2017.01414

72. Scott MJ, Hoth JJ, Turina M, Woods DR, Cheadle WG. Interleukin-10 suppresses natural killer cell but not natural killer T cell activation during bacterial infection. *Cytokine* (2006) 33(2):79–86. doi: 10.1016/j.cyto.2005.12.002

73. Parlet CP, Waldschmidt TJ, Schlueter AJ. Chronic ethanol feeding induces subset loss and hyporesponsiveness in skin T cells. *Alcohol Clin Exp Res* (2014) 38 (5):1356–64. doi: 10.1111/acer.12358

74. Lee JH, Shim YR, Seo W, Kim MH, Choi WM, Kim HH, et al. Mitochondrial double-stranded RNA in exosome promotes interleukin-17 production through toll-like receptor 3 in alcohol-associated liver injury. *Hepatology* (2020) 72(2):609–25. doi: 10.1002/hep.31041

75. Zhang Y, et al. Persistent deficiency of mucosa-associated invariant T (MAIT) cells during alcohol-related liver disease. *Cell bioscience* (2021) 11 (1):148–8. doi: 10.1186/s13578-021-00664-8

76. Riva A, Patel V, Kurioka A, Jeffery HC, Wright G, Tarff S, et al. Mucosa-associated invariant T cells link intestinal immunity with antibacterial immune defects in alcoholic liver disease. *Gut* (2018) 67(5):918–30. doi: 10.1136/gutjnl-2017-314458

77. Coleman LG Jr., Crews FT. Innate immune signaling and alcohol use disorders. *Handb Exp Pharmacol* (2018) 248:369–96. doi: 10.1007/164_2018_92

78. Bartemes KR, Kita H. Roles of innate lymphoid cells (ILCs) in allergic diseases: The 10-year anniversary for ILC2s. *J Allergy Clin Immunol* (2021) 147 (5):1531–47. doi: 10.1016/j.jaci.2021.03.015

79. Zisman DA, Strieter RM, Kunkel SL, Tsai WC, Wilkowski JM, Bucknell KA, et al. Ethanol feeding impairs innate immunity and alters the expression of Th1- and Th2-phenotype cytokines in murine klebsiella pneumonia. *Alcohol Clin Exp Res* (1998) 22(3):621–7. doi: 10.1111/j.1530-0277.1998.tb04303.x

80. Santana Carrero RM, Beceren-Braun F, Rivas SC, Hegde SM, Gangadharan A, Plote D, et al. IL-15 is a component of the inflammatory milieu in the tumor microenvironment promoting antitumor responses. *Proc Natl Acad Sci* (2019) 116 (2):599–608. doi: 10.1073/pnas.1814642116

81. Tosello-Trampont A, Surette FA, Ewald SE, Hahn YS. Immunoregulatory role of NK cells in tissue inflammation and regeneration. *Front Immunol* (2017) 8. doi: 10.3389/fimmu.2017.00301

82. Cui K, Yan G, Xu C, Chen Y, Wang J, Zhou R, et al. Invariant NKT cells promote alcohol-induced steatohepatitis through interleukin-1beta in mice. *J Hepatol* (2015) 62(6):1311–8. doi: 10.1016/j.jhep.2014.12.027

83. Samuelson DR, Gu M, Shellito JE, Molina PE, Taylor CM, Luo M, et al. Pulmonary immune cell trafficking promotes host defense against alcohol-associated klebsiella pneumonia. *Commun Biol* (2021) 4(1):997. doi: 10.1038/s42003-021-02524-0

84. Hartmann P, Chen P, Wang HJ, Wang L, McCole DF, Brandl K, et al. Deficiency of intestinal mucin-2 ameliorates experimental alcoholic liver disease in mice. *Hepatology* (2013) 58(1):108–19. doi: 10.1002/hep.26321

85. Brozinsky S, Fani K, Grosberg SJ, Wapnick S. Alcohol ingestion-induced changes in the human rectal mucosa: light and electron microscopic studies. *Dis Colon Rectum* (1978) 21(5):329–35. doi: 10.1007/BF02586661

86. Grewal RK, Mahmood A. The effects of ethanol administration on brush border membrane glycolipids in rat intestine. *Alcohol* (2010) 44(6):515–22. doi: 10.1016/j.alcohol.2010.07.008

87. Alleyne J, Dopico AM. Alcohol use disorders and their harmful effects on the contractility of skeletal, cardiac and smooth muscles. *Adv Drug Alcohol Res* (2021) 1:10011. doi: 10.3389/adar.2021.10011

88. Draberova L, Paulenda T, Halova I, Potuckova L, Bugajev V, Bambouskova M, et al. Ethanol inhibits high-affinity immunoglobulin e receptor (FcepsilonRI) signaling in mast cells by suppressing the function of FcepsilonRI-cholesterol signalosome. *PloS One* (2015) 10(12):e0144596. doi: 10.1371/journal.pone.0144596

89. Nishida K, Yamasaki S, Ito Y, Kabu K, Hattori K, Tezuka T, et al. Fc{epsilon}RI-mediated mast cell degranulation requires calcium-independent microtubule-dependent translocation of granules to the plasma membrane. *J Cell Biol* (2005) 170 (1):115–26. doi: 10.1083/jcb.200501111

90. Toivari M, Maki T, Suutarla S, Eklund KK. Ethanol inhibits IgE-induced degranulation and cytokine production in cultured mouse and human mast cells. *Life Sci* (2000) 67(23):2795–806. doi: 10.1016/S0024-3205(00)00863-8

91. Brown SD, Brown LA. Ethanol (EtOH)-induced TGF-beta1 and reactive oxygen species production are necessary for EtOH-induced alveolar macrophage dysfunction and induction of alternative activation. *Alcohol Clin Exp Res* (2012) 36 (11):1952–62. doi: 10.1111/j.1530-0277.2012.01825.x

92. Pan XY, Wang L, You HM, Cheng M, Yang Y, Huang C. Alternative activation of macrophages by prostacyclin synthase ameliorates alcohol induced liver injury. *Lab Invest* (2021) 101(9):1210–24. doi: 10.1038/s41374-021-00531-7

93. Subramanian VS, Subramanya SB, Ghosal A, Said HM. Chronic alcohol feeding inhibits physiological and molecular parameters of intestinal and renal

riboflavin transport. American journal of physiology. *Cell Physiol* (2013) 305(5): C539–46. doi: 10.1152/ajpcell.00089.2013

94. Parlesak A, Schäfer C, Schütz T, Bode JC, Bode C. Increased intestinal permeability to macromolecules and endotoxemia in patients with chronic alcohol abuse in different stages of alcohol-induced liver disease. *J Hepatol* (2000) 32 (5):742–7. doi: 10.1016/S0168-8278(00)80242-1

95. Bode C, Kugler V, Bode JC. Endotoxemia in patients with alcoholic and non-alcoholic cirrhosis and in subjects with no evidence of chronic liver disease following acute alcohol excess. *J Hepatol* (1987) 4(1):8–14. doi: 10.1016/S0168-8278 (87)80003-X

96. Leeansyah E, Ganesh A, Quigley MF, Sönnerborg A, Andersson J, Hunt PW, et al. Activation, exhaustion, and persistent decline of the antimicrobial MR1-restricted MAIT-cell population in chronic HIV-1 infection. *Blood* (2013) 121 (7):1124–35. doi: 10.1182/blood-2012-07-445429

97. Rodin W, Sundström P, Ahlmanner F, Szeponik L, Zajt KK, Wettergren Y, et al. Exhaustion in tumor-infiltrating mucosal-associated invariant T (MAIT) cells from colon cancer patients. *Cancer Immunol Immunother* (2021) 70(12):3461–75. doi: 10.1007/s00262-021-02939-y

98. Zhang X. Regulatory functions of innate-like b cells. *Cell Mol Immunol* (2013) 10(2):113–21. doi: 10.1038/cmi.2012.63

frontiers | Frontiers in Immunology

TYPE Brief Research Report
PUBLISHED 05 April 2023
DOI 10.3389/fimmu.2023.1128352

OPEN ACCESS

EDITED BY
Samantha Yeligar,
Emory University, United States

REVIEWED BY
Liz Simon,
Louisiana State University, United States
Rachel McMahan,
University of Colorado Anschutz Medical Campus, United States

*CORRESPONDENCE
Frederico Marianetti Soriani
fredsori@icb.ufmg.br

SPECIALTY SECTION
This article was submitted to Nutritional Immunology, a section of the journal Frontiers in Immunology

RECEIVED 20 December 2022
ACCEPTED 06 March 2023
PUBLISHED 05 April 2023

CITATION
Pontes Pereira TT, Fideles Duarte-Andrade F, Gardone Vitório J, do Espírito Santo Pereira T, Braga Martins FR, Marques Souza JA, Malacco NL, Mathias Melo E, Costa Picossi CR, Pinto E, Santiago Gomez R, Martins Teixeira M, Nori de Macedo A, André Bautista Canuto G and Soriani FM (2023) Chronic alcohol administration alters metabolomic profile of murine bone marrow. *Front. Immunol.* 14:1128352. doi: 10.3389/fimmu.2023.1128352

Chronic alcohol administration alters metabolomic profile of murine bone marrow

Tássia Tatiane Pontes Pereira[1], Filipe Fideles Duarte-Andrade[2], Jéssica Gardone Vitório[2], Taiane do Espírito Santo Pereira[3], Flavia Rayssa Braga Martins[1], Jéssica Amanda Marques Souza[1], Nathália Luisa Malacco[4], Eliza Mathias Melo[5], Carolina Raíssa Costa Picossi[6], Ernani Pinto[7], Ricardo Santiago Gomez[2], Mauro Martins Teixeira[5], Adriana Nori de Macedo[8], Gisele André Baptista Canuto[3] and Frederico Marianetti Soriani[1]*

[1]Department of Genetics, Ecology and Evolution, Universidade Federal de Minas Gerais, Belo Horizonte, Brazil, [2]Department of Clinic, Pathology and Dental Surgery, Universidade Federal de Minas Gerais, Belo Horizonte, Brazil, [3]Department of Analytical Chemistry of the Institute of Chemistry, Universidade Federal da Bahia, Salvador, Brazil, [4]Department of Microbiology and Immunology, McGill University, Montreal, QC, Canada, [5]Department of Biochemistry and Immunology, Federal University of Minas Gerais, Belo Horizonte, Brazil, [6]Chemistry Institute, University of São Paulo, São Paulo, Brazil, [7]Nuclear Energy Center in Agriculture, Escola Superior de Agricultura Luiz de Queiroz, University of São Paulo, Piracicaba, Brazil, [8]Chemistry Department, Universidade Federal de Minas Gerais, Belo Horizonte, Brazil

Introduction: People with hazardous alcohol use are more susceptible to viral, bacterial, and fungal infections due to the effect of alcohol on immune system cell function. Metabolized ethanol reduces NAD^+ to NADH, affecting critical metabolic pathways. Here, our aim was to investigate whether alcohol is metabolized by bone marrow cells and if it impacts the metabolic pathways of leukocyte progenitor cells. This is said to lead to a qualitative and quantitative alteration of key metabolites which may be related to the immune response.

Methods: We addressed this aim by using C57BL/6 mice under chronic ethanol administration and evaluating the metabolomic profile of bone marrow total cells by gas chromatography–coupled mass spectrometry (GC–MS).

Results: We identified 19 metabolites. Our data demonstrated that chronic ethanol administration alters the metabolomic profile in the bone marrow, resulting in a statistically diminished abundance of five metabolites in ethanol-treated animals: uracil, succinate, proline, nicotinamide, and tyrosine.

Discussion: Our results demonstrate for the first time in the literature the effects of alcohol consumption on the metabolome content of hematopoietic tissue and open a wide range of further studies to investigate mechanisms by which alcohol compromises the cellular function of the immune system.

KEYWORDS

alcoholism, bone marrow, metabolome, cell function, metabolites, immune system

1 Introduction

Alcohol use disorder (AUD) is characterized by an impaired ability to stop or control alcohol use, despite adverse social, occupational, or health consequences. AUD is one of the most common psychiatric disorders and is a leading cause of mortality worldwide (1).

Considerable evidence indicates that alcohol abuse results in clinical abnormalities of the immune system (2, 3). Hematopoietic stem cells differentiate into myeloid progenitor cells, which are the precursor cells of granulocytes, the major type of phagocyte, constituting the front line of innate immune defense (4, 5).

Multiple lines of clinical and experimental evidence demonstrate that chronic alcohol consumption is linked to increased risks of infections, such as pneumonia. This effect has been related to alcohol's effect on the immune system (6, 7), such as alterations in the production of bone marrow immune cells and impairment of their effector functions (3, 5).

Although there is a vast literature describing the effect of alcohol on the immune system (2, 3), there is a limitation in our understanding of the effect of alcohol on the bone marrow, and it is not known whether the cells of this system are affected by alcohol in the bloodstream or if this deleterious effect occurs inside the bone marrow microenvironment.

The majority of ingested alcohol is metabolized in the liver by hepatocytes, but immune cells such as macrophages and neutrophils can also metabolize it (8). Regardless of cell type, alcohol metabolism involves the action of alcohol dehydrogenase (ADH) and aldehyde dehydrogenase (ALDH2). The ADH enzyme is present in the cytoplasm of cells and is responsible for the oxidation reaction of ethanol that results in acetaldehyde. ADH2 is present in the mitochondria and converts acetaldehyde to acetate. These reactions involve the reduction of nicotinamide adenine dinucleotide (NAD^+) to NADH, increasing the NADH : NAD^+ ratio, and leading to a cellular environment vulnerable to damages caused by metabolites and adducts from ethanol metabolism and reactive oxygen species (ROS) (9).

The NADH : NAD^+ ratio is an important parameter for the maintenance of several metabolic enzymes, and its disbalance is known to disturb cell metabolism (10), such as decreased glycolysis (11), decreased Krebs cycle (12, 13), and decreased gluconeogenesis (13, 14).

Immune cells have distinct metabolic configurations that allow them to balance energy demands and molecular biosynthesis. However, beyond that, it is now becoming clear that cellular metabolism has direct roles in regulating immune cell function, and disturbances in these metabolic configurations limit the functionality of these cells (15–17). The field of immunometabolism has advanced our understanding of how cell metabolism plays a central role in cell function, such as phagocytosis, ROS production, cell differentiation/maturation, and consequent host defenses (18–20).

In this study, we applied a metabolomic approach using gas chromatography–mass spectrometry (GC–MS) to characterize metabolic changes in the bone marrow microenvironment to test the hypothesis that alcohol could change metabolic pathways in the bone marrow and leukocyte progenitor cells, leading to a qualitative and quantitative alteration of metabolites that may be directly or indirectly related to the immune response.

We obtained a snapshot of the distinct changes in the metabolite composition of bone marrow cellular content in mice chronically exposed to ethanol. The identified metabolites suggest that chronic alcohol consumption would disrupt several metabolic pathways, such as glycolysis, the Krebs cycle, and amino acid synthesis, that could interfere with immune cell function.

Our results represent the first step toward understanding the dysfunction of the immune system due to alcohol consumption because of bone marrow microenvironment alteration of metabolite content.

2 Methods

2.1 Ethics statement and mouse model of chronic ethanol consumption

Animal experiments received approval from the Animal Ethics Committee (CEUA) of the Universidad Federal de Minas Gerais (UFMG), Brazil (Protocol 337/2018), which is in accordance with Brazilian guidelines (CONCEA) and international standards. Six-week-old male C57BL/6J mice were divided into EtOH and H_2O groups and maintained in specific pathogen-free conditions. Animals in the EtOH group received ethanol at a rate of 5% (v/v) in the first week, followed by 10% (v/v) in the second week, and were treated for 10 weeks with 20% (v/v) of ethanol in their drinking water. The H_2O group received water. This model, standardized by Yeligar et al. (21), generates similar blood alcohol levels to those observed in humans under chronic consumption.

2.2 Sample preparation for flow cytometry

Bone marrow was harvested from the femurs of six animals in each group using 0.5% BSA in 1× phosphate buffered saline (PBS). A sample for the ethanol group was lost during analysis. Total bone marrow cells were subjected to hypotonic lysis to remove residual erythrocytes. The samples were filtered in a 40 µm cell strainer, centrifuged, resuspended in 0.5% BSA in 1× PBS, fixed with 1× PBS solution containing 4% formaldehyde for 20 min, and then the cells in 0.5% BSA in 1× PBS were subjected to flow cytometry analysis on the FACSCanto II cytometer (Becton Dickinson). The relevant population was gated using accepted criteria for cell complexity and size, excluding debris and singlets (Supplementary Figure 1). FSC and SSC plots were assessed using FlowJo software (Tree Star, Ashland, OR, USA). Graphing and statistical analyses were performed using GraphPad Prism 8. Differences between different groups were analyzed by a student t-test.

2.3 Sample preparation for GC–MS

Approximately 3×10^7 total bone marrow cells were obtained from three animals pooling samples for each group (H_2O and

EtOH) (n = 8 pools per group). Bone marrow was harvested from the femur and tibia using phosphate buffered saline (PBS). Red blood cells were lysed by osmotic shock. Metabolic quenching was performed using a cooling bath (dry ice/alcohol), and samples containing 1×10^7 cells were centrifuged for 10 min at 225*g* at 4°C, and the completely dry cell pellet was stored in a −80°C freezer for further extraction of metabolites.

2.4 Metabolite extraction and GC–MS system

Metabolite extraction was performed according to modifications to the protocol described by Canuto et al. (22). Technical replicates of 1×10^7 bone marrow cells were produced. Metabolites were extracted with 300 µl of extraction solvent containing methanol:chloroform:water 1:3:1 (v/v/v) followed by 2 min in a vortex mixer, four cycles of freezing and thawing in liquid nitrogen, and centrifugation for 10 min at 16,000*g* at 4°C. The entire supernatant was transferred to the glass insert and completely dried in the vacuum concentrator SpeedVac at 35°C.

Methoximation was performed by adding 20 µl of methoxyamine to pyridine (15 mg/ml). The vials were placed in an ultrasound bath for 10 s, followed by vigorous vortexing for 10 s. The samples were then incubated for 90 min at room temperature and protected from light. For silylation, 20 µl of BSTFA with 1% TCMS were added. The samples were again subjected to an ultrasound bath for 10 s, followed by vigorous vortexing for 10 s. The reaction was processed in a thermostatic bath for 30 min at 40°C. Finally, 100 µl of heptane containing an internal standard (methyl tridecanoate) was added to each sample.

Samples, QCs (quality controls), and a blank were derivatized according to the protocol described above. Samples were analyzed randomly, and QCs were analyzed at the beginning, every five samples, and at the end of the analytical sequence.

For the construction of the identification library, data were corrected for the retention times of hydrocarbon patterns (FAME MIX). Metabolites detected in the blank were removed from the final result.

The analyses were performed in a gas chromatography system (model 5975C, Agilent Technologies) coupled to a quadrupole mass spectrometer (model 7890A, Agilent Technol). A HP5-MS column (30 m, 0.25 i.d., 0.25 mm film, 95% dimethyl/5% diphenylpolysiloxane—Agilent Technologies) was used to perform the separation of the metabolites. High-purity helium was used as a mobile phase at a 1 ml/min flow rate. The injector was maintained at 250°C, and samples were injected with a 1:10 split at 10 ml/min of He. The oven was initially set at 60°C and held for 1 min, and the temperature increased to 300°C at 10°C/min, resulting in 25 min of run time.

The MS was operated in scan mode (50–600 *m/z*). An electron impact ionization source was placed at −70 eV. Detector transfer line, source filament, and quadrupole temperatures are maintained at 290, 230, and 150°C, respectively. Operation and data acquisition using Qualitative Analysis Mass Hunter B05.00 (Agilent Technologies) software.

2.5 GC–MS data processing and statistical analysis

Raw data were converted to *.mzData in Qualitative Analysis software (B.05.00, Agilent Technologies), and the profiles were checked for outlier removal. An optimization of data extraction and processing parameters was performed using the IPO package (isotopologue parameter optimization, version 1.16.0), using QC samples to find the best conditions. Data processing was performed in XCMS software (version 1.24.1) running on the R platform (version 3.2.3, R Core Team). The optimized parameters were as follows: "Matched Filter" method for peak detection using peak width (fwhm) = 7.2, signal/noise ratio (snthresh) = 1.0, minimum difference between m/z's for overlapping peaks (mzdiff) = 0.36, and maximum number of peaks per extracted ion chromatogram (max) = 5. The grouping step used bandwidth correction (bw) = 0.9, width of overlapping bands of m/z (mzwid) = 0.061, minimum number of samples needed in at least one of the sample groups to be a valid group (minsamp) = 1, minimum fraction of detected samples (minfrac) = 0.5, and maximum number of peaks per extracted ion chromatogram (max) = 50 (in the first and second groupings). Alignment using retention time correction was performed using the "obiwarp" method. FillPeaks were applied to remove missing values, and the extracted molecular features (*m/z* ratios, retention times, and intensities) were normalized before statistical analysis. The raw data matrix consisted of eight samples per group, with each sample presenting the average intensity of the referred molecular feature.

Multivariate statistical analyses were performed on the MetaboAnalyst 5.0 platform, in which the data matrix of identified metabolites was normalized by the internal standard, C13 methyl tridecanoate (*m/z* 74, RT 13.73 min), and log transformation and Pareto scaling were also applied. To evaluate instrumental stability, principal component analysis (PCA) was applied, followed by partial least squares discriminant analysis (PLS-DA) to indicate metabolite differences between groups (ethanol *vs.* control), in which a VIP score >1.0 from PLS-DA was used to select discriminants.

2.6 Metabolite annotation

Metabolite annotation was performed in AMDIS (Automated Mass Spectral Deconvolution and Identification System) software using the Fiehn RT Library. Metabolites were annotated based on retention time and mass spectral fragmentation pattern. To do that, retention indexing followed by retention time analysis were performed. The annotated metabolites were then correlated with the raw data matrix extracted from XCMS.

3 Results

3.1 Chronic ethanol consumption does not affect the size and complexity of the bone marrow cells from mice

To assess whether cell number is a suitable parameter for normalization of samples in the study, we evaluated the general

profile of cells by flow cytometry using the complexity (SSC-A) and size (FSC-A) parameters. The gating strategy was able to select around 91% of total bone marrow cells in both experimental groups (Supplementary Figure 1). Figures 1A, B show representative FSC-A and SSC-A histograms from water-treated animals, while Figures 1C, D show representative FSC-A and SSC-A histograms from ethanol-treated animals. Overlapping the histograms (FSC-A in Figure 1E and SSC-A in Figure 1F) demonstrates similar distributions of cells in each parameter. To quantify the distribution of sizes and complexities of cells in both groups, we analyzed the area under the curve (AUC) and the results demonstrated that ethanol treatment did not change the distribution of cell sizes (Figure 1G) or cell complexities (Figure 1H) in the bone marrow.

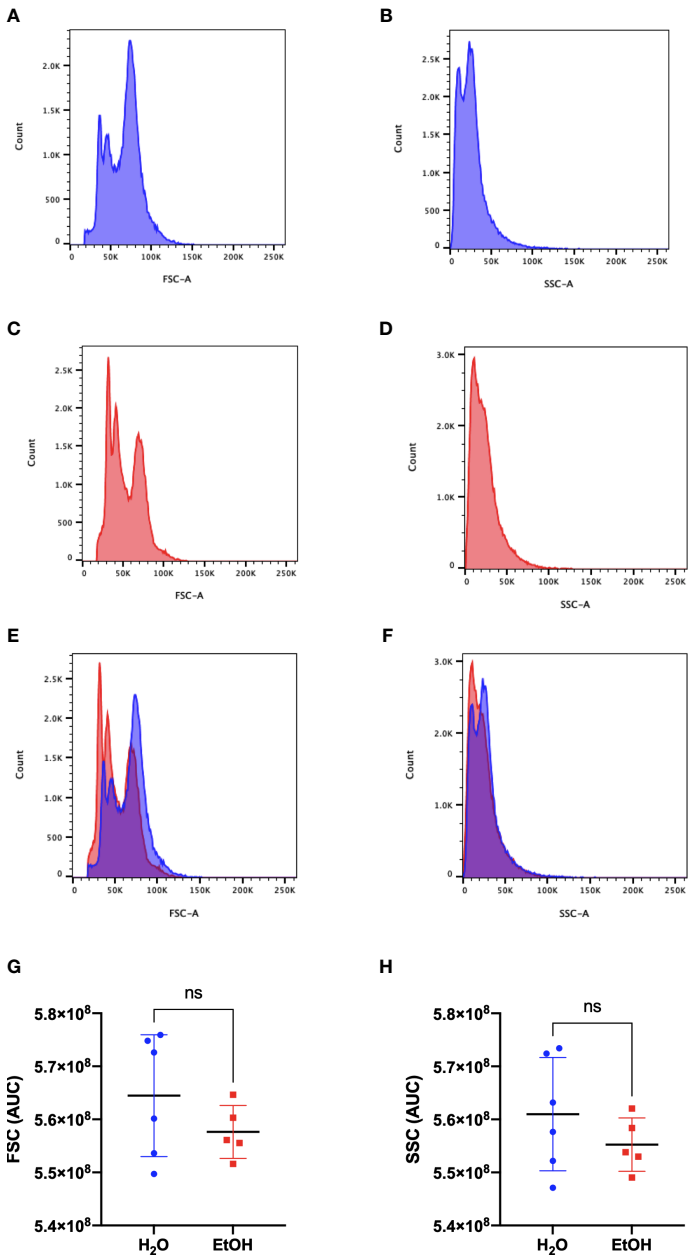

FIGURE 1
Bone Marrow cells analysis. Representative histograms of size and complexity in bone marrow from ethanol- and water-treated animals by flow cytometry. FSC-A represents the discrimination of cells by size, while SSC-A represents the complexity of cells. **(A, C)** represent the frequency of cells related to their size, and **(B, D)** represent the frequency of cells related to their complexity. **(A, B)** water-treated group **(C, D)** ethanol-treated group. **(E)** representative overlapping of **(A, C)** FSC-A graphs and **(F)** representative overlapping of **(B, D)** SSC-A graphs. In blue is the water-treated group, and in red is the ethanol-treated group. The area under the curve (AUC) of the samples was calculated and represents the distribution of the entire population used in metabolomics. A statistical analysis of AUC was conducted for FSC **(G)** and SSC **(H)**. *ns* represents not statistically significant.

3.2 Chronic alcohol consumption alters the metabolomics profile in the bone marrow

Gas chromatography–coupled mass spectrometry was performed using pooled bone marrow cells. After carrying out the identification processes in AMDIS, correlation with the matrix extracted from XCMS, and removal of the analytes present in the blank, our approach was effective in identifying 19 metabolites (Table 1) that were classified into six different Gene Ontology classes: amino acids, organohetetocyclic compounds, monosaccharides, organic acids, and fatty acids alcohols/polyols (Figure 2). Metabolites 3 and 17 present two possibilities for identification.

To evaluate the instrumental performance, principal component analysis (PCA) (Figure 3A) and partial least squares discriminant analysis (PLS-DA) (Figure 3B) was applied, including the QC samples. The supervised model (PLS-DA) was validated using a distance separation method with 100 permutations, considering a p-value of ≤0.05. It is possible to observe an excellent group of QCs demonstrating the quality and reliability of the instrument for data acquisition.

Moreover, to better identify and discriminate metabolites, a new model (PLS-DA) (Figure 3C) was conducted without the QC samples, and a VIP score >1.0 (Figure 3D) was used to consider statistically significant differences in abundance of the metabolites between groups. Five metabolites were identified with statistical significance by multivariate analysis (uracil, L-tyrosine, L-proline, succinic acid, and nicotinamide).

Table 1 presents, in bold, the significantly altered metabolites between groups comparison, in which the statistical results (VIP score) and the variation rate fold change (FC) are presented. These five statistically different abundance metabolites are decreased in the ethanol-treated group at several intensities.

4 Discussion

Metabolic profiles have been explored in many diseases (23), including liver diseases resulting from alcoholism (24–27). This study was the first to investigate the impact of chronic alcohol consumption on the bone marrow metabolic profile using an *in vivo* model of chronic ethanol consumption. The motivation for this study stems from evidence demonstrating that chronic consumption has negative effects on the ability of individuals with hazardous alcohol use to respond properly during infections (2, 28, 29).

TABLE 1 Metabolites identified by GC–MS analysis and statistically significant altered metabolites in bone marrow cell of ethanol-treated mice.

Metabolite	VIP score	FC (EtOH/H_2O)	Chemical Classification
1. Valine	0.63	0.94	Amino acids, peptides, and analogues
2. Alanine	0.99	0.97	Amino acids, peptides, and analogues
3. Leucine/isoleucine	0.06	0.95	Amino acids, peptides, and analogues
4. Benzoic acid	0.62	0.51	Organic acids and derivates
5. Serine	0.82	0.87	Amino acids, peptides, and analogues
6. Proline	**1.26**	**0.98**	**Amino acids, peptides, and analogues**
7. Succinic acid	**1.38**	**0.89**	**Organic acids and derivates**
8. Uracil	**2.90**	**0.71**	**Organoheterocyclic compounds**
9. Fumaric acid	0.54	0.91	Organic acids and derivates
10. Aspartic acid	0.73	0.97	Amino acids, peptides, and analogues
11. Nicotinamide	**1.20**	**0.70**	**Organoheterocyclic compounds**
12. Malic acid	0.28	0.96	Organic acids and derivates
13. Glutamic acid	0.91	0.91	Amino acids, peptides, and analogues
14. Lauric acid	0.28	0.87	Organic acids and derivates
15. Tyrosine	**1.07**	**0.86**	**Amino acids, peptides, and analogues**
16. Hexadecanol	0.01	0.77	Alcohols and Polyols, Other
17. Mannitol/altrose	0.64	1.16	Monosaccharides and Derivatives
18. Linoleic acid	0.34	0.72	Fatty Acids and Fats
19. Oleic acid	0.36	1,11	Fatty Acids and Fats

FC, Fold Change; VIP score, Varial Importance in Projection.
The metabolites present in lines 3 and 17 present two possible identifications. This is due to the analytical impossibility of differentiating these isomers as a function of elution at very close retention times and because they present identical MS fragmentation profiles. Therefore, the identification is presented with both isomers. Statistically significant altered metabolites that are present are shown in bold.

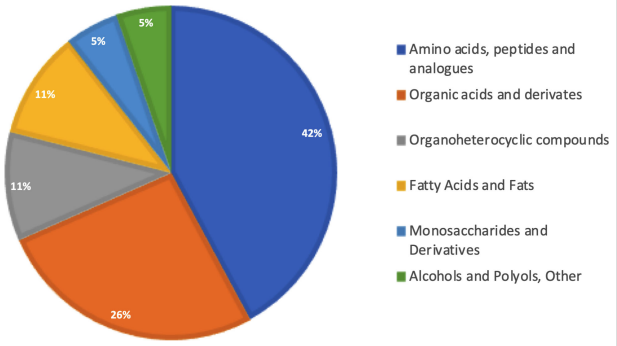

FIGURE 2
Biological categorization of identified metabolites. All 19 identified metabolites were classified according to functional categorization in PubChem (https://pubchem.ncbi.nlm.nih.gov). Percentages represent the number of classified metabolites in each category.

Analytical tools for metabolomics studies have high sensitivity, being able to identify and quantify the presence of analytes at low concentrations (30). Therefore, the first step of the present study was to evaluate, by flow cytometry, whether the parameter number of cells would be adequate, since alcohol could be causing an increase in cell size, resulting in a bias toward greater abundance of the metabolite. The descriptive evaluation obtained from the FSC, and SSC histograms showed that ethanol treatment does not cause changes in the size/volume of cells in the bone marrow, ensuring that the quantitative differences found in this study are because of alcohol on metabolic pathways, resulting in a distinct metabolic profile.

The negative effect of chronic ethanol consumption on the immune system and bone marrow has already been investigated. It is well established that the cells of the immune system of individuals affected by alcoholism have a lower capacity to migrate to the infectious site, phagocyte, and eliminate the pathogen, and the mechanism is often related to the production of cytokines and chemokines that have their levels and activities affected (21, 31–34). In the bone marrow, studies have shown that alcohol consumption promotes important effects on hematopoiesis (35, 36).

In this study, we evaluated the effect of ethanol on bone marrow at the level of metabolites. Once cellular metabolism plays an important role in the functionality of immune cells, changes in the metabolic profile can compromise their functionality (15).

The metabolomics profile revealed significant effects of chronic alcohol consumption on the metabolome of mouse bone marrow. Although the analytical restrictions of the gas chromatography approach limit the scope of the study to volatile compounds and/or volatile compounds through derivatization, it was possible to obtain a holistic approach to the metabolic profile of this tissue as well as the changes resulting from chronic exposure to alcohol.

Nicotinamide ($C_6H_6N_2O$) showed reduced abundance in cells from animals under chronic treatment with ethanol. Nicotinamide is the active form of vitamin B3 and a component of the coenzyme nicotinamide adenine dinucleotide (NAD). When ethanol is metabolized, it generates a reduced cellular environment due to the use of nicotinamide adenine dinucleotide (NAD^+) as an enzymatic cofactor at both stages of its metabolism. The reduced cellular environment has been related to the dysfunctions observed in the cells of the immune system (2, 21, 37, 38). In addition, NAD^+ is an enzyme cofactor used in important metabolic pathways such as glycolysis and the Krebs cycle, which have been reported to be essential for neutrophil and macrophage function (15, 39, 40). We hypothesize that ethanol metabolism limits the availability of NAD^+ for cell metabolism, altering the metabolic profile. This alteration may be related to the negative effect of alcohol on the function of these cells. Our results suggest that this may be part of the mechanism by which alcohol alters metabolism in this tissue. Although functional studies are needed to confirm and elucidate this evidence.

Succinic acid, an important component of the TCA cycle, was recently identified as a modulator of the innate immune response. In lipopolysaccharide (LPS)-activated macrophages, succinate was identified as a key metabolite in innate immune response signaling since its increase is correlated to increased production of interleukin-1b during inflammation (41, 42). Furthermore, lipopolysaccharide-induced succinate stabilizes hypoxia-inducible factor (HIF-1α), an effect that is inhibited by 2-deoxyglucose, with interleukin-1b as an important target (41, 43). HIF-1α is an oxygen-dependent transcriptional activator that plays crucial roles in tumor angiogenesis and mammalian development (44). Furthermore, HIF-1α increases macrophage aggregation, invasion, and motility and boosts the expression of pro-inflammatory cytokines. HIF-1α also increases neutrophil survival by inhibiting apoptosis and triggering NF-κB-dependent neutrophilic inflammation (45). Succinate was also shown to promote hematopoietic cell proliferation by phosphorylation of the ERK1/2 mitogen-activated protein kinase (MAPK) pathway and inositol phosphate accumulation in a pertussis toxin (PTX)-sensitive manner (46). Furthermore, succinate induced activation of ERK1/2, JNK, and p38 MAPK signaling pathways in immortalized retinal ganglion cells (RGC-5) cells in a dose-dependent manner (47). The ERK1/2 and MAPK pathways are related to the activation of the pro-inflammatory response of immune cells (48–50). Therefore, the deregulation in the amount of succinate found in this work can be considered a modulating mechanism of chronic alcohol consumption in the immune response.

In agreement with studies that investigated changes in the metabolome associated with alcohol consumption in humans, amino acids are the most representative chemical class (51). Tyrosine and proline are non-essential amino acids used in protein biosynthesis. Protein tyrosine (PTP) phosphorylation is an important post-translational modification that controls cell signaling involved in the regulation of a variety of biological processes, including cell growth, proliferation, differentiation, migration, survival, and death. The negative effect of downregulating these amino acids in the ethanol-treated group can impair an important biological process since tyrosine phosphorylation is considered one of the fundamental steps in signal transduction and regulation of enzymatic activity (52). However, studies that investigate the relationship between quantitative alterations of amino acids and the function of immune system cells were not found in the literature. The results

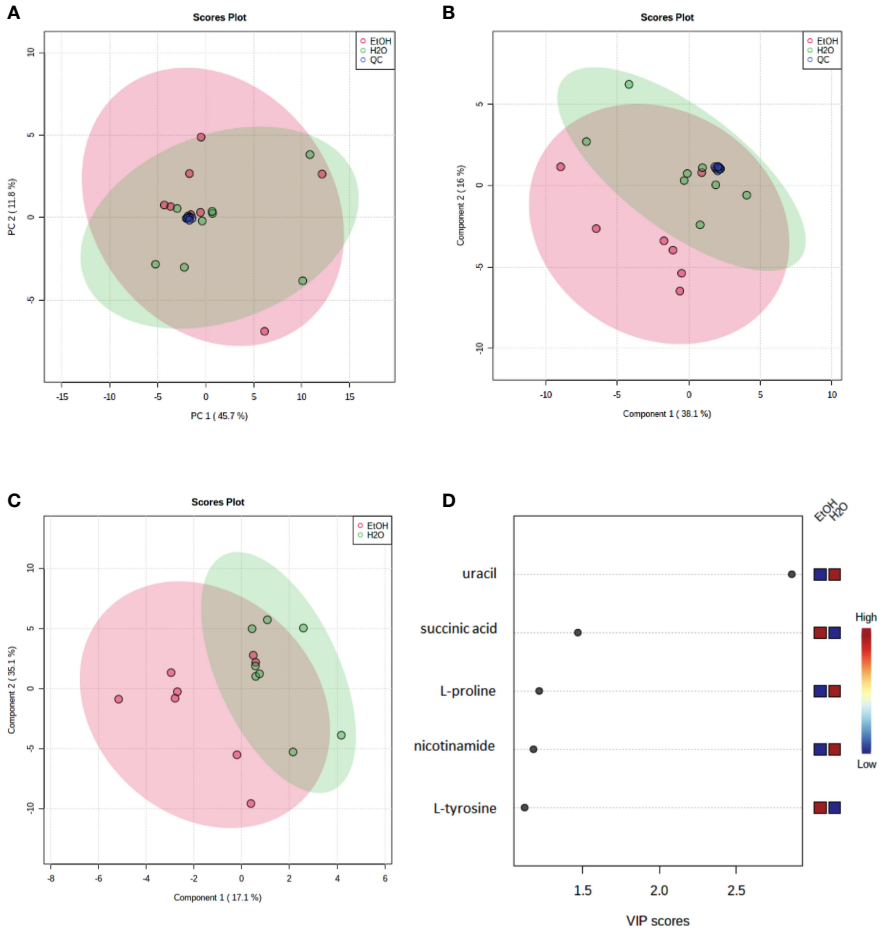

FIGURE 3
Multivariate models (Pareto scaling) of metabolites identified in cell samples analyzed by GC–MS and discriminating metabolites between ethanol-treated and control groups by GC–MS. **(A)** Principal component analysis (PCA) and **(B)** partial least squares discriminant analysis (PLS-DA). Each dot represents one sample, and **(A, B)** show a separation of the groups and a robust clustering of the Quality Controls (QC). PSL-DA model parameters: R2 = 0.58 and Q2 = 0.26). Quality controls (QC—blue dots), a water-treated control group (H_2O—green dots), and ethanol-treated experimental group (EtOH—red dots). **(C)** The PLS-DA Model (Pareto scale) shows a separation between the groups; **(D)** the VIP Score Chart contains the discriminating metabolites between groups. A VIP score >1 is considered significant. A red (high) to blue (low) scale indicates the relative abundance of metabolites in the ethanol-treated group compared to the water-treated control group. The green ellipses represent the water-treated control group, and the red ellipses represent the ethanol-treated experimental group.

found here suggest that investigations in this direction may be promising for understanding the mechanism behind the harmful effect of alcohol on immune response. Once some amino acids like tyrosine can be catabolized all the way down into intermediaries of the Krebs cycle, especially into fumarate and acetoacetate (53).

Uracil is a common natural pyrimidine found in RNA and was found to be downregulated in the bone marrow of ethanol-treated mice. Despite not finding in the literature a direct relationship between this nucleotide and the function of immune cells, it is known that uracil helps to carry out the synthesis of many enzymes necessary for cell function through the interaction with ribose and phosphates and serves as an allosteric regulator and a coenzyme for many important biochemical reactions (54).

A wide variety of types of RNAs act in the regulation of the immune system. microRNAs, RNA-binding proteins that control the stability and translation of messenger RNA (mRNA) and RNA interference (RNAi) are examples of RNAs that act by controlling the gene expression of cytokines and chemokines responsible for the intercellular communication of the immune system (55, 56). The decrease in uracil levels resulting from the chronic consumption of ethanol in the bone marrow may indirectly compromise the entire elaboration of the immune response.

Metabolic profiles can be considered a phenotypic state that undergoes variations under the influence of changes in the genome, proteome, transcriptome, metabolism, and modifications in the microenvironment where they are found (57). In our approach, we demonstrate for the first time that chronic ethanol consumption can alter the bone marrow microenvironment, and this can be associated with altered immune cell metabolism, leading to a programmed alteration function of the mature circulating cells. However, this is an initial, exploratory metabolomics study that brings important insights into cellular metabolism under alcohol exposure. We are aware of some limitations of our approach, such as the influence of animal gender in metabolism and susceptibility to alcohol, the use of other analytical platforms that should improve the number of identified metabolites, and the need for functional

studies to demonstrate the role of metabolic pathways in the immune response. In addition, the effects of blood alcohol concentration and the effects of the products of its metabolism (e.g., acetaldehyde) can also be considered. Complementary studies will allow greater coverage of the metabolome, in addition to confirming and validating the hypotheses raised in this work.

Data availability statement

The original contributions presented in the study are included in the article/Supplementary Material. Further inquiries can be directed to the corresponding author.

Ethics statement

The animal study was reviewed and approved by Animal Ethics Committee (CEUA) of Universidad Federal de Minas Gerais (UFMG), Brazil (Protocol 337/2018) which are in accordance to the Brazilian guidelines (CONCEA) and international standards.

Author contributions

Conception of the study: FS. Designed the experiments: TP, FA, JV, and FS. Performed the experiments: TP, JS, FM, CP, and EP. Interpretation of the results and data analysis: TP, TS, GC, AM, NM, and FS. Contributed reagents/materials/analysis tools: MT, FS, and RG. Wrote the manuscript: TP and FS. Helped in animal experiments: EM. All authors contributed to the article and approved the submitted version.

Funding

This work was supported by the Pró-Reitoria de Pesquisa at the Universidade Federal de Minas Gerais, Conselho Nacional de Desenvolvimento Científico e Tecnológico (474528-2012-0 and 483184-2011-0), and the Fundação de Amparo à Pesquisa do Estado de Minas Gerais (APQ- 01756-10; APQ-02198-14; APQ-03950-17; and APQ-01899-18). This study was financed in part by the Coordenação de Aperfeiçoamento de Pessoal de Nível Superior —Brasil (CAPES)—Finance Code 001 and the Instituto Nacional de Ciência e Tecnologia em Dengue e Interação Microrganismo Hospedeiro (INCT em Dengue). The funders had no role in study design, data collection and analysis, decision to publish, or preparation of the manuscript.

Acknowledgments

We would like to thank the Universidade Federal de Minas Gerais for the opportunity to develop this work. We are thankful to Ilma Marçal S. and Rosemeire A. Oliveira.

Conflict of interest

The authors declare that the research was conducted in the absence of any commercial or financial relationships that could be construed as a potential conflict of interest.

Publisher's note

Supplementary material

The Supplementary Material for this article can be found online at: https://www.frontiersin.org/articles/10.3389/fimmu.2023.1128352/full#supplementary-material

References

1. Alcoholism NI. Understanding alcohol use disorder. *Natl Inst Alcohol Abus Alcohol* (2019), 4–6. https://www.niaaa.nih.gov/sites/default/files/publications/Alcohol_Use_Disorder.pdf.

2. Le Daré B, Lagente V, Gicquel T. Ethanol and its metabolites: update on toxicity, benefits, and focus on immunomodulatory effects. *Drug Metab Rev* (2019) 51:545–61. doi: 10.1080/03602532.2019.1679169

3. Shi X, Delucia AL, Bao J, Zhang P. Alcohol abuse and disorder of granulopoiesis. *Physiol Behav* (2019) 63:1–18. doi: 10.1016/j.pharmthera.2019.03.001

4. Kellie S, Al-Mansour Z. Overview of the immune system. *Micro- Nanotechnol. Vaccine Dev* (2017) 357:63–81. doi: 10.1016/B978-0-323-39981-4.00004-X

5. Shi X, DeLucia AL, Bao J, Zhang P. Alcohol abuse and disorder of granulopoiesis. *Pharmacol Ther* (2019) 198:206–19. doi: 10.1016/j.pharmthera.2019.03.001

6. Sarkar D, Jung MK, Wang HJ. Alcohol and the immune system. *Alcohol Res Curr Rev* (2015) 37:153–5. doi: 10.1136/bmj.298.6673.543

7. Szabo G, Saha B. Alcohol's effect on host defense. *Alcohol Res Curr Rev* (2015) 37:159–70.

8. Wickramasinghe SN. Rates of metabolism of ethanol to acetate by human neutrophil precursors and macrophages. *Alcohol Alcohol* (1985) 20:299–303. doi: 10.1093/oxfordjournals.alcalc.a044537

9. Zakhari S. Overview: How is alcohol metabolized by the body? *Alcohol Res Heal* (2006) 29:245–54.

10. Cederbaum AI. Alcohol metabolism. *Clin Liver Dis* (2012) 16:667–85. doi: 10.1016/j.cld.2012.08.002

11. Bradford BU, Rusyn I. Swift increase in alcohol metabolism (SIAM): Understanding the phenomenon of hypermetabolism in liver. *Alcohol* (2005) 35:13–7. doi: 10.1016/j.alcohol.2004.12.001

12. Hawkins RD, Kalant H. No title. *Pharmacol Rev* (1972) 24:67–157.

13. Zakhari S, Li TK. Determinants of alcohol use and abuse: impact of quantity and frequency patterns on liver disease. *Hepatology* (2007) 46:2032–9. doi: 10.1002/hep.22010

14. Lieber CS. Ethanol metabolism, cirrhosis and alcoholism. *Clin Chim Acta* (1997) 257:59–84. doi: 10.1016/S0009-8981(96)06434-0

15. Loftus RM, Finlay DK. Immunometabolism: Cellular metabolism turns immune regulator. *J Biol Chem* (2016) 291:1–10. doi: 10.1074/jbc.R115.693903

16. Al-Khami AA, Rodriguez PC, Ochoa AC. Energy metabolic pathways control the fate and function of myeloid immune cells. *J Leukoc Biol* (2017) 102:369–80. doi: 10.1189/jlb.1VMR1216-535R

17. Buck MD, Sowell RT, Kaech SM, Pearce EL. Metabolic instruction of immunity. *Cell* (2017) 169:570–86. doi: 10.1016/j.cell.2017.04.004

18. Wang A, Luan HH, Medzhitov R. An evolutionary perspective on immunometabolism. *Science* (2019) 80-):363. doi: 10.1126/science.aar3932

19. Artyomov MN, Van den Bossche J. Immunometabolism in the single-cell era. *Cell Metab* (2020) 32:710–25. doi: 10.1016/j.cmet.2020.09.013

20. Cichon I, Ortmann W, Kolaczkowska E. Metabolic pathways involved in formation of spontaneous and lipopolysaccharide-induced neutrophil extracellular traps (Nets) differ in obesity and systemic inflammation. *Int J Mol Sci* (2021) 22:1–29. doi: 10.3390/ijms22147718

21. Yeligar SM, Harris FL, Hart CM, Brown LAS. Ethanol induces oxidative stress in alveolar macrophages *via* upregulation of NADPH oxidases. *J Immunol* (2012) 188:3648–57. doi: 10.4049/jimmunol.1101278

22. Canuto GAB, Castilho-Martins EA, Tavares MFM, Rivas L, Barbas C, López-Gonzálvez Á. Multi-analytical platform metabolomic approach to study miltefosine mechanism of action and resistance in leishmania. *Anal Bioanal Chem* (2014) 406:3459–76. doi: 10.1007/s00216-014-7772-1

23. Andrisic L, Dudzik D, Barbas C, Milkovic L, Grune T, Zarkovic N. Short overview on metabolomics approach to study pathophysiology of oxidative stress in cancer. *Redox Biol* (2018) 14:47–58. doi: 10.1016/j.redox.2017.08.009

24. Yang Z, Kusumanchi P, Ross RA, Heathers L, Chandler K, Oshodi A, et al. Serum metabolomic profiling identifies key metabolic signatures associated with pathogenesis of alcoholic liver disease in humans. *Hepatol Commun* (2019) 3:542–57. doi: 10.1002/hep4.1322

25. Kim SJ, Jung YS, Kwon DY, Kim YC. Alleviation of acute ethanol-induced liver injury and impaired metabolomics of s-containing substances by betaine supplementation. *Biochem Biophys Res Commun* (2008) 368:893–8. doi: 10.1016/j.bbrc.2008.02.003

26. Li S, Liu H, Jin Y, Lin S, Cai Z, Jiang Y. Metabolomics study of alcohol-induced liver injury and hepatocellular carcinoma xenografts in mice. *J Chromatogr. B Anal Technol BioMed Life Sci* (2011) 879:2369–75. doi: 10.1016/j.jchromb.2011.06.018

27. Manna SK, Patterson AD, Yang Q, Krausz KW, Li H, Idle JR, et al. Identification of noninvasive biomarkers for alcohol-induced liver disease using urinary metabolomics and the ppara -null mouse. *J Proteome Res* (2010) 9:4176–88. doi: 10.1021/pr100452b

28. Yeligar SM, Chen MM, Kovacs EJ, Sisson JH, Burnham EL, Ann L, et al. Alcohol and lung injury and immunity HHS public access. *Alcohol* (2016) 55:51–9. doi: 10.1016/j.alcohol.2016.08.005

29. Malacco NLS de O, Souza JAM, Martins FRB, Rachid MA, Simplicio JA, Tirapelli CR, et al. Chronic ethanol consumption compromises neutrophil function in acute pulmonary aspergillus fumigatus infection. *Elife* (2020) 9:1–23. doi: 10.7554/eLife.58855

30. Dunn WB, Ellis DI. Metabolomics: Current analytical platforms and methodologies. *TrAC - Trends Anal Chem* (2005) 24:285–94. doi: 10.1016/j.trac.2004.11.021

31. Kasicka-Jonderko A. Alcohol and the digestive system – should it always be blamed? *Prz Gastroenterol* (2012) 7:264–75. doi: 10.5114/pg.2012.32064

32. Mehta AJ, Guidot DM. Alcohol abuse, the alveolar macrophage and pneumonia. *Am J Med Sci* (2012) 343:244–7. doi: 10.1097/MAJ.0b013e31823ede77

33. Luong TT, Kim EH, Bak JP, Nguyen CT, Choi S, Briles DE, et al. Ethanol-induced alcohol dehydrogenase e (AdhE) potentiates pneumolysin in streptococcus pneumoniae. *Infect Immun* (2015) 83:108–19. doi: 10.1128/IAI.02434-14

34. Rao R, Topiwala A. Alcohol use disorders and the brain. *Addiction* (2020) 115:1580–9. doi: 10.1111/add.15023

35. Latvala J, Parkkila S, Niemelä O. Excess alcohol consumption is common in patients with cytopenia: Studies in blood and bone marrow cells. *Alcohol Clin Exp Res* (2004) 28:619–24. doi: 10.1097/01.ALC.0000122766.54544.3B

36. Di Rocco G, Baldari S, Pani G, Toietta G. Stem cells under the influence of alcohol: effects of ethanol consumption on stem/progenitor cells. *Cell Mol Life Sci* (2019) 76:231–44. doi: 10.1007/s00018-018-2931-8

37. Martinez SR, Maresha S, Gay and LZ. Nicotinamide riboside, an NAD+ precursor, attenuates the development of liver fibrosis in a diet-induced mouse model of liver. *Physiol Behav* (2016) 176:139–48. doi: 10.1016/j.bbadis.2019.06.009.Nicotinamide

38. Garaycoechea JI, Crossan GP, Langevin F, Mulderrig L, Louzada S, Yang F, et al. Alcohol and endogenous aldehydes damage chromosomes and mutate stem cells. *Nature* (2018) 553:171–7. doi: 10.1038/nature25154

39. Van den Bossche J, O'Neill LA, Menon D. Macrophage immunometabolism: Where are we (Going)? *Trends Immunol* (2017) 38:395–406. doi: 10.1016/j.it.2017.03.001

40. Wang F, Zhang S, Vuckovic I, Jeon R, Lerman A, Folmes CD, et al. Glycolytic stimulation is not a requirement for M2 macrophage differentiation. *Cell Metab* (2018) 28:463–475.e4. doi: 10.1016/j.cmet.2018.08.012

41. Tannahill GM, Curtis AM, Adamik J, Palsson-McDermott EM, McGettrick AF, Goel G, et al. Succinate is an inflammatory signal that induces IL-1β through HIF-1α. *Nature* (2013) 496:238–42. doi: 10.1038/nature11986

42. Viola A, Munari F, Sánchez-Rodríguez R, Scolaro T, Castegna A. The metabolic signature of macrophage responses. *Front Immunol* (2019) 10:1–16. doi: 10.3389/fimmu.2019.01462

43. Jiang M, Chen Z, Li H, Zhang T, Yang M, Peng X, et al. Succinate and inosine coordinate innate immune response to bacterial infection. *PloS Pathog* (2022) 18:e1010796. doi: 10.1371/journal.ppat.1010796

44. Lee JW, Bae SH, Jeong JW, Kim SH, Kim KW. Hypoxia-inducible factor (HIF-1)α: Its protein stability and biological functions. *Exp Mol Med* (2004) 36:1–12. doi: 10.1038/emm.2004.1

45. Palazon A, Goldrath AW, Nizet V, Johnson RS. HIF transcription factors, inflammation, and immunity. *Immunity* (2014) 41:518–28. doi: 10.1016/j.immuni.2014.09.008

46. Hakak Y, Lehmann-Bruinsma K, Phillips S, Le T, Liaw C, Connolly DT, et al. The role of the GPR91 ligand succinate in hematopoiesis. *J Leukoc Biol* (2009) 85:837–843. doi: 10.1189/jlb.1008618

47. Raucci A, Laplantine E, Mansukhani A, Basilico C. Activation of the ERK1/2 and p38 mitogen-activated protein kinase pathways mediates fibroblast growth factor-induced growth arrest of chondrocytes. *J Biol Chem* (2004) 279:1747–56. doi: 10.1074/jbc.M310384200

48. Nadra I, Mason JC, Philippidis P, Florey O, Smythe CDW, McCarthy GM, et al. Proinflammatory activation of macrophages by basic calcium phosphate crystals *via* protein kinase c and MAP kinase pathways: A vicious cycle of inflammation and arterial calcification? *Circ Res* (2005) 96:1248–56. doi: 10.1161/01.RES.0000171451.88616.c2

49. Thakur V, McMullen MR, Pritchard MT, Nagy LE. Regulation of macrophage activation in alcoholic liver disease. *J Gastroenterol Hepatol* (2007) 22:53–6. doi: 10.1111/j.1440-1746.2006.04650.x

50. Hazeldine J, Hampson P, Opoku FA, Foster M, Lord JM. N-formyl peptides drive mitochondrial damage associated molecular pattern induced neutrophil activation through ERK1/2 and P38 MAP kinase signalling pathways. *Injury* (2015) 46:975–84. doi: 10.1016/j.injury.2015.03.028

51. Voutilainen T, Kärkkäinen O. Changes in the human metabolome associated with alcohol use: A review. *Alcohol Alcohol* (2019) 54:225–34. doi: 10.1093/alcalc/agz030

52. Ardito F, Giuliani M, Perrone D, Troiano G, Muzio L. The crucial role of protein phosphorylation in cell signalingand its use as targeted therapy (Review). *Int J Mol Med* (2017) 40:271–80. doi: 10.3892/ijmm.2017.3036

53. National Center for Biotechnology Information. *PubChem pathway summary for pathway SMP0000006, tyrosine metabolism, source: PathBank* (2023). Available at: https://pubchem.ncbi.nlm.nih.gov/pathway/PathBank:SMP0000006.

54. Kaphalia AL, Calhoun WJ. Alcoholic Lung Injury: Metabolic, Biochemical and Immunological Aspects. *Toxicol Lett* (2013) 24:1–21. doi: 10.1016/j.toxlet.2013.07.016

55. Ansel KM. RNA Regulation of the immune system. *Immunol Rev* (2013) 253:5–11. doi: 10.1111/imr.12062

56. Xie Y, Wei Y. A novel regulatory player in the innate immune System : Long non-coding RNAs. *Int J Mol Sci* (2021). doi: 10.3390/ijms22179535

57. Dudzik D, Barbas-Bernardos C, García A, Barbas C. Quality assurance procedures for mass spectrometry untargeted metabolomics. a review. *J Pharm BioMed Anal* (2018) 147:149–73. doi: 10.1016/j.jpba.2017.07.044

frontiers | Frontiers in Immunology

TYPE Original Research
PUBLISHED 19 May 2023
DOI 10.3389/fimmu.2023.1175275

OPEN ACCESS

EDITED BY
Samantha Yeligar,
Emory University, United States

REVIEWED BY
Rachel McMahan,
University of Colorado Anschutz Medical Campus, United States
Robert Wade Siggins,
Louisiana State University, United States

*CORRESPONDENCE
Frederico Marianetti Soriani
fredsori@icb.ufmg.br

†These authors have contributed equally to this work and share last authorship

RECEIVED 27 February 2023
ACCEPTED 05 May 2023
PUBLISHED 19 May 2023

CITATION
Martins FRB, de Oliveira MD, Souza JAM, Queiroz-Junior CM, Lobo FP, Teixeira MM, Malacco NL and Soriani FM (2023) Chronic ethanol exposure impairs alveolar leukocyte infiltration during pneumococcal pneumonia, leading to an increased bacterial burden despite increased CXCL1 and nitric oxide levels.
Front. Immunol. 14:1175275.
doi: 10.3389/fimmu.2023.1175275

Chronic ethanol exposure impairs alveolar leukocyte infiltration during pneumococcal pneumonia, leading to an increased bacterial burden despite increased CXCL1 and nitric oxide levels

Flávia Rayssa Braga Martins[1], Maycon Douglas de Oliveira[1], Jéssica Amanda Marques Souza[1], Celso Martins Queiroz-Junior[2], Francisco Pereira Lobo[1], Mauro Martins Teixeira[3], Nathalia Luisa Malacco[4†] and Frederico Marianetti Soriani[1*†]

[1]Department of Genetics, Ecology and Evolution, Institute of Biological Sciences, Federal University of Minas Gerais, Belo Horizonte, Minas Gerais, Brazil, [2]Department of Morphology, Institute of Biological Sciences, Federal University of Minas Gerais, Belo Horizonte, Minas Gerais, Brazil, [3]Department of Biochemistry and Immunology, Institute of Biological Sciences, Federal University of Minas Gerais, Belo Horizonte, Minas Gerais, Brazil, [4]Department of Microbiology and Immunology, McGill University, Montreal, QC, Canada

Ethanol abuse is a risk factor for the development of pneumonia caused by *Streptococcus pneumoniae*, a critical pathogen for public health. The aim of this article was to investigate the inflammatory mechanisms involved in pneumococcal pneumonia that may be associated with chronic ethanol exposure. Male C57BL6/J-Unib mice were exposed to 20% (v/v) ethanol for twelve weeks and intranasally infected with $5x10^4$ CFU of *S. pneumoniae*. Twenty-four hours after infection, lungs, bronchoalveolar lavage and blood samples were obtained to assess the consequences of chronic ethanol exposure during infection. Alcohol-fed mice showed increased production of nitric oxide and CXCL1 in alveoli and plasma during pneumococcal pneumonia. Beside this, ethanol-treated mice exhibited a decrease in leukocyte infiltration into the alveoli and reduced frequency of severe lung inflammation, which was associated with an increase in bacterial load. Curiously, no changes were observed in survival after infection. Taken together, these results demonstrate that chronic ethanol exposure alters the inflammatory response during *S. pneumoniae* lung infection in mice with a reduction in the inflammatory infiltrate even in the presence of higher levels of the chemoattractant CXCL1.

KEYWORDS

alcohol, nitric oxide, pneumonia, streptococcus pneumoniae, CXCL1

1 Introduction

Alcohol abuse is one of the risk factors associated with premature death and disability worldwide (1). Digestive disease, injuries, cardiovascular diseases, cancer, and infectious diseases are the major causes of deaths associated with harmful alcohol consumption (1). During the severe acute respiratory syndrome virus (SARS-CoV-2) pandemic, an increased volume and frequency of alcohol consumption were observed within the group of people under isolation, which may have direct consequences for the health of the populations during the pandemic recovery (2, 3).

Effects of alcohol metabolism and its consequences in the immune system have been extensively studied, however differences and similarities between acute and chronic exposure during viral, fungal, and bacterial infections are vastly discussed (4–9). Despite this, literature consensus related to ethanol effects relies on the modulation of the inflammatory response during infection, modifying its normal course (8, 10). Chronic alcohol consumption, as reviewed by Malherbe and Messaoudi, is associated with an increase in the systemic inflammatory response through a direct effect on epigenetic changes in progenitor, circulating and tissue-resident cells, which will have a direct effect during an infection disease (11).

According to the World Health Organization, *S. pneumoniae*, which is included in the group of gram-positive bacteria, is associated with thousands of deaths yearly and one of the risk factors for this infection is alcohol abuse (12–14). Detection of pathogen associated molecular patterns of *S. pneumoniae* by intra- and extracellular pattern recognition receptors on immune cells initiates a proinflammatory response that includes the production of cytokines, chemokines, nitric oxide (NO) and leukocyte recruitment (15, 16). Resident macrophages are essential in this process, coordinating the correct recruitment of neutrophils and the resolution process (17). Neutrophils, in turn, will be the vast majority of migrating cells during pneumococcal pneumonia and their effector functions are essential to limit bacterial spread (18, 19). The C-X-C motif chemokine receptor 2 (CXCR2) ligands, CXCL1 and CXCL2, are critical molecules for neutrophil chemoattraction and host defense against bacterial pneumonia (20, 21).

Pneumococcal infection also induces production of NO mostly by the inducible NO synthase isoform (NOS2), supporting the orchestration of cellular activities during inflammatory response, which includes the production of several cytokines and chemokines such as TNF-α, interleukin 8, and CXCL2 (22–24). In addition to the importance of NO to control pneumococcal viability into the lungs, NOS2 deficient mice are protected during bacteremia caused by *S. pneumoniae*, revealing a contrast effect of NO (25).

Hulse bus and cols., recently demonstrated that moderate intoxication with ethanol increased expression of *Cxcl1* and *Cxcl2*, neutrophil infiltration, and bacterial load into the lungs of mice infected with *S. pneumoniae* infection (5). The aim of this article was to investigate the inflammatory mechanisms involved in pneumococcal pneumonia, such as NO and chemokine production, and cellular infiltration to infectious sites, that may be associated with the chronic ethanol exposure. Our data revealed that following chronic ethanol exposure, mice produced increased amounts of CXCL1 in serum and bronchoalveolar lavage fluid (BALF) after *S. pneumoniae* infection along with increased NO levels. Although we observed higher levels of CXCL1 in ethanol infected mice, our results demonstrated decreased neutrophil and macrophage infiltration into the airways of infected alcohol-fed mice. Decreased amounts of leukocytes into the airways were associated with a higher bacterial burden in alcohol-fed mice, however no changes in lethality of infected mice were observed.

2 Material and methods

2.1 Animals and chronic ethanol exposure

Male C57BL/6J-Unib mice were purchased from the Central Animal Facility of the Federal University of Minas Gerais, Brazil. All experiments received prior approval from the Ethics Committee on the Use of Animals (protocol number: 4/2015) and followed the guidelines of the National Council for the Control of Animal Experimentation (CONCEA, Brazil). Mice were specific pathogen-free and were randomly allocated to polysulfone minisolators, without environmental enrichment and filtered air. Dry food was freely available, light was sustained at 12 hours light/12 hours dark, and temperature was maintained 23 ± 2°C.

Five-week-old mice were initiated to ethanol exposure with a 5% (v/v) ethanol solution in their freely available drinking water during the first week of treatment, 10% (v/v) ethanol in the second week, and 20% (v/v) ethanol solution from the third to the twelfth week (26). Control mice had free access to water during the same period. According to Malacco et al., 2020, the ethanol exposure protocol did not change mice weight gain and generated an average blood alcohol concentration of 200 milligrams per deciliter at the end of twelve weeks exposure. Ethanol treatment was suspended immediately prior infection.

2.2 Bacterial culture and infection

Culture of *S. pneumoniae* (ATCC 6303 serotype 3) was performed following protocols established by Tavares et al., 2016 (27). The bacterial inoculum was measured by absorbance until reaching the mid-log phase, centrifuged, and diluted in sterile saline to a concentration of approximately $5x10^4$ CFU in 40 μL. The inoculum was instilled intranasally into mice anaesthetized by inhalation of 3% isoflurane. The inoculum was confirmed by plating serial dilutions of the bacterial suspension on blood agar.

2.3 Colony forming unit (CFU)

One day post infection mice were euthanized with ketamine (100 mg/kg) and xylazine (6 mg/Kg) and the lungs were sterile harvested. Bacterial load was analyzed from lung tissue macerated in sterile phosphate-buffered saline (PBS), diluted and plated on blood agar. CFUs were counted after overnight incubation at 37°C, 5% CO_2 atmosphere.

2.4 Histopathological analysis

Left lung lobes were fixed in 4% formalin for 24 hours, progressively dehydrated in alcohol and embedded in paraffin blocks. 5 µm sections were cut from each tissue, placed on slides and stained with hematoxylin and eosin (H&E). Histopathological score analyses of lung slides were performed using the intensity criteria of (i) vascular inflammation (0–4), (ii) airway inflammation (0-4), (iii) parenchymal inflammation (0-5) and (iv) polymorphonuclear cell infiltrate (0-5) (28). The severity of the inflammatory lesions was then classified as absent (0-1), mild (2-5), moderate (6-9), intense (10-13) and severe (14-18). Representative images of the slides were taken under a light microscope at 10x and 40x magnification to better illustrate the phenotypes. Data are expressed as a percentage of animals showing the degree of histopathological lesion described above.

2.5 Cellular infiltrate analysis

Blood plasma and bronchoalveolar fluid (BALF) were obtained as previously described (29). Briefly, blood was harvested from inferior cava vein with heparinized Pasteur's pipette and bronchoalveolar lavage were realized with 2 milliliters of cold PBS, after trachea exposure. BALF was centrifuged 320 *x g* for 10 min at 4°C, and the supernatant was stored at -20°C for chemokine analysis. Total cells in BALF were analyzed by counting in the Neubauer chamber with Turk's solution. Differential cell counts were obtained by rapid panoptic-stained cytospin preparation (Laborclin) and double-blind observation under light microscopy using cell morphology (nuclear shape and nucleus/cytoplasm ratio) and staining criteria.

Myeloperoxidase (MPO) and N-acetylglucosaminidase (NAG) were used as indirect measures of neutrophil and macrophage accumulation in the lungs, respectively, following the established protocols of Barcelos et al, 2005. Briefly, the collected lungs were homogenized, the contents of the cell granules were released after three rounds of freezing in liquid nitrogen and the supernatant contents were used for the assay. The MPO and NAG standard curves were quantified from a known amount of each cell in a parallel experiment. The resulting colorimetric reaction was read in a spectrophotometer and the results were expressed in relative units per mg of tissue (30, 31).

2.6 Blood cells counting

Blood was collected in EDTA tubes. Leukocyte quantification and differentiation was performed using a Celltac MEK-6500K hemocytometer (Nihon Kohden). Plasma was obtained after centrifugation at 600 x g for 10 min at 4°C and stored at -20°C until further investigation.

2.7 Nitric Oxide (NO) measurement

NO production in BALF was evaluated indirectly through nitrite formation, by Griess method (32). Briefly, 50 µL of Griess reagent (1% sulfanilamide and 0.1% naphthylethylenediamine in 2.5% phosphoric acid) was added to 100 µL of BALF samples. After 10 min, the absorbance of the samples was measured at 540 nm. Nitrite quantification was done using a nitrite standard curve.

2.8 Chemokine measurement

Levels of CXCL1 in plasma and BALF and IL-6, TNF-α and CCL2 in BALF were obtained using DuoSet Enzyme-Linked Immunosorbent Assay kits (R&D 348 Systems). The assays followed the manufacturer's instructions. The absorbance found in the samples was compared to the specific standard curve of known values for each cytokine/chemokine evaluated.

2.9 Statistical analysis

Experiments were done at least twice and randomically and double-blind analyzed. Graphs and statistical analysis were performed using Graph Pad Prism 8. Differences between different groups were analyzed by Two-way analysis of variance (ANOVA) and Tukey's *post hoc* test. Statistical significance was considered when $p<0.05$. Survival analysis used the Log Rank test.

3 Results

3.1 Chronic ethanol exposure is related to increased bacterial load into the lungs

Proper bacterial clearance is critical for the improvement in the progression of infectious diseases (19). To assess the impact of chronic ethanol exposure on bacterial clearance, at the end of twelve weeks treatment, mice were intranasally infected with *S. pneumoniae* and twenty-four hours later were euthanized, lungs and plasma were harvested (Figure 1A). Results demonstrate recovery of bacteria from both infected groups, demonstrating an established infection. Nevertheless, alcohol-fed mice had a higher number of viable bacteria into the lungs compared to untreated mice (Figure 1B). We hypothesized that these animals would be more susceptible to infection, since bacterial clearance was greatly damped in alcohol-fed mice. We evaluated mice survival after *S. pneumoniae* infection and, curiously, we did not observe significant differences between groups (Figure 1C). These results encouraged us to investigate the inflammatory mechanisms that might be involved in mice survival even with increased bacterial load.

Histopathological analyses of the inflammatory process into the lungs were observed and uninfected animals in the ethanol-exposed and unexposed groups showed little or no severity of lung injury (Figures 1D, E). In contrast, after twenty-four hours of infection with *S. pneumoniae*, we observed an increase in the frequency of mice with increased severity of inflammatory lesions in the lung tissue (Figure 1D). The frequency of severe inflammatory lesions was higher in the infected group not exposed to ethanol (Figure 1D). Images of representative tissue sections show a more prominent

10.3389/fimmu.2023.1175275

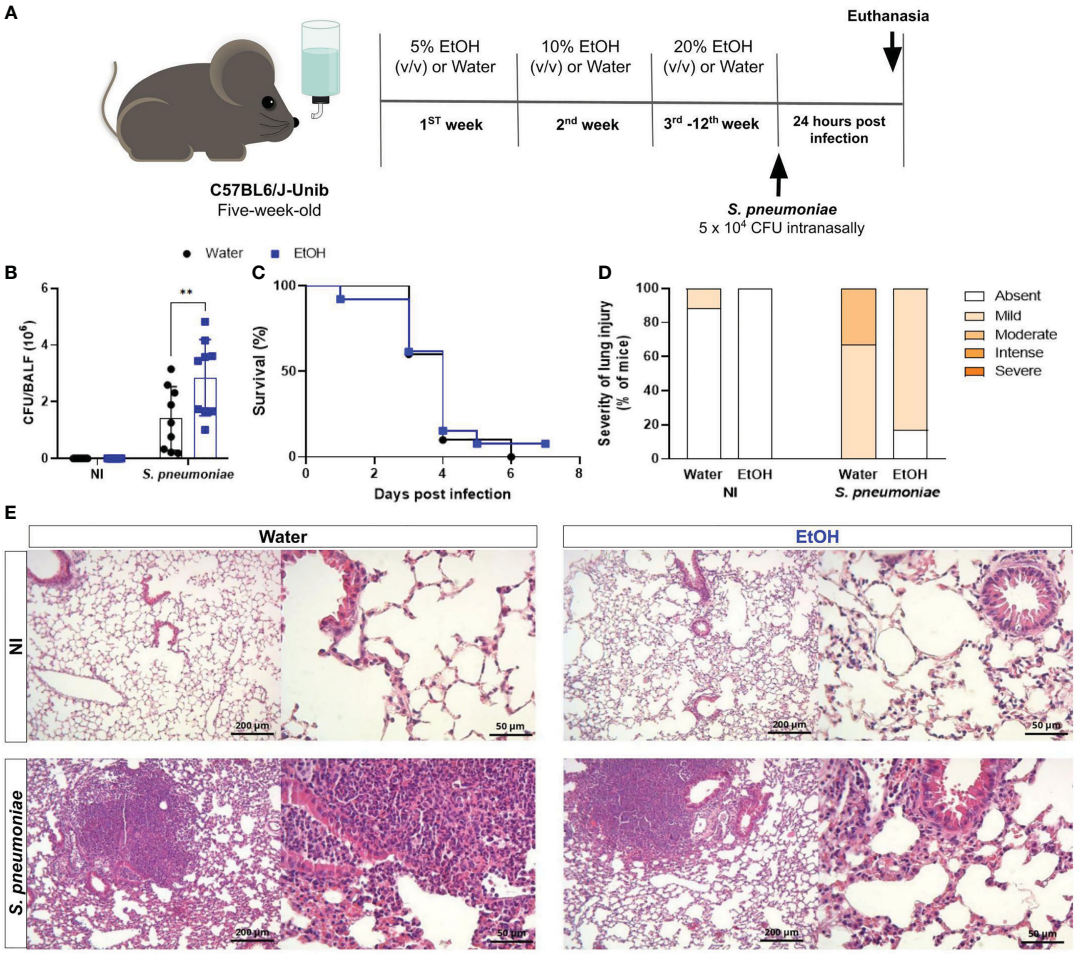

FIGURE 1
Chronic alcohol exposure impaired bacterial clearance with no effects on survival rate after *S. pneumoniae* infection. **(A)** Methodological scheme of exposure to ethanol and infection. Five-week-old male C57BL6/J-Unib mice started the chronically exposure to ethanol with a 5% (v/v) alcoholic solution. Alcohol concentration doubled after one week until the third week and remained stable (20% v/v) at the end of treatment. After alcohol treatment, mice were infected with 5 x 10^4 CFU of *S. pneumoniae*. After 24h hours of infection, mice were euthanized. **(B)** Bacterial Load into the lungs after infection. **(C)** Lethality curves. **(D)** Percentage of mice with different severity of lung inflammatory lesions and **(E)** representative H&E stained lung section images under light microscopy at 10x and 40x magnification. Data are presented as the mean ± SD (6 to 9 mice per group). ** Significantly different ($p < 0.01$) by two-way ANOVA analysis test.

inflammatory infiltrate into the lungs of water-treated infected mice compared to ethanol-exposed infected mice (Figure 1E).

3.2 Increased NO production is associated with chronic ethanol exposure

Chronic ethanol consumption is associated with increased NO production in liver, kidney, and lung (33–35). Although cellular NO signaling has an ambiguous role during pneumococcal infection, we investigated whether chronic exposure would alter this inflammatory mechanism (25). To understand NO production in the alveoli of ethanol-exposed mice, we assessed NO production through nitrite formation. Twenty-four hours post-infection, alcohol-fed mice produced increased amounts of NO in BALF, whereas untreated infected mice showed a similar NO production to uninfected mice (Figure 2A). As NO signaling has been linked to production of other inflammatory mediators, we investigated whether this increase in BALF NO levels would also be associated with an increase in CXCL1 (16, 23, 24, 36).

3.3 Chronic alcohol exposure increases CXCL1 released in BALF and blood in pneumococcal infection

The orchestration of the inflammatory response is essential for the removal of bacteria from the infectious site (19). This process ranges from pathogen recognition to the recruitment and activation of phagocytes (37). CXCL1 is an important chemokine responsible for the influx of neutrophils into the lungs during Gram-positive bacterial pneumonia (20). Twenty-four hours after infection, alcohol-fed mice produced significantly higher amounts of CXCL1 in BALF compared to infected untreated mice

10.3389/fimmu.2023.1175275

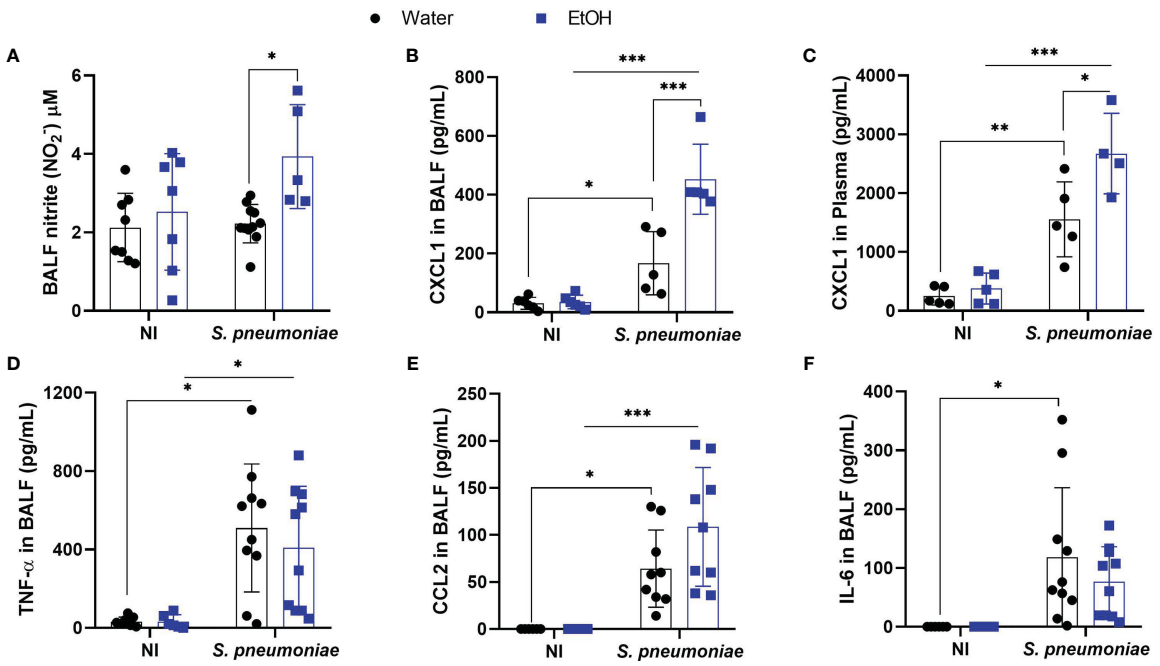

FIGURE 2
Alcohol-fed mice had higher production of NO, CXCL1 in BALF and plasma 24 hours after pneumococcal infection. After alcohol treatment, mice were infected with *S. pneumoniae* and 24h hours post infection mice were euthanized, BALF and blood plasma was collected to determine **(A)** NO production through Griess reaction and for analysis of pró-inflammatory mediators. CXCR2 ligand, chemokine **(B)** CXCL1 on BALF supernatant and **(C)** plasma, **(D)** TNF-α in BALF, **(E)** CCL2 in BALF and **(F)** IL-6 in BALF. Data are presented as the mean ± SD (4 to 9 mice per group). *Significantly different ($p < 0.05$), **Significantly different ($p < 0.01$) by two-way ANOVA analysis test. ***Significantly different ($p < 0.001$) by two-way ANOVA analysis test.

(Figure 2B). At the same time point, the release of CXCL1 in plasma increased in both infected mice, with alcohol-fed mice showing higher levels of this chemokine (Figure 2C). Although CXCL2 is also a CXCR2 ligand and plays an important role in neutrophil recruitment to sites of infection, CXCL2 levels did not change in the blood or alveoli of both infected or uninfected groups. (Supplementary Figure 1). We also assessed BALF levels of other important pro-inflammatory mediators during pneumococcal pneumonia such as TNF-α, IL-6 and CCL2. The levels of these mediators increased in the alveoli twenty-four hours after infection, but there were no statistical differences between ethanol-treated infected mice and water-treated infected mice groups (Figures 2D–F).

3.4 Decreased neutrophil and macrophage migration to alveoli is associated with ethanol exposure also in the presence of high levels of chemokines

To understand the significantly increased bacterial load into alcohol-fed mice even in the presence of higher levels of NO and CXCL1, we decided to investigate inflammatory cell influx into the infection site. Ethanol consumption did not affect the total cell amount in alveoli before the bacterial challenge (Figure 3A). After infection, alcohol-fed mice demonstrated a significantly decreased number of cells into the airways compared to non-treated infected mice (Figure 3A). To analyze the immune cell profile that migrates to alveoli during *S. pneumoniae* infection, we performed a double-blind differential cell count. Both groups of infected mice showed a massive neutrophil and macrophage infiltration, even though alcohol-fed mice presented a decreased migration of both cell types into alveoli (Figures 3B, C).

Despite the reduced migration of leukocytes into the BALF of infected mice exposed to ethanol, the total amount of circulating leukocytes in the blood was not altered in any of the experimental groups (Figure 3D). When polymorphonuclear and mononuclear cells in the blood were assessed, no differences were observed between any of the groups (Figures 3E, F). At the same time post-infection, we also observed no difference in the indirect quantification of neutrophils or macrophages in the lung parenchyma by the NAG and MPO assays (Figures 3G, H).

4 Discussion

Alcohol exposure is already known as a risk factor for *S. pneumoniae* infection by affecting the immune response during pneumococcal pneumonia, although the mechanisms involved with chronic alcohol consumption are not yet fully understood (9, 38–40). Here we demonstrated that increased bacterial load in alcohol-fed mice is associated with decreased leukocyte migration into the alveoli, reduced frequency of severe lung inflammation and systemic and local CXCL1 release during infection (Figure 4).

10.3389/fimmu.2023.1175275

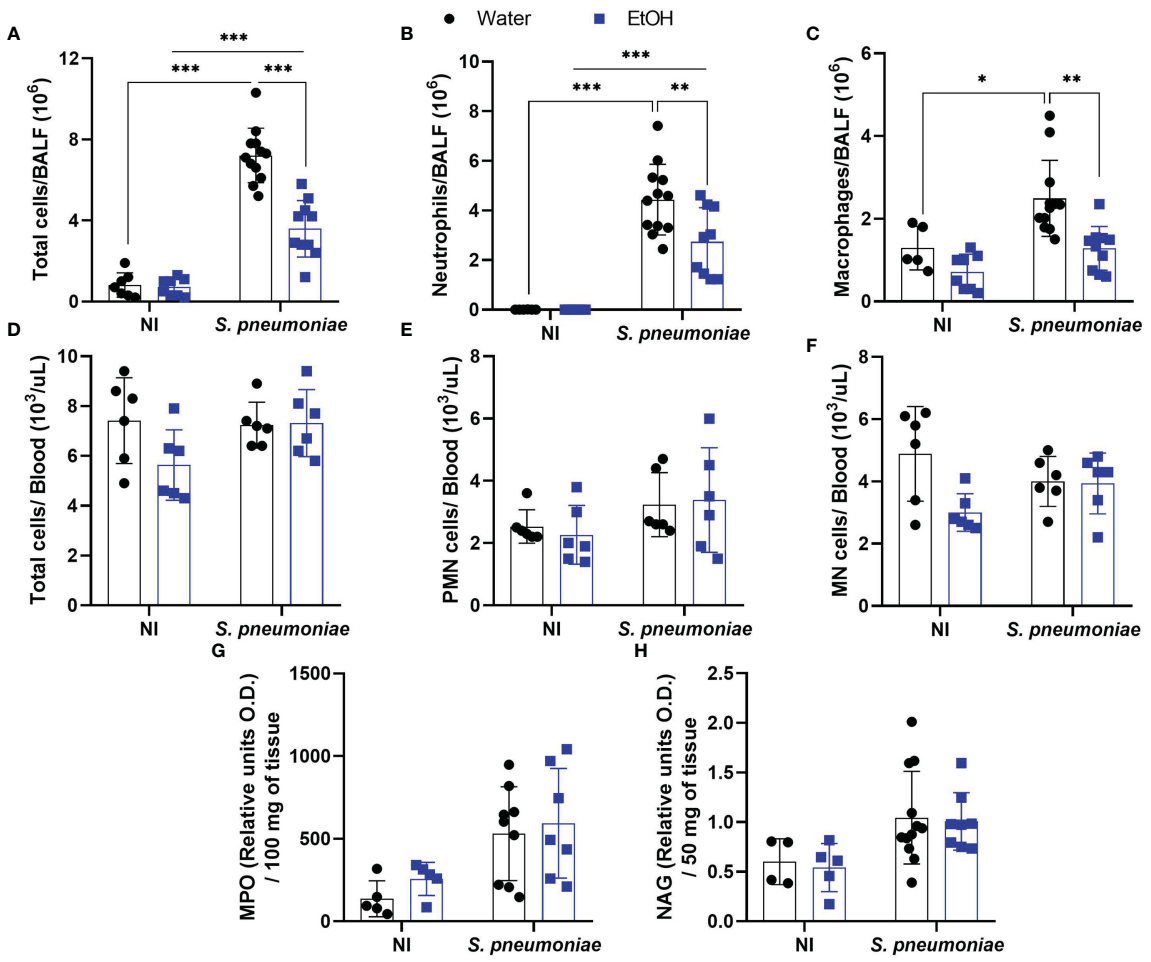

FIGURE 3
Alcohol-fed mice have decreased neutrophil and macrophage infiltration into airways 24 hours post pneumococcal infection. After alcohol treatment, mice were infected with *S. pneumoniae*. After 24h hours of infection, mice were euthanized, BALF, blood and lungs were collected to determine the infiltration of inflammatory cells. **(A)** Total cells, **(B)** Neutrophils and **(C)** Macrophages count in BALF. **(D)** Total cells, **(E)** polymorphonuclear cells and **(F)** mononuclear cells into the blood. **(G)** Neutrophils and **(H)** macrophages infiltrated into the lung parenchyma. Data are presented as the mean ± SD (7 to 11 mice per group). * Significantly different ($p < 0.05$), **Significantly different ($p < 0.01$), ***Significantly different ($p < 0.001$) by two-way ANOVA analysis test.

Neutrophil migration into the lungs is a critical mechanism during pneumococcal infection. Neutrophil depletion reduced clearance of *S. pneumoniae* in a mouse model of infection (41). In addition, antimicrobial mechanisms released by activated neutrophils are critical for controlling bacterial growth in the lung, as serine protease-deficient animals have impaired antimicrobial defense and increased mortality after infection (37, 42). Here, we associate the reduced number of alveolar neutrophils with the higher bacterial load in chronically alcohol-fed mice. We observed that the decreased leukocyte amounts in the alveoli of chronically ethanol-exposed and infected mice was reflected as a decrease in the frequency of inflammatory lesions in the lungs. These data show that even when the bacterial load was increased in animals chronically exposed to ethanol, the severity of the lung lesions, observed 24 hours after infection with *S. pneumoniae*, was smaller due to the reduced migration of leukocytes to the site of infection.

Curiously, this phenotype did not affect mortality. This could be due to the balance between an excessive inflammatory response and microbial burden control, or it could be related to higher mortality rate found in this inoculum (43). The ambiguous role of neutrophils in microbial inflammation is also still under investigation. Studies have already shown that attenuation of neutrophil migration is associated with reduced lung injury by preventing the damage caused by neutrophil activation and migration (44). However, the mechanisms related to the survival of alcohol-fed animals with fewer neutrophils and higher fungal load need to be further investigated. Furthermore, one of the limitations of this article is the observation window of leukocyte migration, which is limited to the first 24 hours of infection.

Recently, Hulsebus et al. (2022) demonstrated that moderate alcohol consumption increased the expression of *Cxcl1* in mice lung tissue during pneumococcal infection and was accompanied by the increase in neutrophil infiltrate (5). However, previous results from our research group have shown that although chronic ethanol exposure induces elevated levels of CXCL1 in serum and BALF during *Aspergillus fumigatus* infection, it is also associated with a decrease in neutrophil infiltration, due to a decrease in CXCR2

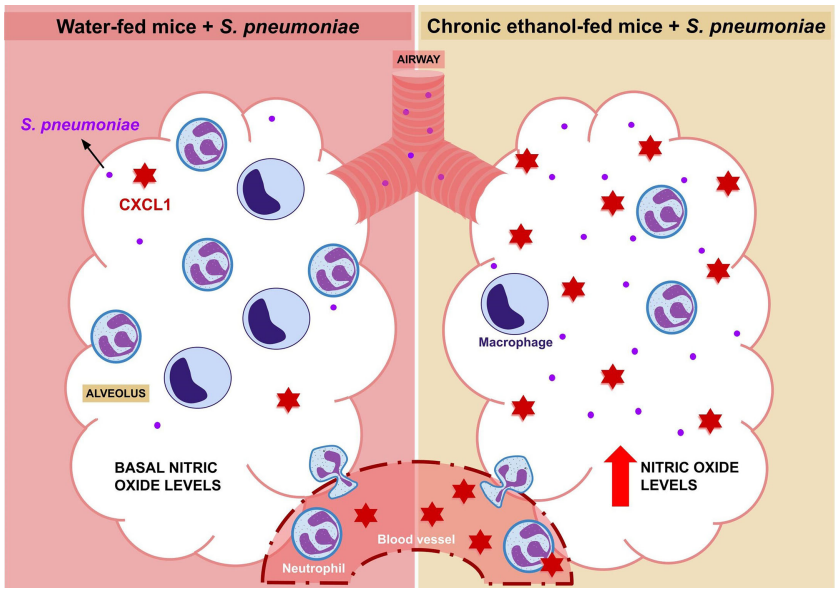

FIGURE 4
Elucidative Design. After 24 hours of infection with Streptococcus pneumoniae, an increase in the migration of macrophages and neutrophils into the alveolus is observed. However, this migration is reduced in alcohol-fed mice, although this group also shows an increase in CXCL1 in plasma and BALF. In contrast to water-fed mice, which have low levels of nitric oxide at baseline, alcohol-fed mice have a higher bacterial load and higher alveolar nitric oxide production compared to untreated mice.

expression in these cells (7). Moreover, we also demonstrated an impairment in neutrophil effector functions and a higher susceptibility to fungal infection (7). Without altering mice susceptibility to pneumococcal pneumonia, our data together suggest that chronic ethanol exposure induces important inflammatory changes during acute pneumonia, impairing adequate neutrophil migration to the site of infection. This phenotype is also observed in sepsis, a decreased neutrophil migration which is associated with increased NO release and consequent overproduction of pro-inflammatory mediators, resulting in failure of neutrophil response and lethality (45, 46).

Acute exposure to ethanol decreases granulocyte migration to the lungs during pneumococcal infection that is related to a decrease in granulopoiesis in the bone marrow (BM) of ethanol-exposed mice (47). Recently, we demonstrated that the same regimen of ethanol exposure used here does neither change the number of circulating cells in treated animals, nor the number of granulocyte precursors in BM (7). Here, we did not observe any change in the number or cell type of circulating leukocytes that could be altered by chronic exposure to ethanol. These data do not exclude the possibility that these cells have altered functionality, but highlight the fact that the decrease in cell migration to the alveoli occurs independently of the number of circulating cells. After our analyses also revealed an equal number of neutrophils and macrophages in the lung parenchyma, we can assume that the chronic effect of ethanol observed is related to the lack of migration of these cells directly to the alveoli.

Ethanol exposure increases NO released from endothelial cells and is associated with liver injury in alcoholic hepatitis (33, 48, 49). NO is known to have a role in controlling cytokine and chemokine expression (50), which could be a promising target for inflammatory diseases. This important biological mediator alters the expression pattern of genes by disrupting the activity of enzymes responsible for post-transcriptional modifications of histones, such as histone acetyltransferases and methyltransferases (51). The modification of the epigenetic code and the interaction of the transcriptional machinery with gene promoters is a determining factor for the inflammatory cell profile (52). In conjunction with the increased production of NO in the BALF of ethanol-exposed mice during pneumococcal infection, we observed a significant increase in the amount of CXCL1 in the blood and BALF. This increased production of chemokine may be due to nitric oxide and its role in epigenetic modulation during the inflammatory response, but this relationship needs to be further investigated during chronic ethanol treatment. Indeed, as highlighted by Malherbe and Messaoudi, the systemic effects of ethanol metabolism and its by-products in regulating gene expression through epigenetic modifications will be extremely important during infection and homeostasis (11).

The development of invasive pneumococcal disease is more common in people with a history of alcohol abuse, about 21% compared with 6% in the general population (53). Therefore, it is important to search and understand the pathophysiology of pneumococcal infection in patients with a history of alcohol abuse, to improve therapeutic interference and preventive measures for those affected. Health surveillance is also important to ensure that alcoholics receive adequate medical care and have a better outcome during pneumococcal pneumonia.

In conclusion, we demonstrate that chronic ethanol exposure in mice is associated with increased bacterial load and decreased leukocyte migration during pneumococcal pneumonia, even in the presence of higher levels of CXCL1. This profile may be also associated with increased BALF NO production, highlighting the ambiguous role of NO during pneumococcal infection.

Data availability statement

The datasets presented in this study can be found in online repositories. The names of the repository/repositories and accession number(s) can be found in the article/Supplementary Material.

Ethics statement

The animal study was reviewed and approved by Ethics Committee on the Use of Animals at Federal University of Minas Gerais - CEUA UFMG.

Author contributions

FS and NM guided the development of the project and the writing of the manuscript. FM, NM and JS collected the samples and performed the experiments. MO performed the bioinformatics analysis and participated in statistical analysis. FM analyzed the data results and statistical analysis, illustrated the results and wrote the manuscript. CQ-J performed the histopathological analyses. FL and MT participated intellectually in the development of the project. All authors contributed to the article and approved the submitted version.

Funding

This work was supported by Pró-Reitoria de Pesquisa - Universidade Federal de Minas Gerais, Conselho Nacional de Desenvolvimento Científico e Tecnológico - 474528-2012-0; 483184-2011-0. Fundação de Amparo à Pesquisa do Estado de Minas Gerais - APQ- 01756-10; APQ-02198-14; APQ-03950-17; APQ-01899-18. This study was financed in part by the Coordenação de Aperfeiçoamento de Pessoal de Nível Superior - Brasil (CAPES) - Finance Code 001 and Instituto Nacional de Ciência e Tecnologia em Dengue e Interação Microrganismo Hospedeiro (INCT em Dengue). The funders had no role in study design, data collection and analysis, decision to publish, or preparation of the manuscript.

Acknowledgments

We would like to thank Universidade Federal de Minas Gerais for the opportunity to develop this work. We are thankful to Ilma Marçal S. and Rosemeire A. Oliveira.

Conflict of interest

The authors declare that the research was conducted in the absence of any commercial or financial relationships that could be construed as a potential conflict of interest.

Publisher's note

Supplementary material

The Supplementary Material for this article can be found online at: https://www.frontiersin.org/articles/10.3389/fimmu.2023.1175275/full#supplementary-material

References

1. World Health Organization. *Alcohol: fact sheet* (2018-). Available at: https://www.who.int/en/news-room/fact-sheets/detail/alcohol (Accessed February 7, 2023).

2. Killgore WDS, Cloonan SA, Taylor EC, Lucas DA, Dailey NS. Alcohol dependence during COVID-19 lockdowns. *Psychiatry Res* (2021) 296:113676. doi: 10.1016/j.psychres.2020.113676

3. Bailey KL, Samuelson DR, Wyatt TA. Alcohol use disorder: a pre-existing condition for COVID-19? *Alcohol* (2021) 90:11–7. doi: 10.1016/j.alcohol.2020.10.003

4. Morris NL, Michael DN, Crotty KM, Chang SS, Yeligar SM. Alcohol-induced glycolytic shift in alveolar macrophages is mediated by hypoxia-inducible factor-1 alpha. *Front Immunol* (2022) 13:865492. doi: 10.3389/fimmu.2022.865492

5. Hulsebus HJ, Najarro KM, McMahan RH, Boe DM, Orlicky DJ, Kovacs EJ. Ethanol intoxication impairs respiratory function and bacterial clearance and is associated with neutrophil accumulation in the lung after *Streptococcus pneumoniae* infection. *Front Immunol* (2022) 13:884719. doi: 10.3389/fimmu.2022.884719

6. Xu HQ, Wang CG, Zhou Q, Gao YH. Effects of alcohol consumption on viral hepatitis b and c. *World J Clin cases* (2021) 9(33):10052–63. doi: 10.12998/wjcc.v9.i33.10052

7. Malacco NLSO, Souza JAM, Martins FRB, Rachid MA, Simplicio JA, Tirapelli CR, et al. Chronic ethanol consumption compromises neutrophil function in acute pulmonary *Aspergillus fumigatus* infection. *Elife* (2020) 239:e58855. doi: 10.7554/eLife.58855

8. Kany S, Janicova A, Relja B. Innate immunity and alcohol. *J Clin Med* (2019) 8 (11):1981. doi: 10.3390/jcm8111981

9. Yeligar SM, Chen MM, Kovacs EJ, Sisson JH, Burnham EL, Brown LA. Alcohol and lung injury and immunity. *Alcohol* (2016) 55:51-9. doi: 10.1016/j.alcohol.2016.08.005

10. Dai Q, Pruett SB. Different effects of acute and chronic ethanol on LPS-induced cytokine production and TLR4 receptor behavior in mouse peritoneal macrophages. *J Immunotoxicol* (2006) 3(4):217–25. doi: 10.1080/15476910601080156

11. Malherbe DC, Messaoudi I. Transcriptional and epigenetic regulation of monocyte and macrophage dysfunction by chronic alcohol consumption. *Front Immunol* (2022) 13:911951. doi: 10.3389/fimmu.2022.911951

12. Gupta NM, Lindenauer PK, Yu PC, Imrey PB, Haessler S, Deshpande A, et al. Association between alcohol use disorders and outcomes of patients hospitalized with community-acquired pneumonia. *JAMA Netw Open* (2019) 2(6):e195172. doi: 10.1001/jamanetworkopen.2019.5172

13. Wahl B, O'Brien KL, Greenbaum A, Majumder A, Liu L, Chu Y, et al. Burden of streptococcus pneumoniae and haemophilus influenzae type b disease in children in the

era of conjugate vaccines: global, regional, and national estimates for 2000-15. *Lancet Glob Health* (2018) 6(7):e744–57. doi: 10.1016/S2214-109X(18)30247-X

14. World Health Organization. *Pneumococcus: vaccine preventable diseases surveillance standards* (2018). Available at: https://www.who.int/publications/m/item/vaccine-preventable-diseases-surveillance-standards-pneumococcus (Accessed February 7, 2023).

15. Koppe U, Suttorp N, Opitz B. Recognition of *Streptococcus pneumoniae* by the innate immune system. *Cell Microbiol* (2012) 14(4):460–6. doi: 10.1111/j.1462-5822.2011.01746.x

16. Marriott HM, Hellewell PG, Whyte MK, Dockrell DH. Contrasting roles for reactive oxygen species and nitric oxide in the innate response to pulmonary infection with streptococcus pneumoniae. *Vaccine* (2007) 25(13):2485–90. doi: 10.1016/j.vaccine.2006.09.024

17. Knapp S, Leemans JC, Florquin S, Branger J, Maris NA, Pater J, et al. Alveolar macrophages have a protective antiinflammatory role during murine pneumococcal pneumonia. *Am J Respir Crit Care Med* (2003) 167(2):171–9. doi: 10.1164/rccm.200207-698OC

18. Schrottmaier WC, Kral-Pointner JB, Salzmann M, Mussbacher M, Schmuckenschlager A, Pirabe A, et al. Platelet p110β mediates platelet-leukocyte interaction and curtails bacterial dissemination in pneumococcal pneumonia. *Cell Rep* (2022) 41(6):111614. doi: 10.1016/j.celrep.2022.111614

19. Van der Poll T, Opal SM. Pathogenesis, treatment, and prevention of pneumococcal pneumonia. *Lancet* (2009) 374(9700):1543–56. doi: 10.1016/S0140-6736(09)61114-4

20. Paudel S, Baral P, Ghimire L, Bergeron S, Jin L, DeCorte JA, et al. CXCL1 regulates neutrophil homeostasis in pneumonia-derived sepsis caused by streptococcus pneumoniae serotype 3. *Blood* (2019) 133(12):1335–45. doi: 10.1182/blood-2018-10-878082

21. Phillipson M, Kubes P. The neutrophil in vascular inflammation. *Nat Med* (2011) 17(11):1381–90. doi: 10.1038/nm.2514

22. Marriott HM, Ali F, Read RC, Mitchell TJ, Whyte MK, Dockrell DH. Nitric oxide levels regulate macrophage commitment to apoptosis or necrosis during pneumococcal infection. *FASEB J* (2004) 18(10):1126–8. doi: 10.1096/fj.03-1450fje

23. Pfeilschifter J, Eberhardt W, Beck KF. Regulation of gene expression by nitric oxide. *Pflugers Arch* (2001) 442(4):479–86. doi: 10.1007/s004240100586

24. Fang FC. Perspectives series: host/pathogen interactions. mechanisms of nitric oxide-related antimicrobial activity. *J Clin Invest* (1997) 99:2818–25. doi: 10.1172/JCI119473

25. Kerr AR, Wei XQ, Andrew PW, Mitchell TJ. Nitric oxide exerts distinct effects in local and systemic infections with streptococcus pneumoniae. *Microbial Pathogenesis* (2004) 36(6):303–10. doi: 10.1016/j.micpath.2004.02.001

26. Yeligar SM, Harris FL, Hart CM, Brown LA. Ethanol induces oxidative stress in alveolar macrophages via upregulation of NADPH oxidases. *J Immunol* (2012) 188 (8):3648–57. doi: 10.4049/jimmunol.1101278

27. Tavares LP, Garcia CC, Vago JP, Queiroz-Junior CM, Galvão I, David BA, et al. Inhibition of phosphodiesterase-4 during pneumococcal pneumonia reduces inflammation and lung injury in mice. *Am J Respir Cell Mol Biol* (2016) 55(1):24–34. doi: 10.1165/rcmb.2015-0083OC

28. Horvat JC, Beagley KW, Wade MA, Preston JA, Hansbro NG, Hickey DK, et al. Neonatal chlamydial infection induces mixed T-cell responses that drive allergic airway disease. *Am J Respir Crit Care Med* (2007) 176(6):556–64. doi: 10.1164/rccm.200607-1005OC

29. Malacco NLSO, Souza JA, Mendes AC, Rachid MA, Kraemer LR, Mattos MS, et al. Acute lung injury and repair induced by single exposure of *Aspergillus fumigatus* in immunocompetent mice. *Future Microbiol* (2019) 14:1511–25. doi: 10.2217/fmb-2019-0214

30. de Francischi JN, Queiroz-Junior CM, Pacheco CMDF, Fonseca AH, Klein A, Caliari MV. Myeloperoxidase content is a marker of systemic inflammation in a chronic condition: the example given by the periodontal disease in rats. *Mediators Inflammation* (2009) 60837. doi: 10.1155/2009/760837.760837

31. Barcelos LS, Talvani A, Teixeira AS, Vieira LQ, Cassali GD, Andrade SP, et al. Impaired inflammatory angiogenesis, but not leukocyte influx, in mice lacking TNFR1. *J Leukocyte Biol* (2005) 78(2):352–8. doi: 10.1189/jlb.1104682

32. Tsikas D. Analysis of nitrite and nitrate in biological fluids by assays based on the griess reaction: appraisal of the griess reaction in the l-arginine/nitric oxide area of research. *J Chromatogr B Anal Technol Biomed Life Sci* (2007) 851:51–70. doi: 10.1016/j.jchromb.2006.07.054

33. Tirapelli LF, Batalhão ME, Jacob-Ferreira AL, Tirapelli DP, Carnio EC, Tanus-Santos JE, et al. Chronic ethanol consumption induces histopathological changes and increases nitric oxide generation in the rat liver. *Tissue Cell* (2011) 43(6):384–91. doi: 10.1016/j.tice.2011.08.003

34. Tirapelli LF, Martins-Oliveira A, Batalhão ME, Tirapelli DP, Carnio EC, Tanus-Santos JE, et al. Ethanol consumption increases the expression of endothelial nitric oxide synthase, inducible nitric oxide synthase and metalloproteinases in the rat kidney. *J Pharm Pharmacol* (2012) 64(1):68–76. doi: 10.1111/j.2042-7158.2011.01396.x

35. Polikandriotis JA, Rupnow HL, Brown LA, Hart CM. Chronic ethanol ingestion increases nitric oxide production in the lung. *Alcohol* (2007) 41(5):309–16. doi: 10.1016/j.alcohol.2007.03.012

36. Vasudevan D, Hickok JR, Bovee RC, Pham V, Mantell LL, Bahroos N, et al. Nitric oxide regulates gene expression in cancers by controlling histone posttranslational modifications. *Cancer Res* (2015) 75(24):5299–308. doi: 10.1158/0008-5472.CAN-15-1582

37. Domon H, Terao Y. The role of neutrophils and neutrophil elastase in pneumococcal pneumonia. *Front Cell Infect Microbiol* (2021) 11:615959. doi: 10.3389/fcimb.2021.615959

38. de Roux A, Cavalcanti M, Marcos MA, Garcia E, Ewig S, Mensa J, et al. Impact of alcohol abuse in the etiology and severity of community-acquired pneumonia. *Chest* (2006) 129:1219–25. doi: 10.1378/chest.129.5.1219

39. Garcia-Vidal C, Ardanuy C, Tubau F, Viasus D, Dorca J, Liñares J, et al. Pneumococcal pneumonia presenting with septic shock: host- and pathogen-related factors and outcomes. *Thorax* (2010) 65:77–81. doi: 10.1136/thx.2009.123612

40. Bhatty M, Pruett SB, Swiatlo E, Nanduri B. Alcohol abuse and streptococcus pneumoniae infections: consideration of virulence factors and impaired immune responses. *Alcohol* (2011) 45(6):523–39. doi: 10.1016/j.alcohol.2011.02.305

41. Garvy BA, Harmsen AG. The importance of neutrophils in resistance to pneumococcal pneumonia in adult and neonatal mice. *Inflammation* (1996) 20:499–512. doi: 10.1007/BF01487042

42. Hahn I, Klaus A, Janze AK, Steinwede K, Ding N, Bohling J, et al. Cathepsin G and neutrophil elastase play critical and nonredundant roles in lung-protective immunity against streptococcus pneumoniae in mice. *Infect Immun* (2011) 79 (12):4893–901. doi: 10.1128/IAI.05593-11

43. Casadevall A, Pirofski L-A. The damage-response framework of microbial pathogenesis. *Nat Rev Microbiol* (2003) 1:17–24. doi: 10.1038/nrmicro732

44. Kovtun A, Messerer DAC, Scharffetter-Kochanek K, Huber-Lang M, Ignatius A. Neutrophils in tissue trauma of the skin, bone, and lung: two sides of the same coin. *J Immunol Res* (2018) 8173983:12. doi: 10.1155/2018/8173983

45. Zhang F, Liu A-L, Gao S, Ma S, Guo S-B. Neutrophil dysfunction in sepsis. *Chin Med J* (2016) 129(22):2741–4. doi: 10.4103/0366-6999.193447

46. Benjamim CF, Ferreira SH, Cunha FQ. Role of nitric oxide in the failure of neutrophil migration in sepsis. *J Infect Dis* (2000) 182:214–23. doi: 10.1086/315682

47. Raasch CE, Zhang P, Siggins RWII, LaMotte LR, Nelson S, Bagby GJ. Acute alcohol intoxication impairs the hematopoietic precursor cell response to pneumococcal pneumonia. *Alcohol Clin Exp Res* (2010) 34(12):2035–43. doi: 10.1111/j.1530-0277.2010.01291.x

48. Kaewphaleuk T, Watanapa WB, Panich U. Ethanol enhances endothelial ionic currents and nitric oxide release via intermediate-conductance calcium-activated potassium channel. *Life Sci* (2019) 228:21–9. doi: 10.1016/j.lfs.2019.04.052

49. Deng XS, Deitrich R. Ethanol metabolism and effects: nitric oxide and its interaction. *Curr Clin Pharmacol* (2007) 2(2):145–53. doi: 10.2174/157488407780598135

50. Kobayashi Y. The regulatory role of nitric oxide in proinflammatory cytokine expression during the induction and resolution of inflammation. *J Leukoc Biol* (2010) 88(6):1157–62. doi: 10.1189/jlb.0310149

51. Socco S, Bovee RC, Palczewski MB, Hickok JR, Thomas DD. Epigenetics: the third pillar of nitric oxide signalling. *Pharmacol Res* (2017) 121:52–8. doi: 10.1016/j.phrs.2017.04.011

52. Fyodorov DV, Zhou BR, Skoultchi AI, Bai Y. Emerging roles of linker histones in regulating chromatin structure and function. *Nat Rev Mol Cell Biol* (2018) 192–206. doi: 10.1038/nrm.2017.94

53. Grau I, Ardanuy C, Calatayud L, Schulze MH, Liñares J, Pallares R. Smoking and alcohol abuse are the most preventable risk factors for invasive pneumonia and other pneumococcal infections. *Int J Infect Dis* (2014) 25:59–64. doi: 10.1016/j.ijid.2013.12.013

Frontiers in Immunology

Explores novel approaches and diagnoses to treat immune disorders.

The official journal of the International Union of Immunological Societies (IUIS) and the most cited in its field, leading the way for research across basic, translational and clinical immunology.

Discover the latest Research Topics

See more →

Frontiers

Avenue du Tribunal-Fédéral 34
1005 Lausanne, Switzerland
frontiersin.org

Contact us

+41 (0)21 510 17 00
frontiersin.org/about/contact